Sediment Routing and Recycling through Multiple Basins from Palaeozoic to Mesozoic Times: a Provenance Study of the Devonian Old Red Sandstone of Southern Ireland and Neighbouring Offshore Mesozoic Basins.

Brenton J. Fairey, BSc (Hons), MSc

A thesis submitted for the degree of
Doctor of Philosophy

November, 2017

National University of Ireland, Cork
Geology, School of Biological, Earth and Environmental Sciences

Principal supervisor: Dr. Patrick A. Meere
Co-supervisor: Dr. Kieran F. Mulchrone
Advisor: Dr. David E. Jarvis
Head of Discipline: Prof. Andrew J. Wheeler
Head of School: Prof. Sarah C. Culloty

Table of Contents

List of Figures

List of Abbreviations

AFT	Apatite Fission Track
BT	Bellewstown Terrane
°C	Degrees Celcius
CBB	Cardigan Bay Basin
CDF	Cumulative Distribution Function
CG	Carnsore Granite
CISB	Central Irish Sea Basin
CKL	Cork-Kenmare Line
CL	Cathodoluminescence
DB	Dingle Basin
DBGML	Dingle Bay-Galtee Mountain Line
FB	Fastnet Basin
Ga	Giga-annum/billion years ago
GG	Galway Granite
GSB	Goban Spur Basin
GT	Grangegeeth Terrane
ISZ	Iapetus Suture Zone
KBB	Kish Bank Basin
KDE	Kernel Density Estimation
KMFZ	Killarney-Mallow Fault Zone
K-S	Kolmogorov-Smirnov
LA-ICP-MS	Laser Ablation-Sector Field-Inductively Coupled Plasma-Mass Spectrometry/Spectrometer
LA-SF-ICP-MS	Laser Ablation-Sector Field-Inductively Coupled Plasma-Mass Spectrometry/Spectrometer
LB	Labadie Bank

LORS	Lower Old Red Sandstone
NIC	Newry Igneous Complex
Ma	Mega-annum/million years ago
MDS	Multi-Dimensional Scaling
N	number of samples
n	number of grains analysed
NCSB	North Celtic Sea Basin
NKL	North Kerry Lineament
ORS	Old Red Sandstone
PDP	Probability Density Plot
PR	Pembrokeshire Ridge
SCSB	South Celtic Sea Basin
SEM	Scanning Electron Microscope
SG	Saltees Granite
SGSB	St. Georges Channel Basin
SMB	South Munster Basin
TD	Total depth
TIC	Tyrone Igneous Complex
UORS	Upper Old Red Sandstone
VR	Vitrinite Reflectance

Declaration

I hereby declare that this thesis has not been submitted for another degree at University College Cork or any other university. The work described in this thesis is entirely that of the author except where otherwise stated.

This thesis is submitted in fulfilment of the requirement of the degree of Doctor of Philosophy at the National University of Ireland, Cork in the School of Biological, Earth and Environmental Sciences (Discipline of Geology), College of Science, Engineering and Food Science.

Signed…….. Date……

Brenton J. Fairey

Acknowledgements

The work presented in this thesis is the culmination of a long journey to Ireland to undertake four years of research. I could not, however, have come this far without the guidance, friendship, support and kindness of many people that I have met along the way. Of course, none of it would have been possible without the guidance and supervision of Drs Pat Meere and Kieran Mulchrone. I am indebted to Pat for familiarising me with Irish geology (and pronunciation of Irish words) and having an open-door policy. Your patience is truly admirable to say the least! I have learnt a lot from you, not least in relation to correctly applying a handbrake in the field. I don't think I have met a more accommodating person – I really am extremely grateful for all you have done Pat.

Kieran has also shown amazing support, having made all those strenuous trips to far-away lands to support me at conferences. Your knack for finding an Irish pub in foreign countries is impressive. Our discussions during early phases of the project really helped to shape the thesis and your support and feedback throughout is very much appreciated.

I would also like to thank my advisor, Dr Ed Jarvis. I took the term 'advisor' quite literally and you always kindly obliged. Thank you for your help with field work and for keeping me entertained on those not-so-productive days. Perhaps one day you will succumb to my incessant requests for that mini barrel of oil. Mary McSweeney, Elaine Kelly and Sinead Smith are thanked for all their help with administrative affairs – and there were many. Mary Lehane and Stuart Warner are thanked for their technical assistance and always being able to help at the drop of a hat. Dr. John Reevey is thanked for his help with all things granitic and Prof. Emeritus Ken Higgs for his useful discussions on Munster Basin stratigraphy. A special mention must also go to Prof. Hari Tsikos who took a chance on me and taught me how to undertake research. Without his mentorship and encouragement, I would not have made it this far.

I would like to thank Dr. Daniel Pastor-Galán for his sampling and geochronological advice during the early stages of the project and for introducing us to the teams in Dresden and Amsterdam. Mr. Keith Byrne is thanked for his advice about all things offshore and for many useful comments

and discussions. Mr Charlie Carlisle is thanked for his assistance in sampling offshore material.

A number of people at the Vrije Universteit Amsterdam were instrumental in sample preparation and data acquisition. Mr. Roel van Elsas is warmly thanked for his patience and humour in assisting with mineral separation and teaching me the many steps involved. Dr Klaudia Kuiper is thanked for her expertise and acquisition of Ar-Ar data and for feedback on early manuscripts. Prof. Jan Wijbrans is also thanked for being so accommodating and granting the use of his laboratories and office space.

In Dresden, Prof. Dr. Ulf Linnemann is thanked for accommodating me in his laboratory and helping with the ICP-MS. A special thank you, also, to Mandy Hofmann who gave up a lot of her time, and had to wake up extra early, to ready the laboratory for each day's zapping. She is also thanked for translating the lunch menu to English every day and teaching me how to reduce the ICP-MS data. The entire Dresden team, which also includes Mr. Andreas Gärtner and Ms. Benita-Lisette Sonntag are thanked for their efforts in reducing the detrital zircon data and for helping with any zircon-related queries. Andreas is also thanked for generously making available his compilation of Avalonian zircon age data.

I would also like to thank Drs Dave Chew, Chris Mark and Nathan Cogné for providing unpublished apatite age data and for constructive comments on early drafts of two of the manuscripts. Thank you, also, to Mr. Colin Reid and Ms. Leona O'Connor for their assistance with CL imaging. Dr. Meg Ennis is thanked for her advice and comments and for providing data and thin sections from her thesis.

I started this project with a partner-in-crime – Mr. Aidan Kerrison. Thank you for all your help in the field, laboratory and office, and for teaching me all your strange Australian ways. Thank you also for putting up with my terrible Australian accent. We certainly had our ups and downs, but I cannot deny the extremely important part you played in bringing this work to fruition. To all the other people I had the privilege of sharing office space with – Dr. Greg Beechinor, proto-Dr Nidia Alavarez-Armada, Dr. Dave McCarthy (briefly), Dr. Aaron Lim and proto-Dr. Mohit Tunwal. A-a-ron and Mo – thank you both for

putting up with all my nonsense and keeping things interesting in the office. Dave – your help with settling, providing papers and geological insight right at the beginning of it all is much appreciated. Dr. Will McCarthy gave me a place to stay in St. Andrews and attempted to cook me some haggis. Thank you for being so accommodating Will.

To the members of the “Upside-Down-House”, Aidan, Mohit, Ben Philip and Juergen Lang, thank you all for making it so easy to live in Cork City. Ben – thank you for being our personal chauffeur! It was good to have someone to reminisce about Africa with and think about how we can make money with snakes and beer cans.

To my family, especially my mother, Anne, and sister, Sam, thank you for supporting me and seeing me whenever you were on this end of the planet. Sam and Howard – thank you for accommodating me when I have come back to South Africa, and for driving me everywhere. You have no idea how much I appreciate you all.

Last, but most certainly not least, thank you to my partner, Bryony, who has stuck with me through years of living apart. Your support has been invaluable to me and I am so grateful that you have stuck by me through all the fossil talk, Ryanair travel, pretending to be clever, stopping to look at rocks, stressing for no apparent reason.

Acknowledgement of Funding

This project was funded by the Irish Shelf Petroleum Studies Group (ISPSG) of the Irish Petroleum Infrastructure Programme (PIP) Group 4 (project code IS 12/05 UCC). The ISPSG comprises: Atlantic Petroleum (Ireland) Ltd, Cairn Energy Plc, Chrysaor E&P Ireland Ltd, Chevron North Sea Limited, ENI Ireland BV, Europa Oil & Gas, ExxonMobil E&P Ireland (Offshore) Ltd., Husky Energy, Kosmos Energy LLC, Maersk Oil North Sea UK Ltd, Petroleum Affairs Division of the Department of Communications, Energy and Natural Resources, Providence Resources Plc, Repsol Exploración SA, San Leon Energy Plc, Serica Energy Plc, Shell E&P Ireland Ltd, Sosina Exploration Ltd, Tullow Oil Plc and Woodside Energy (Ireland) Pty Ltd.

ABSTRACT

This study presents the first dataset of detrital zircon U-Pb ages from the Devonian Old Red Sandstone (ORS) in the Dingle and Munster Basins as well as the offshore Mesozoic North Celtic Sea Basin (NCSB), South Celtic Sea Basin (SCSB), Goban Spur Basin (GSB) and Fastnet Basin (FB). This large dataset is complimented by new detrital white mica Ar-Ar ages in both onshore and offshore basins as well as apatite U-Pb ages in the Dingle and Munster Basins. Previous work (Ennis et al., 2015; Soper and Woodcock, 2003) has indicated the possibility of recycling of Lower ORS (LORS) into the Upper ORS (UORS) due to mid-Devonian Acadian deformation and basin inversion. By exploring the possible sediment sources for each basin, the study aims to investigate the role of recycling in sediment provision to answer two main questions:

1) Does the UORS in southern Ireland represent large-scale recycling of LORS from the Dingle Basin?
2) Does the southern Irish ORS act as a major source of detritus for Triassic to Cretaceous sediments of the NCSB, SCSB, GSB and FB?

Sedimentary rocks in the LORS have similar detrital zircon age distributions which are dominated by ca. 1.2 Ga zircons as well as late Neoproterozoic grains. These age distributions suggest a dominant contribution of detritus of Laurentian affinity as well as contributions from westerly and southerly derived Ganderian (peri-Gondwanan) detritus. Caledonian uplift of the area north of the Iapetus Suture would have allowed for a large contribution of Laurentian material. The majority of UORS samples contain very few late Neoproterozoic grains and are instead dominated by early Palaeozoic and ca. 1.1 Ga zircons. These detrital zircon age distributions represent recycling of northerly-derived Ordovician to Silurian sedimentary rocks of the Southern Uplands – Longford Down terrane, which are of Laurentian affinity, and not recycling of LORS as previously suggested. The western Toe Head and Old Head Sandstone Formations, which represent the transition from terrestrial ORS to Carboniferous marine environments, are dominated by zircons of Acadian (410-390 Ma) age as well as late Neoproterozoic zircons, suggesting a western offshore Acadian granite

source. Clastic rocks of the eastern Old Head Sandstone Formation have a Laurentian provenance like that of the underlying UORS. Detrital apatite and white micas from the ORS indicate Late Caledonian (430-420 Ma) to Acadian sources which were generally not recorded by detrital zircon ages.

The majority of samples in the offshore basins of southern Ireland have complex detrital zircon age distributions which indicate a mixture of sources. Most samples contain an abundance of late Neoproterozoic zircons of peri-Gondwanan affinity. Potential candidates for these zircons include Ganderia, Megumia, Avalonia and Cadomia but distinguishing between these is problematic – especially given the likely mixture of sources. The abundance of late Mesoproterozoic detrital zircons in some samples indicates the presence of a Laurentian source with the most likely delivery method for such zircons being recycling of UORS sedimentary rocks, simply due to their close proximity (forming the footwall to the NCSB) to the Mesozoic basins. Two detrital white mica samples have dominant Late Caledonian (~430 Ma) ages, one sample has mostly Acadian (~405 Ma) and one sample has a dominant late Neoproterozoic age. Thus, sediments in the southern Irish offshore basins were predominantly sourced from peri-Gondwanan terranes, Caledonian and Acadian granites and recycling of UORS sedimentary rocks.

1 Introduction

The geology south of the Iapetus Suture Zone (ISZ; Figure 1–1) in Ireland is dominated by sedimentary and volcanic successions of the Devonian Old Red Sandstone (ORS). The widespread nature of these predominantly continental deposits in southern Ireland has prompted a number of previous workers to suggest that adjacent offshore Triassic to Cretaceous sedimentary rocks from the Celtic Sea and surrounding areas may represent recycling of ORS rocks (e.g. Caston, 1995; Ewins and Shannon, 1995; Tyrrell, 2005). Even within the ORS successions in southern Ireland and in Britain, workers have suggested that the Lower ORS (LORS), such as that found in the Lower to Middle Devonian Dingle Basin in County Kerry, had been recycled into the Upper ORS (UORS) during a period of Acadian (410-390 Ma) uplift (Ennis et al., 2015; Soper and Woodcock, 2003). Thus, Mesozoic sedimentary rocks of the North Celtic Sea Basin (NCSB), South Celtic Sea Basin (SCSB), Fastnet and Goban Spur basins may represent at least three cycles of erosion and deposition.

The Dingle Basin occupies an area just south of the ISZ in south western Ireland (Figure 1–2). It hosts the only Lower Devonian sedimentary rocks (the LORS) in southern Ireland and its position just south of the ISZ and just north of the traditional Variscan front means that it is likely to record information relating to Caledonian, Acadian and Variscan orogenic activity (Todd, 2015). Of the five tectonostratigraphic units that make up the ORS on the Dingle Peninsula, the Dingle Group constitutes the largest proportion of sedimentary rocks (Todd, 1989). Within the Dingle Group, we analysed one sample each from the Slea Head and Coumeenoole Formations which represent a major axial braided river which flowed toward the northeast (Todd, 2000). Previous provenance studies (e.g. Ennis et al., 2015; Todd, 1989, 2000) have focussed on mica geochronology, conventional petrography, facies analysis, clast composition and Nd isotopes. The natural progression in building upon our understanding of the provenance of these post-Caledonian successions is to integrate apatite and zircon U-Pb ages.

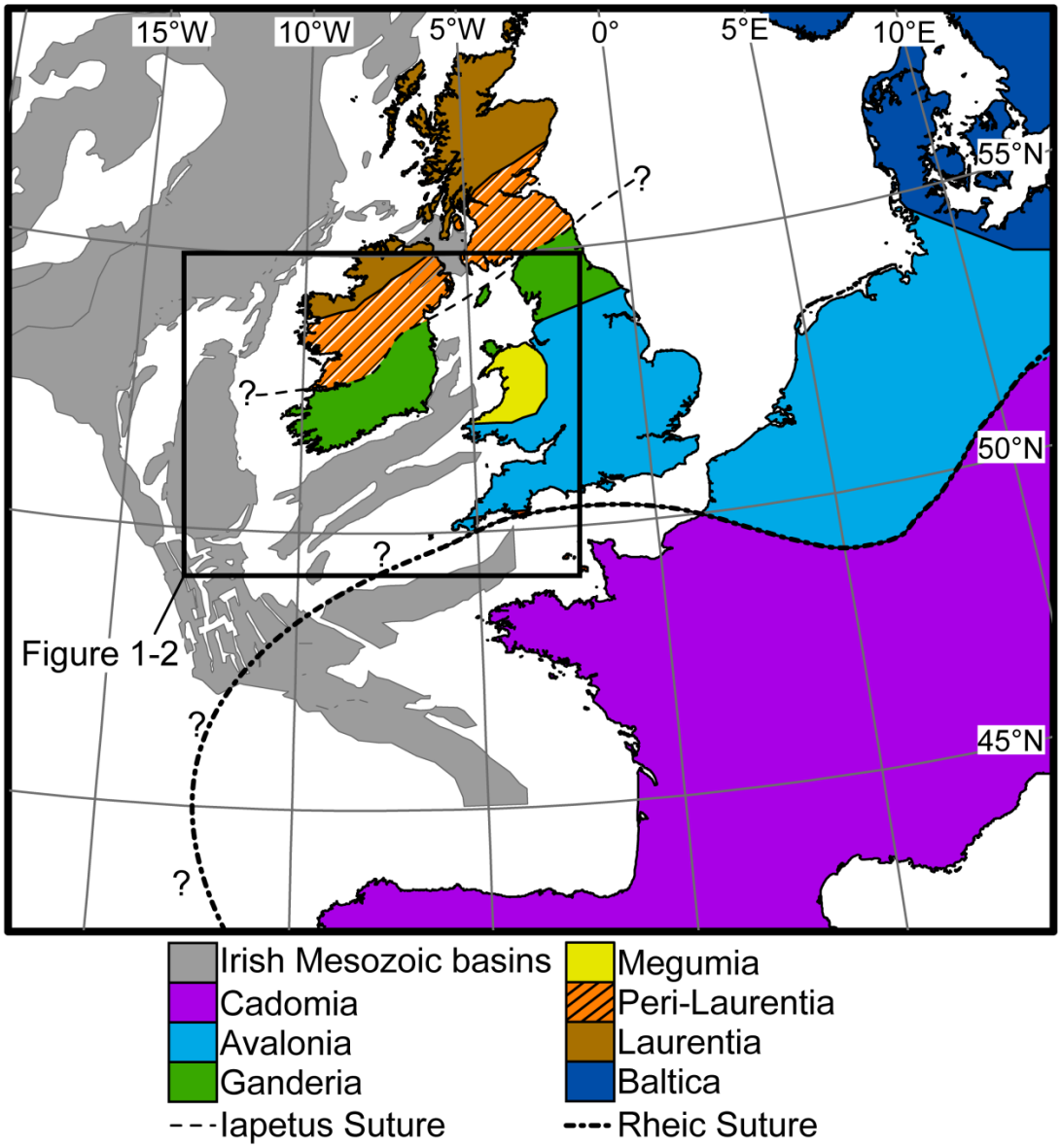

Figure 1–1. Regional map of major tectonic components which represent broad potential sediment source areas for the basins under investigation (modified after Linnemann et al., 2007; Nance et al., 2012; Waldron et al., 2014, 2011, 2009).

Following the deposition of the LORS and subsequent Rheic-Ocean subduction-driven Acadian deformation (Woodcock et al., 2007), widespread Middle to Late Devonian extension allowed for deposition of the UORS in the Munster Basin and, later, the Carboniferous clastic rocks of the South Munster Basin. The Munster Basin contains a thick (>5.7 km in places) succession of continental sedimentary rocks with a subordinate volcanic component (Williams et al., 2000). Provenance studies within the basin have largely been localised (e.g. Carruthers, 1985). Ennis et al. (2015) analysed detrital micas

from the western part of the basin and concluded that they represent recycling of northerly-derived LORS sediments. Other provenance information is largely indirect, for example, facies analysis by MacCarthy (1990) and palaeocurrent analysis by Williams et al. (1989). The work of Ennis et al. (2015) highlighted a gap in our knowledge of the UORS of southern Ireland that prompted further provenance investigations involving the most recent single grain geochronological techniques available.

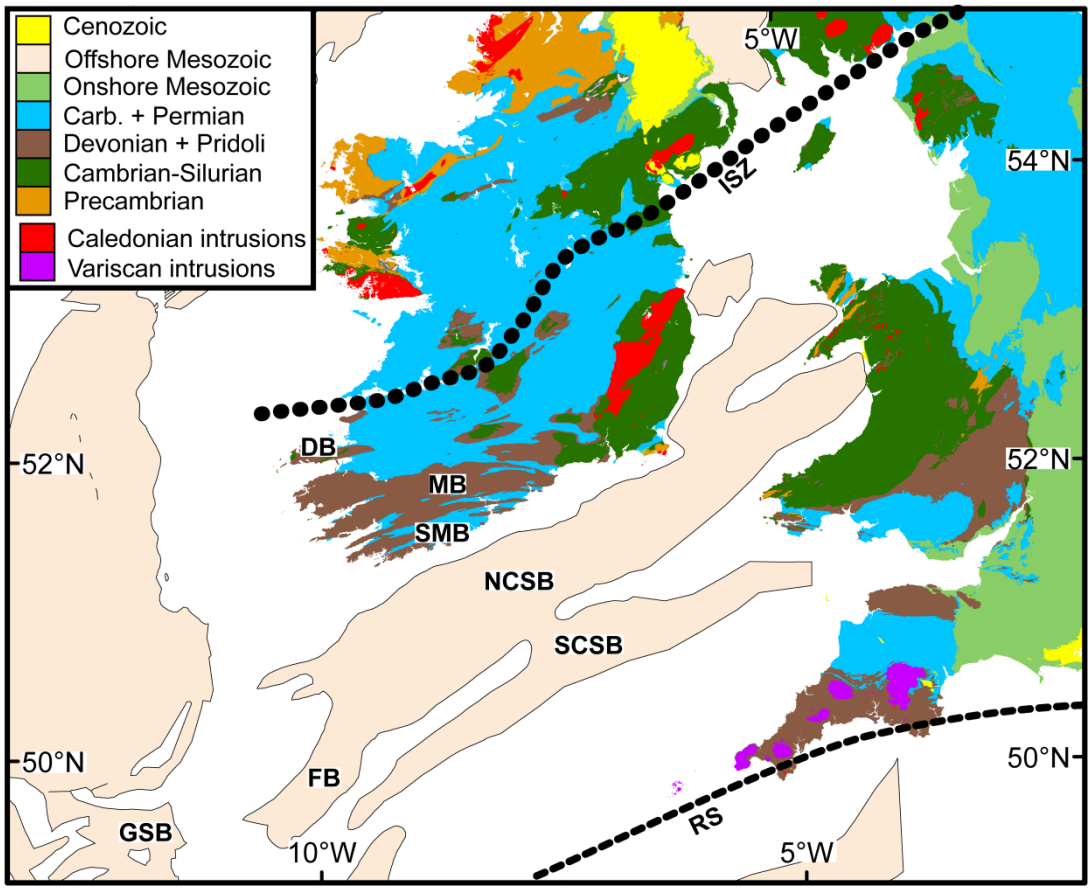

Figure 1–2. Regional map of the study area. All the basins under investigation in this study are labelled. DB, Dingle Basin; FB, Fastnet Basin; GSB, Goban Spur Basin; ISZ, Iapetus Suture Zone; MB, Munster Basin; NCSB, North Celtic Sea Basin; RS, Rheic Suture; SCSB, South Celtic Sea Basin; SMB, South Munster Basin.

In the broadest sense, this thesis aims to determine the sedimentary provenance of the Dingle, Munster, South Munster, North Celtic Sea, Fastnet, Goban Spur and South Celtic Sea basins (Figure 1–2). In so doing, the relationship between the offshore Mesozoic basins and the onshore Palaeozoic basins will be elucidated. Determining the provenance of the oldest

basins allows the establishment of potential source “signals” for provenance studies within the younger basins. This aim necessitates the production of a large dataset of detrital geochronological data from three sediment provenance proxies, namely apatite, white mica and zircon. Although conventional petrographic observations and point counting can provide some broad information on tectonic setting (Dickinson et al., 1983) of basins as well as aid in provenance interpretations, the advent of laser ablation-inductively coupled plasma-mass spectrometry (LA-ICP-MS) allows for rapid analysis of large numbers of detrital grains which can provide insights into the age of source areas and even past tectonic configurations. In the case of U-Pb in zircon, which has a closure temperature of greater than 900°C (Cherniak and Watson, 2001), these source areas are likely to be ultimately restricted to high temperature, predominantly felsic igneous bodies.

In order to ensure that as many potential sediment sources as possible are represented, it is necessary to employ proxies that can provide insights into lower temperature thermal events than those represented by zircon. Therefore, this study uses U-Pb ages of detrital apatites and ^{40}Ar-^{39}Ar ages of detrital white micas to facilitate more robust provenance interpretations of detrital zircon age data. The closure temperature of the U-Pb system in apatites ranges from ca. 375-550°C (Cochrane et al., 2014). White mica ^{40}Ar-^{39}Ar closure temperatures have been recorded as low as 270°C (Snee et al., 1988) and up to 450°C (Scharf et al., 2016).

In the LORS of the Dingle Basin, which represents the first major post-Caledonian continental sediment deposition in southern Ireland, the thesis aims to establish what contributions are made by sources north (Laurentia) and south (Ganderia and other peri-Gondwanan terranes) of the ISZ (Figure 1–1). In the process, the role of Caledonian orogenesis in supplying sediment to the basin will be assessed.

Establishing the sedimentary provenance of rocks within the UORS in the Munster and South Munster basins will:

1. build a picture of the palaeogeography during basin development.
2. establish whether extensive post-Acadian recycling of LORS took place in southern Ireland.

3. produce a potential source “signal” for adjacent Mesozoic sedimentary deposits.

This study also brings with it a number of implications for the hydrocarbon industry in the NCSB, SCSB, Fastnet Basin and Goban Spur Basin. Firstly, the establishment of possible sediment routing pathways during the Mesozoic could feed into reservoir distribution models, thereby de-risking existing hydrocarbon plays. Secondly, the study can shed light on what was a dynamic palaeogeographic environment during Mesozoic times as a result of the breakup of Pangaea and formation of the Atlantic Ocean. Lastly, understanding the extent of sediment recycling in the offshore basins could hint at the level of maturity (and hence reservoir quality) of the sedimentary rocks within the basin. A recent study, however, suggests that sediment recycling and maturity are not necessarily linked (Garzanti, 2017).

The thesis consists of three main chapters written as three separate manuscripts. Two of these manuscripts are under review in international peer-reviewed journals and the third is awaiting publication of the first two before submission. The thesis is structured in order of age of the sedimentary basin being studied so that information obtained from one basin can be fed into the study of the next. This acquisition of possible source signals allows for the assessment of the role of sediment recycling in consecutively younger basins.

1.1 References

Carruthers, R.A., 1985. The Upper Palaeozoic geology of the Glen of Aherlow and the Galtee Mountains, Counties Limerick and Tipperary. PhD thesis. University of Dublin.

Caston, V.N.D., 1995. The Helvick oil accumulation, Block 49/9, North Celtic Sea Basin. Geol. Soc. London, Spec. Publ. 93, 209–226. doi:10.1144/GSL.SP.1995.093.01.15

Cherniak, D.J., Watson, E.B., 2001. Pb diffusion in zircon. Chem. Geol. 172, 5–24. doi:10.1016/S0009-2541(00)00233-3

Cochrane, R., Spikings, R.A., Chew, D.M., Wotzlaw, J.F., Chiaradia, M., Tyrrell, S., Schaltegger, U., Van der Lelij, R., 2014. High temperature (>350°C) thermochronology and mechanisms of Pb loss in apatite. Geochim. Cosmochim. Acta 127, 39–56. doi:10.1016/j.gca.2013.11.028

Dickinson, W.R., Beard, S.L., Brakenridge, R.G., Erjavec, J.L., Ferguson, R.C., Inman, K.F., Knepp, R.A., Lindberg, F.A., Ryberg, P.T., 1983. Provenance of North American Phanerozoic sandstones in relation to tectonic setting. Geol. Soc. Am. Bull. 94, 222. doi:10.1130/0016-7606(1983)94<222:PONAPS>2.0.CO;2

Ennis, M., Meere, P.A., Timmerman, M.J., Sudo, M., 2015. Post-Acadian sediment recycling in the Devonian Old Red Sandstone of Southern Ireland. Gondwana Res. 28, 1415–1433. doi:10.1016/j.gr.2014.10.007

Ewins, N.P., Shannon, P.M., 1995. Sedimentology and diagenesis of the Jurassic and Cretaceous of the North Celtic Sea and Fastnet Basins. Geol. Soc. London, Spec. Publ. 93, 139–169. doi:10.1144/GSL.SP.1995.093.01.12

Garzanti, E., 2017. The maturity myth in sedimentology and provenance analysis. J. Sediment. Res. 87, 353–365.

Linnemann, U., Gerdes, A., Drost, K., Buschmann, B., 2007. The continuum between Cadomian orogenesis and opening of the Rheic Ocean: Constraints from LA-ICP-MS U-Pb zircon dating and analysis of plate-tectonic setting (Saxo-Thuringian zone, northeastern Bohemian Massif, Germany). Geol. Soc. Am. Spec. Pap. 423, 61–96. doi:10.1130/2007.2423(03)

MacCarthy, I.A.J., 1990. Alluvial sedimentation patterns in the Munster Basin, Ireland. Sedimentology 37, 685–712. doi:10.1111/j.1365-3091.1990.tb00629.x

Nance, R.D., Gutiérrez-Alonso, G., Keppie, J.D., Linnemann, U., Murphy, J.B., Quesada, C., Strachan, R.A., Woodcock, N.H., 2012. A brief history of the Rheic Ocean. Geosci. Front. 3, 125–135. doi:10.1016/j.gsf.2011.11.008

Scharf, A., Handy, M.R., Schmid, S.M., Favaro, S., Sudo, M., Schuster, R., Hammerschmidt, K., 2016. Grain-size effects on the closure temperature of white mica in a crustal-scale extensional shear zone - Implications of in-situ 40Ar/39Ar laser-ablation of white mica for dating shearing and cooling (Tauern Window, Eastern Alps). Tectonophysics 674, 210–226. doi:10.1016/j.tecto.2016.02.014

Snee, L.W., Sutter, J.F., Kelly, W.C., 1988. Thermochronology of economic

mineral deposits; dating the stages of mineralization at Panasqueira, Portugal, by high-precision 40 / 39 Ar age spectrum techniques on muscovite. Econ. Geol. 83, 335–354. doi:10.2113/gsecongeo.83.2.335

Soper, N.J., Woodcock, N.H., 2003. The lost Lower Old Red Sandstone of England and Wales : a record of post-Iapetan flexure or Early Devonian transtension? Geol. Mag. 140, 627–647. doi:10.1017/S0016756803008380

Todd, S., 1989. Role of the Dingle Bay Lineament in the evolution of the Old Red Sandstone of southwest Ireland, in: Arthurton, R., Gutteridge, P., Nolan, S. (Eds.), The Role of Tectonics in Devonian and Carboniferous Sedimentation in the British Isles. The Yorkshire Geological Society, Bradford, pp. 35–54.

Todd, S.P., 2015. Structure of the Dingle Peninsula, SW Ireland: evidence for the nature and timing of Caledonian, Acadian and Variscan tectonics. Geol. Mag. 152, 242–268. doi:10.1017/S0016756814000260

Todd, S.P., 2000. Taking the roof off a suture zone: basin setting and provenance of conglomerates in the ORS Dingle Basin of SW Ireland. Geol. Soc. London, Spec. Publ. 180, 185–222. doi:10.1144/GSL.SP.2000.180.01.10

Tyrrell, S., 2005. Investigations of Sandstone Provenance. PhD thesis. University College Dublin.

Waldron, J.W.F., Schofield, D.I., Dufrane, S.A., Floyd, J.D., Crowley, Q.G., Simonetti, A., Dokken, R.J., Pothier, H.D., 2014. Ganderia-Laurentia collision in the Caledonides of Great Britain and Ireland. J. Geol. Soc. London. 171, 555–569. doi:10.1144/jgs2013-131

Waldron, J.W.F., Schofield, D.I., White, C.E., Barr, S.M., 2011. Cambrian successions of the Meguma Terrane, Nova Scotia, and Harlech Dome, North Wales : dispersed fragments of a peri-Gondwanan basin? J. Geol. Soc. London. 168, 83–98. doi:10.1144/0016-76492010-068.Cambrian

Waldron, J.W.F., White, C.E., Barr, S.M., Simonetti, A., Heaman, L.M., 2009. Provenance of the Meguma terrane, Nova Scotia: rifted margin of early Paleozoic Gondwana. Can. J. Earth Sci. 46, 1–8. doi:10.1139/E09-004

Williams, E.A., Sergeev, S.A., Stossel, I., Ford, M., Higgs, K.T., 2000. U-Pb

zircon geochronology of silicic tuffs and chronostratigraphy of the earliest Old Red Sandstone in the Munster Basin, SW Ireland. Geol. Soc. London, Spec. Publ. 180, 269–302. doi:10.1144/GSL.SP.2000.180.01.13

Williams, E., Bamford, M., Cooper, M., Edwards, H., Ford, M., Grant, G., MacCarthy, I., McAfee, A., O'Sullivan, M., 1989. Tectonic controls and sedimentary response in the Devonian-Carboniferous Munster and South Munster basins, south-west Ireland, in: Arthurton, R., Gutteridge, P., Nolan, S. (Eds.), The Role of Tectonics in Devonian and Carboniferous Sedimentation in the British Isles. The Yorkshire Geological Society, Bradford, pp. 120–141.

Woodcock, N.H., Soper, N.J., Strachan, R.A., 2007. A Rheic cause for the Acadian deformation in Europe. J. Geol. Soc. London. 164, 1023–1036. doi:10.1144/0016-76492006-129

2 The provenance of the Devonian Old Red Sandstone of the Dingle Peninsula, SW Ireland – the earliest record of Laurentian and peri-Gondwanan sediment mixing in Ireland.

(Current manuscript status: Accepted, JGSL)

Brenton J. Fairey[1], Aidan Kerrison[1], Patrick A. Meere[1], Kieran F. Mulchrone[2], Mandy Hofmann[3], Andreas Gärtner[3], Benita-Lisette Sonntag[3], Ulf Linnemann[3], Klaudia F. Kuiper[4], Meg Ennis[1], Chris Mark[5], Nathan Cogné[5] and David Chew[5].

[1]School of Biological, Earth and Environmental Sciences, University College Cork, Cork, Ireland.

[2]School of Applied Mathematics, University College Cork, Cork, Ireland

[3]Senckenberg Naturhistorische Sammlungen Dresden, Museum für Mineralogie und Geologie, Königsbrücker Landstraße 159, D-01109 Dresden, Germany.

[4]Faculty of Earth Sciences Vrije Universiteit Amsterdam, De Boelelaan 1085, NL-1081 HV Amsterdam, The Netherlands.

[5]Department of Geology, Museum Building, Trinity College Dublin, Dublin 2, Ireland.

Abstract

The Lower Old Red Sandstone (LORS) in southern Ireland is hosted in the Lower Devonian Dingle Basin which lies immediately south of the Iapetus Suture on the Dingle Peninsula, County Kerry. The basin developed as a post-Caledonian pull-apart structure prior to Acadian deformation which in turn was followed by end-Carboniferous Variscan deformation. Detrital zircon U-Th-Pb geochronology is complimented by mica Ar-Ar and apatite U-Pb geochronology to gain a comprehensive understanding of the provenance of the Lower Devonian LORS of the Dingle Basin and assess contributions of major tectonic components (e.g. Laurentia, Ganderia). Sedimentary rocks in the LORS have similar detrital zircon age distributions which are dominated by ca. 1.2 Ga zircons as well as late Neoproterozoic grains. These age distributions indicate a dominant contribution of detritus of Laurentian affinity

as well as contributions from westerly and southerly derived Ganderian detritus. Caledonian uplift of the area north of the Iapetus Suture would have facilitated a large contribution of (peri-)Laurentian material. The Upper Old Red Sandstone on the Dingle Peninsula has a distinctly different detrital zircon character including few late Neoproterozoic zircons and abundant zircons of ca. 1.05 Ga age, indicating sediment derivation only from Laurentia and no recycling from the LORS.

2.1 Introduction

The Dingle Basin in County Kerry, southwest Ireland represents the only record of Early Devonian sedimentation south of the Iapetus Suture in Ireland. Its structure records a critical period in the tectonic history and development of Ireland, having been affected by both the Acadian and Variscan Orogenies (Meere and Mulchrone, 2006). Furthermore, the basin's sedimentary rocks offer an opportunity to understand its palaeogeography, possibly recording Grampian (475-465 Ma) to Late Caledonian (430-420 Ma) detrital input following the final Silurian accretion of Ganderia to the margin of Laurentia.

Existing provenance studies (Ennis et al., 2015; e.g. Todd, 2000) have greatly improved our understanding of the development and palaeogeography of the Dingle Basin. However, a comprehensive investigation utilising detrital single-grain techniques has yet to be undertaken. Such a study would serve to elucidate regional sediment source contributions in a basin which is intimately associated with the Iapetus Suture (Todd, 2000) – arguably the most important structural entity in the Phanerozoic tectonic history of Ireland.

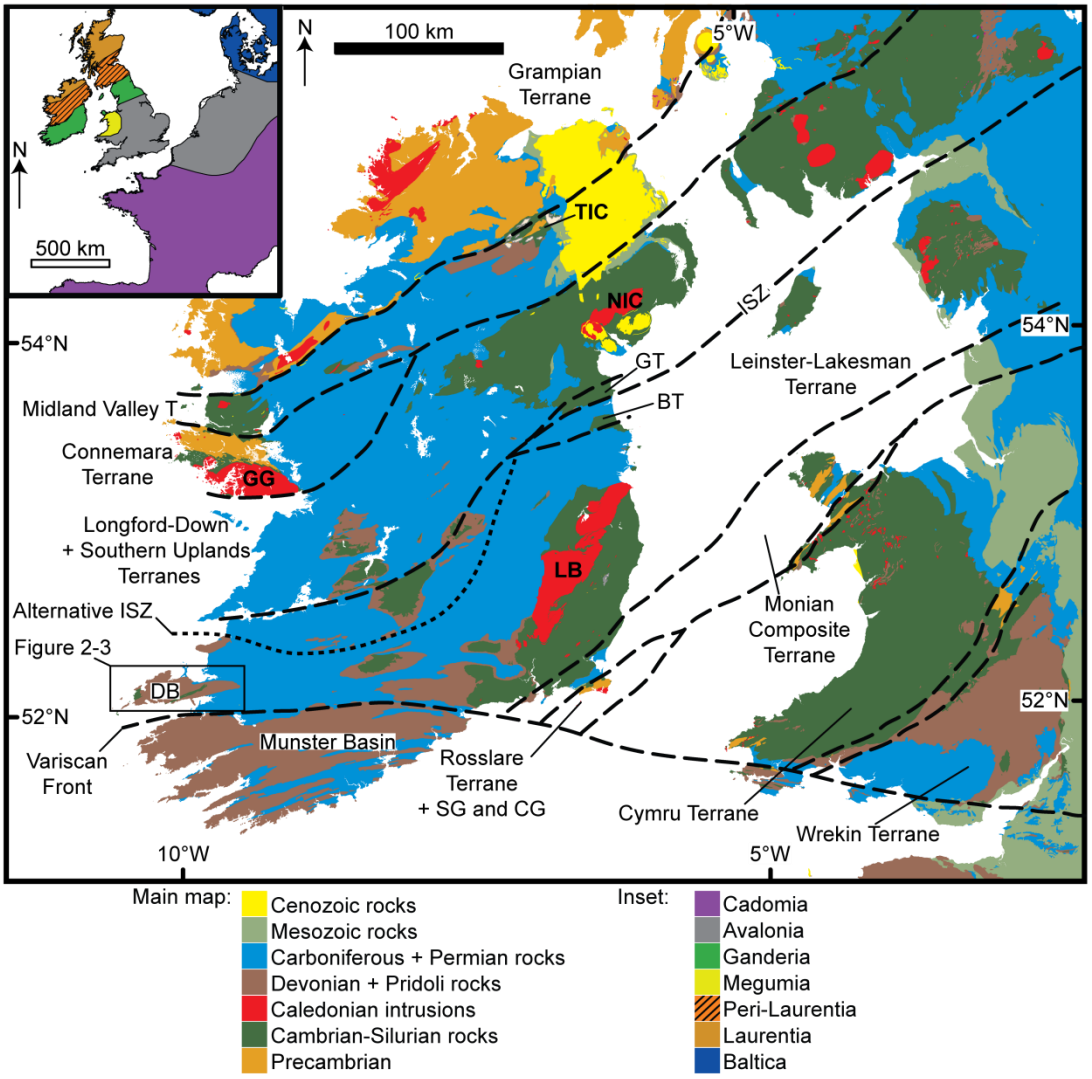

Figure 2–1. Regional map of the British Isles showing the major terranes of Ireland (modified after McIlroy and Horák 2006; Waldron et al., 2014; McConnell et al. 2016; alternative ISZ after Todd et al. 1991). The rectangle indicates the study area shown in Figure 2–3. Inset: regional map showing broad tectonic domains (Linnemann et al., 2007; Nance et al., 2012; Waldron et al., 2014, 2011, 2009) Key: BT, Bellewstown Terrane; CG, Carnsore Granite; DB, Dingle Basin; GG, Galway Granite; GT, Grangegeeth Terrane; ISZ, Iapetus Suture Zone; NIC, Newry Igneous Complex; SG; Saltees Granite; TIC, Tyrone Igneous Complex.

This study provides the first multiproxy (zircon, apatite, mica) single-grain datasets from the area, with the aim of determining the provenance of the Lower Old Red Sandstone (LORS) in the Dingle Group of the Lower Devonian Dingle Basin and assessing the roles of Laurentian and peri-Gondwanan domains in contributing detritus. The study also considers the detrital zircon provenance of the Upper Old Red Sandstone (UORS) on the Dingle Peninsula.

2.2 Regional Geology and Review of Terranes in the British Isles

The oldest potential source of detrital zircons lies to the north of the Iapetus Suture Zone (ISZ) in the form of the Laurentian craton (Figure 2–1). A compilation of existing detrital zircon data of known Laurentian sources (Figure 2–2) shows three broad peaks that correspond to major crust-forming events which contributed to the formation of Laurentia (Cawood et al., 2007). These peaks occur in the Archaean, Palaeoproterozoic and Mesoproterozoic, recording essentially uninterrupted zircon production from 1.9 Ga to 0.9 Ga. A major characteristic of detrital zircon distributions from this sector of the Laurentian continent is the absence of zircons of late Neoproterozoic age due to the absence of an active margin on the Laurentian continent at this time (Pointon et al., 2012). The Rhinns Complex on the island of Inishtrahull off the north coast of County Donegal (Daly et al., 1991) and the Annagh Gneiss Complex in County Mayo comprise the exposed Proterozoic Laurentian basement in Ireland, and are also the oldest rocks exposed in Ireland. The Grenville Orogeny, represented by the large peak in late Mesoproterozoic zircon ages (Figure 2–2), is recorded in the Annagh Gneiss Complex by the 1.17 Ga Doolough gneiss, the 1.01 Ga Doolough Granite and by 0.99 to 0.96 Ga late orogenic pegmatites and migmatitic leucosomes (Daly, 1996). A variety of marine sedimentary (e.g. Clew Bay Complex), ocean-arc-volcanic (e.g. Lough Nafooey Arc – see Chew et al., 2007) and ophiolitic rocks (e.g. Deer Park Complex) make up the material accreted to the margin of Laurentia during the Grampian Orogeny (475-465 Ma) in Ireland which represents the early stage of the Caledonian orogenic cycle (Chew and Stillman, 2009). This early stage was followed by sinistral transpressive docking of a peri-Gondwanan terrane to the newly-accreted Laurentian margin (Dewey and Strachan, 2003).

The term `peri-Gondwanide' was first proposed by Van Der Voo (1988) to describe a number of tectonostratigraphic elements which existed as terranes in the Iapetus Ocean during the Ordovician period. Using palaeomagnetic evidence, Van Der Voo (1988) suggested that these terranes were proximal to northwest African Gondwana, rather than Laurentia. This has since been supported by other studies (see Nance et al., 2008, and references therein).

We use the term *domain* to refer to tectonostratigraphic units consisting of one or more terranes (Hibbard et al., 2007). Peri-Gondwanan domains include Avalonia, Ganderia, Megumia, Carolinia in present-day North America, and Avalonia and Cadomia (including Iberia, Bohemia and Armorica) in Europe (Nance et al., 2008). Those domains that had the potential, given their Devonian positions relative to southern Ireland, to provide sediment to the basin being investigated include Avalonia, Ganderia and Megumia. For a comprehensive review of peri-Gondwanan terranes, the reader is referred to Nance et al. (2008). The correlation of the Meguma terrane to the Harlech Dome is discussed by Waldron et al. (2011), White et al. (2012) and Nance et al. (2015).

The main rock exposures of pre-Devonian basement south of the Iapetus Suture Zone in Ireland are found in the Leinster Massif in the southeastern part of the island. The massif hosts a number of Cambrian to Silurian volcanic and sedimentary units intruded by Caledonian-Acadian granites. There has been wide acceptance that pre-Silurian southern Ireland represents part of Avalonia (e.g. Van Der Voo, 1983; Livermore et al., 1985; Van Der Voo, 1988; Pickering et al., 1988; Ford et al., 1992; Cocks et al., 1997; McConnell and Morris, 1997; Keppie et al., 2003; Tyrrell et al., 2007; Woodcock and Strachan, 2012; Fullea et al., 2014; Todd, 2015), but others have suggested linkages to different peri-Gondwanan domains. One school of thought contends that southern Ireland, Wales and southern England formed part of a number of terranes that collectively formed Cadomia (e.g. Soper and Hutton, 1984; Max et al., 1990).

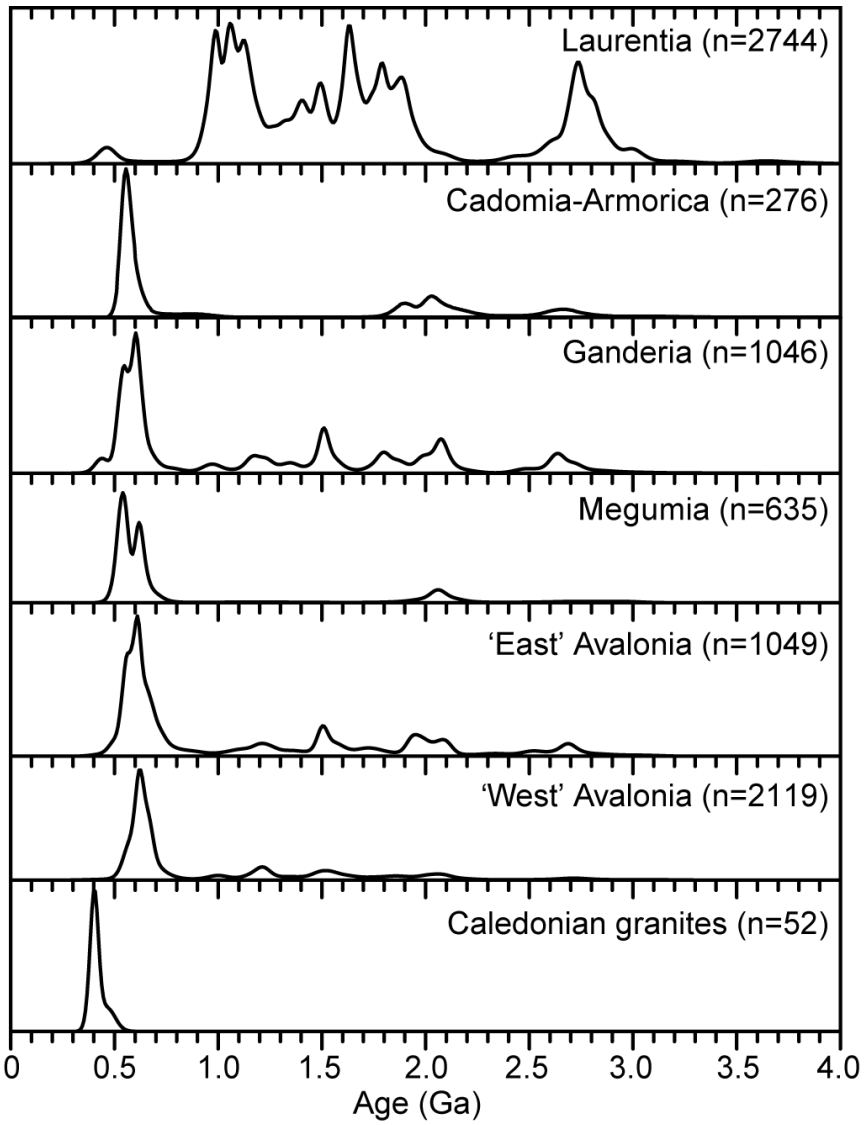

Figure 2–2. Kernel density estimation plots (bandwidth = 20 Ma) of published detrital zircon ages from various potential sources (modified and expanded after Pointon et al., 2012). Laurentia data: Cawood et al. (2003); Friend et al. (2003); Cawood et al. (2007); Kirkland et al. (2008); Waldron et al. (2008); McAteer et al. (2010); Cawood et al. (2012); Strachan et al. (2013); Waldron et al. (2014); Johnson et al. (2016). Cadomia-Armorica data: Fernandez-Suarez et al. (2002); Samson et al. (2005); Linnemann et al. (2008); Strachan et al. (2008). Ganderia data: Fyffe et al. (2009); Waldron et al. (2014); Willner et al. (2014). Megumia data: Krogh and Keppie (1990); Waldron et al. (2009, 2011); Pothier et al. (2015). `East' Avalonia data: Collins and Buchan (2004); Murphy et al. (2004b); Strachan et al. (2007); Linnemann et al. (2012); Willner et al. (2013). `West' Avalonia data: Keppie et al. (1998); Thompson and Bowring (2000); Barr et al. (2003); Murphy et al. (2004a, 2004b); Pollock (2007); Satkoski et al. (2010); Thompson et al. (2012); Dorais et al. (2012); Barr et al. (2012); Force and Barr (2012); Pollock et al. (2012); Willner et al. (2013); Henderson et al. (2016). Caledonian granite ages are from Ireland only and include various isotopic geochronological techniques. Caledonian data: Chew and Stillman (2009).

Kennedy (1979) first implied that southern Ireland is a trans-Atlantic extension of Ganderia. Van Staal et al. (1996) (and references therein) extend the Gander Zone of Newfoundland, where Ganderia was first described, into Ireland, Wales, England and the Isle of Man. As evidence of this they cited a correlation of Cambrian and Ordovician clastic successions, a similarity of overstepping successions, juxtaposition of mafic to ultramafic, possibly ophiolitic rocks (e.g. Rosslare Complex) and a similarity in fossil fauna. This extension of Ganderia into southern Ireland is further supported by van Staal et al. (1998) who suggest that Avalonia and Ganderia may have become juxtaposed at least during the late Cambrian. If this is the case then it was an amalgamated Avalonia-Ganderia microcontinent that collided with Laurentia during the Caledonian Orogeny. More recently, Waldron et al. (2014) have drawn similarities between detrital zircon ages from Monian Composite Terrane (county Wexford) and Leinster-Lakesman samples and samples analysed by Fyffe et al. (2009) for Ganderia in New Brunswick and Maine. The difference between Ganderian detrital zircon samples from Cambrian sedimentary rocks and West Avalonian samples is that the latter are lacking in Mesoproterozoic and Palaeoproterozoic zircons (Waldron et al., 2014). Waldron et al. (2014) attribute these Mesoproterozoic and Palaeoproterozoic zircons in Ganderian sediments to a possible Amazonian source in West Gondwana.

Distinguishing between Avalonia and Ganderia by detrital zircon populations alone is difficult (Figure 2–2). Stratigraphic, faunal and further isotopic evidence is required, as exemplified in a review of the East Avalonian terranes by Schofield et al. (2016). They use geochronological data as well as magmatic whole-rock Sm-Nd and O-isotopes to show that what is currently viewed as East Avalonian basement in England has closer isotopic and age affinities to Ganderia than to West Avalonia. Elimination of East Avalonia in the British Isles simplifies the interpretation of the provenance of Neoproterozoic detrital zircons in Devonian sedimentary rocks in the region. Although Ganderia is the most proximal potential source of Neoproterozoic zircons, one cannot eliminate the possible detrital influence from other peri-Gondwanan sources.

Waldron et al. (2011) proposed that the Cambrian successions of the Meguma terrane of Nova Scotia and the Harlech Dome of Wales be considered a single palaeogeographical domain which they named ‘Megumia’. They show that detrital zircon age distributions from the Harlech Dome have greater similarity to those in the Meguma terrane than those in Avalonia. The major difference in detrital zircon age distributions between Megumia and Avalonia is the significant presence of 1.95 to 2.1 Ga zircons in Megumia and the lack thereof in Avalonia. These zircon ages are believed to be associated with Eburnean orogenic magmatic activity (Waldron et al., 2011). For the purpose of this study, a significant contribution of Neoproterozoic zircon grains to the sediments under investigation is used predominantly as a tool to distinguish between peri-Gondwana-derived and Laurentia-derived zircons, due to the fact that Laurentia is not known to have any major source of Neoproterozoic zircons (Figure 2–2). Furthermore, given the Devonian age and tectonic setting of the sediments, it is likely that they represent heterogeneous source areas. However, the reader is urged to bear in mind the complexities associated with sources of Neoproterozoic zircons in the British Isles, as described above.

The Grampian Orogeny, which occurred in the Ordovician period, is considered to be the first stage of the Caledonian orogenic cycle (Chew and Stillman, 2009) and records the collision of an oceanic arc (recognised in Ireland as the Lough Nafooey Arc) with the Laurentian margin (Chew and Strachan, 2014). Ordovician sediments from the South Mayo Trough record dominant input of zircons in the age range ca. 490 to ca. 467 Ma (McConnell et al., 2009). However, this range bears two populations, one around 487 Ma and one between ca. 474 and ca. 467 Ma, interpreted by McConnell et al. (2009) to be sourced from the Lough Nafooey Arc/Clew Bay Complex and the Connemara orthogneiss suite respectively. The Tyrone Igneous Complex is also of similar age to the Connemara suite (Cooper et al., 2011). The Grangegeeth volcanic terrane in eastern Ireland has a maximum age of ca. 465 Ma and inherited Archean, Palaeoproterozoic and Mesoproterozoic zircon within it indicate that it is of Laurentian origin, perhaps being related to the Tyrone Igneous Complex (McConnell et al., 2010). Its anomalous position

south of the Southern Uplands – Longford Down terrane is attributed to transpressive strike-slip deformation in Middle Silurian times (McConnell et al., 2010). To the south of the Grangegeeth terrane lies the Bellewstown terrane (Figure 2–1). This terrane is considered part of the Ganderian margin and zircons dated from a sandstone within a volcanogenic breccia place the age of volcanism in the terrane at ca. 474 Ma (McConnell et al., 2015).

Plagiogranite boulders from Silurian conglomerates which lie unconformably upon the Lough Nafooey Group are considered to be sourced from the Lough Nafooey Arc (Chew et al., 2007). U-Pb zircon ages of around 490 Ma from these boulders, supported by Nd-isotope data, led Chew et al. (2007) to conclude that the arc had encountered Laurentian margin sediments by this time. This arc material represents a source of Early Ordovician detrital zircons. The Southern Uplands – Longford Down terrane predominantly consists of Ordovician to Silurian metasedimentary rocks that were originally deposited in the Iapetus Ocean on the margin of Laurentia and were subsequently accreted to this margin (McConnell et al., 2016; Waldron et al., 2008). In Ireland, McConnell et al. (2016) found that these rocks contain Palaeoproterozoic and Mesoproterozoic zircons indicative of a Laurentian origin. In addition, their samples contain an abundance of Early to Middle Ordovician zircons which they interpret as representing a volcanic arc source (e.g. Tryrone Igneous Complex, Lough Nafooey Arc). In Scotland, Waldron et al. (2008) and Waldron et al. (2014) found that the majority of detrital zircons are of Proterozoic age and sourced from Laurentia. Generally, samples from these studies produced fewer Early to Middle Ordovician zircons relative to those from the Irish side of the terrane.

Another potentially important Ordovician zircon source occurs in the Duncannon and Ribband Groups in the Leinster Massif. The minor calc-alkaline volcanic rocks in the Ribband Group represent arc development during initial stages of subduction of the Iapetus Ocean crust beneath Ganderia (East Avalonia) in Tremadocian times (Woodcock, 2012). The Duncannon Group volcanic suite consists of basalts and rhyolites, extruded in Caradoc times (Sandbian-Katian) which is considered indicative of a back-arc region (Woodcock, 2012). These volcanic suites have not yet been dated and

their ages are largely constrained by faunal evidence in associated sedimentary successions (e.g. Owen and Parkes, 2000).

The final welding of Ganderia to the margin of Laurentia, which included an accreted ocean arc following the Grampian Orogeny, was achieved during the Caledonian Orogeny, by about 430-425 Ma (Mac Niocaill, 2000; Waldron et al., 2014). However, abundant evidence of Late Caledonian (including Acadian, *sensu* Chew and Stillman, 2009) magmatism exists in the form of widely distributed intrusions in Ireland and Britain. These range in age from ca. 430 Ma to 380 Ma (Figure 2–2). An example of such an intrusion, which has been proposed as a proximal source of detritus to the Munster Basin (e.g. Penney, 1980) and which represents the age of the majority of these intrusions (Figure 2–2), is the Leinster granite batholith. O'Connor et al. (1989) obtained a U-Pb monazite age of 405 ± 2 Ma for the batholith. However, recent work by Fritschle et al. (2017) shows that it was emplaced over an extended period from ca. 417 Ma to 405 Ma. Vermeulen et al. (2000) have shown, by seismic analysis of southern Ireland, that the UORS south of the Killarney-Mallow Fault Zone is likely to be concealing a granitic body. Such an interpretation has been suggested by other studies (e.g. Ford et al., 1991; Meere, 1995; Masson et al., 1998; Vermeulen et al., 2000; Todd, 2000). Todd (2000) suggested that, based on clast analysis of the Trabeg Conglomerate Formation, a granite body similar to the Leinster Batholith was exposed in the southern hinterlands of the Dingle Basin during its development and that the Leinster terrane therefore extends westward following Caledonian trends. Other examples of intrusives of Late Caledonian age in Ireland include the Donegal (418-388 Ma), Galway (412-380 Ma) and Newry Granites (403-387 Ma) and the Carnsore and Saltees Granites (436-428 Ma). The age ranges presented above are, in most cases, the result of dating by multiple geochronogical techniques which yield different ages. The studies from which these ages are obtained are reviewed in Chew and Stillman (2009). The Newry Igneous Complex has recently been redated by Cooper et al. (2016) who showed that, like the Leinster Batholith, the complex was emplaced over a similarly extended period from 414 Ma to 407 Ma.

Following the closure of the Iapetus Ocean, a Silurian to Early Devonian period of sinistral transtension accommodated deposition of the LORS in the Dingle Basin and elsewhere in the southern British Isles (Soper and Woodcock, 2003; Todd, 1989). This Emsian transtension across the ISZ in Ireland and Britain possibly initiated emplacement of granites of similar age on either side of the ISZ (Brown et al., 2008; Cooper et al., 2016). The rocks of the Dingle Basin record an Emsian deformational event which is considered to be part of the Acadian orogenic episode (Meere and Mulchrone, 2006; Todd, 1989, 2015, 2000). Deformation occurred in a transpressive regime but its kinematic character in the Dingle Basin is debated (e.g. Todd, 1989; Meere and Mulchrone, 2006; Todd, 2015) because the structural fabrics within the LORS are complicated by Carboniferous Variscan overprinting.

2.3 Local Geology and Sample Location

The majority of the rocks that crop out on the Dingle Peninsula, southwest Ireland, form part of the Lower to Middle Devonian Lower Old Red Sandstone of the Dingle Basin. Basement to this basin is also exposed on the peninsula in the form of the Ordovician Annascaul Formation and the Silurian Dunquin Group (Todd et al., 2000) (Figure 2–3). These Ordovician to Silurian rocks have been correlated with rocks of comparable age in the Leinster Massif and therefore have a peri-Gondwanan affinity (Todd et al., 2000). The axis of the Dingle Basin approximates the regional northeast-southwest Caledonian trend in Ireland. The basin's sedimentary fill is complicated by a series of unconformities which separate five lithostratigraphic groups (Boyd and Sloan, 2000). Todd et al. (1988) consider the main mechanism of subsidence to be in the form of a sinistral pull-apart structure. Meere and Mulchrone (2006) recognise two broad phases of extension: an Early Devonian phase that accommodated Dingle Basin sediments, and a Late Devonian to Carboniferous phase that accommodated the sediments of the Munster Basin. An intervening Middle Devonian transpression, likely recording the Acadian orogenic event (Dewey and Strachan, 2003; Soper and Woodcock, 2003), led Ennis et al. (2015) to consider the possibility of sedimentary recycling from the

Dingle Basin into the Munster Basin. Such recycling of the Dingle Basin LORS into the UORS of the Munster Basin has also been suggested by Todd (2015).

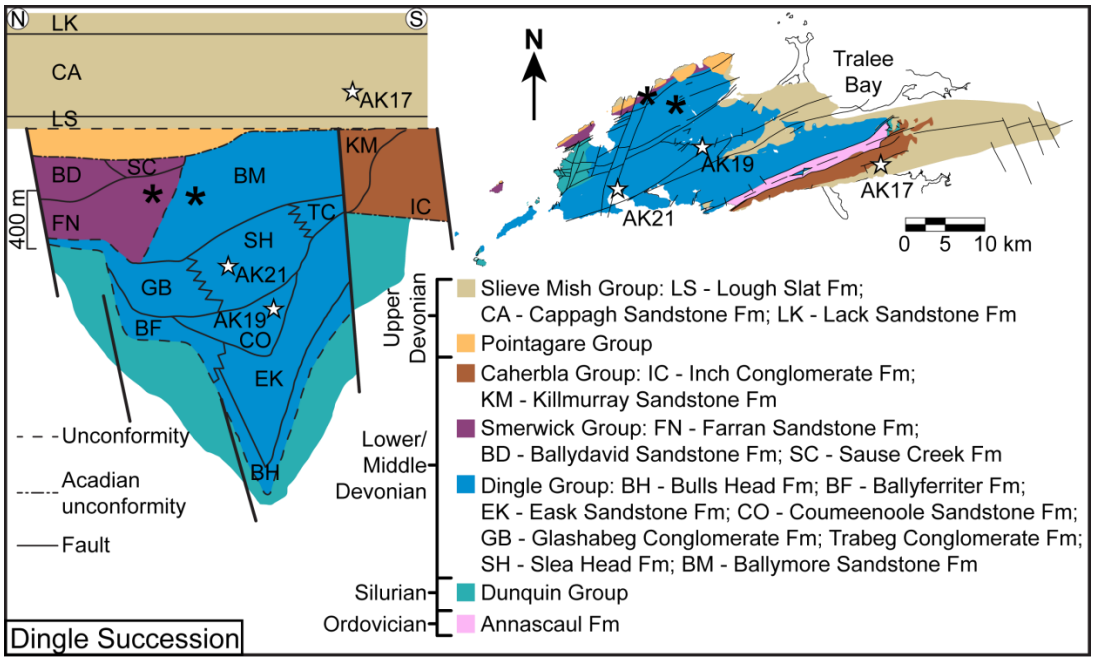

Figure 2–3. Geological map and generalised north-south geological cross section of the Dingle Peninsula showing sample locations (modified after Todd 1989; Ennis et al., 2015). Detrital apatite and detrital zircon sample location marked by bold asterisks and white stars respectively.

Within the Dingle Basin, the Dingle Group, which is the most voluminous, represents a fluvial/alluvial environment in which axial (flowing from southwest to northeast along the basin axis) braid-plains and flood sheets, represented by the Eask, Coumeenoole, Slea Head and Ballymore Formations, were deposited by generally perennial axial river systems that flowed from the southwest (Todd, 2000). These were abutted by alluvial fans, mainly represented by the Glashabeg Conglomerate Formation in the north and the Trabeg Conglomerate Formation in the south, that drained transversely into the basin (Todd, 2000). Spores from the Eask and Slea Head Formation have yielded ages of Early Pragian and Early Emsian respectively (Higgs, 1999). Two samples from the LORS of the Dingle Basin were taken from the Coumeenoole Formation and the overlying Slea Head Formation from the Dingle Group (Figure 2–3) in close proximity to the locations of equivalent samples from Ennis et al. (2015).

Todd (2000) carried out an extensive study of clasts from the correlative Glashabeg Conglomerate, Slea Head and Trabeg Conglomerate Formations in the Lower to Middle Devonian Dingle Basin. Based on the large number of mafic to intermediate volcanic clasts and the presence of limestone clasts in the Glashabeg Conglomerate Formation, he concluded that the source area was dominated by Ordovician volcanic rocks lying in close proximity to the north of the basin and likely intersecting the Iapetus Suture Zone. Rivers feeding the Slea Head Formation (and the conformably underlying Coumeenoole Formation, which has a similar palaeoflow direction) flowed axially through the basin toward the northeast, draining an area to the southwest (Todd, 2000). Pebble clasts indicate sediment derivation from Silurian volcanic rocks and from an extension of the Leinster Massif basement (Todd, 2000). The Trabeg Conglomerate Formation formed the southern flank of the Slea Head system and drained an area to the south and southwest of the basin which was made up of rocks similar to those observed in the Leinster Massif (Todd, 2000).

Unconformably overlying the Dingle Group is the Smerwick Group, which consists of sedimentary rocks of aeolian and fluvial origin (Todd et al., 1988). The two groups are truncated by an unconformity that developed due to erosion during Late Emsian Acadian basin inversion (Meere and Mulchrone, 2006). These strata were followed by deposition of the Pointagare Group, exposed only on the northern coast of the peninsula, and the Caherbla Group to the south which contains the Inch Conglomerate Formation. These formations are thought to have been deposited in Middle Devonian (Eifelian) times, based predominantly on faunal and palynological evidence (Todd, 2015, and references therein). Finally, the overstepping sandstone and conglomerate successions of the Slieve Mish Group were deposited during the Late Devonian and are considered by Williams (2000) to be a correlative of the Ballinskelligs Formation and equivalents in the Munster Basin. Sample AK17 was obtained from a pebbly sandstone of the fluvial to lacustrine (Todd, 2015) Cappagh Sandstone Formation of the Slieve Mish Group.

2.4 Analytical procedures and sampling

The apatite U-Pb data were originally generated as part of a bedrock thermal history study utilising the apatite fission track (AFT) low-temperature thermochronometer (Cogné et al., 2014), because the laser ablation-inductively coupled plasma-mass spectrometry (LA-ICP-MS) approach to AFT analysis permits U-Pb and AFT ages to be determined on the same grains during a single analytical session (Chew and Donelick, 2012). The sampling and separation process is therefore different to the zircon separation process.

2.4.1 Zircon U-Pb

Data to produce the source ‘signals’ shown in Figure 2–2 were derived from a number of sources. Data from samples interpreted to be of Laurentian origin were sourced from Cawood et al. (2003), Friend et al. (2003), Cawood et al. (2007), Kirkland et al. (2008), Waldron et al. (2008), McAteer et al. (2010), Cawood et al. (2012), Strachan et al. (2013), Waldron et al. (2014) and Johnson et al. (2016). Data from samples interpreted from Cadomia-Armorica are from Fernandez-Suarez et al. (2002), Samson et al. (2005), Linnemann et al. (2008) and Strachan et al. (2008). Data from sample of Ganderian association are from Fyffe et al. (2009), Waldron et al. (2014) and Willner et al. (2014). Data from samples interpreted to be of Megumian affinity are from Krogh and Keppie (1990), Waldron et al. (2009, 2011) and Pothier et al. (2015). `East' Avalonia data were taken from Collins and Buchan (2004), Murphy et al. (2004b), Strachan et al. (2007), Linnemann et al. (2012) and Willner et al. (2013). Data from samples interpreted to be sourced from `West' Avalonia are from Keppie et al. (1998), Thompson and Bowring (2000), Barr et al. (2003), Murphy et al. (2004a, 2004b), Pollock (2007), Satkoski et al. (2010), Thompson et al. (2012), Dorais et al. (2012); Barr et al. (2012), Force and Barr (2012), Pollock et al. (2012), Willner et al. (2013) and Henderson et al. (2016). Caledonian granite ages are from Ireland only and include various isotopic geochronological techniques. The granite data were sourced from a compilation by Chew and Stillman (2009).

Sample separation was undertaken at Vrije Universiteit Amsterdam. Detrital zircons were liberated from samples using a jaw crusher and disc mill.

Density separation was achieved using diiodomethane in a centrifuge as per Ijlst (1973) and magnetic separation using a Frantz magnetic separator. Zircons of all morphologies and colours, between 60 and 250 µm, were hand-picked under binocular microscope. Typically, between 120 and 180 zircons per sample were mounted in epoxy disks and ground and polished to expose the approximate centre of the grains. Cathodolumenescence (CL) imaging was undertaken at the University of St. Andrews and at Trinity College Dublin in order to identify optimal positions for laser ablation.

Uranium, thorium and lead isotopes were measured by laser ablation-sector field-inductively coupled plasma-mass spectrometry (LA-SF-ICP-MS) at the Museum für Mineralogie und Geologie (Geoplasma Lab, Senckenberg Naturhistorische Sammlungen Dresden) using a Thermo-Scientific Element 2 XR sector field ICP-MS coupled to a New Wave UP-193 Excimer Laser System. Each analysis consisted of approximately 15 s background acquisition followed by 30 s data acquisition. A common-Pb correction based on the interference- and background-corrected ^{204}Pb signal and a model Pb composition (Stacey and Kramers, 1975) was carried out if necessary. The necessity of the correction is judged on whether the corrected ^{207}Pb/^{206}Pb lies outside of the internal errors of the measured ratios. Raw data were corrected for background signal, common Pb, laser induced elemental fractionation, instrumental mass discrimination, and time-dependant elemental fractionation of Pb/Th and Pb/U using a Microsoft Excel spreadsheet program developed by Axel Gerdes (Institute of Geosciences, Johann Wolfgang Geothe-University Frankfurt, Frankfurt am Main, Germany). Concordia diagrams and concordia ages were produced using Isoplot/Ex 3.7 of Ludwig (2012). Frequency and kernel density estimation (KDE) curves were plotted using DensityPlotter (Vermeesch, 2012). Frequency plots were assigned a binwidth of 25 Ma. KDEs were plotted using a bandwidth of 20 Ma and a Gaussian kernel. This bandwidth was chosen by trial and error (by comparison to histograms and probability density plots) because in many cases the ‘optimal bandwidth’ calculated in DensityPlotter caused severe oversmoothing. More importantly, the same bandwidth was applied to all samples and to detrital zircons from potential source areas so that comparisons were like-for-like.

Multi-dimensional scaling (MDS) analysis was performed using the R package `provenance` by Vermeesch et al. (2016).

2.4.2 White mica Ar-Ar

Detrital white mica Ar-Ar ages for the Coumeenoole Formation in the Dingle Group from Ennis et al. (2015) are recalculated in this study using the 28.201 ± 0.046 Ma age of Kuiper et al. (2008) for the Fish Canyon sanidine standard, generally increasing the age of individual grains by ca. 1 % . This was done to facilitate comparison of future detrital white mica analyses which will be conducted using this age for the standard. Details of analytical procedures can be found in Ennis et al. (2015).

2.4.3 Apatite U-Pb

At each outcrop, ~10 kg of material was collected across several adjacent beds to reduce any bias arising during deposition from localized heavy mineral concentrating processes. Subsequent sample preparation and analysis were conducted at Trinity College Dublin. The sub–300 μm nonmagnetic heavy mineral fraction was obtained by standard jaw crushing, sieving, magnetic, and heavy liquid separation techniques. Grains were mounted in epoxy resin, ground to expose internal surfaces, and polished. To avoid sample bias, no attempt was made to exclude anhedral or inclusion-bearing grains; the LA-ICP-MS technique permits identification and exclusion of U-rich inclusions (e.g., zircon) from the time-resolved (i.e., downhole) ablation signal of the appropriate isotopes.

Analyses were conducted using a Photon Machines Analyte Excite 193 nm ArF Excimer laser ablation system coupled to a Thermo Scientific iCAP Qc ICPMS, employing laser spots of 30 μm, a fluence of 4.5 J cm^{-2}, a repetition rate of 5 Hz, and an ablation time for each spot of 45 s followed by a 25 s background measurement. Repeated measurements of the primary Madagascar apatite mineral standard (Thomson et al., 2012) were used to correct for downhole U-Pb fractionation, mass bias, and intrasession instrument drift using the “VizualAge_UcomPbine” data reduction scheme for IOLITE (Chew et al., 2014; Paton et al., 2011), while the secondary McClure

Mountain and Durango apatite standards were analysed as unknowns (McDowell et al., 2005; Schoene and Bowring, 2006). Unlike phases that exclude common (initial or nonradiogenic) Pb during crystallization, such as zircon, the often high common-Pb content in apatite typically renders apatite grains discordant in the U-Pb system. Common-Pb in the Madagascar apatite primary standard was corrected for using a ^{207}Pb-based correction method using a known initial ^{207}Pb/^{206}Pb ratio (Chew et al., 2014). Variable common-Pb content in the detrital apatite unknowns was corrected using an initial common-Pb composition derived from a terrestrial Pb evolution model (Stacey and Kramers, 1975) applied to an initial estimate for the age of the apatite, and then by adopting an iterative approach based on a ^{207}Pb correction (Chew et al., 2011). The ^{207}Pb-based correction assumes U-Pb* (radiogenic Pb) concordance – a reasonable assumption in the case of standards and magmatic grains, but one which may not be the case for detrital grains that have experienced partial Pb loss. As a result, independent geological evidence is required to discriminate between partially and wholly reset detrital U-Pb ages, similar to partially reset AFT ages (Mark et al., 2016).

Due to the ^{207}Pb-based correction, no apatite U-Pb age data can be excluded based on discordance criteria. However, the relatively low U content of apatite (sometimes <1 ppm) and consequent near-zero radiogenic Pb content of some grains can result in undesirably large analytical uncertainties. We therefore excluded grains with 2σ errors >25%, similar to the approach of Zattin et al. (2012).

As post-deposition temperatures exceeded the thermal sensitivity of the AFT technique (ca. 120-60 °C; e.g., Gallagher et al., 1998), the resultant AFT ages typically defined a single population for each sample. Because only a single AFT age population was defined for each sample, it was only necessary to analyse ca. 20-30 grains for each sample.

2.4.4 Detrital zircon U-Th-Pb results

Two hundred and seventy three zircons were analysed from the Lower Devonian Dingle Group on the Dingle Peninsula. Another 119 detrital zircon grains were analysed from the Upper Devonian Slieve Mish Group on the

Dingle Peninsula. The number of concordant ages obtained from each sample ensures an extremely low probability of missing an age component that contributes 10 % of the detrital zircon age population of the analysed sedimentary rocks (Vermeesch et al., 2016). For all three samples, where age populations contribute over six percent, interpretations can be made at the 95 % confidence level.

Age uncertainties reported in the text are at the 2σ level unless otherwise stated. Core-rim analyses were undertaken where these features could be identified in CL images and where grains were large enough. Only rim ages are used for provenance interpretations in order to determine the most recent source of sediment. The results are presented as Wetherill concordia (Wetherill, 1956), frequency and KDE plots (Figure 2–4 and Figure 2–5). The $^{207}Pb/^{206}Pb$ age is reported where the $^{206}Pb/^{238}U$ age is greater than 1.0 Ga because the $^{207}Pb/^{206}Pb$ age is more precise in older zircon grains (e.g. Gehrels et al., 2008).

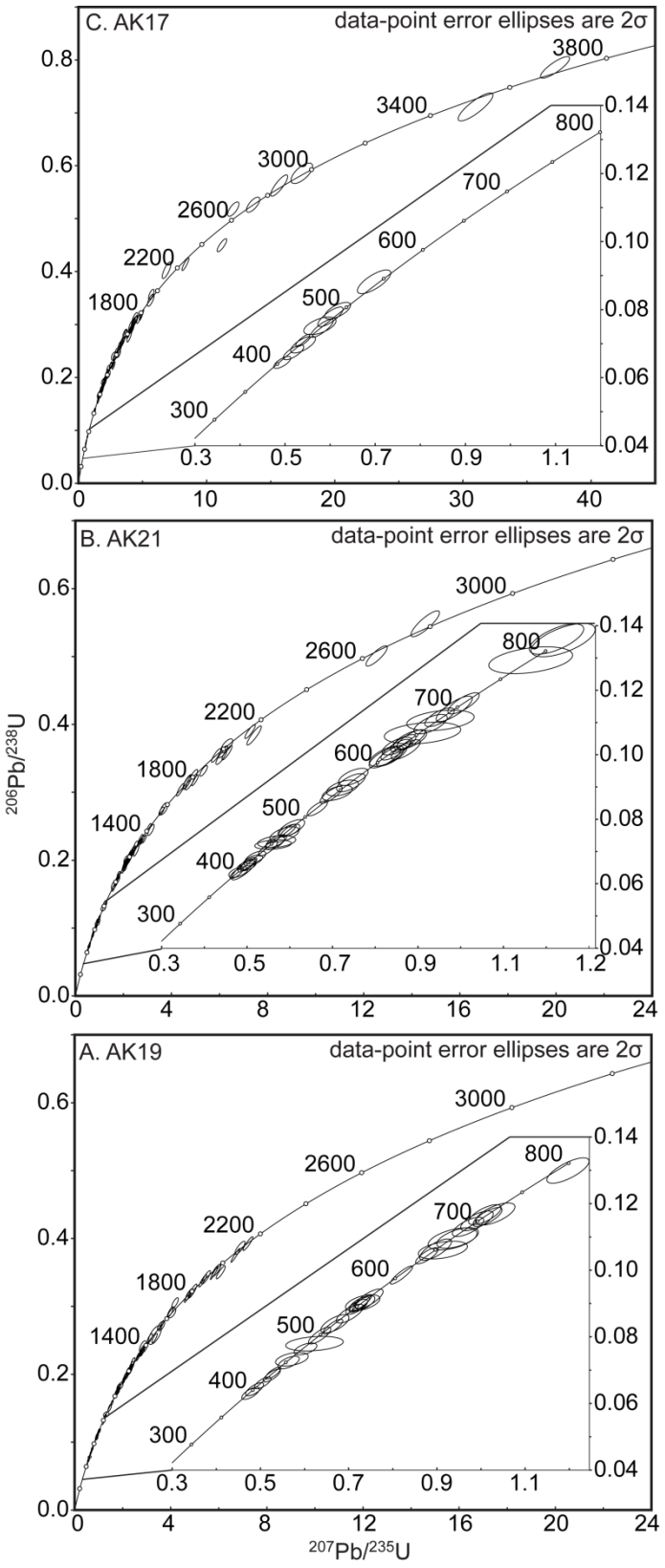

Figure 2–4. Wetherill concordia plots for all detrital zircon samples analysed in this study (youngest ages inset). **A**. Coumeenoole Formation (sample AK19). **B**. Slea Head Formation (sample AK21). **C**. Cappagh White Sandstone Formation (sample AK17).

2.4.4.1 Coumeenoole Formation - Sample AK19

Sample AK19, collected at Connor Pass, consists of grey, moderately sorted, medium- to coarse-grained sandstone and is the stratigraphically oldest sample in the study area. One hundred and fourteen zircon grains were analysed yielding a total of 86 concordant analyses ranging from 394 ± 9 Ma to 2142 ± 16 Ma (Figure 2–4A). Thirty seven grains (43 %) yielded Mesoproterozoic ages which form a major peak at around 1.20 Ga (Figure 2–5A). Neoproterozoic zircons make up 26 % (n = 22) of the sample, the second largest peak in the sample occurring at around 550 Ma. The rest of the sample is composed of 14 (16 %) Palaeoproterozoic zircons and 13 (15 %) Palaeozoic zircons. Of the Palaeozoic grains, four are Cambrian, four are Ordovician, two are Silurian and three are Devonian. Two of the Devonian zircons, the youngest in the sample, have ages of 394 ± 9 Ma and 402 ± 10 Ma and have length:width ratios of 3:1 and 5:1 respectively. Kostov (1973) suggests that high length-width ratios may indicate rapid cooling rates. However, such ratios may simply represent first order detrital zircons that have not been reworked (Poldervaart, 1955).

2.4.4.2 Slea Head Formation - Sample AK21

This sample was taken from Cooleen Pier in Ventry Bay and consists of dark grey, medium- to coarse-grained, pebbly sandstones. Ninety eight concordant ages were obtained from measurement of 159 zircon grains. Ages range from 395 ± 8 Ma to 2765 ± 29 Ma and the largest peak is developed at 1.18 Ga (Figure 2–4B and Figure 2–5B). Mesoproterozoic zircons form the bulk of the sample at 40 % (n = 39). Twenty six zircon grains (27 %) are Neoproterozoic in age, forming a major peak at ca. 630 Ma. Palaeoproterozoic zircons contribute 13 % (n = 13) of the sample. Eighteen grains are Palaeozoic in age, including one Cambrian zircon, eight Ordovician zircons, three Silurian zircons and six Devonian zircons. This sample, unlike sample AK19, also contains Archaean grains (n = 2). A concordia age of 405 ± 4 Ma ($MSWD_{conc}$ = 0.18; p_{conc} = 0.67) was calculated using the six Devonian zircons. Two of these zircons display length:width ratios of greater than 3:1.

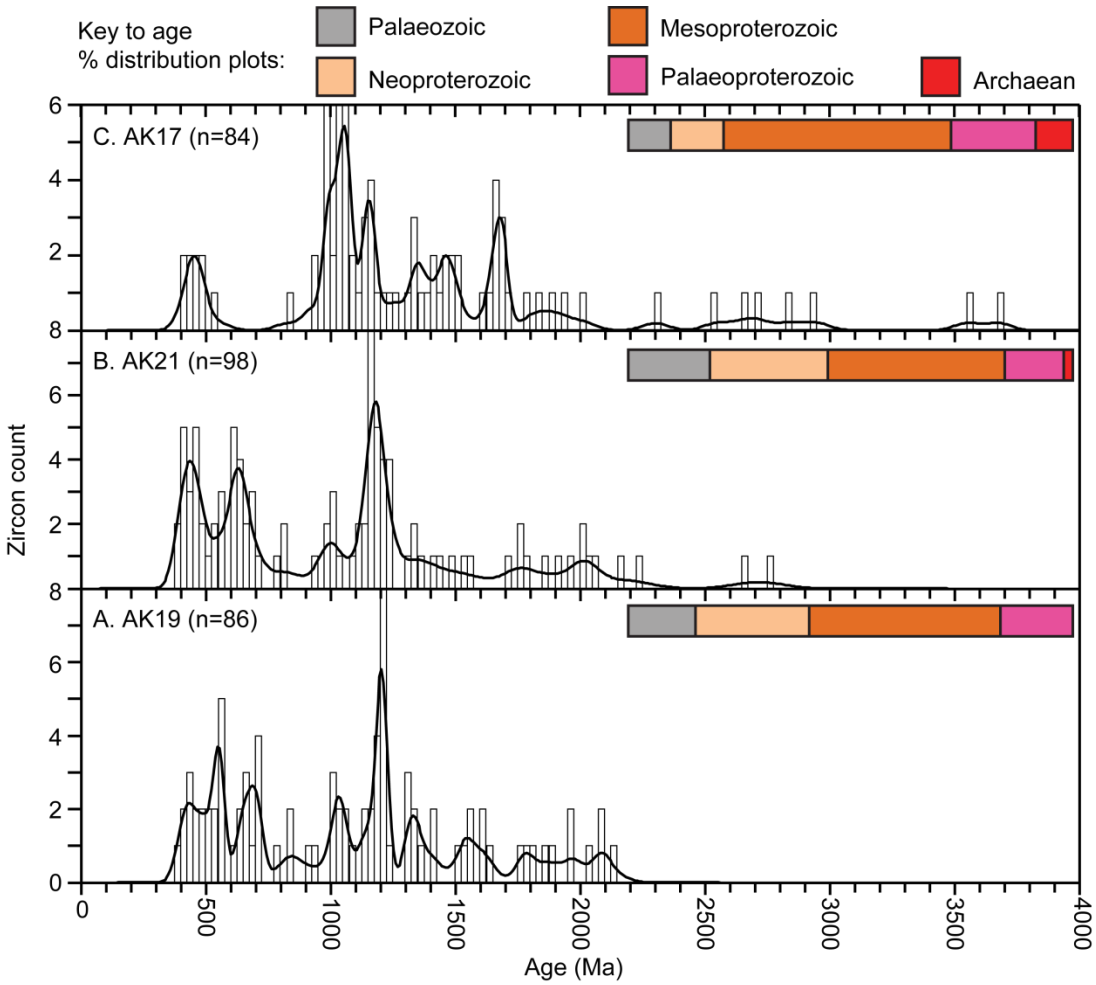

Figure 2–5. Detrital zircon age KDE, histogram plots and age percentage distribution plots from Dingle Peninsula samples. **A**. Coumeenoole Formation (sample AK19). **B**. Slea Head Formation (sample AK21). **C**. Cappagh White Sandstone Formation (sample AK17). n, number of analyses.

2.4.4.3 Cappagh White Sandstone Formation - Sample AK17

This sample, consisting of grey to pink, poorly sorted medium- to coarse-grained, pebbly sandstone, was taken from an outcropping ridge at Aughils, north of the R561. One hundred and nineteen zircons were analysed, producing 84 concordant ages ranging from 403 ± 9 Ma to 3677 ± 21 Ma (Figure 2–4C). The majority of these grains are Mesoproterozoic in age (43 grains representing 51 % of the sample) and the largest peak in the sample is Mesoproterozoic at ca. 1.05 Ga (Figure 2–5C). Sixteen grains (19 %) are Palaeoproterozoic in age and represent the second largest population in the sample. Neoproterozoic zircons represent 12 % (n = 10) of the sample.

Palaeozoic zircons represent 10 %, including one Cambrian zircon, three Ordovician zircons, three Silurian zircons and one Devonian zircon. Seven Archaean zircon grains are present in the sample. There is a paucity of zircon ages (n = 3) between ca. 550 Ma and ca. 980 Ma.

2.5 Apatite U-Pb and Mica $^{40}Ar/^{39}Ar$ Geochronology

2.5.1 Apatite U-Pb

These data were generated concurrently with apatite fission track analyses that were undertaken for bedrock thermal history studies by Cogné et al. (2014), but were not previously published. Due to the low number of detrital apatite grains analysed, the data must be interpreted with caution. In some cases, samples from the same formation are combined to yield the minimum statistical requirement of 60 analyses, as per Dodson et al. (1988). The limited variability in detrital apatite ages in these larger samples suggests that it is unlikely that multiple apatite sources of significantly different age and thermal history were being sampled by the sediments under investigation. The apatite U-Pb ages were not utilised in the aforementioned study. Therefore the data have been included in this study (Figure 2–6) to provide a geochronological proxy which has an intermediate closure temperature (ca. 375-550 °C; Cochrane et al., 2014) between the mica $^{40}Ar/^{39}Ar$ and zircon U-Pb systems. The sampling transect was collected from Mount Brandon on the Dingle Peninsula (Figure 2–3). This transect intersected two formations and includes four samples taken from the Ballymore Sandstone Formation and one sample from the Farran Sandstone Formation.

Combined analyses from four samples (Mb-1, Mb-4, Mb-5 and Mb-7) from the Ballymore Sandstone Formation, the uppermost formation in the Dingle Group, yields a KDE spectrum composed of 70 ages forming a single KDE peak at ca. 420 Ma. Detrital apatite ages in this formation range from 356 ± 80 to 896 ± 30 Ma (Figure 2–6A). However, 63 % of grains have ages between 380 and 440 Ma and 10 % have ages of less than 393 Ma (end-Emsian). Eighteen apatite grains were analysed from the Farran Sandstone Formation (sample Mb-9), the lowest formation in the Smerwick Group. These grains

range in age from 347 ± 58 to 1356 ± 227 Ma. The KDE spectrum (Figure 2–6B) shows the highest age concentration at ca. 420 Ma.

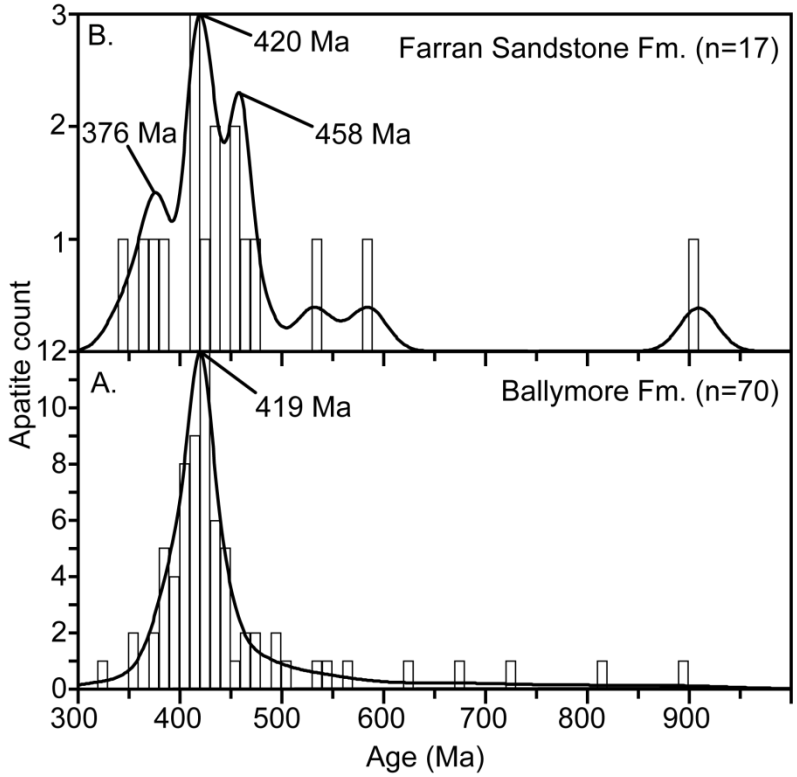

Figure 2–6. KDE and histogram plots for detrital apatite U-Pb ages in (**A**) the Ballymore Formation and (**B**) the Farran Sandstone Formation. n, number of analyses.

2.5.2 Mica $^{40}Ar/^{39}Ar$

Ennis et al. (2015) acquired detrital white mica ages for a sample from the Coumeenoole Formation, at a similar location (Connor Pass) to detrital zircon sample AK19. These ages have been recalculated here using the revised Fish Canyon sanidine standard age of Kuiper et al. (2008). Detrital white mica ages in the sample range from 308 ± 10.3 Ma to 440 ± 7 Ma, including two main age groups forming KDE peaks at ca. 414 Ma and ca. 382 Ma (Figure 2–7).

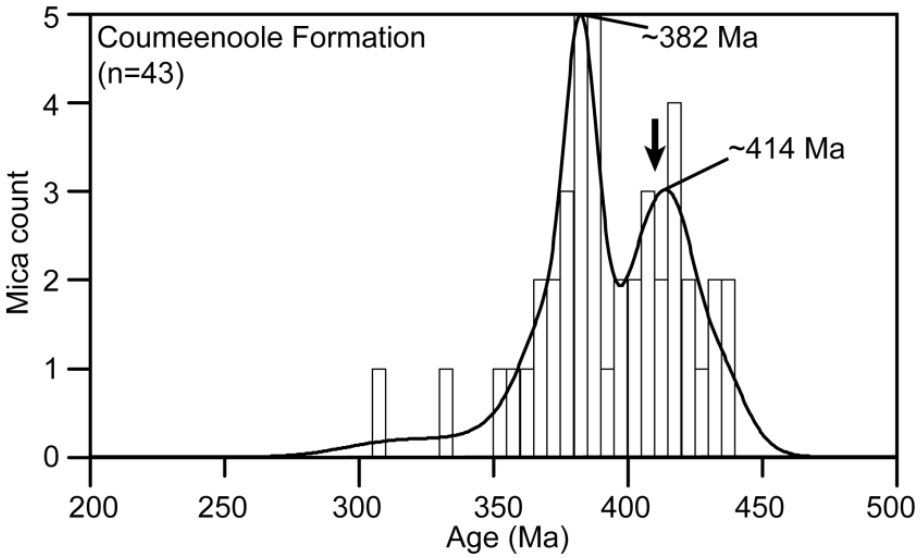

Figure 2–7. Histogram and KDE plots of revised detrital white mica ages from a sample from the Coumeenoole Formation at Connor Pass on the Dingle Peninsula (original data from Ennis et al., 2015). Bold arrow represents approximate depositional age (see text for explanation of 382 Ma peak). n, number of analyses.

2.6 Discussion

The overall age distribution of detrital zircons in samples from the Coumeenoole and Slea Head Formations (similar Proterozoic distributions, a gap in ages between 730 and 940 Ma, mostly continuous distributions between 390 and 730 Ma and major KDE peaks at around 1.2 Ga) suggests a common source throughout their deposition (Kolmogorov-Smirnov test p-value of 0.871). Palaeozoic peaks in both samples, at around 430 Ma, likely correspond to a Caledonian (430-420 Ma) source. A mean $^{207}Pb/^{206}Pb$ age of 432 ± 3 Ma as well as a whole-rock Rb-Sr isochron age of 428 ± 11 Ma was obtained by O'Connor et al. (1988) for the Carnsore granite. A Rb-Sr whole-rock isochron age of 436 ± 7 Ma for the Saltees granite by Max et al. (1979) led O'Connor et al. (1988) to conclude that the two intrusions are genetically related. These intrusions are the only ones of this age in Ireland and the 430 Ma age of detrital zircons from the LORS, as well as the northerly directed palaeoflow of the Trabeg Conglomerate Formation (Todd, 2000), suggests that the intrusions extend westward beneath the Munster Basin along the strike of Caledonian lineaments. The idea of such a buried granite is not new; it was first proposed by Murphy (1960) and has since been expanded upon by

a number of authors (e.g. Ford et al., 1991; Meere, 1995; Masson et al., 1998; Vermeulen et al., 2000; Todd, 2000). Vermeulen et al. (2000) interpreted seismic profiles across southern Ireland as showing a shallow, granitic body buried beneath the UORS just south of the Killarney-Mallow Fault Zone. Todd (2000) suggested that granite clasts within the Trabeg Conglomerate Formation might represent the unroofing of a presently buried granitic intrusion which forms part of an extension of the Leinster terrane.

Detrital apatite ages from the uppermost part of the Dingle Group, in the Ballymore Formation, yield a single peak at ca. 420 Ma (Figure 2–6A) which is compatible with a Late Caledonian granitic source. Williams et al. (1999) obtained a magmatic zircon age of 411 Ma for the Cooscrawn Tuff Bed in the Ballymore Formation which is older than 22 of the 70 detrital apatites analysed in this formation. A concordia age from six zircons in the underlying Slea Head Formation provides a maximum depositional age of 405 ± 4 Ma ($MSWD_{conc}$ = 0.18; p_{conc} = 0.67) and suggests that the Cooscrawn Tuff age is likely erroneous. Palynological evidence places the deposition of the Slea Head Formation in early to possibly middle Emsian times and is compatible with the youngest group of detrital zircons in this formation. The high length to width ratio of some of the youngest zircons in both the Coumeenoole and Slea Head Formations may suggest an igneous source that had cooled rapidly (Kostov, 1973) – possibly a syn-sedimentary volcanic source. Although U-Pb ages of apatite grains from the Ballymore Formation are younger, they are nonetheless indistinguishable from the zircon ages of the Coumeenoole and Slea Head Formations at the 2-sigma level. A dominant age peak of ca. 420 Ma (Figure 2–6B) is also observed for 17 detrital apatite grains in the Farran Sandstone Formation (Smerwick Group) which unconformably overlies the Ballymore Formation.

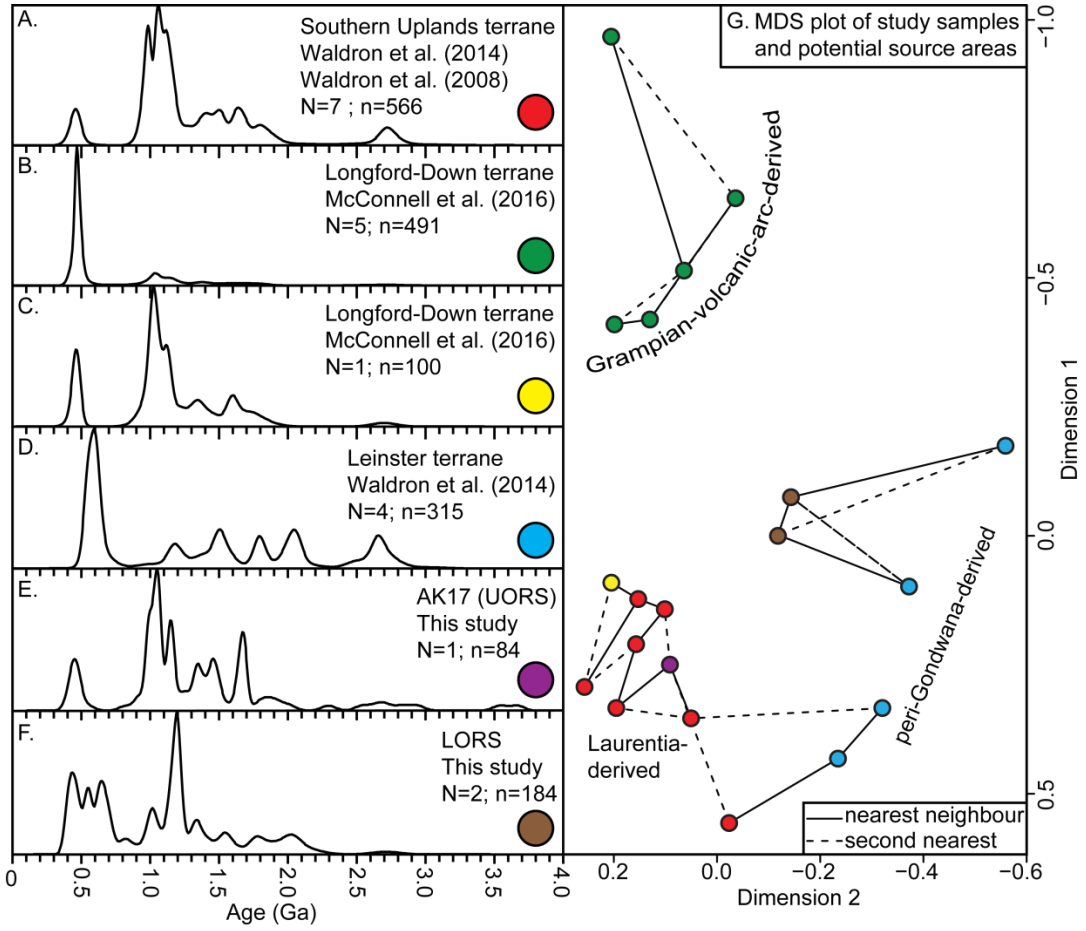

Figure 2–8. KDE plots of detrital zircon ages from various potential local sediment sources as well as age distributions for detrital zircons analysed in this study. **A**. Upper Ordovician to Llandovery sedimentary rocks of the Southern Uplands terrane (Waldron et al., 2008, 2014) with dominant Laurentian provenance. **B**. Upper Ordovician to Llandovery sedimentary rocks of the Longford Down terrane showing peri-Laurentian arc provenance (McConnell et al., 2016). **C**. A single sample from the Llandovery Lough Avaghon Formation in the Longford Down terrane showing dominant Laurentian provenance (McConnell et al., 2016). **D**. Ganderian provenance of Cambrian sedimentary rocks in the Leinster terrane (Waldron et al., 2014). **E**. UORS on the Dingle Peninsula. **F**. Composite of two samples from the LORS Dingle Group. **G**. Multi-dimensional scaling map of individual samples used in plots A-F. Labels indicate broad provenance interpretations from original studies. Axes values are dimensionless K-S effect sizes (Vermeesch, 2013). The most closely related samples are joined by a solid line and the second closest are marked with a dashed line. N, number of samples; n, number of single zircon grain ages.

A lower Palaeozoic source of detrital mica is reflected in the oldest age peak (ca. 414 Ma, Figure 2–7) from a sample from the Coumeenoole Formation. However, the dominant age peak is much younger, at ca. 382 Ma. This peak is much younger than the Emsian depositional age of the host

sedimentary rock and suggests that the LORS experienced a thermal resetting event. A review of the potential causes of resetting is provided in Ennis et al. (2015) and the extension associated with Lough Guitane Volcanism in the Munster Basin is briefly mentioned. Given that Williams et al. (2000) obtained a U-Pb zircon age of 378.5 Ma for the Horses Glen Volcanic Centre and 384.5 Ma for the Killeen Volcanic Centre (which lie to the southeast of the Dingle Basin), it is likely that the younger detrital mica ages represent resetting by high heat flow associated with extension and volcanism which may have been caused by emplacement of a granitic body at depth below the Munster Basin (Avison, 1984). Alternatively, these younger ages could represent partial resetting due to low-grade Variscan metamorphism at the end of the Carboniferous Period.

The low proportion of Palaeozoic zircons in the Dingle Group does not reflect the high proportion of volcanic clasts reported by Todd (2000) and interpreted to have been derived from rocks of Ordovician to Silurian age. This, however, may simply be a function of low zircon fertility in the volcanic source due to the dominant mafic to intermediate compositions (Todd, 2000).

Determination of the ultimate source of late Neoproterozoic detrital zircons in these samples is relatively straightforward because of the lack of abundant known sources of this age on this part of the Laurentian craton (Figure 2–2). The LORS samples also contain some 1.9 to 2.1 Ga zircons, considered to be indicative of the Gondwanan Eburnean Orogeny (Nance et al., 2008). Late Neoproterozoic zircons are ubiquitous in peri-Gondwanan terranes as a result of arc magmatism at that time (Nance et al., 2008) and therefore represent the most likely source. It should be noted, however, that Cawood and Nemchin (2001) report extensional magmatism associated with rifting in Laurentia between 520 and 555 Ma. But sedimentary rocks interpreted to be of Laurentian affinity do not record extensive Neoproterozoic zircon production (Figure 2–2). Combined detrital zircon ages from various Cambrian formations in the Leinster Massif (Waldron et al., 2014) yield a high proportion in the range 500 to 770 Ma forming a peak at around 590 Ma (Figure 2–8D). Waldron et al. (2014) proposed that these zircon ages represent a Ganderian source for the host sediments. If the source of granitic material for the Dingle Group was

indeed Late Caledonian granites as suggested above, then, by extension, the Cambrian to Ordovician rocks into which the granites intrude are also a viable source of detritus. Support for derivation of late Neoproterozoic zircons from recycling of peri-Gondwanan strata can be found in the study by Todd (2000) who found coticule and tourmalinite clasts akin to rocks found in the Ordovician Ribband Group. Todd (2000) also suggests that quartzite clasts in the Trabeg Conglomerate Formation could be related to quartzites of the Cambrian Bray Group. The similarity in the ranges of detrital zircon ages younger than 800 Ma in both the Coumeenoole and Slea Head Formations suggests that this southerly source remained available throughout their deposition.

Zircons with ages in the range of 1.1 to 1.25 Ga, the most abundant in both samples, are likely ultimately sourced from Laurentia. Cawood and Nemchin (2001) consider grains in this age range to be representative of magmatic and metamorphic activity associated with the Grenville Orogeny. Zircons of similar age are present in the Ganderia-derived Cambrian sediments in the Leinster Massif. However, the far greater abundance of zircons of this age range relative to zircons of late Neoproterozoic age in the Dingle Group samples requires an additional source from which the older zircons can be derived.

Constructing a palaeodrainage pattern for the Coumeenoole and Slea Head Formations requires a source (or sources) of detritus that meet the following criteria:

a) Abundant zircons yielding ca. 1.2 Ga U-Pb ages (likely of ultimate Laurentian affinity).
b) Presence of late Neoproterozoic and 1.9 to 2.1 Ga zircons (of peri-Gondwanan affinity)
c) Paucity of zircons between 730 and 940 Ma
d) Low proportion of Palaeozoic zircons
e) Late Caledonian apatite U-Pb and white mica $^{40}Ar/^{39}Ar$ ages (ca. 420 Ma and 414 Ma, respectively).

Transverse drainage, as indicated by palaeocurrent directions (Todd, 2000), particularly from the south but possibly also from the north, was the likely means by which Late Caledonian and peri-Gondwanan material was supplied to the Dingle Basin (Figure 2–9). Evidence of Late Caledonian detrital input to

the basin is given by 420 Ma apatite and 414 Ma mica ages. Although the ultimate source of Mesoproterozoic zircons in the Coumeenoole and Slea Head Formations was probably the Grenville Orogeny, defining the immediate source area is more problematic because a source of abundant 1.2 Ga zircons has not been found in Ireland. Ordovician and Silurian strata from the Southern Uplands – Longford Down terrane show an abundance of 1.1 Ga (Figure 2–8A and C) and Ordovician zircons (Figure 2–8B). This accretionary wedge material is therefore a poor candidate unless the source character of these sedimentary rocks changes westward, along strike. The apparent dissimilarity, revealed by multi-dimensional scaling analysis, between the Dingle Group samples and samples of Laurentian derivation in the Southern Uplands – Longford Down terrane (Figure 2–8G) reflects the lack of 1.2 Ga zircons in the available source data and presence of late Neoproterozoic zircons of peri-Gondwanan affinity in the Dingle Group samples.

Given the bulk northeastward palaeoflow in the Coumeenoole and Slea Head Formations (Todd et al., 1988), it is likely that most of the detritus was deposited as a result of this flow. A source to the southwest of the Dingle Basin must account for the high proportion of Laurentian zircons in the analysed samples. Therefore, although the main river course likely flowed from the west and southwest, we suggest that Caledonian highlands in the north produced a large number of tributaries flowing from north to south, into the main Coumeenoole/Slea Head system (Figure 2–9). Alternatively, it is also possible that the Iapetus Suture forms a regional S-shape and that the strike of the suture swings from roughly east-west onshore to southwest-northeast off the southwest coast of Ireland. This is highly speculative however, as there is no other supporting evidence for such a hypothesis.

Unlike the LORS on the Dingle Peninsula, the UORS, represented by sample AK17 from the Cappagh White Sandstone Formation, contains very few late Neoproterozoic zircons but is instead dominated by Mesoproterozoic grains. Also, unlike the LORS, the UORS contains a dominant 1.05 Ga peak as opposed to the 1.2 Ga peak of the LORS. The lack of late Neoproterozoic grains, dominant 1.05 Ga KDE peak and similarity to detrital zircon age spectra of Laurentian affinity (Figure 2–8A, C and G) indicates a northerly-derived

source area and no input from sources south of the Iapetus Suture. It would also indicate that recycling of the LORS into the UORS in southern Ireland, as previously suggested, is not likely to have occurred. It is more conceivable that this sediment was recycled from material similar to that found in the Longford Down terrane.

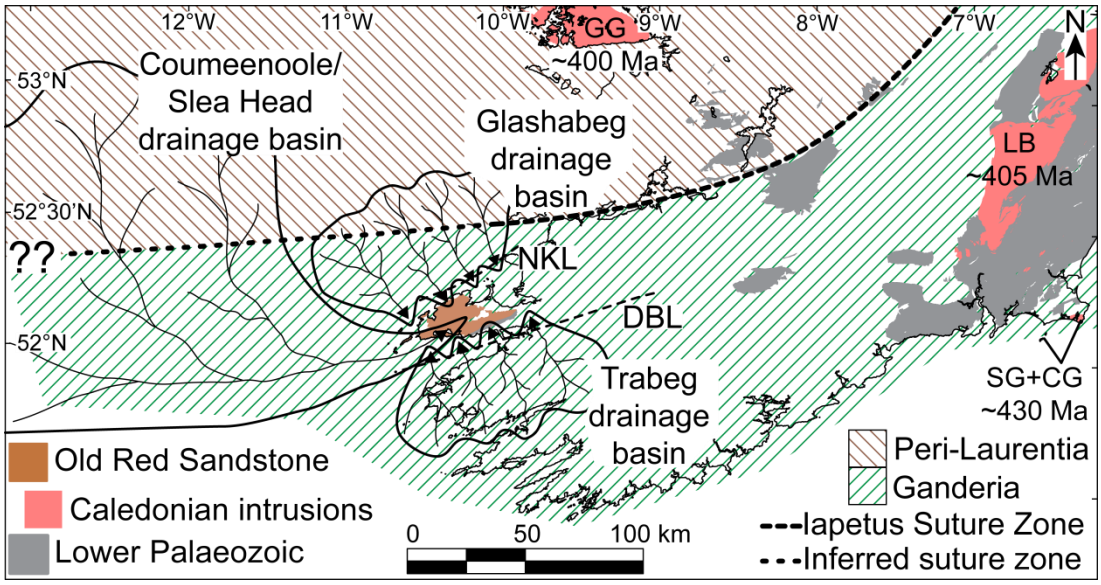

Figure 2–9. Possible palaeodrainage pattern in the Dingle Basin during deposition of the Coumeenoole and Slea Head Formations (modified after Todd 2000). CG, Carnsore Granite; DBL, Dingle Bay Lineament; GG, Galway Granite Batholith; LB, Leinster Batholith; NKL, North Kerry Lineament; SG, Saltees Granite.

It is becoming widely accepted that a period of regional sinistral transtension occurred across the Iapetus Suture Zone in the Early Devonian Period (Brown et al., 2008; Cooper et al., 2016; Dewey and Strachan, 2003; Phillips et al., 1995; Todd, 1989). In the present study, the discrepancy between 1.2 Ga Laurentian zircons found in the Dingle Group and 1.1 Ga Laurentian zircons found in the Longford Down and Southern Uplands terranes as well as the abundance of 1.05 Ga zircons in the UORS of the Dingle Peninsula is supportive of large-scale sinistral transtenional displacement along the Iapetus Suture, removing the 1.2 Ga source of detrital zircon and introducing the 1.05-1.1 Ga source to the UORS in the Late Devonian Period. Of course, this discrepancy may not have tectonic significance and may simply be representative of topographic separation of

sources or complete denudation of the 1.2 Ga source and subsequent exhumation of the 1.1 Ga source. High resolution detrital zircon sampling of younger formations within and overlying the Dingle Group would serve to elucidate the nature and timing of the change in source character. Finally, a minimum depositional age of ca. 405 Ma for the Coumeenoole Formation adds to growing evidence (Soper and Woodcock 2003, and references therein) of a discrete Emsian orogenic event in the British Isles.

2.7 Conclusions

This paper presents the first multi-proxy, single-grain detrital geochronological study of the LORS in the Lower Devonian Dingle Basin in southwestern Ireland which suggests the following:

1) The Dingle Basin sedimentary fill is dominated by Laurentian detritus but also includes a mixture of peri-Gondwanan and Late Caledonian (430-420 Ma) to Acadian (410-390 Ma) source areas.
2) A dominant drainage area lay to the west but the basin must have received much detritus from transverse drainage to the north which intersected Laurentian material.
3) Detrital zircons from the UORS Cappagh White Sandstone Formation show very different characteristics to the LORS where sediment was being supplied solely from detritus of Laurentian affinity.
4) The paucity of late Neoproterozoic zircons in the UORS compared to the high proportion in the LORS suggests that the UORS was not derived from recycling of LORS sediments as previously suggested.
5) Well documented regional sinistral transtension during the Early Devonian Period was likely responsible for a switch in Laurentian source character from the LORS (prevalence of 1.2 Ga detrital zircons) to the UORS (prevalence of 1.1 Ga detrital zircons).

2.8 Acknowledgements

B.J.F, A.K, P.A.M and K.F.M acknowledge the financial support of the Irish Shelf Petroleum Studies Group (ISPSG) of the Irish Petroleum Infrastructure Programme (PIP) Group 4 (project code IS 12/05 UCC). The ISPSG comprises: Atlantic

Petroleum (Ireland) Ltd, Cairn Energy Plc, Chrysaor E&P Ireland Ltd, Chevron North Sea Limited, ENI Ireland BV, Europa Oil & Gas, ExxonMobil E&P Ireland (Offshore) Ltd., Husky Energy, Kosmos Energy LLC, Maersk Oil North Sea UK Ltd, Petroleum Affairs Division of the Department of Communications, Energy and Natural Resources, Providence Resources Plc, Repsol Exploración SA, San Leon Energy Plc, Serica Energy Plc, Shell E&P Ireland Ltd, Sosina Exploration Ltd, Tullow Oil Plc and Woodside Energy (Ireland) Pty Ltd. D.C., C.M. and N.C. acknowledge support from Science Foundation Ireland grant 12/IP/1663 and 13/RC/2092 (iCRAG Research Centre, project HC4.2PD6a). iCRAG is funded under the SFI Research Centres Programme and is co-funded under the European Regional Development Fund. D. Pastor-Galan is thanked for his geochronology and sampling advice. C. Reid and R. van Elsas are thanked for their technical assistance for SEM and sample preparation respectively. J.W.F Waldron and J.F. Dewey are thanked for their constructive reviews which significantly improved the manuscript.

2.9 References

Avison, M., 1984. The Lough Guitane Volcanic Complex, County Kerry: A Preliminary Survey. Irish J. Earth Sci. 6, 127–136.

Barr, S.M., Davis, D.W., Kamo, S., White, C.E., 2003. Significance of U–Pb detrital zircon ages in quartzite from peri-Gondwanan terranes, New Brunswick and Nova Scotia, Canada. Precambrian Res. 126, 123–145. doi:10.1016/S0301-9268(03)00192-X

Barr, S.M., Hamilton, M.A., Samson, S.D., Satkoski, A.M., White, C.E., 2012. Provenance variations in northern Appalachian Avalonia based on detrital zircon age patterns in Ediacaran and Cambrian sedimentary rocks, New Brunswick and Nova Scotia, Canada. Can. J. Earth Sci. 49, 533–546. doi:10.1139/e11-070

Boyd, J.D., Sloan, R.J., 2000. Initiation and early development of the Dingle Basin, SW Ireland, in the context of the closure of the Iapetus Ocean. Geol. Soc. London, Spec. Publ. 180, 123–145. doi:10.1144/GSL.SP.2000.180.01.08

Brown, P.E., Ryan, P.D., Soper, N.J., Woodcock, N.H., 2008. The Newer Granite problem revisited: a transtensional origin for the Early Devonian Trans-Suture Suite. Geol. Mag. 145, 235–256. doi:10.1017/S0016756807004219

Cawood, P.A., Merle, R.E., Strachan, R.A., Tanner, P.W.G., 2012. Provenance of the Highland Border Complex: constraints on Laurentian margin accretion in the Scottish Caledonides. J. Geol. Soc. London. 169, 575–586. doi:10.1144/0016-76492011-076

Cawood, P.A., Nemchin, A.A., 2001. Paleogeographic development of the east Laurentian margin: Constraints from U-Pb dating of detrital zircons in the Newfoundland Appalachians. Geol. Soc. Am. Bull. 113, 1234–1246. doi:10.1130/0016-7606(2001)113<1234:PDOTEL>2.0.CO;2

Cawood, P.A., Nemchin, A.A., Smith, M., Loewy, S., 2003. Source of the Dalradian Supergroup constrained by U-Pb dating of detrital zircon and implications for the East Laurentian margin. J. Geol. Soc. London. 160, 231–246. doi:10.1144/0016-764902-039

Cawood, P.A., Nemchin, A.A., Strachan, R., Prave, T., Krabbendam, M., 2007. Sedimentary basin and detrital zircon record along East Laurentia and Baltica during assembly and breakup of Rodinia. J. Geol. Soc. London. 164, 257–275. doi:10.1144/0016-76492006-115

Chew, D.M., Donelick, R.A., 2012. Combined apatite fission track and U-Pb dating by LA-ICP-MS and its application in apatite provenance analysis, in: Sylvester, P.J. (Ed.), Quantitative Mineralogy and Microanalysis of Sediments and Sedimentary Rocks. Mineralogical Association of Canada, pp. 219–247.

Chew, D.M., Graham, J.R., Whitehouse, M.J., 2007. U-Pb zircon geochronology of plagiogranites from the Lough Nafooey (= Midland Valley) arc in western Ireland: constraints on the onset of the Grampian orogeny. J. Geol. Soc. London. 164, 747–750. doi:10.1144/0016-76492007-025

Chew, D.M., Petrus, J.A., Kamber, B.S., 2014. U–Pb LA–ICPMS dating using accessory mineral standards with variable common Pb. Chem. Geol. 363, 185–199. doi:10.1016/j.chemgeo.2013.11.006

Chew, D.M., Stillman, C.J., 2009. Late Caledonian orogeny and magmatism, in: The Geology of Ireland. pp. 143–174.

Chew, D.M., Strachan, R.A., 2014. The Laurentian Caledonides of Scotland and Ireland. Geol. Soc. London, Spec. Publ. 390, 45–91.

doi:10.1144/SP390.16

Chew, D.M., Sylvester, P.J., Tubrett, M.N., 2011. U-Pb and Th-Pb dating of apatite by LA-ICPMS. Chem. Geol. 280, 200–216. doi:10.1016/j.chemgeo.2010.11.010

Cochrane, R., Spikings, R.A., Chew, D.M., Wotzlaw, J.F., Chiaradia, M., Tyrrell, S., Schaltegger, U., Van der Lelij, R., 2014. High temperature (>350°C) thermochronology and mechanisms of Pb loss in apatite. Geochim. Cosmochim. Acta 127, 39–56. doi:10.1016/j.gca.2013.11.028

Cocks, L.R.M., McKerrow, W.S., Van Staal, C.R., 1997. The margins of Avalonia. Geol. Mag. 134, 627–636.

Cogné, N., Chew, D., Stuart, F.M., 2014. The thermal history of the western Irish onshore. J. Geol. Soc. London. 171, 779–792. doi:10.1144/jgs2014-026

Collins, A.S., Buchan, C., 2004. Provenance and age constraints of the South Stack Group, Anglesey, UK: U–Pb SIMS detrital zircon data. J. Geol. Soc. London. 161, 743–746. doi:10.1144/0016-764904-036

Cooper, M.R., Anderson, P., Condon, D.J., Stevenson, C.T.E., Ellam, R.M., Meighan, I.G., Crowley, Q.G., 2016. Shape and intrusion history of the Late Caledonian, Newry Igneous Complex, Northern Ireland, in: Young, M.E. (Ed.), Unearthed: Impacts of the Tellus Surveys of Ireland. Royal Irish Academy, Dublin, pp. 145–155. doi:DOI:10.3318/ 978-1-908996-88-6.ch11

Cooper, M.R., Crowley, Q.G., Hollis, S.P., Noble, S.R., Roberts, S., Chew, D., Earls, G., Herrington, R., Merriman, R.J., 2011. Age constraints and geochemistry of the Ordovician Tyrone Igneous Complex, Northern Ireland: implications for the Grampian orogeny. J. Geol. Soc. London. 168, 837–850. doi:10.1144/0016-76492010-164

Daly, J.S., 1996. Pre-Caledonian history of the Annagh Gneiss Complex, North-western Ireland, and correlation with Laurentia-Baltica. Irish J. Earth Sci. 15, 5–18.

Daly, J.S., Muir, R.J., Cliff, R.A., 1991. A precise U-Pb zircon age for the Inishtrahull syenitic gneiss, County Donegal, Ireland. J. Geol. Soc. London. 148, 639–642. doi: 10.1144/gsjgs.148.4.0639

Dewey, J.F., Strachan, R.A., 2003. Changing Silurian-Devonian relative plate motion in the Caledonides: sinistral transpression to sinistral transtension. J. Geol. Soc. London. 160, 219–229. doi:10.1144/0016-764902-085

Dodson, M.H., Compston, W., Williams, I.S., Wilson, J.F., 1988. A search for ancient detrital zircons in Zimbabwean sediments. J. Geol. Soc. London. 145, 977–983. doi:10.1144/gsjgs.145.6.0977

Dorais, M.J., Wintsch, R.P., Kunk, M.J., Aleinikoff, J., Burton, W., Underdown, C., Kerwin, C.M., 2012. P-T-t conditions, Nd and Pb isotopic compositions and detrital zircon geochronology of the Massabesic Gneiss Complex, New Hampshire: Isotopic and metamorphic evidence for the identification of Gander basement, central New England. Am. J. Sci. 312, 1049–1097. doi:10.2475/10.2012.01

Ennis, M., Meere, P.A., Timmerman, M.J., Sudo, M., 2015. Post-Acadian sediment recycling in the Devonian Old Red Sandstone of Southern Ireland. Gondwana Res. 28, 1415–1433. doi:10.1016/j.gr.2014.10.007

Fernandez-Suarez, J., Gutierrez Alonso, G., Jeffries, T.E., 2002. The importance of along-margin terrane transport in northern Gondwana: Insights from detrital zircon parentage in Neoproterozoic rocks from Iberia and Brittany. Earth Planet. Sci. Lett. 204, 75–88. doi:10.1016/S0012-821X(02)00963-9

Force, E.R., Barr, S.M., 2012. Provenance of the Lower Carboniferous Horton Group, Petit-de-Grat Island, Nova Scotia, as revealed by detrital zircon ages. Atl. Geol. 48, 137–145. doi:10.4138/atlgeol.2012.007

Ford, M., Brown, C., Readman, P., 1991. Analysis and tectonic interpretation of gravity data over the Variscides of southwest Ireland. J. Geol. Soc. London. 148, 137–148. doi:10.1144/gsjgs.148.1.0137

Ford, M., Klemperer, S.L., Ryan, P.D., 1992. Deep structure of southern Ireland: a new geological synthesis using BIRPS deep reflection profiling. J. Geol. Soc. London. 149, 915–922.

Friend, C.R.L., Strachan, R.A., Kinny, P.D., Watt, G.R., 2003. Provenance of the Moine Supergroup of NW Scotland: evidence from geochronology of detrital and inherited zircons from (meta) sedimentary rocks , granites and migmatites. J. Geol. Soc. London 160, 247–257.

Fritschle, T., Daly, J.S., Whitehouse, M.J., Mcconnell, B., Buhre, S., 2017. Multiple intrusive phases in the Leinster Batholith, Ireland : geochronology, isotope geochemistry and constraints on the deformation history. J. Geol. Soc. London 175, 229–246.

Fullea, J., Muller, M.R., Jones, A.G., Afonso, J.C., 2014. The lithosphere-asthenosphere system beneath Ireland from integrated geophysical-petrological modeling II: 3D thermal and compositional structure. Lithos 189, 49–64. doi:10.1016/j.lithos.2013.09.014

Fyffe, L.R., Barr, S.M., Johnson, S.C., McLeod, M.J., McNicoll, V.J., Valverde-Vaquero, P., van Staal, C.R., White, C.E., 2009. Detrital zircon ages from Neoproterozoic and Early Paleozoic conglomerate and sandstone units of New Brunswick and coastal Maine: implications for the tectonic evolution of Ganderia. Atl. Geol. 45, 110–144. doi:10.4138/atlgeol.2009.006

Gallagher, K., Brown, R., Johnson, C., 1998. Fission track analysis and its applications to geological problems. Annu. Rev. Earth Planet. Sci. 26, 519–572. doi:10.1146/annurev.earth.26.1.519

Gehrels, G.E., Valencia, V.A., Ruiz, J., 2008. Enhanced precision, accuracy, efficiency, and spatial resolution of U-Pb ages by laser ablation-multicollector-inductively coupled plasma-mass spectrometry. Geochemistry, Geophys. Geosystems 9, 1–13. doi:10.1029/2007GC001805

Henderson, B.J., Collins, W.J., Murphy, J.B., Gutierrez-Alonso, G., Hand, M., 2016. Gondwanan basement terranes of the Variscan–Appalachian orogen: Baltican, Saharan and West African hafnium isotopic fingerprints in Avalonia, Iberia and the Armorican Terranes. Tectonophysics 681, 278–304. doi:10.1016/j.tecto.2015.11.020

Hibbard, J.P., van Staal, C.R., Rankin, D.W., 2007. A comparative analysis of pre-Silurian crustal building blocks of the northern and the southern Appalachian orogen. Am. J. Sci. 307, 23–45. doi:10.2475/01.2007.02

Higgs, K.T., 1999. Early Devonian spore assemblages from the Dingle Group, County Kerry, Ireland. Boll. della Soc. Paleontol. Ital. 38, 187–196.

Ijlst, L., 1973. A Laboratory Overflow-Centrifuge for Heavy Liquid Mineral

Separation. Am. Mineral. 58, 1088–1093.

Johnson, T.E., Kirkland, C.L., Reddy, S.M., Evans, N.J., McDonald, B.J., 2016. The source of Dalradian detritus in the Buchan Block, NE Scotland: application of new tools to detrital datasets. J. Geol. Soc. London. 173, 773–782. doi:10.1144/jgs2016-019

Kennedy, M.J., 1979. The continuation of the Canadian Appalachians into the Caledonides of Britain and Ireland. Geol. Soc. London, Spec. Publ. 8, 33–64. doi:10.1144/GSL.SP.1979.008.01.03

Keppie, J.D., Davis, D.W., Krogh, T.E., 1998. U-Pb geochronological constraints on Precambrian stratified units in the Avalon Composite Terrane of Nova Scotia, Canada: tectonic implications. Can. J. Earth Sci. 35, 222–236. doi:10.1139/e97-109

Keppie, J.D., Nance, R.D., Murphy, J.B., Dostal, J., 2003. Tethyan, Mediterranean, and Pacific analogues for the Neoproterozoic–Paleozoic birth and development of peri-Gondwanan terranes and their transfer to Laurentia and Laurussia. Tectonophysics 365, 195–219. doi:10.1016/S0040-1951(03)00037-4

Kirkland, C.L., Strachan, R.A., Prave, A.R., 2008. Detrital zircon signature of the Moine Supergroup, Scotland: Contrasts and comparisons with other Neoproterozoic successions within the circum-North Atlantic region. Precambrian Res. 163, 332–350. doi:10.1016/j.precamres.2008.01.003

Kostov, I., 1973. Zircon morphology as a Crystallogenetic indicator. Krist. und Tech. 8, 11–19. doi:10.1002/crat.19730080103

Krogh, T.E., Keppie, J.D., 1990. Age of detrital zircon and titanite in the Meguma Group, southern Nova Scotia, Canada: Clues to the origin of the Meguma Terrane. Tectonophysics 177, 307–323. doi:10.1016/0040-1951(90)90287-I

Kuiper, K.F., Deino, A., Hilgen, F.J., Krijgsman, W., Renne, P.R., Wijbrans, J.R., 2008. Synchronizing Rock Clocks of Earth History. Science (80-.). 320, 500–504. doi:10.1126/science.1154339

Linnemann, U., Gerdes, A., Drost, K., Buschmann, B., 2007. The continuum between Cadomian orogenesis and opening of the Rheic Ocean: Constraints from LA-ICP-MS U-Pb zircon dating and analysis of plate-

tectonic setting (Saxo-Thuringian zone, northeastern Bohemian Massif, Germany). Geol. Soc. Am. Spec. Pap. 423, 61–96. doi:10.1130/2007.2423(03)

Linnemann, U., Herbosch, A., Liégeois, J.P., Pin, C., Gärtner, A., Hofmann, M., 2012. The Cambrian to Devonian odyssey of the Brabant Massif within Avalonia: A review with new zircon ages, geochemistry, Sm-Nd isotopes, stratigraphy and palaeogeography. Earth-Science Rev. 112, 126–154. doi:10.1016/j.earscirev.2012.02.007

Linnemann, U., Pereira, F., Jeffries, T.E., Drost, K., Gerdes, A., 2008. The Cadomian Orogeny and the opening of the Rheic Ocean: The diacrony of geotectonic processes constrained by LA-ICP-MS U-Pb zircon dating (Ossa-Morena and Saxo-Thuringian Zones, Iberian and Bohemian Massifs). Tectonophysics 461, 21–43. doi:10.1016/j.tecto.2008.05.002

Livermore, R.A., Smith, A.G., Briden, J.C., 1985. Palaeomagnetic Constraints on the Distribution of Continents in the Late Silurian and Early Devonian. Philos. Trans. R. Soc. Lond. B. Biol. Sci. 309, 29–56.

Ludwig, K.R., 2012. User's Manual for Isoplot 3.75. Berkeley Geochronol. Cent. Spec. Publ. 1–72.

Mac Niocaill, C., 2000. A new Silurian palaeolatitude for eastern Avalonia and evidence for crustal rotations in the Avalonian margin of southwestern Ireland. Geophys. J. Int. 141, 661–671. doi:10.1046/j.1365-246X.2000.00101.x

Mark, C., Cogné, N., Chew, D., 2016. Tracking exhumation and drainage divide migration of the Western Alps: A test of the apatite U-Pb thermochronometer as a detrital provenance tool. Bull. Geol. Soc. Am. 128, 1439–1460. doi:10.1130/B31351.1

Masson, F., Jacob, A.W.B., Prodehl, C., Readman, P.W., Shannon, P.M., Schulze, A., Enderle, U., 1998. A wide-angle seismic traverse through the Variscan of southwest Ireland. Geophys. J. Int. 134, 689–705. doi:10.1046/j.1365-246X.1998.00572.x

Max, M.D., Barber, A.J., Martinez, J., 1990. Terrane assemblage of the Leinster Massif , SE Ireland , during the Lower Palaeozoic. J. Geol. Soc. London 147, 1035–1050.

Max, M.D., Ploquin, A., Sonet, J., 1979. The age of the Saltees granite in the Rosslare Complex, in: The Caledonides of the British Isles Reviewed. Geological Society of London, pp. 723–725. doi:10.1144/GSL.SP.1979.008.01.88

McAteer, C.A., Stephen Daly, J., Flowerdew, M.J., Connelly, J.N., Housh, T.B., Whitehouse, M.J., 2010. Detrital zircon, detrital titanite and igneous clast U-Pb geochronology and basement-cover relationships of the Colonsay Group, SW Scotland: Laurentian provenance and correlation with the Neoproterozoic Dalradian Supergroup. Precambrian Res. 181, 21–42. doi:10.1016/j.precamres.2010.05.013

McConnell, B., Crowley, Q.G., Riggs, N., 2010. Laurentian origin of the Ordovician Grangegeeth volcanic arc terrane, Ireland. J. Geol. Soc. London. 167, 469–474. doi:10.1144/0016-76492009-139

McConnell, B., Morris, J., 1997. Initiation of Iapetus subduction under Irish Avalonia. Geol. Mag. 134, 213–218.

McConnell, B., Parkes, M., Crowley, Q., Rushton, A., 2015. No Exploits back-arc basin in the Iapetus suture zone of Ireland. J. Geol. Soc. London. 172, 740–747. doi:10.1144/jgs2015-044

McConnell, B., Riggs, N., Crowley, Q.G., 2009. Detrital zircon provenance and Ordovician terrane amalgamation, western Ireland. J. Geol. Soc. London 166, 473–484. doi:10.1144/0016-76492008-081

McConnell, B., Rogers, R., Crowley, Q., 2016. Sediment provenance and tectonics on the Laurentian margin: implications of detrital zircons ages from the Central Belt of the Southern Uplands–Down–Longford Terrane in Co. Monaghan, Ireland. Scottish J. Geol. 52, 11–17. doi:10.1144/sjg2015-013

McDowell, F.W., McIntosh, W.C., Farley, K.A., 2005. A precise 40Ar–39Ar reference age for the Durango apatite (U–Th)/He and fission-track dating standard. Chem. Geol. 214, 249–263. doi:10.1016/j.chemgeo.2004.10.002

McIlroy, D., Horák, J.M., 2006. Neoproterozoic: the late Precambrian terranes that formed Eastern Avalonia, in: Brenchley, P.J., Rawson, P.F. (Eds.), The Geology of England and Wales. Geological Society of London, pp.

9–24. doi:10.1144/GOEWP.2

Meere, P., 1995. The structural evolution of the western Irish Variscides: an example of obstacle tectonics? Tectonophysics 246, 97–112.

Meere, P.A., Mulchrone, K.F., 2006. Timing of deformation within Old Red Sandstone lithologies from the Dingle Peninsula, SW Ireland. J. Geol. Soc. London. 163, 461–469. doi:10.1144/0016-764905-099

Murphy, J.B., Fernández-Suárez, J., Jeffries, T.E., 2004a. Lithogeochemical and Sm-Nd and U-Pb isotope data from the Silurian–Lower Devonian Arisaig Group clastic rocks, Avalon terrane, Nova Scotia: A record of terrane accretion in the Appalachian-Caledonide orogen. Geol. Soc. Am. Bull. 116, 1183. doi:10.1130/B25423.1

Murphy, J.B., Fernández-Suárez, J., Jeffries, T.E., Strachan, R.A., 2004b. U-Pb (LA-ICP-MS) dating of detrital zircons from Cambrian clastic rocks in Avalonia: erosion of a Neoproterozoic arc along the northern Gondwanan margin. J. Geol. Soc. London. 161, 243–254. doi:10.1144/0016-764903-064

Murphy, T., 1960. Gravity map in Ireland - sheet 5 - south west. Geophys. Bull. 18.

Nance, R., Neace, E., Braid, J., Murphy, J., Dupuis, N., Shail, R., 2015. Does the Meguma Terrane Extend into SW England? Geosci. Canada 42, 61–76. doi:10.12789/geocanj.2014.41.056

Nance, R.D., Gutiérrez-Alonso, G., Keppie, J.D., Linnemann, U., Murphy, J.B., Quesada, C., Strachan, R.A., Woodcock, N.H., 2012. A brief history of the Rheic Ocean. Geosci. Front. 3, 125–135. doi:10.1016/j.gsf.2011.11.008

Nance, R.D., Murphy, J.B., Strachan, R.A., Keppie, J.D., Gutiérrez-Alonso, G., Fernández-Suárez, J., Quesada, C., Linnemann, U., D'lemos, R., Pisarevsky, S.A., 2008. Neoproterozoic-early Palaeozoic tectonostratigraphy and palaeogeography of the peri-Gondwanan terranes: Amazonian v. West African connections, in: Ennih, N., Liégeois, J.-P. (Eds.), The Boundaries of the West African Craton. The Geological Society of London, pp. 345–383. doi:10.1144/SP297.17

O'Connor, P.J., Aftalion, M., Kennan, P.S., 1989. Isotopic U–Pb ages of zircon and monazite from the Leinster Granite, southeast Ireland. Geol. Mag.

126, 725. doi:10.1017/S0016756800007044

O'Connor, P.J., Kennan, P.S., Aftalion, M., 1988. New Rb-Sr and U-Pb Ages for the Carnsore Granite and their bearing on the antiquity of the Rosslare Complex, southeastern Ireland. Geol. Mag. 125, 25–29. doi:10.1017/S0016756800009341

Owen, A.W., Parkes, M.A., 2000. Trilobite faunas of the Duncannon Group: Caradoc stratigraphy, environments and palaeobiogeography of the Leinster terrane, Ireland. Palaeontology 43, 219–269. doi:10.1111/1475-4983.00125

Paton, C., Hellstrom, J., Paul, B., Woodhead, J., Hergt, J., 2011. Iolite: Freeware for the visualisation and processing of mass spectrometric data. J. Anal. At. Spectrom. 26, 2508. doi:10.1039/c1ja10172b

Penney, S., 1980. A new look at the Old Red Sandstone succession of the Comeragh Mountains, County Waterford. J. Earth Sci. 3, 155–178.

Phillips, E.R., Barnes, R.P., Boland, M.P., Fortey, N.J., McMillan, A.A., 1995. The Moniaive Shear Zone: a major zone of sinistral strike-slip deformation in the Southern Uplands of Scotland. Scottish J. Geol. 31, 139–149. doi:10.1144/sjg31020139

Pickering, K.T., Bassett, M.G., Siveter, D.J., 1988. Late Ordovician-early Silurian destruction of the Iapetus Ocean : Newfoundland , British Isles and Scandinavia — a discussion. Trans. R. Soc. Edinb. Earth Sci. 79, 361–382.

Pointon, M.A., Cliff, R.A., Chew, D.M., 2012. The provenance of Western Irish Namurian Basin sedimentary strata inferred using detrital zircon U-Pb LA-ICP-MS geochronology. Geol. J. 47, 77–98. doi:10.1002/gj.1335

Poldervaart, A., 1955. Zircons in rocks; Part 1, Sedimentary rocks; Part 2, Igneous rocks. Am. J. Sci. 253, 433–461. doi:10.2475/ajs.253.8.433

Pollock, J.C., 2007. The Neoproterozoic-Early Paleozoic Tectonic Evolution of the Peri-Gondwanan Margin of the Appalachian Orogen - an Integrated Geochronological, Geochemical and Isotopic Study from North Carolina and Newfoundland. North Carolina State University.

Pollock, J.C., Hibbard, J.P., Van Staal, C.R., 2012. A paleogeographical review of the peri-Gondwanan realm of the Appalachian orogen. Can. J.

Earth Sci. 49, 259–288. doi:10.1139/E11-049

Pothier, H.D., Waldron, J.W.F., Schofield, D.I., DuFrane, S.A., 2015. Peri-Gondwanan terrane interactions recorded in the Cambrian–Ordovician detrital zircon geochronology of North Wales. Gondwana Res. 28, 987–1001. doi:10.1016/j.gr.2014.08.009

Samson, S.D., D'Lemos, R.S., Miller, B. V., Hamilton, M.A., 2005. Neoproterozoic palaeogeography of the Cadomia and Avalon terranes: constraints from detrital zircon U-Pb ages. J. Geol. Soc. London. 162, 65–71. doi:10.1144/0016-764904-003

Satkoski, A.M., Barr, S.M., Samson, S.D., 2010. Provenance of Late Neoproterozoic and Cambrian Sediments in Avalonia: Constraints from Detrital Zircon Ages and Sm-Nd Isotopic Compositions in Southern New Brunswick, Canada. J. Geol. 118, 187–200. doi:10.1086/649818

Schoene, B., Bowring, S.A., 2006. U–Pb systematics of the McClure Mountain syenite: thermochronological constraints on the age of the 40Ar/39Ar standard MMhb. Contrib. to Mineral. Petrol. 151, 615–630. doi:10.1007/s00410-006-0077-4

Schofield, D., Potter, J., Barr, S.M., Horak, J., Millar, I.L., Longstaffe, F., 2016. Reappraising the Neoproterozoic "East Avalonian" terranes of southern Great Britain. Gondwana Res. 35, 257–271. doi:10.1016/j.gr.2015.06.001

Soper, N.J., Hutton, D.H.W., 1984. Late Caledonian sinistral displacements in Britain: Implication for a three-plate model. Tectonics 3, 781–794.

Soper, N.J., Woodcock, N.H., 2003. The lost Lower Old Red Sandstone of England and Wales : a record of post-Iapetan flexure or Early Devonian transtension? Geol. Mag. 140, 627–647. doi:10.1017/S0016756803008380

Stacey, J.S., Kramers, J.D., 1975. Approximation of terrestrial lead isotope evolution by a two-stage model. Earth Planet. Sci. Lett. 26, 207–221. doi:10.1016/0012-821X(75)90088-6

Strachan, R.., 2008. Early Earth history and the development of the Archaean crust, in: Woodcock, N., Strachan, R. (Eds.), Geological History of Britain and Ireland. Blackwell Science Ltd., Oxford, pp. 41–51.

Strachan, R.A., Collins, A.S., Buchan, C., Nance, R.D., Murphy, J.B.,

D'Lemos, R.S., 2007. Terrane analysis along a Neoproterozoic active margin of Gondwana: insights from U-Pb zircon geochronology. J. Geol. Soc. London 164, 57–60.

Strachan, R.A., Prave, A.R., Kirkland, C.L., Storey, C.D., 2013. U–Pb detrital zircon geochronology of the Dalradian Supergroup, Shetland Islands, Scotland: implications for regional correlations and Neoproterozoic–Palaeozoic basin development. J. Geol. Soc. London. 170, 905–916. doi:10.1144/jgs2013-057

Thompson, M.D., Barr, S.M., Grunow, A.M., 2012. Avalonian perspectives on Neoproterozoic paleogeography: Evidence from Sm-Nd isotope geochemistry and detrital zircon geochronology in SE New England, USA. Bull. Geol. Soc. Am. 124, 517–531. doi:10.1130/B30529.1

Thompson, M.D., Bowring, S.A., 2000. Age of the Squantum "Tillite," Boston Basin, Massachusetts: U-Pb zircon constraints on terminal Neoproterozoic glaciation. Am. J. Sci. 300, 630–655. doi:10.2475/ajs.300.8.630

Thomson, S.N., Gehrels, G.E., Ruiz, J., Buchwaldt, R., 2012. Routine low-damage apatite U-Pb dating using laser ablation-multicollector-ICPMS. Geochemistry, Geophys. Geosystems 13. doi:10.1029/2011GC003928

Todd, S., 1989. Role of the Dingle Bay Lineament in the evolution of the Old Red Sandstone of southwest Ireland, in: Arthurton, R., Gutteridge, P., Nolan, S. (Eds.), The Role of Tectonics in Devonian and Carboniferous Sedimentation in the British Isles. The Yorkshire Geological Society, Bradford, pp. 35–54.

Todd, S.P., 2015. Structure of the Dingle Peninsula, SW Ireland: evidence for the nature and timing of Caledonian, Acadian and Variscan tectonics. Geol. Mag. 152, 242–268. doi:10.1017/S0016756814000260

Todd, S.P., 2000. Taking the roof off a suture zone: basin setting and provenance of conglomerates in the ORS Dingle Basin of SW Ireland. Geol. Soc. London, Spec. Publ. 180, 185–222. doi:10.1144/GSL.SP.2000.180.01.10

Todd, S.P., Connery, C., Higgs, K.T., Murphy, F.C., 2000. An Early Ordovician age for the Annascaul Formation of the SE Dingle Peninsula, SW Ireland.

J. Geol. Soc. London. 157, 823–833. doi:10.1144/jgs.157.4.823

Todd, S.P., Murphy, F.C., Kennan, P.S., 1991. On the trace of the Iapetus suture in Ireland and Britain. J. Geol. Soc. London 148, 869–880.

Todd, S.P., Williams, B.P.J., Hancock, P.L., 1988. Lithostratigraphy and structure of the Old Red Sandstone of the Northern Dingle Peninsula, Co. Kerry, southwest Ireland. Geol. J. 23, 107–120.

Tyrrell, S., Haughton, P.D.W., Daly, J.S., 2007. Drainage reorganization during breakup of Pangea revealed by in-situ Pb isotopic analysis of detrital K-feldspar. Geology 35, 971–974. doi:10.1130/G4123A.1

Van Der Voo, R., 1988. Paleozoic paleogeography of North America, Gondwana, and intervening displaced terranes: Comparisons of paleomagnetism with paleoclimatology and biogeographical patterns. Geol. Soc. Am. Bull. 100, 311–324.

Van Der Voo, R., 1983. Paleomagnetic constraints on the assembly of the Old Red Continent. Tectonophysics 91, 271–283.

Van Staal, C.R., Dewey, J.F., Niocaill, C.M., McKerrow, W.S., 1998. The Cambrian-Silurian tectonic evolution of the northern Appalachians and British Caledonides: history of a complex, west and southwest Pacific-type segment of Iapetus. Geol. Soc. London, Spec. Publ. 143, 197–242. doi:10.1144/GSL.SP.1998.143.01.17

Van Staal, C.R., Sullivan, R.W., Whalen, J.B., 1996. Provenance and tectonic history of the Gander Zone in the Caledonian/Appalachian orogen: Implications for the origin and assembly of Avalon. Geol. Soc. Am. Spec. Pap. 304, 347–367.

Vermeesch, P., 2013. Multi-sample comparison of detrital age distributions. Chem. Geol. 341, 140–146. doi:10.1016/j.chemgeo.2013.01.010

Vermeesch, P., 2012. On the visualisation of detrital age distributions. Chem. Geol. 312–313, 190–194. doi:10.1016/j.chemgeo.2013.01.010

Vermeesch, P., Resentini, A., Garzanti, E., 2016. An R package for statistical provenance analysis. Sediment. Geol. 336, 14–25. doi:10.1016/j.sedgeo.2016.01.009

Vermeulen, N.J., Shannon, P.M., Masson, F., Landes, M., 2000. Wide-angle seismic control on the development of the Munster Basin, SW Ireland.

Geol. Soc. London, Spec. Publ. 180, 223–237. doi:10.1144/GSL.SP.2000.180.01.11

Waldron, J.W.F., Floyd, J.D., Simonetti, A., Heaman, L.M., 2008. Ancient Laurentian detrital zircon in the closing Iapetus ocean, Southern Uplands terrane, Scotland. Geology 36, 527–530. doi:10.1130/G24763A.1

Waldron, J.W.F., Schofield, D.I., Dufrane, S.A., Floyd, J.D., Crowley, Q.G., Simonetti, A., Dokken, R.J., Pothier, H.D., 2014. Ganderia-Laurentia collision in the Caledonides of Great Britain and Ireland. J. Geol. Soc. London. 171, 555–569. doi:10.1144/jgs2013-131

Waldron, J.W.F., Schofield, D.I., White, C.E., Barr, S.M., 2011. Cambrian successions of the Meguma Terrane, Nova Scotia, and Harlech Dome, North Wales : dispersed fragments of a peri-Gondwanan basin? J. Geol. Soc. London. 168, 83–98. doi:10.1144/0016-76492010-068.Cambrian

Waldron, J.W.F., White, C.E., Barr, S.M., Simonetti, A., Heaman, L.M., 2009. Provenance of the Meguma terrane, Nova Scotia: rifted margin of early Paleozoic Gondwana. Can. J. Earth Sci. 46, 1–8. doi:10.1139/E09-004

Wetherill, G., 1956. Discordant Uraniam-Lead Ages, I. Trans. Am. Geophys. Union 37, 320–326.

White, C.E., Palacios, T., Jensen, S., Barr, S.M., 2012. Cambrian-Ordovician acritarchs in the Meguma terrane, Nova Scotia, Canada: Resolution of early Paleozoic stratigraphy and implications for paleogeography. Bull. Geol. Soc. Am. 124, 1773–1792. doi:10.1130/B30638.1

Williams, E.A., 2000. Flexural cantilever models of extensional subsidence in the Munster Basin (SW Ireland) and Old Red Sandstone fluvial dispersal systems. Geol. Soc. London, Spec. Publ. 180, 239–268. doi:10.1144/GSL.SP.2000.180.01.12

Williams, E.A., Sergeev, S.A., Stossel, I., Ford, M., Higgs, K.T., 2000. U-Pb zircon geochronology of silicic tuffs and chronostratigraphy of the earliest Old Red Sandstone in the Munster Basin, SW Ireland. Geol. Soc. London, Spec. Publ. 180, 269–302. doi:10.1144/GSL.SP.2000.180.01.13

Williams, E.A., Sergeev, S.A., Stossel, I., Ford, M., Higgs, K.T., 1999. U-Pb Zircon Geochronology of Silicic Tuffs from the Old Red Sandstone of the Dingle and Munster Basins (SW Ireland): Refining the Devonian Time

Scale. EUG J. Conf. Abstr. 4.

Willner, A.P., Barr, S.M., Gerdes, A., Massonne, H.-J., White, C.E., 2013. Origin and evolution of Avalonia: evidence from U–Pb and Lu–Hf isotopes in zircon from the Mira terrane, Canada, and the Stavelot–Venn Massif, Belgium. J. Geol. Soc. 170, 769–784. doi:10.1144/jgs2012-152

Willner, A.P., Gerdes, A., Massonne, H.-J., Van Staal, C.R., Zagorevski, A., 2014. Crustal evolution of the Northeast Laurentian Margin and the Peri-Gondwanan Microcontinent Ganderia Prior to and During Closure of the Iapetus Ocean: Detrital Zircon U-Pb and Hf Isotope Evidence from Newfoundland. Geosci. Canada 41, 345–364.

Woodcock, N.H., 2012. Ordovician Volcanism and Sedimentation on Eastern Avalonia, in: Woodcock, N.H., Strachan, R.A. (Eds.), Geological History of Britain and Ireland. Blackwell Publishing Ltd., pp. 162–176.

Zattin, M., Andreucci, B., Thomson, S.N., Reiners, P.W., Talarico, F.M., 2012. New constraints on the provenance of the ANDRILL AND-2A succession (western Ross Sea, Antarctica) from apatite triple dating. Geochemistry, Geophys. Geosystems 13. doi:10.1029/2012GC004357

3 Sedimentary provenance of the Devonian Old Red Sandstone in southern Ireland: a multi-proxy investigation into the role of sediment recycling.

(Current manuscript status: in prep. for Basin Research)

Brenton J. Fairey[a], Aidan Kerrison[a], Patrick A. Meere[a], Kieran F. Mulchrone[b], Mandy Hofmann[c], Andreas Gärtner[c], Benita-Lisette Sonntag[c], Ulf Linnemann[c], Klaudia F. Kuiper[d], Meg Ennis[a], Chris Mark[e], Nathan Cogné[e] and David Chew[e].

[a]School of Biological, Earth and Environmental Sciences, University College Cork, Cork, Ireland.

[b]School of Applied Mathematics, University College Cork, Cork, Ireland

[c]Senckenberg Naturhistorische Sammlungen Dresden, Museum für Mineralogie und Geologie, Königsbrücker Landstraße 159, D-01109 Dresden, Germany.

[d]Faculty of Earth Sciences, De Boelelaan 1085, NL-1081 HV Amsterdam, The Netherlands.

[e]Department of Geology, Museum Building, Trinity College Dublin, Dublin 2, Ireland.

Abstract

The Devonian Old Red Sandstone (ORS) magnafacies of southern Ireland is hosted in the Lower Devonian Dingle Basin and the Upper Devonian Munster Basin. Following the closure of the Iapetus Ocean during the long-lived Caledonian Orogeny, the Dingle Basin developed as a pull-apart structure before being deformed by Acadian tectonic activity. The Munster Basin developed as a half-graben structure in response to post-Acadian N-S extension in the region. Thus the ORS in Ireland provides important insights into the tectonic history of the region due to its temporal and spatial proximity to the Caledonian (~470-420 Ma), Acadian (~410-390 Ma) and Variscan orogenic events (~390-290 Ma). A multi-proxy geochronological approach is taken to unravel the depositional history of the ORS in terms of sedimentary provenance and to assess the possible role of sedimentary recycling in basin development, utilising detrital zircon U-Th-Pb, detrital mica ^{40}Ar-^{39}Ar and detrital apatite U-Pb geochronology. The majority of Upper ORS (UORS)

samples contain very few late Neoproterozoic grains and are instead dominated by early Palaeozoic and ca. 1.1 Ga zircons. These detrital zircon age distributions represent recycling of northerly-derived Ordovician to Silurian strata of the Southern Uplands – Longford Down terrane which are of Laurentian affinity, and not recycling of Lower ORS (which contain a significant number of late Neoproterozoic detrital zircons) as previously suggested. The western South Munster Basin, which represent the transition from terrestrial ORS to Carboniferous marine environments, is dominated by zircons of Acadian (410-390 Ma) age as well as late Neoproterozoic zircons, suggesting a western offshore Acadian igneous source. Clastic rocks of the eastern South Munster Basin have a Laurentian provenance like that of the underlying UORS. The Late Caledonian to Acadian ages of detrital apatites and micas in the ORS of southern Ireland, which are not apparent in the detrital zircon record, highlights the importance of a multi-proxy approach to sedimentary provenance analysis.

3.1 Introduction

The Devonian Old Red Sandstone (ORS) in Ireland and Britain has the potential to record a wealth of information regarding the Palaeozoic tectonic history of the region, given that it is chronostratigraphically placed between two mountain building events, namely the Caledonian and Variscan Orogenies. The Caledonian Orogeny in Scotland and Ireland consists of three phases (Chew and Strachan, 2014): the Grampian (475-465 Ma), the Scandian (435-425 Ma) and the Acadian (395 Ma). In terms of potential sources, we refer to felsic plutonism of 435-420 Ma age as ‘Late Caledonian’ and that of 410-390 Ma age as ‘Acadian’.

Soper and Woodcock (2003) determined that an extensive Lower ORS (LORS) succession accumulated across England and Wales during a period (ca. 420-400 Ma) of sinistral transtension (Dewey and Strachan, 2003) following the closure of the Iapetus Ocean and associated Caledonian orogenesis. They postulated that the majority of this sediment was recycled into Upper ORS (UORS) basins as a result of uplift by the short-lived Acadian Orogeny. Recent work by Ennis et al. (2015) has suggested that sediments from the Lower Old Red Sandstone (LORS) in southern Ireland, preserved

today in the Lower-Middle Devonian Dingle Basin, had been recycled into the UORS of the Middle-Upper Devonian Munster Basin in a similar fashion to the LORS of England and Wales. However, Fairey et al. (2018) showed that the LORS of the Dingle Basin contained late Neoproterozoic detrital zircons and that the UORS on the Dingle Peninsula was devoid of grains of this age. Thus they concluded that recycling of LORS into the UORS did not take place. This laid the foundation for a rigorous investigation of the provenance of the Munster Basin and the role played by orogenic drivers and sedimentary recycling.

The aim of this paper is to present the first detrital zircon and apatite geochronological data, and additional detrital mica geochronological data, for the Upper Devonian Old Red Sandstone as well as early Carboniferous (Tournaisian) sedimentary rocks of the Munster and South Munster basins in southern Ireland. In so doing, the paper utilises a multi-technique approach of coupling detrital zircon U-Pb with detrital mica $^{40}Ar/^{39}Ar$, and detrital apatite U-Pb geochronological data to elucidate the sedimentary provenance of the UORS in southern Ireland and evaluate the role of Palaeozoic orogenic events in recycling of sediments into the Munster Basin. We demonstrate that such a multiproxy approach is a necessity when dealing with the possibility of large-scale sedimentary recycling.

The southern British Isles occupy an area in which the relative positions, areal extent, and even existence, of a number of peri-Gondwanan terranes remains a contentious issue. While some authors consider the lower crust south of the Iapetus Suture in Ireland to be a part of Avalonia, others now consider this to be an extension of Ganderia (Waldron et al., 2014) – a view which is shared in this paper. Recent work has also provided evidence that a ‘Megumia’ domain may also occur in Britain. Waldron et al. (2011) and Nance et al. (2015) suggest that the Harlech Dome area of Wales has a number of Meguma-like characteristics.

3.2 Regional Geology

The UORS in southern Ireland rests upon Ganderian basement which includes the Cambrian to Ordovician rocks of the Leinster Massif (Waldron et al., 2014). To the north, this basement is bound by the Iapetus Suture Zone

beyond which lie the peri-Laurentian rocks accreted to the margin of Laurentia during the Ordovician to Silurian Caledonian Orogeny (Chew and Strachan, 2014). The basement below offshore Devonian rocks is not known but potential southern sediment sources include Avalonia and/or Megumia. Fairey et al (2018) provide a detailed review of the regional setting of the ORS in southern Ireland and expand upon the complexities of terrane associations in the region. Existing detrital zircon age spectra of potential source terranes are provided for reference (Figure 3–1).

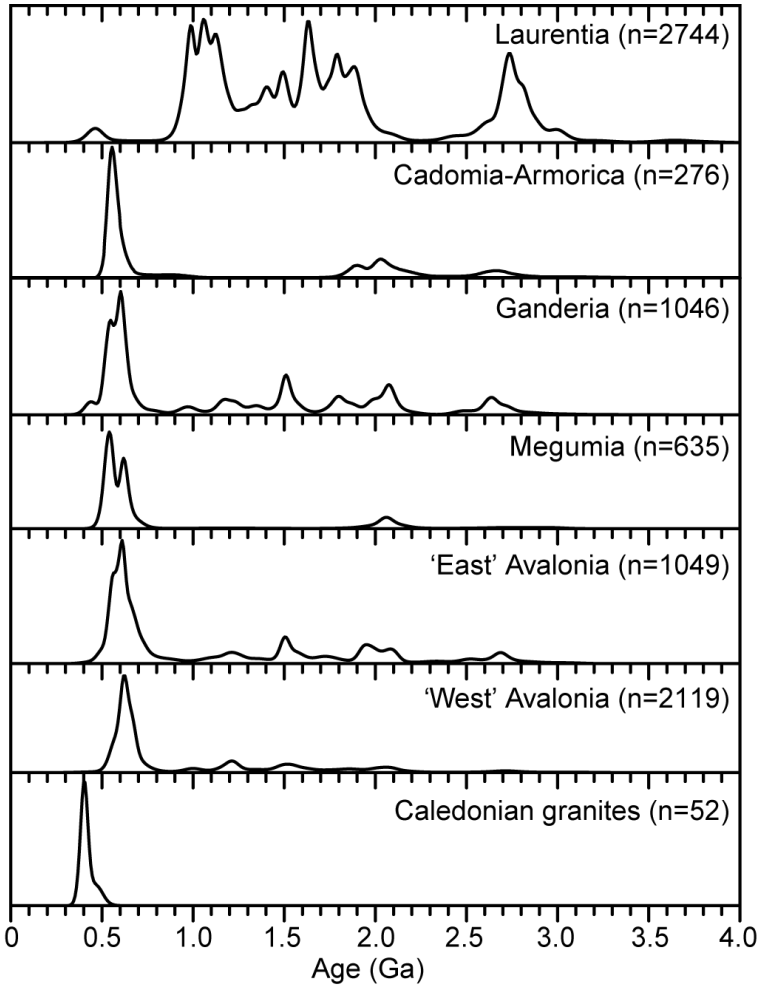

Figure 3–1. Detrital zircon age kernel density estimation (KDE) plots for potential source domains (after Fairey et al. 2018 and references therein).

3.3 Local Geology and Sample Location

The bulk of the UORS in Ireland is preserved in the Munster Basin in the southern part of the island. The sedimentary and volcanic successions that

represent the UORS magnafacies of the Munster Basin were deposited from the earliest late Givetian to early Carboniferous times in an interval that lasted at least ca. 23 Ma (Williams et al., 2000). The base of the UORS in the Munster Basin is not exposed between the Iveragh and Beara Peninsulas, where the sedimentary package is thickest (> 5.7 km, according to Williams et al., 2000) but it can be recognised in the eastern part of the basin, in the Galtee Mountains, as an exposed angular unconformity between Silurian pelitic rocks and the overlying UORS (Carruthers, 1987).

In a study of wide-angle seismic profiles across southern Ireland, Vermeulen et al. (2000) showed that the development of the Munster Basin was strongly influenced by pre-existing Caledonian structures, with the Killarney-Mallow Fault Zone (KMFZ) being the major bounding structure at the northern basin margin (Figure 3–2), although the Dingle Bay-Galtee Mountain Line (DBGML) has also been suggested (Williams et al., 1989; MacCarthy, 1990). The 1000 m isopach has often been regarded as the stratigraphic basin margin and is said to separate the thick intrabasin accumulations of UORS from overstepping successions (Williams et al., 1989). The southern boundary is not seen onshore and has not been delineated to date but extrapolation of the 1000 m isopach suggests that the basin does not extend far offshore (Vermeulen et al., 2000, and references therein). However, Williams (2000) proposed that the Munster Basin must extend for more than tens of kilometres offshore. The structural setting of the Munster Basin has been described as an intracontinental half-graben, with the hinge lying somewhere to the south (e.g. Williams et al., 1989; MacCarthy, 1990; see Williams, 2000 for an alternative model). Subsidence in the southern parts was accommodated by the Dunmanus-Castletown Fault (DCF) (Williams et al., 1989). Vermeulen et al. (2000) suggested that the UORS accumulations in the Munster Basin were predominantly accommodated by N-S extension along listric faults of the KMFZ and Cork-Kenmare Line (CKL), with later contribution from the north-dipping DCF in the southern part of the basin. Extension along the northern basin margin was not uniform - subsidence was greater in the west than in the east - this is reflected in the western position of the depocenter, between the Beara and Iveragh peninsulas (MacCarthy, 1990).

Models for the development of the UORS in the Munster Basin (e.g. Williams et al., 1989; MacCarthy, 1990; Williams, 2000) show that depositional systems may have developed independently in the west and east. In the western part of the basin, two dominant syn-rift phases of fluvial influx are recognised by Williams et al. (1989). The first influx involved the development of an approximately NNE-SSW-draining fan-like system that is represented by the Glenflesk Chloritic Sandstone Formation (proximal) and the Gortanimill and Slaheny Formations (distal) (Figure 3–2, section A-B). Pb-Pb zircon dating of volcanic horizons within the Glenflesk Chloritic Sandstone Formation yielded ages between 385 and 378 Ma (mid-Frasnian to early Givetian), suggesting that the oldest formations, the Valentia Slate and Bird Hill Formations, are likely to have been deposited at the latest during early Givetian times (Williams et al., 2000). The St. Finans Sandstone Formation predominantly crops out on the Iveragh Peninsula and is considered coeval to the Glenflesk Chloritic Sandstone Formation (Williams et al., 1989; MacCarthy, 1990). Carruthers (1985) suggested that the Slievenamuck Conglomerate Formation of the Galtee Mountains succession (Figure 3–2, section C-D) may also be coeval with the Glenflesk Chloritic Sandstone Formation and other correlatives. The gravel braidplain environment of the Slievenamuck Formation has an overall north to south palaeocurrent thus indicating a northern sediment source (Carruthers, 1985).

The second fluvial influx, brought on by a second phase of syn-rift subsidence, involved a western fan system with NNE-SSW directed palaeoflow and an eastern fan system of similarly directed flow (Williams, 2000, and references therein). The western system is represented by the Gun Point Formation (Figure 3–2, section A-B) and the eastern system is represented by the Poulgrania Sandstone Formation (Figure 3–2, section C-D). The southerly limit of the northerly-derived fluvial influxes in the western part of the Munster Basin is marked by the DCF (Williams, 2000). To the south of this fault system, the Sherkin and Castlehaven Formations indicate west to east palaeoflow directions (Williams et al., 1989, and references therein). Williams (2000) suggests that these formations represent a separate fluvial system, areally unrelated to those of the Glenflesk Chloritic Sandstone and

Gun Point Formations. MacCarthy (1990), however, interprets this sudden change in palaeocurrent directions as an indication of merging between the northerly-derived and westerly-derived fluvial systems.

An important discovery of marine palynomorphs towards the base of the Sherkin Formation led Higgs et al. (2000) to conclude that a marine incursion occurred during mid-Frasnian times, and that it is possible that the southern limits of the Munster Basin, today obscured by the Atlantic Ocean and the Celtic Sea, had a marine connection throughout the Late Devonian.

A number of predominantly fine-grained sandstone and siltstone formations in the UORS in the Munster Basin have been termed 'background sedimentation' by Williams et al. (1989) and represent low-energy, unconfined deposition of sediments at the periphery of major fluvial distributary systems. Examples include the Castlehaven, Caha Mountain, Valentia Slate and Ballystrasna Formations and Nier Group (Facies Association D of MacCarthy, 1990). Widespread throughout the eastern part of the Munster Basin, and representing the top of the ORS in these areas, is the Kiltorcan Formation. It caps the Comeragh and Galtee Mountain successions (Figure 3–2, sections C-D and E-F) and is approximately coeval with the Toe Head Formation in south west Co. Cork (LE Biozone - Kiltorcan: Jarvis, 1990; Toe Head: Clayton and Higgs, 1979). MacCarthy (1990) suggests that the appearance of an abundance of feldspar in the Kiltorcan Formation, notably under-represented in underlying formations, represents the earliest unroofing of the Leinster Batholith.

Toward the top of the UORS succession in the south west part of the Munster Basin is the Toe Head Formation - this represents an early transition to marine conditions with tidal to shallow marine conditions represented by the conformably overlying Old Head Sandstone Formation (Williams et al., 1989). Finally, the Harrylock Formation occurs to the east of the eastern margin of the Munster Basin. It is considered to be partially coeval with the Kiltorcan Formation (Higgs et al., 1988). According to MacCarthy (1990), the Harrylock Formation represents a medial facies in a mature drainage system on the fringes of the eastern part of the Munster Basin. Carruthers (1985) considered the Harrylock Formation to be part of a sub-basin that was separated from the

Munster Basin as indicated by palaeoflow toward the southeast in the Knockavelish Member, Dunmore East.

Samples were collected from the UORS in the Munster Basin in such a way as to capture the variability in facies associations while attempting to maintain a wide spatial and temporal extent (stars in map and cross-sections in Figure 3–2). Naturally, this is limited to availability of suitable outcrop - the majority of samples, therefore, are from mountainous or coastal areas.

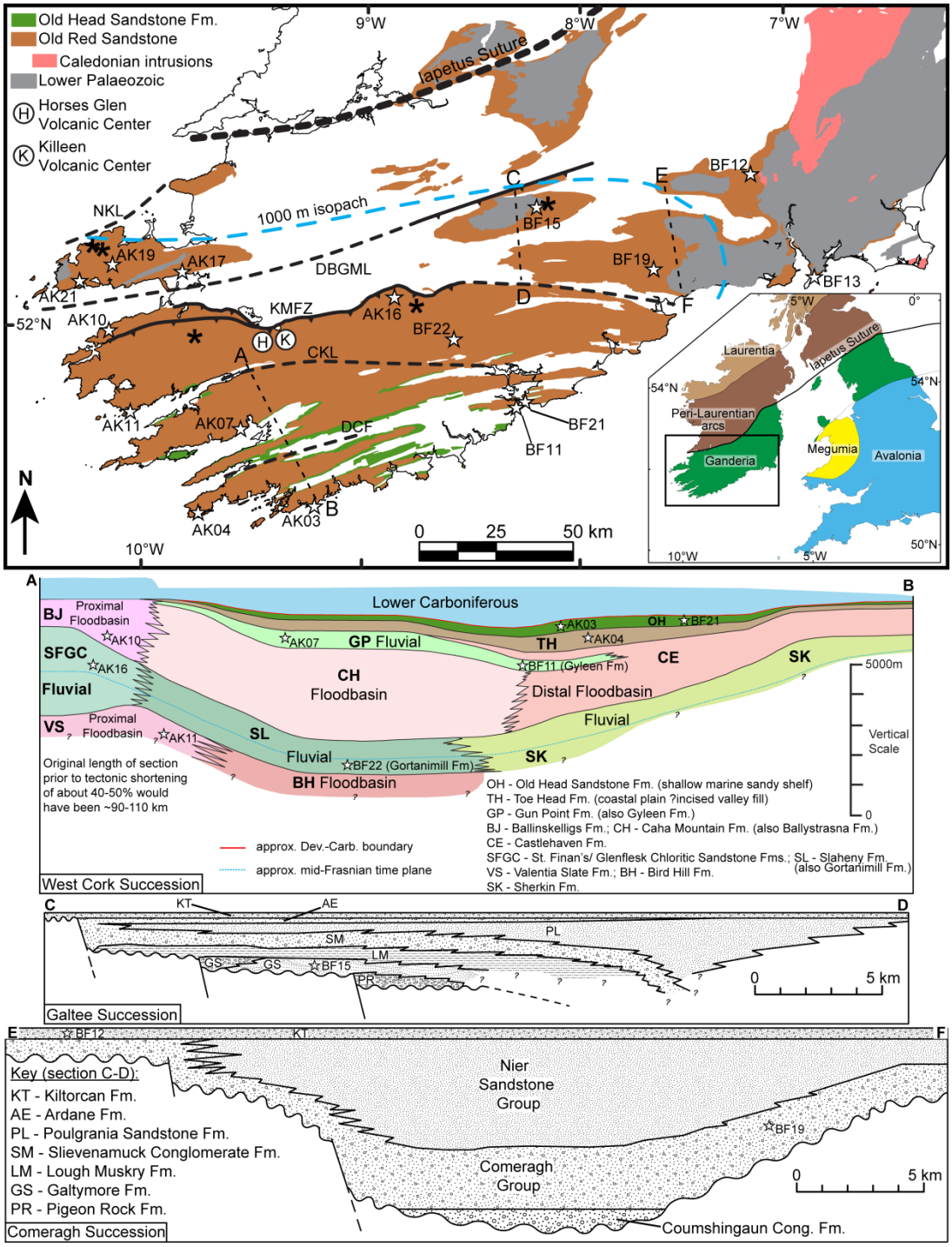

Figure 3–2: Generalised geological map of southern Ireland including idealised cross section for the western (A-B, modified after MacCarthy, 2007) and eastern (C-D, E-F, modified after Carruthers, 1985) Munster Basin. Stars indicate sample locations and approximate stratigraphic position. Asterisks represent detrital apatite sample sites (from west to east: [Mb-9]; [Mb-1, Mb-4, Mb-5, Mb-7]; [Ca-1, Ca-4, Ca-6, Ca-8, Ca-9]; [Bg-1]; [Ga-1, Ga-2, Ga-4]). Sections C-D and E-F are slightly vertically exaggerated. CKL, Cork-Kenmare Line; DBGML, Dingle Bay Galtee Mountain Line; DCF, Dunmanus-Castletown Fault; KMFZ, Killarney-Mallow Fault Zone; NKL, North Kerry Lineament. Faults and isopach modified after Vermeulen et al. (2000) and Carruthers (1987) respectively.

3.4 Post depositional history of the Munster Basin

When dealing with low-temperature geochronometers such as the white mica Ar-Ar system, where loss of argon can occur at temperatures as low as ca. 270°C (Snee et al., 1988) or as high as 450°C (Scharf et al., 2016), subject to variables including grain size and cooling rate, it is necessary to understand the post-depositional history of the basin from which the white micas were sampled. Post-depositional history is essentially irrelevant for zircon and less relevant for apatite given that considerable Pb diffusion in these minerals occurs at temperatures greater than 900°C (Cherniak and Watson, 2001) and 375°C (Cochrane et al., 2014) respectively.

In the case of the Munster Basin, post-depositional history is particularly important due to the potential effects of burial depth (at least 5 km in the depocenter, according to Williams et al., 2000) and the end-Carboniferous Variscan Orogeny, known to be responsible for basin inversion (Price and Todd, 1988). The development of a penetrative cleavage, buckling of the sedimentary strata and fault-reactivation in the central and western parts of the basin indicate the strong influence of the Variscan Orogeny in these areas (Meere and Banks, 1997). Cooper et al. (1986) argued that the Leinster Massif acted as a stable entity during the Variscan Orogeny, resulting in the waning of deformation toward the east. A study of illite crystallinity across the western part of the Munster Basin by Meere (1995) suggests that temperatures may have reached 325 °C as a result of extension before onset of Variscan deformation. Ennis et al. (2015) found that a number of detrital micas from the western part of the basin had ages that were younger than the depositional age of the sedimentary rock from which they were extracted. They suggested that these younger ages reflect a period of thermal rejuvenation of the micas during elevated temperature conditions following the onset of Variscan deformation.

3.5 Analytical procedures and sampling

3.5.1 Zircon U-Pb

Sample separation was undertaken at the Vrije Universiteit Amsterdam. Detrital zircons were liberated from samples using a jaw crusher and disc mill.

Separation was achieved using diiodomethane (density > 3.3 g/cm^3) in a centrifuge as per IJlst (1973) and magnetic separation using a Frantz magnetic separator. Zircons of all morphology and colour, between 60 and 250 µm, were hand-picked under a binocular microscope. Typically, between 120 and 180 zircons per sample were mounted in epoxy disks and ground and polished to expose the approximate center of the grains. Cathodoluminescence (CL) imaging was undertaken at the University of St. Andrews and at Trinity College Dublin in order to identify optimal positions for laser ablation.

U, Th and Pb isotopes were measured by LA-SF-ICP-MS at the Museum für Mineralogie und Geologie (Geoplasma Lab, Senckenberg Naturhistorische Sammlungen Dresden). Further details of laser and ICP-MS parameters, as well as data reduction protocols, can be found in Linnemann et al. (2014) and references therein. Data was reduced using a Microsoft Excel spreadsheet program developed by Axel Gerdes (Institute of Geosciences, Johann Wolfgang Geothe-University Frankfurt). Concordia diagrams and concordia ages were produced using Isoplot/Ex 3.7 of Ludwig (2012). Histograms and kernel density estimation (KDE) curves were plotted using DensityPlotter (Vermeesch, 2012). Histograms were assigned a binwidth of 25 Ma. KDEs were plotted using a bandwidth of 20 Ma and a Gaussian kernel. Multi-dimensional scaling (MDS) plots were constructed using the 'provenance' package of Vermeesch et al. (2016).

3.5.2 White mica Ar-Ar

For white micas, a grain size range of 200 µm to 500 µm was used for separation. Mica-rich samples were processed using a vibrating table. Mica-poor samples were processed on the vibrating table and further separated by density using diiodomethane (density of 2.78 g/cm^3) in a centrifuge. Magnetic separation was undertaken only where abundant impurities were observed, otherwise inclusion- and impurity-free micas were hand-picked under binocular microscope.

Three white mica samples were irradiated together with Fish Canyon sanidine (FCs) for 18 hours at the Oregon State University TRIGA reactor in the cadmium shielded CLICIT facility. $^{40}Ar/^{39}Ar$ analyses were performed at the geochronology laboratory of the VU University on a Helix MC noble gas

mass spectrometer. Single mica grains were fused with a Synrad CO_2 laser beam and released gas was exposed to NP10 and St172 getters and analyzed on the Helix MC. The five argon isotopes were measured simultaneously with ^{40}Ar on the H2-Faraday position with a 10^{13} Ω resistor amplifier, ^{39}Ar on the H1-Faraday with a 10^{13} Ω resistor amplifier, ^{38}Ar on the AX-CDD, ^{37}Ar on the L1-CDD and ^{36}Ar on the L2-CDD (CDD – Compact Discrete Dynode). Gain calibration for the CDDs is done by peak jumping a CO_2 reference beam on all detectors in dynamic mode. All intensities are corrected relative to the L2 detector. Air pipettes are run every ten hours and are used for mass discrimination corrections. The atmospheric air value of 298.56 from Lee et al. (2006) is used. Detailed analytical procedures for the Helix MC are described in Monster (2016). The calibration model of Kuiper et al. (2008) with FCs of 28.201 ± 0.046 Ma and decay constants of Min et al. (2000) are used in age calculations. The correction factors for neutron interference reactions are (2.64 ± 0.02) $x10^{-4}$ for $(^{36}Ar/^{37}Ar)_{Ca}$, (6.73 ± 0.04) $x10^{-4}$ for $(^{39}Ar/^{37}Ar)_{Ca}$, (1.21 ± 0.003) $x10^{-2}$ for $(^{38}Ar/^{39}Ar)_{K}$ and (8.6 ± 0.7) $x10^{-4}$ for $(^{40}Ar/^{39}Ar)_{K}$. All errors are quoted at the 1σ level and include all analytical errors. Relevant analytical data for age calculations can be found in the online supplementary material.

As in Fairey et al. (2018), in order to facilitate a direct comparison with our results, detrital white mica Ar-Ar ages from Ennis et al. (2015) are recalculated in this study using the 28.201 ± 0.046 Ma age of Kuiper et al. (2008) for the Fish Canyon sanidine standard, generally increasing the age of individual grains from those samples by ca. 1 %, approximately 4 Ma.

3.5.3 Apatite U-Pb

At each outcrop, ~10 kg of material was collected across several adjacent beds to reduce any bias arising during deposition from localized heavy mineral concentrating processes. Subsequent sample preparation and analysis were conducted at Trinity College Dublin. The sub–300 μm nonmagnetic heavy mineral fraction was obtained by standard jaw crushing, sieving, magnetic, and heavy liquid separation techniques. Grains were mounted in epoxy resin, ground to expose internal surfaces, and polished. To avoid sample bias, no attempt was made to exclude anhedral or inclusion-bearing grains; the laser ablation-inductively coupled plasma-mass spectrometer (LA-ICP-MS)

technique permits identification and exclusion of U-rich inclusions (e.g., zircon) from the time-resolved (i.e., downhole) ablation signal of the appropriate isotopes.

Analyses were conducted using a Photon Machines Analyte Excite 193 nm ArF Excimer laser ablation system coupled to a Thermo Scientific iCAP Qc ICPMS, employing laser spots of 30 µm, a fluence of 4.5 J cm^{-2}, a repetition rate of 5 Hz, and an ablation time for each spot of 45 s followed by a 25 s background measurement. Repeated measurements of the primary Madagascar apatite mineral standard (Thomson et al., 2012) were used to correct for downhole U-Pb fractionation, mass bias, and intrasession instrument drift using the "VizualAge_UcomPbine" data reduction scheme for IOLITE (Chew et al., 2014; Paton et al., 2011), while the secondary McClure Mountain and Durango apatite standards were analysed as unknowns (Schoene and Bowring, 2006; McDowell et al., 2005). Unlike phases that exclude common (initial or non-radiogenic) Pb during crystallization, such as zircon, the often high common-Pb content in apatite typically renders apatite grains discordant in the U-Pb system. Common-Pb in the Madagascar apatite primary standard was corrected for using a ^{207}Pb-based correction method using a known initial $^{207}Pb/^{206}Pb$ ratio (Chew et al., 2014). Variable common-Pb content in the detrital apatite unknowns was corrected using an initial common-Pb composition derived from a terrestrial Pb evolution model (Stacey and Kramers, 1975) applied to an initial estimate for the age of the apatite, and then adopting an iterative approach based on a ^{207}Pb correction (Chew et al., 2011). The ^{207}Pb-based correction assumes U-Pb* (radiogenic Pb) concordance – a reasonable assumption in the case of standards and magmatic grains, but one which may not be the case for detrital grains that have experienced partial Pb loss. As a result, independent geological evidence is required to discriminate between partially and wholly reset detrital U-Pb ages, similar to partially reset apatite fission track (AFT) ages.

Due to the ^{207}Pb-based correction, no apatite U-Pb age data can be excluded based on discordance criteria. However, the relatively low U content of apatite (sometimes <1 ppm) and consequent near-zero radiogenic Pb content of some grains can result in undesirably large analytical uncertainties.

We therefore excluded grains with 2σ errors >25%, similar to the approach of Zattin et al. (2012). These apatite U-Pb data were originally generated as part of a bedrock thermal history study utilising the AFT low-temperature thermochronometer (Cogné et al., 2016, 2014), because the LA-ICPMS approach to AFT analysis permits U-Pb and AFT ages to be determined on the same grains during a single analytical session (Chew and Donelick, 2012). As post-deposition temperatures exceeded the thermal sensitivity of the AFT technique (ca. 120-60 °C; e.g., Gallagher et al., 1998), the resultant AFT ages typically defined a single population for each sample. Thus, only ca. 20-30 grains were analysed for each sample.

3.6 Detrital zircon U-Th-Pb results

The study aimed to meet the statistical requirements of Vermeesch (2004) of at least 117 analysed grains per sample. In the UORS of the Munster and South Munster Basins, a total of 1886 detrital zircon grains yielded 1493 concordant and precise ages. U-Pb and Pb-Pb ages reported here are within 90% and 110% (inclusive) concordance and are analytically precise to within 10% (2σ). In most samples, this filtering, particularly for concordance, greatly reduced the number of usable analyses but in all cases populations of greater than eight percent can be detected with 95 % confidence.

Age uncertainties reported in the text are at the 2σ level unless otherwise stated. Core-rim analyses were undertaken where these features could be identified in CL images and where grains were large enough. Only rim ages are used for provenance interpretations in order to determine the most recent source of sediment. The results are presented as Wetherill concordia diagrams (Figure 3–3) and frequency and KDE plots (Figure 3–4). The data are presented in order of known stratigraphic age. The $^{207}Pb/^{206}Pb$ age is reported where the $^{206}Pb/^{238}U$ age is greater than 1.0 Ga because the $^{207}Pb/^{206}Pb$ age is more precise in older zircon grains (e.g. Gehrels et al., 2008).

3.6.1 Valentia Slate Formation - Sample AK11

This sample was taken from just east of Rath Strand on the south east coast of the Iveragh Peninsula and consists of medium-grained sandstone.

One hundred and seventy analyses of zircons from this sample yielded 141 concordant ages ranging from 401 ± 5 Ma to 2764 ± 26 Ma (Figure 3–3A). The sample is dominated by Mesoproterozoic zircons which make up 52 % (n = 73) (Figure 3–4C). A major Mesoproterozoic peak occurs at ca. 1.05 Ga. Palaeozoic zircons constitute the second largest component in the sample at 24 % (n = 34). Another major peak occurs in the Palaeozoic at ca. 460 Ma. Cambrian (n = 11) and Ordovician (n = 17) zircons are dominant in the Palaeozoic portion. Five Silurian zircons and one Devonian zircon representing the rest of the population in this age range. Palaeoproterozoic and Neoproterozoic zircons make up 16 % (n = 22) and 7 % (n = 10) of the sample respectively. Two analyses produced Archaean ages. A distinct gap in zircon ages exists between ca. 550 Ma and ca. 950 Ma with the exception of a single zircon at 716 ± 10 Ma.

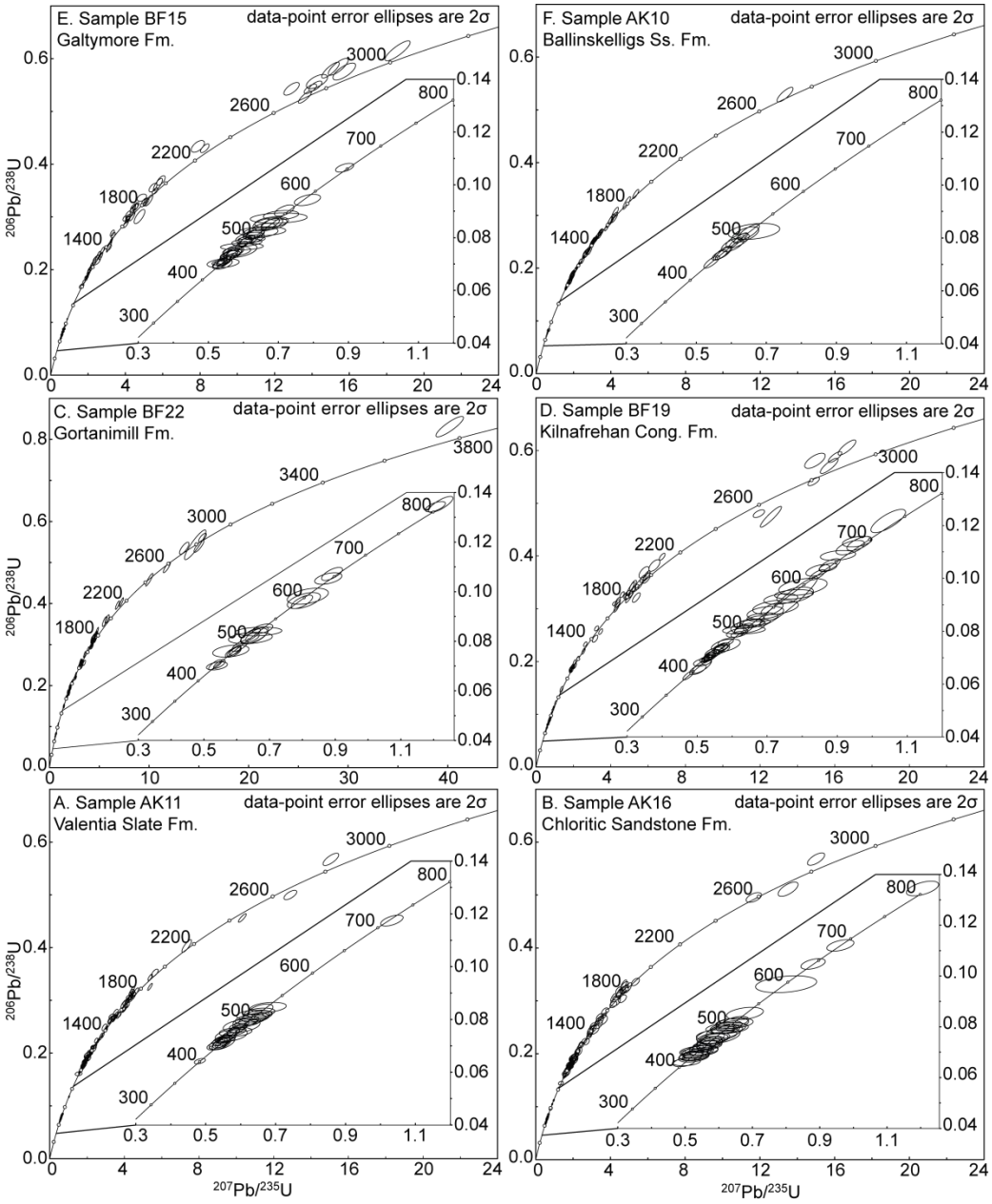

Figure 3–3. Wetherill concordia diagrams for the ORS in southern Ireland. **A**. Valentia Slate Formation (sample AK11). **B**. Chloritic Sandstone Formation (sample AK16). **C**. Gortanimill Formation (sample BF22). **D**. Kilnafrehan Conglomerate Formation (sample BF19). **E**. Galtymore Formation (sample BF15). **F**. Ballinskelligs Sandstone Formation (sample AK10). **G**. Gun Point Formation (sample AK07). **H**. Toe Head Formation (sample AK04). **I**. Gyleen Formation (sample BF11). **J**. Kiltorcan Formation (sample BF12). **K**. Western Old Head Sandstone Formation (sample AK03). **L**. Eastern Old Head Sandstone Formation (sample BF21). **M**. Harrylock Formation (Sample BF13). Data that are more than 10 % discordant and have greater than 10 % (2σ) analytical uncertainty are not shown.

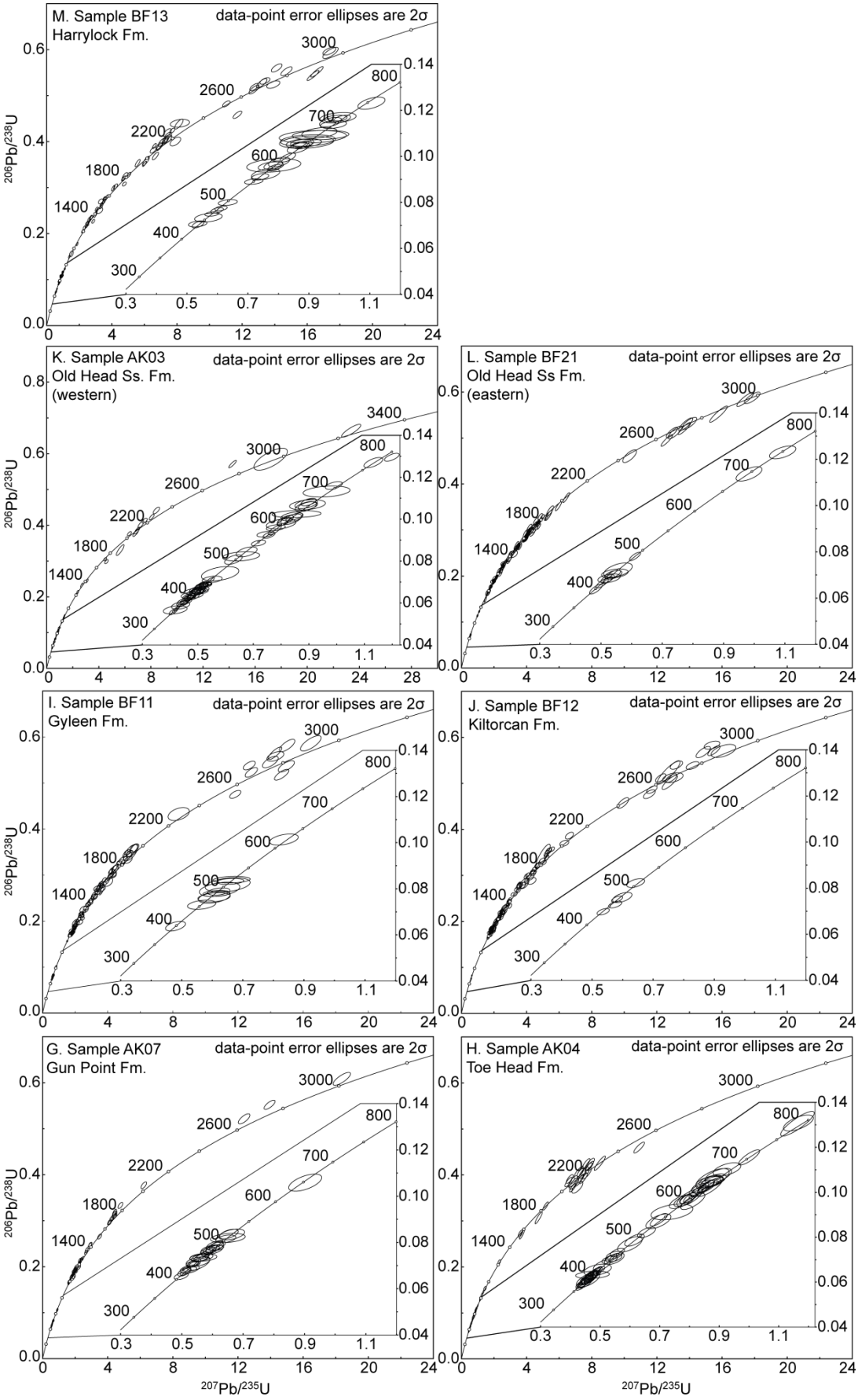

Figure 3–3 (continued)

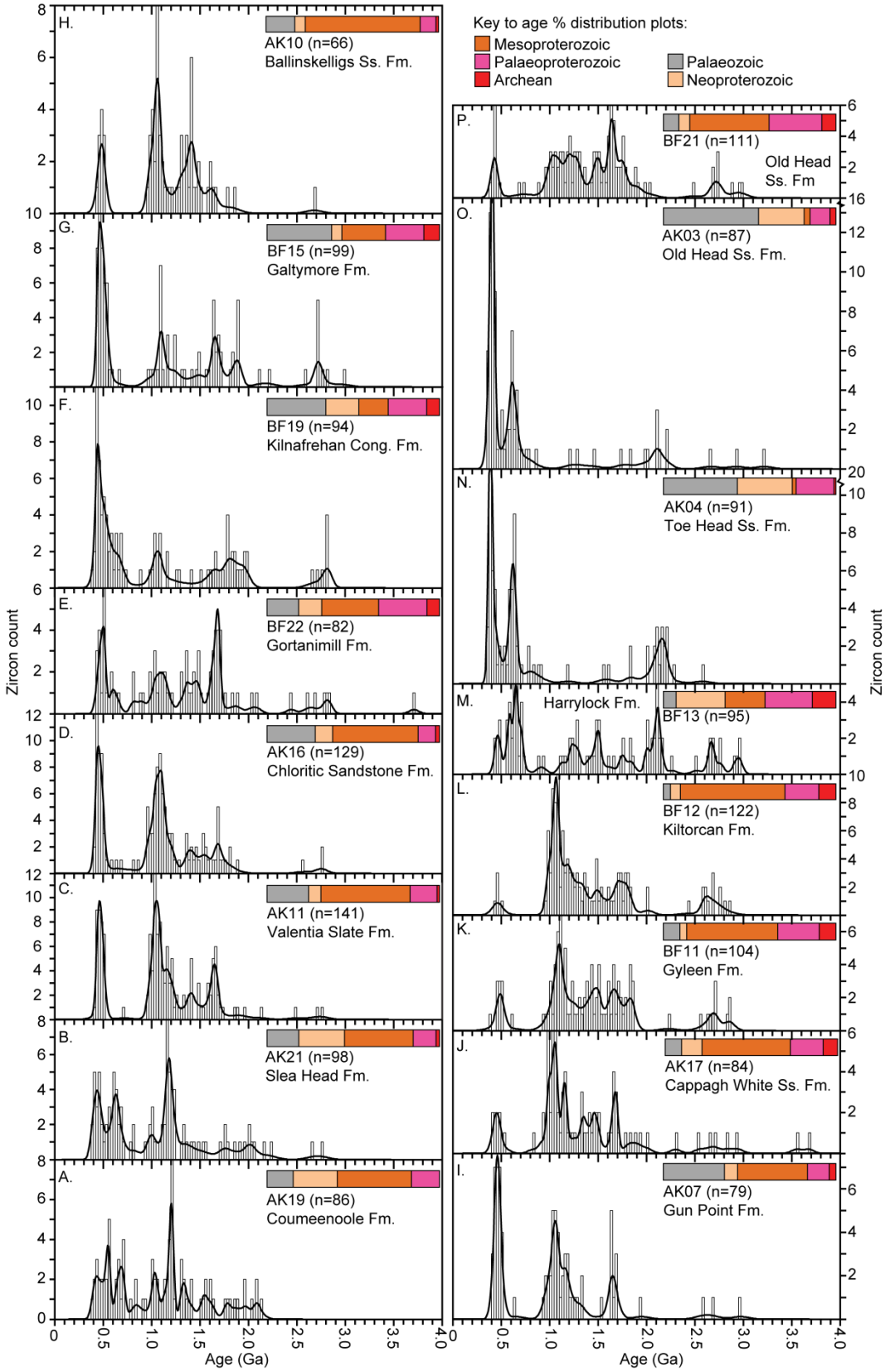

Figure 3–4. Histograms and area-normalised kernel density estimation curves as well as proportions (horizontal bars) of ages (as indicated in the legend) for detrital zircon samples in Dingle (**A**, **B**, **J**), Munster (**C**-**I**, **K**-**M**) and South Munster Basins (**N**-**P**). Data for samples AK19, AK21 and AK17 are taken from Fairey et al. (2018).

3.6.2 Chloritic Sandstone Formation - Sample AK16

This green, medium-grained sandstone was sampled from an abandoned quarry near Glenflesk. A range of ages between 412 ± 9 Ma and 2757 ± 40 Ma was obtained for 129 concordant analyses from 151 zircon grains (Figure 3–3B). The majority of zircon grains (n = 64; 50 %) are Mesoproterozoic in age and form a major peak occurring at ca. 1.09 Ga (Figure 3–4D). Thirty six zircons (28 %) are Palaeozoic in age forming the largest peak in the sample at ca. 450 Ma. Most Palaeozoic zircons are Cambrian, Ordovician or Silurian in age. Only two Devonian zircons are present. These give a concordia age of 413 ± 6 Ma ($MSWD_{conc}$ = 0.027; p_{conc} = 0.87). Equal proportions of Palaeoproterozoic and Neoproterozoic zircons occur in the sample, each representing 10 % (n = 13) of the total. The oldest zircon grains in the sample are represented by three Archaean grains. Two of these grains have an age of ca. 2756 Ma. Although some grains are scattered between ca. 550 Ma and ca. 950 Ma, a general paucity of detritus of this age is noted.

3.6.3 Gortanimill Formation - Sample BF22

This sample was taken from a road cutting on the N20, just west of Kilmona Cross. It consists of greenish grey, medium-grained, well sorted, micaceous sandstone. One hundred and fifty zircon grains in this sample yielded 82 concordant ages ranging from 437 ± 8 Ma to 3710 ± 21 Ma (Figure 3–3C). The majority of these ages (33 %; n = 27) are of Mesoproterozoic age (Figure 3–4E). The largest peak occurs close to the Palaeoproterozoic-Mesoproterozoic boundary at ca. 1.68 Ga. Minor Mesoproterozoic peaks are developed at ca. 1.1 Ga and 1.4 Ga. Palaeoproterozoic zircons form the second largest proportion in the sample at 28 % (n = 23). Fifteen zircons (18 %) are of Palaeozoic age and 11 (13 %) are Neoproterozoic in age. A large Palaeozoic peak occurs at ca. 500 Ma and is composed of Cambrian (n = 7), Ordovician (n = 5) and Silurian (n = 3) zircons. A small peak can be identified in the Neoproterozoic at ca. 600 Ma. Archaean grains form the remainder of the sample (n = 6). The three youngest grains yield a concordia age of 439 ± 5 Ma ($MSWD_{conc}$ = 0.016; p_{conc} = 0.90).

3.6.4 Kilnafrehan Conglomerate Formation (Comeragh Group) - Sample BF19

This grey, poorly-sorted, pebbly sandstone was taken from a road cutting in the Coumaraglin Mountain townland in Co. Waterford. One hundred and thirty eight grains were analysed from the sandstone matrix. One analysis per grain yielded a total of 94 concordant ages ranging from 396 ± 9 Ma to 2822 ± 23 Ma (Figure 3–3D). Thirty two zircons (34 %) are Palaeozoic in age and represent the largest proportion in the sample, forming a major peak at ca. 445 Ma (Figure 3–4F). This peak has a tail which extends into the Neoproterozoic. There are equal proportions of Ordovician and Silurian zircons in the sample at 10 % (n = 9) but the largest Palaeozoic contribution is made by Cambrian aged zircons (n = 11). Three grains are Devonian in age. The second largest contribution is made by Palaeoproterozoic zircons which make up 22 % (n = 21) of the sample. Mesoproterozoic and Neoproterozoic zircons make up 17 % (n = 16) and 19 % (n = 18) of the sample respectively. Seven zircons are Archaean in age, including three zircons with ages between 2820 Ma and 2823 Ma.

3.6.5 Galtymore Formation - Sample BF15

A pinkish orange, medium-grained, moderately sorted sandstone was sampled from the western cliff face at Lough Curra, Galtee Mountains. One hundred and forty eight zircons were analysed yielding a total of 99 concordant analyses (Figure 3–3E). Ages ranges from 436 ± 9 Ma to 2975 ± 26 Ma. Two zircons were suitable for core-rim analyses (Figure 3–5D-E). Palaeozoic aged zircons form the bulk of the sample (n = 37) with Cambrian (n = 17) and Ordovician (n = 14) zircons being particularly dominant (Figure 3–4G). Palaeozoic zircons form the largest peak in the sample at ca. 460 Ma. Mesoproterozoic zircons form 25 % (n = 25) of the sample. A paucity of zircons is recognised between ca. 550 Ma and ca. 950 Ma (n = 4), similar to that in samples AK11 and AK16. Palaeoproterozoic zircons make up 22 % (n = 22) of the sample and Neoproterozoic zircons make up 6 % (n = 6). Nine Archaean zircons are present. The six Silurian-aged zircons form a concordia age of 439 ± 3 Ma ($MSWD_{conc}$ = 0.12; p_{conc} = 0.73).

3.6.6 Ballinskelligs Sandstone Formation - Sample AK10

This sample was taken from Coonanna Beach, north east of Corrigower. Sixty six concordant analyses were obtained from 118 grains in this pinky purple, moderately sorted sandstone. Detrital zircon ages range from 442 ± 12 Ma to 2678 ± 26 Ma (Figure 3–3F). The sample is dominated by Mesoproterozoic zircons (n = 44; 67 %) which form a major peak at around 1.05 Ga (Figure 3–4H). Eleven Palaeozoic zircons constitute the second largest proportion in the sample at 17 %, forming a peak at ca. 480 Ma. These are predominantly Cambrian (n = 6) and Ordovician (n = 4) in age. Palaeoproterozoic zircons make up 9 % (n = 6) and Neoproterozoic zircons make up 6 % (n = 4). A single zircon of Archaean age is present in the sample. No zircons in this sample have ages between ca. 550 Ma and ca. 950 Ma.

3.6.7 Gun Point Formation - Sample AK07

This sample was taken from the road cutting opposite the lookout point on the R572 north east of Garinish West. It consists of medium-grained green sandstone. A total of 120 grains were analysed yielding 79 concordant ages ranging from 409 ± 8 Ma to 2974 ± 24 Ma (Figure 3–3G). The majority of grains (n = 32; 41 %) in this sample are of Mesoproterozoic age, forming a major peak at ca. 1.06 Ga (Figure 3–4I). The largest peak, however, is Palaeozoic in age (at ca. 460 Ma) and represents the second largest proportion of zircons in the sample (n = 28; 35 %). Of the Palaeozoic-aged zircons, six are Cambrian, 13 are Ordovician, seven are Silurian and two are Devonian in age. Palaeoproterozoic zircons make up 13 % (n = 10) and Neoproterozoic zircons make up 8 % (n = 6). Three Archaean zircons are present in the sample. A notable gap in zircon ages is seen between ca. 520 Ma and 940 Ma, with only one zircon occuring at ca. 650 Ma.

3.6.8 Toe Head Formation - Sample AK04

Taken from the western cliff of the isolated cove on the eastern side of Barley Cove Beach, this sample consists of grey, fine- to medium-grained sandstone. A total of 91 concordant ages were produced from analysis of 180 zircon grains (Figure 3–3H). These ages range from 363 ± 8 to 2579 ± 21 Ma with the largest proportion (n = 39; 43 %) of zircons being Palaeozoic in age

(Figure 3–4N). Twenty eight of these are of Devonian age. This is reflected in the largest peak in the sample at ca. 390 Ma. The second largest proportion of zircons in the sample are Neoproterozoic in age, representing 32 % (n = 29) of the sample and forming a peak at around 620 Ma. Palaeoproterozoic zircons make up 22 % (n = 20) of the sample with a significant peak at ca. 2.16 Ga. Two zircons are Mesoproterozoic in age. These are two of only three zircons that occur between ca. 920 Ma and ca. 1.8 Ga. One Archaean-aged zircon is present in the sample.

3.6.9 Gyleen Formation - Sample BF11

Sample BF11 consists of light grey, medium-grained, well-sorted sandstone. It was taken approximately 200 m north east of the entrance to Myrtleville Beach. One hundred and thirty seven zircon grains produced 104 concordant ages ranging from 399 ± 10 Ma to 2870 ± 26 Ma (Figure 3–3I). Fifty five (53 %) zircon grains have Mesoproterozoic ages, forming a major peak at ca. 1.1 Ga (Figure 3–4K). Palaeoproterozoic-aged zircons contribute 24 % (n = 25) of the sample. Equal proportions of Archaean and Palaeozoic zircons are present in the sample (n = 10). Cambrian (n = 5) and Ordovician (n = 4) zircons form the bulk of Palaeozoic zircons in the sample and the remaining grain is Devonian in age. Four zircons are of Neoproterozoic age. Only one zircon in this sample has an age that lies between ca. 520 Ma and ca. 920 Ma.

3.6.10 Kiltorcan Formation - Sample BF12

This light yellow, poorly-sorted, medium- to coarse-grained sandstone was taken from the Kiltorcan Formation type section at the abandoned Kiltorcan Quarry. One hundred and twenty two concordant ages were obtained from 163 analyses of 157 detrital zircon grains. Six zircons were analysed for core-rim analyses and three showed difference in ages outside of error (Figure 3–5.A-C). Zircons in this sample range in age from 435 ± 7 Ma to 2863 ± 54 Ma (Figure 3–3J) with Mesoproterozoic-aged zircons representing the largest proportion in the sample (n = 74; 61 %). The largest peak in the sample occurs at ca. 1.06 Ga (Figure 3–4L). The second largest proportion of zircons, at 20 % (n = 24), are Palaeoproterozoic in age. Archaean- and Neoproterozoic-aged

zircons represent 10 % (n = 12) and 6 % (n = 7) of the sample respectively. Five zircons in the sample are of Palaeozoic age. Three of these are Ordovician in age, one is Silurian and one is Cambrian. This sample contains no zircons that have ages between ca. 510 Ma and ca. 960 Ma.

3.6.11 Western Old Head Sandstone Formation - Sample AK03

This fine-grained sandstone was sampled from an outcrop exposed on the beach south of Lickowen townland near Toe Head. One hundred and thirty five grains were analysed and yielded 87 concordant ages ranging from 351 ± 8 Ma to 3217 ± 21 Ma (Figure 3–3K). Forty eight grains (55 %) are Palaeozoic in age. The majority of these grains (n = 30) being of Devonian age. This Devonian majority corresponds with the largest peak in the sample which occurs at ca. 400 Ma (Figure 3–4O). Neoproterozoic zircons contribute 26 % (n = 23) of the sample and form a significant peak at ca. 615 Ma. Other zircon ages in the sample are sparsely distributed between 800 Ma and 3.3 Ga. Ten zircons (11 %) are Palaeoproterozoic in age forming a minor peak at ca. 2.1 Ga. Three zircons are of Mesoproterozoic age and three are of Archaean age. The two youngest zircons, of Carboniferous age, form a concordia age of 353 ± 6 Ma ($MSWD_{conc}$ = 0.087; p_{conc} = 0.77).

3.6.12 Eastern Old Head Sandstone Formation - sample BF21

This sample was taken from White Bay, near Roches Point. It consists of cream-coloured, medium-grained, well sorted sandstone. Analysis of 150 zircon grains produced 111 concordant ages that range from 399 ± 11 Ma to 2985 ± 22 Ma (Figure 3–3L). This sample differs greatly from sample AK03 in that the majority of zircons (n = 51; 46 %) are of Mesoproterozoic age. Additionally, Neoproterozoic zircons represent a much smaller proportion (n = 7; 6 %) of the sample. The contribution of Palaeozoic-aged zircons is also much lower at 9 % (n = 10). Six of the Palaeozoic grains are Silurian in age, two are Ordovician and two are Devonian. These ages form a narrow peak at around 430 Ma (Figure 3–4P). Palaeoproterozoic zircons represent the second largest contribution to the sample at 31 % (n = 34) and correspond with the largest peak in the sample at ca. 1.64 Ga. A paucity of zircons with ages between ca. 500 Ma and 950 Ma occurs in this sample. Archaean-aged

zircons contribute 8 % (n = 9) with six of these producing a Neoarchaean peak at ca. 2.72 Ga.

3.6.13 Harrylock Formation - sample BF13

This sample consists of red, poorly sorted, pebbly, micaceous, medium-grained channel sandstone and was taken from Sandeel Bay Beach on the western coast of Houseland townland on Hook Head. One hundred and forty grains were analysed, producing 95 concordant ages that range from 438 ± 7 Ma to 2968 ± 13 Ma (Figure 3–3M). This sample has very similar proportions of Palaeoproterozoic- (n = 26; 27 %) and Neoproterozoic-aged (n = 27; 28 %) zircons. Neoproterozoic zircons form the largest peak in the KDE plot at around 645 Ma (Figure 3–4M). The second largest peak occurs at around 2.11 Ga. Twenty two zircons (23 %) have Mesoproterozoic ages. These manifest as two distinct peaks in the KDE plot: one at ca. 1.24 Ga and another at ca. 1.5 Ga. Archaean-aged zircons make up 14 % (n = 13) and are represented as two peaks in the KDE plot: one at ca. 2.67 Ga and the other at ca. 2.95 Ga. Zircons of Palaeozoic age make up 7 % (n = 7). This includes one Cambrian-, four Ordovician- and two Silurian-aged zircons.

3.6.14 Summary of Detrital Zircon Geochronology

Three broad groups can be established for samples of the UORS in southern Ireland based upon the distribution of detrital zircon ages. Samples AK07, AK11, AK16, BF15, and BF19 have similar detrital zircon age distributions. The highest proportion of zircon ages in these samples are Palaeoproterozoic or Mesoproterozoic, including a dominant KDE peak in this age range of between 1.0 and 1.1 Ga and a secondary KDE peak in the Late Palaeoproterozoic (1.6-1.7 Ga, BF19: ca 1.8 Ga). They are also characterised by a dominant Ordovician KDE peak and a paucity of middle to late Neoproterozoic zircons (with the exception of BF19 which has nine late Neoproterozoic zircons). BF15 and BF19 also have significant Archaean KDE peaks at 2.7 and 2.8 Ga respectively, which are not present in the other samples.

Samples BF11, BF12, BF21 and AK10 are characterised by very low proportions of Palaeozoic zircons and a dominant KDE peak of zircons with

ages between 1.0 and 1.1 Ga (except BF21 which has a dominant peak at ca. 1.6 Ga). These samples also contain very few late Neoproterozoic zircons. Samples BF11, BF12 and BF21 also show a grouping of Archaean zircons forming a KDE peak between 2.60 and 2.75 Ga. Sample AK10 has very few zircons in this age range.

Samples AK03 and AK04 are very similar in their zircon age distributions. Both show three conspicuous zircon age groups. The majority of zircons in these samples are Palaeozoic in age forming KDE peaks at ca. 388 Ma and ca. 406 Ma in AK04 and AK03 respectively. Unlike other samples in the UORS, these samples have very few zircons of Mesoproterozoic age and have a clear late Neoproterozoic KDE peak between 610 and 630 Ma. The other conspicuous KDE peak in these samples occurs between 2.1 and 2.2 Ga. Three Archaean zircons are present in sample AK03 compared to one in AK04.

Finally, sample BF13 shows few similarities to other samples in the ORS of southern Ireland. The spectrum of ages is more complex than in other samples, with Neoproterozoic zircons contributing the greatest proportion in the sample and a grouping of zircons between 2.0 and 2.2 Ga producing a major KDE peak at ca. 2.1 Ga. Another difference is the absence of zircons of the age range 1.0 to 1.1 Ga. A Middle Ordovician KDE peak at ca. 464 is also present. Samples AK03, AK04 and BF13 are the only samples in the UORS that contain significant populations of zircons between 2.0 and 2.4 Ga.

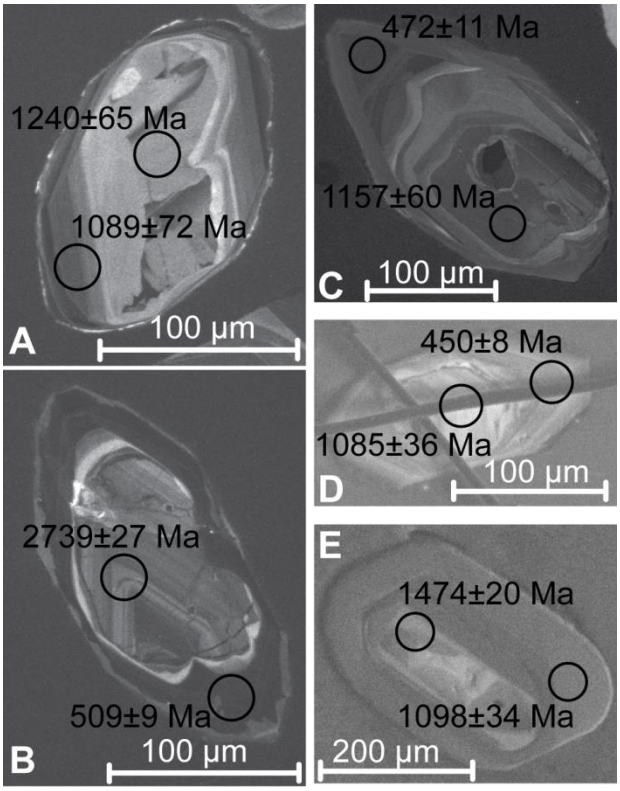

Figure 3–5. CL images showing position and age of zircon core-rim analyses in sample BF12 (**A**-**C**) and BF15 (**D**-**E**).

3.7 Detrital Mica Geochronology

Detrital micas were separated from three of the samples for which detrital zircon data were obtained. The new detrital mica ages reported here build upon an existing database of ages for the Dingle Basin and western part of the Munster Basin (Ennis et al., 2015). A total of 143 single-grain fusion $^{40}Ar/^{39}Ar$ were obtained from the Middle Devonian Gortanimill Formation, the Upper Devonian Old Head Sandstone Formation and the Devonian to Carboniferous Harrylock Formation (Figure 3–6 E-G). We have taken an approach whereby around 30 micas are dated and if the KDE curve showed more than one peak, then another 20 to 30 micas are analysed. However, if little age variation is observed, then thirty grains is deemed sufficient to represent the population.

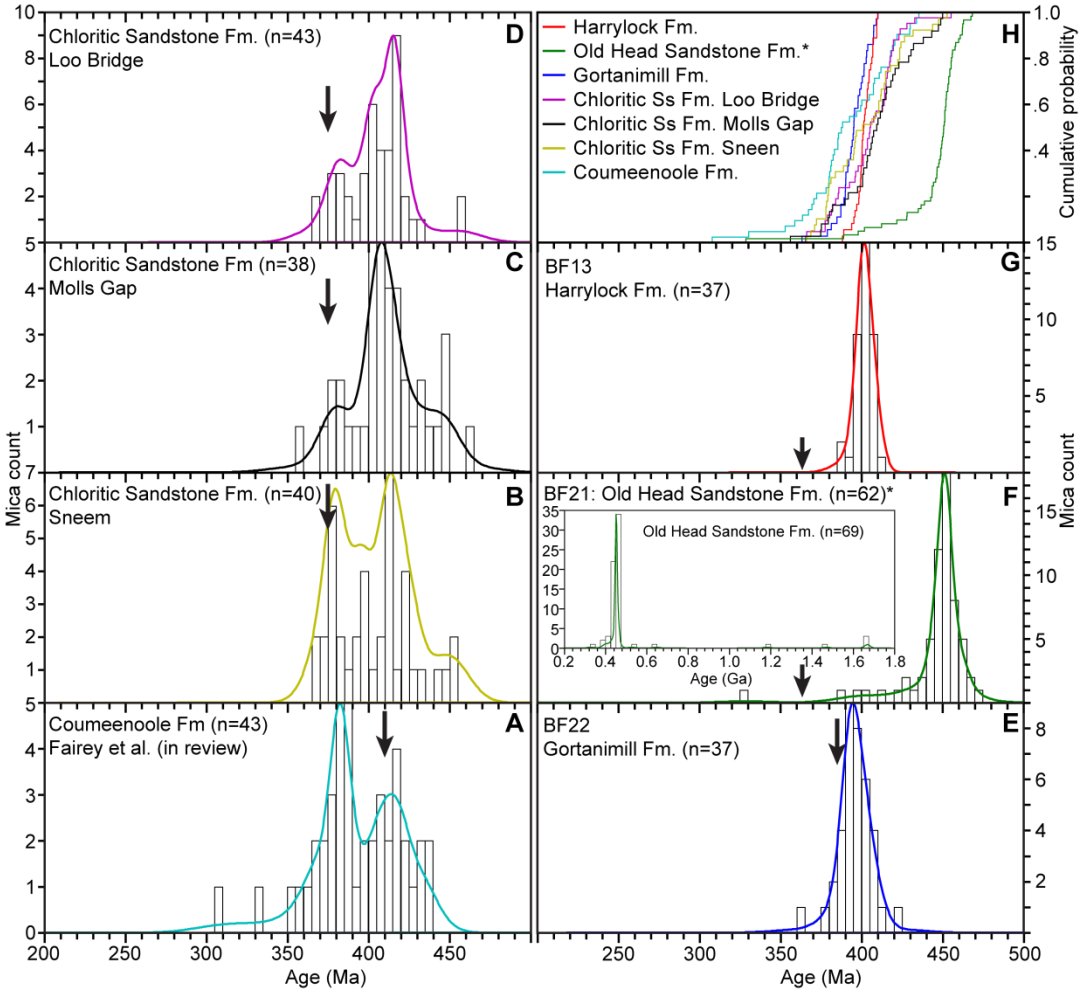

Figure 3–6. Histograms and KDE curves for detrital mica ages in the Dingle (**A**) and the western part of the Munster Basin (**B**-**D**) (Data adjusted from Ennis et al. (2015) – see analytical procedures). Histograms and KDE curves of newly obtained detrital mica ages from the Gortanimill Formation (**E**), Old Head Sandstone Formation and Harrylock Formation (**G**). **H**: combined cumulative probability plot for all detrital mica samples. Bold arrows indicate approximate depositional ages.

*to facilitate comparison of the major component, the small number of ages >0.5 Ga have been removed for the Old Head Sandstone Formation in (**F**) and (**H**). However, the full dataset is shown as an inset in (**F**).

Thirty seven detrital mica grains from the Gortanimill Formation (sample BF22) yielded a range of ages from 363 ± 22 Ma to 422 ± 12 Ma that defines a single KDE peak at ca. 395 Ma (Figure 3–6.E). The KDE peak has a slight tail toward younger ages.

Initially, 37 grains were analysed in sample BF21 from the eastern part of the Old Head Sandstone Formation. A number of older ages were obtained during this initial run. In order to provide improved resolution of mica ages,

another 32 grains were analysed. The additional analyses did not significantly alter the original distribution and relative abundance of detrital mica ages in the sample. In total, 69 grains were analysed and yielded a spread of ages from 329 ± 6 to 1670 ± 6 Ma (Figure 3–6.F inset). The overwhelming majority (ca. 80 %) of grains occur within the range 370 - 500 Ma and form a KDE peak at ca. 451 Ma (Figure 3–6.F). Three grains have ages in the range 1660 - 1671 Ma. Two grains are Mesoproterozoic in age, one is Neoproterozoic and one is Cambrian. An extended tail toward younger ages is also observed in the main peak.

Thirty seven grains from sample BF13, taken from the Harrylock Formation, produced a narrow range of ages from 388 ± 12 to 410 ± 6 Ma and a single KDE peak at ca. 402 Ma. A minor tail toward younger ages is observed in this KDE spectrum.

3.7.1 Comparison with existing mica geochronology for the UORS

Two of the three samples analysed in this study show narrow age ranges around 400 Ma (Figure 3–6.E and G.). The other sample, BF21, shows a spread of ages but a dominant peak at around 450 Ma with a tail toward younger ages as well as a spread of Proterozoic ages (Figure 3–6.F inset). The samples from the Chloritic Sandstone Formation in the western UORS, however, have more complicated mica age distributions (Figure 3–6.B-D). Most show two distinguishable peaks, one between 400 and 415 Ma, and one at ca. 375 Ma.

3.8 Apatite U-Pb Geochronology

These data were generated concurrently with apatite fission track analyses that were undertaken for bedrock thermal history studies by Cogné et al. (2014, 2016), but were not previously published. Samples taken from the same formation have been combined. The limited variability in detrital apatite ages in these larger samples suggests that it is unlikely that multiple apatite sources of vastly different age and thermal history were being sampled by the sediments under investigation. The apatite U-Pb ages were not utilised in the aforementioned studies, therefore the data have been included in this study (Figure 3–7) to provide a geochronological proxy which has an intermediate

closure temperature (ca. 375-550 °C; Cochrane et al., 2014) between the mica $^{40}Ar/^{39}Ar$ and zircon U-Pb systems. Two sampling transects were collected from the Munster Basin: one from Carrauntoohil and one from the Galtee Mountains (Figure 3–2). Five samples were retrieved from the Carrauntoohil section - three from the Lough Acoose Sandstone Formation and two from the Ballinskelligs Sandstone Formation. In the Galtee Mountain transect, three samples were collected, one from each of the Slievenamuck Conglomerate, Lough Muskry and Galtymore Formations. A single sample was also taken from the Ballystrasna Formation in a quarry south of Mallow.

Six formations belonging to the UORS were sampled across the Munster Basin: two from the west, three from the east and one from the central part of the basin. In the west, 47 apatites were dated from the Ballinskelligs Sandstone Formation (samples Ca-1, Ca-6) yielding a range of ages from 339 ± 51 to 2816 ± 225 Ma (Figure 3–7.C). Approximately 40 % of grains have ages between 380 and 440 Ma. The highest KDE peak occurs at ca. 432 Ma but subordinate peaks are developed at ca. 376 and 397 Ma as well as two apatite ages forming a peak at ca. 945 Ma. Three samples (Ca-4, Ca-8, Ca-9) from the Lough Acoose Sandstone Formation give a combined total of 62 detrital apatite ages (Figure 3–7.D). These ages range from 324 ± 64 to 1024 ± 51 Ma with 53 % falling in the range 380 to 440 Ma. A single KDE peak is developed at ca. 423 Ma. Thirteen percent of apatite ages from this formation are younger than the minimum depositional age of 372 Ma (end-Frasnian). A single sample (Bg-1) from the Ballystrasna Formation in the central part of the basin produced 27 detrital apatite ages ranging from 370 ± 71 to 1079 ± 71 Ma. Two broadly continuous ranges occur in this sample, ca. 490 to 590 Ma (37 % of ages in the sample) and ca. 370 to 470 Ma (59 % of ages in the sample). The largest peak in the KDE spectrum occurs at ca. 437 Ma, with two smaller peaks at 511 and 569 Ma.

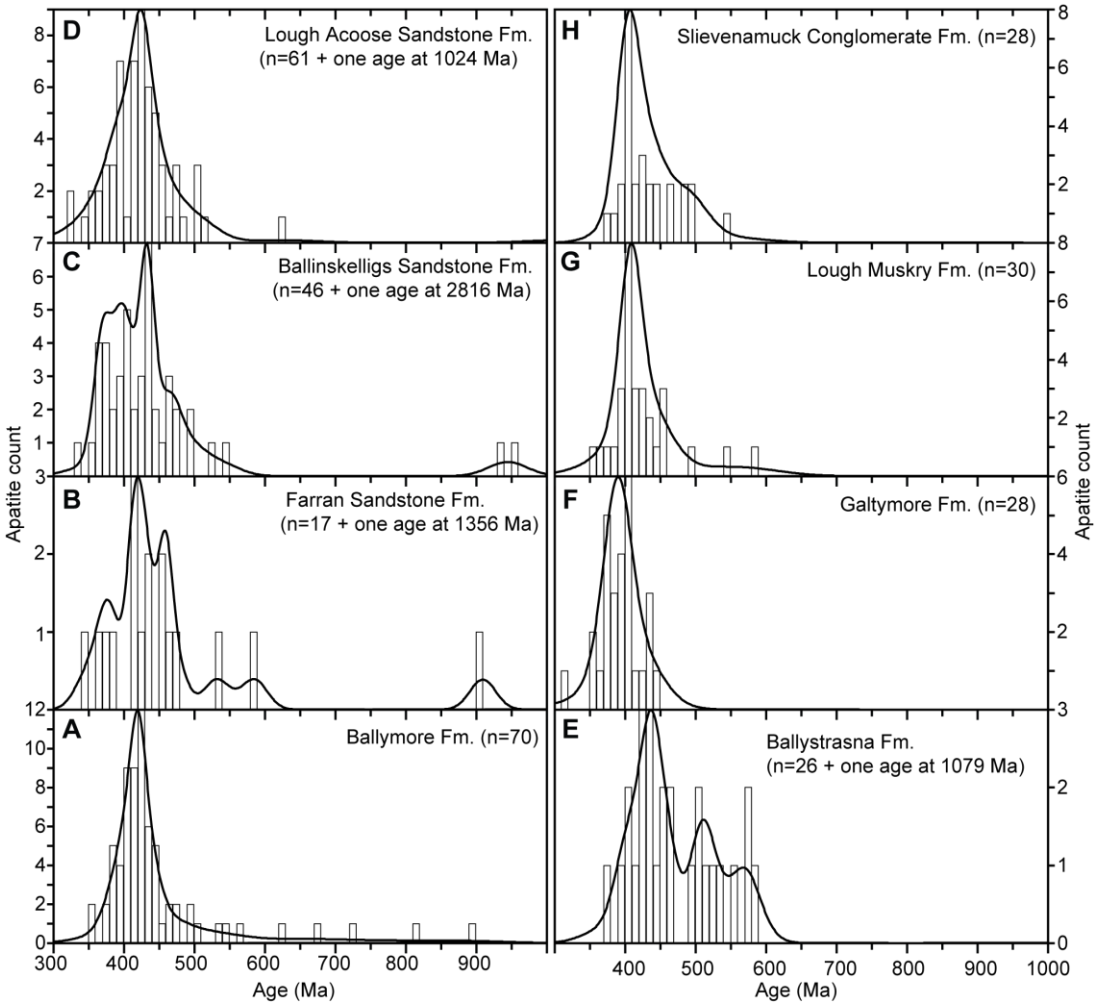

Figure 3–7. Histograms and KDE curves for detrital apatite ages in the Dingle (**A** and **B**, modified after Fairey et al. 2018) and the Munster Basin (**C**-**H**).

In the eastern part of the Munster Basin, three samples were taken from three different formations in the Galtee Mountains succession. A total of 28 ages were obtained from detrital apatites in the Galtymore Formation (sample Ga-2, Figure 3–7.F). These range from 310 ± 67 to 448 ± 37 Ma, forming a single KDE peak at ca. 390 Ma. Sixty four percent of these fall within the range 380 to 440 Ma and 32 % are younger than 380 Ma. Thirty detrital apatite grains from the Lough Muskry Formation (sample Ga-1) yielded a range of ages from 350 ± 76 to 587 ± 66 Ma forming a single KDE peak at ca. 410 Ma which has a tail toward older ages (Figure 3–7.G). The majority of grains (67 %) in this sample fall within the range 380 to 440 Ma. A similar distribution of ages is observed in the sample from the Slievenamuck Conglomerate Formation (sample Ga-4) which consists of 28 detrital apatite ages with a single KDE

peak at ca. 407 Ma that has a tail toward older ages (Figure 3–7.H). Apatite ages range from 380 ± 35 to 550 ± 71 Ma with 64 % of grains in the sample being confined to the 380 to 440 Ma range.

3.9 Discussion

This paper presents the first detrital zircon and apatite U-Pb geochronological data for the UORS in southern Ireland and combines it with detrital white mica $^{40}Ar/^{39}Ar$ geochronological data. This multi-proxy approach is used to evaluate the role of orogenic drivers, especially in terms of possible sedimentary recycling of LORS to UORS.

3.9.1 Provenance of the Upper Old Red Sandstone

It has been shown in Section 3.6.14 that the detrital zircon samples from across the UORS in southern Ireland can be placed, with some exceptions, into three broad groups based on descriptive analysis of the distribution of ages within each sample. Multi-dimensional scaling (MDS) analysis by pair-wise Kolmogorov-Smirnov (K-S) distances (Vermeesch, 2013) allows a more objective approach to describing the relationship between these samples (Figure 3–8). Those samples that are most closely related by K-S distances are grouped together, in this case forming four separate groups. The provenance of the samples in the UORS is described below according to this grouping.

3.9.1.1 Source of detrital zircons in Group 1, 2 and 3

Group 1 samples are all from formations which are stratigraphically confined to the Munster Basin and which either comprise, or are proximal to, the western depocenter of the basin. Group 2 samples are also confined to within the basin margins but are from the eastern part of the basin. With the exception of Sample BF22, the Group 3 samples belong to formations which are representative of the upper-most part of the UORS in southern Ireland. All samples have a concentration of detrital zircon ages between 1.0 and 1.1 Ga (with varying proportions between samples). The ultimate source of these zircons is likely to be the Grenville Orogen within the Laurentian craton (Cawood and Nemchin, 2001). This is supported by the paucity of zircons that

would indicate Trans-Amazonian or Eburnean thermo-tectonic events (2.0-2.1 Ga, Nance et al., 2008). Crucially, with the exception of Sample BF19, all samples contain very few zircons of late Neoproterozoic age, indicating that peri-Gondwanan domains had no significant contribution to the detritus being delivered to the UORS of the Munster Basin. The late Neoproterozoic zircons present in Sample BF19 may represent some influence from a source of peri-Gondwanan affinity - likely from the Leinster terrane.

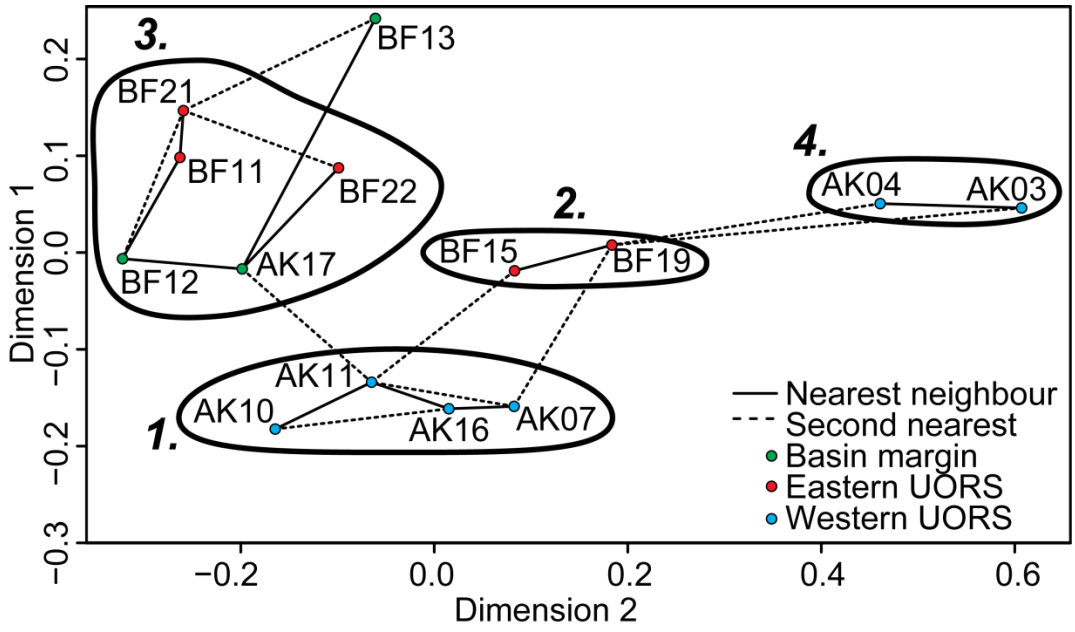

Figure 3–8. Non-metric multi-dimensional scaling map of all UORS detrital zircon samples. Four main groups are highlighted by bold circles. Sample AK17 is taken from Fairey et al. (2018). Axes values are dimensionless K-S distances (Vermeesch, 2013). The most closely related samples are joined by a solid line and the second closest are marked with a dashed line.

The proportion of Palaeozoic detrital zircon grains in these samples differs considerably. Due to the similarity in Proterozoic zircon distributions, the relative contribution of zircons of Palaeozoic age is vitally important for understanding their sedimentary provenance. The variability of Palaeozoic contributions is reflected in the groupings established by MDS analysis. Group 3 samples generally contain low proportions of Palaeozoic grains relative to Group 1 and 2 samples. Group 1 and 2 show Palaeozoic KDE peaks which lie between 445 and 465 Ma, with the exception of Sample AK10 which has a

Cambrian KDE peak at ca. 486 Ma. A striking similarity is seen between a number of Group 3 samples and a compilation of detrital zircon ages measured by Waldron et al. (2008, 2014) for Upper Ordovician to Silurian rocks in the Southern Uplands terrane as well as a single Silurian-aged sample from the Gala Group in the Longford-Down terrane analysed by McConnell et al. (2016)(Figure 3–9.A and C.). This similarity suggests that detrital zircon age distributions in samples from Group 3, particularly Samples AK17, BF11 and BF12, can be explained entirely by recycling of strata analogous to those in the Southern Uplands terrane. The high proportion of Palaeozoic zircons in Group 1 and Group 2 samples may be attributed to the higher contribution of detritus from lithologies that are poor in Precambrian zircons such as most of those analysed by McConnell et al. (2016) in the Longford-Down terrane (Figure 3–9.B) which are said to be sourced from peri-Laurentian arc material accreted during the Grampian Orogeny. This interpretation is supported by the fact that the oldest sedimentary rocks of the north eastern Munster Basin rest, with angular unconformity, on Silurian basement (Carruthers, 1985). Although detrital zircons from these Silurian rocks have not been analysed, broad correlatives in the Lake District have been analysed by Waldron et al. (2014) who interpret them to be a southerly continuation of Silurian Southern Upland terrane deposits with similar Laurentian sediment derivation. Approximate north to south palaeocurrents in the uppermost Silurian turbiditic sedimentary rocks of the Galtee succession (Sleeman and McConnell, 1995) suggest a similar situation in southern Ireland. The Ordovician sedimentary rocks that lie to the south of the Iapetus Suture (e.g. Skiddaw Group of the Lake District) could not have acted as a source of detritus for Group 1-3 samples because these rocks were found to contain an abundance of late Neoproterozoic zircons indicative of a peri-Gondwanan provenance (Waldron et al., 2014).

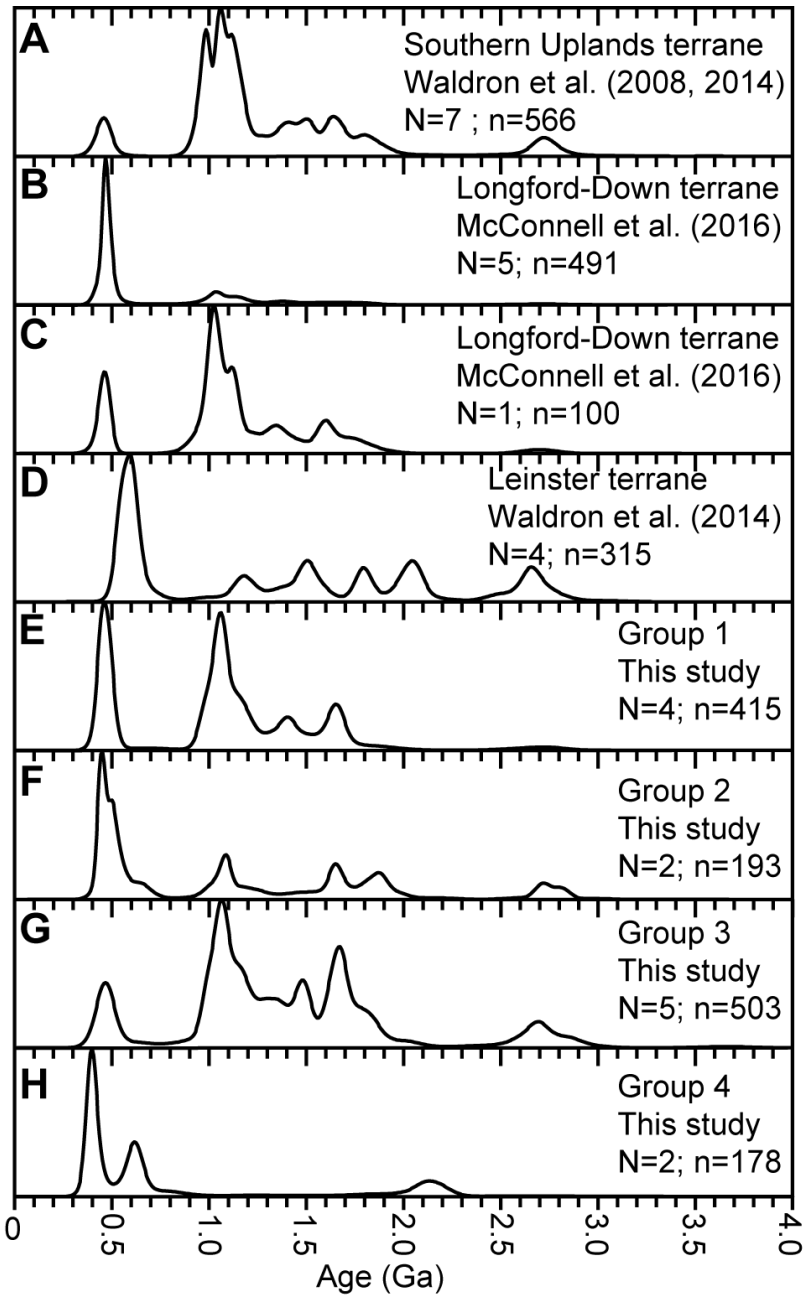

Figure 3–9. KDE plots of detrital zircon ages from various potential local sediment sources as well as for composite plots for each group of samples from this study. **A**. Upper Ordovician to Llandovery sedimentary rocks of the Southern Uplands terrane (Waldron et al., 2008, 2014) with dominant Laurentian provenance. **B**. Upper Ordovician to Llandovery sedimentary rocks of the Longford-Down terrane showing peri-Laurentian arc provenance (McConnell et al., 2016). **C**. A single sample from the Llandovery Lough Avaghon Formation in the Longford-Down terrane showing dominant Laurentian provenance (McConnell et al., 2016). **D**. Ganderian provenance of Cambrian sedimentary rocks in the Leinster terrane (Waldron et al., 2014). **E**. Combined analyses from Group 1 samples. **F**. Combined analyses from Group 2 samples. **G**. Combined analyses from Group 3 samples. **H**. Combined analyses from Group 4 samples. Key: N = number of samples; n = number of zircon grain ages.

3.9.1.2 Source of detrital zircons in Group 4

Samples AK04 and AK03 are from the Toe Head and Old Head Sandstone Formations respectively. MDS analysis (Figure 3–8) shows that these samples represent an entirely different source to the rest of the samples in the study. The formations represent the upper limits of the UORS in southwest Ireland and record a transition from terrestrial to marine conditions (MacCarthy, 1990). The detrital zircon age distribution within these samples is dominated by Palaeozoic zircons. However, unlike in Group 1-3 samples, where the large majority of Palaeozoic zircons are Ordovician to Silurian in age, Group 4 samples contain an abundance of zircons of Early Devonian age (Figure 3–9H). These zircons of Early Devonian age are interpreted here to represent a major Acadian igneous source. Two other conspicuous peaks are present in the detrital zircon distributions in Group 4 samples. One is Palaeoproterozoic (ca. 2.2 Ga) and the other is late Neoproterozoic (ca. 620 Ma). The difference in the overall age of Palaeozoic detrital zircons, paucity of Mesoproterozoic zircons and significant presence of zircons at around 2.2 Ga and 620 Ma suggests an entirely different sediment provenance for the Group 4 samples.

Palaeocurrents in the Toe Head Formation indicate dominant flow toward the northeast (Graham, 1975). This direction contrasts with the southeast-, south- and southwest-directed palaeocurrents of the formations from which Group 1, 2 and 3 samples were collected. For the western Old Head Sandstone Formation, the similarity in detrital zircon populations to those of the underlying Toe Head Formation suggests a continued sediment supply from the southwest. However, Sample BF21 was taken from the eastern part of the same formation and shows a detrital age distribution consistent with derivation from the north. A similar depositional model to that of Episode 4 of MacCarthy (1990) is invoked for the development of the Toe Head and Old Head Sandstone Formations whereby a marine incursion from the southeast creates a geographical separation of sandstones from different source regions. Therefore, those sandstones deposited on the north shore of the sea have a distinctly Laurentian affinity, either by re-working of underlying ORS sandstones or by derivation from similar northerly sources, whereas the sandstones deposited on the western shore are derived from the southwest.

A similar scenario is also suggested by Williams et al. (1989) whereby the east-west oriented Castletown-Ringabella Fault System was the main subsidence-controlling mechanism creating a depocenter to the south of the fault with an axis of similar orientation.

Geophysical studies have shown that a large granitic body possibly lies approximately 125 km off the coast of south west Ireland (Conroy and Brock, 1989). This granite could provide a source for the abundant Acadian-aged zircons in Group 4 samples. The source of late Neoproterozoic zircons is difficult to determine, especially given the low number of Proterozoic grains. The zircon age distributions, with a single peak at 2.2 Ga and sparse number of Mesoproterozoic grains, have greater affinity with Cadomia-Armorica than with Ganderia or Avalonia (Figure 3–1). However, the more likely scenario is that the sparse number of Precambrian zircons in these samples is a function of dilution by the large number of Palaeozoic grains and that the late Neoproterozoic zircons are likely sourced from Ganderian country rock into which the Acadian granites have intruded.

3.9.1.3 Source of detrital zircons in the Harrylock Formation (Sample BF13)

Detrital zircons from Sample BF13 from the Harrylock Formation on Hook Head indicate a very different sedimentary provenance to the rest of the UORS (Figure 3–8). The dominant late Neoproterozoic peak and general paucity of Mesoproterozoic zircons, particularly between 1.0 and 1.2 Ga, indicates sources of Laurentian affinity were likely not providing sediment to this formation. Additionally, the abundance of zircons between the ages of 2.0 and 2.2 Ga, typically absent from Laurentian sedimentary rocks, is characteristic of Ganderian derivation (Waldron et al., 2014). Therefore, the spectrum of ages seen in the Harrylock Formation can simply be explained by a local recycling of Cambrian sediments to the northeast in the Leinster Massif which are known to be of Ganderian affinity (Figure 3–9.D, Waldron et al., 2014). This requires a drainage area that was separate from the dominant source areas feeding the rest of the basin and included the area around the Leinster Batholith possibly acting as a watershed.

3.9.2 Additional provenance perspectives of the UORS based on mica and apatite geochronology

Three white mica samples were collected from the central and eastern UORS to complement published white mica ages for the western UORS (Munster Basin) and LORS of the Dingle Basin acquired by Ennis et al. (2015). Those from the LORS and the western UORS show two distinct peaks which vary in proportion between samples. The older peaks in these samples are taken to represent the crystallisation ages of the micas. These peaks range in age between 400 and 415 Ma. The younger peaks, however, all occur between a narrow age range of 375 to 379 Ma. This lends further support to the suggestion by Fairey et al. (2018) that volcanism and high heatflow and fluid flow associated with granite emplacement below the western Munster Basin at this time was responsible for resetting of the white mica ^{40}Ar-^{39}Ar system in sedimentary rocks of the LORS and UORS.

The most likely source of detrital micas, certainly in the eastern UORS, is the Leinster Batholith and equivalents which are two-mica granites with coarse-grained white micas (Roycroft, 1991) and has a crystallisation age of 405 Ma (O'Connor et al., 1989). However, most UORS samples have very few zircons of this age. The youngest zircon in the Kiltorcan Formation, for example, has an age of 435 Ma. This formation is the uppermost part of the ORS and has been interpreted to represent the first unroofing of the Leinster Batholith, according to MacCarthy (1990). The dearth of zircons of this age most likely reflects a hydrodynamic biasing during transportation toward the much lighter white mica as well as the far greater modal abundance of micas in the source region. In the case of the eastern Old Head Sandstone, the major detrital mica age peak occurs at 450 Ma. Mineral cooling ages (from hornblende, biotite and muscovite) for the Dalradian Supergroup and Clew Bay Complex fall between approximately 455 and 465 Ma (Chew et al., 2010). Therefore, these rocks are a likely source of micas in the Old Head Sandstone Formation. This source is consistent with a northern derivation of detrital zircons in this sample. The lack of zircons of Grampian age (475-465 Ma) further suggests a metamorphic rather than magmatic origin of the micas.

The apatite ages presented in this study have larger errors than those exhibited by zircon U-Pb data because the U content of apatite is typically 1-2 orders of magnitude less than that of zircon, resulting in correspondingly lower radiogenic Pb contents, combined with the presence of initial Pb. Many of the single-grain central ages, therefore, are younger than the depositional age, but nonetheless overlap at the 2-sigma level. As a whole, however, the major peaks are still viable indicators of the age of the apatite sources. Dominant peaks for detrital apatite ages in UORS samples differ from the dominant western UORS detrital mica ages (which are younger) and the youngest detrital zircon age peaks for the majority of the UORS (which are older). In addition, there is a difference in peak ages between samples in the western UORS, which have ages of ca. 423 and 432 Ma, and those from the eastern UORS in the Galtee Mountains succession, which have ages ranging from 385 to 415 Ma. A single sample from the central part of the Munster Basin, in the Ballystrasna Formation, has a dominant peak age of ca. 437 Ma. The western detrital apatite ages reflect a dominant source similar in age to the Saltees and Carnsore granites which have ages of 436 ± 7 Ma (Max et al., 1979) and 428 ± 11 Ma (O'Connor et al., 1989) respectively. However, given the palaeocurrents are south- or southeasterly-directed, a mechanism for acquiring detritus of this age in the western part of the basin is difficult to explain, even if these granites extend below the Munster Basin. The eastern samples, however, are of Acadian age and may have been sourced from the proximal Leinster Batholith.

Taken together, the detrital apatite and mica geochronology of the UORS in southern Ireland record an important proximal Late Caledonian source of detritus that otherwise would have been missed by analysis of detrital zircons only. It remains unclear as to why Late Caledonian to Acadian zircons are rare in the UORS. The consistent Acadian age of micas across the basin is also problematic, considering that apatite ages vary considerably in the western and eastern parts of the UORS. If, despite having different crystallisation ages, the Carnsore and Leinster Granites, for example, both produce an Acadian age range for white micas then a post-crystallization re-heating event must have occurred, perhaps related to Acadian deformation. In the Leinster terrane

such deformation is considered to be contemporaneous with intrusion of the Leinster Granite (Chew and Stillman, 2009, and references therein). Although long-range subaqueous transport of white micas is conceivable (see, for example, Anderson et al. 2017), the absence of micas of early Palaeozoic age and Proterozoic age such as those found by Mange et al. (2010) in the South Mayo Trough precludes long-range northern sourcing of micas in the southern Irish ORS. The absence of Mesoproterozoic apatite and micas in the UORS indicates that a direct source of Mesoproterozoic zircons is unlikely and is consistent with recycling of Silurian sedimentary rocks as a source of zircons. Therefore, combined detrital zircon, apatite and mica geochronology shows that the majority of the UORS in southern Ireland was sourced from mixing of medial Silurian sediments of predominantly Laurentian affinity with proximal Late Caledonian (~430-420 Ma) to Acadian (~410-390 Ma) igneous sources.

3.9.3 Summary of palaeodrainage during deposition of UORS in southern Ireland

Much work has been undertaken in trying to understand the provenance of the large accumulation of UORS in the Munster Basin. Early studies focussed on localised successions (e.g. Capewell, 1956; 1965; Penney, 1980; Carruthers, 1985) but MacCarthy (1990) described the basin in terms of facies associations and suggested its development involved four depositional episodes. In this model, a northern and western source of detritus was dominant. Proximal sources were dominant during earliest deposition and become more distal as the depositional system matured (MacCarthy, 1990). Williams (2000) described sediment deposition into the Munster Basin as two major ‘fluvial dispersal systems’ that mostly flowed from north to south. The larger of the two systems was in the northwestern part of the basin, where the succession is thickest, and the smaller system was in the northeastern part.

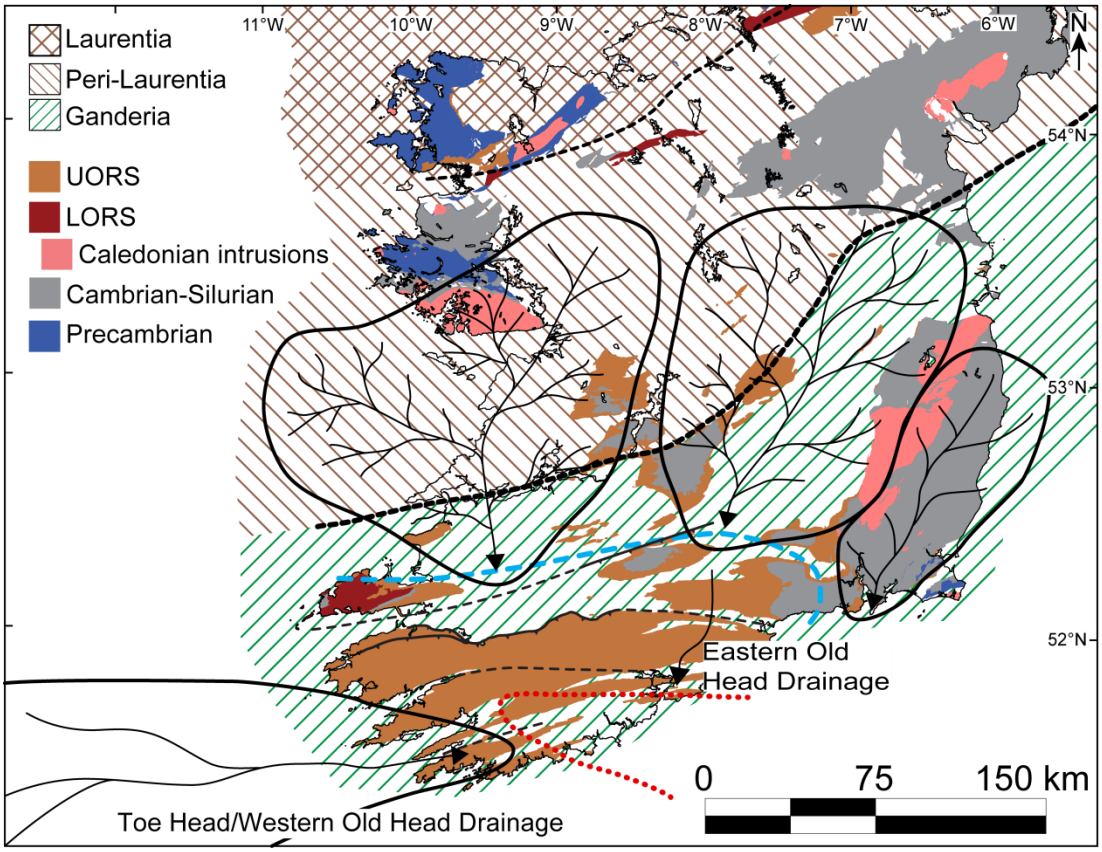

Figure 3–10. Possible palaeodrainage patterns during deposition of the UORS in the Munster Basin. The basin margin is taken as the 1000m isopach (blue dashed line). Possible shoreline of transgressive sea during Old Head Sandstone deposition shown as dotted red line (Modified after MacCarthy, 1990).

Overall, detrital zircon, mica and apatite geochronology for the bulk of the UORS indicates a dominant input of Laurentian and Caledonian detritus and very little influence from the underlying peri-Gondwanan basement. The Laurentian component was likely derived from peri-Laurentian Silurian sedimentary rocks to the north of the Munster Basin which contain abundant northerly-derived turbiditic successions of Laurentian affinity (Figure 3–9; McConnell et al., 2016; Waldron et al., 2014, 2008). The inferred drainage for northerly derived sediment is based upon the fluvial distributary systems of Williams (2000). What is important to note is that the systems probably did not come into direct contact with peri-Laurentian arc volcanic material or sediments akin to those in the South Mayo Trough which contain abundant early Palaeozoic to Precambrian white micas (Mange et al., 2010). Exactly how the rocks of the South Mayo Trough were shielded from denudation into

the Munster Basin system is not clear. The two simplest explanations are either that the drainage system did not intersect the South Mayo Trough (as depicted in Figure 3–10) or that the rocks of the South Mayo Trough were not voluminous enough to provide significant quantities of sediment. Another explanation is that during UORS deposition the South Mayo Trough was concealed beneath Late Caledonian thrust sheets.

The Toe Head Formation and the western Old Head Formation were likely sourced from the west as indicated by northeasterly-directed palaeoflow (Graham, 1975). Off the west coast of southern Ireland a presumed granitic body was imaged by Conroy and Brock (1989) and, if Acadian in age, would account for the abundant detrital zircons of this age (ca. 400 Ma). The eastern Old Head Sandstone Formation shows very similar detrital zircon distributions to the older formations in the UORS and was therefore probably sourced from the north. This differing provenance within the same formation might simply be a function of the shape and orientation of the basin (red dotted line, Figure 3–10).

Finally, the Harrylock Formation is derived from a very different source to the rest of the UORS in southern Ireland as it consists of a dominant input of late Neoproterozoic zircons associated with peri-Gondwanan terranes. Thus, a separate palaeodrainage pattern is envisaged (Figure 3–10) which drained from the north and northeast and denuded Ganderia-derived Cambrian sedimentary rocks (Waldron et al., 2014) as well as the Leinster Batholith.

3.9.4 Drivers of sedimentation and the role of recycling

It has been suggested by Ennis et al. (2015) that the Dingle Basin represents only a portion of the original extent of LORS sedimentation in southern Ireland and that, based on age-equivalence of detrital micas and an increase in sediment maturity, the UORS resulted from recycling of LORS sediments. Such a situation has also been proposed for similar-aged sediments in southern Britain by Soper and Woodcock (2003) who suggested that this recycling was driven by Acadian inversion of LORS basins. Detrital zircon age data presented in this study for the Dingle Group shows an appreciable late Neoproterozoic source which is not present in the majority of samples in the UORS. If the UORS is a product of recycling of LORS similar

to that preserved in the Dingle Basin, then a significant proportion of late Neoproterozoic zircons would be expected in the former. This, however, is not the case. Instead recycling of Ordovician to Silurian sedimentary rocks can account for the distribution of detrital zircon ages seen in UORS succession.

MacCarthy (1990) suggested that large granitic intrusions, such as the Leinster Batholith, resisted subsidence during deposition of the UORS, thus creating an elevated area from which detritus was shed. The Late Caledonian age of detrital micas and apatites in the UORS adds further plausibility to this suggestion. However, relatively high relief of Silurian rocks akin to those in the Longford-Down and Leinster terranes (which contain abundant zircons of Laurentian affinity) would be required to supply Laurentian detrital zircons. The Early Devonian timing of Acadian deformation and contemporaneous granite emplacement (Chew and Stillman, 2009) in Ireland is in agreement with the timing of deposition of the earliest known sediments in the Munster Basin (likely of Eifelian age, according to Williams et al., 1997). It is possible that active uplift of the source region was accomplished as a result of deformation accompanied by intrusion of magmas during the Acadian Orogeny. The Newry Igneous Complex, for example, which intrudes Silurian sedimentary rocks in the Longford Down terrane has recently been redated by Cooper et al. (Cooper et al., 2016) and shows that the complex was emplaced over a seven million year period from 414 to 407 Ma. Such emplacement could result in substantial uplift of the surrounding country rock and resultant exhumation (Kimbrough et al., 2001).

3.10 Conclusions

This paper presents the first multi-proxy, single-grain detrital geochronological study of the ORS in the Upper Devonian Munster Basin and early Carboniferous rocks of the South Munster Basin in southern Ireland. A multi-proxy approach to investigating the provenance of these basins allowed us to test the extent of recycling and to better understand the Devonian palaeogeography of a region which has a complex geological history involving multiple orogenies. This study indicates the following:

(1) The detrital zircon record of the UORS shows very little contribution from peri-Gondwanan rocks. Instead the majority of samples indicate

Laurentian affinity – likely as a result of recycling of northerly-derived Ordovician to Silurian marine sedimentary rocks of the Southern Uplands – Longford Down terrane and westward extension thereof.

(2) The scarcity of late Neoproterozoic zircons in the UORS compared to the high proportion in the LORS supports the suggestion that the LORS did not act as a source of sediment for the UORS and that the LORS in southern Ireland probably did not extend much further beyond what is presently exposed in the Dingle Basin. Thus the notion of a regionally interconnected, areally extensive LORS across the southern British Isles is not supported.

(3) Detrital zircons from the western Toe Head and Old Head Sandstone Formations indicate differing sediment derivation to that of the rest of the UORS (as well as the eastern Old Head Sandstone Formation) with dominance of 390 to 400 Ma zircons and a conspicuous late Neoproterozoic zircon peak. Taking into account west to east palaeocurrent data as well as offshore geophysical anomalies from previous studies, a western offshore Acadian granitic source is suggested. The eastern Old Head Sandstone indicates an ultimate Laurentian sediment source – possibly from reworking of the underlying portions of the UORS sediments.

(4) Detrital apatite U-Pb ages and detrital mica Ar-Ar ages indicate Late Caledonian and Acadian sources in both the LORS and UORS that would have otherwise been missed by detrital zircon analysis only. We therefore recommend that provenance studies employ multiple geochronological techniques with different temperature sensitivities when assessing the sedimentary provenance of basins. This recommendation is particularly pertinent when dealing with sediments that are suspected to have undergone multiple cycles of sedimentation.

3.11 Acknowledgments

B.J.F, A.K, P.A.M and K.F.M acknowledge the financial support of the Irish Shelf Petroleum Studies Group (ISPSG) of the Irish Petroleum Infrastructure Programme (PIP) Group 4 (project code IS 12/05 UCC). The ISPSG comprises: Atlantic Petroleum (Ireland) Ltd, Cairn Energy Plc, Chrysaor E&P Ireland Ltd, Chevron North

Sea Limited, ENI Ireland BV, Europa Oil & Gas, ExxonMobil E&P Ireland (Offshore) Ltd., Husky Energy, Kosmos Energy LLC, Maersk Oil North Sea UK Ltd, Petroleum Affairs Division of the Department of Communications, Energy and Natural Resources, Providence Resources Plc, Repsol Exploración SA, San Leon Energy Plc, Serica Energy Plc, Shell E&P Ireland Ltd, Sosina Exploration Ltd, Tullow Oil Plc and Woodside Energy (Ireland) Pty Ltd. D.C., C.M. and N.C. acknowledge support from Science Foundation Ireland grant 12/IP/1663 and 13/RC/2092 (iCRAG Research Centre, project HC4.2PD6a). iCRAG is funded under the SFI Research Centres Programme and is co-funded under the European Regional Development Fund. K.K. acknowledges financial support of NWO grant 864.12.005. D. Pastor-Galan is thanked for his geochronology and sampling advice. C. Reid and R. van Elsas are thanked for their technical assistance for SEM and sample preparation respectively.

3.12 References

Anderson, C.J., Struble, A., Whitmore, J.H., 2017. Abrasion resistance of muscovite in aeolian and subaqueous transport experiments. Aeolian Res. 24, 33–37. doi:10.1016/j.aeolia.2016.11.003

Capewell, J.G., 1965. The Old Red Sandstone of Slieve Mish, Co. Kerry. Proc. R. Ir. Acad. B. 64, 165–174.

Capewell, J.G., 1956. The stratigraphy, structure and sedimentation of the Old Red sandstone of the Comeragh mountains and adjacent areas, County Waterford, Ireland. Q. J. Geol. Soc. 112, 393–412. doi:10.1144/GSL.JGS.1956.112.01-04.19

Carruthers, R.A., 1987. Aeolian sedimentation from the Galtymore Formation (Devonian), Ireland. Geol. Soc. London, Spec. Publ. 35, 251–268. doi:10.1144/GSL.SP.1987.035.01.17

Carruthers, R.A., 1985. The Upper Palaeozoic geology of the Glen of Aherlow and the Galtee Mountains, Counties Limerick and Tipperary. PhD thesis. University of Dublin.

Cawood, P.A., Nemchin, A.A., 2001. Paleogeographic development of the east Laurentian margin: Constraints from U-Pb dating of detrital zircons in the Newfoundland Appalachians. Geol. Soc. Amer. Bull. 113, 1234–1246. doi:10.1130/0016-7606(2001)113<1234:PDOTEL>2.0.CO;2

Cherniak, D.J., Watson, E.B., 2001. Pb diffusion in zircon. Chem. Geol. 172,

5–24. doi:10.1016/S0009-2541(00)00233-3

Chew, D.M., Daly, J.S., Magna, T., Page, L.M., Kirkland, C.L., Whitehouse, M.J., Lam, R., 2010. Timing of ophiolite obduction in the Grampian orogen. Bull. Geol. Soc. Amer. 122, 1787–1799. doi:10.1130/B30139.1

Chew, D.M., Donelick, R.A., 2012. Combined apatite fission track and U-Pb dating by LA-ICP-MS and its application in apatite provenance analysis, in: Sylvester, P.J. (Ed.), Quantitative Mineralogy and Microanalysis of Sediments and Sedimentary Rocks. Mineral. Assoc. of Can., pp. 219–247.

Chew, D.M., Petrus, J.A., Kamber, B.S., 2014. U–Pb LA–ICPMS dating using accessory mineral standards with variable common Pb. Chem. Geol. 363, 185–199. doi:10.1016/j.chemgeo.2013.11.006

Chew, D.M., Stillman, C.J., 2009. Late Caledonian orogeny and magmatism, in: The Geology of Ireland. pp. 143–174.

Chew, D.M., Strachan, R.A., 2014. The Laurentian Caledonides of Scotland and Ireland. Geol. Soc. London, Spec. Publ. 390, 45–91. doi:10.1144/SP390.16

Chew, D.M., Sylvester, P.J., Tubrett, M.N., 2011. U-Pb and Th-Pb dating of apatite by LA-ICPMS. Chem. Geol. 280, 200–216. doi:10.1016/j.chemgeo.2010.11.010

Clayton, G., Higgs, K., 1979. The Tournaisian Marine Transgression in Ireland. J. Earth Sci. 2, 1–10.

Cochrane, R., Spikings, R.A., Chew, D.M., Wotzlaw, J.F., Chiaradia, M., Tyrrell, S., Schaltegger, U., Van der Lelij, R., 2014. High temperature (>350°C) thermochronology and mechanisms of Pb loss in apatite. Geochim. Cosmochim. Acta 127, 39–56. doi:10.1016/j.gca.2013.11.028

Cogné, N., Chew, D., Stuart, F.M., 2014. The thermal history of the western Irish onshore. J. Geol. Soc. London. 171, 779–792. doi:10.1144/jgs2014-026

Cogné, N., Doepke, D., Chew, D., Stuart, F.M., Mark, C., 2016. Measuring plume-related exhumation of the British Isles in Early Cenozoic times. Earth Planet. Sci. Lett. 456, 1–15. doi:10.1016/j.epsl.2016.09.053

Conroy, J., Brock, A., 1989. Gravity and magnetic studies of crustal structure

across the Porcupine basin west of Ireland. Earth Planet. Sci. Lett. 93, 371–376.

Cooper, M.A., Collins, D.A., Ford, M., Murphy, F.X., Trayner, P.M., O'Sullivan, M., 1986. Structural evolution of the Irish Variscides. J. Geol. Soc. London. 143, 53–61. doi:10.1144/gsjgs.143.1.0053

Cooper, M.R., Anderson, P., Condon, D.J., Stevenson, C.T.E., Ellam, R.M., Meighan, I.G., Crowley, Q.G., 2016. Shape and intrusion history of the Late Caledonian, Newry Igneous Complex, Northern Ireland, in: Young, M.E. (Ed.), Unearthed: Impacts of the Tellus Surveys of Ireland. Royal Irish Academy, Dublin, pp. 145–155. doi:DOI:10.3318/ 978-1-908996-88-6.ch11

Dewey, J.F., Strachan, R.A., 2003. Changing Silurian-Devonian relative plate motion in the Caledonides: sinistral transpression to sinistral transtension. J. Geol. Soc. London. 160, 219–229. doi:10.1144/0016-764902-085

Ennis, M., Meere, P.A., Timmerman, M.J., Sudo, M., 2015. Post-Acadian sediment recycling in the Devonian Old Red Sandstone of Southern Ireland. Gondwana Res. 28, 1415–1433. doi:10.1016/j.gr.2014.10.007

Fairey, B.J., Kerrison, A., Meere, P.A., Mulchrone, K.F., Gartner, A., Sonntag, B.-L., Linnemann, U., Kuiper, K.F., Ennis, M., Mark, C., Cogne, N., Chew, D., 2018. The provenance of the Devonian Old Red Sandstone of the Dingle Peninsula, SW Ireland; the earliest record of Laurentian and peri-Gondwanan sediment mixing in Ireland. J. Geol. Soc. London. doi: 10.1144/jgs2017-099.

Gallagher, K., Brown, R., Johnson, C., 1998. Fission track analysis and its applications to geological problems. Annu. Rev. Earth Planet. Sci. 26, 519–572. doi:10.1146/annurev.earth.26.1.519

Gehrels, G.E., Valencia, V.A., Ruiz, J., 2008. Enhanced precision, accuracy, efficiency, and spatial resolution of U-Pb ages by laser ablation-multicollector-inductively coupled plasma-mass spectrometry. Geochem., Geophys. Geosys. 9, 1–13. doi:10.1029/2007GC001805

Graham, J.R., 1975. Deposits of a near-coastal fluvial plain - the Toe Head Formation (Upper Devonian) of southwest Cork, Eire. Sediment. Geol. 14, 45–61.

Higgs, K.T., Clayton, G., Keegan, J.B., 1988. Stratigraphic and systematic palynology of the Tournaisian rocks of Ireland. Geol. Surv. Irel. Spec. Pap. 7, 5–83.

Higgs, K.T., MacCarthy, I.A.J., O'Brien, M.M., 2000. A mid-Frasnian marine incursion into the southern part of the Munster Basin: evidence from the Foilcoagh Bay Beds, Sherkin Formation, SW County Cork, Ireland. Geol. Soc. Lond., Spec. Publ. 180, 319–332. doi:10.1144/GSL.SP.2000.180.01.15

Ijlst, L., 1973. A Laboratory Overflow-Centrifuge for Heavy Liquid Mineral Separation. Am. Mineral. 58, 1088–1093.

Jarvis, E., 1990. New palynological data on the age of the Kiltorcan Flora of Co. Kilkenny, Ireland. J. Micropalaeontology 9, 87–94. doi:10.1144/jm.9.1.87

Kimbrough, D.L., Smith, D.P., Mahoney, J.B., Moore, T.E., Grove, M., Gastil, R.G., Ortega-Rivera, A., Fanning, C.M., 2001. Forearc-basin sedimentary response to rapid Late Cretaceous batholith emplacement un the peninsular ranges of southern and baja california. Geology 29, 491–494. doi:10.1130/0091-7613(2001)029<0491

Kuiper, K.F., Deino, A., Hilgen, F.J., Krijgsman, W., Renne, P.R., Wijbrans, J.R., 2008. Synchronizing Rock Clocks of Earth History. Science 320, 500–504. doi:10.1126/science.1154339

Lee, J.Y., Marti, K., Severinghaus, J.P., Kawamura, K., Yoo, H.S., Lee, J.B., Kim, J.S., 2006. A redetermination of the isotopic abundances of atmospheric Ar. Geochim. Cosmochim. Acta 70, 4507–4512. doi:10.1016/j.gca.2006.06.1563

Linnemann, U., Gerdes, A., Hofmann, M., Marko, L., 2014. The Cadomian Orogen: Neoproterozoic to Early Cambrian crustal growth and orogenic zoning along the periphery of the West African Craton-Constraints from U-Pb zircon ages and Hf isotopes (Schwarzburg Antiform, Germany). Precambrian Res. 244, 236–278. doi:10.1016/j.precamres.2013.08.007

Ludwig, K.R., 2012. User's Manual for Isoplot 3.75. Berkeley Geochronol. Cent. Spec. Publ. 1–72.

MacCarthy, I.A.J., 2007. The South Munster Basin of southwest Ireland. J.

Maps 3, 149–172. doi:10.1080/jom.2007.9710835

MacCarthy, I.A.J., 1990. Alluvial sedimentation patterns in the Munster Basin, Ireland. Sedimentology 37, 685–712. doi:10.1111/j.1365-3091.1990.tb00629.x

Mange, M., Idleman, B., Yin, Q.-Z., Hidaka, H., Dewey, J., 2010. Detrital heavy minerals, white mica and zircon geochronology in the Ordovician South Mayo Trough, western Ireland: signatures of the Laurentian basement and the Grampian orogeny. J. Geol. Soc. London. 167, 1147–1160. doi:10.1144/0016-76492009-091

Max, M.D., Ploquin, A., Sonet, J., 1979. The age of the Saltees granite in the Rosslare complex. Geol. Soc. London, Spec. Publ. 8, 723–725. doi:10.1144/GSL.SP.1979.008.01.88

McConnell, B., Rogers, R., Crowley, Q., 2016. Sediment provenance and tectonics on the Laurentian margin: implications of detrital zircons ages from the Central Belt of the Southern Uplands–Down–Longford Terrane in Co. Monaghan, Ireland. Scottish J. Geol. 52, 11–17. doi:10.1144/sjg2015-013

McDowell, F.W., McIntosh, W.C., Farley, K.A., 2005. A precise 40Ar–39Ar reference age for the Durango apatite (U–Th)/He and fission-track dating standard. Chem. Geol. 214, 249–263. doi:10.1016/j.chemgeo.2004.10.002

Meere, P.A., 1995. Sub-greenschist facies metamorphism from the Variscides of SW Ireland: an early syn-extensional peak thermal event. J. Geol. Soc. London. 152, 511–521. doi:10.1144/gsjgs.152.3.0511

Meere, P.A., Banks, D.A., 1997. Upper crustal fluid migration: an example from the Variscides of SW Ireland. J. Geol. Soc. London. 154, 975–985. doi:10.1144/gsjgs.154.6.0975

Min, K., Mundil, R., Renne, P.R., Ludwig, K.R., 2000. A test for systematic errors in 40Ar/39Ar geochronology through comparison with U/Pb analysis of a 1.1-Ga rhyolite. Geochim. Cosmochim. Acta 64, 73–98. doi:10.1016/S0016-7037(99)00204-5

Monster, M., 2016. Multi-method palaeointensity data of the geomagnetic field during the past 500 kyrs from European volcanoes. Utr. Stud. Earth Sci.

117, 103–123.

Nance, R.D, Neace, E., Braid, J., Murphy, J.B, Dupuis, N., Shail, R., 2015. Does the Meguma Terrane Extend into SW England? Geosci. Canada 42, 61–76. doi:10.12789/geocanj.2014.41.056

Nance, R.D., Murphy, J.B., Strachan, R.A., Keppie, J.D., Gutierrez-Alonso, G., Fernandez-Suarez, J., Quesada, C., Linnemann, U., D'lemos, R., Pisarevsky, S.A., 2008. Neoproterozoic-early Palaeozoic tectonostratigraphy and palaeogeography of the peri-Gondwanan terranes: Amazonian v. West African connections. Geol. Soc. London, Spec. Publ. 297, 345–383. doi:10.1144/SP297.17

O'Connor, P.J., Aftalion, M., Kennan, P.S., 1989. Isotopic U–Pb ages of zircon and monazite from the Leinster Granite, southeast Ireland. Geol. Mag. 126, 725. doi:10.1017/S0016756800007044

Paton, C., Hellstrom, J., Paul, B., Woodhead, J., Hergt, J., 2011. Iolite: Freeware for the visualisation and processing of mass spectrometric data. J. Anal. At. Spectrom. 26, 2508. doi:10.1039/c1ja10172b

Penney, S., 1980. A new look at the Old Red Sandstone succession of the Comeragh Mountains, County Waterford. J. Earth Sci. 3, 155–178.

Price, C.A., Todd, S.P., 1988. A model for the development of the Irish Variscides. J. Geol. Soc. London. 145, 935–939. doi:10.1144/gsjgs.145.6.0935

Roycroft, P., 1991. Magmatically zoned muscovite from the peraluminous two-mica granites of the Leinster batholith, southeast Ireland. Geology 19, 437–440. doi:10.1130/0091-7613(1991)019<0437

Scharf, A., Handy, M.R., Schmid, S.M., Favaro, S., Sudo, M., Schuster, R., Hammerschmidt, K., 2016. Grain-size effects on the closure temperature of white mica in a crustal-scale extensional shear zone - Implications of in-situ 40Ar/39Ar laser-ablation of white mica for dating shearing and cooling (Tauern Window, Eastern Alps). Tectonophysics 674, 210–226. doi:10.1016/j.tecto.2016.02.014

Schoene, B., Bowring, S.A., 2006. U–Pb systematics of the McClure Mountain syenite: thermochronological constraints on the age of the 40Ar/39Ar standard MMhb. Contrib. to Mineral. Petrol. 151, 615–630.

doi:10.1007/s00410-006-0077-4

Sleeman, A.G., McConnell, B., 1995. A geological description of East Cork, Waterford and adjoining parts of Tipperary and Limerick to accompany the bedrock geology 1:100,000 scale map series, sheet 22, East Cork - Waterford with contributions by K. Claringbold, P. O'Connor, W.P. Warren and . Geological Survey of Ireland, Dublin.

Snee, L.W., Sutter, J.F., Kelly, W.C., 1988. Thermochronology of economic mineral deposits; dating the stages of mineralization at Panasqueira, Portugal, by high-precision 40 / 39 Ar age spectrum techniques on muscovite. Econ. Geol. 83, 335–354. doi:10.2113/gsecongeo.83.2.335

Soper, N.J., Woodcock, N.H., 2003. The lost Lower Old Red Sandstone of England and Wales : a record of post-Iapetan flexure or Early Devonian transtension? Geol. Mag. 140, 627–647. doi:10.1017/S0016756803008380

Stacey, J.S., Kramers, J.D., 1975. Approximation of terrestrial lead isotope evolution by a two-stage model. Earth Planet. Sci. Lett. 26, 207–221. doi:10.1016/0012-821X(75)90088-6

Thomson, S.N., Gehrels, G.E., Ruiz, J., Buchwaldt, R., 2012. Routine low-damage apatite U-Pb dating using laser ablation-multicollector-ICPMS. Geochemistry, Geophys. Geosystems 13. doi:10.1029/2011GC003928

Vermeesch, P., 2013. Multi-sample comparison of detrital age distributions. Chem. Geol. 341, 140–146. doi:10.1016/j.chemgeo.2013.01.010

Vermeesch, P., 2012. On the visualisation of detrital age distributions. Chem. Geol. 312–313, 190–194. doi:10.1016/j.chemgeo.2013.01.010

Vermeesch, P., 2004. How many grains are needed for a provenance study? Earth Planet. Sci. Lett. 224, 441–451. doi:10.1016/j.epsl.2004.05.037

Vermeesch, P., Resentini, A., Garzanti, E., 2016. An R package for statistical provenance analysis. Sediment. Geol. 336, 14–25. doi:10.1016/j.sedgeo.2016.01.009

Vermeulen, N.J., Shannon, P.M., Masson, F., Landes, M., 2000. Wide-angle seismic control on the development of the Munster Basin, SW Ireland. Geol. Soc. London, Spec. Publ. 180, 223–237. doi:10.1144/GSL.SP.2000.180.01.11

Waldron, J.W.F., Floyd, J.D., Simonetti, A., Heaman, L.M., 2008. Ancient Laurentian detrital zircon in the closing Iapetus ocean, Southern Uplands terrane, Scotland. Geology 36, 527–530. doi:10.1130/G24763A.1

Waldron, J.W.F., Schofield, D.I., Dufrane, S.A., Floyd, J.D., Crowley, Q.G., Simonetti, A., Dokken, R.J., Pothier, H.D., 2014. Ganderia-Laurentia collision in the Caledonides of Great Britain and Ireland. J. Geol. Soc. London. 171, 555–569. doi:10.1144/jgs2013-131

Waldron, J.W.F., Schofield, D.I., White, C.E., Barr, S.M., 2011. Cambrian successions of the Meguma Terrane, Nova Scotia, and Harlech Dome, North Wales : dispersed fragments of a peri-Gondwanan basin? J. Geol. Soc. London. 168, 83–98. doi:10.1144/0016-76492010-068.Cambrian

Williams, E.A., 2000. Flexural cantilever models of extensional subsidence in the Munster Basin (SW Ireland) and Old Red Sandstone fluvial dispersal systems. Geol. Soc. London, Spec. Publ. 180, 239–268. doi:10.1144/GSL.SP.2000.180.01.12

Williams, E.A., Sergeev, S.A., Stossel, I., Ford, M., 1997. An Eifelian U–Pb zircon date for the Enagh Tuff Bed from the Old Red Sandstone of the Munster Basin in NW Iveragh, SW Ireland. J. Geol. Soc. London 154, 189–193. doi:10.1144/gsjgs.154.2.0189

Williams, E.A., Sergeev, S.A., Stossel, I., Ford, M., Higgs, K.T., 2000. U-Pb zircon geochronology of silicic tuffs and chronostratigraphy of the earliest Old Red Sandstone in the Munster Basin, SW Ireland. Geol. Soc. London, Spec. Publ. 180, 269–302. doi:10.1144/GSL.SP.2000.180.01.13

Williams, E., Bamford, M., Cooper, M., Edwards, H., Ford, M., Grant, G., MacCarthy, I., McAfee, A., O'Sullivan, M., 1989. Tectonic controls and sedimentary response in the Devonian-Carboniferous Munster and South Munster basins, south-west Ireland, in: Arthurton, R., Gutteridge, P., Nolan, S. (Eds.), The Role of Tectonics in Devonian and Carboniferous Sedimentation in the British Isles. The Yorkshire Geological Society, Bradford, pp. 120–141.

Zattin, M., Andreucci, B., Thomson, S.N., Reiners, P.W., Talarico, F.M., 2012. New constraints on the provenance of the ANDRILL AND-2A succession (western Ross Sea, Antarctica) from apatite triple dating. Geochemistry,

4 Deciphering Laurentian, peri-Gondwanan, Caledonide and Variscide sediment sources in the offshore Mesozoic basins of southern Ireland using detrital zircon U-Pb and detrital white mica ^{40}Ar-^{39}Ar ages.

(Current manuscript status: ready for submission, JGSL)

Brenton Fairey[1], Aidan Kerrison[1], Patrick A. Meere[1], Kieran F. Mulchrone[2], Mandy Hofmann[3], Andreas Gärtner[3], Benita-Lisette Sonntag[3], Ulf Linnemann[3] and Klaudia F. Kuiper[4]

[1]School of Biological, Earth and Environmental Sciences, University College Cork, Cork, Ireland.

[2]School of Applied Mathematics, University College Cork, Cork, Ireland

[3]Senckenberg Naturhistorische Sammlungen Dresden, Museum für Mineralogie und Geologie, Königsbrücker Landstraße 159, D-01109 Dresden, Germany.

[4]Faculty of Earth Sciences Vrije Universiteit Amsterdam, De Boelelaan 1085, NL-1081 HV Amsterdam, The Netherlands.

Abstract

The North Celtic Sea Basin (NCSB), South Celtic Sea Basin (SCSB), Fastnet and Goban Spur basins are extensional basins in a failed rift setting which preserve Permian to Cenozoic sedimentary successions. These successions provide a record of Pangaea breakup and Alpine compression and inversion. This study presents the first detrital zircon U-Pb and mica ^{40}Ar-^{39}Ar ages for Triassic to Cretaceous sedimentary rocks in this region with the aim of not only establishing sediment sources and pathways, but developing a better understanding of regional palaeogeography with respect to adjacent major tectonostratigraphic units. Using a combination of multidimensional scaling analysis and inverse Monte-Carlo modelling, we find that Triassic sediments in the NCSB and Fastnet Basins were likely sourced from areas to the south and to the northwest respectively. Recycling of Upper Old Red

Sandstone (UORS) of Laurentian affinity played a major role in providing sediment to the Jurassic NCSB and Lower Cretaceous northeastern NCSB. The Lower Jurassic sediments of the Fastnet Basin and Middle Jurassic sediments of the Goban Spur Basin show similar Laurentian detrital zircon distributions, including an absence of late Neoproterozoic zircons, which precludes a Flemish Cap/Orphan Knoll connection during these times. Sediment sources for the Lower Cretaceous sandstones in the NCSB, SCSB and Fastnet Basin were probably situated to the south or east of these basins and were either of Cadomian/East Avalonian affinity or recycled from early Carboniferous sandstones. The complexity and variability of sediment sources for these basins highlights the need for further detailed provenance investigations within the Celtic Sea region.

4.1 Introduction

The provenance of sedimentary rocks can become increasingly difficult to constrain with decreasing age of deposition. This is due to the increasing likelihood of having clastic sedimentary sources (i.e. sediment recycling). The offshore sedimentary basins of southern Ireland, which preserve Mesozoic to Cenozoic sedimentary successions, lie in a region in which a number of major tectonostratigraphic units are proximal enough to be considered potential sediment sources (Figure 4–1). These terranes and/or domains (*sensu* Hibbard et al., 2007) host a variety of potential sources - from Mesoproterozoic Laurentian igneous suites to Carboniferous shallow-marine carbonates. Mesozoic basin-forming processes in this region involve a number of transtensional and transpressional (and resulting inversion) cycles associated with the opening of the Atlantic Ocean and breakup of the Pangean supercontinent (Shannon, 1991). In the offshore basins of southern Ireland (Figure 4–2), structures tend to develop along pre-existing zones of crustal weakness inherited from the Caledonian and Variscan orogenic events (Ewins and Shannon, 1995) . The style of sedimentation and the potential sediment source areas would have been dictated by such tectonic activity.

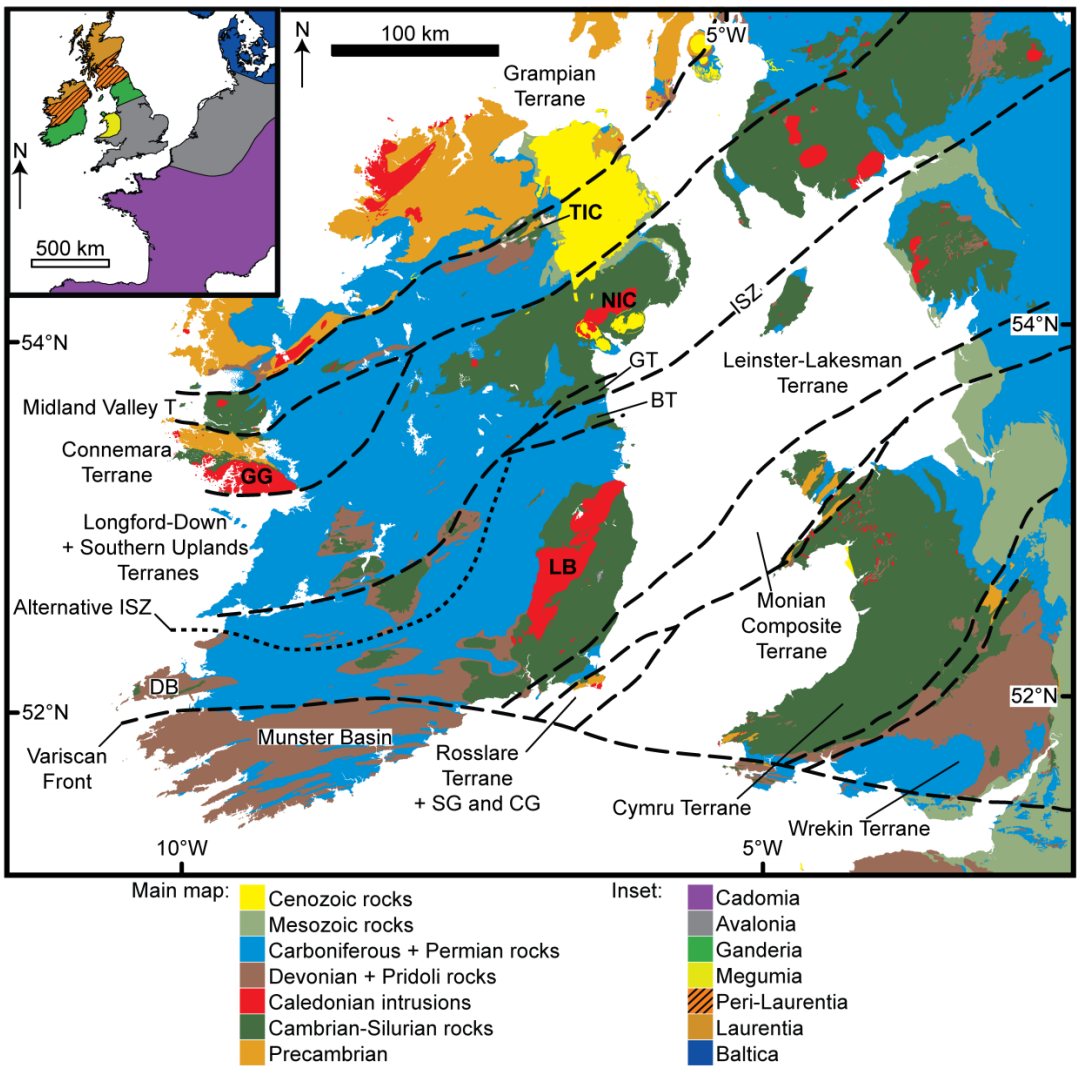

Figure 4–1. Regional map of the British Isles showing the major terranes of Ireland (modified after McIlroy and Horák 2006; Waldron et al., 2014; McConnell et al., 2016; alternative ISZ after Todd et al., 1991). Inset: regional map showing broad tectonic domains (Linnemann et al., 2007; Nance et al., 2012; Waldron et al., 2014, 2011, 2009) Key: BT, Bellewstown Terrane; CG, Carnsore Granite; DB, Dingle Basin; GG, Galway Granite; GT, Grangegeeth Terrane; ISZ, Iapetus Suture Zone; NIC, Newry Igneous Complex; SG; Saltees Granite; TIC, Tyrone Igneous Complex.

Most studies undertaken in the area of interest have focussed on depositional setting and palaeoenvironments along with the structural characteristics and structural evolution of the basins. Examples include Petrie et al. (1989), Naylor (1992), McCann and Shannon (1994), Rowell (1995), Ewins and Shannon (1995), Caston (1995) and Shannon and Naylor (1998). Petrie et al. (1989), Ewins and Shannon (1995) and Caston (1995) did some provenance analysis for Jurassic and Cretaceous sediments in the NCSB (Figure 4–2) and other

offshore southern Irish basins but in all cases this was not the focus of these studies and no single grain geochronological techniques were applied.

From the literature it is evident that no studies have focussed entirely on the analysis of sediments in the southern Irish Mesozoic offshore basins with the goal of determining their provenance. Further empirical evidence is required to better constrain potential Mesozoic source areas for the southern Irish offshore basins. The geochronological analysis of detrital zircons has become an important proxy for sediment provenance in recent years as a result of laser-ablation-inductively coupled-mass spectrometry (LA-ICP-MS) which facilitates rapid analysis of a large number of grains. Complimenting this common provenance proxy with the lower closure temperature of the ^{40}Ar-^{39}Ar system in white micas (350-420 °C according to Von Eynatten and Wijbran, 2003 and references therein) ensures that the youngest possible sediment sources are captured. This study considers the sediment provenance of Triassic to Cretaceous basins that lie to the south and southwest of the Irish mainland, namely, the Celtic Sea basins, the Fastnet Basin and the Goban Spur Basin. We present the first set of single-grain detrital zircon U-Pb ages and single-grain total fusion ^{40}Ar-^{39}Ar ages of detrital white micas from the southern Irish offshore basins in order to determine the source of Triassic to Cretaceous sandstones in these basins and to test the hypothesis that sediment was recycled from the Old Red Sandstone (ORS) of southern Ireland. Determining the provenance of these basins can also aid in understanding the palaeogeography of the region during the Mesozoic. The study has the potential to answer the following questions relating to the development of the southern Irish offshore Mesozoic basins:

1) What role did the ORS of southern Ireland play in providing sediment to the basins?
2) What role is played by potential southern sources such as Cadomia?
3) Do we see evidence of a western, trans-Atlantic source (e.g. Flemish Cap or Orphan Knoll)?

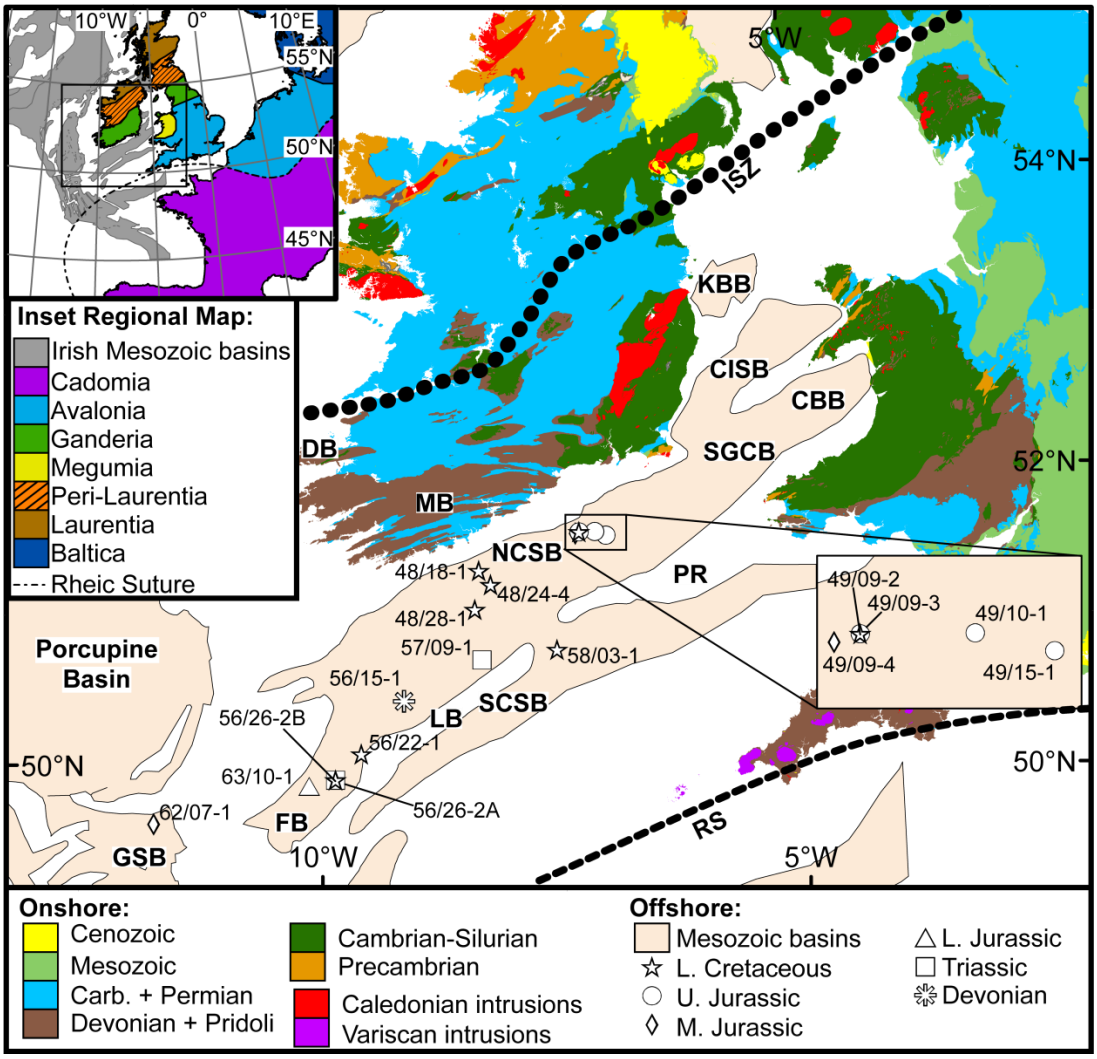

Figure 4–2. Geological map of southern Ireland and southwest United Kingdom also showing the extent of Mesozoic offshore basins in the study region. Inset, top left: broad tectonic framework of Ireland, the British Isles and parts of western Europe (modified after Linnemann et al., 2007; Nance et al., 2012; Waldron et al., 2014, 2011, 2009). Inset, bottom right: magnification of License Block 49. CBB, Cardigan Bay Basin; CISB, Central Irish Sea Basin; DB, Dingle Basin; FB, Fastnet Basin; GSB, Goban Spur Basin; ISZ, Iapetus Suture Zone; KBB, Kish Bank Basin; MB, Munster Basin; NCSB, North Celtic Sea Basin; RS, Rheic Suture; SCSB, South Celtic Sea Basin; SGCB, St. George's Channel Basin.

4.2 Geological Background

4.2.1 Regional Context and Possible Source Areas

The post-Variscan geological history of the United Kingdom and Ireland is defined by the breakup of Pangea, opening of the Tethys Ocean and rifting of the North Atlantic (Tucker and Arter, 1987) from Permian to Quaternary times.

The modern configuration of domains in the region involves peri-Gondwanan elements such as Ganderia, Megumia, Avalonia, Cadomia and, further afield, long-lived cratonic elements such as Laurentia and Baltica (Figure 4–2 inset). These domains had the potential, either directly or indirectly (through recycling), to contribute to sediment accumulation in southern Irish offshore basins during Mesozoic time.

Terranes of Laurentian affinity are abundant on the Irish mainland and many host detrital zircons of Ordovician and Silurian age (Figure 4–3). Therefore, they represent sources of Archaean, Palaeoproterozoic, Mesoproterozoic and early Palaeozoic detrital zircons. These terranes include the Grampian (e.g. Cawood et al., 2003; Chew et al., 2010; Daly, 1996; Daly et al., 1991), Connemara (e.g. Chew et al., 2010), Midland Valley (e.g. Phillips et al., 2009), Longford Down – Southern Uplands (e.g. McConnell et al., 2016; Waldron et al., 2014, 2008), Grangegeeth (e.g. McConnell et al., 2010) and Bellewstown (e.g. McConnell et al., 2015) terranes (Figure 4–1).

Rocks containing abundant detrital zircons of Laurentian origin also occur much closer to the Celtic Sea basins. To the north of the North Celtic Sea Basin (NCSB) lies the Devonian to Carboniferous rocks of the Upper Old Red Sandstone (UORS) which are underlain by Ganderian basement (Waldron et al., 2014). The proximity to the NCSB and considerable extent of the Upper Devonian UORS rocks of the Munster Basin as well as the Fammenian to Tournaisian sandstones of the South Munster Basin (SMB) make them an excellent candidate for providing sediment, particularly to the NCSB. These rocks also unconformably overlie the Mesozoic sedimentary rocks of the NCSB (Rowell, 1995). Fairey et al. (in prep.) analysed detrital zircons from the UORS in the Munster Basin and Carboniferous sandstones from the South Munster Basin and found that four groups could be distinguished based on the age distribution of detrital zircons. These groups were simply named Groups 1, 2, 3 and 4 (here called ORS Group-1, ORS Group-2, ORS Group-3 and SMB Group-4; Figure 4–3B-E) as well as a sample from the extrabasinal Harrylock Formation on Hook Head in County Wexford that did not conform to these groupings (Figure 4–3A). Group 1, 2 and 3 sedimentary rocks were interpreted to be of Laurentian affinity and included varying input of Palaeozoic

and Palaeo- and Mesoproterozoic detrital zircons from a source north of the Iapetus Suture Zone (ISZ). Group 4 sedimentary rocks are from the western part of the South Munster Basin and are interpreted by Fairey et al. (in prep.) to have been sourced predominantly from an Acadian (410-390 Ma) granitic intrusion lying off the southwest coast of Ireland (Conroy and Brock, 1989) as well as from Ganderia.

Basement for the basins in this study consists of Carboniferous sedimentary rocks similar to those found onshore (Higgs, 1983). Pre-Devonian basement, if present, has not been intersected by any of the wells drilled in the area. To the northeast of the NCSB lies the adjoining Cardigan Bay and St. George's Channel basins (Figure 4–2). These basins lie adjacent to Cambrian rocks of the Harlech Dome which have been associated with the peri-Gondwanan Meguma terrane (Waldron et al., 2011) but which were previously considered to be part of the surrounding Eastern Avalonia (e.g. Landing et al., 2000).

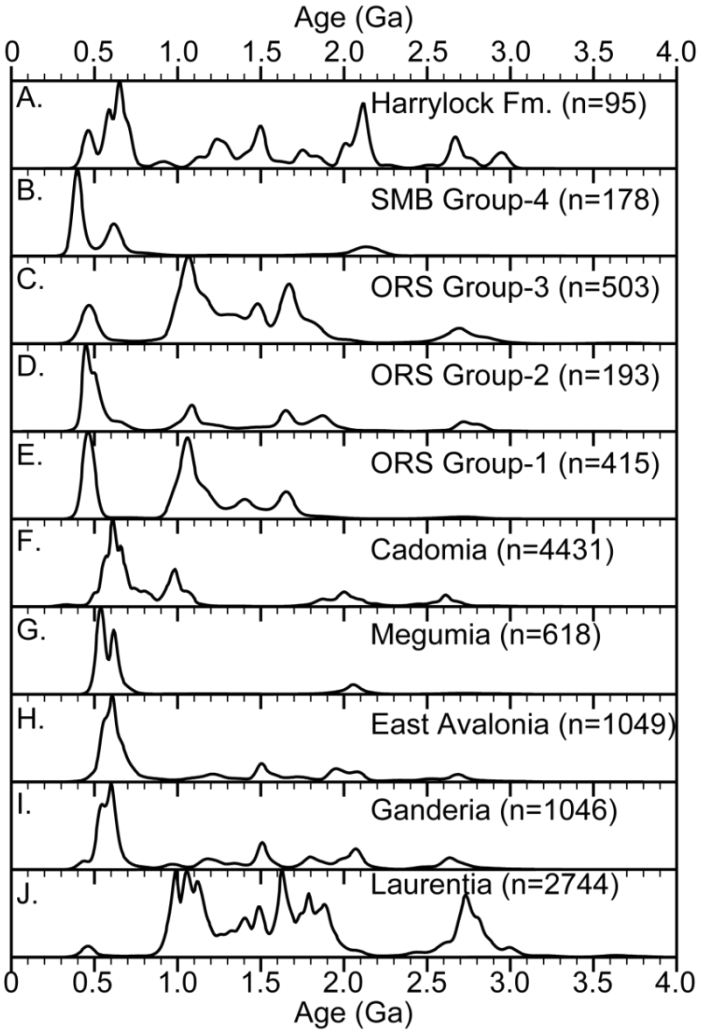

Figure 4–3. Kernel density estimation (KDE) plots of detrital zircon ages from potential source areas for offshore Mesozoic basins of southern Ireland. **A**-**E.** Provenance groupings from samples taken from the ORS and South Munster Basin of southern Ireland (Data and grouping from Fairey et al., in prep.). **F**. Detrital zircon age data interpreted to be of Cadomian affinity (data from Fernandez-Suarez et al., 2002; Fernández-Suárez et al., 2014, 2000; Henderson et al., 2016; Linnemann et al., 2008; Pastor-Galán et al., 2013; Samson et al., 2005; Strachan et al., 2014). **G**. Detrital zircon age data interpreted to be of Megumian affinity (data from Krogh and Keppie, 1990; Waldron et al., 2009, 2011; Pothier et al., 2015). **H**. Detrital zircon age data interpreted to be of East Avalonian affinity (data from Collins and Buchan, 2004; Murphy et al., 2004; Strachan et al., 2007; Linnemann et al., 2012; Willner et al., 2013). **I**. Detrital zircon age data interpreted to be of Ganderian affinity (data from Fyffe et al., 2009; Waldron et al., 2014; Willner et al., 2014). **J**. Detrital zircon age data interpreted to be of Eastern Laurentian affinity (data from Cawood et al., 2003; Friend et al., 2003; Cawood et al., 2007; Kirkland et al., 2008; Waldron et al., 2008; McAteer et al., 2010b; Cawood et al., 2012; Strachan et al., 2013; Waldron et al., 2014; Johnson et al., 2016). ORS, Old Red Sandstone; SMB, South Munster Basin.

An important regional structure lies somewhere to the south of the NCSB and South Celtic Sea Basin (SCSB) in the form of the Rheic Suture. This feature represents the remnants of the Rheic Ocean – the closure of which saw the amalgamation of Laurussia (Laurentia, Baltica, Avalonia and Ganderia) and Gondwana to form the Pangean supercontinent and associated Variscides (Nance et al., 2010). The suture's position could dictate the contribution made by Cadomian-type (see Murphy et al., 2006) stratas during Mesozoic times. It is commonly placed just south of the south coast of England where a zone of approximately east-striking Variscan thrust faults form the boundary between the Armorican Massif and Avalonia (e.g. Andonaegui et al., 2016; McKerrow et al., 2000). It extends to the southwest before swinging south and forming the boundary between the South Portuguese Zone and the Ossa-Morena Complex in southwest Iberia. It is clear that the geology surrounding the offshore basins of the Celtic Sea area is undoubtedly complex. However, in an attempt to simplify matters, we delineate five broad domain associations according to detrital zircon age distributions (Figure 4–3F-J): Cadomia (which includes northwestern Iberia as it lies south of the supposed Rheic Suture), Megumia, East Avalonia, Ganderia and Laurentia.

Other important potential source areas of peri-Gondwanan affinity are those off the coast of Newfoundland. The tectonic histories of the Orphan Knoll and Flemish Cap have become important in understanding the history of opening of the North Atlantic Ocean (e.g. Hopper et al., 2004; Mohn et al., 2015; Sibuet et al., 2007). Their Mesozoic positions with respect to the western and southwestern Irish offshore basins could play a role in the supply of sediment during that time. Zircons from a large granodiorite intrusion within the Flemish Cap yielded upper intercept ages between 751 Ma and 833 Ma, leading King et al. (1985) to conclude that the knoll is part of Avalonia. One would therefore expect to find abundant zircons of this age in sandstones derived from the Flemish Cap.

4.2.2 Exhumation history of southern Ireland and Wales

In order to determine the source of Mesozoic sediments in the southern Irish offshore basins, it is necessary, where possible, to establish what areas

were uplifted to form positive relief required for exhumation and erosion to take place. Mesozoic outliers identified in southern Ireland include the Upper Cretaceous Ballydeenlea outlier in Killarney (Evans and Clayton, 1998; Walsh, 1966), the Jurassic clays in karst cave structures in Cloyne (Higgs and Beese, 1986) and the (likely) Permo-Triassic Killag Formation outlier in County Wexford (Clayton et al., 1986). These suggest that at least some parts of the present-day land surface in southern Ireland were, at times, zones of deposition during the Mesozoic.

A number of apatite fission track (AFT) and vitrinite reflectance (VR) studies in Ireland have revealed important information on the exhumation history of the onshore areas. Green et al. (2000) concluded that AFT and VR data indicate similar post-Carboniferous burial and exhumation histories across onshore Ireland, including cooling intervals in the late Carboniferous to Permian, Middle Jurassic and Early Cretaceous, as well as two Cenozoic episodes. This represents a minimum total of 1.5 km of overburden removed since the Jurassic (Green et al., 2000) . In a more extensive AFT study of Ireland, Allen et al. (2002) developed denudation maps for onshore Ireland from Triassic to Middle Jurassic times. Their modelling for the Mesozoic era records the most wide-spread and highest rates of denudation in southern Ireland during Triassic to Middle Jurassic times. Southern Ireland during Cretaceous time, however, was largely a zone of deposition because only minor cooling around the southwest peninsulas and the northern part of the Leinster Massif was observed (Allen et al., 2002).

Cogné et al. (2014), using AFT as well as apatite (U+Th)/He dating, record a Late Jurassic to Early Cretaceous episode of exhumation of a ca. 2.5 km thick package of Devonian and Carboniferous rocks in southwest Ireland. In the eastern part of southern Ireland, around the Galtee Mountains and Leinster Massif, Cogné et al. (2016) show that a significant exhumation event took place during the Early Jurassic. They link this to the thick Lower Jurassic sedimentary successions in the NCSB. In Wales, Mesozoic exhumation took place in Permo-Triassic times around the areas of Snowdonia and Pembrokeshire, in Early to Middle Jurassic times around Anglesey and in Late Triassic times around the Brecon Beacons area (Cogné et al., 2016). Although

exhumation of these areas in Wales has direct implications for sedimentation in proximal basins (e.g. St. Georges Channel, Cardigan Bay, Central Irish Sea), its relevance to the NCSB and SCSB is dependent upon the along-axis interconnectivity of proximal and distal basins during the Mesozoic.

4.2.3 Local Geology

The choice of southern Irish offshore sedimentary basins on which to focus this study was largely dictated by the availability of sample material for analysis. Therefore, the NCSB forms the main topic of this paper. Sampling rationale and sample descriptions are discussed in greater detail in the next section.

4.2.3.1 NCSB, SCSB and Fastnet Basin

The NCSB, like most other offshore Irish basins, is developed in a failed-rift environment associated with the breakup of Pangaea and the formation of the North Atlantic Ocean (Petrie et al., 1989). The structure of the basement in this area is particularly important in terms of basin development. The architecture of the NCSB, SCSB and Fastnet Basin is controlled by pre-existing Caledonian (roughly northeast-southwest) and Variscan (roughly east-west thrust faults and northwest-southeast strike-slip faults) structural trends (Rowell, 1995; Shannon and Naylor, 1998). This is evident in the general northeast-southwest trends of the basin axes. The basement, affected by these major orogenic events, is likely to be a continuation of onshore Upper Devonian to Carboniferous sedimentary rocks (Higgs, 1983) as well as Variscan-related (e.g. Cornubian Batholith) granitic intrusions. The NCSB and Fastnet Basin are separated from the SCSB by a structural high known as the Labadie Bank – Pembrokeshire Ridge (Shannon and Naylor, 1998).

Although sediment began to accumulate in the SCSB during the Permian, widespread sedimentation in the NCSB and Fastnet Basin did not take place until the Late Triassic (Shannon, 1991). Tyrrell et al. (2012) support this in their palaeogeographic reconstruction of the region at this time. Permian sedimentation was restricted to localised intermontane basins associated with Variscan topographic elevation (Shannon, 1995). The Triassic

palaeoenvironments of the NCSB and Fastnet Basin, in which the Sherwood Sandstone Group and the Mercia Mudstone Group were deposited, is said to have included arid alluvial and fluvial systems, floodplain and sabhka systems and coastal settings (Shannon, 1995). Therefore, depositional environments were largely continental at this time and sediment accumulation was accommodated by synrift extension and, later, thermal subsidence (Shannon, 1995). Triassic deposits in the SCSB are dominated by thick salt successions with interbedded red mudstone beds, representing deposition in a shallow, hypersaline lacustrine environment (Shannon, 1995).

In Early Jurassic times, the NCSB and SCSB were largely characterised by near-coastal environments as well as open-marine conditions (Ewins and Shannon, 1995; Petrie et al., 1989). The Fastnet Basin was largely a deltaic environment during this time (Ewins and Shannon, 1995), although Petrie et al. (1989) suggest that the Lower Jurassic sedimentary rocks in the Fastnet Basin represent a shallow marine environment. The early Middle Jurassic was dominated by open-marine conditions in the NCSB followed by a marine regression which led to the development of continental facies toward the end of the Middle Jurassic and into the Late Jurassic (Petrie et al., 1989). According to Shannon (1991), the Early to Middle Jurassic was a time of tectonic quiescence in the Celtic Sea area. Petrie et al. (1989) suggest that, although subsidence was passive (thermal) at this time, the adjacent massifs were uplifted as a prologue to major rifting in the Late Jurassic. Middle Jurassic successions in the Fastnet Basin are poorly and intermittently developed and generally not present in the SCSB, either representing non-deposition or Early Cretaceous inversion (Shannon, 1991). The end of the Middle Jurassic in the NCSB is marked by a major unconformity and onset of Late Jurassic syn-rift alluvial, fluvial and shallow marine sedimentation (Shannon, 1991). Rifting became the major contributor of subsidence at this time and, as a result, evidence of eustatic sea-level changes were often overprinted (Ewins and Shannon, 1995). Upper Jurassic successions are absent in the SCSB and Fastnet Basin.

The onset of Cretaceous basin development in the NCSB, SCSB and Fastnet Basin is marked by an unconformity followed by fluvial and alluvial

sedimentation (Shannon, 1991). These Cretaceous sedimentary rocks consist of the non-marine Middle to Upper Purbeck successions which were overlain by rocks of the Wealden Facies (Caston, 1995). An episode of rifting during the Early Cretaceous meant that these sediments were being deposited in a synrift setting dominated by fluvial and alluvial environments (Shannon, 1991). The Wealden Facies in the Fastnet Basin represents deposition, at first, in fluvial and alluvial environments, and later, in lagoonal settings (Ainsworth et al., 1985). The waning of rifting and onset of thermal subsidence is marked at the top of the Lower Cretaceous by the Greensand Group consisting of glauconitic sandstones of shallow marine influence (Shannon, 1991). The Upper Cretaceous successions in the NCSB, SCSB and Fastnet Basin are dominated by deep marine chalks (Shannon, 1991).

Cenozoic sedimentation is complicated by the effects of Alpine compression which caused basin inversion in the Celtic Sea area (Shannon, 1991). At least one kilometer of stratigraphy was removed in two uplift events (Shannon and Naylor, 1998). As a result, Palaeogene sedimentary rocks are poorly represented in the NCSB (Shannon and Naylor, 1998).

4.2.3.2 Goban Spur Basin

Rifting in the Goban Spur Basin area began in mid-Triassic times, according to Naylor and Shannon (2005). The basin is separated from the Fastnet Basin by the Fastnet High to the east (Naylor and Shannon, 2011) and from the Porcupine Basin by the Porcupine Fault to the north (Dingle and Scrutton, 1979). The basement has been identified through dredging (Auffret et al., 1979) and from drilling in the Deep Sea Drilling Project (De Graciansky et al., 1985) which show that it predominantly consists of Upper Devonian to Carboniferous sedimentary rocks intruded by Variscan granitoids. The granitoids, sampled by dredging, were dated by Auffret et al. (1979), yielding ages of between 275 Ma (whole rock Rb-Sr) and 290 Ma (K-Ar biotite).

The Lower to Middle Jurassic successions are said to have been deposited in a continental shelf environment (Naylor and Shannon, 2011). These were overlain by a thick succession of Middle Jurassic basalts (Naylor and Shannon, 2011). Upper Jurassic stratigraphy is not present in the Goban

Spur, instead the basalts are unconformably overlain by Lower Cretaceous sedimentary rocks (Naylor and Shannon, 2005) that are of shallow marine origin (Shannon, 1991).

4.3 Sampling and methods

Original well logs from the 1970s and 1980s were analysed to determine which wells were best suited for sampling. Fifteen samples were taken for geochronological analysis from 14 wells across the North Celtic Sea, South Celtic Sea, Fastnet and Goban Spur Basins (Figure 4–4 and Figure 4–5). Petrographic samples were taken from four wells in the NCSB and the only well in the Goban Spur Basin.

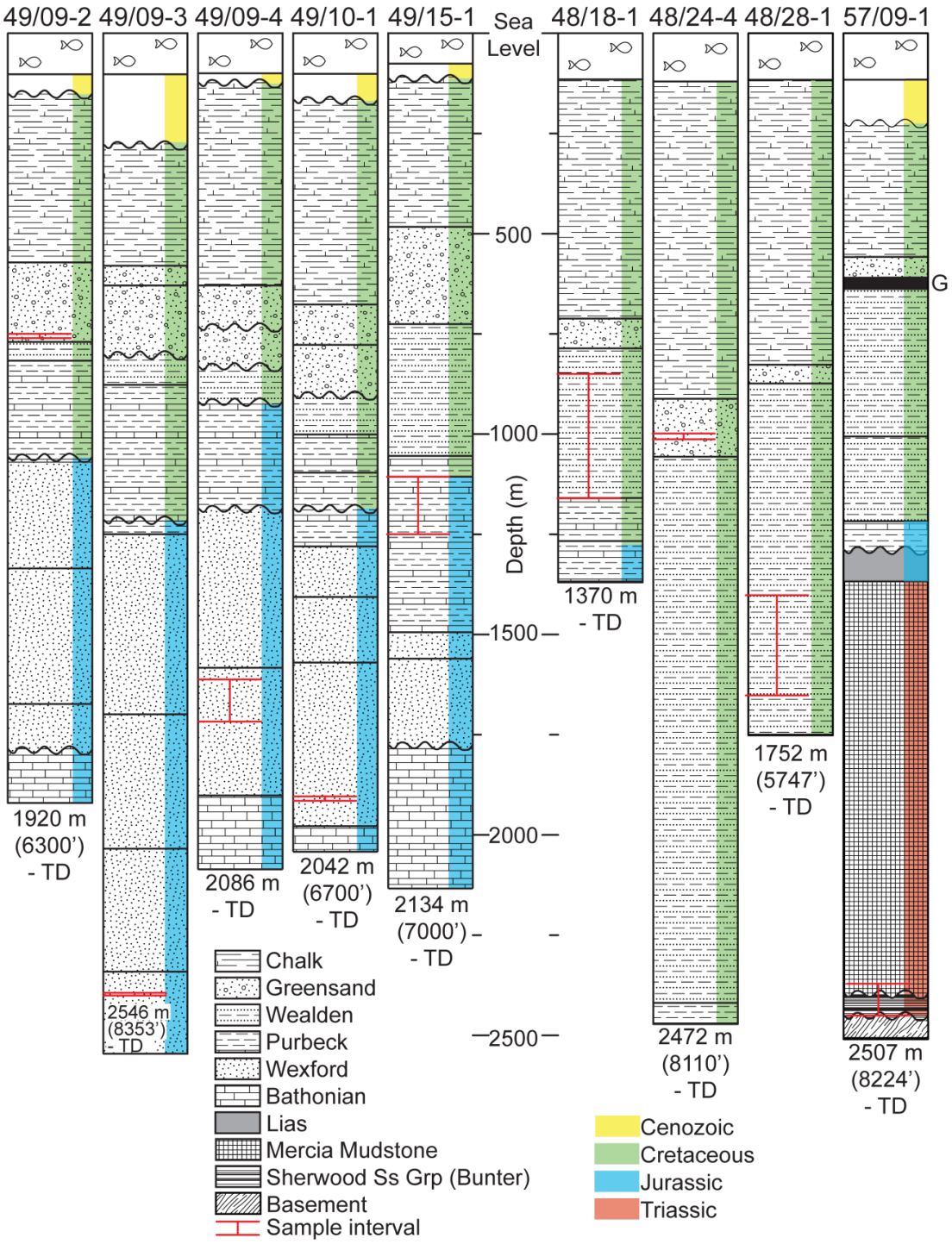

Figure 4–4. Generalised stratigraphic logs of sampled wells in the NCSB showing sample intervals (adapted from composite logs compiled by BP, Marathon, Esso and Gulf). G, Gault clay; TD, total depth.

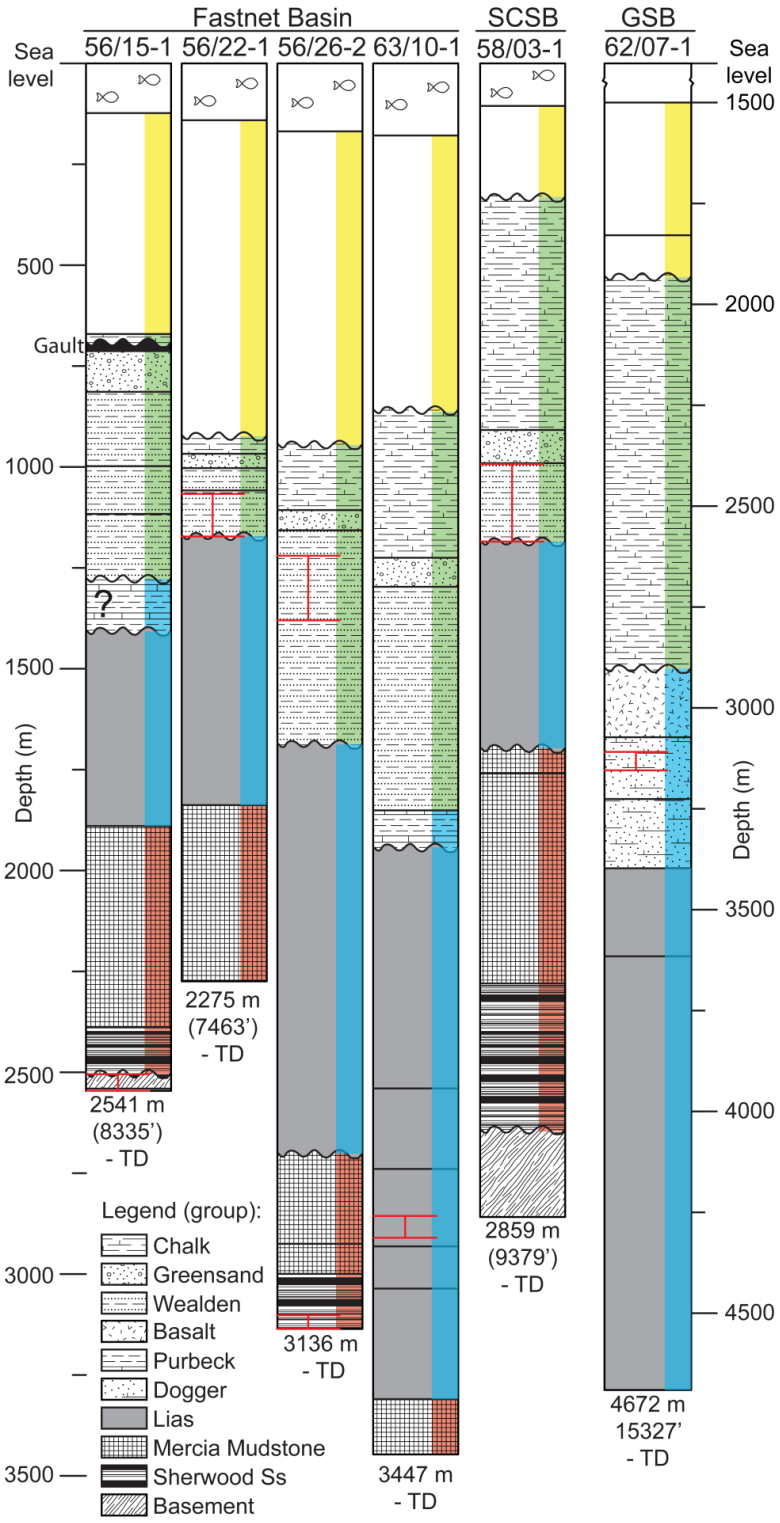

Figure 4–5. Generalised stratigraphic logs of sampled wells in the Fastnet, Goban Spur and South Celtic Sea Basins showing sampled intervals (adapted from composite logs compiled by BP, Chevron, Conoco, Esso, Ireland Cities Services, Schlumberger and Texaco). GSB, Goban Spur Basin ; SCSB, South Celtic Sea Basin. See Figure 4–4 for colour code.

4.3.1 Detrital zircon samples

Uranium, thorium and lead isotopes were measured by LA-SF-ICP-MS at the Museum für Mineralogie und Geologie (Geoplasma Lab, Senckenberg Naturhistorische Sammlungen Dresden). Further details of laser and ICP-MS parameters, as well as data reduction protocols, can be found in Linnemann et al. (2014) and references therein. Concordia diagrams and concordia ages were produced using Isoplot/Ex 3.7 of Ludwig (2012). Frequency and relative probability plots (both probability density plots [PDP] and kernel density estimation [KDE]) were plotted using DensityPlotter (Vermeesch, 2012). Frequency plots were assigned a bandwidth of 25 Ma. KDEs were plotted using a bandwidth of 20 Ma and a Gaussian kernel. The $^{207}Pb/^{206}Pb$ age was used for zircons older than 1.0 Ga whereas the $^{206}Pb/^{238}U$ age was used for zircons that were younger than 1.0 Ga. Statistical tests for measuring the relationship between samples were undertaken using DZstats v2.0 (Saylor and Sundell, 2016) and mixture modelling was done using DZMix v1.1.3 (Sundell and Saylor, 2017). The mixture modelling was undertaken using 10 000 model trials of which 1 % best fits were used. KDE density distributions were set at a bandwidth of 20 Ma for the cross correlation coefficient statistic. Optimization was not undertaken on the results. In this study we used the K-S test D statistic as our main means of comparing detrital zircon source contributions as it utilises cumulative density functions which avoid the oversmoothing pitfalls of both probability density plots and KDE plots.

4.3.2 Detrital white mica samples

Due to the common use of mica as a means of preventing loss of circulation during drilling, precaution was taken when selecting samples for mica geochronology. Therefore, only core material was used or cuttings where micas could be macroscopically identified within them. Of the samples that met these criteria, five yielded enough grains for provenance analysis. The five samples are from wells 56/26-2, 56/15-1, 49/9-3, 49/9-2 and 48/24-4. A full methodology can be found in Fairey et al. (in prep.).

4.3.3 Petrographic samples

Drill cores that contained coarse and pebbly sandstones were of particular interest for petrographic analysis. Petrographic samples were taken from the Middle Jurassic in 62/7-01, Upper Jurassic in 49/10-01 and 49/9-3 and Lower Cretaceous in 48/24-04. Polished thin sections were produced from these samples and observed under a light microscope as well as a scanning electron microscope (SEM) at the iCRAG Laboratory, Trinity College Dublin.

4.4 Results

4.4.1 Petrography

Here we describe petrographic samples from drill core samples only – where the sample being described is well contextualised. The sample from a Middle Jurassic section in well 62/07-1 consists of very fine quartz arenite (mean grain size: ~ 80 µm) with minor feldspar (Figure 4–6A). Overall, it is moderately- to well sorted, although grain size ranges from ca. 20 µm to ca. 200 µm. The brownish, extremely fine-grained matrix makes up less than 10 % of the rock and reduces primary porosity. Accessory phases include zircon, tourmaline and muscovite. The grain size and sorting suggest a low- to moderate-energy depositional environment. The majority of quartz grains are spherical and sub-angular, suggesting high transport distances in a subaqueous environment.

Two lithologies were sampled from the Upper Jurassic drill core in well 49/10-1. The first is a fine sublitharenite (mean grain size: ~ 150 µm) that is poorly sorted (grain size range: ~ 30 to ~ 300 µm) (Figure 4–6B). Many grains have quartz overgrowths which obscure the grain shape. Some calcite cement is present. Accessory minerals include tourmaline, zircon and muscovite.

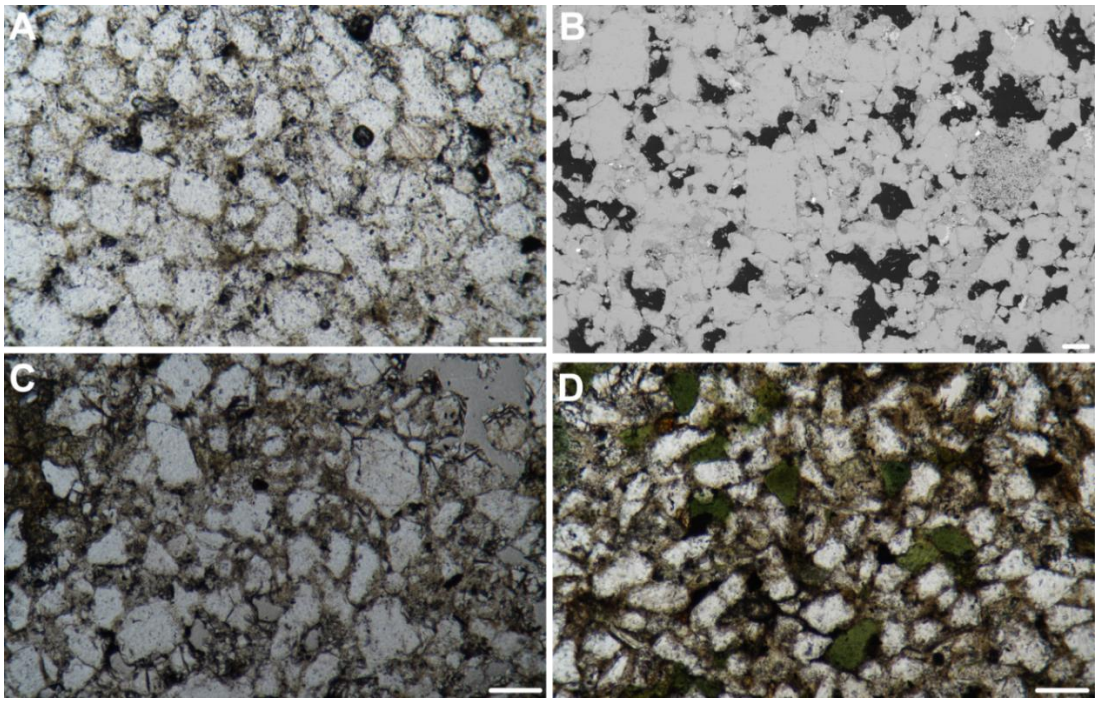

Figure 4–6. Representative petrographic images from drill core samples. **A**. Plane-polarised light photomicrograph of sample 62/07-1 (Middle Jurassic, Fastnet Basin). **B**. Scanning electron microscope back scattered electron image of sandstone from sample 49/10-1 (Upper Jurassic, NCSB). **C**. Plane-polarised light photomicrograph of sample 49/09-3 (Upper Jurassic, NCSB). **D**. Plane-polarised light photomicrograph of greensand from sample 48/24-4 (Lower Cretaceous, NCSB). White bar measures 100 µm.

The second lithology is a pebble conglomerate. In hand specimen, pebbles include jasper, coal, shale, quartz and quartzite. In thin section, the majority of clasts (mean grain size of ca. 500 µm) consist of monocrystalline quartz. Lithic fragments are present and are mostly composed of fine-grained sedimentary rocks including shale, chert, limestone, as well as vein quartz. Poikilotopic calcite forms the dominant cement and significantly reduces porosity. The rock is generally poorly sorted (50 µm to 1.5 cm) and clast roundness ranges from sub-angular to well-rounded. Both lithologies from well 49/10-1 represent deposition in a braided river environment.

Sample 49/09-3 consists of very fine-grained, poorly sorted quartz arenite (mean grain size: ~ 140 µm) (Figure 4–6C). Grain boundaries are obscured by quartz overgrowths. Tourmaline and zircon are present as accessory phases

and carbonate forms the dominant cement. The poor sorting suggests a proximal source of quartz in this sandstone.

A sample from the Lower Cretaceous section of well 48/24-4 is composed of glauconite-rich, bioturbated (on a macroscopic scale), well sorted, very fine-grained (mean grain size: ~ 63 µm) quartz arenite (Figure 4–6D). The majority of quartz grains are angular and overgrown by dusty quartz. Accessory minerals include zircon, muscovite and tourmaline. Small amounts of plant material are also present. The pervasive bioturbation, fine grain size and dominance of glauconite are suggestive of a shallow inner shelf environment with low sedimentation rates.

4.4.2 Zircon U-Pb Geochronology

4.4.2.1 57/09-1 (Lower Triassic – NCSB)

Approximately 18 m of Lower Triassic interbedded red to brown claystones and sandstones were sampled from well 57/09-1 in the NCSB. One hundred and seven concordant analyses ranging in age from 297 ± 4 Ma to 3311 ± 25 Ma were obtained from 136 grains. Sixty one grains (57 %) have Neoproterozoic ages, forming the largest KDE peak at ca. 602 Ma (Figure 4–7A). The second largest proportion of grains are Palaeozoic in age (22 %, n = 24) and include the second largest KDE peak, developed around 320 Ma. The majority of Palaeozoic grains are Carboniferous (n = 9) and Devonian (n = 6) in age. Two minor KDE peaks are developed at ca. 950 Ma and ca. 1.91 Ga. A spread of single grains occurs with Mesoproterozoic and Palaeoproterozoic ages but these do not form any conspicuous KDE peaks. Three Archaean grains are present in the sample. The three youngest grains give a concordia age of 299 ± 3 Ma ($MSWD_{conc}$ = 0.018; p_{conc} = 0.89).

4.4.2.2 49/09-4 (Middle Jurassic – NCSB)

Drill cuttings taken from a 105 m Middle Jurassic section in well 49/09-4 from the NCSB intersected interbeds of sandstones and mudstones with minor limestone and conglomerate. One hundred and forty six analyses produced 99 concordant ages ranging from 320 ± 7 Ma to 3019 ± 35 Ma. The largest proportion of grains (33 %; n = 33) are Mesoproterozoic in age and form a

major KDE peak at ca. 1.04 Ga and a less prominent peak at ca. 1.26 Ga (Figure 4–7B). Zircons of Neoproterozoic age make up the second largest proportion at 26 % (n = 26), forming the largest KDE peak at ca. 626 Ma and a secondary peak at ca. 545 Ma. A similar proportion (25 %; n = 25) of zircons in the sample are Palaeoproterozoic in age and form a major peak at ca. 1.66 Ga and a minor peak at ca. 1.76 Ga. Four of the eight Archaean grains have ages between 2.67 Ga and 2.78 Ga. Of the seven Palaeozoic grains, three are Cambrian, two are Silurian, one is Devonian and one is Carboniferous in age.

4.4.2.3 49/15-1 (Upper Jurassic – NCSB)

Approximately 140 m of drill cuttings were sampled from an Upper Jurassic section in well 49/15-1 in the NCSB. The section is dominated by sandstone but includes minor intercalations of mudstone, siltstone and limestone. The large volume of drilling mud present in the original sample left uncertainty as to the final yield of drill cuttings – hence a large interval was taken to produce enough zircons for provenance analysis. One hundred and twenty concordant ages were obtained from 156 grains. These ages range from 355 ± 10 Ma to 2908 ± 21 Ma. Mesoproterozoic (40 %; n = 48) and Palaeoproterozoic (30 %; n = 36) grains make up the bulk of the sample, producing major KDE peaks at ca. 1.08 Ga and ca. 1.66 Ga (Figure 4–7C). Neoproterozoic grains make up 14 % (n = 17) of the sample and a single KDE peak is developed at ca. 600 Ma. Palaeozoic grains make up 11 % (n = 13) forming a single KDE peak at ca. 447 Ma. Six Archaean grains are present in the sample, forming a broad KDE peak at ca. 2.82 Ga.

4.4.2.4 49/10-1 (Upper Jurassic – NCSB)

This sample was taken from a ca. 11 m drill core section that intersected interbedded pebble conglomerates and medium- to coarse-grained sandstone. One hundred and forty seven grains were analysed yielding 82 concordant ages ranging from 349 ± 6 Ma to 2794 ± 21 Ma. The bulk of grains have Proterozoic ages, Palaeoproterozoic grains making up 37 % (n = 30), Neoproterozoic grains making up 27 % (n = 22) and Mesoproterozoic grains

making up 17 % (n = 14) of the sample. Archaean grains make up 11 % (n = 9), producing minor KDE peaks at 2.55 Ga and 2.77 Ga (Figure 4–7D). The largest KDE peak in the sample is developed at ca. 638 Ma. The second largest peak occurs at ca. 2.08 Ga. Secondary KDE peaks also occur at ca. 1.07 Ga and ca. 1.66 Ga. Palaeozoic grains represent the lowest proportion (9 %; n = 7) in the sample producing one KDE peak at ca. 368 Ma. A paucity of ages is noted between 2.2 Ga and 2.5 Ga as well as between 750 Ma and 950 Ma.

4.4.2.5 49/09-3 (Upper Jurassic – NCSB)

This sample was taken from a ca. 7 m drill core section (Core #2) consisting of fine- to medium-grained massive, cream-coloured sandstone of Late Jurassic age. Ninety six concordant ages were obtained from 126 detrital zircon analyses in this sample. These ages range from 176 ± 3 Ma to 3010 ± 17 Ma. Palaeoproterozoic zircons and Mesoproterozoic zircons are equally abundant in the sample, each representing 27 % (n = 24). Palaeoproterozoic KDE peaks occur at 1.64 Ga, 1.97 Ga and 2.15 Ga. The largest KDE peak occurs at ca. 1.04 Ga and a secondary Mesoproterozoic peak occurs at 1.18 Ga (Figure 4–7E). Neoproterozoic zircons account for 19 % (n = 17) of the sample and a major Neoproterozoic peak occurs at ca. 655 Ma. Thirteen zircon grains (15 %) are of Palaeozoic age and form a major KDE peak at ca. 470 Ma and a secondary peak at ca. 540 Ma. Eight zircons are Archaean in age, including five grains with ages between 2.72 Ga and 2.85 Ga. The three youngest zircons in the sample form a concordia age of 176 ± 2 Ma ($MSWD_{conc}$ = 0.013; p_{conc} = 0.91).

4.4.2.6 48/28-1 (Lower Cretaceous – NCSB)

A 250 m section of drill cuttings was taken from the Lower Cretaceous of well 48/28-1. Ninety five concordant ages ranging from 254 ± 16 Ma to 2861 ± 26 Ma were obtained from 134 zircon grains. The highest proportion of zircons in the sample are Neoproterozoic in age (29 %; n = 28) and the largest KDE peak is developed at ca. 580 Ma (Figure 4–7F). The second largest proportion (23 %; n = 22) consists of Palaeozoic zircons and has a

corresponding KDE peak at ca. 359 Ma as well as a secondary peak at ca. 446 Ma. Mesoproterozoic zircons make up 24 % (n = 23), including two KDE peaks at ca. 1.05 Ga and ca. 1.13 Ga. Palaeoproterozoic zircons make up 18 % of the sample. A number of minor KDE peaks occur in this age range but the largest of them is at ca. 1.95 Ga. Five Archaean zircons have a spread of ages between 2.40 Ga and 2.87 Ga. Gaps in age distributions occur between 1.15 Ga and 1.40 Ga and between 2.00 Ga and 2.40 Ga.

4.4.2.7 48/18-1 (Lower Cretaceous – NCSB)

The sampled section consists of 310 m of drill cuttings taken from interbedded mudstones, sandstones and conglomerates of Early Cretaceous age. One hundred and thirty zircon grains yielded 83 concordant ages ranging from 383 ± 6 Ma to 3162 ± 27 Ma. More than half of the zircons in the sample (53 %; n = 44) are Neoproterozoic in age and contribute to a dominant KDE peak at ca. 613 Ma (Figure 4–7G). Palaeozoic zircons make up 20 % (n = 17) of the sample and form the second largest KDE peak at 428 Ma. Sixteen percent (n = 13) are Palaeoproterozoic in age, 7 % (n = 6) are Mesoproterozoic and three of the zircon are Archaean in age. Very minor KDE peaks occur at ca. 783 Ma, 955 Ma and 2.1 Ga. A general paucity of ages is noted between 1.02 Ga and 2.04 Ga. The two youngest grains in the sample yield a concordia age of 384 ± 6 Ma ($MSWD_{conc}$ = 0.005; p_{conc} = 0.94).

4.4.2.8 48/24-4 (Lower Cretaceous – NCSB)

A 14 m drill core interval of grey, fine-grained, glauconitic sandstone of Early Cretaceous age was sampled from well 48/24-4 in the NCSB. One hundred and forty one analysed grains produced concordant ages ranging from 373 ± 8 Ma to 3513 ± 30 Ma. The highest proportion of grains (31 %, n = 27) are Neoproterozoic in age and represent the largest KDE peak in the sample at ca. 624 Ma (Figure 4–7H). Twenty two grains (25 %) are Palaeoproterozoic in age. These are represented by KDE peaks at ca. 1.78 Ga and ca. 2.08 Ga. Palaeozoic grains make up 22 % of the sample (n = 19) in which the second largest KDE peak is developed at ca. 409 Ma. A broad KDE peak is developed at ca. 1.60 Ga and consists of Meso- and

Palaeoproterozoic grains. Mesoproterozoic grains contribute 15 % (n = 13) of the sample but do not produce any conspicuous KDE peaks. Three zircon grains form a minor KDE peak at ca. 988 Ma. Six Archaean grains occur in the sample. Five of these have ages between 2.67 Ga and 2.88 Ga. No zircons in the sample have ages between 2.18 Ga and 2.67 Ga. A single grain has an age of 3513 ± 30 Ma.

4.4.2.9 49/09-2 (Lower Cretaceous – NCSB)

Eleven meters of dark grey, glauconite-rich, fine-grained sandstone was sampled from a Lower Cretaceous drill core section of well 49/09-2 in the NCSB. One hundred and forty analyses yielded 98 concordant ages ranging from 128 ± 3 Ma to 2888 ± 26 Ma. Mesoproterozoic grains dominate the sample (n = 41). The largest KDE peak occurs at ca. 1.09 Ga but secondary Mesoproterozoic peaks also occur at ca. 1.24 Ga and 1.50 Ga (Figure 4–7I). Twenty four Palaeoproterozoic grains are present in the sample, forming a single, broad KDE peak at 1.70 Ga. Fifteen grains are Neoproterozoic in age and form KDE peaks at ca. 576 Ma and ca. 978 Ma. Archaean grains constitute 11 % (n = 11) of the sample and form a minor KDE peak at 2.70 Ga. The six Palaeozoic grains in the sample form a minor KDE peak at 467 Ma. The KDE peak at ca. 128 Ma is a poor candidate for maximum depositional age of the sediment as it consists of a single analysis but gives a tentative Barremian age. There is a paucity of ages between 670 Ma and 940 Ma as well as between 1.88 Ga and 2.46 Ga.

4.4.2.10 56/26-2A (Lower Triassic – Fastnet Basin)

Thirty four meters of Lower Triassic sandstone with minor siltstone interbeds was sampled from drill cuttings in well 56/26-2 from the Fastnet Basin. Of the 125 detrital zircon analyses conducted on the sample, 77 yielded concordant ages ranging from 301 ± 9 Ma to 3127 ± 42 Ma. In the KDE spectrum, two dominant peaks are present: one at ca. 397 Ma and one at ca. 669 Ma. The largest proportions of zircon ages correspond to these peaks, including 31 % (n = 24) Neoproterozoic zircons and 27 % (n = 21) Palaeozoic zircons (Figure 4–7J). Thirteen of the Palaeozoic zircons are Devonian in age,

four are Silurian and four are Carboniferous. Palaeoproterozoic aged zircons make up 25 % (n = 19) and include small KDE peaks at ca. 1.91 and 2.15 Ga. Mesoproterozoic zircons constitute 13 % (n = 10) of the sample. Three zircons of Archaean age are present.

4.4.2.11 63/10-1 (Lower Jurassic – Fastnet Basin)

This sample consists of drill cuttings from a 54 m Sinemurian section in well 63/10-1 from the Fastnet Basin. The dominant lithology consists of poorly- to moderately sorted fine-grained sandstone with interbedded shales. One hundred and sixty four analyses yielded 135 concordant ages ranging from 419 ± 8 Ma to 3051 ± 23 Ma. The overwhelming majority of zircon grains have Palaeoproterozoic (43 %; n = 58) and Mesoproterozoic (33 %; n = 44) ages. The largest KDE peak occurs at ca. 1.73 Ga but subordinate peaks occur at 441 Ma, 1.12 Ga, 1.42 Ga, 1.49 Ga, 1.96 Ga and 2.77 Ga (Figure 4–7K). Archaean grains make up 14 % (n = 19) of the sample and Palaeozoic zircons make up the remainder (6 %; n = 8). Three grains are Ordovician, four are Silurian and one is Devonian. A paucity of zircon ages occurs between 500 and 900 Ma and between 2.08 and 2.66 Ga.

4.4.2.12 56/26-2B (Lower Cretaceous – Fastnet Basin)

One hundred and thirty detrital zircons were analysed from this sample, yielding 91 concordant analyses which range in age from 306 ± 8 Ma to 3076 ± 42 Ma. A 160 m section of Lower Cretaceous, moderately- to well-sorted sandstone with minor interbedded mudstones was sampled from drill cuttings from well 56/26-2 in the Fastnet Basin. Detrital zircons of Palaeoproterozoic age make up the largest proportion in the sample at 30 % (n = 27) and the third largest KDE peak occurs at ca. 1.74 Ga (Figure 4–7L). The largest and second largest peaks, however, have ages of ca. 397 Ma and 597 Ma respectively. Mesoproterozoic zircons constitute 24 % (n = 22) of the sample and form minor KDE peaks at ca. 1.39 Ga and 1.53 Ga and a broad peak at ca. 1.15 Ga. Seventeen zircons (19 %) are Neoproterozoic in age. Nineteen zircons (21 %) are Palaeozoic in age (one Ordovician, three Silurian, 11

Devonian and three Carboniferous). A spread of Archaean grains occurs between 2.5 and 3.1 Ga (n = 6).

4.4.2.13 56/22-1 (Lower Cretaceous – Fastnet Basin)

The sample consists of drill cuttings from a 106 m Lower Cretaceous section of predominantly sandstone lithology with interbedded mudstone and minor coal beds. Seventy three concordant detrital zircon ages were extracted from a total of 106 analyses. These ages range from 377 ± 6 Ma to 2632 ± 31 Ma. Neoproterozoic ages are the most abundant in the sample (37 %; n = 27) and form a major KDE peak at ca. 623 Ma (Figure 4–7M). Palaeoproterozoic grains represent 29 % (n = 21) of the sample but have widely distributed ages and form diffuse KDE peaks at ca. 2.07 and 1.68 Ga. Palaeozoic grains make up 25 % (n = 18) and form a major peak at ca. 429 Ma. Mesoproterozoic grains (7 %; n = 5) form a broad peak at ca. 1.13 Ga. Two Neoarchaean grains are present. Only one grain age occurs between 750 Ma and 1.09 Ga and there are no zircons with ages between 1.23 and 1.64 Ga.

4.4.2.14 58/03-1 (Lower Cretaceous – SCSB)

Approximately 200 m of drill cuttings were sampled, yielding ca. 200 g of sample (after removal of drilling mud). The sampled interval is composed of sandstones with intercalated mudstones and coal seams. One hundred and forty one zircon grains yielded 85 concordant ages ranging from 326 ± 7 Ma to 2968 ± 15 Ma. Thirty four grains (40 %) are Neoproterozoic in age, forming a major KDE peak at ca. 598 Ma (Figure 4–7N). Equal numbers of Palaeoproterozoic and Mesoproterozoic grains occur in the sample (n = 18; 21 %). Palaeozoic grains form the second largest KDE peak at ca. 421 Ma and make up 15 % (n = 13) of the sample. Minor KDE peaks occur at ca. 839 Ma, 943 Ma, 1.04 Ga, 1.49 Ga, 1.64 Ga, 1.94 Ga and 2.09 Ga. Two Archaean grains are present in the sample.

4.4.2.15 62/07-1 (Middle Jurassic - Goban Spur Basin)

This sample constitutes ca. 46 m of drill cuttings from well 62/07-1 which is Middle Jurassic in age and consists of fine- to medium-grained, moderately-

to well-sorted sandstone with interbedded siltstone. Well 62/07-1 is the only existing well in the Goban Spur Basin. Ninety two concordant detrital zircon ages were acquired from 108 analyses ranging from 396 ± 10 Ma to 3631 ± 25 Ma. The largest proportion (39 %; n = 36) of zircons is Palaeoproterozoic in age, corresponding to the dominant KDE peak at ca. 1.63 Ga and a secondary KDE peak at 1.95 Ga (Figure 4–7O). Mesoproterozoic-aged zircons make up the second largest proportion at 33 % (n = 30). A conspicuous Archaean KDE peak is present at ca. 2.78 Ga and is made up of a spread of ages between 2.65 and 2.90 Ga. Archaean grains represent 15 % (n = 14). There is a notable lack of zircons between 2.05 and 2.50 Ga as well as between 475 and 930 Ma. A dominant peak occurs at ca. 441 Ma and makes up the 9 % of Palaeozoic zircons. Of these, five are Ordovician, two are Silurian and one is Devonian in age.

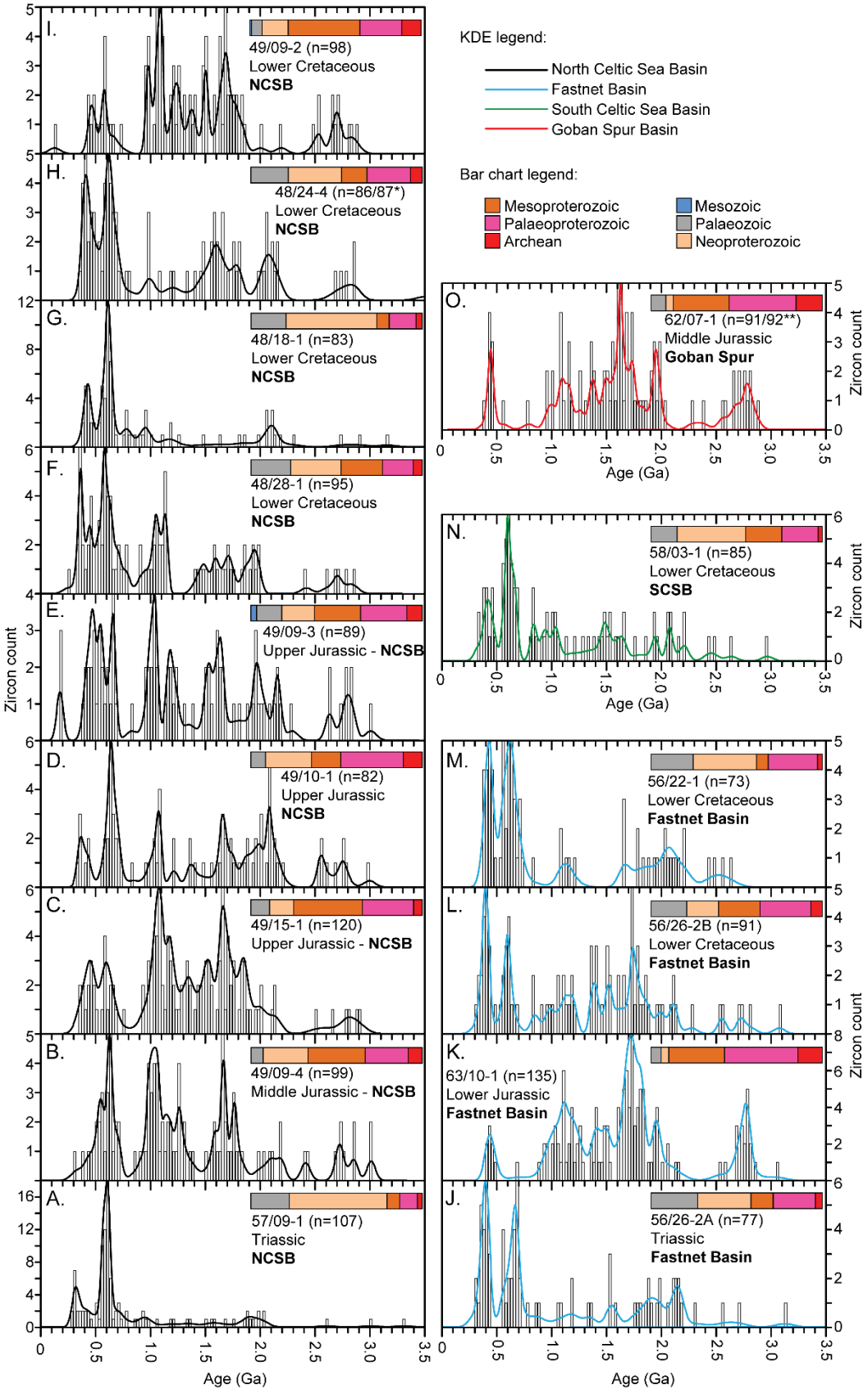
KDE legend:
North Celtic Sea Basin
Fastnet Basin
South Celtic Sea Basin
Goban Spur Basin
Bar chart legend:
Mesoproterozoic
Palaeoproterozoic
Archean
Mesozoic
Palaeozoic
Neoproterozoic
I.
49/09-2 (n=98)
Lower Cretaceous
NCSB
H.
48/24-4 (n=86/87*)
Lower Cretaceous
NCSB
G.
48/18-1 (n=83)
Lower Cretaceous
NCSB
F.
48/28-1 (n=95)
Lower Cretaceous
NCSB
E.
49/09-3 (n=89)
Upper Jurassic - NCSB
D.
49/10-1 (n=82)
Upper Jurassic
NCSB
C.
49/15-1 (n=120)
Upper Jurassic - NCSB
B.
49/09-4 (n=99)
Middle Jurassic - NCSB
A.
57/09-1 (n=107)
Triassic
NCSB
O.
62/07-1 (n=91/92**)
Middle Jurassic
Goban Spur
N.
58/03-1 (n=85)
Lower Cretaceous
SCSB
M.
56/22-1 (n=73)
Lower Cretaceous
Fastnet Basin
L.
56/26-2B (n=91)
Lower Cretaceous
Fastnet Basin
K.
63/10-1 (n=135)
Lower Jurassic
Fastnet Basin
J.
56/26-2A (n=77)
Triassic
Fastnet Basin
Zircon count
Age (Ga)

Figure 4–7

4.4.2.16 Summary

A total of 1764 detrital zircon grains were analysed from thirteen samples from across the NCSB and Fastnet Basin as well one sample each from the Goban Spur and SCSB. These yielded 1415 ages that are 90-110 % concordant. From the NCSB one sample is Triassic in age, one is Middle Jurassic in age, three are of Late Jurassic age and four are of Early Cretaceous depositional age. From the Fastnet Basin one sample is of Triassic age, one is of Early Jurassic age and two are of Early Cretaceous depositional age. The sample from the Goban Spur has a Middle Jurassic depositional age and the single sample from the SCSB has an Early Cretaceous depositional age. The samples therefore cover a time span of approximately 100 Ma.

All samples, with the exception of 63/10-1 and 62/07-1, contain late Neoproterozoic detrital zircons that form a conspicuous KDE peak. Samples 49/09-4, 49/09-3, 49/09-2, 63/10-1 and 62/7-01 have distinct Archaean KDE peaks between 2.65 Ga and 2.9 Ga that are made up of four or more zircons. Conversely, samples 57/09-1, 48/18-01, 56/25-2A, 56/22-1 and 58/03-1 have a total of three zircons or less that are Archaean in age. Samples 49/09-4, 49/15-1, 49/09-3 and 49/09-2 have dominant KDE peaks between 1.0 Ga and 1.2 Ga. Samples 48/24-1, 56/26-2A, 56/26-2B and 56/22-1 have dominant 400 Ma KDE peaks.

Figure 4–7. KDE plots (bandwidth = 20 Ma) and histograms (binwidth = 25 Ma) for Mesozoic samples taken from the NCSB (**A**-**I**), Fastnet Basin (**J**-**M**), SCSB (**N**) and Goban Spur Basin (**O**). The plots have not been normalised to equal areas but histogram counts are provided to facilitate comparison. Proportions of zircon ages are also shown. *one zircon age not shown in the plot occurs at ca. 3.5 Ga. **one zircon age not shown in the plot occurs at ca. 3.6 Ga.

4.4.3 White mica ^{40}Ar-^{39}Ar Geochronology

With the exception of sample 49/15-1 from the well of the same name, all the samples described are taken from the same intervals as those analysed for detrital zircon geochronology. In total, five samples produced 282 ^{40}Ar-^{39}Ar ages (Figure 4–8). Sixty eight white micas from a Triassic section of well 56/26-2 in the Fastnet Basin produced ages ranging from 308 ± 1 Ma to 607 ± 4 Ma and a single KDE peak at ca. 579 Ma (Figure 4–8A). Forty white micas from a section thought to be equivalent of the Old Head Sandstone Formation (of the onshore Munster Basin) in well 56/15-1 yielded ages ranging from 282 ± 1 Ma to 1424 ± 5 Ma. Twenty two of these have ages between 350 Ma and 400 Ma and form a major KDE peak at 368 Ma (Figure 4–8B). Other very minor, broad KDE peaks occur at ca. 290, 491 and 561 Ma. Sixty eight white mica grains were analysed from an Upper Jurassic sample from well 49/09-3 in the NCSB and produced ages ranging from 303 ± 3 Ma to 684 ± 2 Ma. A dominant KDE peak is developed at ca. 405 Ma and a minor peak at ca. 429 Ma (Figure 4–8C).

Thirty seven white mica grains from a Lower Cretaceous sample in well 49/09-2 yielded ages between 406 ± 6 Ma and 473 ± 11 Ma. These ages form a single KDE peak at ca. 431 Ma (Figure 4–8D). Another Lower Cretaceous sample taken from well 48/24-4 yielded 69 detrital mica ages which range from 367 ± 12 Ma to 687 ± 7 Ma. These form a dominant KDE peak at ca. 431 Ma and minor peaks at ca. 404 and 458 Ma (Figure 4–8E).

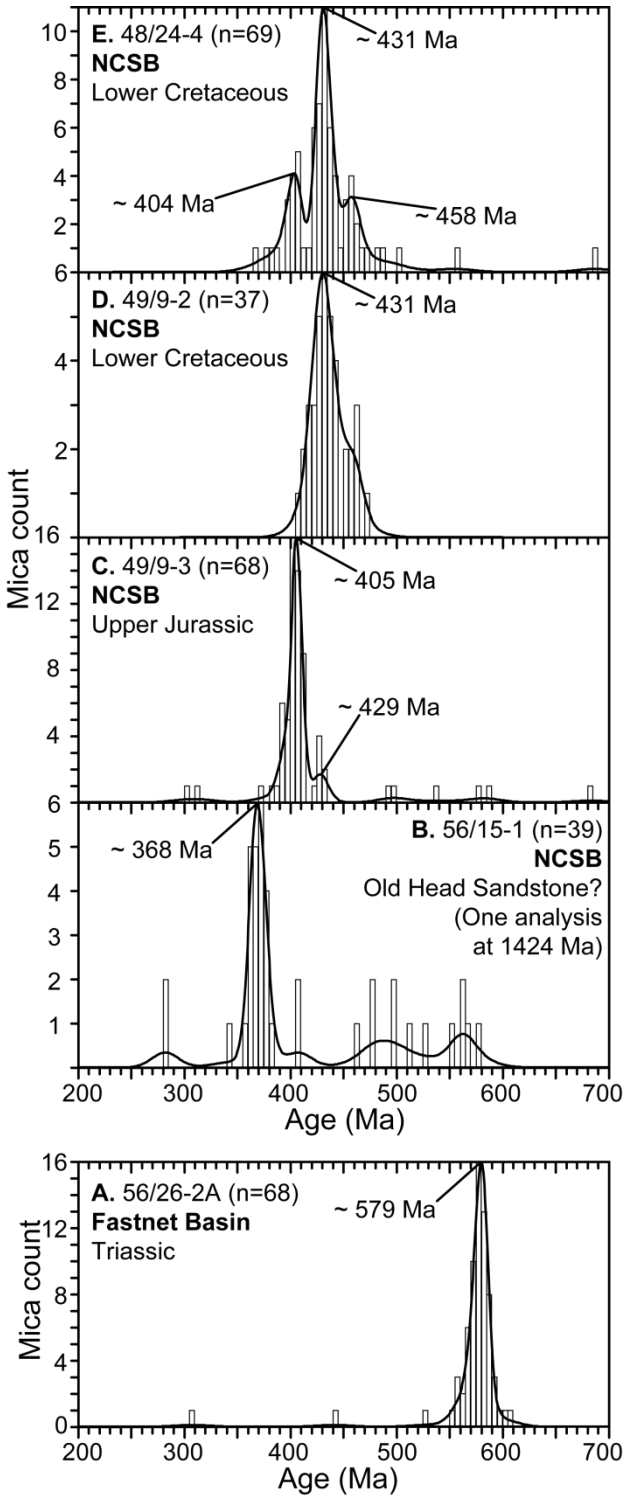

Figure 4–8. Kernel density estimation plots (bandwidth = 5 Ma) and histograms (binwidth = 5 Ma) for white mica ages in well samples from the Fastnet (**A**) and North Celtic Sea (**B**-**E**) basins.

4.5 Discussion: Mesozoic palaeodrainage configurations in the Fastnet, Goban Spur and Celtic Sea basins

In the following sections we consider the provenance of each basin within the study area and provide a summary of possible palaoedrainage patterns throughout the Mesozoic for the southern Irish offshore basins. We have used inverse Monte Carlo modelling implemented in DZMix v1.1.3 (Sundell and Saylor, 2017) to determine the proportions of potential detrital zircon sources (those shown in Figure 4–3) that contributed to each sample (Figure 4–9). Due to the low number of zircons analysed (<100) in some of the samples, we use the method only to determine which potential sources were major contributors and place no particular importance on the specific relative contribution of each source. The method also assumes that all potential sources have been accounted for, but this assumption cannot be made with full confidence for ancient samples.

4.5.1 Triassic

One sample of Triassic depositional age was recovered from the southern margin of the NCSB. The age distribution of its zircons is simple, relative to those taken from higher up in the NCSB stratigraphy (a major peak at ca. 602 Ma and a much smaller, but conspicuous peak at ca. 320 Ma; Figure 4–10). The location of the well, proximal to the southern margin of the basin, would suggest that the source lay to the south of the basin. This suggestion is further supported by evidence of onlap of Triassic sediments onto basement rocks of the Labadie Bank, indicating that this feature formed a positive ridge in the area during the Triassic (Shannon, 1995). Inverse Monte Carlo modelling of potential source contributions (Figure 4–9A) suggests that a mixed source of Tournaisian rocks of the South Munster Basin (SMB Group-4) and detrital zircons of Meguma affinity may have been the main contributors. However, the 320 Ma Palaeozoic KDE peak is a diagnostic component.

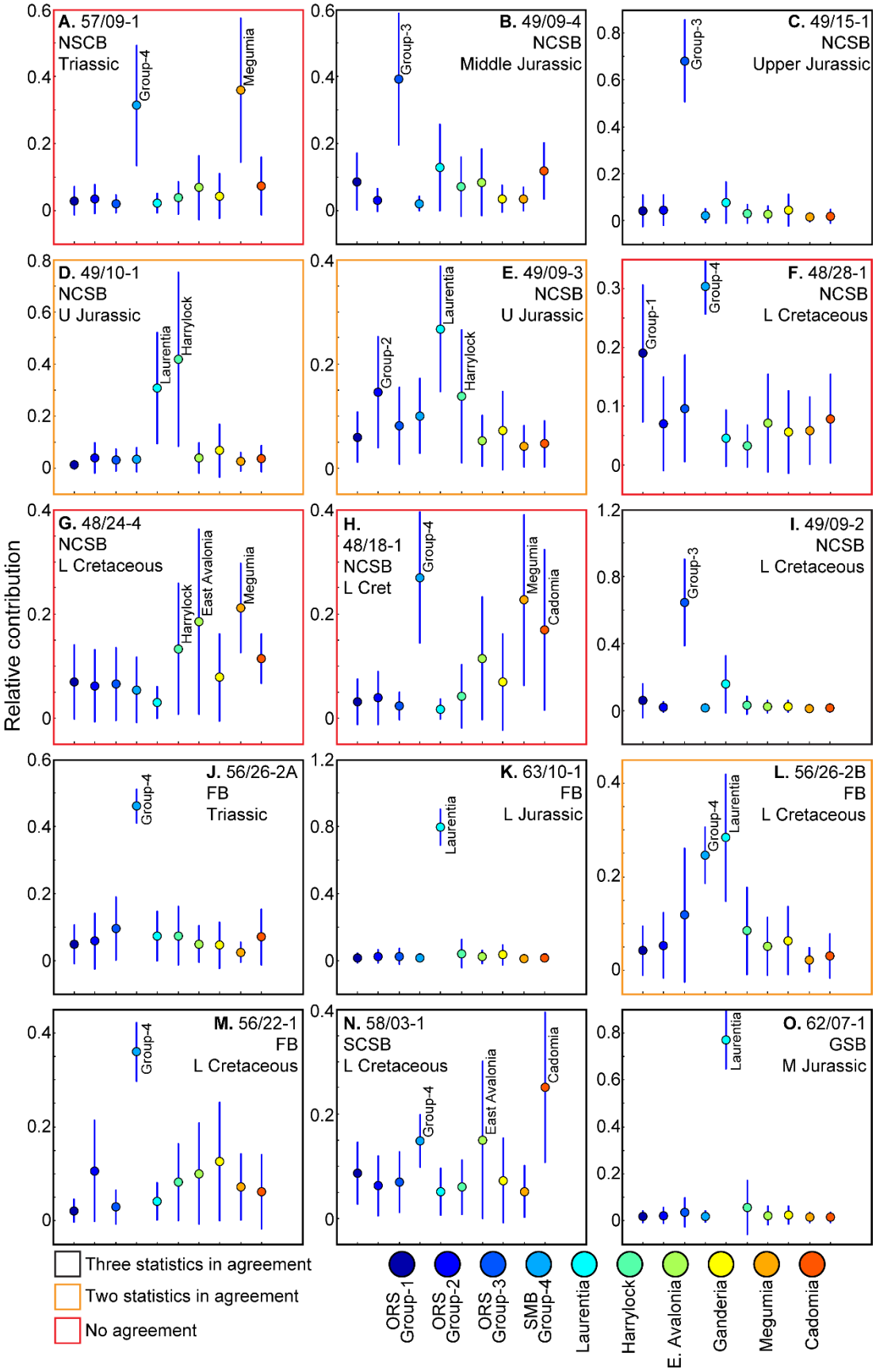
A. 57/09-1
NSCB
Triassic
Group-4
Megumia
B. 49/09-4
NCSB
Middle Jurassic
Group-3
C. 49/15-1
NCSB
Upper Jurassic
Group-3
D. 49/10-1
NCSB
U Jurassic
Laurentia
Harrylock
E. 49/09-3
NCSB
U Jurassic
Group-2
Laurentia
Harrylock
F. 48/28-1
NCSB
L Cretaceous
Group-1
Group-4
G. 48/24-4
NCSB
L Cretaceous
Harrylock
East Avalonia
Megumia
H.
48/18-1
NCSB
L Cret
Group-4
Megumia
Cadomia
I. 49/09-2
NCSB
L Cretaceous
Group-3
J. 56/26-2A
FB
Triassic
Group-4
K. 63/10-1
FB
L Jurassic
Laurentia
L. 56/26-2B
FB
L Cretaceous
Group-4
Laurentia
M. 56/22-1
FB
L Cretaceous
Group-4
N. 58/03-1
SCSB
L Cretaceous
Group-4
East Avalonia
Cadomia
O. 62/07-1
GSB
M Jurassic
Laurentia
Relative contribution
Three statistics in agreement
Two statistics in agreement
No agreement
ORS Group-1
ORS Group-2
ORS Group-3
SMB Group-4
Laurentia
Harrylock
E. Avalonia
Ganderia
Megumia
Cadomia

Figure 4–9

Although minor trachytic dykes ranging in age from 314 Ma to 296 Ma intrude UORS sedimentary rocks in southwest Ireland (Quinn et al., 2005), the nearest significant potential source of zircons of 320 Ma age lies to the south in the form of Variscan-related granitoid intrusions. These are present in northwest Iberia (Fernandez-Suarez et al., 2000) as well as in Armorican terranes (Augier et al., 2015; Ducassou et al., 2011; Tartèse et al., 2011). Therefore, the source area likely lay to the south, south of the Rheic Suture but also incorporated proximal detritus from the Labadie Bank and possibly sediment from the Harlech Dome (Megumia, according to Waldron et al., 2011) to the northeast (Figure 4–11A).

Detrital zircon age spectra from Triassic samples from the western margin of the Wessex Basin in the United Kingdom show very similar age distributions to the NCSB sample of this study (Figure 4–10). These were interpreted by Morton et al. (2016) to represent a Cadomian source with very minor contribution from Variscan granites. This interpretation supports a southern source, although the Variscan granitoids have played a greater role in supplying sediment to the NCSB than in the Wessex Basin.

In the Fastnet Basin, sample 56/26-2A was taken from the Triassic Sherwood Sandstone Formation. The sample shares few similarities with the Sherwood Sandstone Formation sample taken from the NCSB. The late Neoproterozoic KDE peak is shifted toward older ages, Early Devonian zircons are dominant and a conspicuous KDE peak occurs at around 2.1 Ga (Figure 4–10). The implication is that different source areas were operating for each basin during the deposition of the Sherwood Sandstone Formation. Mixture modelling for sample 56/26-2A (Figure 4–9J) shows that South Munster Basin sedimentary rocks were a major contributor during Triassic times.

Figure 4–9. Relative contributions of known potential source regions modelled using an inverse Monte Carlo approach implemented in DZMix v1.1.3 of Sundell and Saylor (2017). Three statistics are measured (cross-correlation coefficient, Kuiper test V statistic and K-S test D statistic) but here we show only the K-S test D statistic. Border colours indicate observed level of agreement between the three statistics based on all statistics showing the same highest contributing source.

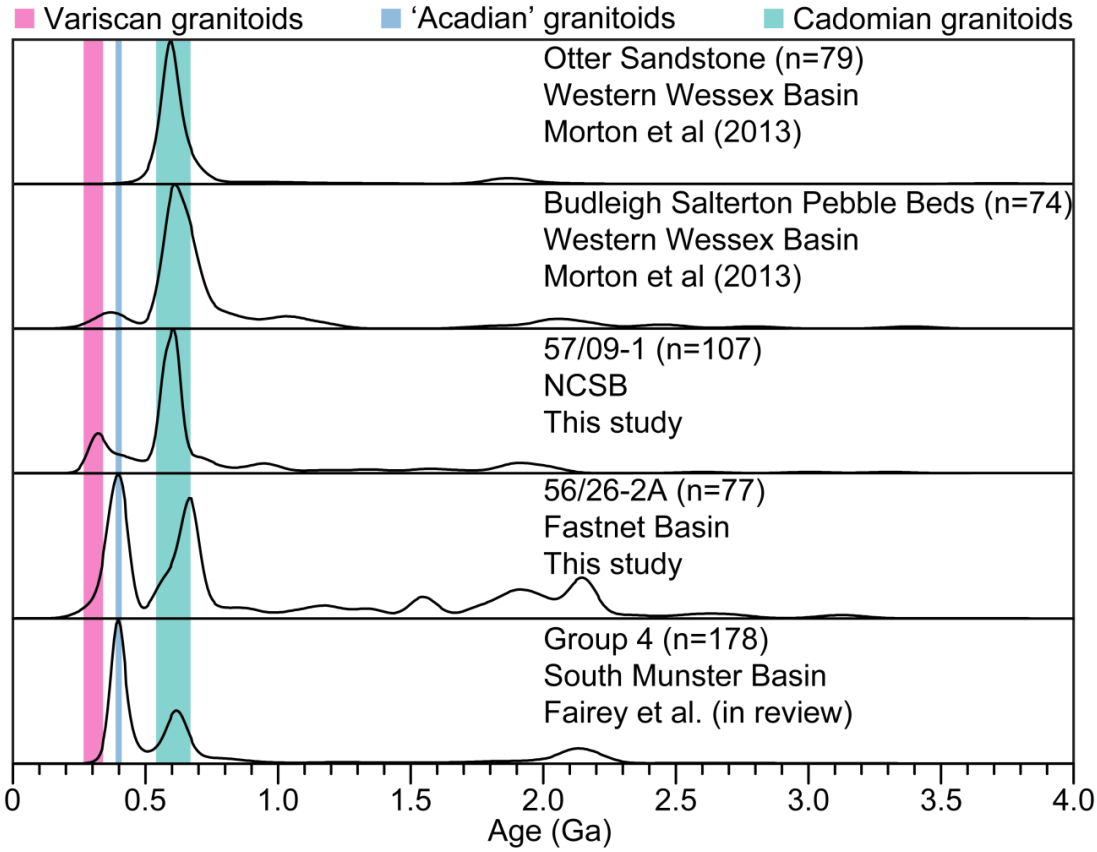

Figure 4–10. KDE plots (bandwidth = 20 Ma) of detrital zircon ages from Triassic samples in the western Wessex basin compared to the Triassic samples taken in the NCSB and Fastnet Basin in this study. n = number of zircon grains.

Of particular interest in sample 56/26-2A is the distribution of detrital mica ages which produce a major KDE peak at around 579 Ma. There are only 3 grains that have ages younger than 550 Ma. This indicates that the source area from which these micas were derived did not experience temperatures higher than the closure temperature for the $^{40}Ar/^{39}Ar$ isotopic system (as high as 450°C, according to Scharf et al., 2016). Thus the sediment source area could not have been subjected to higher than greenschist facies metamorphism after late Neoproterozoic times. A northern source for these micas is unlikely given that no detrital micas of late Neoproterozoic age were found in the Munster and South Munster Basin (Fairey et al., in prep.; Ennis et al., 2015) or in samples from the northern margin of the NCSB. Detrital micas in Ediacaran slates in northwest Iberia (Gutiérrez-Alonso et al., 2005) preserve late Neoproterozoic ages considered to be of Cadomian origin (albeit older than the ages obtained in this study – 590-783 Ma) which suggests that

Cadomia may have been a source of detritus. However, unlike the Triassic sample from the NCSB, the southern source in the Fastnet Basin must have been devoid of Variscan-aged granitoids as these are under-represented in the detrital zircon age distribution.

Mixture modelling for the Lower Triassic sample from the Fastnet Basin does not display the mixed source that is evident in the NCSB (Figure 4–9). Instead the modelling suggests that the dominant contribution is from sandstones of the South Munster Basin (SMB Group-4, Figure 4–10). Indeed, the source area would need to account for a high number of Acadian-aged detrital zircons (410-390 Ma) as well as a high proportion of late Neoproterozoic detrital zircons. The late Neoproterozoic age of detrital micas, however, is suggestive of a southern source. To account for the high number of Acadian-aged detrital zircons as well as the high proportion of late Neoproterozoic zircons and late Neoproterozoic age of detrital micas, a mixed source area is required that consisted of a proximal northern source of Acadian granitic material as well as a distal source from south of the Rheic Suture (Figure 4–11A).

4.5.2 Jurassic

A single Lower Jurassic sample, taken from the Fastnet Basin, was analysed in this study. The Lower Jurassic sedimentary rocks of the Fastnet Basin are considered to have been deposited in a deltaic environment (Ewins and Shannon, 1995). The sample (sample 63/10-1) contains no detrital zircons of late Neoproterozoic age and therefore could not have been sourced from peri-Gondwanan material. This precludes a southwest source area (Murphy and Ainsworth, 1991) and sedimentological connection to the Flemish Cap. Instead, given the abundance of Palaeo- and Mesoproterozoic detrital zircon ages, the sample was likely derived from a northern source of Laurentian affinity. Although the Munster Basin ORS was ultimately sourced from Laurentia (Fairey et al., in prep), it is an unlikely source of sediment because the proportions of Mesoproterozoic and Palaeoproterozoic zircons in the UORS are different to those in the Lower Jurassic Fastnet Basin. The dominant ca. 1.7 Ga detrital zircon KDE peak in the Lower Jurassic sample

can be attributed to magmatism of this age in Labrador, Canada (Cawood et al., 2007 and references therein) and has been found as the major detrital zircon component in Dalradian metasedimentary rocks in County Mayo, northwest Ireland (McAteer et al., 2010a). Mixture modelling also clearly indicates a dominant Laurentian source (Figure 4–9K). The Porcupine Basin may have provided a sedimentological link to northern Laurentian sources during that time (Figure 4–11B).

The Middle Jurassic sediments of the Goban Spur Basin were derived from a very similar source to that of the Lower Jurassic sediments in the Fastnet Basin. This similarity is evident in the similar detrital zircon age distributions from both samples (Figure 4–7K and O). Mixture modelling for the Goban Spur sediments indicates a dominant Laurentian source rather than recycling of UORS sediments (Figure 4–9O). This Laurentian source suggests that a very similar palaeodrainage to that of the Lower Jurassic Fastnet Basin was in operation in the Middle Jurassic Goban Spur Basin in order to deliver a similar spectrum of detrital zircons (Figure 4–11C). The paucity of late Neoproterozoic zircons indicates that peri-Gondwanan sources to the south (Cadomia) and to the west (Flemish Cap/Avalonia) could not have been operating as sediment source areas during the Early to Middle Jurassic periods in the Fastnet and Goban Spur basins respectively. A Laurentian source for the Middle Jurassic Goban Spur Basin sediments could indicate a connection with the Porcupine Basin to the north which may have acted as a sediment pathway. For such a connection to exist, the basement high which separated the Porcupine and Goban Spur basins (Dingle and Scrutton, 1979) must have been discontinuous at this time.

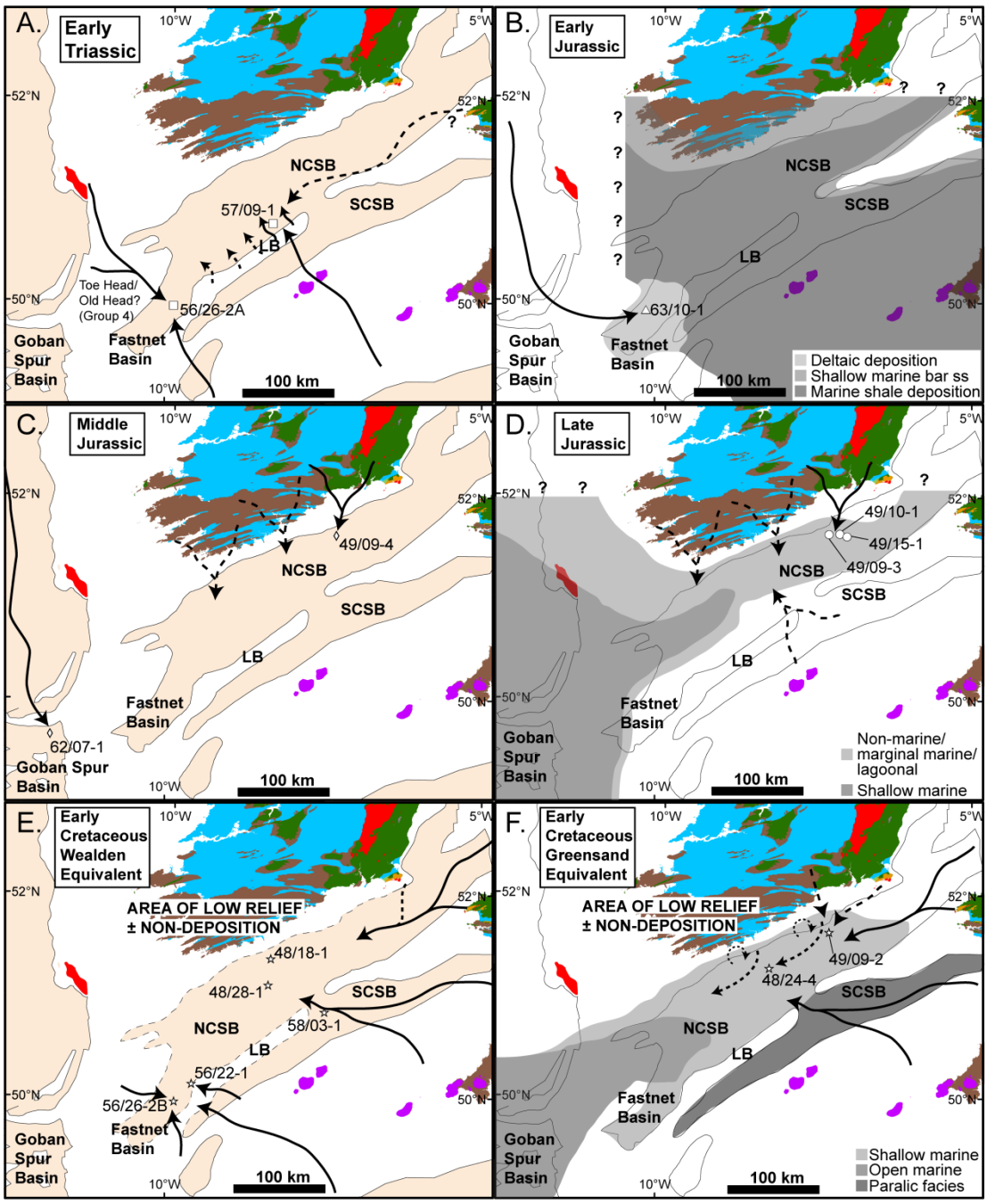

Figure 4–11. Palaeodrainage patterns in the North Celtic Sea, South Celtic Sea, Fastnet and Goban Spur basins during **A**. Early Triassic, **B**. Early Jurassic, **C**. Middle Jurassic, **D**. Late Jurassic, **E**. Early Cretaceous (Wealden) and **F**. Early Cretaceous (Greensand). Depositional environments are adapted from Ewins and Shannon (1995) and Naylor and Shannon (2011). Abbr.: NCSB – North Celtic Sea Basin, SCSB – South Celtic Sea Basin, LB – Labadie Bank. For geological legend, refer to Figure 4–2.

The dominant Palaeo- and Mesoproterozoic KDE peaks in Middle to Upper Jurassic samples from the NCSB (samples 49/09-4, 49/15-1 and 49/09-3; Figure 4–7B, C and E) are typical of Laurentia-derived sediments (Cawood et

al., 2007a). However, these samples also have a significant proportion of late Neoproterozoic zircons which require an additional source. Cambrian sedimentary rocks from the Leinster terrane are dominated by late Neoproterozoic zircons derived from Ganderia (Waldron et al., 2014) but zircons of this age are also abundant in other peri-Gondwanan domains such as Megumia and Avalonia. Detrital zircon age spectra for the different peri-Gondwanan domains are impossible to distinguish when mixing with Laurentian detritus obscures the Precambrian part of the spectra. In any case, mixture modelling for these samples shows a major contribution from sources of Laurentian affinity (Figure 4–9B-E and I). The dominant contribution of ORS sedimentary rocks (ORS Group-2, ORS Group-3 and the Harrylock Formation) suggests that sedimentary recycling from onshore upper Palaeozoic sedimentary rocks played a significant role in sediment accumulation in this part of the NCSB (Figure 4–11C and D).

Palaeozoic detrital zircon KDE peaks at around 470 Ma for sample 49/9-3 also support a northern source. McConnell et al. (2016) found an abundance of zircons of this age in Silurian clastic rocks from the Longford-Down terrane (Figure 4–1) and attributed these to Laurentian margin magmatic activity during the Ordovician Period. Sources for Palaeozoic detrital zircons in samples 49/10-1 (ca. 365 Ma) and 49/15-1 (ca. 450 Ma) have not been identified, although Chew and Strachan (2014) allude to a potential late-stage Grampian accretionary event occurring in the Late Ordovician – this may be a potential source of ca. 450 Ma zircons. However, no direct evidence of such an event exists in Ireland.

Sample 49/10-1 differs from the other samples in the northeast NCSB in that the Palaeoproterozoic and Mesoproterozoic KDE peaks are not as pronounced. A similar spectrum is observed in sandstones of the onshore, Upper Devonian Harrylock Formation which was interpreted by Fairey et al. (in prep.) to be derived from Cambrian sediments of the Leinster Massif. This sample, therefore, may represent recycling of Cambrian or Upper Devonian sedimentary rocks. The detrital zircon age spectra of samples in the northeastern part of the NCSB can be explained by northern derivation of sedimentary rocks from the UORS of the Munster Basin and Cambrian

sedimentary rocks of Ganderian association (Figure 4–11). Significant Ganderian contributions, however, are not evident in the relative contributions calculated by mixture modelling (Figure 4–9B-E and I). A northern source is also supported by apatite fission track data which suggest that a significant period of cooling occurred in the Galtee Mountains and Leinster Massif areas during Early Jurassic times (Cogné et al., 2016). Given the thick accumulations of Upper Jurassic sedimentary rocks, it is likely that erosion of these onshore areas continued throughout the Jurassic.

Detrital white mica ages taken from sample 49/09-3, which has dominant KDE peak ages of ca. 405 Ma, supports a Leinster Massif source area. This age corresponds to the youngest phase of (two-mica) granite emplacement in the Leinster Batholith (ca. 404 Ma; Fritschle et al., 2017). Fairey et al (in prep.) found coarse-grained detrital white micas in the Upper Devonian Harrylock Formation at Hook Head which yielded a KDE peak age of ca. 402 Ma. Further west in the Devonian Munster Basin, the same authors found that sandstone from the Gortanimill Formation contained detrital white micas with a KDE peak age of ca. 395 Ma. The similarity between the observed detrital mica ages in onshore and offshore samples provides further support for the findings of Caston (1995) of recycling of UORS sediments as a major source of detritus in the NCSB during the Late Jurassic.

In summary, Middle to Upper Jurassic samples from the northeastern NCSB indicate a dominant northern source of Upper Devonian ORS which contain detrital zircons of ultimate Laurentian affinity. However, in order to account for the abundance of late Neoproterozoic detrital zircons, a mixed source area must have been exposed to the north of the NCSB during this time. A Ganderian provenance for late Neoproterozoic zircons is likely. Although this is not evident from the mixture modelling, the proximity to the Leinster Massif, which hosts Cambrian sediments of Ganderian affinity (Waldron et al., 2014), as well as the dominant contribution from ORS sedimentary rocks suggests that a northern source is most likely. We also suggest that this northern source was probably in operation all along the northern margin of the NCSB during the Middle to Late Jurassic (Figure 4–11C and D).

4.5.3 Cretaceous

A total of seven Lower Cretaceous samples were taken across the study area. Three wells were sampled from the Lower Cretaceous succession in the central part of the NCSB and one from the northeastern part (Figure 4–2, Figure 4–4). Two Lower Cretaceous samples were taken from the Fastnet Basin and one from SCSB. Five of those samples are from Wealden-type continental-paralic facies (samples 58/03-1, 56/26-2B, 56/26-2, 48/18-1 and 48/28-1) and two from the shallow marine Lower Greensand Group (samples 48/24-4 and 49/09-2). Like most of the Jurassic samples taken in the NCSB, late Neoproterozoic detrital zircons are abundant in the Cretaceous samples.

4.5.3.1 Wealden Group

Supply of late Neoproterozoic detrital zircons resumed during deposition of the Wealden Group in the Fastnet Basin, although sample 56/26-2B contains a much higher proportion of Palaeo- and Mesoproterozoic detrital zircons than sample 56/22-1 and a lower proportion of late Neoproterozoic zircons. This difference may reflect the position of the samples, sample 56/26-2B being in a more central part of the basin and sample 56/22-1 being very close to the northern limit of the southeastern basin margin. Sediment in the central part of the basin would have a greater likelihood of reworking underlying sediments than on the margins and is thus more likely to rework detrital zircons. Sample 56/26-2B could have reworked similar sediment to that of sample 63/10-1 that contained an abundance of Laurentian zircons.

Cretaceous and Triassic samples from well 56/26-2 both contain detrital zircon KDE peaks at ca. 397 Ma which are difficult to assign to a possible southern source. Examples of granitoids of this approximate Acadian age are abundant in Ireland (e.g. Leinster Batholith, Galway Granites and Donegal Granites – see Chew and Stillman, 2009 and references therein). Such granitoids are also abundant in Maine and New Brunswick (Bradley et al., 2000) but granitoids with ages around 370 Ma are also widespread in those areas and these ages would be expected in detritus derived from there. The Iberian Massif is unlikely to have been a possible source of zircons of this age because that region was undergoing extension during Emsian times

(Gutiérrez-Alonso et al., 2008) and although volcanic rocks of that age are present, their generally mafic composition makes them poor candidates to contain zircon.

A possible source of zircons of Emsian age is the Upper Devonian to Carboniferous sandstone of the South Munster Basin which, on the western side of the basin, record a dominant ca. 400 Ma source of detrital zircons as well as late Neoproterozoic detrital zircons (Figure 4–10). Recycling of South Munster Basin detrital zircons into the Fastnet Basin is further supported by mixture modelling which shows a dominant input from SMB Group-4 sedimentary rocks (Figure 4–9J, L and M). In summary, sample 56/26-2B represents dominant input from proximal Tournaisian sedimentary rocks surrounding the basin whereas sample 56/22-1 represents a mixture of proximal Tournaisian sedimentary sources and distal, southern peri-Gondwanan sources (Figure 4–11E).

Sample 48/28-1 in the NCSB has a high proportion of Palaeozoic detrital zircons relative to sample 48/18-1. Palaeozoic KDE peak ages are different in these samples and identifying a source is difficult. The Saltees and Carnsore granites are the only known candidates for the ca. 430 Ma KDE peak age of sample 48/18-1. Sample 48/28-1 has a dominant Palaeozoic peak age of ca. 359 Ma and only two zircons with ages around 430 Ma. The Upper Jurassic sample 49/10-1 also shows a KDE peak at around 360 Ma, albeit a minor one. A source of these detrital zircons is difficult to pinpoint because no rocks of this age have been dated in Ireland. Given the Late Devonian extension and development of the Munster Basin to the north of the NCSB, one might expect extensional magmatism to provide a potential source. However, the rocks of the Lough Guitane Volcanic Complex, which are interbedded within lower sedimentary successions of the Munster Basin, have been dated between 384 Ma and 378 Ma (Williams et al., 2000). A KDE detrital mica peak age of 368 Ma for basement (possible Old Head Sandstone equivalent) sandstones in well 56/15-1 (Figure 4–8) possibly represent a similar source area to detrital zircons of similar age in samples 49/10-1 and 48/28-1.

Pointon et al. (2012) also found Late Devonian detrital zircons in their provenance study of the Western Irish Namurian Basin which straddles the

Iapetus Suture Zone. They considered zircons of this age not to be specific to either a Laurentian or peri-Gondwanan provenance. In this study, however, we believe that the absence of detrital zircons of this age in Upper Devonian to Early Carboniferous sedimentary rocks of the Munster and South Munster basins (Fairey et al. in prep.) – an obvious potential sediment source – may be an important additional indicator that sediment was not sourced from the north.

Mixture modelling of potential source areas was largely inconclusive for samples from the central NCSB (Figure 4–9F-H) but does point to a general southern source area for sample 48/18-01. Mixture modelling for sample 48/28-1, however, indicates a proximal source area to the north in the form of a mixture of Munster Basin (ORS Group-1) and South Munster Basin (SMB Group-4) sedimentary rocks. In all cases, the three statistics used in the models produced different major source contributions and must thus be interpreted extremely cautiously.

The single sample from the SCSB reveals detrital zircons dominated by late Neoproterozoic ages, producing a similar age distribution to that in Cretaceous samples in the central NCSB, particularly sample 48/18-1. Sample 58/03-1, however, contains a higher proportion of Mesoproterozoic grains and a KDE peak at ca. 1.5 Ga which is not present in sample 48/18-1. Mixture modelling indicates that the highest detrital zircon contributions to the sample were made by Cadomian, East Avalonian and SMB Group-4 sources (Figure 4–9N). A Cadomian source would indicate a southern sediment derivation whereas an East Avalonian source could indicate a southeastern or eastern derivation (Figure 4–11E). An SMB Group-4 source could also be explained by a southern derivation if, as suggested by Higgs (1983), the basement consists of early Carboniferous sandstones.

4.5.3.2 Greensand Group

Two samples from the Greensand Group in the NCSB were taken, one from the central part of the basin (sample 48/24-4) and one from the northeastern part (sample 49/09-2). Sample 49/09-2 has a similar detrital zircon age distribution to Jurassic samples in the same area (especially

samples 49/15-01, 49/09-4 and 49/09-3). This similarity suggests that the northern mixed UORS-Ganderian source that operated during Jurassic times in this area was still available during the Early Cretaceous. The KDE spectrum for sample 48/24-4 (as well as the other Cretaceous samples from the central NCSB), however, contain much lower proportions of pre-Neoproterozoic zircons (Figure 4–7F-G). These lower proportions suggest that zircons of Laurentian affinity were not being deposited in this area during the Early Cretaceous and that, given the strong Laurentian association of the UORS abutting the northern margin of the NCSB, a northern source was not likely during this time. This suggestion suits the Cretaceous denudation models by Allen et al. (2002) for southern Ireland where apatite fission track analysis indicates a mostly depositional rather than erosional environment (Figure 4–11E and F). Mixture modelling indicates that ORS Group-3 contributed the largest proportion of detrital zircons during this time (Figure 4–9I). The detrital zircon age spectrum in 49/09-2 could also be explained by reworking of underlying sediments in a shallow marine environment (Figure 4–11F).

Detrital mica ages from the Lower Greensand Group of sample 48/24-4 produce a KDE peak of the same age (431 Ma) as that in the Lower Greensand Group of sample 49/09-2 (Figure 4–8). Given that granitic rocks of this age are not exposed in the ORS of the southwestern part of onshore Ireland, this area was not a likely source. Instead, weak longshore drift may have played a role in delivering micas of this age from the same source as those micas found in sample 49/09-2 (Figure 4–11F). The two samples do, however, have very different detrital zircon age spectra (K-S test p-value < 0.05). Sample 49/09-2 shows a definitive input of Laurentian zircons that does not occur in the central part of the basin. This difference suggests that two different sources which contained similarly-aged detrital micas were delivering detritus to the two locations or that the detrital zircon ages represent reworking of underlying sediments with additional contributions being made from rocks of similar age to the Saltees and Carnsore granites.

Significantly, the mica ages obtained from sample 49/09-2 provide a means by which to distinguish between sediment derived from southern Ireland and that derived from Wales (i.e. the Avalonian and Megumia domains) because

no significant sources of 430 Ma age have been identified in Wales. Therefore, transverse drainage played a much greater role in sediment provision to the basin than axial drainage during the Late Jurassic (sample 49/09-3) and during the Early Cretaceous (sample 49/09-2).

4.6 Conclusions

This study presents the first detrital zircon and mica geochronological data for the Mesozoic NCSB, SCSB, Fastnet Basin and Goban Spur Basin. From analysis of this geochronological dataset we can draw the following conclusions:

1) Southern sources operating during Triassic times in the NCSB were probably located south of the Rheic Suture in terranes in northwest Iberia and Armorica. The Triassic sediments in the Fastnet Basin, however, consist of mixed sources of distal southern origins and proximal western/northern origins. The Lower Cretaceous Wealden Facies in the Fastnet, SCSB and possibly NCSB may also represent distal southern or southeastern source areas.
2) The ORS of southern Ireland played a significant role in providing sediment to the northern margin and central parts of the North Celtic Sea Basin in Middle to Late Jurassic times and, in the northeastern part of the basin, during Early Cretaceous times. Jurassic to Lower Cretaceous sedimentary rocks in the northeast, therefore, are, at least in part, the product of multiple erosional-depositional cycles. However, the general lack of Laurentian derived detrital zircons in Lower Cretaceous sandstones from the central part of the NCSB suggests that a significant northern ORS source was unlikely and that relief in the southwestern part of Ireland was subdued or below sea level at that time.
3) A Laurentian provenance for Middle Jurassic sedimentary rocks in the Goban Spur Basin precludes a connection to the Flemish Cap and/or Orphan Knoll during this time. Instead, the sediments must have been ultimately sourced from north of the Iapetus Suture Zone, with the Porcupine Basin possibly acting as a sediment pathway. Although of

ultimate Laurentian origin, the sedimentary rocks of the UORS in Ireland do not contain the high proportion of Late Palaeoproterozoic detrital zircons required to explain the dominant KDE peaks of that age in both the Lower Jurassic sediments from the Fastnet Basin and the Middle Jurassic sediments from the Goban Spur Basin.

These sediment provenance proxies reveal a high spatial and temporal variability of source areas across the southern Irish offshore Mesozoic basins, attesting to the complex nature of basin formation in the Celtic Sea region during Pangaea breakup. Further provenance work in the Celtic Sea region can benefit from higher resolution spatial and temporal (stratigraphic) sampling for detrital geochronology studies, from detailed heavy mineral analysis and from further characterisation of basement and source areas.

4.7 Acknowledgement

B.J.F, A.K, P.A.M and K.F.M acknowledge the financial support of the Irish Shelf Petroleum Studies Group (ISPSG) of the Irish Petroleum Infrastructure Programme (PIP) Group 4 (project code IS 12/05 UCC). The ISPSG comprises: Atlantic Petroleum (Ireland) Ltd, Cairn Energy Plc, Chrysaor E&P Ireland Ltd, Chevron North Sea Limited, ENI Ireland BV, Europa Oil & Gas, ExxonMobil E&P Ireland (Offshore) Ltd., Husky Energy, Kosmos Energy LLC, Maersk Oil North Sea UK Ltd, Petroleum Affairs Division of the Department of Communications, Energy and Natural Resources, Providence Resources Plc, Repsol Exploración SA, San Leon Energy Plc, Serica Energy Plc, Shell E&P Ireland Ltd, Sosina Exploration Ltd, Tullow Oil Plc and Woodside Energy (Ireland) Pty Ltd. K.K. acknowledges financial support of NWO grant 864.12.005. D. Pastor-Galan is thanked for his geochronology and sampling advice. C. Reid and R. van Elsas are thanked for their technical assistance for SEM and sample preparation respectively. The Petroleum Affairs Division of Ireland is thanked for providing well samples and assisting with logistics in that regard.

4.8 References

Ainsworth, N.R., Horton, N.F., Penney, R.A., 1985. Lower Cretaceous micropaleontology of the Fastnet Basin, offshore south-west Ireland. Mar. Pet. Geol. 2, 341–349.

Allen, P.A., Bennett, S.D., Cunningham, M.J.M., Carter, A., Gallagher, K.,

Lazzaretti, E., Galewsky, J., Densmore, A.L., Phillips, W.E.A., Naylor, D., Hach, C.S., 2002. The post-Variscan thermal and denudational history of Ireland. Geol. Soc. London, Spec. Publ. 196, 371–399. doi:10.1144/GSL.SP.2002.196.01.20

Andonaegui, P., Arenas, R., Albert, R., Sánchez Martínez, S., Díez Fernández, R., Gerdes, A., 2016. The last stages of the Avalonian–Cadomian arc in NW Iberian Massif: isotopic and igneous record for a long-lived peri-Gondwanan magmatic arc. Tectonophysics 681, 6–14. doi:10.1016/j.tecto.2016.02.032

Auffret, G.-A., Pastouret, L., Cassat, G., de Charpal, O., Cravatte, J., Guennoc, P., 1979. Dredged Rocks From the Armorican and Celtic Margins. Initial Reports Deep Sea Drill. Proj. XLVIII, 473–491.

Augier, R., Choulet, F., Faure, M., Turrillot, P., 2015. A turning-point in the evolution of the Variscan orogen: the ca. 325 Ma regional partial-melting event of the coastal South Armorican domain (South Brittany and Vendée, France). Bull. la Société Géologique Fr. 186, 63–91. doi:10.2113/gssgfbull.186.2-3.63

Bradley, D., Tucker, R., Lux, D.R., Harris, A.G., McGregor, C.D., 2000. Migration of the Acadian Orogen and foreland basin across the Northern Appalachians of Maine and adjacent areas. U.S. Geol. Surv. Prof. Pap.

Caston, V.N.D., 1995. The Helvick oil accumulation, Block 49/9, North Celtic Sea Basin. Geol. Soc. Lond., Spec. Publ. 93, 209–226. doi:10.1144/GSL.SP.1995.093.01.15

Cawood, P.A., Merle, R.E., Strachan, R.A., Tanner, P.W.G., 2012. Provenance of the Highland Border Complex: constraints on Laurentian margin accretion in the Scottish Caledonides. J. Geol. Soc. London. 169, 575–586. doi:10.1144/0016-76492011-076

Cawood, P.A., Nemchin, A.A., Smith, M., Loewy, S., 2003. Source of the Dalradian Supergroup constrained by U-Pb dating of detrital zircon and implications for the East Laurentian margin. J. Geol. Soc. London. 160, 231–246. doi:10.1144/0016-764902-039

Cawood, P.A., Nemchin, A.A., Strachan, R., 2007a. Provenance record of Laurentian passive-margin strata in the northern Caledonides:

Implications for paleodrainage and paleogeography. Geol. Soc. Amer. Bull. 119, 993–1003. doi:10.1130/B26152.1

Cawood, P.A., Nemchin, A.A., Strachan, R., Prave, T., Krabbendam, M., 2007b. Sedimentary basin and detrital zircon record along East Laurentia and Baltica during assembly and breakup of Rodinia. J. Geol. Soc. Lond. 164, 257–275. doi:10.1144/0016-76492006-115

Chew, D.M., Daly, J.S., Magna, T., Page, L.M., Kirkland, C.L., Whitehouse, M.J., Lam, R., 2010. Timing of ophiolite obduction in the Grampian orogen. Bull. Geol. Soc. Am. 122, 1787–1799. doi:10.1130/B30139.1

Chew, D.M., Stillman, C.J., 2009. Late Caledonian orogeny and magmatism, in: The Geology of Ireland. pp. 143–174.

Chew, D.M., Strachan, R.A., 2014. The Laurentian Caledonides of Scotland and Ireland. Geol. Soc. London, Spec. Publ. 390, 45–91. doi:10.1144/SP390.16

Clayton, G., Sevastopulo, G.D., Sleeman, A.G., 1986. Carboniferous (Dinantian and Silesian) and Permo-Triassic rocks in south County Wexford, Ireland. Geol. J. 21, 355–374. doi:10.1002/gj.3350210402

Cogné, N., Chew, D., Stuart, F.M., 2014. The thermal history of the western Irish onshore. J. Geol. Soc. London. 171, 779–792. doi:10.1144/jgs2014-026

Cogné, N., Doepke, D., Chew, D., Stuart, F.M., Mark, C., 2016. Measuring plume-related exhumation of the British Isles in Early Cenozoic times. Earth Planet. Sci. Lett. 456, 1–15. doi:10.1016/j.epsl.2016.09.053

Collins, A.S., Buchan, C., 2004. Provenance and age constraints of the South Stack Group, Anglesey, UK: U–Pb SIMS detrital zircon data. J. Geol. Soc. London. 161, 743–746. doi:10.1144/0016-764904-036

Conroy, J., Brock, A., 1989. Gravity and magnetic studies of crustal structure across the Porcupine basin west of Ireland. Earth Planet. Sci. Lett. 93, 371–376.

Daly, J.S., 1996. Pre-Caledonian history of the Annagh Gneiss Complex, North-western Ireland, and correlation with Laurentia-Baltica. Irish J. Earth Sci. 15, 5–18.

Daly, J.S., Muir, R.J., Cliff, R. A., 1991. A precise U-Pb zircon age for the

Inishtrahull syenitic gneiss, County Donegal, Ireland. J. Geol. Soc. London. 148, 639–642. doi:10.1144/gsjgs.148.4.0639

De Graciansky, P.C., Poag, C.W., Cunningham, R., Loubere, P., Masson, D.G., Mazzulo, J.M., Montadert, L., Muller, C., Otsuka, K., Reynolds, L.A., Sigal, J., Snyder, S.W., Townsend, H.A., Vaos, S.P., Waples, D., 1985. The Goban Spur transect: geologic evolution of a sediment-starved passive continental margin (DSDP Leg 80, Irish Sea). Geol. Soc. Am. Bull. 96, 58–76. doi:10.1130/0016-7606(1985)96<58:TGSTGE>2.0.CO;2

Dingle, R. V, Scrutton, R.A., 1979. Sedimentary successions and tectonic history of a marginal plateau (Goban Sour, Southwest of Ireland). Mar. Geol. 33, 45–69.

Ducassou, C., Poujol, M., Hallot, E., Bruguier, O., Ballevre, M., 2011. Petrology and geochronology of the high-K calc-alkaline Mésanger magmatism (Armorican massif, France): A ca. 320 Ma old volcano-plutonic association. Bull. la Soc. Geol. Fr. 182, 467–477. doi:10.2113/gssgfbull.182.6.467

Ennis, M., Meere, P.A., Timmerman, M.J., Sudo, M., 2015. Post-Acadian sediment recycling in the Devonian Old Red Sandstone of Southern Ireland. Gondwana Res. 28, 1415–1433. doi:10.1016/j.gr.2014.10.007

Evans, A., Clayton, G., 1998. The geological history of the Ballydeenlea Chalk Breccia, County Kerry, Ireland. Mar. Pet. Geol. 15, 299–307. doi:10.1016/S0264-8172(98)00024-5

Ewins, N.P., Shannon, P.M., 1995. Sedimentology and diagenesis of the Jurassic and Cretaceous of the North Celtic Sea and Fastnet Basins. Geol. Soc. Lond., Spec. Publ. 93, 139–169. doi:10.1144/GSL.SP.1995.093.01.12

Fairey, B.J., Kerrison, A., Meere, P.A., Mulchrone, K.F., Gartner, A., Sonntag, B.-L., Linnemann, U., Kuiper, K.F., Ennis, M., Mark, C., Cogne, N., Chew, D., in review. Sedimentary provenance of the Devonian Old Red Sandstone in southern Ireland: a multi-proxy investigation into the role of sediment recycling. In preparation.

Fernandez-Suarez, J., Dunning, G.R., Jenner, G. a., Gutierrez-Alonso, G., 2000. Variscan collisional magmatism and deformation in NW Iberia:

constraints from U-Pb geochronology of granitoids. J. Geol. Soc. London. 157, 565–576. doi:10.1144/jgs.157.3.565

Fernández-Suárez, J., Gutiérrez-Alonso, G., Jenner, G.A., Tubrett, M.N., 2000. New ideas on the Proterozoic-Early Palaeozoic evolution of NW Iberia: Insights from U-Pb detrital zircon ages. Precambrian Res. 102, 185–206. doi:10.1016/S0301-9268(00)00065-6

Fernández-Suárez, J., Gutiérrez-Alonso, G., Pastor-Galán, D., Hofmann, M., Murphy, J.B., Linnemann, U., 2014. The Ediacaran-Early Cambrian detrital zircon record of NW Iberia: Possible sources and paleogeographic constraints. Int. J. Earth Sci. 103, 1335–1357. doi:10.1007/s00531-013-0923-3

Fernandez-Suarez, J., Gutierrez Alonso, G., Jeffries, T.E., 2002. The importance of along-margin terrane transport in northern Gondwana: Insights from detrital zircon parentage in Neoproterozoic rocks from Iberia and Brittany. Earth Planet. Sci. Lett. 204, 75–88. doi:10.1016/S0012-821X(02)00963-9

Friend, C.R.L., Strachan, R.A., Kinny, P.D., Watt, G.R., 2003. Provenance of the Moine Supergroup of NW Scotland: evidence from geochronology of detrital and inherited zircons from (meta) sedimentary rocks , granites and migmatites. J. Geol. Soc. London 160, 247–257.

Fritschle, T., Daly, J.S., Whitehouse, M.J., McConnell, B., Buhre, S., 2017. Multiple intrusive phases in the Leinster Batholith, Ireland : geochronology, isotope geochemistry and constraints on the deformation history. J. Geol. Soc. London 175, 229–246.

Fyffe, L.R., Barr, S.M., Johnson, S.C., McLeod, M.J., McNicoll, V.J., Valverde-Vaquero, P., van Staal, C.R., White, C.E., 2009. Detrital zircon ages from Neoproterozoic and Early Paleozoic conglomerate and sandstone units of New Brunswick and coastal Maine: implications for the tectonic evolution of Ganderia. Atl. Geol. 45, 110–144. doi:10.4138/atlgeol.2009.006

Green, P.F., Duddy, I.R., Hegarty, K.A., Bray, R.J., Sevastopulo, G., Clayton, G., Johnston, D., 2000. The post-Carboniferous evolution of Ireland: evidence from Thermal History Reconstruction. Proc. Geol. Assoc. 111,

307–320. doi:10.1016/S0016-7878(00)80087-5

Gutiérrez-Alonso, G., Fernández-Suárez, J., Collins, A.S., Abad, I., Nieto, F., 2005. Amazonian Mesoproterozoic basement in the core of the Ibero-Armorican Arc: 40Ar/39Ar detrital mica ages complement the zircon's tale. Geology 33, 637–640. doi:10.1130/G21485.1

Gutiérrez-Alonso, G., Murphy, J.B., Fernández-Suárez, J., Hamilton, M. a., 2008. Rifting along the northern Gondwana margin and the evolution of the Rheic Ocean: A Devonian age for the El Castillo volcanic rocks (Salamanca, Central Iberian Zone). Tectonophysics 461, 157–165. doi:10.1016/j.tecto.2008.01.013

Henderson, B.J., Collins, W.J., Murphy, J.B., Gutierrez-Alonso, G., Hand, M., 2016. Gondwanan basement terranes of the Variscan–Appalachian orogen: Baltican, Saharan and West African hafnium isotopic fingerprints in Avalonia, Iberia and the Armorican Terranes. Tectonophysics 681, 278–304. doi:10.1016/j.tecto.2015.11.020

Hibbard, J.P., van Staal, C.R., Rankin, D.W., 2007. A comparative analysis of pre-Silurian crustal building blocks of the northern and the southern Appalachian orogen. Am. J. Sci. 307, 23–45. doi:10.2475/01.2007.02

Higgs, K., 1983. Palynological evidence for Carboniferous strata in two wells drilled in the Celtic Sea area. Geol. Surv. Irel. Bull. 3, 107–112.

Higgs, K., Beese, A.P., 1986. A Jurassic Microflora from the Colbond Clay of Cloyne, County Cork. Irish J. Earth Sci. 7, 99–109.

Hopper, J.R., Funck, T., Tucholke, B.E., Larsen, H.C., Holbrook, W.S., Louden, K.E., Shillington, D., Lau, H., 2004. Continental break-up and the onset of ultraslow seafloor spreading off Flemish Cap on the Newfoundland rifted margin. Geology 32, 93–96. doi:10.1130/G19694.1

Johnson, T.E., Kirkland, C.L., Reddy, S.M., Evans, N.J., McDonald, B.J., 2016. The source of Dalradian detritus in the Buchan Block, NE Scotland: application of new tools to detrital datasets. J. Geol. Soc. London. 173, 773–782. doi:10.1144/jgs2016-019

King, L.H., Fader, G.B., Poole, W.H., Wanless, R.K., 1985. Geological setting and age of the Flemish Cap granodiorite, east of the Grand Banks of Newfoundland. Can. J. Earth Sci. 22, 1286–1298. doi:10.1139/e85-133

Kirkland, C.L., Strachan, R.A., Prave, A.R., 2008. Detrital zircon signature of the Moine Supergroup, Scotland: Contrasts and comparisons with other Neoproterozoic successions within the circum-North Atlantic region. Precambrian Res. 163, 332–350. doi:10.1016/j.precamres.2008.01.003

Krogh, T.E., Keppie, J.D., 1990. Age of detrital zircon and titanite in the Meguma Group, southern Nova Scotia, Canada: Clues to the origin of the Meguma Terrane. Tectonophysics 177, 307–323. doi:10.1016/0040-1951(90)90287-I

Landing, E., Bowring, S.A., Davidek, K.L., Rushton, A.W.A., Fortey, R.A., Wimbledon, W.A.P., 2000. Cambrian–Ordovician boundary age and duration of the lowest Ordovician Tremadoc Series based on U–Pb zircon dates from Avalonian Wales. Geol. Mag. 137, 485–494. doi:10.1017/S0016756800004507

Linnemann, U., Gerdes, A., Drost, K., Buschmann, B., 2007. The continuum between Cadomian orogenesis and opening of the Rheic Ocean: Constraints from LA-ICP-MS U-Pb zircon dating and analysis of plate-tectonic setting (Saxo-Thuringian zone, northeastern Bohemian Massif, Germany). Geol. Soc. Am. Spec. Pap. 423, 61–96. doi:10.1130/2007.2423(03)

Linnemann, U., Herbosch, A., Liégeois, J.P., Pin, C., Gärtner, A., Hofmann, M., 2012. The Cambrian to Devonian odyssey of the Brabant Massif within Avalonia: A review with new zircon ages, geochemistry, Sm-Nd isotopes, stratigraphy and palaeogeography. Earth-Science Rev. 112, 126–154. doi:10.1016/j.earscirev.2012.02.007

Linnemann, U., Pereira, F., Jeffries, T.E., Drost, K., Gerdes, A., 2008. The Cadomian Orogeny and the opening of the Rheic Ocean: The diacrony of geotectonic processes constrained by LA-ICP-MS U-Pb zircon dating (Ossa-Morena and Saxo-Thuringian Zones, Iberian and Bohemian Massifs). Tectonophysics 461, 21–43. doi:10.1016/j.tecto.2008.05.002

McAteer, C.A., Daly, J.S., Flowerdew, M.J., Whitehouse, M.J., Kirkland, C.L., 2010a. A Laurentian provenance for the Dalradian rocks of north Mayo, Ireland, and evidence for an original basement-cover contact with the underlying Annagh Gneiss Complex. J. Geol. Soc. London. 167, 1033–

1048. doi:10.1144/0016-76492009-147

McAteer, C.A., Daly, J.S., Flowerdew, M.J., Connelly, J.N., Housh, T.B., Whitehouse, M.J., 2010b. Detrital zircon, detrital titanite and igneous clast U-Pb geochronology and basement-cover relationships of the Colonsay Group, SW Scotland: Laurentian provenance and correlation with the Neoproterozoic Dalradian Supergroup. Precambrian Res. 181, 21–42. doi:10.1016/j.precamres.2010.05.013

McCann, T., Shannon, P.M., 1994. Late Mesozoic reactivation of Variscan faults in the North Celtic Sea Basin, Ireland. Mar. Pet. Geol. 11, 94–103. doi:10.1016/0264-8172(94)90012-4

McConnell, B., Crowley, Q.G., Riggs, N., 2010. Laurentian origin of the Ordovician Grangegeeth volcanic arc terrane, Ireland. J. Geol. Soc. London. 167, 469–474. doi:10.1144/0016-76492009-139

McConnell, B., Parkes, M., Crowley, Q., Rushton, A., 2015. No Exploits back-arc basin in the Iapetus suture zone of Ireland. J. Geol. Soc. London. 172, 740–747. doi:10.1144/jgs2015-044

McConnell, B., Rogers, R., Crowley, Q., 2016. Sediment provenance and tectonics on the Laurentian margin: implications of detrital zircons ages from the Central Belt of the Southern Uplands–Down–Longford Terrane in Co. Monaghan, Ireland. Scot. J. Geol. 52, 11–17. doi:10.1144/sjg2015-013

McIlroy, D., Horák, J.M., 2006. Neoproterozoic: the late Precambrian terranes that formed Eastern Avalonia, in: Brenchley, P.J., Rawson, P.F. (Eds.), The Geology of England and Wales. Geol. Soc. Lond., pp. 9–24. doi:10.1144/GOEWP.2

McKerrow, W.S., Mac Niocaill, C., Ahlberg, P.E., Clayton, G., Eagar, R.M.C., 2000. The Late Palaeozoic relations between Gondwana and Laurussia. Geol. Soc. London, Spec. Publ. 179, 9–20. doi:10.1144/GSL.SP.2000.179.01.03

Mohn, G., Karner, G.D., Manatschal, G., Johnson, C.A., 2015. Structural and stratigraphic evolution of the Iberia–Newfoundland hyper-extended rifted margin: a quantitative modelling approach. Geol. Soc. London, Spec. Publ. 413, 53–89. doi:10.1144/SP413.9

Morton, A., Knox, R., Frei, D., 2016. Heavy mineral and zircon age constraints on provenance of the Sherwood Sandstone Group (Triassic) in the eastern Wessex Basin, UK. Proc. Geol. Assoc. 127, 514–526. doi:10.1016/j.pgeola.2016.06.001

Murphy, J.B., Fernández-Suárez, J., Jeffries, T.E., Strachan, R.A., 2004. U-Pb (LA-ICP-MS) dating of detrital zircons from Cambrian clastic rocks in Avalonia: erosion of a Neoproterozoic arc along the northern Gondwanan margin. J. Geol. Soc. London. 161, 243–254. doi:10.1144/0016-764903-064

Murphy, J.B., Gutierrez-Alonso, G., Nance, R.D., Fernández-Suárez, J., Keppie, J.D., Quesada, C., Strachan, R.A., Dostal, J., 2006. Origin of the Rheic Ocean: Rifting along a Neoproterozoic suture? Geology 34, 325–328. doi:10.1130/G22068.1

Murphy, N.J., Ainsworth, N.R., 1991. Stratigraphy of the Triassic, Lower Jurassic and Middle Jurassic (Aalenian) from the Fastnet Basin, Offshore South-west Ireland. Mar. Pet. Geol. 8. doi:10.1016/0264-8172(91)90064-8

Nance, R.D., Gutiérrez-Alonso, G., Keppie, J.D., Linnemann, U., Murphy, J.B., Quesada, C., Strachan, R.A., Woodcock, N.H., 2012. A brief history of the Rheic Ocean. Geosci. Front. 3, 125–135. doi:10.1016/j.gsf.2011.11.008

Nance, R.D., Gutiérrez-Alonso, G., Keppie, J.D., Linnemann, U., Murphy, J.B., Quesada, C., Strachan, R. a., Woodcock, N.H., 2010. Evolution of the Rheic Ocean. Gondwana Res. 17, 194–222. doi:10.1016/j.gr.2009.08.001

Naylor, D., 1992. The post-Variscan history of Ireland. Geol. Soc. London, Spec. Publ. 62, 255–275.

Naylor, D., Shannon, P.M., 2011. Petroleum Geology of Ireland. Dunedin Academic Press Ltd., Edinburgh.

Naylor, D., Shannon, P.M., 2005. The structural framework of the Irish Atlantic Margin, in: Petroleum Geology Conference Series. Geological Society of London, pp. 145–158. doi:10.1144/0060389

Pastor-Galán, D., Gutiérrez-Alonso, G., Murphy, J.B., Fernández-Suárez, J., Hofmann, M., Linnemann, U., 2013. Provenance analysis of the Paleozoic

sequences of the northern Gondwana margin in NW Iberia: Passive margin to Variscan collision and orocline development. Gond. Res. 23, 1089–1103. doi:10.1016/j.gr.2012.06.015

Petrie, S.H., Brown, J.R., Granger, P.J., Lovell, J.P.B., 1989. Mesozoic History of the Celtic Sea Basins. AAPG Mem. 46, 433–444.

Phillips, E.R., Smith, R.A., Stone, P., Pashley, V., Horstwood, M., 2009. Zircon age constraints on the provenance of Llandovery to Wenlock sandstones from the Midland Valley terrane of the Scottish Caledonides. Scottish J. Geol. 45, 131–146. doi:10.1144/0036-9276/01-383

Pointon, M.A., Cliff, R.A., Chew, D.M., 2012. The provenance of Western Irish Namurian Basin sedimentary strata inferred using detrital zircon U-Pb LA-ICP-MS geochronology. Geol. J. 47, 77–98. doi:10.1002/gj.1335

Pothier, H.D., Waldron, J.W.F., Schofield, D.I., DuFrane, S.A., 2015. Peri-Gondwanan terrane interactions recorded in the Cambrian–Ordovician detrital zircon geochronology of North Wales. Gond. Res. 28, 987–1001. doi:10.1016/j.gr.2014.08.009

Quinn, D., Meere, P., Wartho, J., 2005. A chronology of foreland deformation: ultra-violet laser 40 Ar/ 39 Ar dating of syn/late-orogenic intrusions from the Variscides of southwest. J. Struct. Geol. 27, 1413–1425. doi:10.1016/j.jsg.2005.02.003

Rowell, P., 1995. Tectono-stratigraphy of the North Celtic Sea Basin. Geol. Soc. Lond., Spec. Publ. 93, 101–137. doi:10.1144/GSL.SP.1995.093.01.11

Samson, S.D., D'Lemos, R.S., Miller, B. V., Hamilton, M.A., 2005. Neoproterozoic palaeogeography of the Cadomia and Avalon terranes: constraints from detrital zircon U-Pb ages. J. Geol. Soc. London. 162, 65–71. doi:10.1144/0016-764904-003

Saylor, J.E., Sundell, K.E., 2016. Quantifying comparison of large detrital geochronology data sets. Geosphere 12, GES01237.1. doi:10.1130/GES01237.1

Scharf, A., Handy, M.R., Schmid, S.M., Favaro, S., Sudo, M., Schuster, R., Hammerschmidt, K., 2016. Grain-size effects on the closure temperature of white mica in a crustal-scale extensional shear zone - Implications of

in-situ 40Ar/39Ar laser-ablation of white mica for dating shearing and cooling (Tauern Window, Eastern Alps). Tectonophysics 674, 210–226. doi:10.1016/j.tecto.2016.02.014

Shannon, P.M., 1995. Permo-Triassic development of the Celtic Sea region, offshore Ireland. Geol. Soc. London, Spec. Publ. 91, 215–237. doi:10.1144/GSL.SP.1995.091.01.11

Shannon, P.M., 1991. The development of Irish offshore sedimentary basins. J. Geol. Soc. London. 148, 181–189. doi:10.1144/gsjgs.148.1.0181

Shannon, P.M., Naylor, D., 1998. An assessment of Irish offshore basins and petroleum plays. J. Pet. Geol. 21, 125–152. doi:10.1306/BF9AB7A1-0EB6-11D7-8643000102C1865D

Sibuet, J.-C., Srivastava, S.P., Enachescu, M., Karner, G.D., 2007. Early Cretaceous motion of Flemish Cap with respect to North America: implications on the formation of Orphan Basin and SE Flemish Cap–Galicia Bank conjugate margins. Geol. Soc. London, Spec. Publ. 282, 63–76. doi:10.1144/SP282.4

Strachan, R.A., Collins, A.S., Buchan, C., Nance, R.D., Murphy, J.B., D'Lemos, R.S., 2007. Terrane analysis along a Neoproterozoic active margin of Gondwana: insights from U-Pb zircon geochronology. J. Geol. Soc. London 164, 57–60.

Strachan, R.A., Linnemann, U., Jeffries, T., Drost, K., Ulrich, J., 2014. Armorican provenance for the melange deposits below the Lizard ophiolite (Cornwall, UK): Evidence for Devonian obduction of Cadomian and Lower Palaeozoic crust onto the southern margin of Avalonia. Int. J. Earth Sci. 103, 1359–1383. doi:10.1007/s00531-013-0961-x

Strachan, R.A., Prave, A.R., Kirkland, C.L., Storey, C.D., 2013. U–Pb detrital zircon geochronology of the Dalradian Supergroup, Shetland Islands, Scotland: implications for regional correlations and Neoproterozoic–Palaeozoic basin development. J. Geol. Soc. Lond. 170, 905–916. doi:10.1144/jgs2013-057

Sundell, K., Saylor, J.E., 2017. Unmixing detrital geochronology age distributions. Geochem., Geophys. Geosyst.. doi:10.1002/2016GC006774

Tartèse, R., Poujol, M., Ruffet, G., Boulvais, P., Yamato, P., Košler, J., 2011. New U-Pb zircon and 40Ar/39Ar muscovite age constraints on the emplacement of the Lizio syn-tectonic granite (Armorican Massif, France). Comptes Rendus Geosci. 343, 443–453. doi:10.1016/j.crte.2011.07.005

Todd, S.P., Murphy, F.C., Kennan, P.S., 1991. On the trace of the Iapetus suture in Ireland and Britain. J. Geol. Soc. London 148, 869–880.

Tucker, R.M., Arter, G., 1987. The tectonic evolution of the North Celtic Sea and Cardigan Bay basins with special reference to basin inversion. Tectonophysics 137, 291–307.

Tyrrell, S., Haughton, P.D.W., Souders, A.K., Daly, J.S., Shannon, P.M., 2012. Large-scale, linked drainage systems in the NW European Triassic: insights from the Pb isotopic composition of detrital K-feldspar. J. Geol. Soc. London. 169, 279–295. doi:10.1144/0016-76492011-104

Von Eynatten, H., Wijbrans, J.R., 2003. Precise tracing of exhumation and provenance using 40 Ar/ 39 Ar geochronology of detrital white mica: the example of the Central Alps. Geol. Soc. London, Spec. Publ. 208, 289–305. doi:10.1144/GSL.SP.2003.208.01.14

Waldron, J.W.F., Floyd, J.D., Simonetti, A., Heaman, L.M., 2008. Ancient Laurentian detrital zircon in the closing Iapetus ocean, Southern Uplands terrane, Scotland. Geology 36, 527–530. doi:10.1130/G24763A.1

Waldron, J.W.F., Schofield, D.I., Dufrane, S.A., Floyd, J.D., Crowley, Q.G., Simonetti, A., Dokken, R.J., Pothier, H.D., 2014. Ganderia-Laurentia collision in the Caledonides of Great Britain and Ireland. J. Geol. Soc. Lond.. 171, 555–569. doi:10.1144/jgs2013-131

Waldron, J.W.F., Schofield, D.I., White, C.E., Barr, S.M., 2011. Cambrian successions of the Meguma Terrane, Nova Scotia, and Harlech Dome, North Wales : dispersed fragments of a peri-Gondwanan basin? J. Geol. Soc. London. 168, 83–98. doi:10.1144/0016-76492010-068.Cambrian

Waldron, J.W.F., White, C.E., Barr, S.M., Simonetti, A., Heaman, L.M., 2009. Provenance of the Meguma terrane, Nova Scotia: rifted margin of early Paleozoic Gondwana. Can. J. Earth Sci. 46, 1–8. doi:10.1139/E09-004

Walsh, P.T., 1966. Cretaceous outliers in south-west Ireland and their implications for Cretaceous palaeogeography. J. Geol. Soc. London 122,

63–84.

Williams, E.A., Sergeev, S.A., Stossel, I., Ford, M., Higgs, K.T., 2000. U-Pb zircon geochronology of silicic tuffs and chronostratigraphy of the earliest Old Red Sandstone in the Munster Basin, SW Ireland. Geol. Soc. Lond., Spec. Publ. 180, 269–302. doi:10.1144/GSL.SP.2000.180.01.13

Willner, A.P., Barr, S.M., Gerdes, A., Massonne, H.-J., White, C.E., 2013. Origin and evolution of Avalonia: evidence from U–Pb and Lu–Hf isotopes in zircon from the Mira terrane, Canada, and the Stavelot–Venn Massif, Belgium. J. Geol. Soc. Lond. 170, 769–784. doi:10.1144/jgs2012-152

Willner, A.P., Gerdes, A., Massonne, H.-J., Van Staal, C.R., Zagorevski, A., 2014. Crustal evolution of the Northeast Laurentian Margin and the Peri-Gondwanan Microcontinent Ganderia Prior to and During Closure of the Iapetus Ocean: Detrital Zircon U-Pb and Hf Isotope Evidence from Newfoundland. Geosci. Canada 41, 345–364.

5 Synthesis and Conclusions

5.1 Synthesis of core findings

This thesis presents the first detrital zircon U-Pb geochronological study for seven sedimentary basins in southern Ireland that span a history of an approximately 300 million years from Early Devonian to Early Cretaceous times. In addition, the first apatite U-Pb ages and new mica ^{40}Ar-^{39}Ar total fusion ages add an extra dimension for provenance interpretation by allowing the detection of sources that were subjected to lower temperatures than can be recorded in zircon. Sediments deposited during this 300 million year period have the potential to record a wealth of information on the eventual formation (Caledonian, Acadian and Variscan orogenies) and subsequent breakup up of Pangaea. By studying the provenance of each basin, the thesis tests whether sediments in the Mesozoic basins off the coast of southern Ireland were the product of multiple cycles of erosion and deposition. This chapter brings together and discusses the major findings of the thesis in line with the aims presented in Chapter 1.

The Lower to Middle Devonian Lower Old Red Sandstones of the Dingle Basin are the oldest rocks studied in this thesis. The Early Devonian timing of their deposition and proximity to the ISZ provides an opportunity to assess the role of the Caledonian Orogeny in providing sediments to the basin. Two detrital zircon samples from successive formations in the most voluminous of the Dingle Basin groups, the Lower Devonian Dingle Group, reveal a dominant Laurentian source component for both formations. This interpretation is supported by the abundance of Mesoproterozoic detrital zircon grains, especially around the age of 1.2 Ga. The Dingle Group, however, also contains detrital zircons of late Neoproterozoic age which are typical of peri-Gondwanan terranes and, apart from within rift-related magmatism (Cawood and Nemchin, 2001), are under-represented within Laurentia. This late Neoproterozoic component suggests a mixing of Laurentian and peri-Gondwanan detritus in the LORS.

The pre-UORS surface to the south of the Dingle Basin likely consisted of similar geology to that in the Leinster Massif (part of Ganderia, according to (Waldron et al., 2014), with Cambrian to Silurian sedimentary and volcanic

rocks intruded by granitoids ranging in age from 430 Ma (e.g. Carnsore Granite) to 405 Ma (e.g. Leinster Granite). Geochronological evidence for this pre-UORS surface in the Dingle Group is given not only by late Neoproterozoic zircon ages which suggest a proximal Ganderian source, but also by the ca. 420 Ma KDE peak ages for detrital apatites from the Ballymore Formation which are consistent with a Late Caledonian (430-420 Ma) source.

The Dingle Group data are consistent with a palaeodrainage model of a major drainage basin to the south west and transverse drainage from the north and south, as proposed by Todd (2000). However, a significant proportion of the sediment delivered to the basin would have had to be Laurentian in origin. Therefore, the drainage system of the major axial river into the basin must have extended to include the Caledonian highlands to the north.

A detrital zircon age spectrum from a single sample from the UORS on the Dingle Peninsula shows a dominant Laurentian affinity. In contrast to the LORS, this sample is dominated by zircons of around 1.05 Ga age and contains very few late Neoproterozoic zircons. The change in Laurentian source character from the LORS (dominated by 1.2 Ga zircons) to the UORS (dominated by 1.05 Ga zircons) lends support to the model of regional sinistral transtension across the ISZ during the Early Devonian Period (Brown et al., 2008; Cooper et al., 2016; Dewey and Strachan, 2003; Phillips et al., 1995; Todd, 1989) as the 1.2 Ga source was removed and the 1.05 Ga source was introduced. The paucity of late Neoproterozoic zircons in the UORS sample suggests that recycling of LORS into the UORS (Ennis et al., 2015; Soper and Woodcock, 2003) was unlikely.

The evidence given above that the LORS was not recycled into the UORS is further supported by a comprehensive detrital zircon, apatite and mica gechronological study of the UORS of the Middle to Upper Devonian Munster Basin as presented in Chapter 3. The Munster Basin is dominated by sedimentary rocks that are ultimately derived from Laurentia and that generally contain very few late Neoproterozoic zircons that could indicate a peri-Gondwanan association. In addition, detrital zircon KDE spectra for the UORS show Mesoproterozoic peaks between 1.05 Ga and 1.1 Ga as opposed to the 1.2 Ga peaks in the LORS. Extensive recycling of LORS was unlikely. The fact

that the LORS was not recycled implies, then, that the LORS in Ireland did not extend far beyond its present-day location on the Dingle Peninsula and was not continuous across the southern British Isles.

Four groups could be distinguished in samples from the UORS of southern Ireland based on MDS analysis of detrital zircon ages. Groups 1, 2 and 3 are linked in their northern derivation and association with Laurentia. However, their distinction lies in their stratigraphic and/or geographic position in relation to the Munster Basin. Group 1 samples are stratigraphically confined to within the margins of the western part of the Munster Basin. Group 2 samples are stratigraphically confined to within the margins of the eastern Munster Basin and, with the exception of one sample, Group 3 samples are from the uppermost formations within the UORS succession.

Although unlikely to be recycled from the LORS, the bulk of the sedimentary rocks of the Munster Basin represent recycling of clastic sequences. The remarkable similarities between detrital zircon age distributions of Group 1 and 3 samples with samples from the Laurentia-derived sedimentary rocks of the Southern Uplands (Waldron et al., 2014, 2008) and Longford Down (McConnell et al., 2016) terranes suggest that these terranes acted as a major source of detritus during deposition of the UORS. Enigmatically, granitoids of 430-400 Ma, which are proximal to the UORS (e.g. Leinster Batholith and Carnsore/Saltees granites) are not represented by detrital zircon ages in the UORS. Instead, the majority of samples show Ordovician KDE peaks which can also be explained by recycling of sedimentary rocks in the Longford Down terrane. The late Silurian to Early Devonian ages are, however, captured by both detrital white mica and apatite ages within the UORS. In terms of palaeodrainage, two major drainage systems are envisaged that cover a wide area to the north of the basin and crosses the ISZ. A third, smaller drainage system, separate from the main basin, is envisaged for the extrabasinal Harrylock Formation which contains an abundance of late Neoproterozoic zircons.

The detrital zircon provenance of the Carboniferous sedimentary rocks in the South Munster Basin is different in the eastern and western parts of the basin. The Toe Head Formation and Old Head Sandstone Formation in the

western part of the basin shared a common sediment source area throughout their deposition. This source area was very different to that of the underlying UORS of the Munster Basin. Very few pre-Neoproterozoic zircons are present in these samples. Instead they are dominated by zircons of ages between 410 and 390 Ma – an Acadian age. Late Neoproterozoic detrital zircons also form conspicuous KDE peaks suggesting a peri-Gondwanan contribution. The detrital zircons are interpreted to be derived predominantly from an Acadian granitic source that intruded Ganderian basement somewhere off the present southwest coast of Ireland. By contrast, in the eastern part of the basin, the Old Head Sandstone Formation shows a dominant Laurentian character which is interpreted here to represent either distal northern sources across the ISZ or reworking of the underlying UORS of Laurentian affinity. The stark difference in provenance from the western to the eastern ends of the basin can be explained by a physical separation of the two areas by a transgressing seaway.

Following provenance work by, for example, Caston (1995), Ewins and Shannon (1995) and Tyrrell (2005), who agreed that the southern part of Ireland acted as a source of sediment for the North Celtic Sea Basin during the Mesozoic, it was necessary to build a database of geochronological provenance proxies for the voluminous UORS of southern Ireland. In this way the database could be used as an analogue of possible sediment sources for the southern Irish offshore basins. The detrital zircon U-Pb dataset for the NCSB, SCSB, FB and GSB is considerably complex. One major difference between detrital zircon samples from the offshore basins and those from the UORS is that most of the offshore samples contain a significant proportion of late Neoproterozoic zircons which indicates a substantial contribution of peri-Gondwanan material. Determining the source of this material, however, is challenging because (i) the Celtic Sea region is tectonostratigraphically complex, with a number of peri-Gondwanan terranes being possible sediment source candidates; (ii) these sources are difficult to distinguish by their detrital zircon ages only. In addition, many of the samples in the offshore basins contain large proportions of Mesoproterozoic and Palaeoproterozoic detrital zircons that can only be explained by input of a Laurentian source, thereby

obscuring potential distinguishing characteristics of the various peri-Gondwanan terranes. Chapter 4 attempts to deconvolve these detrital zircon age distributions by the use of inverse Monte Carlo modelling (Sundell and Saylor, 2017) to compare and apportion existing detrital zircon ages of various potential sources to the offshore samples.

Two Triassic samples were taken in the study area: one from the FB and one from close to the southern margin of the NCSB. The distribution of detrital zircon ages from the Triassic sample in the NCSB is very similar to samples from the western Wessex Basin which have been interpreted as originating to the south, in Cadomia. Certainly, the presence of detrital zircons forming a KDE peak at ca. 320 Ma in the NCSB and the dominant late Neoproterozoic age of detrital micas in the FB, suggest that these Triassic sediments were being sourced from south of the Rheic Suture. In the case of the NCSB, the source area included Variscan granitoids. However, in the FB, a large proportion of detrital zircons are Acadian in age – similar to samples taken from the western South Munster Basin. Therefore, the Triassic sedimentary rocks in the FB must be a product of mixing of proximal northern sources consisting of sedimentary rocks similar to those of the western South Munster Basin and Cadomian sources which are not intruded by Variscan granitoids (or the granitoids were not exhumed in that area at that time).

The Middle to Upper Jurassic detrital zircon samples of the NCSB indicate a mixed source of both Laurentian and peri-Gondwanan affinity. The Laurentian component is significant because it likely represents recycling of the proximal UORS in southern Ireland. In the northeastern NCSB, a single Lower Cretaceous sample also indicates a similar scenario, however, detrital muscovites indicate that rocks of similar age to the ca. 430 Ma Carnsore and Saltees granites were providing micas to the NCSB during Early Cretaceous deposition of the Greensand Group. Detrital zircons from Lower Cretaceous rocks in the central part of the NCSB, however, indicate that sediment of Laurentian affinity did not play a major role in that area. This observation implies that the southwestern part of Ireland was not being eroded during this time as suggested by apatite fission track data (Allen et al., 2002). The Lower Cretaceous sedimentary rocks of the NCSB and SCSB are tentatively

attributed to southeastern and northeastern source areas in Eastern Avalonia and the Harlech Dome (Megumia). However, these areas cannot account for the 360-430 Ma detrital zircons found in these samples. A 360 Ma source is difficult to pinpoint but sources of 410 Ma and 430 Ma zircons are found in southeast Ireland in the form of the Leinster Batholith and Carnsore and Saltees granites.

A single detrital zircon sample taken from the Middle Jurassic succession in the GSB produced a spectrum of ages that is typical of a Laurentian derivation. However, unlike the Laurentia-derived Group 1, 2 and 3 samples of the UORS in the Munster Basin, the GSB sample is dominated by late Palaeoproterozoic zircons. This difference suggests that it is not likely to be the product of recycling of UORS sedimentary rocks. Instead, a distal source north of the ISZ is suggested, with the Porcupine Basin acting as a conduit for sediment transport. A similar scenario is envisaged for a Lower Jurassic sample in the FB which shows a strikingly similar detrital zircon age distribution. The lack of late Neoproterozoic zircons in the Lower to Middle Jurassic sedimentary rocks in this region is of particular importance as it indicates that the Flemish Cap and/or Orphan Knoll, both associated with Avalonia, could not have acted as sediment sources during that time.

5.2 Concluding remarks and future work

By determining the provenance of onshore Devonian and offshore Mesozoic basins, this thesis broadly tests the hypothesis that the Mesozoic deposits of the NCSB, SCSB, FB and GSB were the product of multiple erosional and depositional cycles. As is common in studies of natural samples, the provenance of sedimentary rocks within these basins is complex. A simple true or false assessment of the hypothesis is, therefore, untenable.

Although it is shown in this thesis that the UORS of the Munster and South Munster basins does not represent reworking of LORS such as that found in the Dingle Basin, it is likely that a large proportion of these sedimentary rocks represent recycling of Ordovician to Silurian metasedimentary rocks in the Longford Down and Southern Uplands terranes. Detrital zircons from the UORS would therefore represent at least two cycles of resedimentation.

Certainly for the Upper Jurassic rocks in the NCSB, there is strong evidence that the UORS acted as a major sediment source. Although the Lower Jurassic of the Fastnet Basin and the Middle Jurassic of the Goban Spur Basin displays a Laurentian affinity, detrital zircon age spectra suggest a different Laurentian source to that in the UORS. Triassic sedimentary rocks in the FB may have been, at least partially, derived from reworking of similar sediments to those in the western South Munster Basin – this would account for the high number of zircons of ca. 400 Ma age. The Triassic rocks in the southern margin of the NCSB were not sourced from recycling of any UORS sediments. Instead, a southern source beyond the Rheic Suture is likely. The provenance of Lower Cretaceous samples in the NCSB, SCSB and FB is difficult to constrain. The generally low proportions of pre-Neoproterozoic detrital zircon grains suggests that a Laurentian source was unlikely to have contributed significantly, if at all. However, the presence of detrital zircons with ages between 430-400 Ma in some Lower Cretaceous samples requires sources that are presently only exposed in Ireland.

Sediment recycling can be well constrained if sufficient geochronological data is available for the sedimentary rocks from which the sediments are thought to have been derived. Unfortunately, one paradoxical problem in provenance studies that will never be overcome is that we are searching for a source for sediment which has been removed from its original location, that is, the source itself has been removed. Building a geochronological database of possible “source areas” that may be analogous to the original source remains our best option. In addition, using geochronology and other isotopic data of multiple mineral proxies is necessary to capture the full array of possible source areas. These proxies must cover a range of temperature sensitivities in order to benefit the study.

The interpretations developed in this thesis can benefit from a high resolution detrital zircon study of the entire succession in the Dingle Basin, from the Lower Ordovician rocks – which would provide valuable insight into collisional processes in western Ireland during the Caledonian Orogeny – to the Upper Devonian rocks. Seeing how detrital age distributions would differ through time in the Dingle Basin would aid in better understanding its

development and the evolution of its surroundings. Coupling these ages with detrital zircon Hf isotopes in all the studied basins might help understand the evolution of the source from which the zircons came, although this method requires better zircon Hf isotopic characterisation of source areas to facilitate comparison. Detailed heavy mineral analysis would also place better constraint on possible source regions in all the studied basins. This project has inspired the development of a new PhD project which is already underway which will determine the provenance and basin evolution of the eastern-most part of the NCSB as well as the St. George's Channel Basin.

5.3 References

Allen, P.A., Bennett, S.D., Cunningham, M.J.M., Carter, A., Gallagher, K., Lazzaretti, E., Galewsky, J., Densmore, A.L., Phillips, W.E.A., Naylor, D., Hach, C.S., 2002. The post-Variscan thermal and denudational history of Ireland. Geol. Soc. London, Spec. Publ. 196, 371–399. doi:10.1144/GSL.SP.2002.196.01.20

Brown, P.E., Ryan, P.D., Soper, N.J., Woodcock, N.H., 2008. The Newer Granite problem revisited: a transtensional origin for the Early Devonian Trans-Suture Suite. Geol. Mag. 145, 235–256. doi:10.1017/S0016756807004219

Caston, V.N.D., 1995. The Helvick oil accumulation, Block 49/9, North Celtic Sea Basin. Geol. Soc. London, Spec. Publ. 93, 209–226. doi:10.1144/GSL.SP.1995.093.01.15

Cawood, P.A., Nemchin, A.A., 2001. Paleogeographic development of the east Laurentian margin: Constraints from U-Pb dating of detrital zircons in the Newfoundland Appalachians. Geol. Soc. Am. Bull. 113, 1234–1246. doi:10.1130/0016-7606(2001)113<1234:PDOTEL>2.0.CO;2

Cooper, M.R., Anderson, P., Condon, D.J., Stevenson, C.T.E., Ellam, R.M., Meighan, I.G., Crowley, Q.G., 2016. Shape and intrusion history of the Late Caledonian, Newry Igneous Complex, Northern Ireland, in: Young, M.E. (Ed.), Unearthed: Impacts of the Tellus Surveys of Ireland. Royal Irish Academy, Dublin, pp. 145–155. doi:DOI:10.3318/ 978-1-908996-88-6.ch11

Dewey, J.F., Strachan, R.A., 2003. Changing Silurian-Devonian relative plate

motion in the Caledonides: sinistral transpression to sinistral transtension. J. Geol. Soc. London. 160, 219–229. doi:10.1144/0016-764902-085

Ennis, M., Meere, P.A., Timmerman, M.J., Sudo, M., 2015. Post-Acadian sediment recycling in the Devonian Old Red Sandstone of Southern Ireland. Gondwana Res. 28, 1415–1433. doi:10.1016/j.gr.2014.10.007

Ewins, N.P., Shannon, P.M., 1995. Sedimentology and diagenesis of the Jurassic and Cretaceous of the North Celtic Sea and Fastnet Basins. Geol. Soc. London, Spec. Publ. 93, 139–169. doi:10.1144/GSL.SP.1995.093.01.12

McConnell, B., Rogers, R., Crowley, Q., 2016. Sediment provenance and tectonics on the Laurentian margin: implications of detrital zircons ages from the Central Belt of the Southern Uplands–Down–Longford Terrane in Co. Monaghan, Ireland. Scottish J. Geol. 52, 11–17. doi:10.1144/sjg2015-013

Phillips, E.R., Barnes, R.P., Boland, M.P., Fortey, N.J., McMillan, A.A., 1995. The Moniaive Shear Zone: a major zone of sinistral strike-slip deformation in the Southern Uplands of Scotland. Scottish J. Geol. 31, 139–149. doi:10.1144/sjg31020139

Soper, N.J., Woodcock, N.H., 2003. The lost Lower Old Red Sandstone of England and Wales : a record of post-Iapetan flexure or Early Devonian transtension? Geol. Mag. 140, 627–647. doi:10.1017/S0016756803008380

Sundell, K., Saylor, J.E., 2017. Unmixing detrital geochronology age distributions. Geochemistry, Geophys. Geosystems. doi:10.1002/2016GC006774

Todd, S., 1989. Role of the Dingle Bay Lineament in the evolution of the Old Red Sandstone of southwest Ireland, in: Arthurton, R., Gutteridge, P., Nolan, S. (Eds.), The Role of Tectonics in Devonian and Carboniferous Sedimentation in the British Isles. The Yorkshire Geological Society, Bradford, pp. 35–54.

Todd, S.P., 2000. Taking the roof off a suture zone: basin setting and provenance of conglomerates in the ORS Dingle Basin of SW Ireland. Geol. Soc. London, Spec. Publ. 180, 185–222.

doi:10.1144/GSL.SP.2000.180.01.10

Tyrrell, S., 2005. INVESTIGATIONS OF SANDSTONE PROVENANCE. PhD thesis. University College Dublin.

Waldron, J.W.F., Floyd, J.D., Simonetti, A., Heaman, L.M., 2008. Ancient Laurentian detrital zircon in the closing Iapetus ocean, Southern Uplands terrane, Scotland. Geology 36, 527–530. doi:10.1130/G24763A.1

Waldron, J.W.F., Schofield, D.I., Dufrane, S.A., Floyd, J.D., Crowley, Q.G., Simonetti, A., Dokken, R.J., Pothier, H.D., 2014. Ganderia-Laurentia collision in the Caledonides of Great Britain and Ireland. J. Geol. Soc. London. 171, 555–569. doi:10.1144/jgs2013-131

Appendices

Explanation of Appendices

The appendices presented here consist of an account of the contribution of all authors to this work (Appendix A), text that was excluded from manuscripts during the editing process (to shorten manuscripts for publication; Appendix B), sample selection and preparation methods as well as sample descriptions (Appendix C), list of conference presentations (Appendix D), a list of courses and workshops attended (Appendix E) and a reference list of references cited herein (Appendix F). All geochronological data can be found in Excel files on the included CD-ROM.

Appendix A

This appendix documents the contribution of all authors involved in the entire thesis project. Multiple authors have contributed to three major chapters presented in this thesis. The original project ideas were conceived by the supervisors of the project, Drs. Patrick Meere and Kieran Mulchrone. They applied for and were awarded full funding for the project by the Petroleum Infrastructure Program of Ireland. Their role as supervisors meant that they were involved in editorial advice and discussions involving interpretation of data.

Brenton Fairey and Aidan Kerrison worked together in the field to acquire all the samples used in this thesis. Drs. Pat Meere and Kieran Mulchrone were also involved in some of the initial field work.

All the major interpretations and conclusions in this thesis are the work of the lead author on all papers, Brenton Fairey. Apart from suggesting the removal of some sections to make the manuscripts more succinct, very little text has been adjusted by the other authors involved in the work. Aidan Kerrison, involved in the project as an MSc student, contributed significantly to detrital zircon sample preparation and analysis. For onshore work, he prepared and analysed all samples from the Dingle Peninsula and western part of the Munster Basin (nine of the sixteen onshore samples). For offshore work, he prepared and analysed six of the fifteen samples. All detrital mica samples were separated by Brenton Fairey. Dr. Klaudia Kuiper analysed the detrital mica samples and reduced the resulting data. She was also responsible for recalculating the data from Ennis et al. (2015). Meg Ennis assisted with editorial matters and provided thin sections for some of the Munster Basin and Dingle Basin formations. Her detrital mica total fusion ages were recalculated and reinterpreted in this thesis, bearing in mind the newly acquired data.

Under the supervision of Prof. Ulf Linnemann, Mandy Hoffman and Andreas Gartner, Aidan Kerrison and Brenton Fairey performed analyses of all detrital zircon samples in the study. Although Aidan Kerrison and Brenton Fairey performed data reduction on a number of samples to learn the

process, this task was ultimately done by Prof. Ulf Linnemann, Mandy Hoffman, Andreas Gartner and Benita-Lisette Sonntag as they were more experienced with the process and would produce more consistent results.

The apatite data presented in Chapter 2 and Chapter 3 were the unpublished 'by-product' of a thermal modelling project (Cogné et al., 2016, 2014) that was undertaken by Drs. David Chew, Chris Mark and Nathan Cogné. These authors are therefore responsible the acquisition of apatite U-Pb data.

All interpretations presented in this thesis are the work of the PhD candidate, Brenton Fairey.

Appendix B

This section presents work that was eventually removed from the manuscripts presented in the main body of the thesis.

B.1.Detailed review of the Munster Basin sedimentary successions

The sedimentary and volcanic successions of the Munster Basin were deposited from the earliest late Givetian to early Carboniferous times in a period that lasted at least ca. 23 Ma (Williams et al., 2000). The base of the Munster Basin succession is not seen between the Iveragh and Beara Peninsulas, where the sedimentary package is thickest (>5.7 km, according to Williams et al., 2000). Correlating units from west to east in the Munster Basin is problematic due to the fact that most of the formations are areally restricted tongues (Williams et al., 1989) and depositional ages are difficult to constrain due to a lack of distinctive palynological and palaeontological evidence. Furthermore, there are few datable volcanic horizon in the eastern part of the basin. There is, therefore, a large number of formation that do not have basin-wide correlatives.

The Munster Basin is structurally bound to the north by the Dingle Bay-Galtee Fault Zone (Williams et al., 2000). The 1000 m isopach has often been regarded as the stratigraphic basin margin and is said to separate the thick intrabasin accumulations of ORS from overstepping successions (Williams et al., 1989). The southern boundary is not seen onshore and has not been delineated to date but if one extrapolates the 1000 m isopach following onshore trends then the basin does not extend far offshore.

B.1.1.Western Munster Basin - Formations and correlations

B.1.1.1.Valentia Slate, Lower Slate and Bird Hill Formation

The oldest exposed formation in the Munster Basin is the Valentia Slate Fm which crops out on Valentia Island and the Iveragh Peninsula. This formation is comprised of purple to greenish-grey siltstones as well as subordinate fine- to medium-grained sandstones (Capewell, 1975). Minor pebble conglomerates also occur in the Valentia Slate Fm and Capewell

(1975) drew similarities between metamorphic clasts in these conglomerates and those in the St. Finans Sandstone Formation, suggesting that these clasts had a similar provenance. Average grain size increases upwards until a significant increase in the number of sandstone units indicates the base of the conformably overlying St. Finan's Sandstone Formation (Capewell, 1975). Graham (1983) described the Valentia Slate Fm as being part of a fine-grained fluvial facies which is the most voluminous in the Munster Basin. Similarly, MacCarthy (1990) included the formation in a facies association which represented floodplain sheetfloods and ephemeral lakes.

A pyroclastic bed known as the Enagh Tuff Bed occurs toward the top of the Valentia Slate Fm (Williams et al., 1997). In dating magmatic zircons from this bed, Williams et al. (1997) established that the minimum depositional age of the Valentia Slate Fm must be ca. 385 Ma. Dating of the Keel Tuff and bulk rock geochemical analysis on both the Enagh Tuff and Keel Tuff led Williams et al. (2000) to propose that the two beds are correlated. This correlation allowed Williams et al. (2000) to rename the tuff as the Keel-Enagh Tuff Bed.

The Valentia Slate Fm has been correlated with the Lower Slate Formation of Sneem (Capewell, 1975; Williams et al., 1989) as well as the Bird Hill Formation which forms part of successions found in south Derrynasaggart Mountains, Beara Peninsula and Shehy Mountains (Williams et al., 1989).

B.1.1.2. St. Finan's Sandstone, Chloritic Sandstone and Green and Grey Sandstone Formations

These formations have been correlated on lithological bases by Capewell (1975) and are also accepted to be correlatives by Williams et al. (1989) They conformably overly the Valentia Slate and Lower Slate Formations (Williams et al., 1989). The Chloritic Sandstone Formation, as the name implies, is predominantly composed of chlorite-rich, green medium- to coarse-grained sandstones as well as polymictic orthoconglomerates (Williams et al., 1989). A small proportion of the formation is composed of thick beds of siltstone (Williams et al. 1989). According to Williams et al.

(1989), this formation represents the proximal facies of a terminal fan-type depositional environment in which sediment was being sourced from the north (the distal end-member being represented by the Gotanimill Fm). Williams (1993) argued that the areally restricted Grey Sandstone Fm, like the Green Sandstone Fm, be considered part of the Chloritic Sandstone Formation. He reasoned that the combined thickness of the Green and Grey Sandstone Formations is similar to the general thickness of the Chloritic Sandstone Fm and that the sedimentary structures and lithologies of the Grey Sandstone Fm are similar to those of the Green Sandstone Fm. Pracht (1997) adopted the name Glenflesk Chloritic Sandstone Formation to include the Chloritic Sandstone and Green and Grey Sandstone Formations. The St. Finan's Sandstone Fm occurs on the Iveragh Peninsula. It mainly comprises medium-grained grey and green sandstones with subordinate purplish-grey to grey siltstones (Capewell, 1975). Capewell (1975) also describes polymictic conglomerates and pebbly sandstones from the St. Finan's Sandstone Fm which included sedimentary clasts as well as some metamorphic clasts. He equated these conglomerates to those of the Inch Conglomerate on the Dingle Peninsula but a number of authors later suggested that, rather than being correlated, the conglomerates in the St. Finan's Sandstone Fm represent recycling of clasts from the Inch Conglomerate (see Todd, 2000 and references therein). Williams et al. (1989) include the St. Finan's Sandstone Formation as a western part of the terminal fan depositional environment that comprises the Chloritic Sandstone and Gortanimill Formations.

B.1.1.3.Gortanimill and Slaheny Formations

Green, very fine- to medium-grained sandstones are the dominant lithology in the Gortanimill Formation with the deficit being made up by siltstone (Williams et al., 1989). The depositional environments in which these lithologies occur include high energy sheetfloods as well as shallow, low-sinuosity fluvial channels flowing across active floodplains (Williams et al., 1989). According to Williams et al. (1989), this floodplain environment terminated by infiltration as no evidence of a terminal, extensive lacustrine

environment exists. The Slaheny Formation is equated with the Gortanimill Formation by Williams et al. (1989) and Williams (1993). Williams (1993) describes Slaheny and Gortanimill 'environmental complexes' and equates them both laterally and temporally. He does indicate, however, that the Slaheny complex has less diverse sedimentary environments than the Gortanimill system. The Slaheny Fm consists of purple siltstones alternating with medium- to coarse-grained micaceous sandstones with minor intraformational conglomerates (Pracht and Sleeman, 2002). In the Derrynasagart Mountains, Beara Peninsula and East Shehy Moutains, these formations conformably overly the Bird Hill Formation (Williams et al., 1989). The Gortanimill Formation represents a distal end member of the Glenflesk Chloritic Sandstone Formation (Williams et al., 1989).

B.1.1.4.Caha Mountain Formation

The Caha Mountain Fm can be found on the Sheep's Head and Beara Peninsulas as well as the NW Shehy Mountains. According to Williams (1993), the formation also extends northward in to the Iveragh Peninsula and is there represented by the lower most 470 m of the Purple Sandstone Formation. Williams (1993) also extends the formation in to the bottom 400 m of the Ballinskelligs Sandstone Fm in west Iveragh. The formation forms part of the 'background' sedimentation of Williams et al. (1989). It overlies the Gortanimill and Slaheny Formations and its base is marked by the appearance of fine-grained purple sandstones with red siltstone interbeds (Pracht and Sleeman, 2002). Pracht and Sleeman (2002) describe intraformational breccias toward the top of the formation with the inclination of clasts indicating transport direction from the NW. The depositional environment is said to be one of distal braided river channels with unconfined sheet floods with coarser-grained sandstone bodies representing active river channels in a flood plain environment (Pracht and Sleeman, 2002)

B.1.1.5. Gun Point, Lower Purple Sandstone, Purple Sandstone and Ballinskelligs Sandstone Formations

The Gun Point Fm can be found in the Derrynasaggart and east Shehy Mountains and the Beara Peninsula. It is dominated by fine- to medium-grained red to purple sandstones and purple siltstones and can be distinguished from the underlying Bird Hill and Caha Mountain Formations based on the relative abundance of coarse-grained sandstone units (Williams, 1993). Intraformational conglomerates have also been noted by (Williams, 1993). The Purple Sandstone Fm around Sneem and the Lower Purple Sandstone Fm of NE Iveragh have been correlated with the Ballinskelligs Sandstone Fm and the Gun Point Formation (Williams et al., 1989; Williams, 1993). More recently, Pracht (1997) reassigned the Lower Purple Sandstone and Purple Sandstone Formations to the Ballinskelligs Fm and this is maintained in the present study. The Ballinskelligs Formation conformably overlies the St. Finnan's Sandstone Fm (Capewell, 1975; Williams et al., 1989). Although, if the northern extension of the Caha Mountain Fm by Williams (1993) is to be considered, then this formation is underlying the Ballinskelligs Sandstone Fm in Sneem and west Iveragh. The Ballinskelligs Sandstone Fm is dominated by bright purple, medium-grained sandstones with subordinate siltstones and minor conglomerate (Capewell, 1975).

B.1.1.6. The Sherkin and Castlehaven Formations

Present outcrop of the Sherkin Fm is restricted to SW County Cork and is the lowest part of the Old Red Sandstone Succession in this area (Higgs et al., 2000). The formation is composed of grey and green, fine- to medium-grained sandstones as well as subordinate grey-green and purple mudstones (Higgs et al., 2000). The lowest exposed unit in the Sherkin Fm, the Foilcoagh Bay Beds, has been shown by Higgs et al. (2000) to have be influenced by a marine incursion during mid-Frasnian times. This has provided a later depositional age for the Sherkin Formation than the existing age of late Givetian-early Frasnian provided by the miospore assemblage

studied by Clayton and Graham (1974). MacCarthy (1990) suggests that the Sherkin Fm is a distal part of the depositional environment that makes up the Chloritic Sandstone and Gortanimill Formations with the palaeodrainage swinging from south and SE to east. However, Williams (1993) suggests that, although the Sherkin system and the Chloritic Sandstone-Gortanimill system were coeval, they were separate systems; an unknown sediment and water source lying to the ENE is suggested for the Sherkin system. Higgs et al. (2000) support and reinforce MacCarthy's interpretation and adds that the Sherkin Fm represents a transition from marine influenced depositional environments at the base to continental red bed conditions toward the top. Conformably overlying the Sherkin Fm in SW County Cork is the Castlehaven Fm. This formation thins to the north and is absent beyond the Beara Peninsula. In the Beara Peninsula and east Shehy Mountains the Castlehaven Formation conformably overlies the Gun Point Fm (Williams et al., 1989). According to Graham and Reilly (1976), the Castlehaven Fm is dominated by purple mudrocks with minor sandstones. It thus forms part of the 'background' sedimentation of Williams et al. (1989). The depositional environment was fluvial with minor river channels in a floodplain (Graham and Reilly, 1976).

B.1.1.7.Toe Head Formation and equivalents

The Toe Head Fm overlies the Castlehaven Fm and is dominated by fine- to medium-grained, grey-green sandstone units (Graham, 1975). Its base is defined by the appearance of sandstone units which are over two meters in thickness and have large-scale cross beds and flat beds (Graham, 1975). The loss of purple mudrocks, abundant in the Castlehaven Fm, is another indicator of the base of the Toe Head Fm (Graham, 1975). Graham (1975) recorded an overall fining upward sequence in the Toe Head Fm which he interpreted as a broad transgressive regime. Evidence of only unidirectional palaeoflow, lack of marine fossils and the lack of heterolithic facies allowed Graham (1975) to interpret the Toe Head Fm as terrestrial and he further suggests that the environment was one of meandering rivers in a coast-proximal fluvial plain environment. Williams et al. (1989), however, describe

the presence of heterolithic lithologies and suggest that at least some parts of the formation were influenced by marine interactions. The formation is considered to be transitional from terrestrial (i.e. Castlehaven Formation) to marine conditions due to the fact that the conformably overlying formation, the Old Head Sandstone Fm, was deposited in a marine environment (Graham, 1975; Williams et al., 1989). According to Williams et al. (1989), palaeocurrent directions in the Toe Head Fm are different across the Dunmanus Fault. North of this fault, the dominant palaeocurrent direction is south whereas to the south of the fault, palaeocurrents were directed east and northeast. Substantial thickening of the formation is seen south of the Dunmanus Fault (Williams et al., 1989). In Williams et al. (1989) and Williams (1993), the Toe Head Formation is equated to the Derryquin Sandstone Fm at Sneem and in NE Iveragh by the Ardnagluggen and Upper Purple Sandstone Formations. The Toe Head Fm *sensu stricto* is recognised as far north as the Beara Peninsula (Williams, 1993).

B.2.1. Eastern Munster Basin - Formations and Correlations

B.1.2.1. The Comeragh Mountains Succession

The Coumshingaun Conglomerate Fm forms the lowest Devonian stratigraphic unit of the Comeragh Mountains succession, where it lies unconformably on Lower Palaeozoic slates (Penney, 1980). It is dominated by poorly-bedded, coarse conglomeratic lithologies with minor lenses of coarse sandstone (Penney, 1980). A maximum thickness of 850 m was calculated by Penney (1980) who also noted that the formation rapidly thins to the northeast and south of the Lower Palaeozoic inlier. Two volcanic members that occur within the Coumshingaun Conglomerate Fm have been described by Penney (1980), namely the Coolnahorna Volcanic Member and the Carrigduff Volcanic Member. He interpreted these volcanic rocks as basaltic aa flows. The conglomerates of this formation contain clasts that resemble sedimentary and volcanic rocks of the underlying Lower Palaeozoic formations (Penney, 1980). But Penney (1980) also found granitic, quartzitic and tourmaline-bearing clasts. The overall depositional

environment has been interpreted as one of proximal braided streams (Penney, 1980).

The Comeragh Conglomerate-Sandstone Fm comformably overlies the Coumshingaun Conglomerate Fm and is distinguished from the latter by increased abundance of sandstone and silstone units, absence of polymict conglomerate clasts and its predominantly well-bedded character (Penney, 1980). Furthermore, bedding tends to be thinner in the Comeragh Conglomerate-Sandstone Fm than in the Coumshingaun Conglomerate Fm (Penney, 1980). In places where the Coumshingaun Conglomerate Fm is not represented, the Comeragh Conglomerate-Sandstone Fm lies unconformably upon Lower Palaeozoic strata (Penney, 1980). The maximum thickness of the formation, as given by Penney (1980), is 610 m. According to Penney (1980), the clasts in this formation are predominantly composed of quartz but a provenance is not suggested. This author does not propose a depositional environment for the formation but the presence of imbricated conglomerate clasts and interbedded, cross-bedded sandstones and conglomerates suggests a continuation of a braided stream setting. The increased presence of finer-grained rocks may be indicative of a slightly less proximal setting. The increased abundance of sandstone and siltstone units in the succession as well as the decrease in conglomerate bed thicknesses, marks the base of the conformably overlying Nier Formation (Penney, 1980). However, Penney (1980) also suggests that, in places, the Nier Fm represents a distal facies equivalent of the Comeragh Conglomerate-Sandstone Fm.

The Croughaun Formation is considered by Penney (1980) to be a lateral equivalent of the Comeragh Conglomerate-Sandstone Fm. A discussion of the evidence for and against this can be found in Gardiner et al. (1983). The formation is approximated to be about 1040 m thick and is dominated by quartz pebble conglomerates and coarse sandstones with some siltstones (Penney, 1980). According to Penney (1980), the Croughan Fm differs from the Comeragh Conglomerate-Sandstone Fm only in that the rocks within it are predominantly green and folded, as opposed to red and largely undeformed.

The Nier Sandstone Formation varies in thickness from a maximum of around 2210 m to completely absent in some places (Penney, 1980). The dominant lithologies consist of red sandstones and mudstones with minor pebble conglomerates (Penney, 1980). This predominantly finer-grained character is one of the factors that distinguishes the Nier Sandstone Fm from the Comeragh Conglomerate-Sandstone Formation which both conformably overlies and laterally grades into the former (Penney, 1980).

B.1.2.2. The Galtee Mountain Succession

This succession predominantly crops out in the Galtee Mountains but also crops out around Slievereagh and Slievenamuck. The most comprehensive study undertaken to date on this succession is by Carruthers (1985) and Carruthers (1987). Carruthers (1985) recognised seven formations in the Galtee Mountains succession, the oldest of which lies, with angular unconformity, upon Silurian rocks. This lower most formation is the Pigeon Rock Formation. It consists of poorly sorted pebble and boulder conglomerates and breccias which are dominated by fine-grained sedimentary clasts (Carruthers, 1985). Carruthers (1985) also noted minor lenses of sandstone throughout the succession. This formation was likely to have been deposited in an alluvial fan environment (Carruthers, 1987).

The Pigeon Rock Fm is conformably overlain by the Galtymore Fm, a sandstone-dominated formation which oversteps the Pigeon Rock Fm and thus also unconformably overlies Silurian rocks in some places (Carruthers, 1987). The sandstones are largely pale red and fine- to medium-grained (Carruthers, 1987). Carruthers (1987) identified two aeolian and four fluvial lithofacies within the Galtymore Fm which he interpreted as representing erg and alluvial fan environments respectively. Palaeoflow was from the north in the alluvial fans whereas an opposing (south-southeasterly) palaeowind direction is interpreted for the erg environment (Carruthers, 1987). Carruthers (1987) suggested that the source of alluvial detritus was localised and thus consists of Silurian metasediments. He further suggests that immaturity of aeolian sediments within the Galtymore Fm as well as low degree of grain rounding indicates a local source for the erg deposits. The

Galtymore Fm is conformably overlain by a thin sequence of interbedded conglomerates, purple and red sandstones and mudrocks of the Lough Muskry Fm, as defined by Carruthers (1985). These deposits have been interpreted as being of ephemeral stream and flood plain origin (Carruthers, 1985).

The Lough Muskry Fm conformably transitions upwards into the Slievenamuck Conglomerate Fm which is marked at its base by the presence of resistate conglomerates and course-grained purple sandstones (Carruthers, 1985). Purple-red mudrocks are also present and show abundant bioturbation in the form of rootlets and burrows (Carruthers, 1985). Common clast compositions in the conglomerates include vein quartz, jasper and chert as well as tourmalinised chert (Sleeman and McConnell, 1995). Carruthers (1985) suggests that the Slievenamuck Conglomerate Fm was deposited upon a gravel braidplain with sediment being sourced from a distant source to the north.

The Slievenamuck Conglomerate Fm conformably transitions upward into the Poulgrania Fm. This formation was formerly known as the Ballydavid Sandstone Fm (Carruthers, 1985) but was renamed by Sleeman and McConnell (1995). It is dominated by fine- to medium-grained red sandstones with minor, bioturbated, purple-red mudrocks and rare conglomerates containing resistate clasts (Carruthers, 1985). These units were deposited in a medial braided stream environment on a sandy alluvial plain with palaeoflow being from north to south (Carruthers, 1985). Carruthers (1985) suggested that the maturity of the sediments in the Poulgrania Fm indicate a distant sediment source.

The incoming of coarse-grained sandstones and resistate conglomerates marks the base of the conformably overlying Ardane Conglomerate Formation (Carruthers, 1985). Clast composition in the conglomerates is dominated by vein quartz and quartzite (Carruthers, 1985). Carruthers (1985) interpreted this formation as a gravel braidplain which results from progradation related to slowing of subsidence along the northern controlling fault system.

B.1.2.3.The Kiltorcan Formation

The Kiltorcan Formation is the most widespread formation in the eastern part of the Munster Basin. It represents the top of the Old Red Sandstone succession in the Comeragh Mountains area - overlying the Nier Sandstone and Comeragh Conglomerate-Sandstone Fms (Penney, 1980). This formation is not restricted to this area and is more widely distributed in the eastern Munster Basin than other formations described in this section. Colthurst (1978) identified five lithologies in the formation: conglomerate with intraformational mudstone clasts, coarse-grained white to yellow sandstone, medium- to fine-grained micaceous red to yellow sandstone, yellow to green silty mudstone and unbedded dark red to green mudstone. The influx of white, feldspar-rich sands during deposition of the Kiltorcan Formation represents the unroofing of the Leinster Granite at this time, according to Penney (1980). Colthurst (1978) suggested that the Kiltorcan Fm was deposited in 'low-sinuosity, unbraided' streams, meandering streams and ephemeral lakes. However, Jarvis (2000) suggests that at least parts of the Kiltorcan Fm were deposited in high-sinuosity rivers in an alluvial plain environment and, furthermore, that no evidence could be found for a lacustrine environment.

B.2.Petrography and Mica Chemistry of the ORS in southern Ireland

B.1.2.Petrography

Petrographic characteristics of the Dingle Basin and western part of Munster Basin are covered in detail in previous work (Ennis et al., 2015). Modal abundances of samples from the LORS and the UORS in southern Ireland from Ennis et al. (2015) are included in this section for comparison. This paper presents a short synopsis of petrographic analyses of samples from the eastern and central parts of the Munster Basin that were used for single-grain analyses. According to the classification scheme of Pettijohn et al (1987), four of the samples are wackes and one, from the Harrylock Formation is subarkose to sublitharenite (red pentagon symbols in Figure I).

Two of the wackes, one from the Galtymore Formation and one from the Kilnafrehan Conglomerate Formation, plot in the lithic greywacke field. The other two, from the Gortanimill Formation and Old Head Sandstone Formation, are quartzwackes. Sericite is commonly found as a major component of the matrix in the studied samples. It also commonly occurs as an alteration product of potassium feldspars. Authigenic quartz overgrowth and cementation (Figure II.D) is typical of most samples, sometimes obscuring the original grain boundaries (Figure II.A). In some sandstones, such as those from the Kiltorcan Formation, feldspar overgrowths are also present (Figure II.C). All samples contain at least minor modal amounts of detrital white mica. In the case of the Harrylock Formation, coarse-grained micas exceeding 500 µm are abundant (Figure II.C).

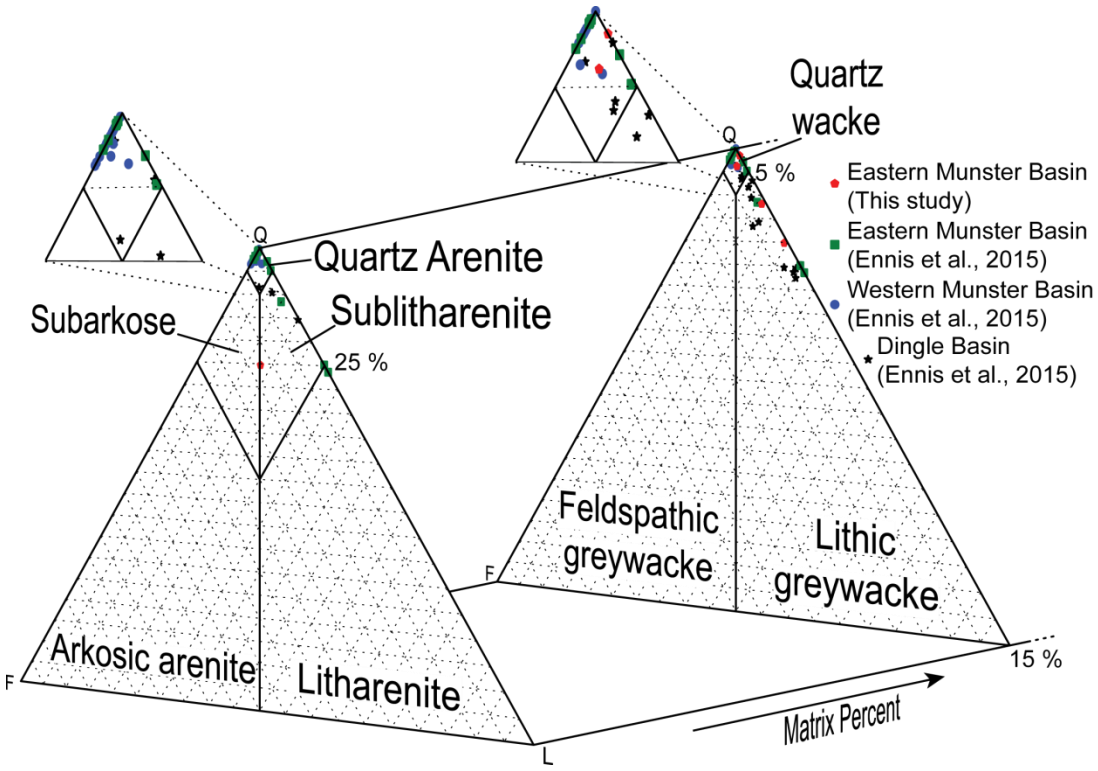

Figure I. Classification of sandstones in the Munster Basin (modified after Pettijohn et al., 1987).

Chlorite-mica stacks are present in varying proportions throughout the Munster Basin. The explanation of how these stacks were produced could impact interpretation of detrital white mica ages if one adopts an explanation

involving temperatures high enough to reset the Ar-Ar system. Such stacks have been identified by Craig et al. (1982) in Lower Palaeozoic metasedimentary rocks in Wales. Craig et al. (1982) suggested that they formed during diagenesis and low-grade metamorphism. More recent studies have suggested that the stacks represent an alteration/replacement product of detrital biotite and other mafic minerals (Milodowski and Zalasiewicz, 1991; Li et al., 1994). In the Munster Basin, chlorite-mica stacks do not contain inclusions that would suggest porphyroblastic growth. Furthermore, many stacks show deformation around more competent clasts (Figure II.E). Thus an ultimate detrital origin for these stacks is supported herein.

Lithic fragments in these samples are dominated by chert and shale. No volcanic clasts were identified in any of the studied samples. Accessory minerals can provide a means of assessing detrital input from various sources (e.g. mafic versus felsic, or high-grade metamorphic versus igneous). A common accessory phase present in all samples is zircon. White mica is also a very common accessory phase. Tourmaline is present in some samples. Opaque phases are also present but have not been identified in this study.

Modal abundances of framework grains in the LORS of the Dingle Basin predominantly populate the recycled orogen and quartzose recycled fields of Dickinson et al. (1983) (Figure 7). This is in contrast to the UORS which predominantly plots in the craton interior field, with the exception of some samples from the eastern part of the Munster Basin, which plot in the recycled orogen and quartzose recycled fields. Three of the five samples analysed in this study also plot in these fields.

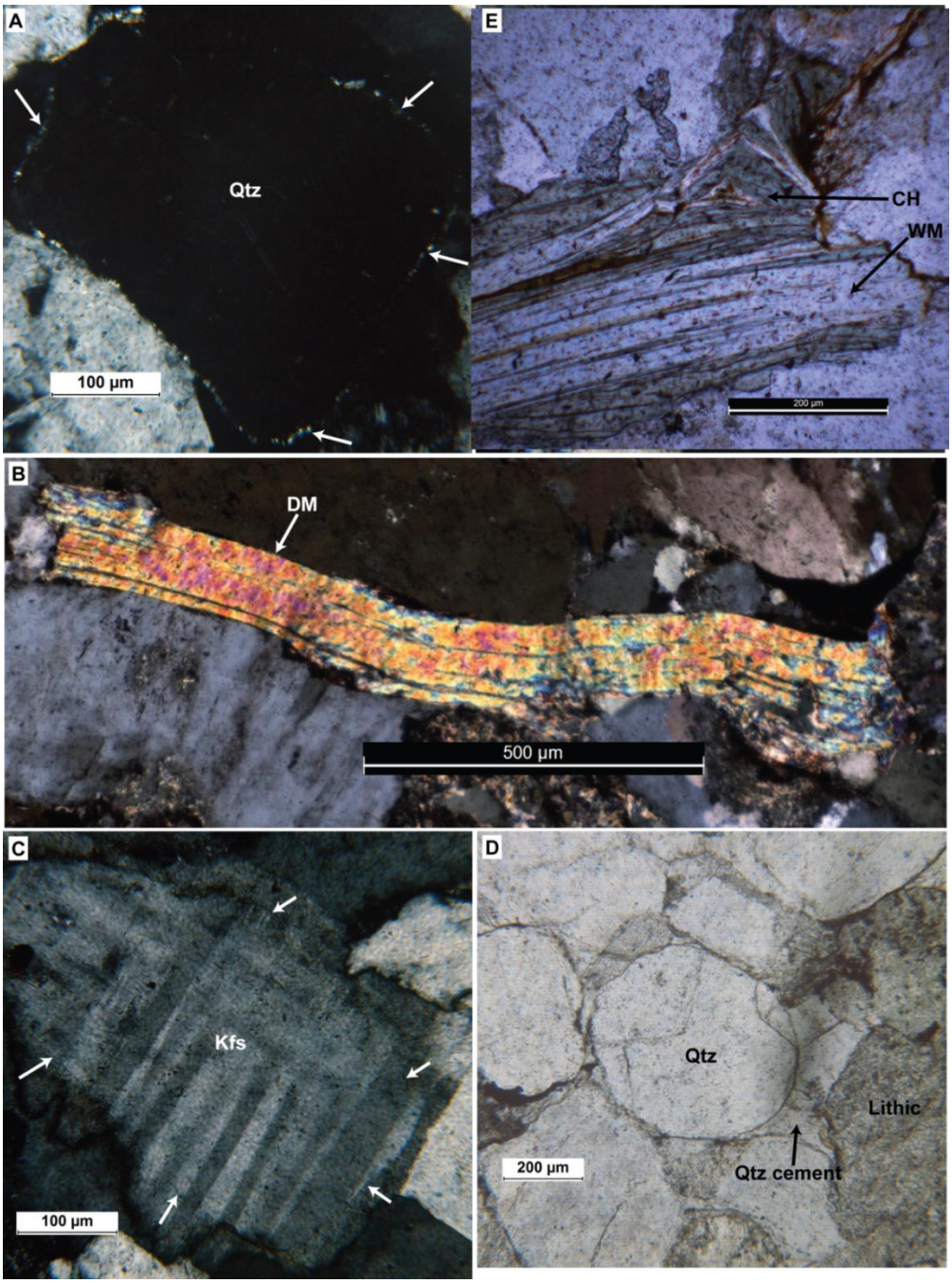

Figure II. Photomicrographs of samples from the eastern UORS in the Munster Basin. **A**. Extinct quartz grain with quartz overgrowth. Arrows indicate original grain boundary lined by sericite (cross-polarised light, sample BF12, Kiltorcan Formation). **B**. Coarse-grained detrital mica (DM) typical of the Harrylock Formation (cross-polarised light, sample BF13). **C**. Potassium feldspar with feldspar overgrowth. Arrows point to original grain boundary (cross-polarised light, sample BF12, Kiltorcan Formation). **D**. Well-rounded, high sphericity quartz grains as well as irregular-shaped, rounded fragments of shale. Quartz forms the dominant cement type. (plane-polarised light, sample BF19, Kilnafrehan Conglomerate Formation). **E**. Deformation of chlorite-mica stacks due to pressure from neighbouring quartz grains (WM: white mica, CH: chlorite; plane-polarised light, sample 220514-4, Coumaraglin Formation).

B.2.2.Mica Chemistry

Of the three detrital mica samples that were dated, two were selected (BF13 and BF22) for electron microprobe analysis in order to compare their geochemistry with that produced by Ennis et al. (2015) for the western part of the Munster Basin and for the Dingle Basin. Comparison of major element constituents on a per-formula-unit basis shows that the two samples broadly overlap with the chemistry of micas from the western part of the basin (Figure IV). Slightly elevated aluminium content relative to micas in the western Munster Basin is noted. Micas in the western Munster Basin also show a greater variability in Fe, Al an Ti content relative to the two samples analysed in this study. This difference in variability may indicate a corresponding difference in variability of sources of detrital micas from the central and eastern parts of the basin and those from the western part. However, a more thorough study of detrital micas from the basin and from potential sources (e.g. Leinster and Galway Granites) would be required to substantiate this statement.

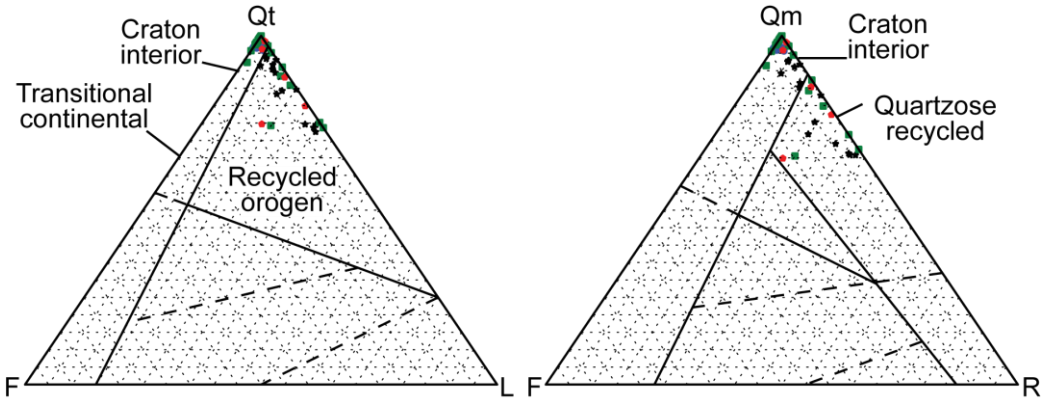

Figure III. Provenance of the LORS in the Dingle Basin and UORS in the Munster Basin based upon modal abundance of framework grains. See Figure I for legend.

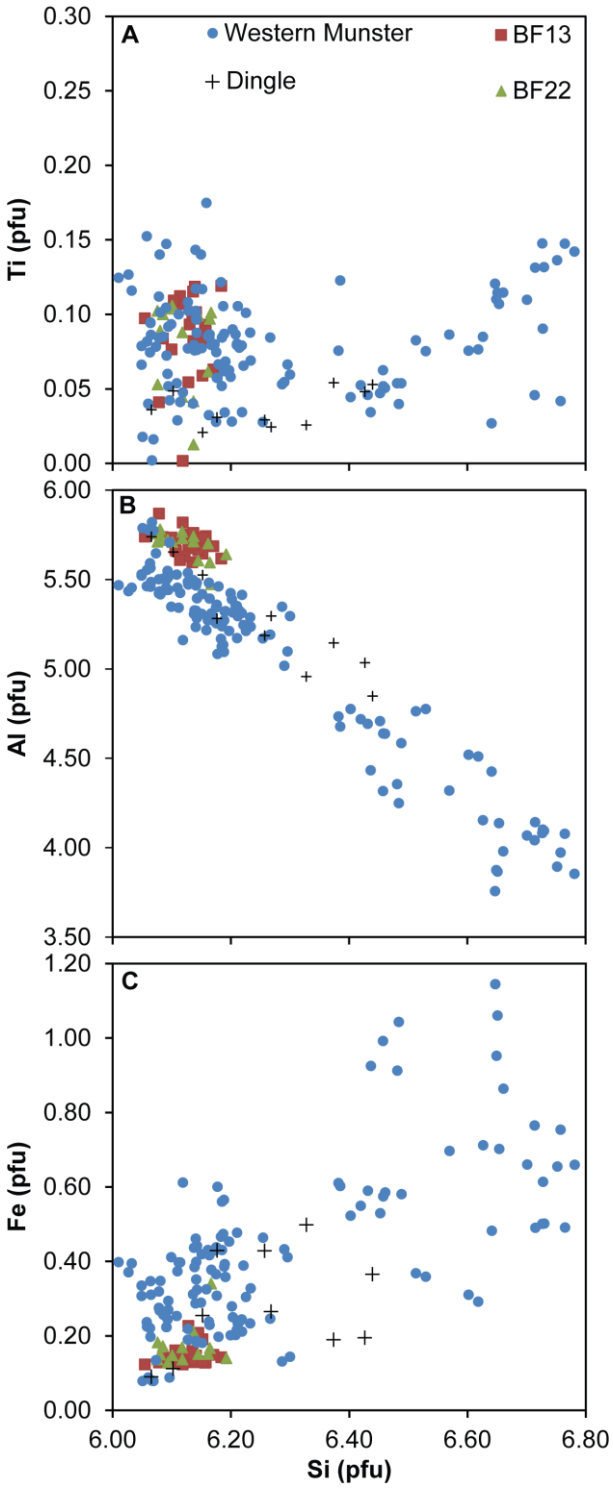

Figure IV. Variation of Ti (**A**), Al (**B**) and Fe (**C**) versus Si for the Dingle and western Munster Basin (data source: Ennis et al., 2015) and from this study (BF13 and BF22). All data is represented as atoms per formula unit based on 22 oxygens.

Appendix C

This section presents the detailed sample selection and preparation methods that were not included in the main body of the thesis. Analytical methods are presented in the thesis and references therein. Table I shows details for all samples used for detrital zircon and mica geochronology in this study. For details of detrital apatite samples the reader is referred to Cogné et al. (2016, 2014).

Onshore samples were collected from outcrop across southern Ireland. Typically between 5 kg to 10 kg samples were collected from outcrop with care taken, where possible, to avoid weathered material. The onshore samples were then cleaned with water in a high pressure hose to remove any unwanted, loose material. After being left to dry, the samples were split using a hydraulic splitter and crushed at a coarse setting in a jaw crusher. Although the jaw crusher was cleaned between samples, further precaution was taken to avoid cross-contamination by rinsing the rock chips with water. The chips were then dried at 50°C.

Offshore samples were obtained from the Petroleum Affairs Division sample storage facility in Dublin. In order to ensure that a sufficient number of zircons and micas would be obtained, a minimum sample size of 1 kg was obtained where possible. True sample size was difficult to estimate where drilling mud (and, in some cases, water) was still present in the samples. In order to meet this minimum requirement, sampling intervals for some samples was increased while still remaining within the same formation. Those drill-cutting samples that still contained drilling mud had to be cleaned. This was done by carefully washing the sample through a 100 µm sieve to remove the drilling mud and retain only the rock chips. Careful attention was paid to the contents of the drilling mud which can contain a muscovite additive. Therefore only samples that contained rock chips with macroscopically visible white micas in them were used for mica geochronology. The chip samples were then dried at 50°C. All samples were then packed and shipped to the Vrije Universiteit Amsterdam for further preparation as detailed below.

C.1.1. Detrital zircon sample preparation

Sample preparation was undertaken at Vrije Universiteit Amsterdam. Samples were crushed using a jaw crusher and disc mill. During both crushing and milling, the aperture size was incrementally reduced and the sample was sieved after each increment in order to prevent breakage of coarse-grained zircons. Clay-sized material was removed by flotation in water. The clean samples were placed in an oven at 50°C to dry overnight.

Once the samples were dry and cool they were subjected to two stages of heavy mineral separation with heavy liquid (diiodomethane). Both stages used a centrifuge for rapid separation of heavy minerals as outlined in IJlst, 1973. The first stage was to separate the bulk of the sample. Diiodomethane of density 3.0 $g.mL^{-1}$ was used at this stage. Diidomethane of density 3.3 $g.mL^{-1}$ was used in the second stage to further purify the heavy mineral separate. These separates were sieved into five size fractions: 60 μm; 60-90 μm; 90-120 μm; 120-180 μm; >180 μm. Each size fraction was passed through a Frantz magnetic separator in order to further concentrate zircons.

Zircons of all morphology, grain size and colour were hand-picked under a binocular microscope. Typically, between 120 and 180 zircons per sample were mounted in epoxy disks and ground and polished to expose the approximate center of the grains. Cathodoluminescent (CL) imaging was undertaken at the University of St. Andrews and at Trinity College Dublin in order to identify optimal positions for laser ablation.

C.2.1.Detrital mica sample preparation

White micas were liberated using a jaw crusher and a disc mill with sieving taking place between each incremental decrease in crush size to preserve coarse grains. Grain sizes range from 200 μm to 500 μm. Mica-rich samples were processed using an angled, stainless steel, vibrating table which concentrated flat minerals. Mica-poor samples were processed on the vibrating table and further separated by density using diiodomethane of density 2.78 $g.mL^{-1}$ in a centrifuge. A frantz magnetic separator was used where impurities were observed under a binocular microscope to retain the least magnetic fraction. One sample (BF21) was washed gently in three percent HNO_3 to remove impurities from grain surfaces. Finally, grains were hand-picked to avoid inclusions and other impurities.

Table I. Details of all samples collected and analysed in this study.

Well No.	Sample No.	Sample interval (m) Upper	Lower	Total depth (m)	Core No.	Coordinates y	x	Basin	Dep. Age	Group/Formation	Detrital Geochron.
N/A	AK19	N/A	N/A	N/A	N/A	52.181960	-10.205780	DB	E. Dev.	Coumeenoole Fm	zircon
N/A	AK21	N/A	N/A	N/A	N/A	52.131480	-10.359050	DB	E. Dev.	Slea Head Fm	zircon
N/A	AK17	N/A	N/A	N/A	N/A	52.166880	-9.874711	UORS DB	L. Dev.	Cappagh White Ss. Fm.	zircon
N/A	AK11	N/A	N/A	N/A	N/A	51.755630	-10.101230	MB	M. Dev.	Valentia Slate Fm.	zircon
N/A	BF22	N/A	N/A	N/A	N/A	51.983600	-8.586383	MB	M. Dev.	Gortanimill Fm.	zircon + mica
N/A	BF19	N/A	N/A	N/A	N/A	52.184167	-7.638517	MB	M./L. Dev.	Kilnefrehan Cong. Fm	zircon
N/A	BF15	N/A	N/A	N/A	N/A	52.369067	-8.198133	MB	M./L. Dev.	Galtymore Fm.	zircon
N/A	AK16	N/A	N/A	N/A	N/A	52.086730	-8.830000	MB	M./L. Dev.	Chloritic Ss. Fm.	zircon
N/A	AK10	N/A	N/A	N/A	N/A	51.990900	-10.212830	MB	L. Dev.	Ballinskelligs Ss. Fm.	zircon
N/A	AK07	N/A	N/A	N/A	N/A	51.713280	-9.582383	MB	L. Dev.	Gun Point Fm.	zircon
N/A	BF11	N/A	N/A	N/A	N/A	51.785808	-8.291022	MB	L. Dev.	Gyleen Fm.	zircon
N/A	BF12	N/A	N/A	N/A	N/A	52.462867	-7.179900	MB	L. Dev.	Kiltorcan Fm.	zircon
N/A	BF13	N/A	N/A	N/A	N/A	52.161017	-6.882650	MB	L. Dev.	Harrylock Fm.	zircon + mica
N/A	AK04	N/A	N/A	N/A	N/A	51.467460	-9.772069	SMB	E. Carb.	Toe Head Fm.	zircon
N/A	AK03	N/A	N/A	N/A	N/A	51.492470	-9.231367	SMB	E. Carb.	Old Head Ss Fm.	zircon
N/A	BF21	N/A	N/A	N/A	N/A	51.802517	-8.249017	SMB	E. Carb.	Old Head Ss Fm.	zircon + mica
48/18-1	48/18-1	850	1160	1370	Cuttings	51.425047	-8.422678	NCSB	E. Cret.	Wealden Gp.	zircon
48/24-4	48/24-4	999	1013	2472	1	51.331365	-8.296366	NCSB	E. Cret.	Greensand Gp.	zircon + mica
48/28-1	48/28-1	1402	1652	1752	Cuttings	51.164750	-8.462889	NCSB	E. Cret.	Wealden Gp.	zircon
49/09-2	49/09-2	750	761	1919	1	51.683958	-7.346094	NCSB	E. Cret.	Greensand Gp.	zircon + mica
49/09-3	49/09-3	2394	2401	2546	2	51.683950	-7.346061	NCSB	L. Jur.	Wexford Beds	zircon + mica
49/09-4	49/09-4	1612	1717	2078	Cuttings	51.671311	-7.384328	NCSB	M. Jur.	Wexford Beds	zircon
49/10-1	49/10-1	1904	1915	2042	1	51.684850	-7.176539	NCSB	L. Jur.	Purbeck	zircon
49/15-1	49/15-1	1106	1250	2134	Cuttings	51.658739	-7.059775	NCSB	L. Jur.	Purbeck	zircon
57/09-1	57/09-1	2371	2451	2507	Cuttings	50.827880	-8.381836	NCSB	E. Trias.	Sherwood Ss. Gp.	zircon
58/03-1	58/03-1	993	1192	2859	Cuttings	50.891993	-7.585781	SCSB	E. Cret.	Wealden Gp.	zircon
56/15-1	56/15-1	2499	2541	2541	Cuttings	50.544720	-9.197453	NCSB/FB	E. Carb.	Old Head Ss Fm.	mica
56/22-1	56/22-1	1067	1172	2266	Cuttings	50.185710	-9.636133	FB	E. Cret.	Wealden Gp.	zircon
56/26-2	56/26-2A	3102	3136	3136	Cuttings	50.007130	-9.897846	FB	E. Trias.	Sherwood Ss. Gp.	zircon + mica
56/26-2	56/26-2B	1220	1380	3136	Cuttings	50.007130	-9.897846	FB	E. Cret.	Wealden Gp.	zircon
63/10-1	63/10-1	2856	2910	3447	Cuttings	49.961360	-10.171140	FB	E. Jur.	Lias Gp.	zircon
62/07-1	62/07-1	3109	3155	4672	Cuttings	49.667300	-11.763030	GSB	M. Jur.	Dogger Fm.	zircon

DB, Dingle Basin; FB, Fastnet Basin; GSB, Goban Spur Basin; MB, Munster Basin ; NCSB, North Celtic Sea Basin; SCSB, South Celtic Sea Basin; UORS, Upper Old Red Sandstone

Appendix D

Below is a list of first author conference and workshop presentations relating to work undertaken during this thesis.

Fairey B., Tunwal M., Meere P., Mulchrone K., 2017. Coupling colour CL of quartz with multiple geochronological proxies in an attempt to determine extent of sediment recycling in Devonian and Mesozoic basins of southern Ireland. Poster presentation at the Atlantic Ireland Conference, Dublin, 31 October – 1 November, 2017.

Fairey B., 2017. Overview of sedimentary provenance activities at University College Cork. Oral presentation at the iCRAG sediment tracking meeting, University College Dublin, Dublin, 7 June 2017.

Fairey B., Tunwal M., Meere P., Mulchrone K., 2017. Coupling colour CL of quartz with multiple geochronological proxies in an attempt to determine extent of sediment recycling in Devonian and Mesozoic basins of southern Ireland. Poster presentation at the European Geosciences General Assembly, Vienna, 8 – 13 April 2017.

Fairey B., Meere P., Mulchrone K., Kerrison A., Kuiper K., Linnemann U., Hofmann M., Gärtner A. and Sonntag B., 2016. Detrital mica and zircon geochronology as evidence for the Devonian-Carboniferous “Old Red Staging Area” and development of super-mature sediments in the southern Irish offshore. Oral presentation at the British Sedimentological Research Group Annual General Meeting, Cambridge, 18 – 20 December 2016.

Fairey B., Meere P., Mulchrone K., Kerrison A., Kuiper K., Linnemann U., Hofmann M., Gärtner A. and Sonntag B., 2016. First detrital mica Ar-Ar ages from Devonian and Mesozoic sediments of onshore and offshore southern Ireland. Poster presentation at the Atlantic Ireland Conference, Dublin, 1 – 2 November, 2016.

Fairey B., Kerrison A., Meere P., Mulchrone K., Linnemann U., Hofmann M., Gärtner A., Sonntag B. and Byrne K., 2016. A provenance study of the Mesozoic North Celtic Sea Basin and eastern sector of the Upper Devonian Munster: insights from detrital zircon U-Pb ages. Oral

presentation at the 35th International Geological Congress, Cape Town, 27 August – 5 September 2016.

Fairey B., Kerrison A., Meere P., Mulchrone K., Linnemann U., Hofmann M., Gärtner A., Sonntag B. and Byrne K., 2016. Three cycles of sedimentation in ancient sedimentary basins of southern Ireland: insights from detrital zircon U-Pb ages. Oral presentation delivered at the European Geosciences General Assembly, Vienna, 17 – 22 April 2016.

Fairey B., Kerrison A., Meere P., Mulchrone K., Linnemann U., Hofmann M., Gärtner A., Sonntag B. and Byrne K., 2016. A provenance study of ancient sedimentary basins of southern Ireland: insights from detrital zircon U-Pb ages. Oral presentation delivered at the Irish Geological Research Meeting, Galway, 19 – 21 February 2016

Fairey B., Kerrison A., Meere P., Mulchrone K., Linnemann U., Hofmann M., Gärtner A., Sonntag B. and Byrne K., 2015. Sedimentary provenance of the Devonian Munster Basin and the Mesozoic North Celtic Sea Basin: evidence from detrital zircons. Poster presented at the Atlantic Ireland Conference, Dublin, 27 October 2015.

Fairey B., Hofmann M., Gärtner A., Sonntag B.-L., Linnemann U., Byrne K., Meere P., Mulchrone K. and Kerrison A., 2015. Evidence from detrital zircons for sedimentary links between the onshore Palaeozoic and offshore Mesozoic basins of southern Ireland. Poster presented at the AAPG European Regional Conference, Lisbon, 18 – 19 May 2015.

Fairey B., Kerrison A., Tunwal M., Meere P. and Mulchrone K., 2014. Use of thermochronology and quantitative sandstone petrology in establishing provenance links between onshore and offshore sedimentary basins of southern Ireland. Poster presented at the Irish Geological Research Meeting, Dublin, 28 Feb – 2 March 2014.

.

Appendix E

Below is a list of courses and workshops undertaken during the duration of this thesis:

- 2016: CASP Sandstone Provenance Workshop, United Kingdom
- 2016: Introduction to LaTeX, University College Cork, Ireland.
- 2016: Statistics and Data Analysis for Postgraduate Research Students, University College Cork, Ireland.
- 2015: Sedimentary Provenance Analysis Workshop, University of Gottingen, Germany.
- 2014: Teaching and Learning, University College Cork, Ireland.
- 2014: GIS Clinic, University College Cork, Ireland.

Appendix F

References used in the appendices are listed below.

Capewell, J.G., 1975. The Old Red Sandstone Group of Iveragh, Co. Kerry. Proc. R. Ir. Acad. B. 75, 155–171.

Carruthers, R.A., 1987. Aeolian sedimentation from the Galtymore Formation (Devonian), Ireland. Geol. Soc. London, Spec. Publ. 35, 251–268. doi:10.1144/GSL.SP.1987.035.01.17

Carruthers, R.A., 1985. The Upper Palaeozoic geology of the Glen of Aherlow and the Galtee Mountains, Counties Limerick and Tipperary. University of Dublin.

Clayton, G., Graham, J.R., 1974. Miospore assemblages from the Devonian Sherkin Formation of southwest County Cork, Republic of Ireland. Pollen et Spores 16, 565–588.

Cogné, N., Chew, D., Stuart, F.M., 2014. The thermal history of the western Irish onshore. J. Geol. Soc. London. 171, 779–792. doi:10.1144/jgs2014-026

Cogné, N., Doepke, D., Chew, D., Stuart, F.M., Mark, C., 2016. Measuring plume-related exhumation of the British Isles in Early Cenozoic times. Earth Planet. Sci. Lett. 456, 1–15. doi:10.1016/j.epsl.2016.09.053

Colthurst, J.R.J., 1978. Old Red Sandstone Rocks Surrounding the Slievenamon Inlier, Counties Tipperary and Kilkenny. J. Earth Sci. R. Dublin Soc. 1, 77–103.

Craig, J., Fitches, W.R., Maltman, A.J., 1982. Chlorite-mica stacks in low-strain rocks from central Wales. Geol. Mag. 119, 243. doi:10.1017/S0016756800026066

Dickinson, W.R., Beard, L.S., Brakenridge, G.R., Erjavec, J.L., Ferguson, R.C., Inman, K.F., Knepp, R.A., Lindberg, F.A., Ryberg, P.T., 1983. Provenance of North American Phanerozoic sandstones in relation to tectonic setting. Geol. Soc. Am. Bull. 94, 222–235. doi:10.1130/0016-7606

Ennis, M., Meere, P.A., Timmerman, M.J., Sudo, M., 2015. Post-Acadian sediment recycling in the Devonian Old Red Sandstone of Southern Ireland. Gondwana Res. 28, 1415–1433. doi:10.1016/j.gr.2014.10.007

Gardiner, P., MacCarthy, I., Penney, S., 1983. Discussion of: A new look at the Old Red Sandstone succession of the Comeragh mountains, county Waterford. J. Earth Sci. 5, 241–246.

Graham, J.R., 1983. Analysis of the Upper Devonian Munster Basin, an Example of a Fluvial Distributary System, in: Modern and Ancient Fluvial Systems. Blackwell Publishing Ltd., Oxford, UK, pp. 473–483. doi:10.1002/9781444303773.ch38

Graham, J.R., 1975. Analysis of an Upper Palaeozoic transgressive sequence in southwest County Cork, Eire. Sediment. Geol. 13, 267–290.

Graham, J.R., Reilly, T.A., 1976. The Stratigraphy of the Area around Clonakilty Bay, South County Cork. Proc. R. Irish Acad. Sect. B … 76, 379–391.

Higgs, K.T., MacCarthy, I.A.J., O'Brien, M.M., 2000. A mid-Frasnian marine incursion into the southern part of the Munster Basin: evidence from the Foilcoagh Bay Beds, Sherkin Formation, SW County Cork, Ireland. Geol. Soc. London, Spec. Publ. 180, 319–332. doi:10.1144/GSL.SP.2000.180.01.15

Jarvis, D.E., 2000. Palaeoenvironment of the plant bearing horizons of the Devonian-Carboniferous Kiltorcan Formation, Kiltorcan Hill, Co. Kilkenny, Ireland. Geol. Soc. London, Spec. Publ. 180, 333–341. doi:10.1144/GSL.SP.2000.180.01.16

Li, G., Peacor, D.R., Merriman, R.J., Roberts, B., van der Pluijm, B.A., 1994. TEM and AEM constraints on the origin and significance of chlorite-mica stacks in slates: an example from Central Wales, U.K. J. Struct. Geol. 16, 1139–1157. doi:10.1016/0191-8141(94)90058-2

MacCarthy, I.A.J., 1990. Alluvial sedimentation patterns in the Munster Basin, Ireland. Sedimentology 37, 685–712. doi:10.1111/j.1365-3091.1990.tb00629.x

Milodowski, A.E., Zalasiewicz, J.A., 1991. The origin and sedimentary, diagenetic and metamorphic evolution of chlorite–mica stacks in Llandovery sediments of central Wales, U.K. Geol. Mag. 128, 263. doi:10.1017/S0016756800022111

Penney, S., 1980. A new look at the Old Red Sandstone succession of the Comeragh Mountains, County Waterford. J. Earth Sci. 3, 155–178.

Pettijohn, F.J., Potter, P.E., Siever, R., 1987. Petrography of Common Sands and Sandstones, in: Sand and Sandstone. pp. 139–213. doi:10.1007/978-1-4615-9974-6_6

Pracht, M., 1997. A geological description to accompany the Bedrock Geology 1:100000 Scale Map Series, Sheet 21, Kerry-Cork, with contributions by G. Wright (Groundwater), G. Stanley and K. Claringbold (Minerals) and W.P. Warren (Quaternary). Geological Survey of Ireland, Dublin.

Pracht, M., Sleeman, A.G., 2002. A geological description of West Cork and adjacent parts of Kerry to accompany the bedrock geology 1:100000 scale map series, sheet 24, West Cork, With contributions by G.Wright (Groundwater) and W. Cox (Minerals). Geological Survey of Ireland, Dublin.

Sleeman, A.G., McConnell, B., 1995. A geological description of East Cork, Waterford and adjoining parts of Tipperary and Limerick to accompany

the bedrock geology 1:100,000 scale map series, sheet 22, East Cork - Waterford with contributions by K. Claringbold, P. O'Connor, W.P. Warren and . Geological Survey of Ireland, Dublin.

Todd, S.P., 2000. Taking the roof off a suture zone: basin setting and provenance of conglomerates in the ORS Dingle Basin of SW Ireland. Geol. Soc. London, Spec. Publ. 180, 185–222. doi:10.1144/GSL.SP.2000.180.01.10

Williams, E.A., 1993. The stratigraphy, fluvial sedimentology and structural geology of the Old Red Sandstone in the Derrynasaggart Mountains, Counties Cork and Kerry. University College Cork.

Williams, E.A., Sergeev, S.A., Stossel, I., Ford, M., 1997. An Eifelian U–Pb zircon date for the Enagh Tuff Bed from the Old Red Sandstone of the Munster Basin in NW Iveragh, SW Ireland. J. Geol. Soc. London 154, 189–193. doi:10.1144/gsjgs.154.2.0189

Williams, E.A., Sergeev, S.A., Stossel, I., Ford, M., Higgs, K.T., 2000. U-Pb zircon geochronology of silicic tuffs and chronostratigraphy of the earliest Old Red Sandstone in the Munster Basin, SW Ireland. Geol. Soc. London, Spec. Publ. 180, 269–302. doi:10.1144/GSL.SP.2000.180.01.13

Williams, E., Bamford, M., Cooper, M., Edwards, H., Ford, M., Grant, G., MacCarthy, I., McAfee, A., O'Sullivan, M., 1989. Tectonic controls and sedimentary response in the Devonian-Carboniferous Munster and South Munster basins, south-west Ireland, in: Arthurton, R., Gutteridge, P., Nolan, S. (Eds.), The Role of Tectonics in Devonian and Carboniferous Sedimentation in the British Isles. The Yorkshire Geological Society, Bradford, pp. 120–141.

Explanation of supplementary data for Fairey, 2018. PhD thesis.

The following section contains the underlying data that was used to produce this thesis as well as confidence levels at which the detrital zircon age data can be interpreted (Table I). Table II shows detrital zircon U-Th-Pb data for samples from the Dingle Peninsula. Table III contains detrital zircon U-Th-Pb data for all samples from the UORS. Table IV contains detrital zircon U-Th-Pb data for all samples from the offshore basins observed in this study. Table V contains all detrital apatite U-Pb data used in this study from the LORS on the Dingle Peninsula. Table VI contains all detrital apatite U-Pb data used in this study from the UORS of southern Ireland. Table VII shows the adjusted detrital mica ages from the study by Ennis et al. (2015).Table VIII presents the new detrital mica total fusion 40Ar/39Ar data obtained from the eastern UORS and the offshore basins in this study.

Table I. The number of concordant and precise detrital zircon ages for each sample and corresponding probabilities of missing a five and ten percent fraction of the population as well as the smallest fraction that can be confidently interpreted.

Sample number	Number of concordant and precise ages	Probability of missing 5%	Probability of missing 10%	Percentage minimum fraction that can be resolved at the 95 % confidence level
AK19	86	0.2217	0.001161	6.44
AK21	98	0.1251	0.000328	5.78
AK11	141	0.0144	0.000004	4.26
AK16	129	0.0265	0.000013	4.59
BF22	82	0.2663	0.001769	6.70
BF19	94	0.1518	0.000500	5.98
BF15	99	0.1192	0.000295	5.73
AK17	84	0.2431	0.001433	6.56
AK10	66	0.5190	0.009532	8.00
AK07	79	0.3045	0.002427	6.91
AK04	91	0.1753	0.000686	6.14
BF11	104	0.0932	0.000174	5.50
BF12	122	0.0378	0.000026	4.81
AK03	87	0.2116	0.001045	6.38
BF21	111	0.0658	0.000083	5.21
BF13	95	0.1447	0.000450	5.93
57/09-1	107	0.0803	0.000127	5.37
49/09-4	99	0.1192	0.000295	5.73
49/15-1	120	0.0418	0.000032	4.88
49/10-1	82	0.2663	0.001769	6.70
49/09-3	89	0.1927	0.000846	6.26
48/28-1	95	0.1447	0.000450	5.93
48/24-4	86	0.2217	0.001161	6.44
48/18-1	83	0.2545	0.001592	6.63
49/09-2	96	0.1379	0.000405	5.88
56/26-2A	77	0.3323	0.002995	7.05
63/10-1	135	0.0195	0.000007	4.42
56/26-2B	91	0.1753	0.000686	6.14
56/22-1	73	0.3938	0.004564	7.37
58/03-1	85	0.2322	0.001290	6.50
62/07-1	91	0.1753	0.000686	6.14

Table II. LA ICP MS U, Pb and Th isotopic data for detrital zircons from all three samples from the Dingle Peninsula

Number	$^{207}Pb^{a}$ (cps)	U^{b} (ppm)	Pb^{b} (ppm)	Th^{b} / U	^{206}Pb / ^{204}Pb	$^{206}Pb^{c}$ / ^{238}U	2 s %	$^{207}Pb^{c}$ / ^{235}U	2 s %	$^{207}Pb^{c}$ / ^{206}Pb	2 s %	rho[d]	^{206}Pb / ^{238}U	2 s (Ma)	^{207}Pb / ^{235}U	2 s (Ma)	^{207}Pb / ^{206}Pb	2 s (Ma)	conc %
Sample AK19	Coumeenoole Formation					Location (decimal degrees):				52.18196 N 10.20578 W		Datum: IRENET95							
AK19-seq1-a01	9982	37	11	0.27	4893	0.2903	2.1	4.0494	3.3	0.1012	2.6	0.63	1643	30	1644	27	1645	48	100
AK19-seq1-a02	6269	53	10	0.32	8744	0.1732	2.5	1.7424	3.4	0.0730	2.3	0.72	1030	23	1024	22	1013	48	102
AK19-seq1-a03	1722	14	3	0.55	1542	0.1861	2.4	1.7404	5.9	0.0678	5.4	0.40	1100	24	1024	39	863	112	127
AK19-seq1-a04	5327	48	10	0.65	7827	0.1808	2.2	1.7225	3.9	0.0691	3.2	0.58	1071	22	1017	25	902	65	119
AK19-seq1-a05	1816	21	4	0.66	2742	0.1408	2.3	1.3144	7.1	0.0677	6.7	0.32	849	18	852	42	860	140	99
AK19-seq1-a06	12042	191	28	0.89	19540	0.1148	2.1	0.9907	3.1	0.0626	2.2	0.69	701	14	699	16	694	47	101
AK19-seq1-a07	7988	48	11	0.51	9989	0.2071	2.3	2.3157	3.3	0.0811	2.3	0.70	1213	25	1217	23	1224	46	99
AK19-seq1-a08	5904	127	14	0.65	10785	0.0902	2.3	0.6863	3.5	0.0552	2.6	0.66	557	12	531	14	420	58	133
AK19-seq1-a09	3771	19	5	0.30	4516	0.2413	2.8	2.8377	4.1	0.0853	3.1	0.67	1393	35	1366	31	1322	59	105
AK19-seq1-a10	7191	46	11	0.52	9162	0.2052	2.3	2.2557	3.1	0.0797	2.1	0.74	1203	25	1199	22	1190	41	101
AK19-seq1-a11	23401	149	33	0.28	29241	0.2068	2.6	2.3194	2.8	0.0814	1.2	0.90	1212	29	1218	20	1230	24	99
AK19-seq1-a12	5333	31	7	0.42	1800	0.2060	2.7	2.2959	3.9	0.0808	2.7	0.71	1208	30	1211	28	1217	53	99
AK19-seq1-a13	17670	307	33	0.33	29419	0.1043	1.9	0.8775	2.4	0.0610	1.4	0.80	640	12	640	11	639	31	100
AK19-seq1-a14	1304	33	3	0.72	2696	0.0881	3.0	0.5993	9.2	0.0493	8.7	0.33	544	16	477	36	164	203	332
AK19-seq1-a15	27459	102	27	0.54	6055	0.2159	3.8	2.9181	4.5	0.0980	2.5	0.84	1260	43	1387	35	1587	46	79
AK19-seq1-a16	9477	73	15	0.62	13030	0.1799	2.1	1.8362	3.2	0.0740	2.4	0.67	1067	21	1058	21	1042	48	102
AK19-seq1-a17	18843	121	27	0.39	24031	0.2032	2.3	2.2330	2.8	0.0797	1.6	0.81	1193	25	1191	20	1189	32	100
AK19-seq1-a18	8535	260	20	0.71	15773	0.0631	2.4	0.4777	3.4	0.0550	2.5	0.69	394	9	397	11	410	56	96
AK19-seq1-a19	10389	244	19	0.14	18457	0.0804	2.6	0.6343	3.3	0.0572	2.0	0.79	498	12	499	13	501	44	100
AK19-seq1-a20	19254	229	32	0.42	24506	0.1311	2.1	1.4425	2.7	0.0798	1.8	0.76	794	16	907	16	1192	35	67
AK19-seq1-a21	6613	46	9	0.21	8533	0.1978	2.2	2.1463	3.6	0.0787	2.8	0.62	1164	24	1164	25	1164	56	100
AK19-seq1-a22	21658	621	52	0.34	12001	0.0830	2.2	0.6643	2.7	0.0580	1.6	0.80	514	11	517	11	531	36	97
AK19-seq1-a23	5531	169	13	0.40	10568	0.0702	2.4	0.5147	3.6	0.0531	2.7	0.66	438	10	422	13	335	62	131
AK19-seq1-a24	8435	232	20	0.84	15551	0.0643	2.5	0.4867	3.4	0.0549	2.4	0.72	401	10	403	11	410	53	98
AK19-seq1-a25	2891	34	6	0.75	4694	0.1407	2.3	1.2402	5.6	0.0639	5.1	0.42	848	19	819	32	740	108	115
AK19-seq1-a26	16368	76	21	0.53	19221	0.2322	2.0	2.7637	2.4	0.0863	1.4	0.82	1346	24	1346	18	1346	27	100
AK19-seq1-a27	10045	40	14	0.82	10638	0.2711	2.1	3.5944	3.4	0.0962	2.6	0.63	1547	29	1548	27	1551	50	100
AK19-seq1-a28	64009	164	66	0.49	53853	0.3490	2.2	5.8095	2.3	0.1207	0.6	0.96	1930	37	1948	20	1967	11	98
AK19-seq1-a29	79062	223	88	0.53	70088	0.3377	2.2	5.3318	2.4	0.1145	1.0	0.92	1876	37	1874	21	1872	18	100
AK19-seq1-a30	12337	264	28	0.66	21395	0.0890	2.1	0.7183	2.8	0.0585	1.9	0.73	550	11	550	12	550	42	100
AK19-seq1-a31	23592	158	34	0.20	29854	0.2096	2.0	2.3209	2.6	0.0803	1.5	0.80	1227	23	1219	18	1204	30	102
AK19-seq1-a32	4409	94	10	0.63	3426	0.0923	2.4	0.7074	4.3	0.0556	3.6	0.57	569	13	543	18	436	79	131
AK19-seq1-a33	10598	133	22	0.73	16041	0.1299	2.4	1.1971	3.3	0.0668	2.2	0.73	787	18	799	18	832	46	95
AK19-seq1-a34	18889	132	28	0.28	23915	0.2065	1.9	2.2818	2.4	0.0802	1.4	0.82	1210	21	1207	17	1201	27	101
AK19-seq1-a35	5900	40	8	0.37	1303	0.1833	2.4	1.9135	4.5	0.0757	3.8	0.53	1085	24	1086	30	1087	75	100
AK19-seq1-a36	18682	329	37	0.49	17832	0.0986	2.2	0.8198	2.5	0.0603	1.1	0.89	606	13	608	12	615	25	98
AK19-seq1-a37	11128	317	23	0.38	20401	0.0691	2.1	0.5287	2.7	0.0555	1.7	0.78	431	9	431	9	431	37	100

AK19-seq1-a38	57583	176	64	0.47	53971	0.3151	2.4	4.7108	2.6	0.1084	1.0	0.92	1766	37	1769	22	1773	18	100
AK19-seq1-a39	3804	81	9	0.58	7057	0.0916	2.8	0.6869	5.2	0.0544	4.4	0.53	565	15	531	22	387	99	146
AK19-seq1-a40	1360	30	4	1.29	2554	0.0907	2.8	0.6847	7.5	0.0547	6.9	0.38	560	15	530	31	401	155	139
AK19-seq1-a41	6389	49	10	0.48	8714	0.1770	2.4	1.8159	3.2	0.0744	2.1	0.75	1050	23	1051	21	1053	42	100
AK19-seq1-a42	6021	37	9	0.51	4228	0.2055	2.1	2.2506	3.4	0.0794	2.7	0.60	1205	23	1197	24	1183	54	102
AK19-seq1-a43	4200	118	10	0.55	8168	0.0749	2.5	0.5396	3.7	0.0523	2.7	0.69	465	11	438	13	298	61	156
AK19-seq1-a44	5745	48	9	0.34	7973	0.1809	2.3	1.8274	3.5	0.0733	2.7	0.65	1072	22	1055	23	1022	54	105
AK19-seq1-a45	7853	43	12	0.55	8231	0.2522	2.6	2.8488	3.3	0.0819	2.1	0.77	1450	34	1368	25	1244	42	117
AK19-seq1-a46	2835	47	6	0.60	4683	0.1094	2.5	0.9355	4.8	0.0620	4.2	0.51	669	16	671	24	675	89	99
AK19-seq1-a47	41640	357	61	0.17	58411	0.1687	2.2	1.6870	2.6	0.0725	1.4	0.85	1005	21	1004	17	1001	28	100
AK19-seq1-a48	20911	165	33	0.50	28825	0.1746	2.4	1.7739	3.1	0.0737	1.9	0.80	1037	23	1036	20	1033	37	100
AK19-seq1-a49	4394	33	8	0.44	2635	0.2190	2.4	2.1847	4.4	0.0724	3.7	0.54	1277	28	1176	31	996	76	128
AK19-seq1-a50	8027	123	16	0.56	13096	0.1130	2.1	0.9706	3	0.0623	2.1	0.70	690	14	689	15	684	46	101
AK19-seq1-a51	33717	192	47	0.35	40482	0.2258	2.2	2.6353	2.6	0.0847	1.4	0.84	1312	26	1311	19	1308	28	100
AK19-seq1-a52	26074	130	38	0.71	30309	0.2339	2.5	2.8216	3	0.0875	1.7	0.84	1355	31	1361	23	1371	32	99
AK19-seq1-a53	22647	65	25	0.72	21150	0.3177	2.1	4.7653	2.6	0.1088	1.5	0.81	1778	33	1779	22	1779	28	100
AK19-seq1-a54	2222	41	6	1.18	3991	0.1107	2.2	0.8374	5	0.0549	4.4	0.45	677	14	618	23	407	99	166
AK19-seq1-a55	6924	112	13	0.42	11455	0.1062	2.5	0.8970	3.3	0.0613	2.2	0.75	651	15	650	16	648	47	100
AK19-seq1-a56	20436	599	43	0.17	37870	0.0723	2.1	0.5638	3.5	0.0566	2.8	0.61	450	9	454	13	475	62	95
AK19-seq1-a57	4458	126	10	0.54	8360	0.0678	2.4	0.5024	4.1	0.0537	3.3	0.58	423	10	413	14	360	75	117
AK19-seq1-a58	12835	333	24	0.11	20298	0.0733	2.3	0.5713	5.3	0.0566	4.8	0.43	456	10	459	20	474	106	96
AK19-seq1-a59	13869	325	27	0.14	24382	0.0839	2.6	0.6688	3.9	0.0578	2.9	0.68	520	13	520	16	522	63	100
AK19-seq1-a60	14178	225	26	0.19	23622	0.1169	2.3	1.0321	3.5	0.0641	2.7	0.66	713	16	720	18	743	57	96
AK19-seq2-b01	11990	168	21	0.31	19431	0.1167	2.1	1.0087	3	0.0627	2.1	0.70	711	14	708	15	698	45	102
AK19-seq2-b02	58574	247	71	0.26	61901	0.2725	2.1	3.6135	2.2	0.0962	0.8	0.93	1554	29	1553	18	1551	15	100
AK19-seq2-b03	19287	119	24	0.18	25013	0.1965	2.4	2.1197	2.9	0.0782	1.5	0.85	1157	26	1155	20	1153	30	100
AK19-seq2-b04	6430	98	11	0.31	11383	0.1061	2.1	0.9135	5	0.0625	4.5	0.41	650	13	659	24	690	97	94
AK19-seq2-b05	7859	32	8	0.57	9825	0.2123	2.5	2.3717	3.5	0.0810	2.5	0.71	1241	29	1234	26	1222	49	102
AK19-seq2-b06	12167	81	16	0.24	7182	0.1909	2.3	2.0442	2.9	0.0777	1.7	0.80	1126	24	1130	20	1138	34	99
AK19-seq2-b07	4621	80	10	0.46	8157	0.1107	2.0	0.8824	3.7	0.0578	3.1	0.54	677	13	642	18	523	68	130
AK19-seq2-b08	9367	252	21	0.64	17228	0.0662	2.2	0.5052	3	0.0554	2.1	0.72	413	9	415	10	427	47	97
AK19-seq2-b09	19194	137	29	0.33	25145	0.1928	1.8	2.0528	2.5	0.0772	1.7	0.73	1136	19	1133	17	1127	34	101
AK19-seq2-b10	4972	150	12	0.34	9963	0.0780	2.3	0.6225	8.6	0.0579	8.3	0.27	484	11	491	34	527	181	92
AK19-seq2-b11	14404	91	21	0.40	18374	0.2066	2.3	2.2723	2.8	0.0798	1.7	0.81	1211	25	1204	20	1191	33	102
AK19-seq2-b12	11662	69	18	0.54	14737	0.2191	2.0	2.4319	2.8	0.0805	1.9	0.73	1277	24	1252	20	1209	37	106
AK19-seq2-b13	2925	12	4	0.77	1503	0.2579	4.4	3.3383	6.6	0.0939	4.9	0.66	1479	58	1490	53	1506	93	98
AK19-seq2-b14	89769	212	84	0.20	24864	0.3751	2.2	6.6931	2.3	0.1294	0.6	0.96	2053	39	2072	21	2090	11	98
AK19-seq2-b15	66303	372	84	0.13	79264	0.2271	2.0	2.6655	2.4	0.0851	1.2	0.86	1319	24	1319	18	1319	24	100
AK19-seq2-b16	12469	156	25	0.54	18917	0.1381	2.1	1.2758	2.8	0.0670	1.9	0.74	834	17	835	16	838	40	100
AK19-seq2-b17	12869	195	24	0.33	10124	0.1160	2.0	1.0147	2.7	0.0635	1.8	0.75	707	13	711	14	724	37	98
AK19-seq2-b18	28568	80	28	0.34	24267	0.3100	2.5	5.1211	2.9	0.1198	1.4	0.86	1741	38	1840	25	1954	26	89
AK19-seq2-b19	4828	137	11	0.33	9284	0.0753	2.5	0.5486	4.1	0.0529	3.2	0.62	468	11	444	15	322	74	145

AK19-seq2-b20	58325	185	16	0.62	25414	0.0210	52.5	0.3408	52.5	0.1175	1.3	1.00	134	70	298	145	1919	23	7
AK19-seq2-b21	156094	342	141	0.17	32350	0.3925	2.2	7.2139	2.3	0.1333	0.9	0.92	2135	39	2138	21	2142	16	100
AK19-seq2-b22	21347	448	41	0.27	36951	0.0896	2.1	0.7244	2.6	0.0586	1.5	0.82	553	11	553	11	553	32	100
AK19-seq2-b23	23459	111	29	0.34	26844	0.2396	2.5	2.9364	3.2	0.0889	1.9	0.79	1384	31	1391	24	1402	37	99
AK19-seq2-b24	17605	356	37	0.49	30520	0.0902	2.1	0.7304	2.4	0.0587	1.2	0.87	557	11	557	10	556	26	100
AK19-seq2-b25	18165	114	25	0.28	22870	0.2085	2.1	2.3267	2.7	0.0809	1.7	0.77	1221	23	1220	19	1220	33	100
AK19-seq2-b26	33346	108	39	0.35	30777	0.3226	2.6	4.9111	3	0.1104	1.4	0.88	1802	41	1804	25	1806	25	100
AK19-seq2-b27	33033	138	39	0.36	9617	0.2534	2.3	3.3270	2.7	0.0952	1.5	0.84	1456	30	1487	21	1533	27	95
AK19-seq2-b28	32262	79	33	0.44	27077	0.3530	2.1	5.8960	2.6	0.1211	1.4	0.82	1949	36	1961	22	1973	26	99
AK19-seq2-b29	2081	35	4	0.46	3654	0.1165	2.3	0.9275	5.6	0.0577	5.1	0.41	710	15	666	28	520	111	137
AK19-seq2-b30	8526	241	17	0.34	15534	0.0684	2.3	0.5258	3	0.0558	2.0	0.76	426	10	429	11	443	43	96
AK19-seq2-b31	15870	86	20	0.14	18743	0.2356	2.3	2.7971	2.9	0.0861	1.7	0.80	1364	29	1355	22	1341	34	102
AK19-seq2-b32	3602	63	8	0.45	6377	0.1099	2.5	0.8634	5.4	0.0570	4.8	0.47	672	16	632	26	491	106	137
AK19-seq2-b33	5652	57	9	0.24	8148	0.1509	2.8	1.4647	4	0.0704	2.9	0.69	906	23	916	24	940	59	96
AK19-seq2-b34	77129	195	73	0.23	62299	0.3501	2.2	6.0821	2.5	0.1260	1.2	0.88	1935	37	1988	22	2043	21	95
AK19-seq2-b35	557123	673	328	0.06	63088	0.4495	5.5	14.0680	7.1	0.2270	4.5	0.78	2393	112	2754	70	3031	71	79
AK19-seq2-b36	44171	1327	82	0.07	68767	0.0651	2.1	0.5063	2.6	0.0564	1.5	0.82	406	8	416	9	469	32	87
AK19-seq2-b37	10869	262	28	0.61	19650	0.0902	2.2	0.7318	4.3	0.0588	3.7	0.51	557	12	558	19	561	81	99
AK19-seq2-b38	24809	174	38	0.28	31432	0.2046	2.3	2.2635	2.7	0.0802	1.5	0.84	1200	25	1201	19	1203	29	100
AK19-seq2-b39	6894	149	15	0.42	11865	0.0900	2.1	0.7304	3.3	0.0589	2.5	0.66	555	11	557	14	562	54	99
AK19-seq2-b40	25782	54	25	0.56	8570	0.3863	2.0	6.8813	2.5	0.1292	1.4	0.82	2106	37	2096	22	2087	25	101
AK19-seq2-b41	4791	91	12	0.58	8760	0.1128	2.1	0.8653	3.1	0.0556	2.3	0.68	689	14	633	15	437	51	158
AK19-seq2-b42	8487	185	19	0.63	14712	0.0870	2.7	0.7026	3.6	0.0586	2.4	0.74	538	14	540	15	552	53	97
AK19-seq2-b43	1327	32	3	0.55	2418	0.0866	2.4	0.6620	6.3	0.0555	5.8	0.38	535	12	516	26	430	130	124
AK19-seq2-b44	15007	73	20	0.28	17010	0.2531	2.1	3.1342	2.8	0.0898	1.9	0.75	1454	28	1441	22	1422	36	102
AK19-seq2-b45	12248	48	18	0.72	12539	0.3052	2.0	4.1799	2.7	0.0993	1.8	0.75	1717	30	1670	22	1612	33	107
AK19-seq2-b46	14411	88	21	0.16	18270	0.2439	1.9	2.6962	2.4	0.0802	1.6	0.77	1407	24	1327	18	1201	31	117
AK19-seq2-b47	56340	163	67	0.55	49444	0.3429	2.3	5.4712	2.7	0.1157	1.3	0.87	1901	39	1896	23	1891	24	100
AK19-seq2-b48	3930	31	6	0.28	2072	0.1975	2.3	2.0205	3.9	0.0742	3.2	0.59	1162	25	1122	27	1047	64	111
AK19-seq2-b49	15405	236	24	0.02	3696	0.1097	2.3	0.9470	4.1	0.0626	3.4	0.57	671	15	677	20	695	72	96
AK19-seq2-b50	22385	521	52	0.38	16842	0.0914	2.6	0.7458	3.5	0.0592	2.3	0.75	564	14	566	15	574	50	98
AK19-seq2-b51	8514	68	14	0.56	11589	0.1749	2.3	1.7992	3.4	0.0746	2.6	0.67	1039	22	1045	23	1058	52	98
AK19-seq2-b52	4363	103	10	0.60	7718	0.0764	1.9	0.6021	3.5	0.0572	2.9	0.54	474	9	479	13	498	65	95
AK19-seq2-b53	35922	141	43	0.21	36640	0.2917	2.2	3.9828	2.7	0.0990	1.5	0.83	1650	32	1631	22	1606	27	103
AK19-seq2-b54	10257	98	15	0.10	7052	0.1581	2.0	1.5556	2.6	0.0714	1.8	0.75	946	18	953	17	968	36	98
Sample AK21		Slea Head Formation				Location (decimal degrees):			52.13	10.35905 W		Datum:	IRENET95 Irish Transverse Mercator						
AK21-seq1-a01	3676	92	9	0.45	6432	0.0931	2.3	0.7487	3.8	0.0583	3.0	0.61	574	13	567	17	541	66	106
AK21-seq1-a02	3884	137	11	0.88	7184	0.0655	2.0	0.4992	3.6	0.0553	3.0	0.54	409	8	411	12	422	68	97
AK21-seq1-a03	9518	336	25	0.62	17818	0.0633	2.1	0.4755	2.7	0.0545	1.6	0.79	395	8	395	9	393	37	101
AK21-seq1-a04	7661	257	18	0.19	14360	0.0699	2.3	0.5246	3.4	0.0544	2.5	0.66	436	10	428	12	388	57	112
AK21-seq1-a05	20838	709	48	0.33	6427	0.0636	2.7	0.5254	4.5	0.0600	3.6	0.60	397	10	429	16	602	77	66

AK21-seq1-a06	3151	101	8	0.39	5680	0.0766	2.0	0.5995	3.3	0.0568	2.7	0.60	476	9	477	13	483	59	98
AK21-seq1-a07	4582	153	12	0.45	4134	0.0697	2.5	0.4943	3.6	0.0514	2.7	0.68	434	10	408	12	260	61	167
AK21-seq1-a08	6393	229	17	0.44	11567	0.0682	2.3	0.5198	3.8	0.0553	3.0	0.61	425	10	425	13	424	67	100
AK21-seq1-a09	14123	520	35	0.23	14253	0.0660	2.1	0.5016	2.7	0.0551	1.8	0.76	412	8	413	9	417	40	99
AK21-seq1-a10	1708	67	5	0.47	906	0.0705	2.4	0.4797	8	0.0493	7.6	0.31	439	10	398	27	163	178	269
AK21-seq1-a11	34728	184	52	0.23	37479	0.2723	1.8	3.5829	2.4	0.0954	1.6	0.75	1552	25	1546	20	1537	31	101
AK21-seq1-a12	8755	295	23	0.68	5858	0.0636	2.1	0.4796	3.8	0.0547	3.2	0.55	398	8	398	13	399	72	100
AK21-seq1-a13	12597	115	24	0.41	16257	0.1925	2.4	2.0790	3.2	0.0784	2.1	0.74	1135	25	1142	22	1156	42	98
AK21-seq1-a14	4728	187	14	0.45	9299	0.0662	2.4	0.4729	4.4	0.0519	3.7	0.55	413	10	393	14	279	84	148
AK21-seq1-a15	4726	184	13	0.39	8579	0.0673	2.0	0.5142	3.6	0.0554	2.9	0.57	420	8	421	12	430	65	98
AK21-seq1-a16	14497	159	22	0.17	4717	0.1368	3.6	1.3625	4	0.0722	1.8	0.89	827	28	873	24	993	37	83
AK21-seq1-a17	11915	75	21	0.43	13557	0.2472	2.2	3.0543	2.7	0.0896	1.4	0.84	1424	29	1421	21	1417	27	100
AK21-seq1-a18	3547	103	8	0.40	6773	0.0719	2.7	0.5290	4.6	0.0534	3.7	0.59	447	12	431	16	345	84	130
AK21-seq1-a19	60284	147	65	0.42	43759	0.3836	3.0	7.4387	3.3	0.1406	1.4	0.90	2093	54	2166	30	2235	25	94
AK21-seq1-a20	13293	109	23	0.21	17050	0.2056	2.1	2.2515	2.9	0.0794	1.9	0.75	1205	24	1197	20	1183	38	102
AK21-seq1-a21	11856	92	20	0.25	14671	0.2136	2.3	2.4175	2.8	0.0821	1.6	0.82	1248	26	1248	20	1248	32	100
AK21-seq1-a22	5893	215	15	0.20	11381	0.0721	1.7	0.5609	6.3	0.0564	6.0	0.27	449	7	452	23	468	133	96
AK21-seq1-a23	33400	130	47	0.48	29926	0.3176	2.1	4.9847	2.3	0.1138	1.1	0.89	1778	32	1817	20	1861	19	96
AK21-seq1-a24	5274	181	16	0.63	8494	0.0782	2.1	0.5754	3.6	0.0533	3.0	0.58	486	10	462	14	343	67	141
AK21-seq1-a25	2573	120	9	0.27	5565	0.0720	2.4	0.6807	12.6	0.0685	12.4	0.19	448	10	527	53	885	256	51
AK21-seq1-a26	4238	163	12	0.44	7994	0.0696	2.2	0.5143	4.2	0.0536	3.5	0.52	433	9	421	14	356	80	122
AK21-seq1-a27	29677	294	51	0.19	15867	0.1698	2.4	1.8382	2.8	0.0785	1.5	0.85	1011	22	1059	18	1161	29	87
AK21-seq1-a28	19498	87	31	0.52	18047	0.3186	3.9	4.8301	4.4	0.1100	2.0	0.89	1783	61	1790	37	1799	37	99
AK21-seq1-a29	1945	69	6	0.64	3767	0.0811	2.4	0.5855	6.2	0.0524	5.7	0.39	502	12	468	24	302	131	166
AK21-seq1-a30	1692	65	5	0.60	3303	0.0700	4.0	0.5039	10.1	0.0522	9.3	0.39	436	17	414	35	294	213	148
AK21-seq1-a31	10099	81	21	0.52	12560	0.2229	1.9	2.5218	2.8	0.0821	2.0	0.69	1297	23	1278	21	1247	40	104
AK21-seq1-a32	2605	90	11	0.96	5259	0.0930	2.2	0.7658	12.9	0.0597	12.7	0.17	573	12	577	58	593	275	97
AK21-seq1-a33	37004	108	44	0.20	27875	0.3895	2.2	7.2717	2.5	0.1354	1.1	0.89	2121	39	2145	22	2169	20	98
AK21-seq1-a34	14774	539	38	0.04	26637	0.0765	2.0	0.5966	2.5	0.0566	1.4	0.82	475	9	475	9	475	31	100
AK21-seq1-a35	11304	268	29	0.31	19014	0.1036	2.1	0.8655	2.8	0.0606	1.9	0.73	636	13	633	13	624	42	102
AK21-seq1-a36	17529	132	34	0.47	20453	0.2300	2.4	2.7755	2.9	0.0875	1.7	0.81	1335	29	1349	22	1372	33	97
AK21-seq1-a37	3194	129	10	0.66	6183	0.0658	2.0	0.4761	3.3	0.0525	2.7	0.59	411	8	395	11	307	61	134
AK21-seq1-a38	6402	51	10	0.27	7077	0.1958	2.5	2.1183	3.3	0.0785	2.2	0.74	1153	26	1155	23	1158	44	100
AK21-seq1-a39	8840	335	23	0.04	15924	0.0726	2.2	0.5654	3.3	0.0565	2.4	0.69	452	10	455	12	473	52	95
AK21-seq1-a40	2995	27	8	1.41	1052	0.2068	2.1	2.2795	3.8	0.0800	3.1	0.55	1212	23	1206	27	1196	62	101
AK21-seq1-a41	4380	215	16	0.34	8642	0.0704	2.2	0.5433	11	0.0559	10.8	0.20	439	9	441	40	450	239	97
AK21-seq1-a42	26974	97	41	0.52	22204	0.3597	2.0	6.1486	2.5	0.1240	1.5	0.81	1981	34	1997	22	2014	26	98
AK21-seq1-a43	7785	94	17	0.33	10738	0.1657	2.1	1.6911	3.1	0.0740	2.3	0.68	988	19	1005	20	1043	46	95
AK21-seq1-a44	3946	101	12	0.39	6889	0.1107	2.3	0.8896	3.8	0.0583	3.0	0.61	677	15	646	18	541	65	125
AK21-seq1-a45	3613	114	11	0.40	6711	0.0923	2.2	0.6973	3.6	0.0548	2.9	0.62	569	12	537	15	405	64	141
AK21-seq1-a46	2784	94	11	1.07	5002	0.0882	2.4	0.6906	4.6	0.0568	3.9	0.52	545	12	533	19	483	86	113
AK21-seq1-a47	8552	229	19	0.13	486	0.0808	2.4	0.8702	4.5	0.0781	3.8	0.53	501	11	636	21	1149	75	44

AK21-seq1-a48	18938	207	37	0.23	25636	0.1717	2.0	1.7914	2.6	0.0757	1.6	0.77	1021	19	1042	17	1087	33	94
AK21-seq1-a49	26819	250	57	0.32	32993	0.2123	2.2	2.4048	2.7	0.0822	1.5	0.83	1241	25	1244	20	1249	29	99
AK21-seq1-a50	16900	178	38	0.24	21393	0.2047	2.1	2.2756	2.7	0.0806	1.7	0.78	1201	23	1205	20	1212	34	99
AK21-seq1-a51	3332	403	27	0.25	6460	0.0670	2.9	0.4837	5.1	0.0523	4.2	0.57	418	12	401	17	300	95	140
AK21-seq1-a52	5779	476	45	0.39	10229	0.0897	2.2	0.7235	4.2	0.0585	3.6	0.53	554	12	553	18	549	78	101
AK21-seq1-a53	7381	91	22	0.82	10252	0.1966	2.8	1.9876	4.1	0.0733	3.1	0.67	1157	29	1111	28	1023	62	113
AK21-seq1-a54	369	10	2	1.53	611	0.1124	5.6	0.9880	22.7	0.0638	22.0	0.25	687	36	698	122	734	467	94
AK21-seq1-a55	2488	116	9	0.53	5010	0.0694	2.0	0.4799	4.5	0.0502	4.0	0.44	432	8	398	15	203	93	213
AK21-seq1-a56	4818	52	12	0.50	6233	0.1958	2.6	2.1206	4	0.0785	2.9	0.67	1153	28	1156	28	1160	58	99
AK21-seq1-a57	5035	133	16	0.51	8540	0.1027	2.2	0.8511	3.3	0.0601	2.5	0.66	630	13	625	16	608	54	104
AK21-seq1-a58	47203	210	85	0.63	41280	0.3315	1.9	5.3385	2.4	0.1168	1.4	0.80	1846	31	1875	21	1908	26	97
AK21-seq1-a59	7726	85	17	0.31	10009	0.1880	1.9	2.0457	3.3	0.0789	2.7	0.58	1111	20	1131	23	1170	53	95
AK21-seq1-a60	6640	334	27	0.53	12577	0.0714	2.2	0.5262	3.3	0.0534	2.5	0.65	445	9	429	12	348	57	128
AK21-seq2-b01	6756	168	19	0.41	11176	0.1046	2.3	0.8817	3.6	0.0611	2.7	0.66	642	14	642	17	643	58	100
AK21-seq2-b02	2599	75	8	0.37	4779	0.1067	2.6	0.9106	8	0.0619	7.6	0.32	654	16	657	40	670	163	98
AK21-seq2-b03	1841	24	4	0.29	2635	0.1635	3.3	1.6059	5.4	0.0713	4.3	0.62	976	30	973	34	965	87	101
AK21-seq2-b04	1017	43	4	0.58	2141	0.0762	3.9	0.5067	10.7	0.0482	10.0	0.36	474	18	416	37	109	236	435
AK21-seq2-b05	29386	226	47	0.19	37088	0.2040	2.7	2.2782	3.3	0.0810	1.9	0.81	1197	29	1206	24	1221	38	98
AK21-seq2-b06	18689	39	31	1.06	9923	0.5482	2.8	14.5579	3.3	0.1926	1.8	0.85	2818	65	2787	32	2764	29	102
AK21-seq2-b07	16920	1081	79	0.30	14310	0.0710	2.7	0.5490	3.4	0.0561	2.0	0.81	442	12	444	12	457	44	97
AK21-seq2-b08	4260	170	19	0.41	7423	0.1004	2.3	0.8071	3.7	0.0583	2.9	0.63	617	14	601	17	541	63	114
AK21-seq2-b09	4041	121	12	0.47	6993	0.0882	2.2	0.7111	4.1	0.0585	3.4	0.53	545	11	545	17	549	75	99
AK21-seq2-b10	11941	400	28	0.12	1658	0.0711	2.1	0.6204	3.3	0.0633	2.6	0.63	443	9	490	13	718	55	62
AK21-seq2-b11	3115	98	10	0.65	5823	0.0871	2.4	0.6554	4.8	0.0546	4.1	0.50	539	13	512	19	394	93	137
AK21-seq2-b12	15626	148	33	0.40	20048	0.2029	2.4	2.2273	3	0.0796	1.9	0.78	1191	26	1190	21	1187	38	100
AK21-seq2-b13	1713	69	9	0.24	5864	0.1293	2.6	1.1639	6.9	0.0653	6.4	0.38	784	19	784	38	784	134	100
AK21-seq2-b14	920	26	3	0.60	1855	0.1117	2.6	0.7903	8.8	0.0513	8.4	0.29	683	17	591	40	255	193	268
AK21-seq2-b15	5979	64	14	0.23	9150	0.2137	2.7	1.9647	4.2	0.0667	3.3	0.63	1249	31	1104	29	828	68	151
AK21-seq2-b16	48124	257	117	0.78	24088	0.3542	2.3	5.8613	2.7	0.1200	1.4	0.87	1955	40	1956	24	1957	24	100
AK21-seq2-b17	10579	645	49	0.24	20030	0.0753	2.6	0.5874	4.8	0.0566	4.0	0.54	468	12	469	18	475	88	98
AK21-seq2-b18	4869	48	10	0.27	6634	0.2100	2.6	2.1658	3.9	0.0748	2.8	0.68	1229	30	1170	27	1063	57	116
AK21-seq2-b19	15398	176	31	0.21	21233	0.1758	2.1	1.7928	2.9	0.0740	2.0	0.73	1044	21	1043	19	1041	40	100
AK21-seq2-b20	30286	230	55	0.24	34161	0.2314	2.1	2.8803	2.4	0.0903	1.1	0.88	1342	26	1377	18	1431	21	94
AK21-seq2-b21	7147	171	21	0.54	9832	0.1116	2.1	0.9505	3	0.0618	2.1	0.71	682	14	678	15	666	45	102
AK21-seq2-b22	23111	605	58	0.50	1619	0.0834	2.3	0.6646	2.9	0.0578	1.9	0.77	516	11	517	12	523	41	99
AK21-seq2-b23	3878	162	13	0.60	3943	0.0671	2.8	0.4853	4.3	0.0525	3.2	0.66	419	11	402	14	305	73	137
AK21-seq2-b24	5261	115	14	0.43	8856	0.1140	2.6	0.9499	4.1	0.0604	3.1	0.64	696	17	678	20	619	67	112
AK21-seq2-b25	2139	50	6	0.42	3888	0.1098	2.5	0.8484	6	0.0560	5.4	0.41	672	16	624	28	453	121	148
AK21-seq2-b26	15595	177	44	1.14	21764	0.1679	2.3	1.6820	3	0.0727	1.8	0.79	1000	22	1002	19	1005	37	100
AK21-seq2-b27	3762	83	19	0.30	5115	0.2257	2.1	2.3292	3.7	0.0749	3.1	0.57	1312	25	1221	27	1065	62	123
AK21-seq2-b28	2480	106	8	0.57	5143	0.0684	2.5	0.5267	13.6	0.0558	13.4	0.18	427	10	430	49	446	297	96
AK21-seq2-b29	28608	260	55	0.34	36428	0.1962	2.3	2.1672	2.7	0.0801	1.4	0.86	1155	25	1171	19	1200	27	96

AK21-seq2-b30	11781	265	25	0.02	19141	0.1016	2.4	0.8716	3.2	0.0622	2.0	0.77	624	15	636	15	681	44	92
AK21-seq2-b32	5688	136	17	0.52	10071	0.1106	2.3	0.9526	6.8	0.0624	6.3	0.35	676	15	679	34	689	135	98
AK21-seq2-b33	7510	159	21	0.66	12505	0.1095	2.3	0.9295	3.4	0.0616	2.6	0.66	670	14	667	17	659	55	102
AK21-seq2-b34	6847	61	13	0.44	8831	0.1954	3.1	2.1262	4	0.0789	2.5	0.78	1151	33	1157	28	1170	49	98
AK21-seq2-b35	6913	193	20	0.58	12582	0.0899	2.6	0.6900	3.7	0.0557	2.6	0.70	555	14	533	15	440	58	126
AK21-seq2-b36	1671	31	5	0.60	3027	0.1362	2.8	1.0509	5.8	0.0560	5.1	0.48	823	22	729	31	451	113	182
AK21-seq2-b37	11167	225	30	0.59	18380	0.1159	2.3	1.0066	3	0.0630	1.9	0.77	707	16	707	15	708	40	100
AK21-seq2-b38	4833	173	14	0.41	8751	0.0732	2.2	0.5684	3.4	0.0563	2.6	0.65	455	10	457	13	465	58	98
AK21-seq2-b39	7304	60	14	0.34	9331	0.2092	2.5	2.3006	3.5	0.0798	2.4	0.72	1225	28	1212	25	1191	48	103
AK21-seq2-b40	4409	103	13	0.68	7477	0.0996	2.6	0.8266	4	0.0602	3.0	0.65	612	15	612	18	610	65	100
AK21-seq2-b41	15710	114	25	0.21	18650	0.2135	2.9	2.5298	3.5	0.0859	1.9	0.83	1247	33	1281	26	1337	38	93
AK21-seq2-b42	10151	108	21	0.32	8695	0.1791	2.0	1.7990	2.8	0.0729	1.9	0.73	1062	20	1045	18	1010	39	105
AK21-seq2-b43	4365	108	15	0.99	3223	0.1016	2.5	0.7992	4	0.0570	3.2	0.62	624	15	596	18	493	70	126
AK21-seq2-b44	5105	115	13	0.38	8812	0.1095	2.5	0.8795	3.9	0.0582	3.0	0.64	670	16	641	19	539	66	124
AK21-seq2-b45	4413	42	10	0.49	6290	0.2189	2.5	2.1503	4.7	0.0713	4.0	0.53	1276	29	1165	33	965	82	132
AK21-seq2-b46	5073	214	16	0.34	10285	0.0731	2.1	0.5695	6.4	0.0565	6.0	0.33	455	9	458	24	474	133	96
AK21-seq2-b47	11809	137	22	0.21	4920	0.1584	2.2	1.5788	3	0.0723	2.0	0.74	948	20	962	19	994	41	95
AK21-seq2-b48	6357	129	15	0.30	10352	0.1142	2.8	0.9848	3.5	0.0625	2.1	0.80	697	19	696	18	692	44	101
AK21-seq2-b49	19212	140	37	0.51	12269	0.2270	2.3	2.7000	2.7	0.0863	1.5	0.84	1319	27	1328	20	1344	28	98
AK21-seq2-b50	2435	95	7	0.38	4726	0.0671	2.5	0.4858	5	0.0525	4.4	0.49	418	10	402	17	309	100	136
AK21-seq2-b51	5884	87	12	0.27	9333	0.1359	2.8	1.2242	4.2	0.0653	3.2	0.67	821	22	812	24	785	67	105
AK21-seq2-b52	17249	144	33	0.43	15756	0.2007	2.5	2.2227	3.5	0.0803	2.4	0.72	1179	27	1188	25	1205	48	98
AK21-seq2-b53	40358	161	56	0.34	38430	0.3143	2.6	4.6479	3.1	0.1073	1.7	0.84	1762	41	1758	27	1753	31	100
AK21-seq2-b54	6755	239	17	0.42	3810	0.0661	2.6	0.5014	3.5	0.0550	2.3	0.74	412	10	413	12	414	52	100
AK21-seq2-b55	3304	132	9	0.35	6623	0.0685	2.3	0.5473	9.4	0.0580	9.2	0.24	427	9	443	34	528	201	81
AK21-seq2-b56	36736	157	51	0.29	35921	0.3036	2.5	4.3698	2.9	0.1044	1.5	0.86	1709	38	1707	24	1703	27	100
AK21-seq2-b57	17571	65	24	0.59	16728	0.3160	2.6	4.6689	3.2	0.1072	1.8	0.82	1770	40	1762	27	1751	33	101
AK21-seq2-b58	80852	230	90	0.27	64409	0.3582	2.4	6.3107	2.8	0.1278	1.3	0.89	1974	42	2020	24	2068	22	95
AK21-seq2-b59	24984	176	42	0.22	30002	0.2306	2.7	2.7068	3.1	0.0852	1.5	0.87	1337	32	1330	23	1319	29	101
AK21-seq2-b60	84470	128	74	0.38	47489	0.5008	2.4	12.5364	2.9	0.1816	1.6	0.84	2617	53	2645	28	2667	26	98
AK21-seq3-c01	11056	282	30	0.61	19500	0.0876	2.4	0.6967	3	0.0577	1.8	0.80	541	13	537	13	518	40	104
AK21-seq3-c02	9196	69	15	0.35	6728	0.1962	2.8	2.1164	4	0.0783	2.8	0.70	1155	30	1154	28	1153	56	100
AK21-seq3-c03	10848	361	23	0.13	19763	0.0645	4.1	0.4927	4.9	0.0554	2.6	0.84	403	16	407	16	430	59	94
AK21-seq3-c04	22913	126	32	0.24	25050	0.2445	2.7	3.1483	3.5	0.0934	2.1	0.80	1410	35	1445	27	1496	40	94
AK21-seq3-c05	8209	170	20	0.48	13706	0.1048	2.3	0.8836	3.1	0.0612	2.0	0.76	642	14	643	15	645	43	100
AK21-seq3-c06	10166	86	18	0.24	4420	0.2042	2.3	2.2251	3.4	0.0790	2.4	0.69	1198	25	1189	24	1173	48	102
AK21-seq3-c07	13309	313	27	0.19	22537	0.0849	2.8	0.7051	3.2	0.0602	1.6	0.87	525	14	542	14	612	34	86
AK21-seq3-c08	11776	95	22	0.43	14771	0.2152	2.3	2.4111	3.2	0.0813	2.2	0.73	1256	26	1246	23	1228	43	102
AK21-seq3-c09	7624	159	18	0.47	12752	0.0997	2.7	0.8383	3.5	0.0610	2.3	0.76	613	16	618	16	638	49	96
AK21-seq3-c10	2207	60	6	0.44	4030	0.0935	3.1	0.7242	6.5	0.0562	5.7	0.48	576	17	553	28	460	126	125
AK21-seq3-c11	7091	229	20	0.49	12202	0.0774	2.9	0.6374	5.1	0.0597	4.2	0.57	481	13	501	20	593	91	81
AK21-seq3-c12	32826	699	60	0.16	1047	0.0844	2.6	0.8561	3.4	0.0736	2.2	0.77	522	13	628	16	1030	44	51

AK21-seq3-c13	11533	97	21	0.38	14767	0.1997	2.6	2.1777	3.5	0.0791	2.4	0.73	1174	28	1174	25	1175	47	100
AK21-seq3-c14	12632	148	26	0.26	17610	0.1711	2.7	1.7174	3.2	0.0728	1.8	0.83	1018	25	1015	21	1009	36	101
AK21-seq3-c15	8616	199	23	0.52	14518	0.1016	2.6	0.8477	3.3	0.0605	2.1	0.78	624	15	623	16	623	45	100
AK21-seq3-c16	22460	214	39	0.11	29536	0.1867	2.7	1.9989	3.3	0.0777	2.0	0.80	1103	27	1115	23	1138	40	97
AK21-seq3-c17	5920	60	10	0.31	7991	0.1510	3.2	1.5467	4.6	0.0743	3.2	0.71	907	27	949	28	1049	65	86
AK21-seq3-c18	20473	842	47	0.13	10517	0.0578	4.2	0.4460	4.8	0.0560	2.4	0.87	362	15	374	15	451	52	80
AK21-seq3-c19	9822	198	20	0.22	15888	0.0970	2.3	0.8428	2.9	0.0630	1.8	0.79	597	13	621	14	709	38	84
AK21-seq3-c20	27053	233	49	0.29	34334	0.1996	2.6	2.2111	2.9	0.0803	1.4	0.88	1173	28	1185	21	1205	28	97
AK21-seq3-c21	7618	190	22	0.55	3186	0.0992	2.7	0.8227	3.7	0.0602	2.5	0.73	610	16	610	17	610	55	100
AK21-seq3-c22	5811	55	11	0.19	7654	0.2008	2.5	2.1309	4.3	0.0770	3.5	0.58	1180	27	1159	30	1120	70	105
AK21-seq3-c23	4053	62	9	0.42	6194	0.1356	3.1	1.2398	4.9	0.0663	3.8	0.63	819	24	819	28	817	80	100
AK21-seq3-c24	6012	152	18	0.65	10509	0.1013	2.5	0.8092	3.3	0.0579	2.1	0.78	622	15	602	15	527	45	118
AK21-seq3-c25	2146	82	6	0.54	3305	0.0670	3.3	0.4651	10	0.0503	9.4	0.33	418	13	388	33	210	218	199
AK21-seq3-c26	1372	40	4	0.41	893	0.1054	2.5	0.7688	8.1	0.0529	7.7	0.30	646	15	579	36	325	174	199
AK21-seq3-c27	8489	356	25	0.34	14875	0.0664	3.3	0.5280	4.6	0.0576	3.1	0.72	415	13	430	16	516	69	80
AK21-seq3-c28	11912	431	34	0.48	3871	0.0750	2.8	0.6216	4.7	0.0601	3.7	0.60	466	13	491	18	608	81	77
AK21-seq3-c29	7193	257	19	0.13	12920	0.0772	2.9	0.6036	4.2	0.0567	3.1	0.67	479	13	480	16	480	69	100
AK21-seq3-c30	9673	348	27	0.09	6467	0.0824	2.5	0.6306	3.3	0.0555	2.1	0.77	511	12	496	13	431	46	118
AK21-seq3-c31	7344	73	15	0.26	9653	0.1958	3.1	2.0888	4	0.0774	2.6	0.77	1153	33	1145	28	1131	52	102
AK21-seq3-c32	3708	114	12	0.59	6871	0.0894	2.6	0.6672	4.7	0.0542	4.0	0.54	552	14	519	19	378	90	146
AK21-seq3-c33	27504	91	37	0.38	22661	0.3684	2.3	6.2977	3.3	0.1240	2.3	0.70	2022	40	2018	29	2014	41	100
AK21-seq3-c34	5582	149	19	0.85	9695	0.1017	2.5	0.8215	4.3	0.0586	3.5	0.58	624	15	609	20	553	77	113
AK21-seq3-c35	13713	153	32	0.37	18190	0.1906	2.4	2.0216	3	0.0770	1.8	0.80	1124	25	1123	21	1120	36	100
AK21-seq3-c36	4585	146	14	0.38	7464	0.0913	2.5	0.7431	3.7	0.0590	2.7	0.68	563	13	564	16	567	59	99
AK21-seq3-c37	71043	274	105	0.28	31372	0.3521	2.6	6.0778	3	0.1252	1.6	0.85	1944	44	1987	27	2032	28	96
AK21-seq3-c38	30500	587	51	0.09	8963	0.0882	4.0	0.8128	4.6	0.0669	2.2	0.88	545	21	604	21	833	45	65
AK21-seq3-c39	7672	46	15	0.56	8077	0.2757	2.6	3.6840	3.8	0.0969	2.8	0.69	1570	37	1568	31	1565	52	100
AK21-seq3-c40	7874	99	23	1.18	1856	0.1483	3.4	1.6251	4.3	0.0795	2.7	0.79	891	28	980	28	1184	53	75
Sample AK17		Cappagh White Sandstone Form			Location (decimal degrees):				52.16	9.874711 W		Datum:	IRENET95 Irish Transverse Mercator						
AK17-seq1-a01	22198	90	31	0.35	19170	0.3113	3.0	4.4024	4.2	0.1026	3.0	0.70	1747	45	1713	36	1671	56	105
AK17-seq1-a02	1884	54	5	0.66	884	0.0827	3.4	0.6193	9.6	0.0543	9.0	0.35	512	17	489	38	384	202	133
AK17-seq1-a03	6873	65	13	0.47	9437	0.1808	2.5	1.8474	3.8	0.0741	2.8	0.67	1071	25	1062	25	1044	57	103
AK17-seq1-a04	1839	56	5	0.47	3517	0.0776	2.7	0.5692	8.1	0.0532	7.7	0.33	482	12	458	30	338	174	142
AK17-seq1-a05	7967	86	15	0.22	11683	0.1775	2.2	1.6995	3.0	0.0694	2.0	0.74	1054	21	1008	19	911	41	116
AK17-seq1-a06	15508	151	27	0.21	21643	0.1766	2.2	1.7762	3.1	0.0729	2.2	0.70	1049	21	1037	20	1012	45	104
AK17-seq1-a07	9551	335	26	0.40	17946	0.0699	2.4	0.5221	3.1	0.0542	2.0	0.76	436	10	427	11	377	45	116
AK17-seq1-a08	83901	365	108	0.24	82325	0.2774	3.1	3.9665	3.8	0.1037	2.3	0.80	1578	43	1627	32	1692	42	93
AK17-seq1-a09	8249	11	7	0.38	5032	0.5180	2.1	12.0800	3.0	0.1691	2.1	0.72	2691	47	2611	29	2549	35	106
AK17-seq1-a10	33448	304	60	0.30	45297	0.1849	2.7	1.9148	3.1	0.0751	1.6	0.86	1094	27	1086	21	1071	32	102
AK17-seq1-a11	5923	213	15	0.30	6610	0.0680	2.1	0.4993	3.4	0.0533	2.6	0.64	424	9	411	11	340	59	125
AK17-seq1-a12	8617	45	15	0.58	3383	0.2819	2.7	3.6176	3.9	0.0931	2.8	0.69	1601	38	1553	31	1489	53	108

AK17-seq1-a13	37035	41	27	0.37	18686	0.5625	2.9	15.6598	3.5	0.2019	1.8	0.85	2877	68	2856	34	2842	30	101
AK17-seq1-a14	3000	105	9	0.53	1293	0.0717	2.6	0.5101	4.9	0.0516	4.1	0.53	446	11	419	17	268	95	166
AK17-seq1-a15	9004	83	17	0.38	12061	0.1845	2.8	1.9343	4.2	0.0760	3.1	0.67	1092	28	1093	28	1096	62	100
AK17-seq1-a16	15073	125	27	0.29	19762	0.2096	2.3	2.2417	3.0	0.0776	1.9	0.77	1227	26	1194	21	1136	38	108
AK17-seq1-a17	9724	318	21	0.18	11164	0.0660	2.3	0.5473	3.8	0.0601	3.0	0.61	412	9	443	14	608	65	68
AK17-seq1-a18	16118	53	21	0.48	13861	0.3459	2.7	5.6422	3.8	0.1183	2.6	0.73	1915	46	1923	33	1931	46	99
AK17-seq1-a19	10753	104	19	0.09	14568	0.1951	2.5	2.0185	3.4	0.0750	2.3	0.74	1149	27	1122	24	1069	46	107
AK17-seq1-a20	6635	217	14	0.00	12451	0.0733	2.4	0.5476	3.4	0.0542	2.4	0.71	456	11	443	12	380	55	120
AK17-seq1-a21	15949	84	24	0.35	17717	0.2658	2.7	3.3591	3.4	0.0917	2.0	0.81	1519	37	1495	27	1461	37	104
AK17-seq1-a22	43142	295	70	0.28	4771	0.2226	2.7	2.7375	3.3	0.0892	2.0	0.80	1296	31	1339	25	1408	38	92
AK17-seq1-a23	15083	458	43	0.46	10973	0.0882	3.2	0.6974	4.3	0.0574	2.9	0.74	545	17	537	18	505	64	108
AK17-seq1-a24	16910	80	24	0.49	17069	0.2545	2.1	3.5346	2.4	0.1007	1.3	0.84	1462	27	1535	19	1637	24	89
AK17-seq1-a26	7587	42	13	0.61	8505	0.2530	2.5	3.1774	3.7	0.0911	2.8	0.67	1454	32	1452	29	1449	53	100
AK17-seq1-a27	4673	141	14	1.00	8829	0.0732	2.9	0.5450	3.7	0.0540	2.2	0.79	455	13	442	13	371	50	123
AK17-seq1-a28	20814	111	32	0.31	22622	0.2690	2.6	3.4812	3.3	0.0939	2.0	0.79	1535	36	1523	27	1506	39	102
AK17-seq1-a29	4419	157	12	0.47	8392	0.0709	2.7	0.5238	3.3	0.0536	1.9	0.82	442	12	428	12	354	43	125
AK17-seq1-a30	11703	97	22	0.42	12008	0.2040	2.3	2.2198	3.0	0.0789	2.0	0.76	1197	25	1187	21	1170	39	102
AK17-seq1-a31	2589	30	5	0.29	3710	0.1669	3.4	1.6385	8.4	0.0712	7.7	0.40	995	31	985	54	963	156	103
AK17-seq1-a32	3445	107	9	0.27	4558	0.0797	2.5	0.6166	3.8	0.0561	2.9	0.66	494	12	488	15	457	63	108
AK17-seq1-a33	2757	93	8	0.48	5292	0.0778	3.4	0.5690	6.6	0.0531	5.6	0.52	483	16	457	25	331	128	146
AK17-seq1-a34	6649	55	11	0.08	2380	0.2059	3.1	2.2849	6.9	0.0805	6.2	0.45	1207	34	1208	50	1209	122	100
AK17-seq1-a35	9030	92	18	0.35	8834	0.1778	2.8	1.7753	3.7	0.0724	2.5	0.75	1055	27	1036	24	998	50	106
AK17-seq1-a36	2118	21	4	0.49	988	0.1790	2.4	1.8225	5.2	0.0738	4.6	0.46	1061	23	1054	35	1037	93	102
AK17-seq1-a37	24429	136	42	0.55	26918	0.2608	2.4	3.3221	3.0	0.0924	1.8	0.80	1494	32	1486	24	1476	34	101
AK17-seq1-a38	9286	52	14	0.24	3078	0.2453	2.7	3.0894	5.0	0.0914	4.2	0.54	1414	35	1430	39	1454	81	97
AK17-seq1-a39	27860	121	42	0.45	27238	0.3081	2.4	4.4283	2.9	0.1043	1.5	0.85	1731	37	1718	24	1701	28	102
AK17-seq1-a40	23028	238	45	0.28	31931	0.1778	2.5	1.7979	2.8	0.0734	1.3	0.89	1055	24	1045	18	1024	25	103
AK17-seq1-a41	2109	71	5	0.21	4112	0.0765	2.0	0.5496	4.4	0.0521	3.9	0.46	475	9	445	16	290	89	164
AK17-seq1-a42	4317	148	13	0.41	8389	0.0799	2.3	0.5786	4.1	0.0525	3.4	0.57	496	11	464	15	308	77	161
AK17-seq1-a43	11942	72	23	0.68	13603	0.2603	2.3	3.2071	3.1	0.0894	2.1	0.74	1492	30	1459	24	1412	39	106
AK17-seq1-a44	31871	316	56	0.15	42854	0.1786	2.2	1.8659	2.7	0.0758	1.5	0.83	1059	22	1069	18	1089	30	97
AK17-seq1-a45	49391	84	47	0.50	14232	0.4497	2.2	11.1951	2.7	0.1805	1.5	0.83	2394	45	2540	26	2658	25	90
AK17-seq1-a46	25820	234	46	0.21	33618	0.1903	2.5	2.0471	3.1	0.0780	1.8	0.81	1123	26	1131	21	1147	36	98
AK17-seq1-a47	4666	55	12	0.74	6924	0.1744	2.7	1.6359	3.6	0.0680	2.5	0.73	1036	26	984	23	870	51	119
AK17-seq1-a48	10633	55	16	0.27	11437	0.2825	2.2	3.6880	3.2	0.0947	2.3	0.70	1604	32	1569	26	1521	43	105
AK17-seq1-a49	14750	569	43	0.64	18591	0.0673	2.3	0.5397	3.0	0.0582	1.9	0.78	420	9	438	11	537	41	78
AK17-seq1-a50	6554	70	13	0.24	8969	0.1780	3.6	1.8326	5.7	0.0747	4.5	0.62	1056	35	1057	38	1060	90	100
AK17-seq1-a51	28002	112	38	0.28	25956	0.3117	2.6	4.7217	3.1	0.1099	1.8	0.82	1749	39	1771	27	1797	33	97
AK17-seq1-a52	6275	17	8	0.53	5155	0.4026	3.2	6.8804	4.1	0.1240	2.5	0.79	2181	59	2096	37	2014	45	108
AK17-seq1-a53	5290	63	11	0.22	7694	0.1673	2.9	1.6103	4.4	0.0698	3.3	0.66	997	27	974	28	923	68	108
AK17-seq1-a54	5395	116	14	0.44	9273	0.1101	2.5	0.8991	3.3	0.0592	2.2	0.74	674	16	651	16	575	49	117
AK17-seq1-a55	17354	137	31	0.16	21639	0.2222	2.7	2.5093	3.5	0.0819	2.3	0.76	1294	31	1275	26	1243	44	104

AK17-seq1-a56	10103	110	22	0.41	14025	0.1803	2.6	1.8251	3.8	0.0734	2.7	0.70	1069	26	1055	25	1025	54	104
AK17-seq1-a57	2656	28	5	0.29	3849	0.1838	2.7	1.7678	4.6	0.0698	3.7	0.58	1087	27	1034	30	922	77	118
AK17-seq1-a58	10489	50	18	0.62	10741	0.2975	2.5	4.0740	3.1	0.0993	1.9	0.79	1679	37	1649	26	1611	36	104
AK17-seq1-a59	3932	64	10	0.68	6007	0.1380	2.6	1.2693	4.3	0.0667	3.5	0.60	833	20	832	25	829	72	101
AK17-seq1-a60	69092	43	41	0.60	22283	0.7111	3.0	30.9855	3.6	0.3160	1.9	0.85	3463	82	3519	36	3551	29	98
AK17-seq2-b01	4338	158	12	0.33	7782	0.0718	2.7	0.5250	4.1	0.0530	3.2	0.64	447	12	428	15	330	72	135
AK17-seq2-b02	1472	63	5	0.33	3116	0.0717	3.3	0.4767	8.3	0.0482	7.6	0.39	446	14	396	28	110	180	405
AK17-seq2-b03	658	23	2	0.49	1385	0.0828	2.5	0.5582	8.6	0.0489	8.2	0.29	513	12	450	32	143	192	358
AK17-seq2-b04	2601	75	7	0.38	4916	0.0935	2.4	0.6956	4.7	0.0540	4.0	0.51	576	13	536	20	370	90	156
AK17-seq2-b05	4926	52	11	0.63	7019	0.1743	2.6	1.7303	4.4	0.0720	3.5	0.59	1036	25	1020	29	986	72	105
AK17-seq2-b06	62970	146	71	0.47	43965	0.4138	2.4	8.3452	2.7	0.1463	1.2	0.89	2232	45	2269	25	2303	21	97
AK17-seq2-b07	2086	76	7	0.75	4165	0.0791	2.8	0.5609	8.2	0.0514	7.7	0.34	491	13	452	30	259	176	190
AK17-seq2-b08	20460	764	57	0.42	11738	0.0674	2.6	0.5188	3.6	0.0558	2.4	0.74	421	11	424	12	444	54	95
AK17-seq2-b09	9193	62	16	0.29	10950	0.2485	2.2	2.9578	3.4	0.0863	2.6	0.65	1431	29	1397	26	1346	50	106
AK17-seq2-b10	9558	62	19	0.80	1583	0.2402	2.8	2.7942	6.6	0.0844	5.9	0.42	1388	35	1354	50	1301	116	107
AK17-seq2-b11	19604	99	33	0.56	19973	0.2847	3.1	3.9559	3.5	0.1008	1.6	0.89	1615	44	1625	29	1638	29	99
AK17-seq2-b12	136970	454	130	0.43	86780	0.2301	3.1	5.1358	3.6	0.1619	1.8	0.86	1335	38	1842	31	2475	31	54
AK17-seq2-b13	5546	216	17	0.43	11135	0.0708	2.6	0.4982	4.3	0.0510	3.4	0.61	441	11	410	15	242	79	182
AK17-seq2-b14	8601	64	16	0.49	10627	0.2222	2.2	2.5405	3.5	0.0829	2.7	0.63	1294	26	1284	26	1267	53	102
AK17-seq2-b15	9225	337	25	0.37	16869	0.0697	2.9	0.5399	4.2	0.0562	3.0	0.70	434	12	438	15	459	67	95
AK17-seq2-b16	5892	72	12	0.19	8404	0.1697	2.5	1.6808	4.0	0.0718	3.1	0.62	1011	23	1001	26	981	64	103
AK17-seq2-b17	20317	225	41	0.27	27005	0.1784	2.7	1.8481	3.5	0.0751	2.2	0.78	1058	26	1063	23	1072	44	99
AK17-seq2-b18	62727	252	85	0.24	14881	0.3178	2.6	4.9187	2.9	0.1123	1.2	0.92	1779	41	1805	25	1836	21	97
AK17-seq2-b19	2835	79	8	0.34	5172	0.0957	2.0	0.7404	3.7	0.0561	3.2	0.52	589	11	563	16	456	71	129
AK17-seq2-b20	79909	742	145	0.15	103908	0.1950	2.0	2.1199	2.4	0.0789	1.3	0.84	1148	21	1155	17	1169	26	98
AK17-seq2-b21	16559	180	34	0.27	23105	0.1846	2.2	1.8711	2.9	0.0735	1.9	0.75	1092	22	1071	19	1029	39	106
AK17-seq2-b22	15882	146	30	0.27	20586	0.1972	2.6	2.1516	3.2	0.0791	1.9	0.80	1160	27	1166	23	1175	38	99
AK17-seq2-b23	67186	37	37	0.29	16697	0.7859	2.1	37.1866	2.5	0.3432	1.4	0.84	3739	60	3699	25	3677	21	102
AK17-seq2-b24	36438	391	67	0.05	50410	0.1810	2.6	1.8517	3.2	0.0742	1.8	0.83	1072	26	1064	21	1047	36	102
AK17-seq2-b25	25903	36	22	0.32	14144	0.5264	2.2	13.6261	3.1	0.1877	2.2	0.71	2726	49	2724	30	2722	37	100
AK17-seq2-b26	2556	91	8	0.66	5149	0.0749	2.7	0.5244	4.6	0.0508	3.7	0.58	465	12	428	16	232	86	201
AK17-seq2-b27	2433	23	5	0.29	3343	0.1918	2.8	1.9749	7.6	0.0747	7.0	0.37	1131	29	1107	52	1060	142	107
AK17-seq2-b28	23034	107	35	0.41	22759	0.2923	2.5	4.1824	3.2	0.1038	2.0	0.77	1653	36	1671	27	1693	38	98
AK17-seq2-b29	46425	322	92	0.53	54052	0.2456	2.2	2.9820	2.5	0.0881	1.3	0.85	1415	28	1403	19	1384	26	102
AK17-seq2-b30	16818	552	40	0.04	30820	0.0779	3.0	0.6005	3.8	0.0559	2.3	0.79	483	14	478	15	449	52	108
AK17-seq2-b31	30723	148	50	0.47	30669	0.2910	2.2	4.1209	2.8	0.1027	1.7	0.80	1646	33	1658	23	1674	31	98
AK17-seq2-b32	3252	38	8	0.67	4648	0.1647	3.1	1.6096	6.2	0.0709	5.4	0.49	983	28	974	40	954	111	103
AK17-seq2-b33	2377	92	8	0.79	4621	0.0735	2.4	0.5340	4.4	0.0527	3.7	0.54	457	11	434	16	316	85	144
AK17-seq2-b34	31488	1221	82	0.09	58428	0.0709	2.1	0.5405	2.6	0.0553	1.5	0.81	442	9	439	9	423	34	104
AK17-seq2-b35	1530	69	5	0.32	3243	0.0645	2.5	0.4307	4.1	0.0485	3.2	0.62	403	10	364	13	122	76	330
AK17-seq2-b36	1587	20	3	0.28	2454	0.1676	2.7	1.5469	6.9	0.0670	6.3	0.40	999	25	949	43	837	132	119
AK17-seq2-b37	28646	33	22	0.26	13540	0.5857	2.7	17.4279	4.0	0.2158	2.9	0.68	2972	64	2959	39	2950	47	101

AK17-seq2-b38	7537	73	15	0.25	2954	0.1984	2.2	2.0957	3.1	0.0766	2.1	0.73	1167	24	1147	21	1111	42	105
AK17-seq2-b39	7182	63	13	0.25	9418	0.1999	2.7	2.1504	4.0	0.0780	3.0	0.68	1175	29	1165	28	1147	59	102
AK17-seq2-b40	1587	21	4	0.50	695	0.1776	2.3	1.5273	6.2	0.0624	5.8	0.37	1054	23	941	39	687	123	153
AK17-seq2-b41	9271	107	18	0.20	13248	0.1684	2.5	1.6259	5.0	0.0700	4.3	0.50	1003	23	980	32	930	88	108
AK17-seq2-b42	20944	234	41	0.19	28565	0.1718	2.4	1.7756	3.3	0.0750	2.3	0.71	1022	22	1037	22	1068	47	96
AK17-seq2-b43	3646	126	11	0.45	6973	0.0758	2.1	0.5577	4.0	0.0534	3.4	0.53	471	10	450	15	344	77	137
AK17-seq2-b44	17765	86	30	0.61	17865	0.2903	2.4	4.0633	2.9	0.1015	1.7	0.82	1643	34	1647	24	1652	31	99
AK17-seq2-b45	11334	82	20	0.30	13523	0.2379	2.4	2.8213	2.8	0.0860	1.6	0.84	1376	30	1361	22	1339	30	103
AK17-seq2-b46	63419	473	109	0.18	74587	0.2243	2.0	2.6977	2.4	0.0872	1.2	0.87	1305	24	1328	18	1365	22	96
AK17-seq2-b47	1319	40	4	0.41	2533	0.0959	1.9	0.7066	9.0	0.0534	8.8	0.21	591	10	543	38	347	198	170
AK17-seq2-b48	10206	45	16	0.53	10063	0.3060	2.5	4.3787	3.4	0.1038	2.3	0.73	1721	37	1708	28	1693	43	102
AK17-seq2-b49	4328	38	9	0.52	5651	0.2164	2.6	2.3363	4.5	0.0783	3.7	0.58	1263	30	1223	33	1155	73	109
AK17-seq2-b50	4250	92	10	0.20	7788	0.1157	3.3	0.8868	5.5	0.0556	4.3	0.61	706	22	645	26	436	96	162
AK17-seq2-b51	17491	64	25	0.34	15522	0.3568	2.2	5.6820	3.1	0.1155	2.2	0.71	1967	38	1929	27	1888	39	104
AK17-seq2-b52	19518	186	37	0.28	24325	0.1887	2.1	2.0330	2.7	0.0782	1.8	0.75	1114	21	1127	19	1151	36	97
AK17-seq2-b53	12939	165	25	0.47	15275	0.1383	3.0	1.6545	3.6	0.0867	1.9	0.84	835	24	991	23	1355	38	62
AK17-seq2-b54	6238	43	11	0.37	5491	0.2384	2.6	2.8345	3.9	0.0862	3.0	0.65	1378	32	1365	30	1343	58	103
AK17-seq2-b55	9927	131	22	0.33	14346	0.1555	2.4	1.5234	3.9	0.0711	3.0	0.62	932	21	940	24	959	62	97
AK17-seq2-b56	16965	79	26	0.28	17061	0.3048	2.2	4.2850	2.8	0.1020	1.8	0.77	1715	33	1690	24	1660	34	103
AK17-seq2-b57	8171	86	18	0.35	11283	0.1914	2.5	1.9602	3.6	0.0743	2.6	0.69	1129	25	1102	24	1049	52	108
AK17-seq2-b58	4357	151	13	0.51	8027	0.0752	2.8	0.5772	5.0	0.0557	4.2	0.56	468	13	463	19	439	93	107
AK17-seq2-b59	6384	253	19	0.56	11793	0.0645	2.2	0.4936	3.1	0.0555	2.2	0.71	403	9	407	11	433	49	93
AK17-seq2-b60	13668	477	42	0.58	24743	0.0745	2.9	0.5817	3.5	0.0566	2.0	0.82	463	13	466	13	477	44	97

[a] within-run background-corrected mean ^{207}Pb signal in counts per second

[b] U and Pb content and Th/U ratio were calculated relative to GJ-1 and are accurate to approximately 10%.

[c] corrected for background, mass bias, laser induced U-Pb fractionation and common Pb (if detectable, see analytical method) using Stacey & Kramers (1975) model Pb composition. $^{207}Pb/^{235}U$ calculated using $^{207}Pb/^{206}Pb/(^{238}U/^{206}Pb \times 1/137.88)$. Errors are propagated by quadratic addition of within-run errors (2SE) and the reproducibility of GJ-1 (2SD).

[d] Rho is the error correlation defined as $err^{206}Pb/^{238}U/err^{207}Pb/^{235}U$.

Table III. LA ICP MS U, Pb and Th isotopic data for detrital zircons from all 13 samples from the UORS of the Munster and South Munster basins.

Number	^{207}Pb[a] (cps)	U[b] (ppm)	Pb[b] (ppm)	Th[b] U	^{206}Pb ^{204}Pb	^{206}Pb[c] ^{238}U	2 s %	^{207}Pb[c] ^{235}U	2 s %	^{207}Pb[c] ^{206}Pb	2 s %	rho[d]	^{206}Pb ^{238}U	2 s (Ma)	^{207}Pb ^{235}U	2 s (Ma)	^{207}Pb ^{206}Pb	2 s (Ma)	conc %
Sample AK03	western Old Head Sandstone Form Location (decimal degrees) 51.492 9.231367 W											Datum: IRENET95							
AK03-seq1-a01	8935	261	19	0.59	16790	0.0624	1.4	0.4662	3.2	0.0542	2.9	0.43	390	5	389	10	380	64	102
AK03-seq1-a02	1134	23	2	0.53	2032	0.0823	2.2	0.6559	8.3	0.0578	8.0	0.26	510	11	512	34	523	176	97
AK03-seq1-a03	18217	218	19	0.11	264	0.0741	1.5	1.1422	6.8	0.1118	6.6	0.21	461	6	774	37	1829	120	25
AK03-seq1-a04	62761	989	67	0.19	442	0.0629	1.5	0.4766	3.0	0.0549	2.5	0.51	393	6	396	10	409	57	96
AK03-seq1-a05	6741	173	16	0.89	2738	0.0682	1.6	0.5319	2.9	0.0566	2.4	0.54	425	6	433	10	475	54	90
AK03-seq1-a06	15442	467	29	0.25	28103	0.0607	1.6	0.4684	2.8	0.0559	2.3	0.57	380	6	390	9	450	50	84
AK03-seq1-a07	7030	199	13	0.27	2811	0.0628	1.5	0.4674	3.0	0.0540	2.6	0.52	393	6	389	10	370	57	106
AK03-seq1-a08	9255	250	16	0.25	17223	0.0624	2.1	0.4710	2.8	0.0547	1.8	0.76	390	8	392	9	402	41	97
AK03-seq1-a09	20277	515	43	0.60	26827	0.0675	1.8	0.5194	2.5	0.0558	1.8	0.70	421	7	425	9	446	40	94
AK03-seq1-a10	2348	55	4	0.33	3778	0.0666	2.1	0.5400	4.0	0.0588	3.3	0.53	416	8	438	14	560	73	74
AK03-seq1-a11	5184	80	11	0.73	9129	0.1054	1.5	0.8378	3.2	0.0576	2.8	0.48	646	9	618	15	516	61	125
AK03-seq1-a12	9925	280	18	0.19	2431	0.0657	1.2	0.4984	3.5	0.0550	3.4	0.33	410	5	411	12	413	75	99
AK03-seq1-a13	4165	65	7	0.36	7004	0.1013	1.6	0.8375	3.8	0.0600	3.4	0.43	622	10	618	18	602	74	103
AK03-seq1-a14	9516	160	17	0.40	5933	0.0993	1.1	0.8131	2.5	0.0594	2.3	0.45	610	7	604	12	581	49	105
AK03-seq1-a15	4190	113	8	0.52	7788	0.0650	1.2	0.4894	3.0	0.0546	2.7	0.41	406	5	405	10	397	60	102
AK03-seq1-a16	4245	104	8	0.51	2330	0.0684	1.7	0.5172	3.2	0.0548	2.6	0.55	426	7	423	11	406	59	105
AK03-seq1-a17	3109	57	6	0.47	5604	0.0996	1.7	0.7739	3.9	0.0564	3.5	0.45	612	10	582	17	467	77	131
AK03-seq1-a18	8803	157	21	1.09	15192	0.0886	1.3	0.7184	2.9	0.0588	2.6	0.44	547	7	550	13	560	58	98
AK03-seq1-a19	8950	250	16	0.18	16781	0.0634	1.3	0.4749	2.5	0.0543	2.1	0.52	396	5	395	8	386	47	103
AK03-seq1-a20	4608	132	9	0.22	8570	0.0660	1.5	0.4973	2.9	0.0547	2.4	0.52	412	6	410	10	398	54	103
AK03-seq1-a21	3784	63	7	0.71	6623	0.0928	1.2	0.7424	3.3	0.0580	3.1	0.36	572	6	564	14	531	67	108
AK03-seq1-a22	8140	228	15	0.13	14971	0.0690	1.3	0.5291	3.2	0.0557	2.9	0.40	430	5	431	11	439	65	98
AK03-seq1-a23	5155	132	10	0.40	4514	0.0711	1.2	0.5304	3.5	0.0541	3.3	0.34	443	5	432	13	375	75	118
AK03-seq1-a24	202059	427	215	0.05	56982	0.5017	1.6	9.3952	3.6	0.1358	3.2	0.46	2621	36	2377	33	2175	55	121
AK03-seq1-a25	2212	65	5	0.70	873	0.0640	1.7	0.4614	5.4	0.0523	5.2	0.30	400	6	385	18	298	118	134
AK03-seq1-a26	2838	77	6	0.43	5297	0.0676	1.4	0.5087	3.4	0.0546	3.1	0.42	422	6	418	12	395	70	107
AK03-seq1-a27	40110	729	64	0.42	617	0.0686	1.6	0.5269	3.7	0.0557	3.4	0.42	428	6	430	13	441	75	97
AK03-seq1-a28	3968	71	9	1.16	3324	0.0914	1.6	0.7072	3.9	0.0561	3.5	0.43	564	9	543	16	457	77	123
AK03-seq1-a29	10020	121	20	0.58	15206	0.1415	5.3	1.3097	5.7	0.0671	2.3	0.92	853	42	850	33	841	47	101
AK03-seq1-a30	6587	104	12	0.34	4125	0.1073	1.7	0.8900	3.7	0.0602	3.3	0.45	657	11	646	18	609	72	108
AK03-seq1-a31	2555	62	5	0.44	1444	0.0740	3.8	0.5803	9.5	0.0569	8.7	0.40	460	17	465	36	487	193	94
AK03-seq1-a32	4950	73	9	0.58	8535	0.1110	1.2	0.9071	3.8	0.0592	3.6	0.32	679	8	656	18	576	78	118
AK03-seq1-a33	9887	182	12	0.36	320	0.0589	1.5	0.7689	5.0	0.0947	4.7	0.31	369	6	579	22	1522	89	24
AK03-seq1-a34	59154	1466	84	0.08	1217	0.0588	1.0	0.4370	2.2	0.0539	1.9	0.47	368	4	368	7	366	44	101
AK03-seq1-a35	5836	95	12	0.70	10119	0.1031	1.5	0.8280	2.9	0.0583	2.5	0.51	632	9	613	13	540	54	117
AK03-seq1-a36	3761	246	18	0.35	6898	0.0691	1.2	0.5270	3.2	0.0553	3.0	0.38	431	5	430	11	424	67	102

AK03-seq1-a37	11460	300	23	0.46	21139	0.0682	1.3	0.5184	2.3	0.0551	1.9	0.57	425	5	424	8	416	43	102
AK03-seq1-a38	16359	308	24	0.28	628	0.0712	1.8	0.5517	5.3	0.0562	5.0	0.34	444	8	446	19	459	112	97
AK03-seq1-a39	5360	147	9	0.24	10040	0.0601	1.4	0.4493	2.6	0.0542	2.2	0.53	376	5	377	8	379	50	99
AK03-seq1-a40	12564	364	24	0.27	23285	0.0633	1.5	0.4769	2.7	0.0547	2.2	0.56	395	6	396	9	399	50	99
AK03-seq1-a41	6744	185	15	0.57	12780	0.0700	1.8	0.5172	2.9	0.0536	2.3	0.62	436	8	423	10	355	51	123
AK03-seq1-a42	5852	89	10	0.34	9727	0.1063	1.5	0.8964	3.2	0.0611	2.8	0.48	651	9	650	15	644	60	101
AK03-seq1-a43	47843	82	38	0.29	35089	0.4231	1.6	8.0587	2.0	0.1381	1.2	0.80	2274	30	2238	18	2204	21	103
AK03-seq1-a44	37839	993	72	0.25	35109	0.0710	1.3	0.5459	1.9	0.0558	1.4	0.68	442	6	442	7	444	32	99
AK03-seq1-a45	5083	153	11	0.38	9320	0.0660	1.6	0.5021	4.4	0.0552	4.1	0.35	412	6	413	15	421	92	98
AK03-seq1-a46	243413	619	135	0.41	36	0.1018	3.1	5.6785	11.3	0.4044	10.9	0.27	625	18	1928	102	3926	163	16
AK03-seq1-a47	29445	51	23	0.29	11157	0.4127	1.4	7.5184	2.1	0.1321	1.6	0.64	2227	25	2175	19	2127	29	105
AK03-seq1-a48	2209	106	7	0.29	4363	0.0655	1.9	0.4627	5.9	0.0513	5.6	0.32	409	8	386	19	253	129	162
AK03-seq1-a49	31097	95	35	0.55	29332	0.3053	1.2	4.4888	2.1	0.1066	1.7	0.59	1717	18	1729	17	1743	30	99
AK03-seq1-a50	5425	137	11	0.53	4696	0.0658	2.1	0.5011	4.0	0.0552	3.4	0.51	411	8	412	14	420	76	98
AK03-seq1-a51	6949	83	10	0.23	2373	0.1176	2.1	1.0430	10.6	0.0644	10.4	0.20	716	15	725	57	753	220	95
AK03-seq1-a52	8470	193	16	0.20	15554	0.0843	1.6	0.6448	2.8	0.0555	2.3	0.58	522	8	505	11	431	50	121
AK03-seq1-a53	19358	368	52	1.16	7841	0.0924	1.4	0.7564	2.4	0.0594	1.9	0.58	570	7	572	10	580	42	98
AK03-seq1-a54	8422	136	17	0.57	6138	0.1097	1.4	0.9041	2.6	0.0598	2.3	0.51	671	9	654	13	596	49	113
AK03-seq1-a55	7017	28	9	0.36	4483	0.2871	1.8	3.6473	2.7	0.0921	2.0	0.66	1627	25	1560	22	1470	38	111
AK03-seq1-a56	13205	181	20	0.07	21502	0.1161	1.3	0.9898	2.5	0.0618	2.2	0.52	708	9	699	13	669	46	106
AK03-seq1-a57	7411	216	14	0.18	3709	0.0668	1.2	0.5015	2.7	0.0545	2.4	0.46	417	5	413	9	390	53	107
AK03-seq1-a58	2598	50	5	0.22	4530	0.0988	1.5	0.7873	5.3	0.0578	5.1	0.29	608	9	590	24	521	112	117
AK03-seq1-a59	6983	213	15	0.53	8066	0.0599	1.8	0.4443	3.7	0.0538	3.3	0.48	375	7	373	12	364	73	103
AK03-seq1-a60	8354	126	14	0.48	2444	0.1025	1.3	0.8553	8.5	0.0605	8.3	0.16	629	8	628	40	623	180	101
AK03-seq2-b01	34685	234	51	0.20	45595	0.2149	1.7	2.2929	2.3	0.0774	1.6	0.75	1255	20	1210	17	1131	31	111
AK03-seq2-b02	31871	60	27	0.42	24615	0.3852	2.0	6.9365	2.5	0.1306	1.4	0.82	2100	37	2103	22	2106	25	100
AK03-seq2-b03	28217	320	52	0.72	3391	0.1270	1.6	1.1319	2.5	0.0646	1.9	0.64	771	11	769	13	763	40	101
AK03-seq2-b04	70627	307	69	0.14	26819	0.2087	11.2	3.6903	11.3	0.1283	1.5	0.99	1222	126	1569	94	2074	27	59
AK03-seq2-b05	5782	151	16	0.36	9855	0.0960	1.2	0.7805	3.6	0.0590	3.3	0.35	591	7	586	16	567	73	104
AK03-seq2-b06	17769	65	19	0.11	16170	0.2982	1.6	4.5895	2.5	0.1116	1.9	0.64	1682	23	1747	21	1826	34	92
AK03-seq2-b07	127258	135	105	0.93	71364	0.5710	1.5	14.2637	1.7	0.1812	0.8	0.89	2912	35	2767	16	2664	13	109
AK03-seq2-b08	34205	367	46	0.07	51884	0.1295	1.2	1.1983	1.8	0.0671	1.4	0.66	785	9	800	10	841	28	93
AK03-seq2-b09	13993	387	24	0.09	1745	0.0654	1.5	0.5056	2.6	0.0561	2.1	0.58	408	6	415	9	455	48	90
AK03-seq2-b10	8670	137	17	0.47	14964	0.1087	1.4	0.8828	2.6	0.0589	2.2	0.54	665	9	643	12	563	48	118
AK03-seq2-b11	53678	218	60	0.38	4181	0.2445	1.9	3.0814	2.7	0.0914	1.9	0.70	1410	24	1428	21	1455	36	97
AK03-seq2-b12	13085	209	21	0.06	22396	0.1070	1.5	0.8741	2.5	0.0593	2.1	0.58	655	9	638	12	577	45	114
AK03-seq2-b13	23566	633	41	0.19	3932	0.0633	1.8	0.4778	3.1	0.0548	2.5	0.57	395	7	397	10	403	57	98
AK03-seq2-b14	2129	57	7	0.67	3839	0.1026	1.9	0.7949	5.3	0.0562	4.9	0.36	630	12	594	24	459	109	137
AK03-seq2-b15	81444	542	177	0.15	58977	0.3034	5.4	5.9610	5.6	0.1425	1.5	0.96	1708	81	1970	50	2258	25	76
AK03-seq2-b16	10173	427	27	0.09	5505	0.0664	1.8	0.5234	3.0	0.0572	2.4	0.61	414	7	427	11	498	53	83
AK03-seq2-b17	3205	49	6	0.64	4875	0.1069	1.8	0.8948	5.9	0.0607	5.6	0.31	654	12	649	29	630	121	104
AK03-seq2-b18	20641	573	37	0.17	6751	0.0649	1.3	0.4981	2.0	0.0557	1.6	0.65	405	5	410	7	439	35	92

AK03-seq2-b19	3308	57	7	0.62	5849	0.1022	1.9	0.8107	3.9	0.0575	3.5	0.47	628	11	603	18	511	76	123
AK03-seq2-b20	3700	53	7	0.41	6373	0.1157	1.6	0.9405	3.4	0.0590	2.9	0.48	706	11	673	17	566	64	125
AK03-seq2-b21	11511	184	19	0.25	19614	0.0995	2.0	0.8147	3.0	0.0594	2.2	0.67	611	12	605	14	582	48	105
AK03-seq2-b22	8590	298	20	0.12	437	0.0683	1.4	0.5162	3.7	0.0548	3.5	0.38	426	6	423	13	405	77	105
AK03-seq2-b23	74758	193	92	0.24	54211	0.4414	1.7	8.4200	2.4	0.1384	1.7	0.71	2357	34	2277	22	2207	29	107
AK03-seq2-b24	31264	107	46	0.42	25964	0.3766	1.3	6.3495	2.0	0.1223	1.5	0.65	2060	23	2025	17	1990	27	104
AK03-seq2-b25	4711	82	10	0.44	8255	0.1070	1.9	0.8571	3.4	0.0581	2.8	0.55	656	12	629	16	532	62	123
AK03-seq2-b26	6177	94	13	0.72	10576	0.1125	1.1	0.9212	2.9	0.0594	2.7	0.39	687	7	663	14	582	59	118
AK03-seq2-b27	14039	287	25	0.35	285	0.0796	1.5	0.5885	7.5	0.0536	7.4	0.20	494	7	470	29	354	166	139
AK03-seq2-b28	13261	245	16	0.15	709	0.0656	1.9	0.4949	7.0	0.0548	6.7	0.28	409	8	408	24	402	151	102
AK03-seq2-b29	6322	94	11	0.36	10521	0.1082	1.3	0.8987	2.5	0.0602	2.1	0.54	662	8	651	12	613	46	108
AK03-seq2-b30	2378	35	4	0.31	3950	0.1132	1.9	0.9635	7.2	0.0617	6.9	0.26	691	12	685	36	665	148	104
AK03-seq3-c01	14895	309	19	0.11	27745	0.0648	1.7	0.4905	2.5	0.0549	1.9	0.68	405	7	405	8	408	42	99
AK03-seq3-c02	14263	186	17	0.15	24541	0.0948	2.0	0.7771	2.5	0.0595	1.5	0.79	584	11	584	11	584	34	100
AK03-seq3-c03	48052	190	47	0.28	58037	0.2326	2.1	2.6948	2.8	0.0840	1.8	0.77	1348	26	1327	21	1293	34	104
AK03-seq3-c04	9920	168	24	1.09	16624	0.1060	1.8	0.8887	3.5	0.0608	3.0	0.52	649	11	646	17	633	65	103
AK03-seq3-c05	87632	2133	114	0.05	23630	0.0573	2.0	0.4238	2.3	0.0536	1.1	0.87	359	7	359	7	356	26	101
AK03-seq3-c06	4408	99	6	0.34	8339	0.0608	1.9	0.4527	4.5	0.0540	4.1	0.41	380	7	379	14	373	93	102
AK03-seq3-c07	12859	245	18	0.42	23606	0.0677	2.1	0.5193	3.0	0.0556	2.1	0.71	422	9	425	10	438	47	96
AK03-seq3-c08	14330	188	13	0.28	346	0.0637	2.1	0.4794	6.8	0.0546	6.4	0.31	398	8	398	22	395	144	101
AK03-seq3-c09	8702	98	13	0.79	5733	0.1022	2.1	0.9054	3.7	0.0642	3.0	0.57	628	13	655	18	749	64	84
AK03-seq3-c10	6946	144	11	0.56	12992	0.0687	1.9	0.5171	3.2	0.0546	2.6	0.59	428	8	423	11	396	58	108
AK03-seq3-c11	10060	249	16	0.32	18030	0.0630	2.3	0.4754	5.1	0.0547	4.6	0.46	394	9	395	17	399	102	99
AK03-seq3-c12	3475	68	6	0.45	6276	0.0807	2.3	0.6282	4.2	0.0565	3.5	0.55	500	11	495	16	471	77	106
AK03-seq3-c13	31504	687	48	0.34	1903	0.0644	1.9	0.5412	3.0	0.0610	2.2	0.66	402	8	439	11	639	48	63
AK03-seq3-c14	7176	225	13	0.13	1099	0.0566	2.6	0.5188	4.3	0.0664	3.4	0.61	355	9	424	15	820	71	43
AK03-seq3-c15	35043	152	53	0.32	23235	0.3307	3.8	5.6447	4.4	0.1238	2.2	0.86	1842	60	1923	38	2011	39	92
AK03-seq3-c16	3666	95	9	0.29	6716	0.0882	2.7	0.6806	4.2	0.0560	3.3	0.64	545	14	527	18	452	72	121
AK03-seq3-c17	11459	220	20	0.22	15656	0.0860	5.9	0.9306	8.0	0.0785	5.5	0.73	532	30	668	40	1160	109	46
AK03-seq3-c18	17183	662	45	0.41	31805	0.0626	2.3	0.4735	3.1	0.0548	2.1	0.73	392	9	394	10	405	48	97
AK03-seq3-c19	52485	1004	71	0.38	195	0.0567	2.8	0.4184	8.4	0.0535	7.9	0.33	356	10	355	25	350	179	102
AK03-seq3-c20	24621	549	43	0.46	43378	0.0711	2.0	0.5690	2.6	0.0580	1.7	0.75	443	8	457	10	531	38	83
AK03-seq3-c21	5089	364	22	0.07	9456	0.0650	1.9	0.4917	4.9	0.0549	4.5	0.38	406	7	406	16	408	101	99
AK03-seq3-c22	73903	1905	105	0.03	1054	0.0573	2.2	0.4354	2.7	0.0551	1.5	0.82	359	8	367	8	417	34	86
AK03-seq3-c23	14672	183	20	0.35	798	0.0977	2.0	0.7997	5.4	0.0593	5.1	0.37	601	11	597	25	580	110	104
AK03-seq3-c24	8549	275	17	0.20	16164	0.0613	2.0	0.4575	3.3	0.0542	2.7	0.59	383	7	383	11	377	60	102
AK03-seq3-c25	3213	70	7	0.84	5664	0.0844	2.3	0.6755	4.6	0.0581	3.9	0.51	522	12	524	19	532	86	98
AK03-seq3-c26	91764	916	73	0.12	139	0.0654	1.9	0.4978	4.3	0.0552	3.9	0.43	408	7	410	15	421	86	97
AK03-seq3-c27	891	19	2	0.38	1867	0.0905	2.2	0.6106	9.1	0.0489	8.8	0.24	559	12	484	36	144	207	389
AK03-seq3-c28	8572	152	18	0.66	14372	0.1008	1.8	0.8482	3.0	0.0610	2.4	0.59	619	10	624	14	641	51	97
AK03-seq3-c29	21737	769	43	0.20	41279	0.0560	2.3	0.4122	3.1	0.0534	2.0	0.75	351	8	350	9	346	46	101
AK03-seq3-c30	35012	556	39	0.33	396	0.0576	2.4	0.4558	4.4	0.0574	3.7	0.55	361	9	381	14	507	81	71

AK03-seq3-c31	5537	119	14	0.78	9862	0.1015	2.3	0.8021	3.7	0.0573	2.9	0.62	623	13	598	17	503	64	124
AK03-seq3-c32	24784	59	26	0.35	19382	0.4021	2.1	7.2312	2.6	0.1304	1.6	0.80	2179	39	2140	24	2104	28	104
AK03-seq3-c33	3690	71	9	0.78	6328	0.1077	1.8	0.8887	3.3	0.0599	2.8	0.54	659	11	646	16	598	60	110
AK03-seq3-c34	4333	238	15	0.21	1637	0.0655	2.6	0.4961	4.5	0.0550	3.6	0.59	409	10	409	15	411	80	99
AK03-seq3-c35	20075	148	36	0.58	25433	0.2124	2.2	2.3653	3.0	0.0808	2.1	0.74	1242	25	1232	22	1216	40	102
AK03-seq3-c36	1278	29	3	0.35	2447	0.1080	3.0	0.7944	8.2	0.0533	7.7	0.36	661	19	594	38	342	174	193
AK03-seq3-c37	43925	665	48	0.30	190	0.0588	2.5	0.4380	6.2	0.0540	5.7	0.40	369	9	369	19	371	127	99
AK03-seq3-c38	20405	376	43	0.54	1960	0.1000	2.1	0.8366	3.6	0.0607	3.0	0.56	614	12	617	17	629	65	98
AK03-seq3-c39	2678	96	7	0.35	4981	0.0663	1.9	0.5052	5.6	0.0552	5.3	0.34	414	8	415	19	422	118	98
AK03-seq3-c40	47843	38	30	0.34	19281	0.6643	2.2	23.3731	2.6	0.2552	1.3	0.86	3284	57	3243	25	3217	21	102
AK03-seq3-c41	73685	211	96	0.58	24521	0.3791	2.3	6.8449	2.7	0.1310	1.5	0.84	2072	40	2092	24	2111	26	98
AK03-seq3-c42	30602	805	82	0.30	52735	0.0988	1.7	0.8085	2.3	0.0594	1.5	0.74	607	10	602	10	581	33	104
AK03-seq3-c43	6475	11	7	0.09	780	0.5847	4.3	17.1925	6.1	0.2133	4.3	0.70	2968	103	2946	60	2931	70	101
AK03-seq3-c44	2021	59	6	0.52	3868	0.0965	2.1	0.7075	5.9	0.0532	5.5	0.36	594	12	543	25	337	126	176
AK03-seq3-c45	4379	121	16	1.10	7754	0.0972	1.9	0.7735	3.7	0.0577	3.1	0.53	598	11	582	16	520	68	115
Sample AK04		Toe Head Formation				Location (decimal degrees)		51.467		9.772069 W			Datum: IRENET95						
AK04-seq1-a1	8751	171	11	0.04	16632	0.0666	2.4	0.4924	4.0	0.0536	3.2	0.60	416	10	407	14	355	73	117
AK04-seq1-a2	5965	114	7	0.04	11754	0.0699	2.2	0.4981	3.4	0.0517	2.6	0.66	436	9	410	12	270	59	161
AK04-seq1-a3	3379	62	6	1.11	1924	0.0633	2.1	0.4744	9.8	0.0544	9.5	0.21	395	8	394	32	388	214	102
AK04-seq1-a4	11294	237	15	0.24	6247	0.0607	2.3	0.4509	3.0	0.0539	1.9	0.78	380	8	378	9	368	42	103
AK04-seq1-a5	11453	236	16	0.37	3115	0.0621	2.1	0.4598	3.0	0.0537	2.2	0.68	388	8	384	10	360	50	108
AK04-seq1-a6	41848	815	50	0.06	56881	0.0653	2.2	0.4892	2.5	0.0543	1.3	0.86	408	9	404	8	385	29	106
AK04-seq1-a7	6360	75	8	0.45	11513	0.0972	2.1	0.7539	2.8	0.0563	1.9	0.74	598	12	570	12	463	42	129
AK04-seq1-a8	4677	82	8	0.90	8779	0.0740	2.5	0.5558	4.8	0.0545	4.1	0.52	460	11	449	18	391	92	118
AK04-seq1-a9	14376	283	17	0.06	26585	0.0628	2.1	0.4765	3.1	0.0551	2.3	0.68	392	8	396	10	415	51	95
AK04-seq1-a10	5533	61	11	1.58	9385	0.1060	3.5	0.8774	5.2	0.0600	3.9	0.66	650	21	640	25	604	85	108
AK04-seq1-a11	5979	111	7	0.09	11498	0.0705	1.9	0.5127	3.1	0.0528	2.5	0.61	439	8	420	11	319	56	137
AK04-seq1-a12	477	13	1	0.55	1333	0.1350	11.4	-11.3948	251.0	-0.6123	250.8	0.05	816	88	######	#####	#NUM!	####	#NUM!
AK04-seq1-a13	8250	156	11	0.34	15349	0.0651	1.8	0.4907	2.8	0.0546	2.1	0.65	407	7	405	10	397	48	102
AK04-seq1-a14	9943	190	12	0.36	18924	0.0618	3.0	0.4540	4.1	0.0533	2.7	0.74	387	11	380	13	340	62	114
AK04-seq1-a15	6576	131	9	0.39	12794	0.0676	2.4	0.4878	4.4	0.0523	3.6	0.56	422	10	403	15	298	83	141
AK04-seq1-a16	4111	25	7	1.83	6102	0.1532	2.4	1.4474	4.4	0.0685	3.7	0.55	919	21	909	27	884	76	104
AK04-seq1-a17	20168	396	31	0.50	26256	0.0720	2.0	0.5476	4.0	0.0552	3.5	0.50	448	9	443	15	419	78	107
AK04-seq1-a18	3483	73	6	0.74	7132	0.0646	2.7	0.4412	4.3	0.0495	3.3	0.63	404	11	371	13	173	78	234
AK04-seq1-a19	4533	90	6	0.21	8872	0.0637	3.1	0.4572	5.4	0.0520	4.4	0.58	398	12	382	17	286	100	139
AK04-seq1-a20	3209	63	4	0.14	5923	0.0700	2.0	0.5323	4.0	0.0551	3.5	0.51	436	9	433	14	418	77	104
AK04-seq1-a21	5996	119	8	0.40	11287	0.0613	2.4	0.4554	4.0	0.0539	3.2	0.59	384	9	381	13	365	73	105
AK04-seq1-a22	10083	174	15	0.37	18503	0.0814	2.0	0.6212	3.6	0.0553	3.0	0.56	505	10	491	14	426	66	118
AK04-seq1-a23	34950	52	26	0.83	10893	0.3912	2.0	6.6467	2.6	0.1232	1.6	0.78	2128	37	2066	23	2004	29	106
AK04-seq1-a24	6239	67	9	0.65	10935	0.1185	2.0	0.9494	3.2	0.0581	2.5	0.63	722	14	678	16	534	54	135
AK04-seq1-a25	1757	15	2	0.36	3101	0.1476	2.5	1.1674	5.5	0.0574	5.0	0.44	887	20	785	31	506	109	175

AK04-seq1-a26	64435	93	37	0.15	49919	0.3814	2.7	6.9128	3.5	0.1315	2.2	0.77	2083	48	2100	31	2117	39	98
AK04-seq1-a27	4532	48	6	0.60	7741	0.1120	1.8	0.9238	4.8	0.0598	4.4	0.38	685	12	664	24	597	96	115
AK04-seq1-a28	2942	38	4	0.33	5802	0.1086	2.0	0.7727	3.0	0.0516	2.2	0.68	665	13	581	13	268	50	248
AK04-seq1-a29	117778	148	67	0.24	88110	0.4188	2.1	7.8666	2.5	0.1362	1.3	0.85	2255	41	2216	23	2180	23	103
AK04-seq1-a30	4111	77	6	0.42	4830	0.0707	2.0	0.5449	4.2	0.0559	3.7	0.48	441	9	442	15	447	82	99
AK04-seq2-b01	3635	67	6	0.47	6554	0.0769	3.6	0.5998	5.7	0.0566	4.4	0.63	477	17	477	22	476	97	100
AK04-seq2-b02	5278	106	10	1.02	759	0.0689	3.1	0.6209	7.2	0.0654	6.5	0.43	429	13	490	29	786	137	55
AK04-seq2-b03	35718	543	44	0.03	58374	0.0862	3.7	0.7497	4.3	0.0630	2.2	0.87	533	19	568	19	710	46	75
AK04-seq2-b04	7862	109	16	1.08	13624	0.1064	3.6	0.8695	4.3	0.0593	2.4	0.83	652	22	635	21	578	52	113
AK04-seq2-b05	5575	58	9	0.49	8800	0.1375	3.3	1.2322	4.1	0.0650	2.5	0.81	830	26	815	23	775	52	107
AK04-seq2-b06	3075	51	5	0.48	5499	0.0913	2.9	0.7226	4.4	0.0574	3.3	0.67	563	16	552	19	508	72	111
AK04-seq2-b07	3372	86	6	0.33	6771	0.0681	3.1	0.4802	4.8	0.0511	3.7	0.64	425	13	398	16	247	86	172
AK04-seq2-b08	7124	242	17	0.63	13613	0.0610	4.4	0.4592	7.0	0.0546	5.4	0.63	382	16	384	22	394	121	97
AK04-seq2-b09	1819	57	5	1.00	3983	0.0641	3.3	0.4159	7.9	0.0470	7.2	0.42	401	13	353	24	51	171	783
AK04-seq2-b10	7358	203	14	0.55	13880	0.0604	3.3	0.4523	4.4	0.0543	2.8	0.77	378	12	379	14	386	63	98
AK04-seq2-b11	5956	173	10	0.24	7715	0.0595	3.0	0.4477	4.6	0.0545	3.4	0.66	373	11	376	14	394	77	95
AK04-seq2-b12	5733	190	11	0.11	10866	0.0611	3.0	0.4580	4.6	0.0544	3.6	0.64	382	11	383	15	388	80	99
AK04-seq2-b13	5152	159	13	0.71	3822	0.0672	3.0	0.4861	4.9	0.0524	3.9	0.61	420	12	402	16	304	89	138
AK04-seq2-b14	11827	474	21	0.02	22109	0.0491	4.1	0.3720	6.7	0.0550	5.3	0.62	309	12	321	19	411	118	75
AK04-seq2-b15	13257	518	32	0.34	25193	0.0601	3.3	0.4494	4.2	0.0542	2.6	0.79	376	12	377	13	380	58	99
AK04-seq2-b16	10798	223	24	0.49	3095	0.0959	3.1	0.8114	4.1	0.0614	2.7	0.76	590	17	603	19	652	57	91
AK04-seq2-b17	19432	64	22	0.48	17821	0.3067	3.5	4.7404	3.8	0.1121	1.6	0.91	1724	52	1774	32	1834	29	94
AK04-seq2-b18	3327	80	6	0.68	4682	0.0728	17.7	0.6351	239.7	0.0633	239.0	0.07	453	78	499	2713	717	5076	63
AK04-seq2-b19	11185	165	22	0.32	17797	0.1305	3.4	1.1626	4.0	0.0646	2.0	0.87	791	26	783	22	761	42	104
AK04-seq2-b20	2280	35	5	0.46	3887	0.1335	3.4	1.1030	6.5	0.0599	5.5	0.52	808	26	755	35	601	120	134
AK04-seq2-b21	2263	88	8	1.02	875	0.0683	3.3	0.4933	8.9	0.0524	8.2	0.38	426	14	407	30	302	187	141
AK04-seq2-b22	4427	106	12	0.66	5557	0.0977	3.3	0.8006	4.4	0.0594	3.0	0.74	601	19	597	20	582	64	103
AK04-seq2-b23	8887	170	17	0.22	14419	0.1019	3.7	0.8898	4.2	0.0633	2.0	0.87	626	22	646	20	719	43	87
AK04-seq2-b24	1560	45	5	0.43	3022	0.1165	3.7	0.8500	12.6	0.0529	12.1	0.30	710	25	625	61	326	274	218
AK04-seq2-b25	3176	164	11	0.61	6518	0.0552	3.8	0.3813	6.4	0.0501	5.2	0.59	347	13	328	18	198	121	175
AK04-seq2-b26	10260	499	30	0.16	5911	0.0618	4.0	0.4645	4.8	0.0545	2.7	0.83	387	15	387	16	393	60	98
AK04-seq2-b27	3619	89	12	1.10	6041	0.0981	3.3	0.8418	8.1	0.0622	7.4	0.41	603	19	620	38	682	158	88
AK04-seq2-b28	1655	57	6	0.46	3397	0.0932	3.7	0.6448	7.4	0.0502	6.4	0.49	574	20	505	30	204	149	281
AK04-seq2-b29	6213	81	12	0.27	6364	0.1489	3.9	2.0560	6.3	0.1001	4.9	0.62	895	32	1134	44	1626	91	55
AK04-seq2-b30	4563	231	14	0.28	8637	0.0621	3.4	0.4668	4.8	0.0545	3.4	0.71	389	13	389	16	391	76	99
AK04-seq3-c01	6893	139	10	0.47	12815	0.0632	2.6	0.4709	4.0	0.0540	3.0	0.65	395	10	392	13	371	68	106
AK04-seq3-c02	17465	330	20	0.10	32393	0.0621	3.0	0.4703	3.8	0.0549	2.4	0.79	389	11	391	12	408	53	95
AK04-seq3-c03	24220	492	32	0.47	45169	0.0580	2.3	0.4351	3.1	0.0544	2.0	0.75	363	8	367	9	388	45	94
AK04-seq3-c04	21232	288	26	0.75	9840	0.0778	2.6	0.6422	3.1	0.0599	1.7	0.83	483	12	504	12	599	38	81
AK04-seq3-c05	43899	870	50	0.07	82069	0.0616	2.6	0.4618	3.0	0.0544	1.5	0.87	385	10	386	10	386	34	100
AK04-seq3-c06	5535	56	7	0.35	9315	0.1267	1.9	1.0613	3.3	0.0607	2.6	0.59	769	14	734	17	630	57	122
AK04-seq3-c07	4338	45	6	0.85	4158	0.1102	2.2	0.9261	4.1	0.0610	3.5	0.53	674	14	666	20	638	75	106

AK04-seq3-c08	8042	75	11	0.58	13457	0.1353	2.2	1.1347	3.6	0.0608	2.9	0.61	818	17	770	20	634	62	129
AK04-seq3-c09	7264	132	11	0.79	1959	0.0685	3.9	0.5135	5.3	0.0544	3.6	0.74	427	16	421	18	386	80	111
AK04-seq3-c10	7264	134	11	0.78	12328	0.0675	2.9	0.5056	4.6	0.0544	3.6	0.63	421	12	415	16	386	80	109
AK04-seq3-c11	12632	140	16	0.53	15727	0.1004	2.4	0.8267	2.8	0.0597	1.4	0.87	617	14	612	13	593	30	104
AK04-seq3-c12	14033	136	19	0.68	23481	0.1177	2.0	0.9855	2.6	0.0607	1.7	0.77	717	14	696	13	630	36	114
AK04-seq3-c13	4673	93	6	0.44	9096	0.0631	2.2	0.4548	4.1	0.0523	3.5	0.53	394	8	381	13	299	79	132
AK04-seq3-c14	868	9	1	0.01	1411	0.1051	3.8	0.9228	12.5	0.0637	12.0	0.30	644	23	664	63	730	253	88
AK04-seq3-c15	2569	34	4	0.68	4612	0.0953	3.1	0.7455	6.7	0.0567	5.9	0.47	587	18	566	29	482	131	122
AK04-seq3-c16	15890	307	19	0.27	8400	0.0602	2.2	0.4775	4.1	0.0575	3.5	0.54	377	8	396	14	512	76	74
AK04-seq3-c17	7396	97	9	0.36	13197	0.0914	2.4	0.7179	3.5	0.0570	2.6	0.68	564	13	549	15	491	57	115
AK04-seq3-c18	167441	190	78	0.15	111571	0.3915	2.1	8.2341	2.5	0.1526	1.2	0.87	2130	39	2257	22	2375	21	90
AK04-seq3-c19	945	13	1	0.33	1807	0.0972	2.5	0.7111	8.5	0.0531	8.1	0.29	598	14	545	36	332	184	180
AK04-seq3-c20	54775	106	40	0.46	10887	0.3324	2.2	5.1699	2.6	0.1128	1.4	0.84	1850	35	1848	22	1845	25	100
AK04-seq3-c21	22328	59	18	0.47	23336	0.2726	2.3	3.6242	3.2	0.0964	2.2	0.72	1554	32	1555	26	1556	42	100
AK04-seq3-c22	32019	587	30	0.02	5252	0.0551	2.8	0.4269	3.1	0.0561	1.3	0.90	346	9	361	9	458	29	76
AK04-seq3-c23	3068	45	6	1.03	5914	0.0958	2.5	0.6967	4.3	0.0527	3.5	0.58	590	14	537	18	317	80	186
AK04-seq3-c24	2731	25	3	0.20	1508	0.1218	2.7	1.0364	5.3	0.0617	4.6	0.51	741	19	722	28	664	98	112
AK04-seq3-c25	6950	94	10	0.74	12216	0.0821	2.3	0.6557	3.8	0.0579	2.9	0.62	509	12	512	15	526	65	97
AK04-seq3-c26	143844	190	79	0.21	107825	0.3886	2.8	7.2606	3.1	0.1355	1.4	0.89	2116	50	2144	28	2171	24	98
AK04-seq3-c27	78858	141	62	0.28	62817	0.4053	2.6	7.2153	3.4	0.1291	2.1	0.78	2193	49	2138	30	2086	37	105
AK04-seq3-c28	19810	453	26	0.10	35637	0.0595	5.6	0.4732	13.5	0.0576	12.3	0.42	373	20	393	45	516	270	72
AK04-seq3-c29	152124	210	84	0.25	92007	0.3721	2.0	6.8385	2.4	0.1333	1.3	0.85	2039	35	2091	21	2142	22	95
AK04-seq3-c30	13080	277	17	0.14	24307	0.0621	2.3	0.4687	3.1	0.0547	2.1	0.74	388	9	390	10	401	47	97
AK04-seq3-c31	6248	71	9	0.79	2111	0.1026	2.2	0.8454	3.7	0.0597	2.9	0.60	630	13	622	17	594	64	106
AK04-seq3-c32	27550	340	46	1.08	46881	0.0980	2.2	0.8067	2.7	0.0597	1.6	0.81	603	13	601	13	593	35	102
AK04-seq3-c33	16062	324	21	0.28	29592	0.0653	2.1	0.4983	2.9	0.0553	2.0	0.72	408	8	411	10	426	45	96
AK04-seq3-c34	16705	357	22	0.15	4370	0.0647	2.4	0.5089	4.0	0.0571	3.2	0.60	404	9	418	14	495	70	82
AK04-seq3-c35	9888	173	14	0.48	17295	0.0722	2.0	0.5794	2.9	0.0582	2.1	0.69	449	9	464	11	538	46	83
AK04-seq3-c36	2448	48	11	3.59	4677	0.0678	2.2	0.4974	5.5	0.0532	5.0	0.40	423	9	410	19	337	113	126
AK04-seq3-c37	4254	56	6	0.47	7771	0.1027	2.5	0.7860	4.1	0.0555	3.2	0.62	630	15	589	18	433	72	145
AK04-seq3-c38	123054	165	73	0.34	90248	0.3922	2.4	7.4950	2.7	0.1386	1.2	0.89	2133	43	2172	24	2210	21	97
AK04-seq3-c39	6923	155	11	0.54	13081	0.0593	2.8	0.4400	4.0	0.0538	2.8	0.71	371	10	370	12	365	63	102
AK04-seq3-c40	13973	192	18	0.36	24594	0.0878	2.6	0.6968	3.4	0.0576	2.2	0.77	542	14	537	14	514	48	106
AK04-seq3-c41	5948	74	9	0.50	9085	0.1048	2.2	0.8484	3.5	0.0587	2.7	0.64	643	14	624	16	556	58	116
AK04-seq3-c42	2216	29	3	0.69	3980	0.1024	2.4	0.8043	5.6	0.0570	5.1	0.43	629	14	599	26	490	112	128
AK04-seq3-c43	36020	49	23	0.42	27217	0.4051	2.5	7.5133	3.2	0.1345	1.9	0.79	2192	47	2175	29	2158	34	102
AK04-seq3-c44	4770	83	7	0.69	8788	0.0732	2.1	0.5574	3.6	0.0553	2.9	0.59	455	9	450	13	423	64	108
AK04-seq3-c45	11211	135	18	0.96	8108	0.1014	2.2	0.8322	3.2	0.0595	2.3	0.69	622	13	615	15	587	50	106
AK04-seq3-c46	7797	101	11	0.47	13472	0.0962	2.2	0.7821	3.6	0.0589	2.8	0.63	592	13	587	16	565	60	105
AK04-seq3-c47	8271	110	12	0.63	5313	0.0938	2.1	0.7434	2.8	0.0575	1.9	0.74	578	11	564	12	510	42	113
AK04-seq3-c48	17686	402	29	0.70	23160	0.0603	2.3	0.4476	3.1	0.0539	2.1	0.75	377	8	376	10	365	47	103
AK04-seq3-c49	19773	436	26	0.07	37451	0.0626	2.4	0.4631	3.2	0.0536	2.1	0.75	391	9	386	10	356	47	110

AK04-seq3-c50	7670	106	12	0.42	2726	0.1012	1.8	0.8067	2.8	0.0578	2.2	0.64	622	11	601	13	522	47	119
AK04-seq3-c51	6478	77	9	0.56	10845	0.1053	2.2	0.8823	3.8	0.0608	3.0	0.59	645	14	642	18	631	65	102
AK04-seq3-c52	33284	45	20	0.21	3955	0.4233	2.5	7.8690	3.1	0.1348	1.8	0.82	2275	48	2216	28	2162	31	105
AK04-seq3-c53	9883	131	13	0.07	17213	0.1030	2.1	0.8298	2.9	0.0584	2.0	0.72	632	13	614	13	545	44	116
AK04-seq3-c54	4620	58	6	0.01	3670	0.1050	2.5	0.8485	4.8	0.0586	4.1	0.53	644	15	624	23	552	89	116
AK04-seq3-c55	13724	19	15	2.58	10851	0.3858	2.7	6.8425	3.4	0.1286	2.0	0.80	2103	48	2091	30	2079	36	101
AK04-seq3-c56	16500	201	23	0.45	16462	0.1024	3.4	0.8684	4.1	0.0615	2.4	0.82	628	20	635	20	658	51	96
AK04-seq3-c57	7787	160	16	1.13	13961	0.0704	3.0	0.5476	5.0	0.0564	4.0	0.60	439	13	443	18	468	88	94
AK04-seq3-c58	6347	131	9	0.25	12091	0.0693	2.4	0.5103	3.3	0.0534	2.2	0.74	432	10	419	11	345	51	125
AK04-seq3-c59	36191	374	45	0.28	58456	0.1155	2.4	1.0003	2.9	0.0628	1.6	0.83	705	16	704	15	702	34	100
AK04-seq3-c60	5663	117	10	0.66	10833	0.0730	2.1	0.5342	3.5	0.0531	2.7	0.62	454	9	435	12	333	62	136
AK04-seq4-d01	1467	16	2	0.72	2381	0.1119	2.0	0.9724	11.6	0.0630	11.5	0.17	684	13	690	60	710	244	96
AK04-seq4-d02	3215	53	7	1.07	2711	0.0920	2.1	0.6668	4.4	0.0525	3.9	0.47	568	11	519	18	309	89	184
AK04-seq4-d03	2819	36	4	0.60	1723	0.1016	2.2	0.8133	5.0	0.0581	4.5	0.45	624	13	604	23	533	99	117
AK04-seq4-d04	6091	76	10	0.65	5012	0.1051	2.0	0.8725	3.8	0.0602	3.2	0.52	644	12	637	18	612	70	105
AK04-seq4-d05	22138	36	17	0.69	18210	0.3844	2.2	6.5719	2.7	0.1240	1.6	0.81	2097	39	2056	24	2014	28	104
AK04-seq4-d06	57638	79	39	0.50	44775	0.4244	2.1	7.6552	2.5	0.1308	1.3	0.85	2280	41	2191	23	2109	23	108
AK04-seq4-d07	2813	43	4	0.22	4951	0.0871	3.1	0.6957	4.9	0.0579	3.9	0.62	538	16	536	21	527	85	102
AK04-seq4-d08	1928	28	3	0.56	3389	0.0912	3.2	0.7411	7.8	0.0589	7.1	0.41	563	17	563	34	564	154	100
AK04-seq4-d09	22779	324	35	0.31	40835	0.1048	2.1	0.8223	2.7	0.0569	1.7	0.78	643	13	609	12	487	37	132
AK04-seq4-d10	19094	456	18	0.03	21042	0.0431	29.4	0.3260	30.0	0.0548	6.2	0.98	272	79	287	78	405	140	67
AK04-seq4-d11	7357	75	10	0.41	12169	0.1287	2.5	1.0941	3.6	0.0617	2.6	0.69	780	18	751	19	662	56	118
AK04-seq4-d12	11311	146	15	0.38	5674	0.0974	2.0	0.7943	2.8	0.0592	2.1	0.69	599	11	594	13	573	45	104
AK04-seq4-d13	104774	147	67	0.36	36669	0.4033	2.4	7.7090	2.9	0.1386	1.6	0.83	2184	45	2198	27	2210	28	99
AK04-seq4-d14	21862	289	27	0.05	12723	0.1006	2.1	0.8334	3.0	0.0601	2.1	0.70	618	12	616	14	607	45	102
AK04-seq4-d15	34829	720	53	0.28	63963	0.0710	2.1	0.5451	2.4	0.0556	1.3	0.85	442	9	442	9	438	28	101
AK04-seq4-d16	18228	145	24	0.47	27063	0.1457	1.9	1.3440	2.7	0.0669	1.9	0.70	877	16	865	16	835	40	105
AK04-seq4-d17	16679	214	27	0.67	17236	0.1027	2.4	0.8603	3.1	0.0607	2.0	0.76	630	14	630	15	630	43	100
AK04-seq4-d18	12727	251	16	0.21	2322	0.0670	2.0	0.5681	4.0	0.0615	3.5	0.50	418	8	457	15	655	74	64
AK04-seq4-d19	17380	406	24	0.02	32803	0.0645	2.5	0.4809	3.2	0.0541	2.0	0.79	403	10	399	11	374	44	108
AK04-seq4-d20	12552	162	23	1.01	13993	0.1088	1.8	0.8800	3.1	0.0587	2.5	0.57	666	11	641	15	555	55	120
AK04-seq4-d21	46524	71	34	0.51	36336	0.4055	1.8	7.3048	2.3	0.1306	1.4	0.79	2195	34	2149	21	2107	25	104
AK04-seq4-d22	3143	48	5	0.38	5936	0.1028	1.9	0.7652	3.9	0.0540	3.4	0.49	631	12	577	17	371	76	170
AK04-seq4-d23	36340	478	49	0.21	61184	0.1025	2.4	0.8557	2.7	0.0605	1.4	0.86	629	14	628	13	623	30	101
AK04-seq4-d24	151942	192	100	0.63	107059	0.4254	3.0	8.4970	3.3	0.1448	1.3	0.91	2285	58	2286	30	2286	23	100
AK04-seq4-d25	9508	202	17	0.56	17695	0.0730	2.0	0.5517	3.1	0.0548	2.4	0.65	454	9	446	11	405	53	112
AK04-seq4-d26	6434	174	11	0.58	2216	0.0561	3.7	0.4330	6.7	0.0560	5.5	0.56	352	13	365	21	453	123	78
AK04-seq4-d27	8686	81	11	0.32	12374	0.1308	2.2	1.1659	3.5	0.0646	2.7	0.63	793	17	785	19	763	58	104
AK04-seq4-d28	120986	129	68	0.37	71579	0.4595	2.1	10.9085	2.5	0.1722	1.3	0.86	2437	43	2515	23	2579	21	95
AK04-seq4-d29	5298	59	6	0.15	9626	0.1127	1.8	0.8713	3.3	0.0561	2.8	0.53	688	12	636	16	456	62	151
AK04-seq4-d30	29094	50	22	0.45	21448	0.3732	2.8	7.1212	3.9	0.1384	2.7	0.72	2044	50	2127	35	2207	47	93
AK04-seq4-d31	14557	192	23	0.39	10700	0.1143	1.8	0.9528	2.9	0.0605	2.2	0.64	698	12	680	14	620	48	113

AK04-seq4-d32	38647	114	37	0.52	39596	0.2702	2.9	3.7073	3.3	0.0995	1.6	0.88	1542	40	1573	27	1615	30	95
AK04-seq4-d33	3842	50	7	0.77	6907	0.1158	2.1	0.9045	4.6	0.0566	4.1	0.45	706	14	654	22	478	91	148
AK04-seq4-d34	195666	399	118	0.50	7276	0.2873	4.0	5.1632	4.9	0.1303	2.8	0.82	1628	58	1847	43	2102	49	77
AK04-seq4-d35	4432	98	8	0.59	8390	0.0655	3.2	0.4916	7.7	0.0544	7.0	0.41	409	13	406	26	390	157	105
AK04-seq4-d36	18421	41	16	0.39	17736	0.3496	2.0	5.1095	3.0	0.1060	2.2	0.68	1933	34	1838	26	1731	40	112
AK04-seq4-d37	10756	412	26	0.19	20181	0.0627	3.2	0.4698	4.5	0.0543	3.2	0.71	392	12	391	15	384	72	102
AK04-seq4-d38	7154	108	10	0.23	12512	0.0958	2.6	0.7705	4.1	0.0583	3.1	0.65	590	15	580	18	542	67	109
AK04-seq4-d39	13388	190	19	0.33	23058	0.0974	2.0	0.7956	2.8	0.0593	1.9	0.71	599	11	594	12	577	42	104
AK04-seq4-d40	99076	210	70	0.27	81463	0.3083	2.0	5.2706	2.5	0.1240	1.5	0.80	1732	31	1864	22	2014	27	86
AK04-seq4-d41	18552	424	36	0.89	33911	0.0635	1.9	0.4870	2.5	0.0556	1.7	0.73	397	7	403	8	437	38	91
AK04-seq4-d42	2416	54	5	0.89	1651	0.0631	2.4	0.5157	4.8	0.0593	4.2	0.50	394	9	422	17	578	90	68
AK04-seq4-d43	6934	167	13	0.24	15381	0.0785	1.9	0.4973	4.0	0.0459	3.6	0.47	487	9	410	14	-6	86	-8359
AK04-seq4-d44	6739	144	12	0.44	12055	0.0787	2.8	0.6154	4.4	0.0567	3.3	0.65	489	13	487	17	479	74	102
AK04-seq4-d45	11045	149	19	0.70	18675	0.1045	1.9	0.8708	3.2	0.0604	2.5	0.61	641	12	636	15	619	54	104
AK04-seq4-d46	4163	52	7	0.94	7059	0.1046	2.0	0.8683	4.3	0.0602	3.8	0.47	641	12	635	21	611	83	105
AK04-seq4-d47	2261	58	5	0.80	4583	0.0632	1.8	0.4385	4.3	0.0503	3.9	0.42	395	7	369	13	209	90	189
AK04-seq4-d48	7608	174	13	0.13	14238	0.0748	3.1	0.5619	5.5	0.0544	4.5	0.58	465	14	453	20	389	100	119
AK04-seq4-d49	7810	85	13	0.46	12677	0.1349	2.6	1.1746	3.7	0.0631	2.7	0.70	816	20	789	21	713	56	114
AK04-seq4-d50	5120	72	9	0.78	3820	0.0990	2.1	0.7966	3.4	0.0583	2.7	0.61	609	12	595	15	543	58	112
AK04-seq4-d51	14704	360	21	0.03	27332	0.0628	2.0	0.4741	2.7	0.0547	1.8	0.73	393	7	394	9	401	41	98
AK04-seq4-d52	5193	69	8	0.52	8949	0.1064	2.3	0.8674	3.5	0.0591	2.6	0.66	652	14	634	16	571	56	114
AK04-seq4-d53	23868	601	26	0.06	44690	0.0455	22.1	0.3420	23.2	0.0545	7.1	0.95	287	62	299	62	392	158	73
AK04-seq4-d54	25321	133	31	0.40	19325	0.2107	1.9	2.3213	3.2	0.0799	2.5	0.61	1233	22	1219	23	1194	50	103
AK04-seq4-d55	3042	67	5	0.46	5906	0.0755	2.0	0.5486	5.1	0.0527	4.7	0.39	469	9	444	18	316	106	148
AK04-seq4-d56	3056	71	6	0.53	4176	0.0735	2.0	0.5234	5.4	0.0516	5.0	0.37	457	9	427	19	269	116	170
AK04-seq4-d57	5524	120	9	0.23	10499	0.0732	2.0	0.5415	3.0	0.0536	2.2	0.68	456	9	439	11	355	49	128
AK04-seq4-d58	13103	161	24	0.93	22609	0.1173	2.4	0.9554	3.3	0.0591	2.3	0.72	715	16	681	16	570	50	125
AK04-seq4-d59	48071	74	38	0.64	20338	0.4165	1.9	7.8019	2.3	0.1359	1.3	0.83	2244	37	2208	21	2175	23	103
AK04-seq4-d60	4063	53	6	0.54	6854	0.1074	2.5	0.8965	4.1	0.0605	3.2	0.61	658	15	650	20	623	70	106
Sample AK07	Gun Point Formation					Location (decimal degrees)		51.713	9.582383 W			Datum: IRENET95							
AK07-seq1-a01	18574	65	25	0.82	6285	0.3048	1.5	4.2541	2.5	0.1012	2.0	0.59	1715	22	1685	21	1647	38	104
AK07-seq1-a02	22608	174	33	0.29	4498	0.1784	2.1	1.9265	4.0	0.0783	3.5	0.52	1058	21	1090	27	1155	69	92
AK07-seq1-a03	9646	75	13	0.04	4596	0.1834	1.7	1.8957	2.9	0.0750	2.4	0.57	1085	17	1080	20	1068	49	102
AK07-seq1-a04	8426	233	18	0.39	15580	0.0709	1.9	0.5369	2.9	0.0549	2.2	0.66	441	8	436	10	410	49	108
AK07-seq1-a05	2089	14	4	0.84	2685	0.1990	2.5	2.1442	7.0	0.0782	6.5	0.36	1170	27	1163	50	1151	130	102
AK07-seq1-a06	5535	92	11	0.40	5482	0.1058	2.9	0.9022	4.9	0.0618	4.0	0.59	649	18	653	24	668	85	97
AK07-seq1-a07	6398	47	10	0.35	8602	0.1902	2.0	1.9788	3.9	0.0755	3.3	0.52	1122	21	1108	27	1081	66	104
AK07-seq1-a08	51816	339	71	0.16	66429	0.2091	1.6	2.2812	2.1	0.0791	1.4	0.75	1224	18	1206	15	1175	28	104
AK07-seq1-a09	10646	262	22	0.44	19385	0.0745	1.6	0.5713	3.1	0.0556	2.7	0.51	463	7	459	12	438	60	106
AK07-seq1-a10	2254	22	4	0.44	3536	0.1779	1.6	1.5859	4.8	0.0647	4.6	0.33	1055	15	965	31	763	96	138
AK07-seq1-a11	7048	41	11	0.47	8923	0.2427	1.9	2.6901	3.5	0.0804	3.0	0.53	1401	24	1326	26	1206	58	116

AK07-seq1-a12	1663	11	3	0.39	2296	0.2157	2.1	2.2121	5.9	0.0744	5.5	0.36	1259	24	1185	42	1052	111	120
AK07-seq1-a13	3815	34	6	0.28	2166	0.1681	2.0	1.6386	3.3	0.0707	2.7	0.59	1002	18	985	21	948	55	106
AK07-seq1-a14	5829	10	5	0.70	5852	0.4240	3.1	5.9737	4.0	0.1022	2.5	0.78	2278	60	1972	35	1664	46	137
AK07-seq1-a15	7896	220	17	0.34	14640	0.0736	1.7	0.5565	2.7	0.0549	2.1	0.63	458	7	449	10	406	46	113
AK07-seq1-a16	5714	153	12	0.35	10575	0.0708	1.3	0.5349	3.3	0.0548	3.0	0.41	441	6	435	12	405	66	109
AK07-seq1-a17	4112	107	8	0.29	7554	0.0753	1.7	0.5740	3.1	0.0553	2.6	0.55	468	8	461	12	424	59	110
AK07-seq1-a18	25212	167	37	0.20	32062	0.2154	2.0	2.3689	2.7	0.0798	1.8	0.74	1257	23	1233	19	1191	36	106
AK07-seq1-a19	6412	57	10	0.26	2746	0.1776	2.2	1.7483	3.5	0.0714	2.7	0.63	1054	21	1027	23	969	55	109
AK07-seq1-a20	6872	198	15	0.24	12904	0.0733	2.1	0.5473	3.0	0.0542	2.2	0.69	456	9	443	11	378	48	120
AK07-seq1-a21	6023	159	13	0.36	10740	0.0757	1.7	0.5837	2.7	0.0559	2.1	0.63	470	8	467	10	449	47	105
AK07-seq1-a22	21986	182	36	0.31	30617	0.1866	1.4	1.8745	2.3	0.0729	1.8	0.62	1103	14	1072	15	1010	36	109
AK07-seq1-a23	21545	269	55	0.45	29529	0.1830	1.9	1.8650	2.7	0.0739	1.9	0.70	1084	19	1069	18	1039	38	104
AK07-seq1-a24	22582	80	27	0.29	22018	0.3100	1.6	4.4497	2.0	0.1041	1.2	0.81	1740	25	1722	17	1699	22	102
AK07-seq1-a25	5424	149	12	0.30	9813	0.0769	1.8	0.5955	3.6	0.0561	3.1	0.50	478	8	474	14	458	69	104
AK07-seq1-a26	39537	350	67	0.28	37190	0.1812	1.6	1.8741	2.1	0.0750	1.3	0.76	1074	16	1072	14	1069	27	100
AK07-seq1-a27	8232	242	19	0.46	15446	0.0721	1.2	0.5379	3.0	0.0541	2.7	0.39	449	5	437	11	375	62	120
AK07-seq1-a28	13883	133	22	0.22	15381	0.1640	1.8	1.6127	2.8	0.0713	2.0	0.67	979	17	975	17	966	42	101
AK07-seq1-a29	3710	128	11	0.47	6728	0.0736	1.7	0.5638	5.4	0.0555	5.1	0.32	458	8	454	20	434	115	106
AK07-seq1-a30	6737	203	16	0.42	12687	0.0723	2.6	0.5373	3.7	0.0539	2.6	0.70	450	11	437	13	366	59	123
AK07-seq1-a31	3916	95	7	0.10	7227	0.0793	1.4	0.6015	2.9	0.0550	2.5	0.48	492	7	478	11	412	56	119
AK07-seq1-a32	2997	30	5	0.33	3415	0.1687	1.8	1.5867	4.0	0.0682	3.6	0.46	1005	17	965	25	875	74	115
AK07-seq1-a33	11263	66	16	0.21	13632	0.2308	1.6	2.6692	2.8	0.0839	2.3	0.58	1339	20	1320	21	1290	45	104
AK07-seq1-a34	35926	297	91	1.56	48395	0.1860	1.9	1.9347	2.8	0.0754	2.1	0.67	1100	19	1093	19	1080	41	102
AK07-seq1-a35	6858	108	11	0.14	10649	0.0976	3.2	0.8809	3.7	0.0654	1.8	0.87	601	19	641	18	788	39	76
AK07-seq1-a36	12669	112	22	0.34	17337	0.1813	1.9	1.8563	2.8	0.0743	2.1	0.68	1074	19	1066	19	1049	42	102
AK07-seq1-a37	7763	139	12	0.35	445	0.0751	2.8	0.5883	11.4	0.0568	11.1	0.24	467	13	470	44	484	245	96
AK07-seq1-a38	15344	53	20	0.38	15008	0.3331	1.6	4.7788	2.6	0.1041	2.0	0.64	1853	26	1781	22	1698	36	109
AK07-seq1-a39	3385	30	7	0.70	4838	0.1906	2.3	1.8280	5.5	0.0696	5.0	0.41	1125	23	1056	37	915	103	123
AK07-seq1-a40	9030	107	21	0.30	12928	0.1906	1.6	1.8743	2.8	0.0713	2.3	0.57	1125	17	1072	19	967	48	116
AK07-seq1-a41	25794	390	38	0.16	28029	0.0992	2.1	0.9884	3.3	0.0722	2.5	0.64	610	12	698	17	993	52	61
AK07-seq1-a42	29961	195	44	0.23	27543	0.2179	1.7	2.4630	2.3	0.0820	1.6	0.73	1271	20	1261	17	1245	31	102
AK07-seq1-a43	498	3	1	0.00	630	0.2094	3.9	2.3306	17.1	0.0807	16.6	0.23	1226	44	1222	129	1214	327	101
AK07-seq1-a44	2663	69	5	0.23	1179	0.0787	2.2	0.6109	4.2	0.0563	3.6	0.52	489	10	484	16	463	79	105
AK07-seq1-a45	27254	105	35	0.34	26850	0.3100	1.8	4.4070	2.5	0.1031	1.7	0.72	1741	27	1714	21	1681	31	104
AK07-seq1-a46	7103	60	13	0.36	10024	0.1991	1.4	1.9920	2.8	0.0726	2.4	0.50	1171	15	1113	19	1002	50	117
AK07-seq1-a47	4902	131	11	0.32	8825	0.0779	2.4	0.6078	3.8	0.0566	3.0	0.63	484	11	482	15	474	66	102
AK07-seq1-a48	4571	134	11	0.38	4113	0.0734	1.8	0.5699	6.4	0.0563	6.1	0.28	457	8	458	24	464	135	99
AK07-seq1-a49	6740	67	12	0.33	9606	0.1678	1.8	1.6471	3.4	0.0712	2.9	0.53	1000	17	988	22	963	59	104
AK07-seq1-a50	2845	24	5	0.44	3940	0.1898	2.2	1.9804	6.8	0.0757	6.5	0.32	1120	22	1109	47	1087	130	103
AK07-seq1-a51	16072	745	53	0.20	29143	0.0707	1.5	0.5420	2.8	0.0556	2.3	0.55	440	7	440	10	438	51	101
AK07-seq1-a52	10900	87	17	0.11	14379	0.1972	1.7	2.0952	3.1	0.0770	2.7	0.54	1160	18	1147	22	1122	53	103
AK07-seq1-a53	1064	31	3	0.68	2012	0.0801	2.4	0.5959	7.5	0.0539	7.2	0.31	497	11	475	29	368	161	135

AK07-seq1-a54	46037	326	72	0.26	4193	0.2106	1.9	2.3138	2.9	0.0797	2.2	0.66	1232	22	1217	21	1189	43	104
AK07-seq1-a55	14361	510	35	0.21	26368	0.0675	2.1	0.5119	2.8	0.0550	1.8	0.75	421	8	420	10	413	41	102
AK07-seq1-a56	39313	168	55	0.20	39744	0.3189	1.6	4.4204	2.2	0.1005	1.5	0.74	1784	25	1716	18	1634	27	109
AK07-seq1-a57	73954	108	51	0.43	40413	0.3764	1.9	9.6502	2.6	0.1859	1.7	0.76	2060	34	2402	24	2706	28	76
AK07-seq1-a58	5967	50	10	0.39	8009	0.1950	1.8	2.0015	3.9	0.0745	3.5	0.45	1148	18	1116	27	1054	71	109
AK07-seq1-a59	21090	83	27	0.26	20750	0.3156	1.5	4.4385	2.4	0.1020	1.9	0.62	1768	23	1720	20	1661	35	106
AK07-seq1-a60	6265	196	16	0.30	11618	0.0770	1.4	0.5814	2.6	0.0547	2.1	0.56	478	7	465	10	402	48	119
AK07-seq2-b01	7685	249	18	0.38	14231	0.0672	2.1	0.5082	3.5	0.0549	2.8	0.59	419	9	417	12	406	64	103
AK07-seq2-b02	48667	66	44	0.47	27037	0.5519	1.5	13.9374	2.0	0.1832	1.3	0.75	2833	34	2745	19	2682	22	106
AK07-seq2-b03	4120	120	9	0.27	7535	0.0733	1.9	0.5591	4.2	0.0553	3.7	0.46	456	9	451	15	426	82	107
AK07-seq2-b04	4102	39	7	0.21	5686	0.1825	1.6	1.8489	3.6	0.0735	3.2	0.46	1081	16	1063	24	1027	64	105
AK07-seq2-b05	2383	64	6	0.51	4214	0.0834	2.3	0.6627	5.2	0.0576	4.6	0.44	517	11	516	21	515	102	100
AK07-seq2-b06	2766	81	7	0.60	5072	0.0808	2.3	0.6105	4.9	0.0548	4.4	0.47	501	11	484	19	403	98	124
AK07-seq2-b07	42974	412	70	0.05	59147	0.1793	1.5	1.8277	2.2	0.0739	1.5	0.70	1063	15	1055	14	1040	31	102
AK07-seq2-b08	29665	226	47	0.19	37557	0.2022	1.7	2.2388	2.5	0.0803	1.9	0.67	1187	18	1193	18	1205	37	99
AK07-seq2-b09	5660	167	15	0.52	10107	0.0815	1.7	0.6435	4.1	0.0572	3.8	0.41	505	8	504	17	500	83	101
AK07-seq2-b10	6942	65	13	0.31	9545	0.1922	2.0	1.9610	3.3	0.0740	2.6	0.62	1133	21	1102	22	1041	52	109
AK07-seq2-b11	4814	155	12	0.41	8906	0.0739	1.6	0.5532	3.5	0.0543	3.1	0.46	459	7	447	13	384	70	120
AK07-seq2-b12	3868	29	7	0.56	4991	0.2135	1.9	2.3156	3.8	0.0787	3.3	0.50	1247	22	1217	28	1164	66	107
AK07-seq2-b13	1990	19	4	0.54	2007	0.1932	2.5	1.7803	5.6	0.0668	5.0	0.44	1139	26	1038	37	833	105	137
AK07-seq2-b14	1017	10	2	0.27	1615	0.1595	2.4	1.4738	7.8	0.0670	7.4	0.31	954	21	920	48	839	154	114
AK07-seq2-b15	3438	109	8	0.26	6240	0.0733	1.9	0.5625	3.5	0.0556	2.9	0.54	456	8	453	13	437	64	104
AK07-seq2-b16	12737	100	22	0.23	16645	0.2130	2.0	2.2738	2.9	0.0774	2.1	0.70	1245	23	1204	21	1132	41	110
AK07-seq2-b17	6544	63	15	0.97	9113	0.1825	1.9	1.8323	3.0	0.0728	2.3	0.64	1081	19	1057	20	1009	47	107
AK07-seq2-b18	9525	2	5	0.42	31	0.9142	47.3	83.5685	65.5	0.6630	45.2	0.72	4186	1652	4506	1057	4653	653	90
AK07-seq2-b19	27554	40	25	0.56	16204	0.5214	1.7	12.3733	2.4	0.1721	1.6	0.73	2705	38	2633	22	2578	27	105
AK07-seq2-b20	26842	77	33	0.46	22828	0.3770	1.6	6.2120	2.3	0.1195	1.7	0.69	2062	28	2006	21	1949	30	106
AK07-seq2-b21	9750	106	22	0.67	14234	0.1671	2.0	1.6049	3.1	0.0696	2.4	0.63	996	18	972	20	918	50	109
AK07-seq2-b22	19659	121	28	0.64	389	0.1755	2.7	1.8326	5.7	0.0757	5.0	0.48	1043	26	1057	38	1088	100	96
AK07-seq2-b23	16842	139	29	0.35	17596	0.1924	2.0	2.0654	2.8	0.0779	2.0	0.70	1134	21	1137	20	1144	40	99
AK07-seq2-b24	15930	101	33	0.37	16149	0.2971	1.7	4.1052	2.4	0.1002	1.7	0.71	1677	25	1655	19	1628	31	103
AK07-seq2-b25	11612	68	17	0.22	13674	0.2480	1.7	2.9307	2.9	0.0857	2.3	0.60	1428	22	1390	22	1332	45	107
AK07-seq2-b26	3000	23	6	0.45	4033	0.2195	1.8	2.3086	4.4	0.0763	4.0	0.41	1279	21	1215	32	1102	81	116
AK07-seq2-b27	3158	95	9	1.04	5773	0.0685	2.1	0.5254	4.9	0.0557	4.4	0.44	427	9	429	17	439	97	97
AK07-seq2-b28	33466	32	24	0.48	15494	0.6083	1.9	18.3712	2.4	0.2190	1.5	0.79	3063	46	3009	23	2974	24	103
AK07-seq2-b29	28149	256	32	0.13	8068	0.1243	3.1	1.5136	4.2	0.0883	2.8	0.74	755	22	936	26	1389	54	54
AK07-seq2-b30	3353	276	22	0.55	6080	0.0717	2.4	0.5528	5.7	0.0559	5.2	0.41	446	10	447	21	449	116	99
AK07-seq2-b31	7727	249	20	0.45	14338	0.0707	1.4	0.5328	2.6	0.0547	2.2	0.54	440	6	434	9	400	50	110
AK07-seq2-b32	5230	169	11	0.22	7560	0.0655	2.0	0.4980	3.8	0.0552	3.3	0.51	409	8	410	13	418	74	98
AK07-seq2-b33	1500	46	4	0.93	2780	0.0728	2.0	0.5436	6.2	0.0541	5.9	0.32	453	9	441	22	377	132	120
AK07-seq2-b34	2052	15	2	0.74	406	0.1031	3.2	2.7501	7.5	0.1935	6.8	0.43	632	19	1342	57	2772	111	23
AK07-seq2-b35	6369	176	15	0.28	11349	0.0837	2.0	0.6534	3.8	0.0566	3.2	0.53	518	10	511	15	478	72	108

AK07-seq2-b36	10459	337	21	0.12	17054	0.0644	2.1	0.5011	3.7	0.0565	3.0	0.57	402	8	412	13	470	67	85
AK07-seq2-b37	4661	140	11	0.37	7578	0.0769	2.3	0.5981	5.0	0.0564	4.4	0.46	478	10	476	19	468	98	102
AK07-seq2-b38	4651	142	11	0.32	8686	0.0750	2.0	0.5621	3.6	0.0544	3.0	0.56	466	9	453	13	387	67	121
AK07-seq2-b39	19198	171	37	0.46	25759	0.1957	1.9	2.0294	2.5	0.0752	1.6	0.75	1152	20	1125	17	1074	33	107
AK07-seq2-b40	11096	53	17	0.57	5928	0.2656	1.7	3.5024	2.9	0.0956	2.3	0.59	1518	23	1528	23	1541	44	99
AK07-seq3-c01	31455	78	27	0.39	31453	0.3135	1.9	4.3824	2.4	0.1014	1.5	0.78	1758	29	1709	20	1650	28	107
AK07-seq3-c02	21889	359	28	0.46	716	0.0709	3.4	0.5541	5.6	0.0567	4.4	0.61	442	15	448	20	478	98	92
AK07-seq3-c03	9309	155	13	0.38	16759	0.0792	1.4	0.6155	2.5	0.0564	2.1	0.56	491	7	487	10	467	46	105
AK07-seq3-c04	50017	128	43	0.47	16213	0.2961	1.5	4.1353	2.1	0.1013	1.5	0.71	1672	22	1661	17	1648	27	101
AK07-seq3-c05	12764	58	15	0.34	2711	0.2357	2.0	2.6943	2.8	0.0829	1.9	0.72	1364	25	1327	21	1267	38	108
AK07-seq3-c06	2211	32	3	1.61	1536	0.0834	3.1	0.8352	6.1	0.0727	5.2	0.51	516	15	617	29	1005	106	51
AK07-seq3-c07	9132	149	12	0.41	1010	0.0713	1.5	0.6280	7.9	0.0639	7.8	0.19	444	7	495	32	738	165	60
AK07-seq3-c08	7204	143	11	0.36	13512	0.0762	1.9	0.5700	2.9	0.0543	2.2	0.64	473	8	458	11	382	50	124
AK07-seq3-c09	14787	306	26	0.54	4633	0.0776	1.2	0.6133	3.1	0.0573	2.9	0.39	482	6	486	12	503	63	96
AK07-seq3-c10	14191	224	21	0.63	1648	0.0819	2.0	0.6500	7.1	0.0575	6.8	0.28	508	10	509	29	512	150	99
AK07-seq3-c11	21878	139	31	0.66	30145	0.1847	1.4	1.9004	2.4	0.0746	1.9	0.58	1093	14	1081	16	1059	39	103
AK07-seq3-c12	7596	30	8	0.44	1583	0.2451	2.0	2.9002	3.2	0.0858	2.5	0.62	1413	25	1382	24	1334	49	106
AK07-seq3-c13	9182	193	15	0.34	17066	0.0718	2.1	0.5427	2.9	0.0548	2.1	0.70	447	9	440	11	403	47	111
AK07-seq3-c14	8931	213	16	0.54	10915	0.0685	1.2	0.5248	3.7	0.0556	3.5	0.33	427	5	428	13	435	78	98
AK07-seq3-c15	5850	114	19	0.27	8980	0.1611	2.0	1.4825	3.5	0.0667	2.9	0.56	963	18	923	22	829	61	116
AK07-seq3-c16	4400	92	8	0.54	8031	0.0761	1.8	0.5851	3.5	0.0557	3.0	0.51	473	8	468	13	442	67	107
AK07-seq3-c17	1682	30	3	0.56	3103	0.0831	1.6	0.6259	5.5	0.0546	5.3	0.30	515	8	494	22	396	118	130
AK07-seq3-c18	5798	127	11	0.53	10789	0.0753	2.0	0.5706	3.7	0.0549	3.1	0.53	468	9	458	14	410	70	114
AK07-seq3-c19	2159	47	4	0.64	4149	0.0689	2.8	0.5016	5.9	0.0528	5.2	0.47	429	12	413	20	320	118	134
AK07-seq3-c20	7515	169	16	0.91	13640	0.0771	1.7	0.5955	2.6	0.0560	2.0	0.65	479	8	474	10	453	44	106
Sample AK10	Ballinskelligs Sandstone Formation					Location (decimal degrees) 51.990 10.21283 W						Datum: IRENET95							
AK10-seq1-a01	28829	134	36	0.36	32892	0.2495	2.7	3.0751	3.1	0.0894	1.5	0.88	1436	35	1427	24	1413	28	102
AK10-seq1-a02	20459	95	16	0.20	29202	0.1631	2.6	1.6084	2.9	0.0715	1.4	0.88	974	23	973	19	972	28	100
AK10-seq1-a03	9223	241	19	0.42	16897	0.0709	2.7	0.5442	3.4	0.0556	2.0	0.80	442	12	441	12	438	45	101
AK10-seq1-a04	97044	502	125	0.29	114243	0.2366	2.7	2.8284	3.0	0.0867	1.2	0.91	1369	33	1363	22	1353	24	101
AK10-seq1-a05	6297	166	13	0.34	4273	0.0739	2.8	0.5586	4.4	0.0548	3.3	0.65	459	13	451	16	406	74	113
AK10-seq1-a06	49056	242	63	0.43	55833	0.2335	2.8	2.8843	3.2	0.0896	1.6	0.86	1353	34	1378	24	1416	31	96
AK10-seq1-a07	2408	52	5	0.66	4260	0.0825	3.0	0.6649	9.0	0.0585	8.5	0.33	511	15	518	37	548	186	93
AK10-seq1-a08	12730	99	19	0.24	17885	0.1904	2.7	1.9010	3.5	0.0724	2.3	0.76	1124	28	1081	24	998	46	113
AK10-seq1-a09	3215	17	5	0.75	3935	0.2276	3.0	2.6530	4.8	0.0845	3.7	0.62	1322	35	1315	36	1305	73	101
AK10-seq1-a10	14533	123	24	0.39	20789	0.1794	2.6	1.7598	3.5	0.0712	2.3	0.75	1063	26	1031	23	962	47	111
AK10-seq1-a11	1298	5	1	0.69	762	0.2185	3.3	2.2656	6.6	0.0752	5.7	0.51	1274	39	1202	47	1074	114	119
AK10-seq1-a12	2293	29	3	0.40	4592	0.0844	3.1	0.5846	7.1	0.0503	6.4	0.43	522	15	467	27	207	149	252
AK10-seq1-a13	9935	26	7	0.44	12024	0.2579	2.6	2.9971	3.5	0.0843	2.4	0.74	1479	35	1407	27	1299	46	114
AK10-seq1-a14	7515	109	8	0.28	14102	0.0703	2.8	0.5254	3.7	0.0542	2.4	0.76	438	12	429	13	380	54	115
AK10-seq1-a15	9307	120	10	0.58	16808	0.0744	2.6	0.5790	3.3	0.0565	1.9	0.80	462	12	464	12	470	43	98

AK10-seq1-a16	13249	102	28	0.71	16328	0.2262	3.0	2.5834	3.5	0.0828	1.8	0.85	1315	36	1296	26	1265	36	104
AK10-seq1-a17	10375	44	15	0.63	11579	0.2875	2.9	3.6295	3.8	0.0916	2.4	0.77	1629	42	1556	30	1458	46	112
AK10-seq1-a18	24051	91	26	0.39	26907	0.2574	2.6	3.2336	3.1	0.0911	1.6	0.85	1477	35	1465	24	1449	31	102
AK10-seq1-a19	30958	126	38	0.46	33626	0.2649	2.6	3.4313	3.1	0.0939	1.7	0.84	1515	36	1512	25	1507	32	101
AK10-seq1-a20	2013	51	5	0.78	3931	0.0783	2.6	0.5625	6.4	0.0521	5.8	0.41	486	12	453	24	291	133	167
AK10-seq1-a21	11729	89	16	0.29	16338	0.1731	2.8	1.7431	3.4	0.0730	1.9	0.82	1029	26	1025	22	1015	39	101
AK10-seq1-a22	6430	56	10	0.21	9551	0.1752	2.9	1.6535	3.9	0.0685	2.6	0.75	1041	28	991	25	882	54	118
AK10-seq1-a23	3961	27	6	0.18	4331	0.2173	3.7	2.2206	5.4	0.0741	3.9	0.69	1268	43	1188	39	1045	80	121
AK10-seq1-a24	10422	37	14	0.59	10161	0.3201	2.9	4.2906	3.8	0.0972	2.5	0.76	1790	46	1692	32	1571	46	114
AK10-seq1-a25	7735	189	16	0.38	14005	0.0774	2.7	0.6034	4.3	0.0566	3.4	0.63	480	13	479	17	474	74	101
AK10-seq1-a26	16798	111	28	0.75	21648	0.2031	2.7	2.2105	3.2	0.0789	1.7	0.84	1192	29	1184	22	1170	34	102
AK10-seq1-a27	18025	119	25	0.38	23937	0.1946	2.7	2.0611	3.2	0.0768	1.6	0.86	1146	29	1136	22	1116	33	103
AK10-seq1-a28	9224	68	14	0.48	3379	0.1825	2.5	1.8786	3.5	0.0746	2.4	0.73	1081	25	1074	23	1059	47	102
AK10-seq1-a29	14998	63	20	0.71	16624	0.2615	2.7	3.3105	3.1	0.0918	1.6	0.86	1498	36	1484	25	1463	31	102
AK10-seq1-a30	12338	37	12	0.24	12510	0.3051	2.8	4.2247	3.4	0.1004	2.0	0.81	1717	42	1679	28	1632	37	105
AK10-seq1-a31	29479	90	33	0.46	27619	0.3236	3.0	4.8478	3.5	0.1087	1.7	0.87	1807	48	1793	30	1777	32	102
AK10-seq1-a32	1164	32	3	0.52	1157	0.0836	2.8	0.5391	6.8	0.0468	6.2	0.41	518	14	438	25	38	149	1378
AK10-seq1-a33	6847	54	10	0.27	9519	0.1756	3.3	1.7766	4.4	0.0734	2.8	0.76	1043	32	1037	29	1024	57	102
AK10-seq1-a34	8280	74	19	1.14	11603	0.1739	3.6	1.7532	5.2	0.0731	3.7	0.69	1034	34	1028	34	1017	76	102
AK10-seq1-a35	24475	84	31	0.75	24225	0.2963	2.7	4.1876	3.5	0.1025	2.1	0.79	1673	40	1672	29	1670	39	100
AK10-seq1-a36	23992	141	33	0.35	29139	0.2163	2.9	2.5030	3.3	0.0839	1.7	0.87	1262	33	1273	24	1291	32	98
AK10-seq1-a37	44053	165	49	0.19	45218	0.2876	3.0	3.9379	3.4	0.0993	1.6	0.88	1630	43	1622	28	1611	30	101
AK10-seq1-a38	3378	95	7	0.27	5727	0.0732	2.8	0.5422	4.5	0.0537	3.5	0.62	455	12	440	16	359	80	127
AK10-seq1-a39	2826	67	6	0.53	5441	0.0816	3.1	0.5958	4.9	0.0530	3.8	0.64	506	15	475	19	327	86	155
AK10-seq1-a40	12338	55	14	0.22	14385	0.2496	2.8	3.0168	3.2	0.0876	1.4	0.90	1437	36	1412	24	1375	27	105
AK10-seq1-a41	12235	89	15	0.06	16401	0.1754	2.9	1.8465	3.8	0.0763	2.4	0.76	1042	28	1062	25	1104	49	94
AK10-seq1-a42	3880	112	10	0.76	7766	0.0713	2.8	0.5019	4.7	0.0511	3.7	0.60	444	12	413	16	243	86	183
AK10-seq1-a43	19428	156	29	0.27	25947	0.1801	2.6	1.8399	3.2	0.0741	1.8	0.82	1068	26	1060	21	1044	36	102
AK10-seq1-a44	14138	111	20	0.24	19637	0.1709	2.9	1.7154	3.7	0.0728	2.3	0.79	1017	28	1014	24	1008	46	101
AK10-seq1-a45	3085	87	7	0.65	6148	0.0716	2.8	0.5028	4.7	0.0509	3.7	0.61	446	12	414	16	236	86	189
AK10-seq1-a46	12843	102	19	0.29	17510	0.1828	2.8	1.8818	3.4	0.0747	1.9	0.82	1082	28	1075	23	1060	39	102
AK10-seq1-a47	15086	111	22	0.37	20648	0.1850	2.6	1.8980	3.2	0.0744	1.8	0.83	1094	27	1080	21	1053	36	104
AK10-seq1-a48	7960	56	12	0.48	3776	0.1887	2.8	1.9756	3.7	0.0759	2.3	0.77	1114	29	1107	25	1094	47	102
AK10-seq1-a49	2304	69	7	1.22	4532	0.0758	2.7	0.5415	4.7	0.0518	3.8	0.59	471	12	439	17	278	87	169
AK10-seq1-a50	3923	35	6	0.36	4839	0.1707	3.0	1.7001	4.5	0.0722	3.3	0.67	1016	28	1009	29	992	68	102
AK10-seq1-a51	4846	133	10	0.39	9061	0.0720	3.2	0.5351	5.4	0.0539	4.3	0.59	448	14	435	19	368	98	122
AK10-seq1-a52	9045	231	21	0.45	16917	0.0805	2.8	0.6045	3.7	0.0544	2.4	0.76	499	13	480	14	389	54	128
AK10-seq1-a53	3878	64	7	0.61	2093	0.0995	3.1	0.8916	6.5	0.0650	5.7	0.48	612	18	647	32	773	120	79
AK10-seq1-a54	14133	66	20	0.68	16105	0.2504	2.6	3.0863	3.3	0.0894	1.9	0.81	1440	34	1429	25	1413	37	102
AK10-seq1-a55	8177	67	16	0.70	11451	0.1980	2.8	1.9778	3.4	0.0725	1.9	0.83	1165	30	1108	23	999	38	117
AK10-seq1-a56	8248	220	17	0.38	8853	0.0743	2.9	0.5745	3.6	0.0561	2.1	0.80	462	13	461	13	455	47	102
AK10-seq1-a57	38571	153	51	0.50	28429	0.2918	3.0	4.0226	3.6	0.1000	2.0	0.83	1651	44	1639	30	1624	37	102

AK10-seq1-a58	11620	85	17	0.44	15895	0.1851	2.6	1.9012	3.5	0.0745	2.3	0.76	1095	27	1082	23	1055	45	104
AK10-seq1-a59	3487	86	8	0.64	2306	0.0789	2.8	0.6181	4.4	0.0568	3.3	0.65	490	13	489	17	483	74	101
AK10-seq2-b01	7293	180	16	0.38	12994	0.0813	2.9	0.6397	4.9	0.0571	4.0	0.59	504	14	502	20	494	88	102
AK10-seq2-b02	4108	22	6	0.26	5216	0.2743	2.3	3.0323	4.3	0.0802	3.7	0.53	1563	32	1416	34	1201	72	130
AK10-seq2-b03	10832	57	15	0.47	12889	0.2323	2.2	2.7334	3.0	0.0854	2.0	0.75	1346	27	1338	23	1324	39	102
AK10-seq2-b04	4737	104	10	0.52	8450	0.0822	2.9	0.6492	3.9	0.0573	2.5	0.76	509	14	508	16	503	56	101
AK10-seq2-b05	1659	36	4	0.52	2849	0.0892	2.8	0.7257	13.9	0.0590	13.6	0.20	551	15	554	61	568	297	97
AK10-seq2-b06	12020	298	27	0.59	21595	0.0799	2.0	0.6269	2.6	0.0569	1.6	0.78	496	10	494	10	487	36	102
AK10-seq2-b07	4133	121	13	1.39	7990	0.0713	2.3	0.5194	3.8	0.0528	3.1	0.59	444	10	425	13	322	69	138
AK10-seq2-b08	2169	13	3	0.51	2920	0.2221	2.8	2.3250	5.7	0.0759	5.0	0.49	1293	33	1220	42	1093	100	118
AK10-seq2-b09	33256	845	71	0.39	59994	0.0783	2.1	0.6119	2.5	0.0567	1.2	0.86	486	10	485	9	478	27	102
AK10-seq2-b10	11659	90	17	0.24	16024	0.1845	2.3	1.9082	3.1	0.0750	2.2	0.72	1091	23	1084	21	1069	44	102
AK10-seq2-b11	8678	253	20	0.36	16707	0.0757	2.1	0.5553	3.7	0.0532	3.0	0.58	470	10	448	13	338	68	139
AK10-seq2-b12	1558	48	5	0.82	3223	0.0804	2.7	0.5472	7.8	0.0494	7.3	0.35	498	13	443	29	166	172	300
AK10-seq2-b13	11537	54	15	0.35	13114	0.2539	2.4	3.1502	3.0	0.0900	1.8	0.80	1459	32	1445	24	1425	35	102
AK10-seq2-b14	16738	109	23	0.31	22078	0.1962	2.7	2.0939	3.4	0.0774	2.1	0.80	1155	29	1147	24	1131	41	102
AK10-seq2-b15	3381	84	8	0.51	6356	0.0802	1.9	0.5996	3.7	0.0542	3.1	0.52	497	9	477	14	380	71	131
AK10-seq2-b16	3856	104	9	0.42	7394	0.0776	2.3	0.5704	4.3	0.0533	3.6	0.54	482	11	458	16	342	81	141
AK10-seq2-b17	2169	9	3	0.68	2573	0.3004	2.5	3.5340	6.4	0.0853	5.9	0.39	1693	37	1535	52	1323	114	128
AK10-seq2-b18	30299	77	30	0.47	27297	0.3406	2.1	5.3314	2.5	0.1135	1.4	0.83	1889	34	1874	21	1857	25	102
AK10-seq2-b19	6643	179	14	0.38	12797	0.0741	1.9	0.5407	2.6	0.0529	1.7	0.74	461	9	439	9	325	40	142
AK10-seq2-b20	4961	132	12	0.62	9757	0.0802	2.3	0.5720	4.5	0.0517	3.9	0.50	497	11	459	17	273	88	182
AK10-seq2-b21	8812	231	19	0.49	16147	0.0735	2.1	0.5664	3.1	0.0559	2.2	0.69	457	9	456	11	448	50	102
AK10-seq2-b22	8925	45	11	0.30	3556	0.2271	2.8	2.6501	3.9	0.0846	2.8	0.70	1319	33	1315	29	1307	55	101
AK10-seq2-b23	6464	53	11	0.47	9285	0.1952	2.2	1.9170	3.7	0.0712	2.9	0.61	1150	23	1087	25	964	60	119
AK10-seq2-b24	9403	73	14	0.18	10667	0.1862	2.9	1.9402	5.1	0.0756	4.1	0.58	1101	30	1095	34	1083	83	102
AK10-seq2-b25	459	11	1	0.29	947	0.0897	2.5	0.6179	16.7	0.0499	16.6	0.15	554	13	489	67	192	385	288
AK10-seq2-b26	1826	14	3	0.22	2682	0.2045	3.0	1.9515	7.3	0.0692	6.7	0.41	1200	33	1099	50	905	137	133
AK10-seq2-b27	6042	44	10	0.25	8361	0.2117	2.6	2.1560	3.5	0.0738	2.3	0.75	1238	29	1167	24	1037	46	119
AK10-seq2-b28	3271	21	5	0.42	4492	0.2327	2.5	2.3966	4.9	0.0747	4.2	0.52	1349	31	1242	36	1060	84	127
AK10-seq2-b29	5373	37	9	0.32	7296	0.2241	2.2	2.3268	3.7	0.0753	2.9	0.61	1303	26	1221	26	1077	58	121
AK10-seq2-b30	6139	45	10	0.35	8571	0.1997	2.4	2.0129	3.9	0.0731	3.0	0.62	1174	26	1120	27	1017	61	115
AK10-seq2-b31	8879	58	13	0.43	11444	0.2059	1.9	2.2505	2.6	0.0793	1.8	0.72	1207	21	1197	19	1179	36	102
AK10-seq2-b32	7670	192	16	0.34	14231	0.0796	2.2	0.6043	3.4	0.0550	2.7	0.63	494	10	480	13	414	60	119
AK10-seq2-b33	15698	110	23	0.43	21354	0.1927	1.9	1.9941	2.3	0.0751	1.4	0.80	1136	19	1114	16	1070	28	106
AK10-seq2-b35	3051	28	5	0.35	4438	0.1828	2.1	1.7610	5.8	0.0699	5.4	0.37	1082	21	1031	39	925	112	117
AK10-seq2-b36	5412	51	10	0.48	8220	0.1793	2.6	1.6551	4.1	0.0669	3.2	0.63	1063	25	991	26	836	66	127
AK10-seq2-b37	883	7	3	0.80	673	0.3046	2.9	2.5783	18.8	0.0614	18.6	0.15	1714	43	1294	148	653	399	263
AK10-seq2-b38	3836	29	7	0.53	5278	0.2038	2.9	2.0892	4.6	0.0744	3.6	0.63	1196	31	1145	32	1051	72	114
AK10-seq2-b39	5469	137	13	0.55	10338	0.0801	2.1	0.5954	3.7	0.0539	3.0	0.58	497	10	474	14	368	67	135
AK10-seq2-b40	6782	68	12	0.41	9740	0.1636	2.7	1.6094	4.0	0.0713	3.0	0.68	977	25	974	25	967	61	101
AK10-seq2-b41	7591	54	10	0.28	10324	0.1851	2.3	1.9228	3.3	0.0753	2.4	0.68	1095	23	1089	22	1078	49	102

AK10-seq2-b42	4406	142	10	0.32	8717	0.0697	2.4	0.4965	5.9	0.0516	5.4	0.41	435	10	409	20	269	123	161
AK10-seq2-b43	54224	238	70	0.41	59676	0.2662	2.1	3.4081	2.4	0.0929	1.1	0.88	1522	29	1506	19	1485	22	102
AK10-seq2-b44	11803	46	13	0.34	12887	0.2681	1.9	3.4556	3.1	0.0935	2.4	0.63	1531	27	1517	25	1498	45	102
AK10-seq2-b45	25744	187	42	0.39	34656	0.2088	2.2	2.1879	2.6	0.0760	1.5	0.82	1223	24	1177	19	1095	30	112
AK10-seq2-b46	6700	49	9	0.27	9131	0.1856	2.3	1.9227	3.6	0.0752	2.8	0.63	1097	23	1089	24	1073	56	102
AK10-seq2-b47	64736	524	93	0.15	89075	0.1794	2.2	1.8325	2.5	0.0741	1.3	0.85	1064	21	1057	17	1044	27	102
AK10-seq2-b48	18128	112	26	0.36	17239	0.2121	2.1	2.3606	3.2	0.0807	2.4	0.67	1240	24	1231	23	1214	47	102
AK10-seq2-b49	101240	516	125	0.17	117690	0.2369	2.2	2.8716	2.5	0.0879	1.0	0.91	1370	28	1374	19	1381	19	99
AK10-seq2-b50	14432	55	20	0.47	2246	0.3218	2.4	4.2988	3.7	0.0969	2.9	0.64	1798	37	1693	31	1565	53	115
AK10-seq2-b51	4051	113	10	0.52	7820	0.0767	2.3	0.5584	3.6	0.0528	2.8	0.63	476	10	450	13	321	64	148
AK10-seq2-b52	7910	217	17	0.42	15224	0.0747	2.2	0.5478	3.5	0.0532	2.7	0.64	465	10	444	13	336	60	138
AK10-seq2-b53	51230	206	64	0.43	53013	0.2779	2.2	3.7823	2.6	0.0987	1.5	0.82	1581	30	1589	21	1600	28	99
AK10-seq2-b54	17648	84	24	0.54	20242	0.2478	2.3	3.0439	2.9	0.0891	1.7	0.80	1427	30	1419	23	1406	33	101
AK10-seq2-b55	55086	283	72	0.21	65008	0.2472	2.0	2.9507	2.3	0.0866	1.2	0.85	1424	26	1395	18	1351	24	105
AK10-seq2-b56	7029	64	13	0.71	9976	0.1684	2.3	1.6687	3.3	0.0719	2.3	0.71	1004	22	997	21	982	47	102
AK10-seq2-b57	44202	52	31	0.28	24590	0.5289	2.1	13.3283	2.6	0.1828	1.5	0.81	2737	48	2703	25	2678	26	102
AK10-seq2-b58	5100	41	9	0.40	1975	0.1857	4.4	1.9158	6.4	0.0748	4.7	0.68	1098	44	1087	44	1064	95	103
AK10-seq2-b59	31190	147	43	0.46	35482	0.2535	2.3	3.1406	2.6	0.0898	1.3	0.87	1457	30	1443	20	1422	25	102
Sample AK11	Valentia Slate Formation					Location (decimal degrees)		51.755	10.10123 W			Datum: IRENET95							
AK11-seq1-a01	36226	287	49	0.26	51507	0.1623	1.7	1.5950	2.2	0.0713	1.4	0.77	970	16	968	14	965	29	100
AK11-seq1-a02	32713	100	39	0.76	32454	0.3151	1.1	4.4512	2.1	0.1025	1.8	0.52	1766	17	1722	18	1669	33	106
AK11-seq1-a03	15837	128	23	0.21	18902	0.1768	2.1	1.7912	4.2	0.0735	3.6	0.51	1050	21	1042	27	1027	72	102
AK11-seq1-a04	35844	117	35	0.22	36174	0.2842	1.7	3.9541	2.4	0.1009	1.7	0.70	1613	24	1625	19	1641	31	98
AK11-seq1-a05	4108	90	8	0.45	7758	0.0810	1.5	0.5989	3.2	0.0536	2.8	0.47	502	7	477	12	355	64	141
AK11-seq1-a06	12408	353	23	0.26	23086	0.0642	1.3	0.4832	2.7	0.0546	2.4	0.48	401	5	400	9	396	53	101
AK11-seq1-a07	19473	127	17	0.22	21805	0.1219	7.5	1.5154	7.9	0.0902	2.6	0.95	741	53	937	50	1429	49	52
AK11-seq1-a08	4610	103	8	0.30	7372	0.0691	1.7	0.6076	3.2	0.0637	2.7	0.53	431	7	482	12	733	58	59
AK11-seq1-a09	17411	126	24	0.29	24027	0.1822	1.8	1.8534	2.4	0.0738	1.7	0.72	1079	17	1065	16	1035	34	104
AK11-seq1-a10	5427	139	11	0.58	10015	0.0700	1.9	0.5312	4.3	0.0550	3.8	0.44	436	8	433	15	413	85	106
AK11-seq1-a11	28368	118	32	0.19	32205	0.2625	2.3	3.2405	3.0	0.0895	1.8	0.79	1503	31	1467	23	1416	35	106
AK11-seq1-a12	12108	87	16	0.19	16564	0.1798	1.5	1.8383	2.8	0.0742	2.3	0.55	1066	15	1059	19	1046	47	102
AK11-seq1-a13	12068	70	17	0.39	15236	0.2240	1.6	2.4877	2.9	0.0806	2.3	0.57	1303	19	1268	21	1210	46	108
AK11-seq1-a14	5035	107	9	0.44	3621	0.0765	1.6	0.5925	3.2	0.0561	2.8	0.50	475	7	472	12	458	61	104
AK11-seq1-a15	14270	61	16	0.23	10859	0.2455	2.4	2.9928	2.8	0.0884	1.4	0.87	1415	31	1406	21	1391	26	102
AK11-seq1-a16	1603	35	3	0.64	2848	0.0800	2.0	0.6282	5.7	0.0569	5.3	0.35	496	10	495	23	489	118	101
AK11-seq1-a17	6974	157	13	0.47	12322	0.0753	1.9	0.5856	6.6	0.0564	6.3	0.29	468	9	468	25	469	139	100
AK11-seq1-a18	9949	38	13	0.78	10895	0.2760	2.1	3.5242	3.2	0.0926	2.4	0.66	1571	30	1533	26	1480	46	106
AK11-seq1-a19	23187	141	29	0.23	30134	0.2021	1.7	2.1795	2.8	0.0782	2.2	0.63	1187	19	1175	19	1152	43	103
AK11-seq1-a20	6476	55	10	0.35	9299	0.1645	1.5	1.6068	2.9	0.0708	2.4	0.53	982	14	973	18	953	50	103
AK11-seq1-a21	5870	132	11	0.50	10761	0.0734	2.7	0.5625	3.8	0.0555	2.7	0.71	457	12	453	14	434	59	105
AK11-seq1-a22	10068	68	13	0.16	13538	0.1915	1.6	1.9899	2.6	0.0754	2.1	0.61	1130	16	1112	18	1078	41	105

AK11-seq1-a23	4670	98	9	0.53	8545	0.0773	1.4	0.5939	3.6	0.0558	3.3	0.39	480	7	473	14	443	74	108
AK11-seq1-a24	4958	39	8	0.69	6978	0.1713	1.5	1.7028	3.2	0.0721	2.8	0.47	1019	14	1010	21	988	57	103
AK11-seq1-a25	2403	56	6	0.79	4561	0.0805	2.4	0.5955	5.5	0.0536	5.0	0.44	499	12	474	21	355	112	141
AK11-seq1-a26	13810	61	18	0.22	3812	0.2850	1.6	3.3492	2.7	0.0852	2.1	0.60	1617	23	1493	21	1321	41	122
AK11-seq1-a27	2408	51	5	0.83	4244	0.0790	1.7	0.6170	5.1	0.0566	4.9	0.33	490	8	488	20	477	107	103
AK11-seq1-a28	7606	44	10	0.34	9907	0.2118	1.1	2.2821	3.0	0.0782	2.7	0.38	1238	13	1207	21	1151	54	108
AK11-seq1-a29	13610	100	19	0.30	18530	0.1749	1.6	1.7920	2.9	0.0743	2.4	0.55	1039	15	1043	19	1050	49	99
AK11-seq1-a30	17784	120	24	0.29	4979	0.1896	1.8	2.0031	3.4	0.0766	2.9	0.53	1119	18	1117	23	1111	57	101
AK11-seq1-a31	6720	45	9	0.44	8955	0.1860	1.2	1.9565	3.0	0.0763	2.8	0.40	1099	12	1101	20	1103	55	100
AK11-seq1-a32	11174	138	18	0.40	17783	0.1175	1.4	1.0326	2.5	0.0638	2.1	0.57	716	10	720	13	734	44	98
AK11-seq1-a33	15443	50	17	0.38	15759	0.3057	1.1	4.1873	1.9	0.0993	1.5	0.59	1720	17	1672	16	1612	28	107
AK11-seq1-a34	19441	137	25	0.13	26316	0.1865	2.0	1.9394	2.8	0.0754	1.9	0.73	1103	21	1095	19	1079	39	102
AK11-seq1-a35	21330	129	31	0.48	27354	0.2106	1.8	2.2997	2.6	0.0792	1.8	0.71	1232	21	1212	18	1177	36	105
AK11-seq1-a36	19694	100	29	0.70	23175	0.2314	2.4	2.7447	3.0	0.0860	1.8	0.80	1342	29	1341	23	1339	35	100
AK11-seq1-a37	6783	176	16	0.70	12503	0.0695	1.0	0.5305	3.2	0.0554	3.1	0.30	433	4	432	11	427	69	102
AK11-seq1-a38	18195	116	26	0.35	23245	0.2039	1.8	2.2218	2.7	0.0790	2.1	0.65	1196	19	1188	19	1173	41	102
AK11-seq1-a39	18240	87	25	0.36	21888	0.2588	1.6	3.0254	2.4	0.0848	1.8	0.65	1484	21	1414	19	1311	35	113
AK11-seq1-a40	3957	27	6	0.48	1104	0.1772	1.5	1.8645	3.6	0.0763	3.3	0.42	1052	15	1069	24	1104	66	95
AK11-seq1-a41	10771	35	12	0.36	9533	0.3150	1.6	4.3718	2.4	0.1007	1.8	0.67	1765	25	1707	20	1636	33	108
AK11-seq1-a42	4171	121	8	0.10	7866	0.0670	1.5	0.4978	3.0	0.0539	2.6	0.50	418	6	410	10	366	59	114
AK11-seq1-a43	1092	26	2	0.64	1979	0.0740	2.6	0.5731	6.5	0.0562	6.0	0.40	460	12	460	25	458	133	100
AK11-seq1-a44	3435	92	8	0.66	6248	0.0711	3.0	0.5471	5.5	0.0558	4.6	0.54	443	13	443	20	444	102	100
AK11-seq1-a45	3199	83	7	0.40	3091	0.0721	2.3	0.5475	4.2	0.0551	3.6	0.54	449	10	443	15	416	80	108
AK11-seq1-a46	8019	195	15	0.29	14649	0.0720	1.1	0.5508	2.7	0.0555	2.4	0.41	448	5	446	10	432	54	104
AK11-seq1-a47	84616	344	96	0.24	91063	0.2643	1.6	3.4388	2.1	0.0944	1.3	0.78	1512	22	1513	16	1515	24	100
AK11-seq1-a48	6099	104	11	0.40	10563	0.1003	1.1	0.8116	3.0	0.0587	2.8	0.35	616	6	603	14	555	62	111
AK11-seq1-a49	6696	163	14	0.31	1409	0.0827	1.6	0.6546	5.4	0.0574	5.2	0.30	512	8	511	22	508	114	101
AK11-seq1-a50	8854	74	19	1.33	12379	0.1678	1.7	1.6872	3.2	0.0729	2.7	0.52	1000	15	1004	20	1012	55	99
AK11-seq1-a51	15693	65	20	0.44	17026	0.2680	1.6	3.4557	2.8	0.0935	2.3	0.57	1530	22	1517	22	1499	43	102
AK11-seq1-a52	8404	49	11	0.46	10179	0.1932	2.9	2.2332	3.7	0.0838	2.2	0.80	1139	31	1192	26	1289	43	88
AK11-seq1-a53	170686	444	153	0.19	3769	0.3256	1.7	5.3684	1.9	0.1196	1.0	0.87	1817	27	1880	17	1950	17	93
AK11-seq1-a54	24261	82	28	0.36	23937	0.3025	1.8	4.3027	3.0	0.1032	2.4	0.60	1704	27	1694	25	1682	44	101
AK11-seq1-a55	4623	24	6	0.38	5480	0.2487	2.2	2.9323	3.8	0.0855	3.1	0.58	1432	28	1390	29	1327	61	108
AK11-seq1-a56	11067	82	18	0.57	15195	0.1792	2.1	1.8161	3.3	0.0735	2.5	0.65	1063	21	1051	22	1028	50	103
AK11-seq1-a57	3149	26	5	0.42	4615	0.1864	1.3	1.7830	3.7	0.0694	3.5	0.34	1102	13	1039	24	910	72	121
AK11-seq1-a58	33256	98	33	0.26	32127	0.3080	2.0	4.4625	2.7	0.1051	1.9	0.72	1731	30	1724	23	1716	34	101
AK11-seq1-a59	3022	22	6	0.88	4392	0.1865	2.6	1.7869	5.1	0.0695	4.4	0.51	1102	26	1041	34	914	90	121
AK11-seq1-a60	4051	28	6	0.47	4780	0.1985	2.3	2.0866	3.7	0.0762	2.9	0.62	1167	24	1144	25	1102	57	106
AK11-seq2-b01	3010	18	4	0.44	955	0.2088	2.6	2.3401	5.5	0.0813	4.8	0.48	1222	29	1225	40	1228	94	100
AK11-seq2-b02	4156	31	7	0.60	5778	0.2032	1.8	2.0507	3.7	0.0732	3.2	0.49	1193	20	1133	25	1019	65	117
AK11-seq2-b03	6213	152	12	0.31	11427	0.0720	1.4	0.5493	2.8	0.0553	2.4	0.50	448	6	445	10	425	53	106
AK11-seq2-b04	34386	123	44	0.59	34485	0.3003	1.8	4.2037	2.4	0.1015	1.5	0.75	1693	26	1675	19	1652	29	102

AK11-seq2-b05	4935	40	8	0.42	6904	0.1779	1.8	1.7949	3.8	0.0732	3.3	0.47	1055	17	1044	25	1019	67	104
AK11-seq2-b06	13902	93	19	0.17	17521	0.2009	1.8	2.2352	2.8	0.0807	2.1	0.64	1180	19	1192	20	1214	42	97
AK11-seq2-b07	26650	91	31	0.34	13981	0.3067	1.5	4.3327	2.2	0.1024	1.5	0.71	1725	23	1700	18	1669	28	103
AK11-seq2-b08	69550	191	68	0.18	62318	0.3436	1.5	5.3780	1.9	0.1135	1.2	0.78	1904	24	1881	16	1857	21	103
AK11-seq2-b09	13607	46	15	0.38	13395	0.2906	1.6	4.1390	2.6	0.1033	2.0	0.63	1645	24	1662	21	1684	37	98
AK11-seq2-b10	20527	53	21	0.45	14800	0.3522	1.6	5.6319	2.6	0.1160	2.0	0.64	1945	28	1921	22	1895	35	103
AK11-seq2-b11	1902	15	4	1.10	2867	0.1929	2.1	1.7976	6.5	0.0676	6.1	0.32	1137	22	1045	43	856	127	133
AK11-seq2-b12	20877	89	27	0.33	22399	0.2716	2.0	3.5590	2.9	0.0950	2.1	0.69	1549	27	1540	23	1529	39	101
AK11-seq2-b13	6926	49	11	0.49	9352	0.1908	1.8	1.9854	3.2	0.0755	2.7	0.56	1126	19	1111	22	1081	54	104
AK11-seq2-b14	7502	202	16	0.37	13752	0.0715	2.7	0.5476	4.1	0.0556	3.1	0.66	445	12	443	15	435	68	102
AK11-seq2-b15	2272	52	5	0.46	4151	0.0836	1.7	0.6362	4.2	0.0552	3.8	0.41	517	8	500	17	422	85	123
AK11-seq2-b16	1956	40	4	0.42	3587	0.0844	2.6	0.6452	5.6	0.0555	5.0	0.46	522	13	506	23	431	111	121
AK11-seq2-b17	9481	71	15	0.45	12897	0.1878	1.8	1.9366	3.0	0.0748	2.5	0.58	1110	18	1094	21	1063	50	104
AK11-seq2-b18	6509	153	13	0.31	7236	0.0806	2.1	0.6711	8.0	0.0604	7.7	0.27	500	10	521	33	618	167	81
AK11-seq2-b19	56323	203	64	0.31	56505	0.2875	2.0	4.0194	2.7	0.1014	1.8	0.75	1629	29	1638	22	1650	33	99
AK11-seq2-b20	14351	96	21	0.20	18327	0.2095	1.4	2.3013	2.6	0.0797	2.2	0.53	1226	16	1213	19	1188	44	103
AK11-seq2-b21	11108	52	14	0.26	12666	0.2618	1.5	3.2124	2.6	0.0890	2.1	0.59	1499	21	1460	20	1404	40	107
AK11-seq2-b22	1854	43	4	0.52	3265	0.0807	1.7	0.6415	5.1	0.0577	4.8	0.34	500	8	503	20	518	105	97
AK11-seq2-b23	8835	215	19	0.45	16120	0.0780	1.5	0.6003	3.1	0.0558	2.7	0.50	484	7	477	12	445	60	109
AK11-seq2-b24	5935	48	11	0.76	4572	0.1783	1.5	1.8071	3.1	0.0735	2.8	0.48	1058	15	1048	21	1028	56	103
AK11-seq2-b25	38575	145	53	0.61	39085	0.2982	2.0	4.1306	2.6	0.1004	1.6	0.79	1683	30	1660	21	1632	29	103
AK11-seq2-b26	22923	159	36	0.56	29386	0.1876	1.5	2.0210	2.4	0.0781	1.9	0.62	1108	15	1123	17	1150	38	96
AK11-seq2-b27	7626	192	17	0.44	13837	0.0757	1.9	0.5845	3.3	0.0560	2.7	0.57	471	8	467	12	451	59	104
AK11-seq2-b28	2951	23	5	0.66	4048	0.1810	2.6	1.8811	5.3	0.0754	4.5	0.50	1072	26	1074	35	1079	91	99
AK11-seq2-b29	5449	42	11	0.76	7430	0.1999	1.5	2.0537	3.6	0.0745	3.2	0.42	1175	16	1134	25	1055	65	111
AK11-seq2-b30	14103	40	15	0.17	8755	0.3597	1.3	5.4136	2.4	0.1091	2.1	0.52	1981	22	1887	21	1785	37	111
AK11-seq2-b31	4217	38	7	0.49	6393	0.1706	1.7	1.5687	4.3	0.0667	3.9	0.40	1015	16	958	27	828	82	123
AK11-seq2-b32	1030	9	2	0.77	1553	0.1608	1.8	1.5460	9.7	0.0697	9.5	0.19	961	16	949	62	920	196	104
AK11-seq2-b33	21590	139	29	0.16	28084	0.2081	1.9	2.2426	2.7	0.0781	1.9	0.70	1219	21	1194	19	1150	38	106
AK11-seq2-b34	20417	69	27	0.67	20284	0.3073	1.9	4.3430	2.7	0.1025	2.0	0.68	1727	28	1702	23	1670	37	103
AK11-seq2-b35	3619	97	8	0.34	6676	0.0726	1.8	0.5567	4.2	0.0556	3.8	0.42	452	8	449	15	436	85	104
AK11-seq2-b36	3003	21	5	0.80	4009	0.2015	1.7	2.1092	4.2	0.0759	3.8	0.41	1184	19	1152	29	1092	77	108
AK11-seq2-b37	19851	356	42	0.42	34191	0.1048	1.4	0.8560	2.5	0.0592	2.0	0.58	642	9	628	12	576	44	112
AK11-seq2-b38	58539	125	49	0.11	33973	0.3714	1.4	8.9295	2.9	0.1744	2.6	0.49	2036	25	2331	27	2600	43	78
AK11-seq2-b39	4960	133	11	0.48	9176	0.0724	1.4	0.5496	3.3	0.0550	3.0	0.42	451	6	445	12	413	66	109
AK11-seq2-b40	3865	91	8	0.55	6977	0.0795	1.7	0.6232	3.8	0.0568	3.4	0.45	493	8	492	15	486	74	102
AK11-seq2-b41	5992	151	11	0.25	10809	0.0735	1.6	0.5664	3.2	0.0559	2.8	0.50	457	7	456	12	449	62	102
AK11-seq2-b42	6923	195	15	0.58	13167	0.0660	1.6	0.4877	2.6	0.0536	2.0	0.63	412	6	403	9	354	45	116
AK11-seq2-b43	4999	38	8	0.57	6805	0.1846	1.6	1.9068	3.7	0.0749	3.3	0.44	1092	16	1083	25	1066	67	102
AK11-seq2-b44	29227	109	34	0.42	30022	0.2728	1.3	3.7283	2.1	0.0991	1.6	0.63	1555	19	1577	17	1608	31	97
AK11-seq2-b45	85257	457	118	0.36	26254	0.2333	1.5	2.8324	2.1	0.0880	1.5	0.71	1352	19	1364	16	1383	29	98
AK11-seq2-b46	21214	167	31	0.19	7453	0.1795	1.5	1.8592	2.3	0.0751	1.8	0.63	1064	15	1067	16	1072	36	99

AK11-seq2-b47	9463	63	14	0.34	12116	0.1996	1.3	2.2180	3.2	0.0806	2.9	0.40	1173	14	1187	22	1212	57	97
AK11-seq2-b48	25040	186	39	0.44	33391	0.1830	1.2	1.9025	2.0	0.0754	1.5	0.63	1083	12	1082	13	1079	31	100
AK11-seq2-b49	6845	54	10	0.27	5602	0.1861	1.7	1.8955	3.5	0.0739	3.1	0.48	1100	17	1080	24	1038	62	106
AK11-seq2-b50	54263	257	50	0.15	302	0.1746	2.4	1.7855	5.1	0.0742	4.6	0.46	1037	23	1040	34	1046	92	99
AK11-seq2-b51	1911	17	4	0.45	2507	0.1903	2.4	2.0268	6.8	0.0773	6.3	0.36	1123	25	1125	47	1128	126	100
AK11-seq2-b52	79561	111	58	0.32	20420	0.4561	1.5	10.3143	1.7	0.1640	0.8	0.87	2422	30	2463	16	2497	14	97
AK11-seq2-b53	7601	35	11	0.49	5987	0.2689	1.7	3.3308	4.1	0.0899	3.7	0.41	1535	23	1488	32	1422	71	108
AK11-seq2-b54	1975	46	4	0.63	3475	0.0816	1.8	0.6494	5.2	0.0577	4.9	0.34	506	9	508	21	520	107	97
AK11-seq2-b55	55315	320	82	0.42	66491	0.2242	1.8	2.6099	2.1	0.0844	1.1	0.85	1304	21	1303	16	1303	21	100
AK11-seq2-b56	6043	146	11	0.16	10874	0.0755	1.6	0.5889	3.7	0.0566	3.3	0.45	469	7	470	14	475	72	99
AK11-seq2-b57	14514	123	22	0.21	20174	0.1771	2.0	1.7899	2.9	0.0733	2.1	0.69	1051	20	1042	19	1023	43	103
AK11-seq2-b58	8920	216	20	0.83	16184	0.0708	2.7	0.5458	4.1	0.0559	3.1	0.64	441	11	442	15	448	70	99
AK11-seq2-b59	4280	33	8	0.66	5941	0.1925	1.7	1.9381	3.5	0.0730	3.0	0.50	1135	18	1094	24	1015	62	112
AK11-seq2-b60	9164	254	20	0.37	6278	0.0712	2.1	0.5474	3.1	0.0558	2.2	0.68	443	9	443	11	444	50	100
AK11-seq3-c01	69597	271	75	0.14	71900	0.2727	2.1	3.7017	2.6	0.0985	1.5	0.81	1554	29	1572	21	1595	29	97
AK11-seq3-c02	9555	72	13	0.20	12972	0.1790	2.1	1.8516	2.8	0.0750	1.8	0.75	1061	21	1064	19	1069	37	99
AK11-seq3-c03	3826	33	7	0.51	5432	0.1763	2.0	1.7452	4.1	0.0718	3.5	0.49	1047	19	1025	27	980	72	107
AK11-seq3-c04	2984	23	5	0.33	4121	0.1936	1.5	1.9721	4.1	0.0739	3.9	0.36	1141	16	1106	28	1039	78	110
AK11-seq3-c05	13009	122	23	0.50	18653	0.1647	2.0	1.6056	3.0	0.0707	2.2	0.66	983	18	972	19	949	46	104
AK11-seq3-c06	53379	61	36	0.33	29006	0.4998	1.4	12.8874	2.2	0.1870	1.6	0.66	2613	31	2671	21	2716	27	96
AK11-seq3-c07	19568	482	43	0.46	4318	0.0787	1.3	0.6284	2.4	0.0579	2.0	0.56	488	6	495	9	526	43	93
AK11-seq3-c08	2639	64	6	0.56	4760	0.0818	1.8	0.6380	6.4	0.0565	6.2	0.28	507	9	501	26	474	137	107
AK11-seq3-c09	814	18	1	0.32	1516	0.0781	1.9	0.5899	12.0	0.0548	11.8	0.16	485	9	471	46	403	265	120
AK11-seq3-c10	1484	11	2	0.57	2078	0.1954	2.5	2.0294	7.6	0.0753	7.2	0.33	1151	27	1125	53	1077	144	107
AK11-seq3-c11	10882	292	24	0.40	19873	0.0753	1.6	0.5790	2.6	0.0558	2.1	0.62	468	7	464	10	443	46	106
AK11-seq3-c12	24627	94	28	0.13	25665	0.2919	1.8	3.9202	2.3	0.0974	1.5	0.76	1651	26	1618	19	1575	28	105
AK11-seq3-c13	35331	287	61	0.63	47913	0.1715	1.8	1.7734	2.2	0.0750	1.3	0.80	1020	17	1036	14	1069	26	95
AK11-seq3-c14	2913	23	4	0.24	4100	0.1835	2.0	1.8248	4.3	0.0721	3.8	0.46	1086	20	1054	29	989	78	110
AK11-seq3-c15	51845	309	66	0.16	63278	0.2125	1.6	2.4233	2.1	0.0827	1.4	0.75	1242	18	1250	15	1263	28	98
AK11-seq3-c16	8766	59	12	0.22	11439	0.1932	2.1	2.0597	2.9	0.0773	1.9	0.74	1139	22	1136	20	1129	38	101
AK11-seq3-c17	35717	277	52	0.18	48168	0.1865	1.7	1.9251	2.3	0.0749	1.5	0.75	1102	17	1090	15	1065	31	104
AK11-seq3-c18	38522	191	50	0.28	43935	0.2447	1.3	3.0163	2.2	0.0894	1.8	0.60	1411	17	1412	17	1413	34	100
AK11-seq3-c19	42507	163	60	0.49	43094	0.3195	1.7	4.4252	2.2	0.1004	1.4	0.77	1787	27	1717	18	1632	26	110
AK11-seq3-c20	14493	116	23	0.31	19802	0.1842	1.1	1.8776	2.2	0.0739	1.9	0.49	1090	11	1073	15	1040	38	105
AK11-seq3-c21	4272	96	9	0.45	7485	0.0837	2.1	0.6581	4.3	0.0570	3.8	0.48	518	10	513	17	493	83	105
AK11-seq3-c22	6986	55	13	0.71	9586	0.1811	1.4	1.8397	2.8	0.0737	2.4	0.49	1073	14	1060	18	1033	49	104
AK11-seq3-c23	13146	89	20	0.44	7966	0.2023	1.9	2.2467	3.3	0.0805	2.7	0.57	1188	20	1196	24	1210	54	98
AK11-seq3-c24	3715	32	7	0.68	5376	0.1753	2.3	1.6980	4.6	0.0702	4.0	0.49	1041	22	1008	30	935	83	111
AK11-seq3-c25	6650	45	10	0.28	8521	0.2040	1.8	2.2323	2.9	0.0794	2.3	0.62	1197	20	1191	21	1182	45	101
AK11-seq3-c26	22537	161	33	0.23	29409	0.1974	1.9	2.1276	2.7	0.0782	1.9	0.71	1162	21	1158	19	1151	39	101
AK11-seq3-c27	14825	128	24	0.27	7638	0.1754	1.8	1.7522	2.7	0.0724	2.0	0.67	1042	18	1028	18	998	41	104
AK11-seq3-c28	48377	411	75	0.21	66630	0.1759	1.5	1.7932	2.3	0.0739	1.7	0.67	1044	15	1043	15	1040	35	100

AK11-seq3-c29	13826	108	21	0.26	18893	0.1828	1.5	1.8762	2.2	0.0745	1.6	0.69	1082	15	1073	15	1054	32	103
AK11-seq3-c30	41651	279	55	0.22	53736	0.1924	1.7	2.0721	2.3	0.0781	1.5	0.75	1134	18	1140	16	1150	31	99
AK11-seq3-c31	11108	92	18	0.43	15355	0.1753	2.0	1.7686	2.9	0.0732	2.1	0.69	1041	19	1034	19	1019	42	102
AK11-seq3-c32	21562	77	27	0.45	22311	0.2958	1.4	4.0191	2.2	0.0985	1.8	0.62	1670	20	1638	18	1597	33	105
AK11-seq3-c33	5820	47	9	0.21	8081	0.1814	2.2	1.8279	4.6	0.0731	4.1	0.47	1075	22	1056	31	1016	83	106
AK11-seq3-c34	17396	63	19	0.19	17403	0.2857	2.4	4.0082	3.2	0.1017	2.1	0.76	1620	35	1636	26	1656	38	98
AK11-seq3-c35	5904	25	7	0.30	1010	0.2668	1.7	3.4098	3.7	0.0927	3.2	0.46	1524	23	1507	29	1482	61	103
AK11-seq3-c36	33369	199	46	0.31	40893	0.2141	1.9	2.4498	2.7	0.0830	1.9	0.71	1251	22	1257	20	1269	37	99
AK11-seq3-c37	42946	274	58	0.23	54105	0.2016	1.4	2.2466	2.0	0.0808	1.5	0.70	1184	15	1196	14	1217	29	97
AK11-seq3-c38	5024	122	7	0.05	8336	0.0628	2.1	0.5282	6.6	0.0610	6.3	0.31	393	8	431	24	638	136	62
AK11-seq3-c39	26938	98	36	0.60	26890	0.3052	1.7	4.2932	2.2	0.1020	1.4	0.76	1717	25	1692	18	1661	26	103
AK11-seq3-c40	948	22	2	0.54	1706	0.0779	2.4	0.6021	10.3	0.0561	10.0	0.23	484	11	479	40	455	222	106
AK11-seq3-c41	28431	136	37	0.24	32178	0.2634	2.1	3.2388	2.6	0.0892	1.5	0.82	1507	28	1467	20	1408	28	107
AK11-seq3-c42	2430	18	4	0.54	983	0.2018	2.3	1.9609	5.2	0.0705	4.7	0.44	1185	25	1102	36	942	96	126
AK11-seq3-c43	10836	75	16	0.11	9569	0.2119	1.8	2.2215	2.7	0.0761	2.0	0.67	1239	20	1188	19	1096	40	113
AK11-seq3-c44	1827	37	4	0.62	3182	0.0846	1.8	0.6789	6.2	0.0582	6.0	0.29	523	9	526	26	538	130	97
AK11-seq3-c45	10743	83	18	0.53	14483	0.1825	1.7	1.9011	3.2	0.0755	2.7	0.54	1081	17	1081	22	1083	54	100
AK11-seq3-c46	2699	58	7	1.30	4827	0.0776	2.7	0.6026	7.2	0.0563	6.6	0.37	482	12	479	28	465	147	104
AK11-seq3-c47	26210	52	24	0.38	20161	0.4030	2.4	7.3360	2.9	0.1320	1.6	0.84	2183	45	2153	26	2125	28	103
AK11-seq3-c48	4760	97	9	0.36	2721	0.0810	1.7	0.6549	3.5	0.0587	3.0	0.50	502	8	511	14	555	66	90
AK11-seq3-c49	45998	47	32	0.45	24330	0.5673	1.7	15.0571	2.3	0.1925	1.6	0.73	2897	39	2819	22	2764	26	105
AK11-seq3-c50	46621	162	57	0.40	32782	0.3156	2.1	4.6061	2.6	0.1059	1.5	0.81	1768	33	1750	22	1729	28	102
Sample AK16	Chloritic Sandstone Formation					Location (decimal degrees) 52.086 8.83000 W						Datum: IRENET95							
AK16-seq1-A01	371	21	6	1.33	504	0.1915	3.1	2.0026	8.9	0.0758	8.3	0.35	1130	32	1116	62	1091	166	104
AK16-seq1-A02	4844	297	51	0.03	6684	0.1815	1.8	1.8631	3.2	0.0745	2.7	0.55	1075	18	1068	22	1054	54	102
AK16-seq1-A03	212	50	4	0.53	401	0.0741	2.7	0.5699	11.2	0.0558	10.9	0.24	461	12	458	42	444	242	104
AK16-seq1-A04	842	56	10	0.28	1160	0.1802	2.1	1.8857	6.3	0.0759	5.9	0.33	1068	21	1076	43	1092	119	98
AK16-seq1-A05	2513	73	22	0.22	2550	0.2931	1.6	4.1500	3.8	0.1027	3.4	0.44	1657	24	1664	31	1673	62	99
AK16-seq1-A06	688	71	17	0.82	925	0.1955	1.9	2.0811	7.2	0.0772	6.9	0.27	1151	20	1143	51	1126	138	102
AK16-seq1-A07	1708	114	21	0.25	2365	0.1828	1.7	1.9051	4.2	0.0756	3.9	0.41	1082	17	1083	29	1084	77	100
AK16-seq1-A08	1960	56	20	0.56	1992	0.3059	1.1	4.3358	4.0	0.1028	3.8	0.29	1720	17	1700	33	1675	70	103
AK16-seq1-A09	1955	421	38	0.80	3601	0.0753	2.5	0.5824	4.8	0.0561	4.0	0.53	468	11	466	18	455	90	103
AK16-seq1-A10	443	157	12	0.41	833	0.0704	2.4	0.5407	8.6	0.0557	8.2	0.28	439	10	439	31	440	183	100
AK16-seq1-A11	2834	149	38	0.67	3690	0.2174	2.2	2.4022	3.9	0.0801	3.3	0.55	1268	25	1243	29	1200	65	106
AK16-seq1-A12	485	33	8	1.07	675	0.1789	2.4	1.8419	7.0	0.0747	6.5	0.35	1061	24	1061	47	1060	131	100
AK16-seq1-A13	3164	613	46	0.10	5807	0.0796	1.1	0.6255	3.3	0.0570	3.1	0.33	494	5	493	13	492	69	100
AK16-seq1-A14	349	50	5	0.35	606	0.0968	2.8	0.8001	9.3	0.0600	8.8	0.30	596	16	597	43	602	191	99
AK16-seq1-A15	8698	70	54	0.92	4700	0.5680	1.7	15.0060	2.5	0.1916	1.9	0.67	2900	39	2816	24	2756	31	105
AK16-seq1-A16	3072	179	37	0.25	4109	0.2032	1.3	2.1909	3.2	0.0782	2.8	0.43	1192	15	1178	22	1152	57	103
AK16-seq1-A17	2414	539	46	0.68	4502	0.0728	2.4	0.5639	4.2	0.0562	3.4	0.57	453	10	454	15	461	76	98
AK16-seq1-A18	1887	79	19	0.40	2194	0.2226	2.0	2.7306	4.1	0.0890	3.6	0.49	1296	24	1337	31	1404	69	92

AK16-seq1-A19	999	408	28	0.32	1923	0.0661	2.2	0.4972	5.4	0.0546	5.0	0.40	412	9	410	19	395	112	104
AK16-seq1-A20	4540	158	47	0.43	4957	0.2639	2.2	3.4777	3.7	0.0956	3.0	0.59	1510	29	1522	30	1540	57	98
AK16-seq1-A21	1275	89	15	0.23	1806	0.1681	1.8	1.7111	4.2	0.0738	3.8	0.42	1002	17	1013	27	1037	77	97
AK16-seq1-A22	11034	377	81	0.15	17497	0.2204	1.3	2.0040	2.0	0.0659	1.6	0.62	1284	15	1117	14	805	34	160
AK16-seq1-A23	5352	139	62	1.11	5188	0.3215	2.3	4.7664	3.5	0.1075	2.5	0.68	1797	37	1779	29	1758	47	102
AK16-seq1-A24	2333	169	33	0.56	3334	0.1696	2.1	1.7004	4.3	0.0727	3.7	0.48	1010	19	1009	28	1006	76	100
AK16-seq1-A25	1146	270	20	0.36	2179	0.0691	1.8	0.5236	4.8	0.0549	4.5	0.37	431	7	428	17	409	100	105
AK16-seq1-A26	1831	81	21	0.29	2196	0.2427	2.9	2.9317	5.0	0.0876	4.1	0.58	1401	37	1390	39	1374	78	102
AK16-seq1-A27	659	131	11	0.30	1203	0.0814	2.1	0.6463	7.1	0.0576	6.8	0.29	505	10	506	29	513	148	98
AK16-seq1-A28	3182	214	38	0.21	4534	0.1734	2.0	1.7458	4.3	0.0730	3.8	0.47	1031	19	1026	28	1015	77	102
AK16-seq1-A29	147	29	3	0.58	269	0.0789	2.9	0.6217	16.3	0.0572	16.0	0.18	489	14	491	66	498	353	98
AK16-seq1-A30	2190	456	34	0.07	4031	0.0791	1.8	0.6192	5.7	0.0568	5.4	0.31	491	8	489	22	482	119	102
AK16-seq1-A31	472	36	7	0.47	666	0.1655	4.1	1.6593	9.5	0.0727	8.6	0.43	987	38	993	62	1006	174	98
AK16-seq1-A32	931	34	9	0.28	1029	0.2556	2.6	3.3435	5.4	0.0949	4.7	0.48	1467	34	1491	43	1526	89	96
AK16-seq1-A33	3257	70	20	0.52	3775	0.2472	2.2	3.0819	4.1	0.0904	3.5	0.53	1424	28	1428	32	1434	67	99
AK16-seq1-A34	3706	228	47	0.33	3725	0.1919	2.1	2.0434	5.1	0.0772	4.6	0.41	1132	22	1130	35	1127	92	100
AK16-seq1-A35	1267	261	22	0.37	2306	0.0802	2.1	0.6304	5.0	0.0570	4.5	0.42	498	10	496	20	491	100	101
AK16-seq1-A36	1303	93	17	0.24	1846	0.1820	1.9	1.8652	5.0	0.0743	4.6	0.38	1078	19	1069	34	1050	94	103
AK16-seq1-A37	5840	182	35	0.21	7983	0.1861	1.5	1.9418	2.8	0.0757	2.4	0.51	1100	15	1096	19	1086	49	101
AK16-seq1-A38	19118	646	153	0.21	29518	0.2376	1.9	2.2234	2.5	0.0679	1.7	0.75	1374	23	1188	18	864	35	159
AK16-seq1-A39	1319	162	12	0.39	2469	0.0683	2.0	0.5224	4.9	0.0555	4.4	0.41	426	8	427	17	431	99	99
AK16-seq1-A40	2617	152	33	0.30	3427	0.2002	1.9	2.2101	4.0	0.0800	3.6	0.47	1177	20	1184	29	1198	71	98
AK16-seq1-A41	5581	742	52	0.18	11171	0.0710	1.3	0.5116	2.7	0.0522	2.4	0.48	442	6	420	9	295	55	150
AK16-seq1-A42	8423	132	48	0.46	8649	0.3203	1.6	4.4307	2.7	0.1003	2.2	0.57	1791	25	1718	23	1630	42	110
AK16-seq1-A43	881	33	6	0.32	1235	0.1730	2.2	1.7889	5.5	0.0750	5.0	0.40	1029	21	1041	36	1068	101	96
AK16-seq1-A44	220	47	4	0.53	417	0.0820	2.7	0.6451	13.8	0.0570	13.6	0.19	508	13	505	57	493	300	103
AK16-seq1-A45	3958	133	26	0.30	5480	0.1856	2.3	1.9127	3.6	0.0747	2.8	0.63	1098	23	1086	24	1061	56	103
AK16-seq1-A46	535	37	7	0.28	743	0.1753	2.7	1.8016	7.8	0.0745	7.3	0.35	1042	26	1046	52	1055	147	99
AK16-seq1-A48	5165	198	36	0.29	7610	0.1737	2.5	1.7004	3.4	0.0710	2.4	0.72	1032	24	1009	22	957	48	108
AK16-seq1-A49	871	35	6	0.28	1268	0.1723	2.3	1.7067	5.3	0.0718	4.8	0.42	1025	22	1011	35	981	98	104
AK16-seq1-A50	2448	83	17	0.41	3313	0.1906	2.0	2.0289	4.4	0.0772	3.9	0.47	1125	21	1125	30	1127	77	100
AK16-seq1-A51	940	33	7	0.50	1265	0.1803	1.6	1.9234	6.0	0.0774	5.8	0.27	1068	16	1089	41	1131	115	94
AK16-seq1-A52	2087	451	39	1.09	1730	0.0659	2.6	0.5788	6.0	0.0637	5.4	0.44	411	10	464	22	732	113	56
AK16-seq1-A53	735	25	5	0.48	1001	0.1848	2.8	1.9544	6.7	0.0767	6.0	0.43	1093	29	1100	46	1113	120	98
AK16-seq1-A54	1142	225	19	0.58	2071	0.0734	2.4	0.5721	5.7	0.0566	5.2	0.42	456	10	459	21	474	115	96
AK16-seq1-A55	1317	309	24	0.48	2485	0.0716	1.8	0.5482	5.1	0.0556	4.8	0.35	446	8	444	19	435	107	102
AK16-seq1-A56	427	93	8	0.57	808	0.0767	2.4	0.5933	8.3	0.0561	7.9	0.29	476	11	473	32	456	176	104
AK16-seq1-A57	670	154	12	0.40	1234	0.0708	2.1	0.5496	7.2	0.0563	6.9	0.29	441	9	445	26	463	153	95
AK16-seq1-A58	1093	235	21	0.44	2018	0.0814	2.0	0.6410	6.1	0.0571	5.8	0.32	505	10	503	25	495	128	102
AK16-seq1-A59	2009	62	13	0.32	2634	0.2046	1.5	2.2524	4.3	0.0799	4.1	0.34	1200	16	1198	31	1193	80	101
AK16-seq1-A60	694	50	10	0.55	965	0.1809	2.7	1.8558	5.8	0.0744	5.1	0.46	1072	26	1065	39	1053	103	102
AK16-seq2-B01	526	35	7	0.24	712	0.1902	2.2	2.0185	8.5	0.0770	8.2	0.25	1122	22	1122	59	1121	163	100

AK16-seq2-B02	7212	215	74	0.25	7152	0.3312	2.1	4.7126	2.8	0.1032	1.9	0.74	1844	33	1769	24	1682	35	110
AK16-seq2-B03	359	42	3	0.32	662	0.0765	3.3	0.5984	8.9	0.0568	8.2	0.38	475	15	476	34	482	181	99
AK16-seq2-B04	261	17	4	0.42	353	0.1925	2.9	2.0659	12.8	0.0778	12.4	0.23	1135	31	1138	91	1143	247	99
AK16-seq2-B05	6266	245	48	0.45	8900	0.1787	1.8	1.8099	3.0	0.0735	2.4	0.60	1060	18	1049	20	1027	49	103
AK16-seq2-B06	2047	148	39	0.59	2396	0.2336	1.5	2.8551	3.8	0.0886	3.5	0.40	1353	19	1370	29	1396	68	97
AK16-seq2-B07	1179	74	15	0.34	1513	0.1886	3.2	2.1028	6.1	0.0808	5.2	0.53	1114	33	1150	43	1218	101	91
AK16-seq2-B08	2391	359	44	0.69	4044	0.1048	1.6	0.8804	3.4	0.0609	3.0	0.48	642	10	641	16	637	64	101
AK16-seq2-B09	800	87	8	0.37	1453	0.0853	2.3	0.6778	6.6	0.0577	6.2	0.35	527	12	525	27	517	135	102
AK16-seq2-B10	199	43	5	1.19	349	0.0791	3.7	0.6362	10.6	0.0583	9.9	0.35	491	18	500	43	543	216	90
AK16-seq2-B11	3948	51	21	0.68	3573	0.3358	1.7	5.3391	3.2	0.1153	2.7	0.54	1866	28	1875	28	1885	49	99
AK16-seq2-B12	840	204	16	0.47	1557	0.0739	2.5	0.5730	5.4	0.0562	4.8	0.46	460	11	460	20	461	105	100
AK16-seq2-B13	890	114	9	0.41	1661	0.0727	2.0	0.5661	6.2	0.0565	5.9	0.32	452	9	456	23	472	130	96
AK16-seq2-B14	2652	115	29	0.27	3109	0.2394	2.5	2.9377	4.1	0.0890	3.2	0.61	1383	31	1392	31	1404	62	99
AK16-seq2-B15	6972	67	44	0.71	3760	0.5110	2.2	13.5073	3.2	0.1917	2.4	0.67	2661	47	2716	31	2757	40	97
AK16-seq2-B16	595	132	12	0.71	1114	0.0755	2.5	0.5847	6.7	0.0562	6.3	0.36	469	11	467	26	460	139	102
AK16-seq2-B17	2123	60	21	0.35	2073	0.3212	1.8	4.7095	3.8	0.1063	3.3	0.49	1796	29	1769	32	1738	61	103
AK16-seq2-B18	347	74	7	0.54	636	0.0831	3.1	0.6622	11.7	0.0578	11.3	0.27	514	16	516	48	523	247	98
AK16-seq2-B19	4982	181	49	0.13	5300	0.2720	1.5	3.6357	3.0	0.0969	2.6	0.50	1551	21	1557	24	1566	48	99
AK16-seq2-B20	5187	155	63	0.95	5189	0.3144	2.1	4.4926	3.3	0.1036	2.5	0.65	1762	33	1730	28	1690	46	104
AK16-seq2-B21	1694	70	20	0.30	1907	0.2691	2.1	3.4341	4.6	0.0926	4.1	0.45	1536	29	1512	37	1479	78	104
AK16-seq2-B22	1235	60	16	0.39	1474	0.2428	2.0	2.9255	4.5	0.0874	4.1	0.44	1401	25	1389	35	1369	78	102
AK16-seq2-B23	1315	76	17	0.32	1679	0.2164	2.0	2.4380	4.6	0.0817	4.2	0.43	1263	22	1254	34	1239	81	102
AK16-seq2-B24	2307	183	34	0.37	3290	0.1740	2.4	1.7572	4.3	0.0732	3.6	0.54	1034	23	1030	28	1020	74	101
AK16-seq2-B25	7104	102	34	0.19	6733	0.3247	2.4	4.9255	3.5	0.1100	2.6	0.69	1812	38	1807	30	1800	47	101
AK16-seq2-B26	3297	49	18	0.53	1771	0.3040	2.0	4.6374	3.8	0.1106	3.2	0.52	1711	30	1756	32	1810	58	95
AK16-seq2-B27	12608	74	45	0.54	7714	0.4955	1.5	11.6746	2.9	0.1709	2.4	0.53	2594	33	2579	27	2566	41	101
AK16-seq2-B28	2252	120	28	0.31	2806	0.2238	1.9	2.5928	4.2	0.0840	3.7	0.45	1302	22	1299	31	1293	73	101
AK16-seq2-B29	777	59	11	0.38	1100	0.1769	2.7	1.8002	6.8	0.0738	6.2	0.39	1050	26	1046	45	1036	126	101
AK16-seq2-B30	425	112	8	0.32	800	0.0701	1.5	0.5324	6.8	0.0550	6.7	0.22	437	6	433	24	414	149	106
AK16-seq2-B31	3363	380	50	0.18	5399	0.1345	1.8	1.2054	3.3	0.0650	2.7	0.54	813	13	803	18	775	58	105
AK16-seq2-B32	1810	123	30	1.08	2465	0.1858	2.4	1.9654	5.2	0.0767	4.6	0.47	1099	25	1104	36	1114	92	99
AK16-seq2-B33	1212	88	16	0.28	1663	0.1732	2.4	1.8176	4.9	0.0761	4.3	0.48	1030	22	1052	33	1098	87	94
AK16-seq2-B34	142	27	3	1.95	255	0.0767	3.3	0.5973	18.6	0.0564	18.3	0.18	477	15	476	73	470	405	101
AK16-seq2-B35	792	176	16	0.74	1434	0.0782	3.0	0.6167	7.1	0.0572	6.4	0.43	485	14	488	28	500	141	97
AK16-seq2-B36	459	36	8	0.86	666	0.1791	2.4	1.7824	6.8	0.0722	6.3	0.36	1062	24	1039	45	991	129	107
AK16-seq2-B37	718	158	14	0.63	1311	0.0796	2.3	0.6276	6.9	0.0572	6.5	0.33	494	11	495	28	499	144	99
AK16-seq2-B38	123	30	3	0.74	232	0.0715	3.8	0.5542	11.6	0.0562	11.0	0.33	445	16	448	43	462	244	96
AK16-seq2-B39	1516	111	20	0.28	2137	0.1786	2.5	1.8202	5.7	0.0739	5.1	0.44	1059	25	1053	38	1039	104	102
AK16-seq2-B40	799	49	10	0.31	1032	0.2042	3.3	2.2752	7.1	0.0808	6.3	0.47	1198	37	1205	52	1217	124	98
AK16-seq2-B41	418	198	14	0.34	772	0.0678	11.0	0.5214	16.6	0.0557	12.4	0.66	423	45	426	60	442	277	96
AK16-seq2-B42	485	35	7	0.42	666	0.1753	1.8	1.8396	7.7	0.0761	7.5	0.24	1041	17	1060	52	1098	149	95
AK16-seq2-B43	4882	226	59	0.26	5826	0.2524	2.0	3.0399	3.8	0.0874	3.2	0.53	1451	26	1418	29	1369	62	106

AK16-seq2-B44	531	135	10	0.33	991	0.0686	2.4	0.5276	6.9	0.0558	6.4	0.34	427	10	430	24	445	143	96
AK16-seq2-B45	2028	144	30	0.50	2727	0.1877	1.9	2.0036	3.9	0.0774	3.4	0.48	1109	19	1117	27	1132	68	98
AK16-seq2-B46	4342	144	47	0.25	4453	0.3163	2.1	4.4925	3.0	0.1030	2.1	0.72	1772	33	1730	25	1679	38	106
AK16-seq2-B47	1266	489	32	0.26	2128	0.0636	2.4	0.5592	7.2	0.0638	6.8	0.33	397	9	451	27	735	144	54
AK16-seq2-B48	739	63	11	0.33	1084	0.1693	2.8	1.6705	6.8	0.0716	6.2	0.42	1008	26	997	44	973	126	104
AK16-seq2-B49	2742	993	99	1.05	4910	0.0821	2.0	0.6524	4.6	0.0576	4.1	0.44	509	10	510	18	516	90	99
AK16-seq2-B50	4121	265	56	0.19	5391	0.2111	2.1	2.2922	3.4	0.0788	2.8	0.60	1234	23	1210	25	1166	54	106
AK16-seq2-B51	1129	99	16	0.26	1655	0.1595	2.2	1.5777	5.1	0.0717	4.6	0.44	954	20	961	32	979	94	97
AK16-seq2-B52	777	17	5	0.46	907	0.2460	3.1	3.0951	7.7	0.0913	7.1	0.40	1418	40	1431	61	1452	135	98
AK16-seq2-B53	335	78	6	0.26	614	0.0795	2.2	0.6249	8.3	0.0570	8.0	0.27	493	10	493	33	492	176	100
AK16-seq2-B54	1177	75	16	0.37	1558	0.2045	2.3	2.2343	4.9	0.0792	4.4	0.47	1200	26	1192	35	1178	86	102
AK16-seq2-B55	1257	470	34	0.34	2338	0.0704	1.7	0.5463	5.0	0.0563	4.7	0.34	438	7	443	18	464	103	94
AK16-seq2-B56	4248	274	58	0.26	5642	0.2048	2.2	2.2198	4.0	0.0786	3.3	0.55	1201	24	1187	28	1162	66	103
AK16-seq2-B57	816	202	16	0.48	1513	0.0726	3.2	0.5631	6.1	0.0562	5.2	0.53	452	14	454	23	462	115	98
AK16-seq2-B58	251	12	2	0.72	386	0.1697	3.3	1.5760	8.5	0.0673	7.8	0.39	1011	31	961	54	849	162	119
AK16-seq2-B59	1921	478	42	0.57	3544	0.0788	1.5	0.6147	4.6	0.0566	4.3	0.33	489	7	486	18	475	96	103
AK16-seq2-B60	758	28	6	0.61	1059	0.1767	2.3	1.8045	6.7	0.0740	6.3	0.35	1049	23	1047	45	1043	127	101
AK16-seq3-C01	874	32	6	0.39	1199	0.1793	2.9	1.8840	6.5	0.0762	5.9	0.44	1063	28	1075	44	1100	117	97
AK16-seq3-C02	532	137	10	0.44	992	0.0682	2.6	0.5260	7.1	0.0559	6.7	0.36	425	11	429	25	449	148	95
AK16-seq3-C03	1077	290	23	0.60	1542	0.0687	3.2	0.5558	5.3	0.0587	4.3	0.59	428	13	449	19	556	93	77
AK16-seq3-C04	791	19	6	0.47	659	0.2843	3.7	4.4268	7.4	0.1129	6.4	0.50	1613	53	1717	63	1847	116	87
AK16-seq3-C05	3289	325	65	0.83	4898	0.1611	4.1	1.5570	5.2	0.0701	3.3	0.78	963	37	953	33	931	67	103
AK16-seq3-C06	760	198	15	0.46	1439	0.0701	2.8	0.5376	7.1	0.0556	6.6	0.39	437	12	437	26	437	146	100
AK16-seq3-C07	757	191	15	0.39	1411	0.0754	2.1	0.5853	6.0	0.0563	5.6	0.35	468	9	468	23	465	124	101
AK16-seq3-C08	1726	57	20	0.69	1740	0.2983	2.3	4.2661	5.0	0.1037	4.4	0.47	1683	35	1687	42	1692	81	99
AK16-seq3-C09	2183	85	26	0.37	2381	0.2796	2.2	3.6991	4.1	0.0960	3.5	0.53	1589	31	1571	33	1547	65	103
AK16-seq3-C10	3548	144	40	0.32	4037	0.2599	2.2	3.2965	3.5	0.0920	2.7	0.63	1489	29	1480	27	1467	51	101
AK16-seq3-C11	4446	702	80	0.35	7464	0.1121	1.6	0.9615	3.4	0.0622	3.0	0.47	685	11	684	17	682	64	100
AK16-seq3-C12	146	36	3	0.41	273	0.0806	4.1	0.6384	17.9	0.0574	17.5	0.23	500	20	501	74	507	384	99
AK16-seq3-C13	1105	285	22	0.47	2077	0.0695	2.2	0.5330	5.5	0.0556	5.1	0.40	433	9	434	20	437	112	99
AK16-seq3-C14	4676	138	51	0.47	4680	0.3284	2.0	4.7603	3.5	0.1051	2.8	0.58	1831	32	1778	30	1717	52	107
AK16-seq3-C15	552	148	12	0.81	1052	0.0661	1.8	0.5038	6.7	0.0553	6.5	0.26	413	7	414	23	423	144	98
AK16-seq3-C16	384	33	5	0.26	569	0.1627	2.4	1.5797	8.5	0.0704	8.2	0.29	972	22	962	55	940	168	103
AK16-seq3-C17	496	51	9	0.92	771	0.1446	2.0	1.3459	8.0	0.0675	7.7	0.26	871	17	866	48	853	161	102
AK16-seq3-C18	2563	178	33	0.24	3463	0.1817	1.6	1.8957	3.9	0.0757	3.6	0.40	1076	16	1080	26	1087	72	99
AK16-seq3-C19	504	31	8	1.20	688	0.1903	3.8	1.9877	6.7	0.0758	5.5	0.57	1123	40	1111	46	1089	110	103
AK16-seq3-C20	7724	252	77	0.13	8097	0.3062	2.0	4.1514	2.7	0.0983	1.8	0.74	1722	30	1664	22	1593	34	108
AK16-seq3-C21	2263	402	39	0.51	3816	0.0888	2.4	0.7623	4.2	0.0622	3.5	0.56	549	13	575	19	682	75	80
AK16-seq3-C22	607	134	10	0.29	1090	0.0722	2.3	0.5783	6.2	0.0581	5.8	0.37	449	10	463	23	534	127	84
AK16-seq3-C23	1742	120	23	0.35	2324	0.1839	1.9	1.9541	4.1	0.0771	3.6	0.46	1088	19	1100	28	1123	72	97
AK16-seq3-C24	685	38	11	0.33	738	0.2635	2.9	3.5327	7.0	0.0972	6.4	0.42	1508	39	1535	57	1572	119	96
AK16-seq3-C25	7095	416	134	0.56	8113	0.2908	1.6	3.7037	3.1	0.0924	2.7	0.50	1646	23	1572	25	1475	52	112

AK16-seq3-C26	948	354	29	0.58	1769	0.0744	2.1	0.5758	5.8	0.0562	5.4	0.37	462	10	462	22	458	119	101
AK16-seq3-C27	2247	171	33	0.24	3193	0.1895	1.7	1.9230	3.9	0.0736	3.6	0.42	1119	17	1089	27	1030	72	109
AK16-seq3-C28	499	36	9	1.36	683	0.1884	1.6	1.9868	6.4	0.0765	6.2	0.25	1113	17	1111	44	1108	124	100
AK16-seq3-C29	747	190	14	0.35	1404	0.0687	2.2	0.5261	6.7	0.0555	6.3	0.33	429	9	429	24	433	140	99
AK16-seq3-C30	3655	280	50	0.27	5089	0.1719	1.4	1.7629	3.4	0.0744	3.1	0.41	1023	14	1032	23	1052	63	97
AK16-seq3-C31	1290	94	18	0.29	1789	0.1818	2.4	1.8891	5.0	0.0754	4.4	0.49	1077	24	1077	34	1078	88	100
AK16-seq3-C32	216	46	4	0.42	392	0.0794	2.9	0.6276	13.0	0.0573	12.7	0.22	493	14	495	52	503	279	98
Sample BF11	Gyleen Formation					Location (decimal degrees)		51.785	8.291022 W			Datum: D_WGS_1984							
BF11-seq1-a01	3283	117	56	2.02	3459	0.2871	2.0	3.9338	3.5	0.0994	2.8	0.59	1627	29	1621	28	1612	52	101
BF11-seq1-a02	12786	332	99	0.43	9599	0.2707	2.2	3.4952	8.4	0.0936	8.1	0.26	1544	30	1526	68	1501	153	103
BF11-seq1-a03	1948	22	15	1.49	1734	0.5642	25.2	7.0548	25.6	0.0907	4.4	0.99	2884	615	2118	258	1440	83	200
BF11-seq1-a04	8286	366	88	0.42	9174	0.2193	3.9	2.8477	4.2	0.0942	1.7	0.91	1278	45	1368	32	1512	33	85
BF11-seq1-a05	10089	124	71	0.61	5826	0.4755	1.5	11.8297	2.4	0.1804	1.9	0.62	2508	31	2591	23	2657	31	94
BF11-seq1-a06	2593	111	30	0.30	2932	0.2533	2.0	3.2416	3.8	0.0928	3.2	0.53	1456	26	1467	30	1484	61	98
BF11-seq1-a07	500	39	8	0.42	723	0.1787	2.1	1.8085	8.1	0.0734	7.8	0.26	1060	20	1049	54	1025	158	103
BF11-seq1-a08	10977	401	128	0.59	12393	0.2762	2.0	3.4785	3.0	0.0913	2.2	0.68	1572	28	1522	24	1454	42	108
BF11-seq1-a09	2933	119	43	0.83	3522	0.2898	1.8	3.4605	3.9	0.0866	3.5	0.45	1641	26	1518	31	1352	68	121
BF11-seq1-a10	1073	40	13	0.57	793	0.2846	2.6	4.0260	5.7	0.1026	5.1	0.46	1614	38	1639	48	1672	94	97
BF11-seq1-a11	490	32	7	0.41	634	0.1978	2.5	2.2176	9.2	0.0813	8.9	0.27	1163	27	1187	67	1229	175	95
BF11-seq1-a12	1051	84	15	0.27	1477	0.1757	2.1	1.8049	5.5	0.0745	5.0	0.39	1043	21	1047	36	1055	102	99
BF11-seq1-a13	1874	115	28	0.31	2351	0.2283	1.6	2.6575	4.6	0.0844	4.4	0.35	1325	19	1317	35	1303	85	102
BF11-seq1-a14	1382	423	29	0.49	2641	0.0638	2.7	0.4797	5.6	0.0545	4.9	0.48	399	10	398	18	393	109	101
BF11-seq1-a15	24045	496	180	0.13	25914	0.3641	2.2	4.8512	2.6	0.0966	1.4	0.84	2002	38	1794	22	1560	26	128
BF11-seq1-a16	9436	109	62	0.19	5554	0.5233	1.6	12.8162	2.4	0.1776	1.8	0.67	2713	36	2666	23	2631	30	103
BF11-seq1-a17	1305	96	20	0.41	1771	0.1909	1.8	2.0292	5.5	0.0771	5.2	0.33	1126	19	1125	38	1124	104	100
BF11-seq1-a18	13246	1089	208	0.16	19707	0.1948	1.7	1.8896	2.6	0.0704	2.0	0.65	1147	18	1077	18	939	41	122
BF11-seq1-a19	3229	113	42	0.72	3313	0.2999	1.5	4.2107	3.0	0.1018	2.6	0.50	1691	22	1676	25	1658	48	102
BF11-seq1-a20	2478	116	31	0.27	2868	0.2535	1.8	3.1714	4.1	0.0907	3.6	0.45	1456	24	1450	32	1441	69	101
BF11-seq1-a21	4163	225	47	0.67	5986	0.1745	2.1	1.7537	4.1	0.0729	3.5	0.51	1037	20	1029	27	1011	71	102
BF11-seq1-a23	1644	389	35	0.68	3012	0.0788	1.6	0.6211	4.8	0.0572	4.5	0.34	489	8	491	19	498	100	98
BF11-seq1-a24	8215	405	123	0.45	9842	0.2884	1.7	3.4645	2.3	0.0871	1.6	0.74	1634	25	1519	19	1363	30	120
BF11-seq1-a25	676	57	11	0.47	969	0.1725	2.3	1.7309	6.1	0.0728	5.7	0.37	1026	22	1020	40	1008	116	102
BF11-seq1-a26	683	39	10	0.63	857	0.2253	2.7	2.5552	8.4	0.0823	7.9	0.33	1310	33	1288	63	1252	155	105
BF11-seq1-a27	416	99	10	0.92	757	0.0817	3.1	0.6505	9.2	0.0577	8.7	0.34	506	15	509	38	520	191	97
BF11-seq1-a28	7749	236	81	0.27	7407	0.3261	1.6	4.9302	2.6	0.1096	2.1	0.62	1820	26	1807	22	1794	38	101
BF11-seq1-a29	17805	195	120	0.21	10119	0.5649	2.0	14.2700	2.4	0.1832	1.4	0.82	2887	46	2768	23	2682	23	108
BF11-seq1-a30	1296	101	22	0.62	1768	0.1864	1.8	1.9708	4.9	0.0767	4.6	0.36	1102	18	1106	34	1113	91	99
BF11-seq1-a31	5916	209	68	0.29	6067	0.3129	3.0	4.4516	4.2	0.1032	2.9	0.73	1755	46	1722	35	1682	53	104
BF11-seq1-a32	812	176	15	0.14	1230	0.0865	2.8	0.8052	8.4	0.0675	8.0	0.33	535	14	600	39	855	165	63
BF11-seq1-a33	2083	61	24	0.66	1896	0.3333	1.9	5.2606	3.8	0.1145	3.3	0.49	1854	30	1862	33	1872	59	99
BF11-seq1-a34	6761	185	55	0.32	7478	0.2764	1.3	3.5992	2.9	0.0944	2.6	0.45	1573	18	1549	23	1517	49	104

BF11-seq1-a35	4721	337	72	0.37	6411	0.2006	1.5	2.1250	2.7	0.0768	2.3	0.55	1178	16	1157	19	1117	45	105
BF11-seq1-a36	3677	102	40	0.37	3382	0.3580	2.3	5.5933	3.7	0.1133	2.9	0.61	1972	38	1915	32	1853	53	106
BF11-seq1-a37	1059	83	15	0.28	1437	0.1759	2.1	1.8675	5.5	0.0770	5.1	0.38	1044	20	1070	37	1121	102	93
BF11-seq1-a38	4174	289	56	0.21	5881	0.1939	2.4	2.0426	4.0	0.0764	3.2	0.60	1142	25	1130	27	1106	63	103
BF11-seq1-a39	1000	263	21	0.55	1846	0.0731	2.2	0.5654	6.7	0.0561	6.3	0.33	455	10	455	25	457	140	100
BF11-seq1-a40	1475	279	35	0.89	2583	0.1014	2.0	0.8348	4.6	0.0597	4.1	0.43	622	12	616	21	594	90	105
BF11-seq1-a41	9426	700	128	0.07	12923	0.1913	1.5	1.9942	3.0	0.0756	2.6	0.49	1128	15	1114	20	1084	52	104
BF11-seq1-a42	4363	170	62	0.72	4348	0.3019	1.8	4.3461	3.6	0.1044	3.2	0.48	1701	26	1702	31	1704	59	100
BF11-seq1-a43	2132	126	23	0.40	3080	0.1714	2.1	1.7087	3.9	0.0723	3.3	0.53	1020	19	1012	25	995	67	103
BF11-seq1-a44	2168	129	22	0.23	3063	0.1717	2.6	1.7564	4.9	0.0742	4.1	0.53	1021	24	1030	32	1047	83	98
BF11-seq1-a45	4667	106	43	0.86	4762	0.3173	1.5	4.4747	2.6	0.1023	2.1	0.58	1777	23	1726	21	1666	39	107
BF11-seq1-a46	16123	530	138	0.19	20158	0.2592	2.1	2.9593	2.8	0.0828	1.8	0.75	1486	27	1397	21	1265	36	117
BF11-seq1-a47	2090	116	27	0.98	2926	0.1741	2.3	1.7906	5.4	0.0746	4.9	0.42	1035	22	1042	36	1057	99	98
BF11-seq1-a48	951	51	10	0.34	1332	0.1772	2.2	1.8291	4.4	0.0749	3.9	0.49	1052	21	1056	29	1065	77	99
BF11-seq1-a49	15549	510	188	0.55	15246	0.3457	1.9	5.0767	2.6	0.1065	1.7	0.76	1914	32	1832	22	1741	31	110
BF11-seq1-a50	21703	202	151	0.32	12632	0.7089	2.2	17.5216	2.7	0.1793	1.6	0.81	3454	59	2964	26	2646	26	131
BF11-seq1-a51	9645	96	62	0.22	4962	0.5864	2.3	16.4689	3.2	0.2037	2.1	0.73	2975	55	2904	31	2856	35	104
BF11-seq1-a52	14593	902	173	0.38	23218	0.1823	1.2	1.6520	2.1	0.0657	1.7	0.56	1080	12	990	13	797	36	135
BF11-seq1-a53	11332	489	154	0.51	13047	0.2815	1.7	3.5221	2.8	0.0908	2.2	0.61	1599	24	1532	22	1442	42	111
BF11-seq1-a54	1780	59	22	0.55	1747	0.3279	1.4	4.8269	4.4	0.1068	4.2	0.32	1828	23	1790	38	1745	77	105
BF11-seq1-a55	531	27	5	0.29	727	0.1957	3.4	2.0519	8.7	0.0760	8.0	0.39	1152	36	1133	61	1096	160	105
BF11-seq1-a56	2046	106	21	0.32	2814	0.1889	2.0	1.9702	4.4	0.0756	3.9	0.45	1115	20	1105	30	1086	78	103
BF11-seq1-a57	16870	112	70	0.36	8709	0.5364	1.9	14.9638	2.7	0.2023	2.0	0.68	2768	42	2813	26	2845	32	97
BF11-seq1-a58	14656	269	102	0.37	13559	0.3419	1.9	5.3013	2.5	0.1125	1.7	0.76	1896	32	1869	22	1840	30	103
BF11-seq1-a59	1567	84	16	0.22	2143	0.1841	1.6	1.9315	4.4	0.0761	4.2	0.35	1089	16	1092	30	1098	83	99
BF11-seq1-a60	3947	113	40	0.78	4344	0.2891	1.5	3.7805	2.8	0.0949	2.4	0.55	1637	22	1589	23	1525	44	107
BF11-seq2-b01	2363	84	22	0.34	2810	0.2396	1.5	2.9205	4.6	0.0884	4.3	0.33	1384	19	1387	35	1392	83	99
BF11-seq2-b02	3331	92	26	0.22	3591	0.2777	1.7	3.6908	3.7	0.0964	3.3	0.45	1580	23	1569	30	1555	62	102
BF11-seq2-b03	14212	468	136	0.29	17748	0.2811	1.4	3.2304	2.4	0.0834	1.9	0.61	1597	20	1464	19	1277	37	125
BF11-seq2-b04	2888	120	30	0.59	3726	0.2165	1.6	2.4104	3.9	0.0807	3.6	0.40	1264	18	1246	28	1215	70	104
BF11-seq2-b05	4859	119	44	0.58	4988	0.3146	1.7	4.4065	3.0	0.1016	2.5	0.55	1763	26	1714	25	1653	47	107
BF11-seq2-b06	16418	526	190	0.33	16660	0.3389	1.5	4.7934	1.9	0.1026	1.3	0.76	1881	24	1784	16	1671	23	113
BF11-seq2-b07	9628	79	60	0.57	5205	0.6404	2.6	16.9723	3.3	0.1922	2.0	0.79	3190	66	2933	32	2761	34	116
BF11-seq2-b08	7930	364	103	0.26	9104	0.2706	1.7	3.3921	2.7	0.0909	2.1	0.61	1544	23	1503	21	1445	41	107
BF11-seq2-b09	891	78	15	0.43	1249	0.1718	3.0	1.7628	6.0	0.0744	5.2	0.49	1022	28	1032	40	1053	105	97
BF11-seq2-b10	4215	113	48	0.71	3700	0.3569	1.4	5.6575	25.4	0.1150	25.4	0.06	1967	24	1925	247	1879	458	105
BF11-seq2-b11	1285	91	16	0.25	1746	0.1728	2.1	1.7945	5.8	0.0753	5.4	0.36	1028	20	1043	38	1077	108	95
BF11-seq2-b12	5276	184	66	0.45	5255	0.3260	1.1	4.7117	2.9	0.1048	2.6	0.39	1819	18	1769	24	1711	48	106
BF11-seq2-b13	809	36	8	0.29	1028	0.2108	2.1	2.3872	5.7	0.0821	5.3	0.37	1233	24	1239	42	1249	103	99
BF11-seq2-b14	6153	311	77	0.57	4021	0.2303	13.7	3.4047	14.0	0.1072	2.6	0.98	1336	168	1505	116	1753	47	76
BF11-seq2-b15	2167	60	19	0.60	2435	0.2630	1.5	3.4028	5.1	0.0938	4.9	0.29	1505	20	1505	41	1505	92	100
BF11-seq2-b16	1751	59	15	0.26	2106	0.2387	2.0	2.8478	4.2	0.0865	3.7	0.48	1380	25	1368	32	1350	71	102

BF11-seq2-b17	3837	98	34	0.63	3967	0.2964	2.1	4.1173	3.2	0.1008	2.4	0.65	1673	31	1658	27	1638	45	102
BF11-seq2-b18	3508	140	32	0.21	4371	0.2217	1.7	2.5545	3.2	0.0836	2.7	0.52	1291	19	1288	24	1283	53	101
BF11-seq2-b19	1639	69	15	0.26	2073	0.2117	1.5	2.3877	4.3	0.0818	4.0	0.34	1238	17	1239	31	1241	79	100
BF11-seq2-b20	1107	55	12	0.52	1494	0.1844	1.7	1.9560	5.0	0.0769	4.7	0.34	1091	17	1101	34	1119	94	97
BF11-seq2-b21	1064	42	10	0.56	1305	0.2059	1.6	2.4091	5.6	0.0849	5.4	0.28	1207	17	1245	41	1312	105	92
BF11-seq2-b22	18625	462	189	1.38	19443	0.2923	3.0	4.0208	11.2	0.0998	10.8	0.27	1653	44	1638	96	1620	202	102
BF11-seq2-b23	1756	35	20	1.84	1634	0.3488	4.2	5.4078	6.4	0.1125	4.9	0.65	1929	70	1886	57	1839	89	105
BF11-seq2-b24	24568	166	144	1.20	13427	0.6198	2.9	16.3151	3.4	0.1909	1.8	0.85	3109	71	2895	33	2750	29	113
BF11-seq2-b25	703	37	8	0.41	963	0.1900	2.1	2.0015	6.5	0.0764	6.1	0.32	1121	21	1116	45	1106	123	101
BF11-seq2-b26	3684	88	31	0.51	3828	0.3070	1.6	4.2184	3.4	0.0996	3.0	0.47	1726	24	1678	28	1617	55	107
BF11-seq2-b27	4958	101	38	0.35	4759	0.3495	1.3	5.2341	2.8	0.1086	2.4	0.47	1932	22	1858	24	1777	45	109
BF11-seq2-b28	13072	306	123	0.77	14097	0.3333	1.5	4.4384	2.4	0.0966	1.8	0.63	1854	24	1720	20	1559	35	119
BF11-seq2-b29	2722	119	26	0.31	3595	0.2036	1.9	2.2117	4.1	0.0788	3.7	0.46	1195	20	1185	29	1167	72	102
BF11-seq2-b30	10452	118	83	0.84	5866	0.5458	1.9	13.9830	2.8	0.1858	2.1	0.67	2808	43	2749	27	2705	35	104
BF11-seq2-b31	13123	538	163	0.39	14508	0.2801	2.0	3.6208	2.6	0.0938	1.7	0.76	1592	28	1554	21	1503	31	106
BF11-seq2-b32	4562	236	62	0.28	5376	0.2551	2.5	3.1156	3.7	0.0886	2.7	0.68	1465	33	1437	29	1395	52	105
BF11-seq2-b33	9339	65	46	0.69	5238	0.5580	1.5	14.2928	3.0	0.1858	2.6	0.51	2858	35	2769	29	2705	42	106
BF11-seq2-b34	3618	163	35	0.26	4747	0.2089	1.6	2.2783	3.5	0.0791	3.1	0.46	1223	18	1206	25	1175	61	104
BF11-seq2-b35	14233	102	82	1.13	7957	0.5817	1.9	15.0129	2.6	0.1872	1.8	0.73	2956	45	2816	25	2718	29	109
BF11-seq2-b36	1231	98	20	0.41	1704	0.1893	2.4	1.9796	6.7	0.0758	6.2	0.36	1118	25	1109	46	1091	125	102
BF11-seq2-b37	1456	85	23	0.45	1840	0.2516	2.4	2.8755	4.6	0.0829	4.0	0.51	1447	31	1376	35	1267	77	114
BF11-seq2-b38	869	216	20	0.71	1581	0.0780	1.4	0.6135	5.9	0.0571	5.7	0.24	484	7	486	23	494	126	98
BF11-seq2-b39	840	37	9	0.65	1099	0.2158	1.6	2.3686	5.1	0.0796	4.8	0.31	1259	18	1233	37	1188	96	106
BF11-seq2-b40	1231	343	26	0.45	2239	0.0763	2.2	0.6059	7.1	0.0576	6.8	0.30	474	10	481	28	515	150	92
BF11-seq2-b41	2261	124	35	0.64	2711	0.2441	1.7	2.9455	4.2	0.0875	3.8	0.40	1408	21	1394	32	1372	74	103
BF11-seq2-b42	8281	298	83	0.24	8701	0.2654	2.7	3.6224	3.2	0.0990	1.9	0.82	1517	36	1554	26	1605	35	95
BF11-seq2-b43	4805	226	69	0.13	5329	0.3077	2.7	3.8898	4.5	0.0917	3.6	0.60	1729	40	1612	37	1461	68	118
BF11-seq2-b44	6127	650	120	0.73	9097	0.1564	1.1	1.5108	2.3	0.0701	2.0	0.48	937	9	935	14	930	41	101
BF11-seq2-b45	3302	446	71	0.49	3089	0.1590	14.4	1.7967	14.8	0.0819	3.2	0.98	951	129	1044	101	1244	62	76
BF11-seq2-b46	1694	39	13	0.52	1696	0.2994	1.7	4.3035	4.4	0.1042	4.0	0.38	1689	25	1694	37	1701	74	99
BF11-seq2-b47	1846	57	17	0.35	2114	0.2681	1.2	3.3620	3.7	0.0909	3.5	0.32	1531	16	1496	29	1445	66	106
BF11-seq2-b48	3214	83	38	1.42	3548	0.3253	1.4	4.2272	3.4	0.0943	3.1	0.43	1815	23	1679	28	1513	58	120
BF11-seq2-b49	633	101	10	0.56	1142	0.0840	1.4	0.6633	7.5	0.0573	7.4	0.18	520	7	517	31	503	163	103
BF11-seq2-b50	1534	214	20	0.79	1084	0.0746	2.6	0.7112	12.0	0.0692	11.8	0.22	464	12	545	52	903	242	51
BF11-seq2-b51	480	114	10	0.58	837	0.0782	2.2	0.6476	8.6	0.0600	8.3	0.26	486	10	507	35	605	179	80
BF11-seq2-b52	1010	42	14	0.42	1083	0.3121	2.8	4.1090	5.9	0.0955	5.2	0.48	1751	44	1656	50	1538	98	114
BF11-seq2-b53	848	210	17	0.24	1537	0.0832	1.3	0.6590	5.5	0.0574	5.4	0.23	515	6	514	23	508	118	101
BF11-seq2-b54	992	89	17	0.60	1456	0.1699	2.5	1.6642	5.0	0.0710	4.3	0.50	1012	24	995	32	958	89	106
BF11-seq2-b55	3497	151	47	0.45	3859	0.2817	1.5	3.6328	4.1	0.0935	3.8	0.37	1600	21	1557	33	1499	71	107
BF11-seq2-b56	1523	56	14	0.38	1855	0.2357	1.9	2.7918	5.0	0.0859	4.7	0.37	1364	23	1353	38	1336	91	102
BF11-seq2-b57	8879	273	94	0.08	8589	0.3500	2.3	5.1900	3.1	0.1075	2.1	0.74	1935	39	1851	27	1758	38	110
BF11-seq2-b58	7358	277	117	0.32	7242	0.4042	5.8	5.8984	6.3	0.1058	2.5	0.92	2188	109	1961	56	1729	45	127

BF11-seq2-b59	4071	115	43	0.35	3750	0.3466	1.5	5.3581	3.1	0.1121	2.7	0.48	1918	24	1878	26	1834	49	105
BF11-seq2-b60	10079	81	49	0.31	6133	0.5382	1.4	12.6940	2.4	0.1711	1.9	0.59	2776	32	2657	23	2568	32	108
BF11-seq3-c01	694	109	8	0.25	1254	0.0764	2.8	0.6067	7.0	0.0576	6.4	0.40	474	13	481	27	515	141	92
BF11-seq3-c02	3229	58	30	1.34	2917	0.3580	2.2	5.6564	3.7	0.1146	2.9	0.61	1973	38	1925	32	1873	52	105
BF11-seq3-c03	2884	59	24	0.68	2678	0.3463	1.7	5.3357	3.4	0.1118	2.9	0.51	1917	29	1875	29	1828	52	105
BF11-seq3-c04	17308	188	109	0.42	8736	0.5182	1.9	14.6792	2.5	0.2054	1.6	0.76	2692	41	2795	24	2870	26	94
BF11-seq3-c05	3769	199	38	0.04	5206	0.2048	1.8	2.1205	3.0	0.0751	2.4	0.60	1201	20	1156	21	1071	48	112
BF11-seq3-c06	2279	80	21	0.41	2652	0.2464	2.2	3.0161	4.2	0.0888	3.6	0.52	1420	28	1412	32	1399	68	101
BF11-seq3-c07	3918	181	38	0.31	5187	0.2008	1.9	2.1669	3.2	0.0782	2.6	0.60	1180	21	1170	23	1153	51	102
BF11-seq3-c08	17027	359	129	0.25	16768	0.3453	1.7	4.8937	2.4	0.1028	1.7	0.71	1912	28	1801	20	1675	31	114
BF11-seq3-c09	4229	325	58	0.07	1167	0.1825	3.9	1.9677	4.7	0.0782	2.6	0.83	1081	39	1105	32	1152	52	94
BF11-seq3-c10	8779	331	118	0.62	9236	0.3099	1.5	4.2140	2.3	0.0986	1.8	0.65	1740	23	1677	19	1598	33	109
BF11-seq3-c11	2053	43	16	0.38	1970	0.3330	1.8	4.9655	4.3	0.1081	3.9	0.41	1853	29	1813	37	1768	72	105
BF11-seq3-c12	932	11	6	0.61	693	0.4327	2.7	8.3585	6.4	0.1401	5.8	0.42	2318	52	2271	60	2229	101	104
BF11-seq3-c13	2666	72	22	0.57	2784	0.2672	2.1	3.5949	14.7	0.0976	14.5	0.14	1526	29	1548	124	1579	272	97
BF11-seq3-c14	7820	377	108	0.30	8987	0.2743	2.0	3.4380	2.9	0.0909	2.1	0.68	1563	27	1513	23	1444	40	108
BF11-seq3-c15	3488	239	55	0.39	4583	0.2143	2.3	2.3266	4.0	0.0787	3.3	0.57	1252	26	1220	29	1165	66	107
BF11-seq3-c16	10632	824	172	0.18	14834	0.2108	1.7	2.1595	2.5	0.0743	1.8	0.70	1233	20	1168	17	1050	36	117
BF11-seq3-c17	512	125	11	0.47	933	0.0797	3.2	0.6241	8.7	0.0568	8.1	0.37	495	15	492	34	482	178	103
BF11-seq3-c18	150	7	2	0.59	207	0.1868	3.4	1.9542	15.5	0.0759	15.1	0.22	1104	34	1100	110	1091	303	101
Sample BF12	Kiltorcan Formation					Location (decimal degrees) 52.462 7.1799 W						Datum: D_WGS_1984							
BF12-seq1-A01	3816	351	27	0.37	3690	0.0729	1.6	0.5758	3.1	0.0573	2.6	0.53	454	7	462	11	502	57	90
BF12-seq1-A02	35350	364	152	0.27	38121	0.4049	1.6	5.3650	2.0	0.0961	1.3	0.78	2192	29	1879	17	1550	24	141
BF12-seq1-A03	5589	92	23	0.32	6295	0.2332	1.8	2.9841	3.0	0.0928	2.4	0.60	1351	22	1404	23	1484	45	91
BF12-seq1-A04	2173	59	10	0.00	3021	0.1818	1.6	1.8805	3.7	0.0750	3.3	0.44	1077	16	1074	25	1069	66	101
BF12-seq1-A05	5919	155	29	0.09	8204	0.1928	1.6	1.9721	2.6	0.0742	2.0	0.61	1136	16	1106	17	1047	41	109
BF12-seq1-A06	14704	230	59	0.06	17757	0.2649	1.9	3.1600	2.7	0.0865	2.0	0.69	1515	25	1447	21	1350	38	112
BF12-seq1-A07	4512	80	20	0.22	5356	0.2395	1.9	2.8724	3.1	0.0870	2.4	0.60	1384	23	1375	23	1360	47	102
BF12-seq1-A08	27924	439	128	0.13	35226	0.2969	1.4	3.3825	1.7	0.0826	1.1	0.78	1676	20	1500	14	1260	22	133
BF12-seq1-A09	1204	61	12	0.40	1639	0.1880	1.6	1.9889	5.4	0.0767	5.2	0.29	1111	16	1112	37	1114	104	100
BF12-seq1-A10	2666	69	14	0.40	2472	0.1908	1.5	2.0314	3.9	0.0772	3.6	0.38	1126	16	1126	27	1127	73	100
BF12-seq1-A11	9001	131	40	0.41	10114	0.2760	2.0	3.5272	3.8	0.0927	3.3	0.52	1571	28	1533	31	1481	62	106
BF12-seq1-A12	5295	147	28	0.19	7432	0.1889	1.4	1.9340	2.6	0.0743	2.2	0.54	1115	14	1093	17	1049	44	106
BF12-seq1-A13	7787	228	40	0.23	11228	0.1699	1.5	1.6955	2.8	0.0724	2.4	0.52	1012	14	1007	18	996	49	102
BF12-seq1-A14	24381	857	178	0.34	8593	0.1888	4.0	4.0760	4.7	0.1566	2.4	0.85	1115	41	1650	39	2419	41	46
BF12-seq1-A15	1994	53	10	0.26	2747	0.1897	1.6	1.9803	3.9	0.0757	3.5	0.41	1120	16	1109	26	1088	71	103
BF12-seq1-A16	2067	57	12	0.57	2761	0.1775	1.7	1.9023	3.6	0.0777	3.1	0.47	1053	16	1082	24	1140	62	92
BF12-seq1-A17	1535	65	14	0.16	1954	0.2072	2.3	2.3360	4.0	0.0818	3.3	0.57	1214	25	1223	29	1240	65	98
BF12-seq1-A18	3254	198	37	0.03	4529	0.1979	3.4	2.0671	5.0	0.0758	3.6	0.69	1164	37	1138	35	1089	72	107
BF12-seq1-A19	9746	100	36	0.28	9041	0.3376	1.5	5.2302	2.2	0.1124	1.6	0.69	1875	25	1858	19	1838	29	102
BF12-seq1-A20	6315	193	55	0.23	7224	0.2790	1.9	3.5216	3.1	0.0916	2.4	0.63	1586	27	1532	25	1458	46	109

BF12-seq1-A21	7087	196	58	0.27	7942	0.2787	2.1	3.5751	3.2	0.0930	2.4	0.65	1585	29	1544	26	1489	46	106
BF12-seq1-A22	138	42	4	1.15	260	0.0730	3.6	0.5611	18.1	0.0558	17.7	0.20	454	16	452	68	443	395	103
BF12-seq1-A23	20512	144	95	0.35	11305	0.5679	1.8	14.8463	2.4	0.1896	1.7	0.73	2899	41	2805	23	2739	27	106
BF12-seq1-A24	2907	505	38	0.01	5381	0.0822	1.9	0.6428	3.7	0.0567	3.2	0.51	509	9	504	15	480	71	106
BF12-seq1-A25	9162	104	36	0.27	9010	0.3224	1.8	4.7164	2.8	0.1061	2.2	0.64	1801	28	1770	24	1734	40	104
BF12-seq1-A26	376	11	2	0.53	517	0.1864	1.9	1.9470	10.2	0.0757	10.0	0.19	1102	19	1097	71	1088	201	101
BF12-seq1-A27	483	14	3	0.47	669	0.1784	2.2	1.8706	9.1	0.0761	8.8	0.25	1058	22	1071	62	1096	177	97
BF12-seq1-A28	6452	167	60	0.81	6593	0.2872	2.0	3.9885	3.2	0.1007	2.6	0.61	1627	28	1632	27	1638	48	99
BF12-seq1-A29	34617	137	105	0.90	20043	0.5807	1.6	14.3104	2.2	0.1787	1.5	0.72	2952	37	2771	21	2641	25	112
BF12-seq1-A30	3763	53	17	0.50	3957	0.2790	2.0	3.8063	3.3	0.0990	2.7	0.59	1586	28	1594	27	1605	50	99
BF12-seq1-A31	1782	37	9	0.32	2146	0.2348	1.2	2.7971	4.6	0.0864	4.4	0.27	1359	15	1355	35	1347	85	101
BF12-seq1-A32	2868	98	24	0.20	3394	0.2431	1.6	2.9433	3.8	0.0878	3.4	0.43	1403	20	1393	29	1378	65	102
BF12-seq1-A33	439	14	4	1.47	624	0.1635	2.3	1.6620	10.0	0.0737	9.8	0.23	976	21	994	66	1034	197	94
BF12-seq1-A34	3791	92	20	0.34	4903	0.2036	1.7	2.2371	3.3	0.0797	2.9	0.51	1195	18	1193	24	1189	56	100
BF12-seq1-A35	10092	44	26	0.27	5936	0.5396	1.4	13.1991	2.4	0.1774	1.9	0.57	2782	31	2694	23	2629	32	106
BF12-seq1-A36	7411	192	42	0.33	10064	0.2051	1.4	2.1842	2.7	0.0772	2.3	0.50	1203	15	1176	19	1127	47	107
BF12-seq1-A37	26800	785	183	0.38	40349	0.2260	1.5	1.9978	2.2	0.0641	1.6	0.67	1313	17	1115	15	745	34	176
BF12-seq1-A38	2927	27	14	1.15	2446	0.3698	1.4	6.3137	3.6	0.1238	3.3	0.40	2028	25	2020	32	2012	58	101
BF12-seq1-A39	3396	178	37	0.38	4480	0.1948	2.0	2.1051	3.6	0.0784	3.0	0.55	1147	21	1150	25	1157	59	99
BF12-seq1-A40	1799	321	22	0.00	3285	0.0760	2.4	0.5988	4.3	0.0572	3.7	0.54	472	11	477	17	498	80	95
BF12-seq1-A41	12474	148	53	0.23	12381	0.3463	1.4	5.0148	2.2	0.1050	1.6	0.66	1917	24	1822	19	1715	30	112
BF12-seq1-A42	3358	198	38	0.30	4721	0.1833	1.6	1.8725	3.2	0.0741	2.7	0.51	1085	16	1071	21	1044	55	104
BF12-seq1-A43	6969	143	38	0.44	8463	0.2436	1.6	2.8834	2.9	0.0859	2.4	0.57	1405	21	1378	22	1335	46	105
BF12-seq1-A44	67090	286	214	0.64	42413	0.6255	1.3	14.2261	1.5	0.1649	0.8	0.85	3132	33	2765	15	2507	13	125
BF12-seq1-A45	6390	77	25	0.18	6257	0.3210	1.7	4.7109	2.9	0.1064	2.4	0.59	1795	27	1769	25	1739	44	103
BF12-seq1-A46	15955	183	86	1.10	15116	0.3541	1.4	5.3849	2.1	0.1103	1.6	0.68	1954	24	1882	18	1804	28	108
BF12-seq1-A47	738	17	4	0.59	950	0.2189	2.2	2.4392	6.7	0.0808	6.3	0.33	1276	25	1254	49	1217	124	105
BF12-seq1-A48	461	14	3	0.61	632	0.1844	3.1	1.9178	9.1	0.0754	8.5	0.34	1091	31	1087	62	1080	171	101
BF12-seq1-A49	4845	144	30	0.42	6674	0.1910	1.5	1.9919	2.4	0.0756	1.9	0.61	1127	15	1113	16	1085	38	104
BF12-seq1-A50	36968	166	98	0.40	22245	0.5118	1.4	12.2349	2.1	0.1734	1.6	0.67	2664	31	2623	20	2591	27	103
BF12-seq1-A51	3267	44	15	0.54	3232	0.3040	1.4	4.3865	3.3	0.1046	3.0	0.43	1711	22	1710	28	1708	55	100
BF12-seq1-A52	2099	76	13	0.32	3001	0.1646	1.8	1.6418	4.0	0.0723	3.6	0.45	982	17	986	26	995	73	99
BF12-seq1-A53	10576	337	71	0.47	15417	0.1944	1.3	1.9295	2.6	0.0720	2.2	0.51	1145	14	1091	17	986	45	116
BF12-seq1-A54	6305	127	32	0.25	7594	0.2470	1.5	2.9575	2.8	0.0868	2.4	0.54	1423	19	1397	22	1357	46	105
BF12-seq1-A55	42719	172	115	0.11	24654	0.6307	1.3	15.7269	1.8	0.1809	1.3	0.71	3152	32	2860	17	2661	21	118
BF12-seq1-A56	4678	163	57	0.27	4474	0.3312	1.6	4.9598	3.2	0.1086	2.8	0.49	1844	25	1812	27	1776	51	104
BF12-seq1-A57	5431	135	32	0.36	7056	0.2191	1.5	2.4246	2.6	0.0802	2.1	0.57	1277	17	1250	19	1203	42	106
BF12-seq1-A58	2512	9	6	0.26	1275	0.5705	2.0	16.0905	3.9	0.2046	3.3	0.53	2910	48	2882	38	2863	53	102
BF12-seq1-A59	1738	61	12	0.29	2501	0.1844	1.9	1.8473	4.7	0.0727	4.3	0.39	1091	19	1062	32	1005	88	109
BF12-seq1-A60	20051	210	84	0.10	18927	0.3994	1.3	6.0856	1.8	0.1105	1.2	0.73	2166	25	1988	16	1808	23	120
BF12-seq2-B01	11166	98	39	0.50	10772	0.3479	1.6	5.2100	2.2	0.1086	1.6	0.70	1924	26	1854	19	1776	29	108
BF12-seq2-B02	1227	32	6	0.30	1751	0.1786	2.3	1.8097	5.5	0.0735	5.0	0.42	1059	23	1049	37	1027	102	103

BF12-seq2-B03	9714	194	43	0.12	13076	0.2272	1.3	2.4362	2.0	0.0778	1.6	0.62	1320	15	1253	15	1141	32	116
BF12-seq2-B04	2751	28	10	0.67	2748	0.3074	1.1	4.4275	3.2	0.1045	3.1	0.33	1728	16	1718	27	1705	56	101
BF12-seq2-B05	699	34	8	1.06	968	0.1709	2.0	1.7834	5.9	0.0757	5.5	0.34	1017	19	1039	39	1086	111	94
BF12-seq2-B06	1113	27	5	0.23	1537	0.1769	1.6	1.8406	5.4	0.0755	5.1	0.29	1050	15	1060	36	1081	103	97
BF12-seq2-B07	9782	38	20	0.26	5819	0.4765	1.6	11.5384	2.6	0.1756	2.0	0.64	2512	34	2568	24	2612	33	96
BF12-seq2-B08	3755	73	17	0.46	4832	0.2120	1.3	2.3815	3.0	0.0815	2.7	0.43	1240	14	1237	21	1233	53	101
BF12-seq2-B09	4555	78	18	0.35	5595	0.2178	1.5	2.5625	3.0	0.0853	2.6	0.51	1270	18	1290	22	1323	50	96
BF12-seq2-B10	4107	102	19	0.25	5690	0.1827	1.1	1.8984	2.8	0.0754	2.6	0.37	1082	11	1081	19	1078	53	100
BF12-seq2-B11	6078	143	30	0.35	8552	0.1991	1.2	2.0435	2.4	0.0744	2.0	0.51	1170	13	1130	16	1054	41	111
BF12-seq2-B12	10849	33	25	0.77	5914	0.5831	1.2	15.3821	2.6	0.1913	2.3	0.47	2961	29	2839	25	2754	37	108
BF12-seq2-B13	847	16	4	0.37	1076	0.2087	2.6	2.3799	6.6	0.0827	6.1	0.39	1222	29	1237	48	1262	119	97
BF12-seq2-B16	1999	51	10	0.31	2650	0.1815	1.8	1.9793	4.9	0.0791	4.6	0.37	1075	18	1108	34	1174	90	92
BF12-seq2-B17	1021	35	8	0.44	1264	0.2165	2.6	2.5170	5.4	0.0843	4.8	0.48	1264	30	1277	40	1300	93	97
BF12-seq2-B18	4607	114	24	0.61	6560	0.1802	1.5	1.8308	3.3	0.0737	3.0	0.46	1068	15	1057	22	1033	60	103
BF12-seq2-B19	19016	57	38	0.43	9617	0.5711	1.5	15.5033	2.0	0.1969	1.2	0.78	2912	36	2847	19	2800	20	104
BF12-seq2-B20	5716	484	40	0.49	10695	0.0753	1.5	0.5817	2.6	0.0561	2.1	0.57	468	7	466	10	455	46	103
BF12-seq2-B21	10246	96	33	0.29	10298	0.3217	1.3	4.6239	2.3	0.1043	1.8	0.59	1798	21	1754	19	1701	34	106
BF12-seq2-B22	3461	87	16	0.25	4869	0.1755	1.6	1.8019	3.4	0.0745	3.0	0.47	1042	16	1046	23	1054	61	99
BF12-seq2-B23	2414	114	21	0.24	2730	0.1803	1.7	1.8742	3.8	0.0754	3.4	0.45	1069	17	1072	25	1079	68	99
BF12-seq2-B24	42331	149	103	0.74	25936	0.5498	1.1	12.9520	1.6	0.1709	1.1	0.68	2824	24	2676	15	2566	19	110
BF12-seq2-B25	1566	18	5	0.28	836	0.2879	2.1	4.3072	5.1	0.1085	4.7	0.41	1631	30	1695	43	1774	86	92
BF12-seq2-B26	6702	48	28	1.56	5651	0.3863	1.6	6.6316	3.1	0.1245	2.6	0.52	2105	28	2064	27	2022	47	104
BF12-seq2-B27	2902	72	14	0.30	3965	0.1802	1.4	1.8673	3.5	0.0752	3.2	0.40	1068	14	1070	23	1073	64	100
BF12-seq2-B28	7387	63	25	0.47	6858	0.3567	1.1	5.5521	2.4	0.1129	2.1	0.47	1967	20	1909	21	1846	39	107
BF12-seq2-B29	3224	81	16	0.44	4569	0.1863	1.3	1.8907	3.2	0.0736	2.9	0.40	1101	13	1078	21	1031	59	107
BF12-seq2-B30	20652	556	114	0.30	33189	0.2001	1.4	1.7955	2.3	0.0651	1.8	0.60	1176	15	1044	15	777	39	151
BF12-seq2-B31	5819	105	28	0.55	7349	0.2327	1.0	2.6539	2.8	0.0827	2.6	0.37	1348	13	1316	21	1263	50	107
BF12-seq2-B32	8791	96	34	0.52	8981	0.3076	1.4	4.3490	2.6	0.1026	2.1	0.56	1729	22	1703	21	1671	39	103
BF12-seq2-B33	9595	83	32	0.43	9111	0.3433	1.4	5.2133	2.1	0.1102	1.6	0.67	1902	23	1855	18	1802	28	106
BF12-seq2-B34	8149	41	22	0.55	5419	0.4573	2.1	9.9216	2.9	0.1574	2.0	0.72	2427	43	2428	27	2428	34	100
BF12-seq2-B35	2455	60	11	0.32	3433	0.1749	1.6	1.7901	3.9	0.0742	3.6	0.41	1039	16	1042	26	1048	72	99
BF12-seq2-B36	2288	55	12	0.42	3157	0.1945	1.1	2.0309	3.7	0.0757	3.6	0.28	1146	11	1126	26	1088	71	105
BF12-seq2-B37	3688	103	18	0.24	5416	0.1702	1.5	1.6734	3.2	0.0713	2.8	0.47	1013	14	998	20	967	57	105
BF12-seq2-B38	1265	32	6	0.56	1787	0.1696	1.2	1.7294	4.8	0.0740	4.6	0.25	1010	11	1020	31	1041	93	97
BF12-seq2-B39	10012	80	32	0.23	9212	0.3817	1.3	5.9877	1.9	0.1138	1.4	0.67	2084	22	1974	16	1861	25	112
BF12-seq2-B40	5568	88	27	0.68	6623	0.2584	1.2	3.1344	2.4	0.0880	2.1	0.50	1482	16	1441	19	1382	41	107
BF12-seq2-B41	1779	85	16	0.25	2504	0.1819	2.0	1.8688	4.9	0.0745	4.4	0.42	1077	20	1070	33	1056	89	102
BF12-seq2-B42	639	17	4	1.51	903	0.1832	2.5	1.8902	8.8	0.0748	8.4	0.28	1084	25	1078	60	1064	170	102
BF12-seq2-B43	38798	132	102	1.03	22820	0.5744	1.2	14.0984	2.0	0.1780	1.6	0.61	2926	29	2756	19	2635	27	111
BF12-seq2-B44	7565	76	27	0.49	7133	0.3059	1.7	4.6731	13.1	0.1108	13.0	0.13	1720	25	1762	116	1813	237	95
BF12-seq2-B45	5074	96	22	0.22	6593	0.2223	1.4	2.4788	2.9	0.0809	2.6	0.48	1294	17	1266	22	1218	51	106
BF12-seq2-B46	5782	207	45	0.09	7471	0.2221	1.9	2.4808	3.3	0.0810	2.7	0.57	1293	22	1266	24	1221	53	106

BF12-seq2-B47	7533	80	28	0.51	7645	0.3138	1.3	4.4741	2.4	0.1034	2.0	0.55	1760	21	1726	20	1686	37	104
BF12-seq2-B48	33689	153	110	1.23	19940	0.5237	4.0	12.7232	4.5	0.1762	2.1	0.88	2715	89	2659	43	2618	36	104
BF12-seq2-B49	2741	77	13	0.23	3294	0.1666	1.4	1.6788	3.6	0.0731	3.3	0.38	994	13	1001	23	1016	68	98
BF12-seq2-B50	711	16	3	0.03	951	0.1942	2.4	2.0847	6.3	0.0779	5.8	0.38	1144	26	1144	44	1143	116	100
BF12-seq2-B51	5015	110	28	1.11	3305	0.1880	1.7	1.9245	4.2	0.0742	3.8	0.41	1111	18	1090	28	1048	77	106
BF12-seq2-B52	1101	37	10	0.66	1369	0.2294	2.2	2.6708	6.0	0.0845	5.6	0.36	1331	26	1320	45	1303	109	102
BF12-seq2-B53	9292	200	42	0.30	12590	0.2024	1.1	2.1619	2.3	0.0775	2.0	0.46	1188	12	1169	16	1134	41	105
BF12-seq2-B54	3726	107	20	0.50	5462	0.1667	1.2	1.6466	3.1	0.0716	2.9	0.39	994	11	988	20	976	59	102
BF12-seq2-B55	7742	93	30	0.34	8286	0.3007	1.3	4.0644	2.4	0.0980	1.9	0.56	1695	20	1647	19	1587	36	107
BF12-seq2-B56	2214	81	18	0.13	2379	0.2231	2.8	2.9964	5.4	0.0974	4.7	0.51	1298	32	1407	42	1575	87	82
BF12-seq2-B57	1039	51	10	0.26	1484	0.1818	2.0	1.8328	5.8	0.0731	5.4	0.34	1077	20	1057	39	1017	110	106
BF12-seq2-B58	33257	117	70	0.47	18984	0.5022	2.5	12.7917	3.0	0.1847	1.6	0.84	2623	54	2664	29	2696	27	97
BF12-seq2-B59	904	31	7	0.25	1126	0.2222	3.0	2.5753	7.1	0.0840	6.4	0.42	1294	35	1294	53	1294	125	100
BF12-seq2-B60	54878	165	130	0.67	11926	0.6442	1.5	16.4580	2.2	0.1853	1.6	0.68	3206	38	2904	21	2701	26	119
BF12-seq3-C01	5419	50	20	0.67	5071	0.3275	1.2	5.0361	2.7	0.1115	2.5	0.43	1826	19	1825	23	1825	45	100
BF12-seq3-C02	8481	139	35	0.31	10216	0.2377	1.6	2.8414	2.7	0.0867	2.2	0.59	1374	20	1367	21	1354	43	102
BF12-seq3-C03	3305	69	15	0.28	4388	0.2041	1.0	2.2146	3.0	0.0787	2.8	0.34	1197	11	1186	21	1165	56	103
BF12-seq3-C04	3224	550	36	0.06	6033	0.0698	1.6	0.5365	3.1	0.0558	2.6	0.54	435	7	436	11	443	58	98
BF12-seq3-C05	5177	73	23	0.77	5827	0.2595	1.5	3.3160	2.8	0.0927	2.4	0.52	1487	19	1485	22	1482	46	100
BF12-seq3-C06	299	21	2	0.55	545	0.0805	2.7	0.6331	11.7	0.0571	11.4	0.23	499	13	498	47	494	252	101
BF12-seq3-C07	27467	417	183	0.21	12273	0.4018	1.3	9.3214	2.3	0.1682	1.9	0.57	2177	25	2370	22	2540	32	86
BF12-seq3-C08	6586	93	27	0.31	7572	0.2696	1.3	3.3566	2.5	0.0903	2.2	0.52	1539	18	1494	20	1432	41	107
BF12-seq3-C09	7084	192	35	0.22	10221	0.1783	1.5	1.7826	2.6	0.0725	2.1	0.58	1058	15	1039	17	1000	43	106
BF12-seq3-C10	6412	129	30	0.38	8408	0.2183	1.0	2.3973	2.3	0.0797	2.1	0.41	1273	11	1242	17	1188	42	107
BF12-seq3-C11	53894	198	145	0.70	32837	0.6104	1.4	14.5364	2.1	0.1727	1.5	0.68	3071	35	2785	20	2584	26	119
BF12-seq3-C12	5356	137	25	0.27	7531	0.1782	2.9	1.8346	3.6	0.0746	2.3	0.79	1057	28	1058	24	1059	45	100
BF12-seq3-C13	16198	162	60	0.38	16497	0.3394	1.0	4.8165	1.9	0.1029	1.6	0.53	1884	16	1788	16	1678	30	112
BF12-seq3-C14	15926	196	63	0.35	17380	0.2978	1.4	3.9432	2.1	0.0960	1.6	0.65	1680	21	1623	17	1549	30	108
BF12-seq3-C15	7372	45	26	0.43	3627	0.4907	1.8	14.3652	2.8	0.2123	2.1	0.66	2574	39	2774	27	2923	34	88
BF12-seq3-C16	344	28	6	0.80	490	0.1757	3.1	1.7783	12.8	0.0734	12.5	0.25	1043	30	1038	87	1026	252	102
BF12-seq3-C17	1127	229	14	0.32	2086	0.0586	2.1	0.4588	5.5	0.0568	5.1	0.38	367	8	383	18	485	112	76
BF12-seq3-C18	3443	87	25	0.22	3791	0.2805	1.3	3.6649	3.0	0.0948	2.7	0.44	1594	18	1564	24	1524	50	105
BF12-seq3-C19	1693	62	15	0.39	2123	0.2221	2.1	2.5656	4.8	0.0838	4.3	0.44	1293	25	1291	36	1288	84	100
BF12-seq3-C20	9335	195	41	0.22	12644	0.2071	1.0	2.2074	2.1	0.0773	1.8	0.47	1213	11	1183	15	1129	36	107
BF12-seq3-C21	906	78	15	0.48	1312	0.1757	1.9	1.7384	6.9	0.0718	6.7	0.27	1043	18	1023	46	980	136	107
BF12-seq3-C22	3490	142	31	0.25	4596	0.2138	2.1	2.3442	3.8	0.0795	3.1	0.57	1249	24	1226	27	1185	61	105
BF12-seq3-C23	2720	61	14	0.49	3600	0.1993	1.5	2.1689	4.1	0.0789	3.8	0.36	1172	16	1171	29	1170	76	100
BF12-seq3-C24	2650	78	13	0.20	3820	0.1710	2.0	1.6992	3.8	0.0721	3.2	0.54	1018	19	1008	24	987	65	103
BF12-seq3-C25	13232	45	29	0.41	7158	0.5387	1.3	14.1944	2.3	0.1911	1.9	0.56	2778	29	2763	22	2752	31	101
BF12-seq3-C26	23967	254	94	0.29	25627	0.3542	1.8	4.8094	2.5	0.0985	1.8	0.71	1955	30	1787	21	1595	33	123
BF12-seq3-C27	1022	27	5	0.26	1428	0.1822	1.9	1.8732	5.0	0.0745	4.6	0.38	1079	19	1072	34	1056	94	102
BF12-seq3-C28	2629	58	12	0.24	3416	0.2054	1.7	2.2665	3.7	0.0800	3.3	0.45	1204	18	1202	27	1198	65	101

BF12-seq3-C29	5498	99	44	0.86	5231	0.3531	1.6	5.3541	2.9	0.1100	2.5	0.55	1949	27	1878	25	1799	45	108
BF12-seq3-C30	9595	243	50	0.32	14077	0.1978	1.3	1.9512	2.8	0.0716	2.5	0.47	1163	14	1099	19	973	51	120
BF12-seq3-C31	1251	15	5	0.28	1258	0.2966	1.9	4.2443	4.2	0.1038	3.7	0.45	1675	28	1683	35	1693	69	99
BF12-seq3-C32	1137	30	6	0.64	1585	0.1760	2.2	1.8138	5.5	0.0748	5.0	0.40	1045	21	1050	36	1062	101	98
BF12-seq3-C33	6101	126	30	0.38	7772	0.2191	3.1	2.4826	3.6	0.0822	1.9	0.85	1277	36	1267	27	1250	38	102
BF12-seq3-C34	7588	80	30	0.37	7557	0.3419	6.2	5.0030	7.3	0.1061	3.9	0.85	1896	103	1820	64	1734	71	109
BF12-seq3-C35	12562	312	71	0.57	18200	0.2029	1.2	2.0266	2.2	0.0724	1.8	0.56	1191	13	1124	15	998	37	119
BF12-seq3-C36	6508	160	30	0.22	8911	0.1821	0.9	1.9193	2.3	0.0765	2.1	0.40	1078	9	1088	16	1107	42	97
BF12-seq3-C37	45660	183	107	0.42	20770	0.5115	1.5	12.8805	2.2	0.1826	1.6	0.69	2663	32	2671	21	2677	26	99
BF12-seq3-C38	874	22	4	0.41	1220	0.1801	1.8	1.8605	5.5	0.0749	5.2	0.33	1067	18	1067	37	1066	104	100
BF12-seq3-C39	4184	58	17	0.32	4603	0.2686	2.0	3.5142	3.2	0.0949	2.5	0.63	1534	28	1530	26	1526	47	100
BF12-seq3-C40	11144	49	27	0.36	6688	0.4865	1.4	11.6926	2.3	0.1743	1.8	0.62	2556	30	2580	21	2599	30	98
BF12-seq3-C41	1010	25	8	0.56	1069	0.2823	3.3	3.8635	6.0	0.0993	5.1	0.54	1603	46	1606	50	1610	94	100
BF12-seq3-C42	2884	62	14	0.40	3708	0.2102	1.7	2.3558	3.9	0.0813	3.5	0.44	1230	19	1229	28	1228	69	100
BF12-seq3-C43	3502	27	19	1.01	2008	0.5124	1.7	12.9792	4.0	0.1837	3.6	0.43	2667	38	2678	38	2687	59	99
Sample BF13 fraction			Harrylock Formation			Location (decimal degrees) 52.161 6.88265 W						Datum: D_WGS_1984							
BF13-60-90-seq1-	44075	202	53	0.38	49870	0.2416	2.3	3.0004	2.8	0.0901	1.6	0.81	1395	29	1408	22	1427	31	98
BF13-60-90-seq1-	22244	381	36	0.09	37487	0.0995	1.6	0.8311	2.5	0.0606	1.9	0.63	612	9	614	12	624	42	98
BF13-60-90-seq1-	39400	84	38	0.46	31062	0.3883	1.6	6.9203	2.1	0.1292	1.4	0.76	2115	30	2101	19	2088	24	101
BF13-60-90-seq1-	47193	132	41	0.51	2007	0.2606	3.7	4.6207	3.9	0.1286	1.2	0.95	1493	49	1753	33	2079	21	72
BF13-60-90-seq1-	12923	25	12	0.65	9867	0.4050	1.5	7.4514	2.5	0.1334	2.0	0.61	2192	28	2167	22	2144	34	102
BF13-60-90-seq1-	9656	77	18	0.14	8816	0.2349	1.8	2.7229	2.9	0.0841	2.3	0.61	1360	22	1335	22	1294	45	105
BF13-60-90-seq1-	2216	38	5	0.51	1329	0.1101	1.9	0.8404	5.4	0.0553	5.1	0.34	674	12	619	25	426	113	158
BF13-60-90-seq1-	18536	51	26	0.45	13992	0.4397	1.6	8.1806	5.9	0.1349	5.7	0.27	2349	31	2251	55	2163	100	109
BF13-60-90-seq1-	66746	187	84	0.95	60826	0.3277	1.4	5.0426	2.0	0.1116	1.4	0.71	1827	23	1827	17	1826	26	100
BF13-60-90-seq1-	5355	90	11	0.73	9025	0.1037	1.8	0.8654	3.4	0.0605	2.9	0.53	636	11	633	16	622	63	102
BF13-60-90-seq1-	72337	131	64	0.35	36289	0.4381	2.0	8.1174	2.6	0.1344	1.7	0.76	2342	39	2244	24	2156	30	109
BF13-60-90-seq1-	52555	44	32	0.51	16628	0.5928	1.7	17.4238	2.2	0.2132	1.5	0.75	3001	40	2958	22	2930	24	102
BF13-60-90-seq1-	34324	126	41	0.31	35262	0.2988	1.7	4.0853	2.1	0.0991	1.3	0.80	1686	26	1651	18	1608	24	105
BF13-60-90-seq1-	93043	290	45	0.52	684	0.1397	3.2	2.2892	3.6	0.1189	1.7	0.88	843	25	1209	26	1940	31	43
BF13-60-90-seq1-	8027	193	16	0.38	14321	0.0765	1.3	0.5986	2.8	0.0567	2.5	0.47	475	6	476	11	482	55	99
BF13-60-90-seq1-	4447	164	14	0.41	8196	0.0798	1.7	0.6085	4.1	0.0553	3.8	0.42	495	8	483	16	425	84	116
BF13-60-90-seq1-	4223	164	13	0.40	7849	0.0706	1.5	0.5353	4.6	0.0550	4.4	0.33	440	6	435	17	411	98	107
BF13-60-90-seq1-	22615	75	36	0.58	18024	0.3905	1.6	6.9020	2.2	0.1282	1.6	0.72	2125	29	2099	20	2073	28	103
BF13-60-90-seq1-	-	-	-	-	-	-	-	-	-	-	-	-	-	-	-	-	-	-	-
BF13-60-90-seq1-	11713	289	27	0.59	11586	0.0799	1.3	0.6339	4.1	0.0575	3.8	0.32	496	6	499	16	511	84	97
BF13-60-90-seq1-	4721	85	9	0.52	8137	0.0923	2.1	0.7580	5.0	0.0596	4.6	0.43	569	12	573	22	588	99	97
BF13-60-90-seq1-	2262	38	5	0.56	3965	0.1178	1.9	0.9401	4.7	0.0579	4.2	0.42	718	13	673	23	525	93	137
BF13-60-90-seq1-	5402	104	11	0.37	9327	0.0962	1.6	0.7832	3.2	0.0591	2.8	0.49	592	9	587	14	570	61	104
BF13-60-90-seq1-	25841	141	46	0.28	25893	0.3025	1.6	4.2338	2.3	0.1015	1.7	0.67	1704	23	1681	19	1652	32	103
BF13-60-90-seq1-	11942	205	31	1.19	20231	0.1050	1.1	0.8699	2.6	0.0601	2.3	0.44	643	7	636	12	607	50	106

BF13-60-90-seq1-	90326	103	61	0.30	50642	0.5269	1.5	13.2001	2.0	0.1817	1.3	0.77	2728	35	2694	19	2668	21	102
BF13-60-90-seq1-	16489	56	30	0.81	13302	0.4256	1.4	7.4251	2.2	0.1265	1.7	0.64	2286	27	2164	20	2050	30	111
BF13-60-90-seq1-	6542	30	9	0.39	7459	0.2700	1.7	3.3215	3.6	0.0892	3.2	0.46	1541	23	1486	29	1409	61	109
BF13-60-90-seq1-	5047	96	10	0.55	9189	0.0910	2.4	0.6964	4.2	0.0555	3.4	0.58	561	13	537	18	432	76	130
BF13-60-90-seq1-	47808	159	53	0.22	45409	0.3196	1.5	4.7275	2.1	0.1073	1.4	0.73	1788	23	1772	17	1753	26	102
BF13-60-90-seq1-	34736	131	45	0.31	35797	0.3228	1.4	4.3982	1.9	0.0988	1.3	0.73	1803	22	1712	16	1602	25	113
BF13-60-90-seq1-	29860	190	44	0.23	37627	0.2222	1.6	2.4804	2.2	0.0810	1.4	0.75	1294	19	1266	16	1220	28	106
BF13-60-90-seq1-	87550	159	99	0.22	48772	0.5602	1.3	14.1212	1.9	0.1828	1.4	0.68	2867	30	2758	18	2679	23	107
BF13-60-90-seq1-	8769	84	21	0.34	10913	0.2300	2.0	2.5908	2.8	0.0817	2.0	0.70	1334	24	1298	21	1239	40	108
BF13-60-90-seq1-	11894	38	18	0.47	9439	0.4192	1.7	7.4092	2.7	0.1282	2.1	0.65	2257	33	2162	24	2073	36	109
BF13-60-90-seq1-	25038	147	40	0.58	29994	0.2349	1.6	2.7520	2.4	0.0850	1.7	0.69	1360	20	1343	18	1315	33	103
BF13-60-90-seq1-	94815	242	97	0.43	77965	0.3516	1.4	6.0040	1.6	0.1238	0.9	0.85	1942	23	1976	14	2012	15	97
BF13-60-90-seq1-	8129	162	16	0.19	14150	0.0986	1.7	0.7945	2.7	0.0585	2.1	0.63	606	10	594	12	547	46	111
BF13-60-90-seq1-	156100	187	110	0.31	59827	0.5131	1.5	12.7287	2.0	0.1799	1.3	0.76	2670	33	2660	19	2652	21	101
BF13-60-90-seq1-	4365	82	9	0.36	7665	0.1059	1.6	0.8494	3.7	0.0581	3.4	0.44	649	10	624	18	535	73	121
BF13-60-90-seq1-	9929	52	14	0.40	11468	0.2531	1.5	3.0686	2.4	0.0879	1.8	0.64	1454	20	1425	18	1381	35	105
BF13-60-90-seq1-	29036	88	34	0.35	25800	0.3531	1.9	5.5816	2.3	0.1146	1.3	0.81	1950	31	1913	20	1874	24	104
BF13-60-90-seq1-	23885	266	57	0.28	31395	0.2049	1.4	2.1890	1.9	0.0775	1.3	0.71	1201	15	1178	13	1134	27	106
BF13-60-90-seq1-	8610	190	26	0.31	14027	0.1330	1.7	1.1454	2.7	0.0624	2.1	0.63	805	13	775	14	689	44	117
BF13-60-90-seq1-	13916	415	32	0.16	532	0.0734	2.1	0.5704	6.5	0.0564	6.1	0.33	456	9	458	24	467	136	98
BF13-60-90-seq1-	95789	221	107	0.57	73940	0.4020	1.8	7.3055	2.2	0.1318	1.3	0.81	2178	33	2149	20	2122	22	103
BF13-60-90-seq1-	11150	77	19	0.60	14386	0.2125	1.7	2.3116	2.8	0.0789	2.2	0.62	1242	20	1216	20	1169	43	106
BF13-60-90-seq1-	2126	15	3	0.32	2918	0.2261	2.4	2.3433	6.8	0.0752	6.4	0.36	1314	29	1226	50	1073	128	122
BF13-60-90-seq1-	4219	78	10	0.55	7167	0.1115	2.3	0.9234	4.4	0.0601	3.8	0.52	681	15	664	22	606	81	112
BF13-60-90-seq1-	12468	384	28	0.23	16433	0.0704	1.7	0.5362	3.0	0.0553	2.4	0.58	438	7	436	11	423	54	104
BF13-60-90-seq1-	50059	229	92	0.49	50803	0.3557	2.0	4.9166	2.5	0.1003	1.5	0.80	1962	35	1805	22	1629	28	120
BF13-60-90-seq1-	#DIV/0!	#DIV/0!	#DIV/0!	#####	#DIV/0!	0.0000	####	#DIV/0!	#####	#DIV/0!	####	#####	0	#####	######	#####	#NUM!	####	#NUM!
BF13-90-180-seq1	2649	64	6	0.15	4817	0.1000	2.5	0.7747	4.1	0.0562	3.3	0.61	614	15	582	18	461	72	133
BF13-90-180-seq1	2878	105	8	0.41	5799	0.0717	1.2	0.5007	5.2	0.0507	5.1	0.23	446	5	412	18	225	117	198
BF13-90-180-seq1	341	10	1	0.45	566	0.1104	4.9	0.9306	28.3	0.0611	27.8	0.17	675	31	668	149	643	598	105
BF13-90-180-seq1	1729	38	5	0.85	3200	0.1046	2.1	0.8097	8.7	0.0561	8.5	0.24	642	13	602	40	457	188	140
BF13-90-180-seq1	2123	47	6	0.67	3869	0.1012	1.4	0.7833	5.0	0.0561	4.8	0.27	622	8	587	23	457	107	136
BF13-90-180-seq1	4150	93	9	0.28	7215	0.0957	1.6	0.7753	4.4	0.0587	4.1	0.37	589	9	583	20	558	89	106
BF13-90-180-seq1	17716	76	29	1.26	665	0.2504	2.2	3.2296	5.4	0.0935	4.9	0.42	1441	29	1464	43	1499	92	96
BF13-90-180-seq1	3436	83	8	0.36	6250	0.0931	1.6	0.7216	3.7	0.0562	3.3	0.44	574	9	552	16	460	73	125
BF13-90-180-seq1	4166	97	11	0.66	7591	0.0958	1.8	0.7402	3.2	0.0560	2.6	0.56	590	10	563	14	454	58	130
BF13-90-180-seq1	4435	94	12	0.81	7953	0.1017	1.2	0.7966	4.2	0.0568	4.0	0.30	624	7	595	19	484	88	129
BF13-90-180-seq1	14149	50	19	0.57	13536	0.3245	2.1	4.8043	3.0	0.1074	2.1	0.70	1812	33	1786	25	1755	39	103
BF13-90-180-seq1	201963	288	180	1.00	50877	0.4310	1.7	10.8012	2.2	0.1818	1.3	0.79	2310	33	2506	20	2669	22	87
BF13-90-180-seq1	48796	254	79	0.53	12062	0.2696	1.5	3.5056	2.3	0.0943	1.7	0.66	1539	21	1528	18	1514	32	102
BF13-90-180-seq1	3938	79	10	0.71	6725	0.1056	1.5	0.8709	4.3	0.0598	4.0	0.34	647	9	636	20	596	87	109
BF13-90-180-seq1	57328	78	53	0.73	32039	0.5318	1.1	13.4014	1.9	0.1828	1.5	0.57	2749	24	2708	18	2678	26	103

BF13-90-180-seq1	44984	172	61	0.46	43108	0.3179	0.8	4.6771	1.5	0.1067	1.2	0.57	1780	13	1763	12	1744	22	102
BF13-90-180-seq1	2203	43	5	0.26	3675	0.1102	1.7	0.9348	5.1	0.0615	4.8	0.33	674	11	670	25	657	102	103
BF13-90-180-seq1	9390	179	21	0.51	4106	0.1050	1.3	0.8795	2.9	0.0608	2.6	0.46	644	8	641	14	630	56	102
BF13-90-180-seq1	64482	93	54	0.27	37017	0.5186	1.2	12.7453	1.8	0.1782	1.3	0.69	2693	27	2661	17	2637	22	102
BF13-90-180-seq1	5692	120	16	0.89	9972	0.1060	1.5	0.8511	3.1	0.0582	2.7	0.49	649	9	625	15	539	59	121
BF13-90-180-seq1	13666	31	14	0.36	10901	0.4128	1.5	7.4530	2.4	0.1309	1.9	0.62	2228	28	2167	22	2111	33	106
BF13-90-180-seq1	5610	111	13	0.40	6549	0.1117	1.6	0.9037	3.7	0.0587	3.3	0.44	682	11	654	18	556	73	123
BF13-90-180-seq1	1848	36	4	0.43	3234	0.1142	1.4	0.9144	6.3	0.0581	6.2	0.22	697	9	659	31	533	135	131
BF13-90-180-seq1	9702	177	21	0.27	15770	0.1163	1.2	1.0087	2.3	0.0629	1.9	0.51	709	8	708	12	705	41	101
BF13-90-180-seq1	1443	28	3	0.51	2417	0.1069	1.9	0.8967	8.2	0.0608	8.0	0.23	655	12	650	40	633	173	103
BF13-90-180-seq1	12947	167	24	0.08	19808	0.1495	1.6	1.3777	2.7	0.0668	2.1	0.61	898	14	879	16	832	44	108
BF13-90-180-seq1	6375	123	15	0.35	10971	0.1114	1.5	0.9121	3.2	0.0594	2.8	0.46	681	9	658	15	581	61	117
BF13-90-180-seq1	1782	36	5	0.62	3146	0.1101	1.9	0.9366	14.0	0.0617	13.9	0.14	673	12	671	71	664	298	101
BF13-90-180-seq1	13877	32	15	0.43	10714	0.4055	1.9	7.3968	3.2	0.1323	2.5	0.61	2194	36	2161	29	2129	44	103
BF13-90-180-seq1	11969	348	29	0.38	21523	0.0774	1.1	0.6119	2.7	0.0573	2.5	0.39	481	5	485	11	505	55	95
BF13-90-180-seq1	1967	48	5	0.44	3558	0.0942	2.0	0.7687	12.2	0.0592	12.0	0.16	580	11	579	55	575	261	101
BF13-90-180-seq1	25619	181	41	0.26	15828	0.2191	1.0	2.5216	2.1	0.0835	1.8	0.49	1277	12	1278	15	1281	36	100
BF13-90-180-seq1	5810	141	14	0.27	7800	0.0956	0.9	0.7535	2.7	0.0571	2.6	0.32	589	5	570	12	497	57	119
BF13-90-180-seq1	874	17	2	0.90	1515	0.1142	2.1	0.9799	13.1	0.0622	12.9	0.16	697	14	694	68	682	276	102
BF13-90-180-seq1	2087	46	5	0.47	3763	0.1020	2.0	0.7828	7.1	0.0557	6.9	0.28	626	12	587	32	440	153	142
BF13-90-180-seq1	976	21	2	0.43	1669	0.0961	2.5	0.7847	9.2	0.0592	8.9	0.27	591	14	588	42	576	193	103
BF13-90-180-seq1	33904	88	39	0.41	26846	0.3981	1.8	7.0550	2.4	0.1285	1.6	0.75	2160	34	2118	22	2078	28	104
BF13-90-180-seq1	25698	156	41	0.22	16138	0.2601	2.0	3.3612	2.6	0.0937	1.6	0.77	1490	27	1495	20	1503	31	99
BF13-90-180-seq1	48048	137	60	0.43	40001	0.3904	1.2	6.6077	1.5	0.1228	0.9	0.79	2125	22	2060	14	1997	17	106
BF13-90-180-seq1	72458	111	57	0.27	39769	0.4584	1.4	11.7112	1.9	0.1853	1.2	0.76	2432	29	2582	18	2701	20	90
BF13-90-180-seq1	332827	366	234	0.31	155986	0.5438	1.7	16.3516	1.8	0.2181	0.8	0.90	2799	38	2898	18	2967	13	94
BF13-90-180-seq1	5937	109	13	0.34	9943	0.1164	1.0	0.9875	3.1	0.0615	2.9	0.33	710	7	697	16	657	63	108
BF13-90-180-seq1	29972	38	28	0.95	16161	0.5240	1.3	13.9132	2.4	0.1926	2.0	0.53	2716	28	2744	23	2764	33	98
BF13-90-180-seq1	3570	59	10	1.06	5907	0.1314	2.2	1.1045	3.8	0.0610	3.1	0.58	796	16	756	20	639	66	125
BF13-90-180-seq1	1932	59	7	0.50	3293	0.1061	2.0	0.8924	8.2	0.0610	7.9	0.25	650	13	648	40	638	170	102
BF13-90-180-seq1	50704	212	60	0.17	33315	0.2733	2.8	4.1462	3.2	0.1100	1.4	0.89	1558	39	1663	26	1800	26	87
BF13-90-180-seq1	3321	79	8	0.46	5795	0.0891	1.1	0.7190	3.4	0.0586	3.3	0.32	550	6	550	15	550	71	100
BF13-90-180-seq1	21436	52	23	0.25	16627	0.4239	1.1	7.7127	1.7	0.1320	1.3	0.64	2278	20	2198	15	2124	22	107
BF13-90-180-seq1	13258	463	34	0.21	24159	0.0750	1.1	0.5822	3.3	0.0563	3.1	0.33	466	5	466	12	465	68	100
BF13-90-180-seq1	28758	199	46	0.20	35071	0.2284	1.3	2.6393	2.0	0.0838	1.5	0.66	1326	16	1312	15	1288	30	103
BF13-90-180-seq1	33833	88	40	0.65	26119	0.3685	1.8	6.6749	2.4	0.1314	1.5	0.78	2022	32	2069	21	2116	26	96
BF13-90-180-seq1	11165	100	19	0.37	14895	0.1772	1.7	1.8766	2.4	0.0768	1.7	0.71	1052	17	1073	16	1116	33	94
BF13-90-180-seq1	14121	74	25	0.83	15247	0.2748	1.4	3.5805	2.5	0.0945	2.0	0.58	1565	20	1545	20	1518	38	103
BF13-90-180-seq1	6178	113	15	0.68	10099	0.1138	1.2	0.9803	3.6	0.0625	3.4	0.34	695	8	694	18	690	72	101
BF13-90-180-seq1	3295	60	8	0.35	1713	0.1232	1.6	1.0330	3.7	0.0608	3.3	0.43	749	11	720	19	633	72	118
BF13-90-180-seq1	24291	92	30	0.30	22117	0.3077	1.1	4.7676	2.1	0.1124	1.7	0.55	1729	17	1779	17	1838	31	94
BF13-90-180-seq1	566	11	1	0.24	986	0.1095	2.7	0.9390	18.8	0.0622	18.6	0.15	670	17	672	97	680	398	99

BF13-90-180-seq1	11492	268	29	0.56	4302	0.0950	1.2	0.7870	2.3	0.0601	1.9	0.54	585	7	589	10	605	41	97
BF13-90-180-seq1	17671	93	32	0.83	19435	0.2760	1.3	3.5386	2.1	0.0930	1.6	0.64	1571	18	1536	16	1488	30	106
BF13-90-180-seq1	46913	127	52	0.27	38731	0.3815	1.4	6.5346	2.3	0.1242	1.8	0.61	2083	25	2051	20	2018	32	103
BF13-90-180-seq2	2812	56	6	0.29	4793	0.1119	1.7	0.9089	4.2	0.0589	3.9	0.40	684	11	656	21	563	84	122
BF13-90-180-seq2	9213	165	20	0.30	15338	0.1149	1.5	0.9712	3.1	0.0613	2.7	0.48	701	10	689	16	650	58	108
BF13-90-180-seq2	4205	129	10	0.37	4673	0.0708	1.1	0.5200	3.2	0.0533	3.1	0.33	441	5	425	11	342	69	129
BF13-90-180-seq2	17204	49	21	0.60	14212	0.3579	2.3	6.0939	2.9	0.1235	1.7	0.81	1972	40	1989	25	2007	30	98
BF13-90-180-seq2	18731	220	39	0.55	279	0.1560	3.4	1.5146	6.6	0.0704	5.7	0.52	934	30	936	41	941	116	99
BF13-90-180-seq2	24260	333	47	0.46	1446	0.1231	1.8	1.1052	3.3	0.0651	2.8	0.53	748	12	756	18	778	59	96
BF13-90-180-seq2	3771	114	16	1.00	6365	0.1058	1.4	0.8905	4.7	0.0610	4.5	0.30	649	9	647	23	640	96	101
BF13-90-180-seq2	77607	398	120	0.34	82510	0.2796	1.4	3.6974	2.0	0.0959	1.4	0.71	1589	20	1571	16	1546	27	103
BF13-90-180-seq2	10294	259	23	0.19	17583	0.0911	1.3	0.7398	3.2	0.0589	2.9	0.40	562	7	562	14	563	63	100
BF13-90-180-seq2	1743	33	4	0.36	2939	0.1093	1.5	0.9384	8.1	0.0623	7.9	0.19	668	10	672	41	684	170	98
BF13-90-180-seq2	9719	71	16	0.25	12410	0.2220	1.5	2.4810	3.0	0.0811	2.7	0.48	1292	17	1267	22	1223	53	106
BF13-90-180-seq2	25205	98	32	0.51	21112	0.2796	1.4	4.6941	2.2	0.1218	1.6	0.66	1589	20	1766	18	1982	29	80
BF13-90-180-seq2	31716	77	35	0.41	9613	0.4036	1.3	7.2757	1.9	0.1307	1.4	0.68	2186	24	2146	17	2108	25	104
BF13-90-180-seq2	133	4	0	0.39	349	0.1065	2.3	0.6182	45.4	0.0421	45.3	0.05	652	14	489	193	-221	1140	-296
BF13-90-180-seq2	62130	74	45	0.18	32823	0.5529	1.4	14.7249	1.9	0.1931	1.3	0.73	2837	32	2798	19	2769	22	102
BF13-90-180-seq2	8523	174	19	0.38	14607	0.0975	1.8	0.8022	3.6	0.0596	3.1	0.50	600	10	598	16	591	67	102
BF13-90-180-seq2	40085	495	45	0.07	517	0.0865	1.4	0.8195	4.3	0.0687	4.1	0.33	535	7	608	20	891	84	60
BF13-90-180-seq2	49874	80	49	0.65	30668	0.4819	1.1	11.0266	1.7	0.1659	1.3	0.66	2536	24	2525	16	2517	22	101
BF13-90-180-seq2	747	15	2	0.39	1255	0.1085	2.1	0.9127	9.9	0.0610	9.6	0.21	664	13	659	49	639	207	104
BF13-90-180-seq2	35076	125	22	0.26	30640	0.1497	5.1	2.4114	5.7	0.1168	2.4	0.91	899	43	1246	41	1908	43	47
BF13-90-180-seq2	21323	49	24	0.54	1339	0.4001	1.9	7.9017	3.4	0.1432	2.8	0.57	2170	36	2220	31	2267	48	96
BF13-90-180-seq2	15338	93	23	0.40	6175	0.2267	1.5	2.8557	2.6	0.0914	2.1	0.59	1317	18	1370	20	1454	40	91
BF13-90-180-seq2	99284	97	90	1.26	48101	0.5967	1.2	17.3542	1.9	0.2109	1.5	0.61	3017	28	2955	18	2913	24	104
BF13-90-180-seq2	28687	155	50	0.64	31557	0.2633	1.5	3.3553	2.0	0.0924	1.4	0.74	1507	20	1494	16	1476	26	102
BF13-90-180-seq2	90716	361	104	0.03	77525	0.2960	1.6	4.8702	2.0	0.1193	1.3	0.78	1671	23	1797	17	1946	22	86
BF13-90-180-seq2	4170	77	9	0.33	6844	0.1168	1.6	0.9952	4.9	0.0618	4.6	0.32	712	11	701	25	667	99	107
BF13-90-180-seq2	344749	381	260	0.50	161099	0.5516	1.7	16.5953	1.9	0.2182	0.8	0.90	2832	39	2912	18	2967	13	95
BF13-90-180-seq2	26984	209	46	0.24	33764	0.2157	1.3	2.4300	2.4	0.0817	2.0	0.54	1259	15	1252	17	1238	39	102
BF13-90-180-seq2	216	4	0	0.55	366	0.1084	4.2	0.9137	20.2	0.0611	19.8	0.21	663	27	659	103	644	425	103
Sample BF15	Galtymore Formation					Location (decimal degrees)		52.369	8.198133 W			Datum: D_WGS_1984							
BF15-60-90-seq1-	10124	233	20	0.46	18900	0.0768	1.4	0.5771	2.3	0.0545	1.8	0.62	477	7	463	9	392	41	122
BF15-60-90-seq1-	-	-	-	-	-	-	-	-	-	-	-	-	-	-	-	-	-	-	-
BF15-60-90-seq1-	2575	104	9	0.49	7619	0.0814	2.4	0.3806	9.6	0.0339	9.2	0.26	505	12	328	27	-798	262	-63
BF15-60-90-seq1-	3290	38	7	0.47	4745	0.1678	1.9	1.6388	5.3	0.0708	5.0	0.36	1000	18	985	34	952	102	105
BF15-60-90-seq1-	7939	65	15	0.27	10271	0.2168	1.5	2.3469	2.7	0.0785	2.2	0.56	1265	17	1227	19	1160	44	109
BF15-60-90-seq1-	7969	271	26	0.90	3115	0.0708	2.0	0.5444	3.2	0.0557	2.5	0.63	441	9	441	12	442	56	100
BF15-60-90-seq1-	24296	193	68	0.60	24391	0.2952	1.9	4.1192	2.5	0.1012	1.5	0.78	1668	28	1658	20	1646	29	101
BF15-60-90-seq1-	3336	110	10	0.61	1574	0.0794	1.2	0.6234	5.1	0.0569	4.9	0.23	493	6	492	20	489	109	101

BF15-60-90-seq1-	8267	28	11	0.36	6082	0.3555	1.9	5.4812	3.2	0.1118	2.5	0.60	1961	32	1898	27	1829	46	107
BF15-60-90-seq1-	8734	185	21	0.44	14635	0.1065	1.3	0.8891	2.4	0.0606	2.0	0.53	652	8	646	11	623	44	105
BF15-60-90-seq1-	26433	258	58	0.57	33406	0.1904	1.2	1.9904	2.0	0.0758	1.6	0.59	1123	12	1112	14	1091	33	103
BF15-60-90-seq1-	1416	43	4	0.72	2575	0.0782	1.4	0.6096	5.8	0.0565	5.6	0.25	485	7	483	23	474	124	103
BF15-60-90-seq1-	5026	51	12	0.69	7072	0.1920	1.8	1.9118	3.1	0.0722	2.6	0.57	1132	18	1085	21	992	52	114
BF15-60-90-seq1-	2653	80	7	0.26	4854	0.0846	1.5	0.6494	3.9	0.0557	3.6	0.37	524	7	508	16	439	81	119
BF15-60-90-seq1-	3046	83	8	0.60	5603	0.0799	2.2	0.6188	5.4	0.0562	4.9	0.41	495	10	489	21	460	110	108
BF15-60-90-seq1-	62282	420	101	0.14	3550	0.2440	3.7	3.1315	4.0	0.0931	1.4	0.94	1408	47	1440	31	1489	26	95
BF15-60-90-seq1-	5465	181	19	0.96	10083	0.0794	1.8	0.6019	2.9	0.0550	2.3	0.61	493	8	478	11	410	52	120
BF15-60-90-seq1-	6553	36	12	0.39	7246	0.2993	1.9	3.7909	3.3	0.0919	2.7	0.57	1688	28	1591	27	1465	51	115
BF15-60-90-seq1-	6656	57	13	0.28	2753	0.2181	3.4	2.4650	6.9	0.0820	6.0	0.49	1272	39	1262	51	1245	118	102
BF15-60-90-seq1-	7645	29	12	0.57	7124	0.3728	1.3	5.4772	2.9	0.1066	2.6	0.44	2043	22	1897	25	1741	47	117
BF15-60-90-seq1-	48996	78	61	0.87	25498	0.5845	2.2	15.4069	2.8	0.1912	1.7	0.79	2967	53	2841	27	2752	28	108
BF15-60-90-seq1-	3778	119	10	0.33	6791	0.0857	2.0	0.6660	4.1	0.0563	3.7	0.47	530	10	518	17	466	81	114
BF15-60-90-seq1-	4427	161	15	0.81	8066	0.0766	1.4	0.5957	8.4	0.0564	8.3	0.16	476	6	474	32	468	183	102
BF15-60-90-seq1-	7606	192	21	0.51	12767	0.0942	1.9	0.7829	3.9	0.0602	3.4	0.47	581	10	587	18	612	74	95
BF15-60-90-seq1-	1032	26	3	1.12	1725	0.0943	3.1	0.7763	12.7	0.0597	12.3	0.25	581	17	583	58	594	266	98
BF15-60-90-seq1-	2655	79	7	0.29	5041	0.0876	1.6	0.6496	6.9	0.0538	6.7	0.23	541	8	508	28	362	151	150
BF15-60-90-seq1-	7594	59	24	0.76	7722	0.3323	1.5	4.5598	3.3	0.0995	2.9	0.47	1850	25	1742	28	1615	54	115
BF15-60-90-seq1-	16207	122	45	0.54	15988	0.3185	1.8	4.5481	2.5	0.1036	1.7	0.71	1782	28	1740	21	1689	32	106
BF15-60-90-seq1-	922	53	5	0.74	1762	0.0845	1.8	0.6227	7.4	0.0534	7.2	0.25	523	9	492	29	347	162	151
BF15-60-90-seq1-	4400	146	13	0.43	8213	0.0812	1.7	0.6082	3.8	0.0544	3.4	0.45	503	8	482	15	386	76	130
BF15-60-90-seq1-	1903	62	6	0.63	3458	0.0799	1.9	0.6108	4.5	0.0555	4.1	0.43	495	9	484	18	431	91	115
BF15-60-90-seq1-	18524	154	54	0.57	18635	0.2967	1.4	4.1200	2.1	0.1007	1.5	0.71	1675	21	1658	17	1637	27	102
BF15-60-90-seq1-	14001	93	29	0.59	15916	0.2691	1.8	3.3015	2.8	0.0890	2.1	0.65	1536	25	1481	22	1404	41	109
BF15-60-90-seq1-	51715	77	54	0.71	28259	0.5427	1.4	13.9122	2.0	0.1859	1.4	0.69	2795	31	2744	19	2706	24	103
BF15-60-90-seq1-	13822	87	19	0.37	18433	0.1955	1.8	2.0519	2.9	0.0761	2.3	0.61	1151	19	1133	20	1098	47	105
BF15-60-90-seq1-	48322	113	49	0.61	27496	0.3492	1.4	5.5914	2.2	0.1161	1.8	0.61	1931	23	1915	19	1898	32	102
BF15-60-90-seq1-	2997	49	6	0.37	5202	0.1112	2.1	0.8879	5.2	0.0579	4.8	0.40	680	14	645	25	527	105	129
BF15-60-90-seq1-	4672	8	4	0.50	3607	0.4337	2.1	7.8835	3.6	0.1318	3.0	0.58	2322	41	2218	33	2123	52	109
BF15-60-90-seq1-	9016	47	13	0.68	11216	0.2235	1.6	2.5057	3.1	0.0813	2.7	0.51	1300	19	1274	23	1229	53	106
BF15-60-90-seq1-	16103	79	28	0.54	16554	0.3045	1.8	4.1437	2.7	0.0987	2.1	0.65	1714	27	1663	22	1599	38	107
BF15-60-90-seq1-	18608	139	25	0.22	25975	0.1774	1.5	1.7809	3.1	0.0728	2.7	0.49	1052	15	1039	20	1009	55	104
BF15-60-90-seq1-	17560	442	32	0.23	32309	0.0712	1.7	0.5412	2.3	0.0551	1.6	0.74	443	7	439	8	417	35	106
BF15-60-90-seq1-	911	37	6	1.59	1670	0.1024	2.6	0.7832	7.0	0.0555	6.5	0.38	628	16	587	32	431	145	146
BF15-60-90-seq1-	22253	110	37	0.42	19289	0.3006	3.7	4.7582	4.9	0.1148	3.3	0.75	1694	55	1778	42	1877	59	90
BF15-60-90-seq1-	4715	193	16	0.72	8761	0.0704	1.1	0.5323	3.4	0.0548	3.2	0.32	439	5	433	12	405	72	108
BF15-60-90-seq1-	3268	107	9	0.39	5870	0.0812	1.9	0.6296	3.9	0.0562	3.4	0.49	503	9	496	16	462	76	109
BF15-60-90-seq1-	2283	28	7	1.06	3578	0.1829	2.0	1.6388	5.5	0.0650	5.1	0.37	1083	20	985	35	774	107	140
BF15-60-90-seq1-	13402	62	23	0.55	13166	0.3187	1.5	4.5343	2.6	0.1032	2.2	0.56	1783	23	1737	22	1682	40	106
BF15-60-90-seq1-	1859	15	4	0.49	2577	0.2364	1.9	2.4947	5.4	0.0766	5.0	0.36	1368	24	1270	40	1110	100	123
BF15-60-90-seq1-	3037	42	11	0.41	1446	0.2490	3.3	2.7523	7.3	0.0802	6.5	0.45	1433	42	1343	56	1201	128	119

BF15-60-90-seq1-	9503	67	17	0.86	13299	0.1980	2.1	1.9769	3.1	0.0724	2.2	0.70	1164	23	1108	21	998	45	117
BF15-60-90-seq1-	17595	189	52	0.24	10352	0.2655	1.6	3.3497	2.7	0.0915	2.2	0.60	1518	22	1493	22	1457	42	104
BF15-60-90-seq1-	18823	59	22	0.54	18997	0.3172	1.9	4.4097	2.7	0.1008	1.9	0.71	1776	30	1714	23	1639	35	108
BF15-60-90-seq1-	7840	148	15	0.50	13871	0.0903	1.9	0.7169	3.2	0.0576	2.6	0.59	557	10	549	14	515	57	108
BF15-60-90-seq1-	12660	81	19	0.39	16817	0.2090	1.9	2.2090	2.7	0.0767	2.0	0.68	1223	21	1184	19	1113	40	110
BF15-60-90-seq1-	8983	51	14	0.44	9788	0.2425	2.1	3.1180	3.5	0.0933	2.9	0.59	1400	26	1437	27	1493	54	94
BF15-60-90-seq1-	1569	48	4	0.35	2773	0.0852	2.3	0.6760	5.9	0.0576	5.4	0.38	527	11	524	24	513	119	103
BF15-90-180-seq1	2135	7	2	0.31	2918	0.2279	1.8	2.3713	6.4	0.0755	6.2	0.28	1323	22	1234	47	1081	123	122
BF15-90-180-seq1	2301	19	4	0.76	3730	0.2054	2.4	1.7829	5.8	0.0630	5.3	0.41	1204	26	1039	38	707	112	170
BF15-90-180-seq1	3423	77	7	0.37	6055	0.0839	1.4	0.6596	4.0	0.0570	3.8	0.36	519	7	514	16	492	83	106
BF15-90-180-seq1	11323	352	26	0.34	335	0.0699	2.2	0.5410	4.1	0.0561	3.5	0.52	436	9	439	15	458	78	95
BF15-90-180-seq1	7548	55	11	0.21	10263	0.1991	2.1	2.0607	3.1	0.0751	2.4	0.66	1171	22	1136	22	1070	47	109
BF15-90-180-seq1	3378	44	9	0.93	4774	0.1702	1.6	1.6872	4.5	0.0719	4.1	0.37	1013	15	1004	29	983	84	103
BF15-90-180-seq1	6457	169	13	0.37	11860	0.0730	2.2	0.5578	3.7	0.0554	3.0	0.60	454	10	450	14	429	67	106
BF15-90-180-seq1	14218	15	14	1.93	7799	0.5566	2.0	14.2643	3.3	0.1859	2.6	0.60	2853	45	2767	31	2706	43	105
BF15-90-180-seq1	62006	329	82	0.38	73349	0.2261	2.6	2.6879	3.1	0.0862	1.7	0.83	1314	31	1325	24	1343	34	98
BF15-90-180-seq1	32243	25	19	0.51	15059	0.6149	2.5	18.5879	3.0	0.2192	1.6	0.85	3090	62	3021	29	2975	25	104
BF15-90-180-seq1	2164	80	7	0.47	3836	0.0751	2.8	0.5910	6.6	0.0571	6.0	0.43	467	13	471	25	494	131	94
BF15-90-180-seq1	4473	115	9	0.29	8361	0.0748	2.0	0.5630	3.4	0.0546	2.8	0.58	465	9	453	13	394	62	118
BF15-90-180-seq1	8911	215	18	0.39	16135	0.0788	2.0	0.6098	2.9	0.0561	2.1	0.69	489	9	483	11	457	47	107
BF15-90-180-seq1	26420	76	28	0.44	23874	0.3281	2.0	5.0992	2.6	0.1127	1.7	0.76	1829	32	1836	22	1844	31	99
BF15-90-180-seq1	4334	37	10	1.48	6096	0.1799	2.2	1.7695	4.2	0.0713	3.6	0.53	1067	22	1034	28	967	73	110
BF15-90-180-seq1	2612	59	5	0.50	4512	0.0819	2.0	0.6481	6.4	0.0574	6.1	0.32	508	10	507	26	505	134	100
BF15-90-180-seq1	9579	48	17	0.54	5720	0.3136	1.7	4.3983	2.6	0.1017	2.0	0.64	1759	26	1712	22	1656	37	106
BF15-90-180-seq1	8008	94	20	0.43	4392	0.1941	2.2	2.0258	3.4	0.0757	2.6	0.64	1144	23	1124	23	1087	52	105
BF15-90-180-seq1	29928	85	32	0.46	27508	0.3284	1.9	5.0198	2.7	0.1109	2.0	0.68	1831	30	1823	24	1814	37	101
BF15-90-180-seq1	1438	50	5	0.70	2580	0.0824	1.7	0.6532	8.5	0.0575	8.3	0.20	510	9	510	35	511	182	100
BF15-90-180-seq1	4990	135	11	0.49	9162	0.0704	2.6	0.5371	3.9	0.0553	2.9	0.67	439	11	436	14	424	64	103
BF15-90-180-seq1	5271	138	11	0.57	9726	0.0703	2.0	0.5421	6.9	0.0559	6.6	0.29	438	8	440	25	449	147	98
BF15-90-180-seq1	21247	71	22	0.35	21167	0.2880	2.4	4.0403	3.0	0.1018	1.8	0.79	1631	34	1642	25	1656	34	98
BF15-90-180-seq1	8728	238	20	0.48	16014	0.0741	1.8	0.5679	2.7	0.0556	2.0	0.66	461	8	457	10	435	45	106
BF15-90-180-seq1	2202	53	5	0.42	4301	0.0837	1.8	0.6056	5.2	0.0525	4.9	0.34	518	9	481	20	307	112	169
BF15-90-180-seq1	5152	216	17	0.43	9852	0.0734	1.5	0.5432	3.7	0.0537	3.4	0.40	457	7	441	13	358	77	128
BF15-90-180-seq1	18310	47	21	0.63	16060	0.3691	2.0	5.9077	3.1	0.1161	2.4	0.63	2025	34	1962	27	1897	43	107
BF15-90-180-seq1	5345	141	11	0.29	5432	0.0740	1.8	0.5684	3.8	0.0557	3.4	0.47	460	8	457	14	442	75	104
BF15-90-180-seq1	5345	141	11	0.29	5432	0.0740	1.8	0.5686	3.8	0.0557	3.4	0.47	460	8	457	14	442	75	104
BF15-90-180-seq1	17272	43	19	0.59	15200	0.3613	2.7	5.7420	3.4	0.1153	2.1	0.78	1988	46	1938	30	1884	38	106
BF15-90-180-seq1	11818	17	15	0.57	1470	0.7379	1.9	19.7329	3.2	0.1940	2.6	0.58	3563	51	3078	31	2776	43	128
BF15-90-180-seq1	2428	52	5	0.46	4231	0.0885	1.6	0.7074	5.8	0.0580	5.6	0.28	547	9	543	25	529	123	103
BF15-90-180-seq1	28970	26	17	0.31	14870	0.5756	2.3	15.7303	3.2	0.1982	2.2	0.72	2931	54	2861	31	2811	36	104
BF15-90-180-seq1	1163	18	2	0.78	1940	0.1224	1.8	1.0315	8.2	0.0611	8.0	0.22	744	13	720	43	644	172	116
BF15-90-180-seq1	6696	156	14	0.55	12065	0.0814	1.7	0.6335	3.3	0.0564	2.8	0.52	505	8	498	13	469	62	108

BF15-90-180-seq1	25395	29	19	0.48	15011	0.5428	1.8	12.9039	2.6	0.1724	1.9	0.69	2795	41	2673	25	2581	32	108
BF15-90-180-seq1	1875	14	3	0.45	2828	0.2099	2.7	1.9688	6.4	0.0680	5.8	0.42	1228	30	1105	44	869	120	141
BF15-90-180-seq1	3992	98	10	1.07	7333	0.0733	1.9	0.5622	4.2	0.0556	3.7	0.45	456	8	453	15	436	83	105
BF15-90-180-seq1	9106	58	14	0.50	11643	0.2124	2.1	2.3128	3.2	0.0790	2.4	0.65	1241	24	1216	23	1172	48	106
BF15-90-180-seq1	2372	62	5	0.45	4259	0.0748	1.9	0.5806	5.7	0.0563	5.3	0.34	465	9	465	21	464	118	100
BF15-90-180-seq1	14265	341	26	0.05	25690	0.0812	1.9	0.6299	3.0	0.0563	2.3	0.64	503	9	496	12	463	51	109
BF15-90-180-seq1	2532	54	6	0.93	4321	0.0849	2.8	0.6806	15.4	0.0581	15.1	0.18	526	14	527	65	534	332	98
BF15-90-180-seq1	7243	41	10	0.27	9265	0.2315	2.1	2.5284	3.5	0.0792	2.8	0.60	1342	26	1280	26	1178	56	114
BF15-90-180-seq1	5357	107	11	0.41	9511	0.0988	1.3	0.7727	3.7	0.0567	3.4	0.36	607	8	581	16	481	76	126
BF15-90-180-seq1	16927	147	35	0.33	21183	0.2282	2.4	2.5651	2.9	0.0815	1.8	0.80	1325	28	1291	22	1234	35	107
BF15-90-180-seq1	7144	233	22	0.54	12414	0.0853	1.9	0.6777	3.0	0.0576	2.4	0.63	528	10	525	13	516	52	102
BF15-90-180-seq1	1524	17	4	0.53	2157	0.1946	2.4	1.9369	6.5	0.0722	6.0	0.37	1146	25	1094	44	991	122	116
BF15-90-180-seq1	5056	32	7	0.26	5630	0.2141	2.4	2.7253	4.4	0.0923	3.7	0.55	1251	27	1335	33	1474	69	85
BF15-90-180-seq1	4522	164	14	0.67	8254	0.0744	2.3	0.5730	4.0	0.0559	3.2	0.58	463	10	460	15	447	72	103
BF15-90-180-seq1	3993	18	5	0.22	2783	0.2798	1.6	3.4076	4.0	0.0883	3.7	0.40	1591	23	1506	32	1389	70	114
BF15-90-180-seq1	26322	200	39	0.26	35290	0.1903	1.9	1.9952	2.8	0.0761	2.0	0.69	1123	20	1114	19	1097	41	102
BF15-90-180-seq1	4028	122	14	0.71	3887	0.0960	2.0	0.7472	4.3	0.0564	3.9	0.46	591	11	567	19	469	85	126
BF15-90-180-seq1	4611	167	14	0.34	8020	0.0793	1.8	0.6132	3.8	0.0561	3.4	0.47	492	8	486	15	455	75	108
BF15-90-180-seq1	28132	150	35	0.14	33694	0.2363	2.2	2.7683	2.9	0.0850	1.9	0.77	1367	28	1347	22	1315	36	104
BF15-90-180-seq1	4936	180	15	0.41	9157	0.0812	2.2	0.6144	3.4	0.0549	2.6	0.65	503	11	486	13	408	59	123
BF15-90-180-seq1	3294	135	11	0.53	6414	0.0719	1.9	0.5184	5.1	0.0523	4.8	0.37	447	8	424	18	299	108	150
BF15-90-180-seq1	1701	66	6	0.40	3374	0.0832	2.3	0.5925	5.3	0.0517	4.8	0.43	515	11	472	20	271	109	190
BF15-90-180-seq1	25111	128	50	0.77	24733	0.3204	1.9	4.5716	2.7	0.1035	1.9	0.70	1792	30	1744	23	1688	36	106
BF15-90-180-seq1	1611	19	5	1.26	2293	0.1959	1.5	1.9295	7.6	0.0714	7.5	0.20	1153	16	1091	52	970	153	119
BF15-90-180-seq1	1711	61	6	0.57	3174	0.0840	1.8	0.6342	5.8	0.0548	5.5	0.30	520	9	499	23	402	124	129
BF15-90-180-seq2	133987	96	69	0.75	72767	0.5271	1.8	13.6236	2.1	0.1874	1.2	0.84	2729	40	2724	20	2720	19	100
BF15-90-180-seq2	24952	379	31	0.15	3054	0.0807	3.3	0.8849	8.3	0.0796	7.6	0.40	500	16	644	40	1186	150	42
BF15-90-180-seq2	22507	100	22	0.30	29223	0.2054	1.1	2.2166	2.2	0.0783	1.9	0.50	1204	12	1186	15	1153	37	104
BF15-90-180-seq2	56215	259	69	0.23	51389	0.2552	1.5	3.2480	1.8	0.0923	1.1	0.82	1465	20	1469	14	1474	20	99
BF15-90-180-seq2	68988	510	98	0.27	1576	0.1824	1.5	1.9141	2.3	0.0761	1.7	0.65	1080	15	1086	15	1098	34	98
BF15-90-180-seq2	12466	97	20	0.26	16740	0.1983	1.6	2.0675	2.4	0.0756	1.8	0.66	1166	17	1138	17	1085	37	107
BF15-90-180-seq2	18161	482	35	0.21	32733	0.0723	2.0	0.5612	2.6	0.0563	1.7	0.76	450	9	452	10	463	38	97
BF15-90-180-seq2	1556	10	2	0.61	2472	0.1896	1.7	1.6785	8.9	0.0642	8.7	0.19	1119	18	1000	58	748	185	150
BF15-90-180-seq2	67597	48	32	0.48	24211	0.5480	1.4	14.1794	2.0	0.1877	1.4	0.71	2817	33	2762	19	2722	24	103
BF15-90-180-seq2	9442	48	10	0.37	12636	0.1861	1.8	1.9432	3.1	0.0757	2.5	0.57	1100	18	1096	21	1088	51	101
BF15-90-180-seq2	43475	114	39	0.44	32653	0.2992	1.6	4.1568	2.8	0.1008	2.2	0.58	1687	24	1666	23	1638	42	103
BF15-90-180-seq2	59851	153	53	0.51	60229	0.2959	1.3	4.1170	2.0	0.1009	1.5	0.66	1671	19	1658	16	1641	28	102
BF15-90-180-seq2	762	12	1	0.72	1394	0.0874	1.8	0.7009	9.5	0.0582	9.3	0.19	540	9	539	40	536	204	101
BF15-90-180-seq2	30850	36	22	0.78	28582	0.5271	1.9	7.9751	2.8	0.1097	2.1	0.67	2729	41	2228	25	1795	38	152
BF15-90-180-seq2	18832	323	26	0.25	13799	0.0772	1.5	0.5946	2.4	0.0559	1.8	0.64	479	7	474	9	447	41	107
BF15-90-180-seq2	2190	63	5	0.42	4426	0.0830	1.6	0.5755	4.3	0.0503	4.0	0.38	514	8	462	16	209	92	246
BF15-90-180-seq2	11121	63	13	0.37	15287	0.1849	1.5	1.8813	2.8	0.0738	2.4	0.55	1094	16	1075	19	1036	48	106

BF15-90-180-seq2	9462	157	15	0.44	16453	0.0852	2.1	0.6810	3.8	0.0580	3.1	0.56	527	11	527	16	529	69	100
BF15-90-180-seq2	28129	168	59	0.51	26930	0.3011	2.3	4.3721	2.7	0.1053	1.5	0.83	1697	34	1707	23	1720	28	99
BF15-90-180-seq2	8231	146	12	0.37	14923	0.0785	1.8	0.6056	2.7	0.0560	2.1	0.65	487	8	481	11	451	46	108
BF15-90-180-seq2	18407	36	13	0.25	16131	0.3313	2.6	5.2615	3.3	0.1152	2.0	0.80	1845	42	1863	28	1883	35	98
BF15-90-180-seq2	10345	302	22	0.23	2937	0.0713	1.4	0.5873	3.6	0.0598	3.3	0.40	444	6	469	14	595	71	75
BF15-90-180-seq2	116862	166	79	0.29	85334	0.4301	1.6	8.2560	2.3	0.1392	1.7	0.69	2306	31	2260	21	2217	29	104
BF15-90-180-seq2	96505	73	51	0.49	51587	0.5783	2.1	14.9875	2.6	0.1880	1.4	0.83	2942	51	2814	25	2724	24	108
BF15-90-180-seq2	7040	138	12	0.54	12757	0.0742	2.0	0.5742	3.1	0.0561	2.4	0.64	462	9	461	12	456	53	101
BF15-90-180-seq2	713	18	2	0.86	1235	0.0929	2.4	0.7505	15.6	0.0586	15.4	0.15	573	13	569	70	553	336	104
BF15-90-180-seq2	8196	173	16	0.41	15603	0.0836	1.6	0.6155	3.1	0.0534	2.6	0.52	518	8	487	12	345	59	150
BF15-90-180-seq2	10109	203	14	0.05	18388	0.0718	2.0	0.5497	3.5	0.0555	2.8	0.59	447	9	445	13	433	63	103
BF15-90-180-seq2	14385	40	13	0.35	15056	0.2974	1.4	3.9856	2.5	0.0972	2.2	0.53	1678	20	1631	21	1571	40	107
BF15-90-180-seq2	10713	54	15	0.81	13956	0.2196	1.6	2.3600	2.6	0.0779	2.0	0.63	1280	19	1231	18	1145	39	112
BF15-90-180-seq2	40552	223	46	0.17	54147	0.2054	1.1	2.1544	1.9	0.0761	1.5	0.59	1204	12	1166	13	1097	30	110
BF15-90-180-seq2	2108	33	3	0.56	3711	0.0859	1.9	0.6805	5.8	0.0575	5.4	0.34	531	10	527	24	510	119	104
BF15-90-180-seq2	3307	8	3	0.31	3371	0.3365	1.6	4.8840	4.2	0.1053	3.8	0.39	1870	27	1799	36	1719	71	109
BF15-90-180-seq2	9867	208	16	0.41	18054	0.0706	1.7	0.5418	2.8	0.0556	2.2	0.62	440	7	440	10	437	48	101
Sample BF19	Kilnafrehan Conglomerate Formation					Location (decimal degrees) 52.184 7.638517 W						Datum: D_WGS_1984							
BF19-60-90-seq1-	5293	160	14	0.31	8418	0.0836	2.2	0.6598	4.0	0.0573	3.3	0.55	517	11	514	16	501	73	103
BF19-60-90-seq1-	6322	157	18	0.57	10752	0.1030	1.7	0.8450	3.3	0.0595	2.8	0.52	632	10	622	16	585	62	108
BF19-60-90-seq1-	43230	59	44	0.59	23038	0.6081	1.6	16.0246	2.2	0.1911	1.5	0.73	3063	40	2878	22	2752	25	111
BF19-60-90-seq1-	3437	110	11	0.57	6494	0.0873	1.7	0.6467	4.7	0.0538	4.4	0.37	539	9	506	19	361	99	150
BF19-60-90-seq1-	2532	71	8	0.70	3308	0.0918	1.2	0.7330	12.4	0.0579	12.3	0.10	566	7	558	55	527	270	108
BF19-60-90-seq1-	30254	39	26	0.36	5829	0.5708	2.1	15.7032	2.5	0.1995	1.4	0.83	2911	48	2859	24	2822	23	103
BF19-60-90-seq1-	3920	111	9	0.41	7040	0.0746	2.7	0.5816	5.8	0.0565	5.1	0.46	464	12	465	22	472	113	98
BF19-60-90-seq1-	9865	174	26	0.41	15698	0.1383	1.5	1.2171	3.1	0.0638	2.7	0.49	835	12	808	17	735	56	114
BF19-60-90-seq1-	23024	406	58	0.15	35883	0.1466	1.8	1.3269	2.2	0.0657	1.3	0.80	882	15	858	13	795	28	111
BF19-60-90-seq1-	10802	456	31	0.30	9982	0.0667	3.3	0.5137	4.4	0.0558	2.9	0.74	417	13	421	15	445	65	94
BF19-60-90-seq1-	6124	208	20	0.71	11237	0.0806	1.7	0.6173	3.0	0.0555	2.4	0.58	500	8	488	12	434	54	115
BF19-60-90-seq1-	29477	123	57	1.00	27442	0.3445	2.3	5.1936	2.9	0.1093	1.8	0.79	1908	38	1852	25	1789	32	107
BF19-60-90-seq1-	7154	53	12	0.55	8088	0.1853	7.3	2.2721	9.2	0.0889	5.6	0.79	1096	73	1204	67	1403	107	78
BF19-60-90-seq1-	5345	166	13	0.15	9401	0.0829	1.7	0.6523	4.9	0.0571	4.6	0.34	513	8	510	20	495	101	104
BF19-60-90-seq1-	8248	286	25	0.39	2453	0.0809	2.1	0.6330	3.5	0.0567	2.8	0.59	502	10	498	14	481	62	104
BF19-60-90-seq1-	14339	163	25	0.03	8992	0.1616	2.9	1.6929	3.8	0.0760	2.6	0.74	966	26	1006	25	1094	51	88
BF19-60-90-seq1-	25849	115	41	0.34	23483	0.3265	1.6	5.0350	2.4	0.1119	1.7	0.69	1821	26	1825	20	1830	31	100
BF19-60-90-seq1-	83212	422	129	0.20	80844	0.3033	2.6	4.3284	3.1	0.1035	1.6	0.85	1707	39	1699	26	1688	30	101
BF19-60-90-seq1-	8324	169	19	0.46	697	0.0968	2.7	0.8022	7.0	0.0601	6.5	0.39	596	15	598	32	607	140	98
BF19-60-90-seq1-	9012	339	29	0.66	16926	0.0704	1.8	0.5273	2.7	0.0543	2.1	0.64	439	7	430	10	383	47	115
BF19-60-90-seq1-	14444	101	32	0.72	16445	0.2628	1.5	3.2433	2.8	0.0895	2.3	0.53	1504	20	1468	22	1415	45	106
BF19-60-90-seq1-	28373	206	68	0.18	23768	0.3212	2.3	5.3744	3.2	0.1213	2.2	0.73	1796	36	1881	27	1976	38	91
BF19-60-90-seq1-	4610	202	26	0.73	7958	0.1091	1.1	0.8875	2.9	0.0590	2.7	0.38	668	7	645	14	567	58	118

BF19-60-90-seq1-	4329	95	8	0.26	7990	0.0816	2.2	0.6172	4.5	0.0548	3.9	0.50	506	11	488	18	405	87	125
BF19-60-90-seq1-	22250	121	29	0.35	26851	0.2198	2.2	2.5435	2.9	0.0839	1.9	0.76	1281	25	1285	21	1291	36	99
BF19-60-90-seq1-	7214	293	25	0.53	13326	0.0751	2.2	0.5696	3.8	0.0550	3.0	0.59	467	10	458	14	413	68	113
BF19-60-90-seq1-	9353	205	23	0.19	15413	0.1132	1.9	0.9628	3.0	0.0617	2.3	0.65	691	13	685	15	664	48	104
BF19-60-90-seq1-	12630	131	28	0.39	17074	0.1986	2.0	2.0615	2.9	0.0753	2.1	0.68	1168	21	1136	20	1076	43	108
BF19-60-90-seq1-	4680	126	13	0.66	8095	0.0884	2.1	0.7140	3.6	0.0586	2.9	0.60	546	11	547	15	552	63	99
BF19-60-90-seq1-	72617	328	112	0.25	69237	0.3258	1.4	4.7839	1.7	0.1065	1.1	0.79	1818	22	1782	15	1740	20	104
BF19-60-90-seq1-	2682	61	6	1.27	4277	0.0665	8.4	0.5018	14.8	0.0547	12.1	0.57	415	34	413	51	401	271	103
BF19-60-90-seq1-	33357	150	57	0.49	30224	0.3276	4.1	5.0645	4.5	0.1121	1.8	0.91	1827	65	1830	38	1834	33	100
BF19-60-90-seq1-	6633	81	18	0.53	9666	0.1976	1.5	1.8948	3.3	0.0695	2.9	0.46	1163	16	1079	22	914	61	127
BF19-60-90-seq1-	5701	224	22	0.84	10300	0.0806	1.7	0.6277	2.8	0.0565	2.2	0.61	500	8	495	11	471	49	106
BF19-60-90-seq1-	4872	120	15	0.57	7572	0.1117	2.0	0.9371	3.5	0.0609	2.9	0.56	682	13	671	18	635	63	108
BF19-60-90-seq1-	3144	109	10	0.30	5496	0.0853	1.6	0.6867	5.2	0.0584	5.0	0.30	528	8	531	22	545	109	97
BF19-60-90-seq1-	21988	116	46	0.72	22044	0.3256	1.5	4.5544	2.0	0.1015	1.3	0.75	1817	24	1741	17	1651	25	110
BF19-60-90-seq1-	3987	23	11	1.65	4317	0.3268	1.9	4.2851	4.1	0.0951	3.7	0.47	1823	31	1690	35	1530	69	119
BF19-60-90-seq1-	5792	142	12	0.22	10787	0.0846	1.6	0.6325	3.5	0.0543	3.1	0.47	523	8	498	14	382	70	137
BF19-60-90-seq1-	9499	285	33	0.52	16955	0.1052	1.7	0.8264	2.8	0.0570	2.3	0.60	645	10	612	13	491	50	131
BF19-60-90-seq1-	2274	35	6	0.32	3618	0.1709	1.8	1.5265	4.3	0.0648	3.9	0.41	1017	17	941	27	768	83	132
BF19-60-90-seq1-	28430	147	56	0.57	28167	0.3267	1.4	4.6119	2.1	0.1024	1.6	0.67	1822	22	1751	18	1668	29	109
BF19-60-90-seq1-	22735	277	59	0.51	30689	0.1901	1.7	1.9850	2.4	0.0757	1.7	0.70	1122	18	1110	17	1088	35	103
BF19-60-90-seq1-	39146	462	130	0.41	4958	0.2566	1.7	3.4593	2.6	0.0978	2.0	0.65	1473	22	1518	21	1582	37	93
BF19-60-90-seq1-	11568	445	53	0.15	18923	0.1217	3.0	1.0457	3.9	0.0623	2.5	0.76	740	21	727	20	685	53	108
BF19-60-90-seq1-	10806	301	46	0.58	15885	0.1239	2.6	1.1816	3.3	0.0692	2.1	0.78	753	19	792	19	903	43	83
BF19-60-90-seq1-	1078	60	6	0.39	1866	0.0890	2.5	0.7238	7.4	0.0590	6.9	0.35	550	13	553	32	566	150	97
BF19-60-90-seq1-	8019	331	25	0.33	14769	0.0711	2.1	0.5417	3.4	0.0553	2.6	0.63	443	9	440	12	424	59	104
BF19-60-90-seq1-	35352	110	41	0.47	32810	0.3222	1.4	4.8715	2.3	0.1097	1.9	0.61	1800	23	1797	20	1794	34	100
BF19-60-90-seq1-	9005	244	18	0.27	16623	0.0705	1.7	0.5348	2.7	0.0550	2.0	0.64	439	7	435	9	413	45	106
BF19-60-90-seq1-	2577	98	9	0.55	4962	0.0876	1.9	0.6427	5.2	0.0532	4.8	0.37	541	10	504	21	339	109	160
BF19-60-90-seq1-	46493	374	71	0.20	64184	0.1891	2.7	1.9236	3.2	0.0738	1.6	0.85	1117	28	1089	21	1035	33	108
BF19-60-90-seq1-	39516	71	42	0.58	4461	0.4744	3.4	12.5822	3.7	0.1924	1.4	0.92	2503	71	2649	35	2762	23	91
BF19-60-90-seq1-	7487	65	19	0.88	9217	0.2327	1.6	2.6410	2.9	0.0823	2.4	0.55	1349	20	1312	22	1253	48	108
BF19-60-90-seq1-	7622	556	40	0.22	9652	0.0731	1.8	0.5680	3.6	0.0563	3.1	0.51	455	8	457	13	466	68	98
BF19-60-90-seq1-	3083	98	9	0.27	5404	0.0922	1.8	0.7388	5.4	0.0581	5.1	0.33	569	10	562	23	534	111	106
BF19-60-90-seq1-	24700	162	44	0.38	8044	0.2433	2.3	3.1629	3.7	0.0943	2.9	0.62	1404	29	1448	29	1514	55	93
BF19-60-90-seq1-	5214	89	13	0.25	1624	0.1473	3.1	1.3634	5.0	0.0672	3.9	0.62	886	26	873	30	843	81	105
BF19-60-90-seq1-	4164	106	11	0.35	6967	0.0937	2.6	0.7796	5.5	0.0604	4.8	0.47	577	14	585	25	616	105	94
BF19-90-180-seq1	14966	236	28	0.37	25866	0.1124	1.7	0.9158	2.3	0.0591	1.6	0.72	687	11	660	11	571	34	120
BF19-90-180-seq1	18209	515	35	0.16	33554	0.0710	1.2	0.5388	2.1	0.0550	1.7	0.58	442	5	438	8	413	38	107
BF19-90-180-seq1	15516	80	30	0.67	16055	0.3098	1.0	4.2217	2.3	0.0988	2.1	0.43	1740	15	1678	19	1602	40	109
BF19-90-180-seq1	1700	60	7	1.25	3071	0.0805	1.6	0.6334	7.9	0.0571	7.7	0.20	499	7	498	31	495	170	101
BF19-90-180-seq1	53979	398	79	0.27	72722	0.1904	1.6	1.9940	2.3	0.0760	1.7	0.68	1124	16	1113	16	1094	34	103
BF19-90-180-seq1	130262	124	90	0.53	62675	0.5877	1.4	16.0178	1.8	0.1977	1.1	0.78	2980	34	2878	18	2807	19	106

BF19-90-180-seq1	4067	110	9	0.40	7809	0.0732	1.5	0.5355	3.8	0.0530	3.5	0.39	456	7	435	14	331	79	138
BF19-90-180-seq1	6141	232	19	0.43	11377	0.0768	1.6	0.5874	3.1	0.0555	2.7	0.51	477	7	469	12	431	59	111
BF19-90-180-seq1	2560	169	13	0.06	4526	0.0835	1.2	0.6666	5.2	0.0579	5.0	0.23	517	6	519	21	526	111	98
BF19-90-180-seq1	39369	278	61	0.30	51097	0.2067	1.4	2.2503	2.3	0.0790	1.9	0.59	1211	15	1197	17	1171	37	103
BF19-90-180-seq1	3231	54	7	0.60	5476	0.1087	1.4	0.9021	4.6	0.0602	4.3	0.31	665	9	653	22	611	94	109
BF19-90-180-seq1	7850	38	11	0.21	9229	0.2837	2.0	3.4174	3.2	0.0874	2.6	0.60	1610	28	1508	26	1369	50	118
BF19-90-180-seq1	5943	92	13	0.76	9916	0.1139	1.4	0.9573	3.6	0.0610	3.3	0.40	695	10	682	18	638	71	109
BF19-90-180-seq1	3555	151	12	0.56	6642	0.0682	1.8	0.5150	4.1	0.0547	3.7	0.44	426	7	422	14	401	82	106
BF19-90-180-seq1	7634	66	14	0.66	10467	0.1824	1.7	1.8563	3.0	0.0738	2.5	0.55	1080	17	1066	20	1036	51	104
BF19-90-180-seq1	3639	29	6	0.52	5044	0.2017	1.7	2.0602	4.6	0.0741	4.3	0.37	1185	19	1136	32	1043	86	114
BF19-90-180-seq1	12618	592	45	0.42	23197	0.0700	1.6	0.5354	2.6	0.0555	2.1	0.62	436	7	435	9	431	46	101
BF19-90-180-seq1	4717	131	10	0.28	8674	0.0758	1.5	0.5816	3.1	0.0556	2.7	0.49	471	7	465	12	437	60	108
BF19-90-180-seq1	18345	75	28	0.71	17113	0.3154	1.6	4.3875	2.3	0.1009	1.7	0.68	1767	24	1710	19	1641	32	108
BF19-90-180-seq1	19727	290	28	0.22	29699	0.0950	1.3	0.8883	2.4	0.0678	2.0	0.55	585	7	645	11	863	41	68
BF19-90-180-seq1	8988	79	17	0.57	12240	0.1840	2.2	1.9059	3.9	0.0751	3.3	0.56	1089	22	1083	27	1071	65	102
BF19-90-180-seq1	7616	71	13	0.18	10688	0.1848	1.9	1.8562	3.4	0.0728	2.8	0.56	1093	19	1066	23	1010	57	108
BF19-90-180-seq1	33907	38	27	0.49	5764	0.6056	1.9	16.6547	2.3	0.1994	1.3	0.82	3053	47	2915	23	2822	22	108
BF19-90-180-seq1	2356	101	8	0.15	4225	0.0818	2.5	0.6456	6.2	0.0572	5.7	0.41	507	12	506	25	500	125	101
BF19-90-180-seq1	5769	45	15	0.76	6687	0.2880	1.9	3.4992	3.9	0.0881	3.3	0.50	1631	28	1527	31	1385	64	118
BF19-90-180-seq1	2527	82	10	0.51	4731	0.1067	1.6	0.8034	4.5	0.0546	4.3	0.35	653	10	599	21	397	95	165
BF19-90-180-seq1	25811	128	50	0.44	22780	0.3458	2.3	5.5119	3.2	0.1156	2.2	0.73	1915	39	1902	28	1889	40	101
BF19-90-180-seq1	1163	47	5	0.60	2333	0.0941	2.2	0.6637	7.6	0.0511	7.3	0.29	580	12	517	31	247	168	234
BF19-90-180-seq1	909	45	4	0.34	1825	0.0801	2.5	0.5772	14.2	0.0523	14.0	0.17	497	12	463	54	297	320	167
BF19-90-180-seq1	4990	199	27	1.44	8904	0.0870	2.3	0.6948	6.1	0.0579	5.7	0.37	538	12	536	26	527	125	102
BF19-90-180-seq1	14568	197	39	0.27	19017	0.1917	2.2	2.0785	3.3	0.0786	2.5	0.67	1131	23	1142	23	1163	49	97
BF19-90-180-seq1	21048	73	30	0.66	13586	0.3392	1.7	5.3285	2.8	0.1139	2.2	0.61	1883	27	1873	24	1863	40	101
BF19-90-180-seq1	14724	553	53	1.12	27463	0.0699	1.6	0.5289	2.4	0.0548	1.8	0.66	436	7	431	9	406	41	107
BF19-90-180-seq1	5360	248	19	0.12	9761	0.0793	1.7	0.6141	4.0	0.0561	3.7	0.42	492	8	486	16	458	81	108
BF19-90-180-seq1	13819	314	32	0.15	23221	0.1041	1.2	0.8736	2.4	0.0609	2.1	0.51	639	8	638	12	634	45	101
BF19-90-180-seq1	16253	371	38	0.22	27517	0.1013	1.6	0.8430	2.1	0.0604	1.5	0.73	622	9	621	10	616	31	101
BF19-90-180-seq1	4493	172	14	0.48	8571	0.0737	2.0	0.5382	3.2	0.0530	2.5	0.64	458	9	437	11	328	56	140
BF19-90-180-seq1	1822	62	6	0.51	3546	0.0832	1.2	0.6083	5.5	0.0530	5.4	0.22	515	6	482	21	330	122	156
BF19-90-180-seq1	3581	115	9	0.26	6755	0.0791	1.9	0.5890	4.4	0.0540	3.9	0.44	491	9	470	17	372	88	132
BF19-90-180-seq1	12369	432	32	0.37	22914	0.0694	1.7	0.5271	2.5	0.0551	1.7	0.71	432	7	430	9	416	39	104
BF19-90-180-seq1	20980	134	52	0.62	19725	0.3291	1.5	4.9285	2.2	0.1086	1.6	0.67	1834	23	1807	19	1777	29	103
BF19-90-180-seq1	21714	117	44	0.25	19083	0.3570	1.6	5.7321	2.4	0.1164	1.8	0.68	1968	28	1936	21	1902	32	103
BF19-90-180-seq1	5140	92	20	0.65	7224	0.1856	2.2	1.8529	3.6	0.0724	2.8	0.61	1097	22	1064	24	998	57	110
BF19-90-180-seq1	19990	106	42	0.32	17181	0.3634	1.9	5.9328	2.5	0.1184	1.6	0.78	1998	33	1966	22	1932	28	103
BF19-90-180-seq1	852	71	7	0.46	1567	0.0932	3.0	0.7095	13.6	0.0552	13.3	0.22	575	16	544	59	420	297	137
BF19-90-180-seq1	8277	76	19	0.19	10203	0.2548	1.3	2.9121	3.9	0.0829	3.6	0.34	1463	17	1385	30	1267	71	115
BF19-90-180-seq1	13293	31	22	0.68	7284	0.5805	2.0	14.9416	3.0	0.1867	2.2	0.67	2951	48	2812	29	2713	37	109
BF19-90-180-seq1	7344	25	13	1.08	6234	0.3821	2.4	6.3414	3.8	0.1204	3.0	0.62	2086	42	2024	34	1962	53	106

BF19-90-180-seq1	3927	151	12	0.43	7256	0.0720	2.2	0.5483	3.9	0.0552	3.2	0.56	448	9	444	14	421	72	106
BF19-90-180-seq1	7755	48	20	0.50	6978	0.3691	2.4	5.7842	3.8	0.1136	3.0	0.62	2025	41	1944	34	1858	54	109
BF19-90-180-seq1	1106	36	4	0.59	2287	0.0989	1.6	0.6901	9.4	0.0506	9.2	0.17	608	9	533	40	224	214	272
BF19-90-180-seq1	4053	126	13	0.57	7086	0.0940	1.5	0.7766	5.8	0.0599	5.6	0.26	579	8	584	26	602	122	96
BF19-90-180-seq1	3550	49	9	0.36	5372	0.1793	1.6	1.6651	3.7	0.0673	3.4	0.43	1063	16	995	24	849	70	125
BF19-90-180-seq1	47949	184	86	0.64	39962	0.3986	1.4	6.7575	1.9	0.1230	1.3	0.71	2163	25	2080	17	1999	24	108
BF19-90-180-seq1	10212	538	34	0.50	6855	0.0541	5.5	0.4118	6.2	0.0552	2.8	0.89	340	18	350	18	419	64	81
BF19-90-180-seq1	6000	111	24	0.53	3195	0.1901	2.1	1.9705	4.4	0.0752	3.9	0.47	1122	21	1105	30	1074	78	104
BF19-90-180-seq1	79712	128	84	0.48	40888	0.5411	1.2	14.8718	1.7	0.1993	1.2	0.71	2788	27	2807	16	2821	19	99
BF19-90-180-seq1	15526	651	49	0.30	28182	0.0734	1.9	0.5676	2.9	0.0561	2.2	0.65	457	8	456	11	455	50	101
BF19-90-180-seq1	5216	385	26	0.32	2620	0.0655	2.3	0.5023	3.8	0.0556	3.0	0.62	409	9	413	13	436	66	94
BF19-90-180-seq1	18611	120	44	0.19	15859	0.3583	2.3	5.9290	3.1	0.1200	2.1	0.74	1974	39	1965	28	1956	38	101
BF19-90-180-seq2	4675	115	19	0.83	8144	0.1464	1.5	1.1588	4.4	0.0574	4.1	0.33	881	12	781	24	507	91	174
BF19-90-180-seq2	12872	61	21	0.37	12909	0.3102	2.0	4.3568	2.9	0.1019	2.1	0.69	1742	31	1704	25	1658	39	105
BF19-90-180-seq2	17176	124	24	0.20	23692	0.1898	1.8	1.9346	2.8	0.0739	2.2	0.63	1120	18	1093	19	1040	45	108
BF19-90-180-seq2	20717	322	39	0.43	35818	0.1094	2.1	0.8906	2.8	0.0590	1.8	0.75	669	13	647	13	568	40	118
BF19-90-180-seq2	7613	189	15	0.37	13841	0.0740	1.9	0.5708	3.1	0.0560	2.5	0.59	460	8	459	12	450	56	102
BF19-90-180-seq2	17134	425	32	0.34	31550	0.0717	1.6	0.5463	2.7	0.0553	2.1	0.61	446	7	443	10	424	48	105
BF19-90-180-seq2	13056	286	21	0.08	23518	0.0788	1.1	0.6143	2.4	0.0565	2.1	0.48	489	5	486	9	473	46	103
BF19-90-180-seq2	38506	181	65	0.29	35847	0.3363	3.4	5.0360	3.7	0.1086	1.5	0.92	1869	56	1825	32	1776	27	105
BF19-90-180-seq2	16374	307	39	0.91	27737	0.0913	8.3	0.7616	8.8	0.0605	2.9	0.94	563	45	575	40	621	63	91
BF19-90-180-seq2	9613	355	28	0.58	17875	0.0693	1.1	0.5252	2.9	0.0549	2.7	0.39	432	5	429	10	409	60	106
BF19-90-180-seq2	15453	363	41	0.39	25638	0.1051	1.8	0.8786	2.7	0.0607	2.0	0.68	644	11	640	13	627	43	103
BF19-90-180-seq2	27026	1217	75	0.14	50470	0.0634	2.3	0.4755	2.8	0.0544	1.6	0.82	396	9	395	9	389	37	102
BF19-90-180-seq2	12908	333	24	0.29	24383	0.0701	1.1	0.5205	2.0	0.0539	1.7	0.52	437	4	425	7	365	39	120
BF19-90-180-seq2	29531	32	17	0.28	16693	0.4803	1.2	11.9371	2.1	0.1803	1.7	0.59	2529	26	2599	20	2655	28	95
BF19-90-180-seq2	17076	97	23	0.22	22195	0.2305	1.6	2.4934	2.4	0.0785	1.8	0.66	1337	19	1270	17	1159	35	115
BF19-90-180-seq2	20830	527	43	0.44	38207	0.0741	1.3	0.5670	2.1	0.0555	1.6	0.63	461	6	456	8	433	36	106
BF19-90-180-seq2	21840	547	39	0.23	40050	0.0698	1.4	0.5352	2.2	0.0556	1.7	0.63	435	6	435	8	437	38	100
BF19-90-180-seq2	7236	490	38	0.39	13671	0.0728	1.7	0.5413	3.0	0.0539	2.5	0.56	453	7	439	11	368	56	123
BF19-90-180-seq2	1844	74	7	0.61	3915	0.0741	2.6	0.4892	7.5	0.0479	7.0	0.35	461	12	404	25	93	167	493
BF19-90-180-seq2	8115	327	26	0.45	14604	0.0738	1.5	0.5666	2.9	0.0557	2.5	0.50	459	7	456	11	439	56	104
Sample BF21	Kilnafrehan Conglomerate Formation					Location (decimal degrees) 52.184 7.638517 W						Datum: D_WGS_1984							
BF21-60-90-seq1-	14567	178	37	0.50	20570	0.1875	1.8	1.8727	2.7	0.0724	2.1	0.65	1108	18	1071	18	998	42	111
BF21-60-90-seq1-	6897	69	18	0.79	1114	0.2173	2.3	2.3305	3.5	0.0778	2.7	0.65	1267	26	1222	25	1142	53	111
BF21-60-90-seq1-	10061	92	27	1.23	12705	0.2076	2.6	2.3141	3.3	0.0808	2.0	0.80	1216	29	1217	23	1217	39	100
BF21-60-90-seq1-	8162	66	17	0.55	4685	0.2238	4.1	2.6069	5.0	0.0845	2.7	0.83	1302	49	1303	37	1304	53	100
BF21-60-90-seq1-	10478	48	18	0.77	10548	0.2969	2.1	4.1644	3.0	0.1017	2.2	0.70	1676	31	1667	25	1656	40	101
BF21-60-90-seq1-	1832	18	4	0.47	792	0.1927	2.9	2.0161	5.4	0.0759	4.6	0.53	1136	30	1121	37	1091	92	104
BF21-60-90-seq1-	51553	144	59	0.31	41670	0.3706	2.4	6.4373	2.6	0.1260	1.1	0.90	2032	42	2037	23	2043	20	99
BF21-60-90-seq1-	-	-	-	-	-	-	-	-	-	-	-	-	-	-	-	-	-	-	-

BF21-60-90-seq1-	13863	136	27	0.28	18434	0.1873	2.0	1.9737	2.7	0.0764	1.9	0.73	1107	20	1107	19	1106	37	100
BF21-60-90-seq1-	4030	31	8	0.48	5039	0.2268	1.6	2.5444	4.1	0.0814	3.8	0.40	1318	19	1285	30	1230	74	107
BF21-60-90-seq1-	11460	151	26	0.22	15961	0.1707	1.6	1.7158	2.4	0.0729	1.8	0.66	1016	15	1014	15	1012	37	100
BF21-60-90-seq1-	38952	250	68	0.27	42432	0.2558	1.9	3.2950	2.2	0.0934	1.2	0.85	1468	25	1480	18	1497	23	98
BF21-60-90-seq1-	13045	64	31	1.84	13158	0.2866	2.7	3.9848	3.6	0.1008	2.3	0.77	1624	40	1631	30	1640	43	99
BF21-60-90-seq1-	1912	73	6	0.63	3726	0.0765	1.9	0.5501	5.7	0.0522	5.4	0.33	475	9	445	21	294	124	162
BF21-60-90-seq1-	57173	281	94	0.44	58151	0.2956	2.6	4.0858	2.9	0.1002	1.4	0.88	1670	38	1651	24	1629	26	103
BF21-60-90-seq1-	4116	47	10	0.41	5790	0.1979	2.4	1.9673	5.5	0.0721	4.9	0.44	1164	26	1104	38	988	101	118
BF21-60-90-seq1-	54940	339	121	0.77	55717	0.2854	3.2	3.9306	3.5	0.0999	1.5	0.91	1618	46	1620	29	1622	28	100
BF21-60-90-seq1-	4451	30	7	0.39	3042	0.2060	2.8	2.3763	4.4	0.0837	3.4	0.63	1208	30	1236	32	1284	66	94
BF21-60-90-seq1-	7598	86	16	0.39	10380	0.1713	1.8	1.7255	3.0	0.0730	2.4	0.59	1019	17	1018	20	1015	49	100
BF21-60-90-seq1-	12232	86	23	0.46	6170	0.2354	2.9	2.9245	3.8	0.0901	2.4	0.78	1363	36	1388	29	1428	45	95
BF21-60-90-seq1-	55639	338	87	0.07	38664	0.2634	1.9	3.5159	2.4	0.0968	1.5	0.78	1507	26	1531	19	1563	28	96
BF21-60-90-seq1-	40596	240	68	0.31	43254	0.2642	2.1	3.4821	3.0	0.0956	2.1	0.69	1511	28	1523	24	1540	40	98
BF21-60-90-seq1-	43227	253	76	0.46	35674	0.2650	1.9	3.4600	2.3	0.0947	1.4	0.81	1515	26	1518	18	1522	26	100
BF21-60-90-seq1-	15272	115	29	0.43	17946	0.2263	2.2	2.6613	3.0	0.0853	2.0	0.75	1315	27	1318	22	1322	38	100
BF21-60-90-seq1-	6893	129	17	0.69	11153	0.1137	2.2	0.9829	3.5	0.0627	2.7	0.63	694	15	695	18	698	58	99
BF21-60-90-seq1-	58129	88	51	0.31	19379	0.5122	1.8	12.9221	2.2	0.1830	1.3	0.82	2666	39	2674	21	2680	21	99
BF21-60-90-seq1-	11515	472	31	0.18	20973	0.0677	1.9	0.5211	2.5	0.0558	1.6	0.76	422	8	426	9	444	36	95
BF21-60-90-seq1-	13596	145	27	0.31	18848	0.1770	1.5	1.7911	2.2	0.0734	1.6	0.69	1051	15	1042	15	1024	32	103
BF21-60-90-seq1-	29457	276	64	0.45	12835	0.2111	1.7	2.3432	2.2	0.0805	1.3	0.79	1234	20	1226	16	1210	26	102
BF21-60-90-seq1-	5158	77	16	0.38	1659	0.1883	1.8	1.9437	6.8	0.0749	6.5	0.27	1112	19	1096	46	1065	131	104
BF21-60-90-seq1-	2899	29	6	0.68	1612	0.1669	2.2	1.6834	5.2	0.0731	4.7	0.43	995	20	1002	34	1018	95	98
BF21-60-90-seq1-	44641	158	68	0.69	1060	0.3517	2.3	5.9545	2.6	0.1228	1.3	0.88	1943	38	1969	23	1997	22	97
BF21-60-90-seq1-	67031	278	85	0.09	60540	0.3077	1.6	4.7607	1.9	0.1122	0.9	0.88	1729	25	1778	16	1836	16	94
BF21-60-90-seq1-	1745	17	3	0.04	2478	0.1633	3.1	1.6151	6.6	0.0717	5.9	0.47	975	28	976	43	979	119	100
BF21-60-90-seq1-	36624	482	88	0.31	53564	0.1747	2.8	1.6804	3.5	0.0698	2.0	0.81	1038	27	1001	22	922	42	113
BF21-60-90-seq1-	6017	232	17	0.37	10954	0.0701	2.2	0.5404	4.3	0.0559	3.7	0.51	437	9	439	15	449	81	97
BF21-60-90-seq1-	3991	122	13	1.12	2654	0.0831	2.2	0.6347	4.5	0.0554	4.0	0.48	514	11	499	18	429	88	120
BF21-60-90-seq1-	24892	179	30	0.53	33283	0.1367	1.8	1.4331	2.1	0.0761	1.2	0.82	826	14	903	13	1097	24	75
BF21-60-90-seq1-	42154	171	49	0.32	46637	0.2656	3.0	3.3721	3.6	0.0921	2.0	0.83	1518	40	1498	28	1469	37	103
BF21-60-90-seq1-	8175	52	17	0.56	9370	0.2878	2.8	3.5227	5.0	0.0888	4.2	0.55	1630	40	1532	41	1400	80	116
BF21-60-90-seq1-	14568	70	24	0.64	14758	0.2828	2.4	3.9202	3.5	0.1005	2.5	0.69	1605	34	1618	28	1634	47	98
BF21-60-90-seq1-	734	33	3	0.76	1793	0.0872	2.1	0.8221	66.2	0.0683	66.2	0.03	539	11	609	361	879	1370	61
BF21-60-90-seq1-	10831	87	21	0.44	13226	0.2127	2.7	2.4428	4.2	0.0833	3.2	0.64	1243	31	1255	31	1276	63	97
BF21-60-90-seq1-	2177	71	7	0.97	3966	0.0686	2.3	0.5265	5.7	0.0557	5.2	0.40	428	9	429	20	440	116	97
BF21-60-90-seq1-	8738	170	23	0.46	14482	0.1230	1.8	1.0927	3.2	0.0644	2.6	0.57	748	13	750	17	756	56	99
BF21-60-90-seq1-	17074	83	33	0.72	17922	0.3175	2.2	4.2789	4.1	0.0977	3.4	0.54	1778	34	1689	34	1581	64	112
BF21-60-90-seq1-	49699	77	44	0.33	27269	0.4948	2.1	12.6132	2.3	0.1849	1.0	0.91	2591	45	2651	22	2697	16	96
BF21-60-90-seq1-	57224	308	68	0.14	68932	0.2202	1.9	2.5660	2.4	0.0845	1.5	0.79	1283	22	1291	18	1305	29	98
BF21-60-90-seq1-	40373	405	63	0.09	53363	0.1592	3.5	1.6774	4.7	0.0764	3.1	0.76	953	31	1000	30	1106	61	86
BF21-60-90-seq1-	47703	211	71	0.26	22937	0.3174	1.9	4.7479	2.2	0.1085	1.2	0.84	1777	29	1776	19	1774	22	100

BF21-60-90-seq1-	29439	330	55	0.03	16830	0.1782	2.0	1.8369	2.7	0.0748	1.8	0.73	1057	19	1059	18	1062	37	100
BF21-60-90-seq1-	14777	62	24	0.78	14007	0.3131	1.9	4.6394	2.6	0.1075	1.7	0.75	1756	30	1756	22	1757	31	100
BF21-60-90-seq1-	8003	71	14	0.33	6079	0.1917	1.8	2.2800	2.8	0.0863	2.1	0.65	1131	19	1206	20	1344	41	84
BF21-60-90-seq1-	50105	652	91	0.02	71207	0.1490	3.2	1.4711	3.8	0.0716	2.1	0.84	895	26	919	23	975	42	92
BF21-60-90-seq1-	53555	190	71	0.39	46575	0.3317	2.7	5.3496	3.1	0.1170	1.5	0.87	1847	44	1877	27	1911	28	97
BF21-60-90-seq1-	87548	101	70	0.35	41045	0.5840	2.2	17.4276	2.4	0.2164	1.1	0.88	2965	51	2959	24	2954	18	100
BF21-60-90-seq1-	9272	73	18	0.51	11413	0.2174	1.7	2.4910	3.5	0.0831	3.0	0.50	1268	20	1269	26	1272	59	100
BF21-60-90-seq1-	11804	51	19	0.55	11245	0.3292	1.7	4.8466	2.4	0.1068	1.7	0.71	1835	27	1793	20	1745	30	105
BF21-60-90-seq1-	30785	31	24	0.69	9685	0.5873	1.7	17.8574	2.2	0.2205	1.4	0.79	2979	42	2982	21	2984	22	100
BF21-60-90-seq1-	40726	206	70	0.54	40710	0.2947	1.8	4.1023	2.2	0.1010	1.3	0.82	1665	26	1655	18	1642	23	101
BF21-60-90-seq2-	43172	195	66	0.37	41559	0.3071	3.0	4.4709	3.5	0.1056	1.8	0.86	1727	46	1726	29	1724	33	100
BF21-60-90-seq2-	8092	45	16	0.67	8359	0.3028	2.7	4.4134	4.8	0.1057	4.0	0.57	1705	41	1715	41	1727	73	99
BF21-60-90-seq2-	8190	316	22	0.19	14939	0.0704	2.0	0.5422	3.2	0.0559	2.5	0.63	438	9	440	12	448	56	98
BF21-60-90-seq2-	2592	28	6	0.31	391	0.2117	4.0	2.1411	7.0	0.0734	5.8	0.57	1238	45	1162	50	1024	117	121
BF21-60-90-seq2-	22914	122	41	0.36	23406	0.3039	2.4	4.1689	3.2	0.0995	2.1	0.75	1711	36	1668	26	1614	39	106
BF21-60-90-seq2-	28783	180	52	0.36	31090	0.2657	2.1	3.4500	2.6	0.0942	1.5	0.81	1519	28	1516	20	1512	28	100
BF21-60-90-seq2-	25103	246	57	0.54	32120	0.1975	2.5	2.1611	2.9	0.0794	1.4	0.87	1162	27	1169	20	1181	28	98
BF21-60-90-seq2-	34843	52	33	0.42	18802	0.5297	2.2	13.7726	2.6	0.1886	1.4	0.85	2740	49	2734	25	2730	23	100
BF21-60-90-seq2-	79422	1043	198	0.42	37880	0.1708	2.5	1.7347	3.0	0.0736	1.6	0.84	1017	24	1022	20	1032	33	99
BF21-60-90-seq2-	8626	115	20	0.09	3404	0.1785	2.9	1.6897	4.0	0.0687	2.8	0.71	1059	28	1005	26	889	58	119
BF21-60-90-seq2-	3426	147	11	0.48	6229	0.0707	2.3	0.5452	6.5	0.0560	6.1	0.35	440	10	442	24	451	135	98
BF21-60-90-seq2-	25994	144	52	0.80	19411	0.2856	2.8	3.9995	3.4	0.1016	2.0	0.81	1620	40	1634	28	1653	37	98
BF21-60-90-seq2-	65215	704	124	0.06	87829	0.1850	2.1	1.9274	2.3	0.0755	0.9	0.93	1094	21	1091	15	1083	17	101
BF21-60-90-seq2-	86391	461	116	0.22	80095	0.2373	2.7	3.3550	2.9	0.1025	0.9	0.94	1373	33	1494	23	1670	17	82
BF21-60-90-seq2-	36963	206	69	0.50	25700	0.2915	2.6	4.1070	3.0	0.1022	1.5	0.86	1649	37	1656	25	1664	28	99
BF21-60-90-seq2-	25560	141	47	0.28	26040	0.3213	2.2	4.4313	2.6	0.1000	1.5	0.82	1796	34	1718	22	1624	28	111
BF21-60-90-seq2-	18432	85	29	0.32	18122	0.3183	2.1	4.5592	2.8	0.1039	1.9	0.76	1782	33	1742	24	1694	34	105
BF21-60-90-seq2-	4962	29	11	1.40	5774	0.2402	3.1	2.9553	4.8	0.0892	3.6	0.65	1388	39	1396	37	1409	70	98
BF21-60-90-seq2-	23574	238	48	0.24	30380	0.1972	2.5	2.1175	2.9	0.0779	1.6	0.84	1160	26	1155	20	1143	31	101
BF21-60-90-seq2-	10551	47	19	0.77	10369	0.3246	2.3	4.4916	3.7	0.1004	2.9	0.62	1812	36	1729	31	1631	54	111
BF21-60-90-seq2-	13896	59	24	0.57	12164	0.3412	2.8	5.4383	3.4	0.1156	1.9	0.82	1892	45	1891	29	1889	35	100
BF21-60-90-seq2-	20936	204	49	0.51	8913	0.2087	2.5	2.3252	3.1	0.0808	1.9	0.79	1222	28	1220	22	1217	37	100
BF21-60-90-seq2-	110830	150	137	0.66	56919	0.7508	2.5	20.4817	2.9	0.1979	1.5	0.86	3610	69	3114	28	2809	24	129
BF21-60-90-seq2-	8370	60	15	0.23	9769	0.2360	1.9	2.8298	3.0	0.0869	2.3	0.65	1366	24	1363	23	1359	44	100
BF21-60-90-seq2-	12051	118	27	0.42	15307	0.2052	2.4	2.2672	3.1	0.0801	2.0	0.77	1203	26	1202	22	1201	39	100
BF21-60-90-seq2-	3502	47	11	0.97	5198	0.1743	2.9	1.6658	5.0	0.0693	4.0	0.59	1036	28	996	32	908	83	114
BF21-60-90-seq2-	15290	142	35	0.71	19835	0.1966	2.7	2.1397	3.6	0.0789	2.4	0.75	1157	29	1162	25	1170	47	99
BF21-60-90-seq2-	39739	111	41	0.42	36753	0.3261	1.9	4.9444	2.5	0.1100	1.6	0.77	1819	31	1810	21	1799	29	101
BF21-60-90-seq2-	117457	127	78	0.45	63169	0.5121	2.2	13.1136	2.7	0.1857	1.5	0.82	2666	49	2688	26	2705	25	99
BF21-60-90-seq2-	5647	142	17	0.43	9743	0.1141	2.1	0.9264	3.4	0.0589	2.7	0.62	697	14	666	17	563	58	124
BF21-60-90-seq3-	8691	39	10	0.52	3752	0.2247	1.5	2.5587	3.2	0.0826	2.9	0.47	1307	18	1289	24	1259	56	104
BF21-60-90-seq3-	2535	25	5	0.44	3711	0.1856	2.4	1.7737	6.4	0.0693	5.9	0.37	1098	24	1036	42	908	121	121

BF21-60-90-seq3-	25683	38	21	0.50	6146	0.4606	2.5	10.3272	3.4	0.1626	2.3	0.74	2442	50	2465	32	2483	38	98
BF21-60-90-seq3-	32516	248	61	0.42	28093	0.2231	1.9	2.5814	2.2	0.0839	1.1	0.87	1298	23	1295	16	1291	21	101
BF21-60-90-seq3-	23860	110	31	0.30	3741	0.2610	2.6	3.3830	3.6	0.0940	2.5	0.72	1495	35	1500	29	1508	47	99
BF21-60-90-seq3-	29422	301	58	0.58	42335	0.1656	2.4	1.6564	3.1	0.0726	1.9	0.78	988	22	992	20	1002	39	99
BF21-60-90-seq3-	27789	33	23	0.78	14727	0.5321	2.0	14.0000	2.6	0.1908	1.7	0.77	2750	45	2750	25	2749	28	100
BF21-60-90-seq3-	9620	50	19	1.08	10671	0.2936	1.8	3.6996	2.7	0.0914	1.9	0.69	1659	27	1571	22	1455	37	114
BF21-60-90-seq3-	13323	583	42	0.49	24563	0.0664	2.6	0.5042	3.3	0.0551	2.0	0.78	415	10	415	11	415	45	100
BF21-60-90-seq3-	57043	262	79	0.23	57216	0.2908	2.2	4.0645	2.5	0.1014	1.3	0.86	1646	32	1647	21	1649	24	100
BF21-60-90-seq3-	39622	226	73	0.79	43192	0.2550	1.8	3.2847	2.2	0.0934	1.3	0.82	1464	24	1477	17	1496	24	98
BF21-60-90-seq3-	61340	192	68	0.64	18445	0.2950	2.4	4.1695	2.7	0.1025	1.1	0.90	1667	35	1668	22	1670	21	100
BF21-60-90-seq3-	29623	137	45	0.51	29298	0.2819	2.0	3.9812	2.7	0.1024	1.7	0.77	1601	29	1630	22	1669	32	96
BF21-60-90-seq3-	15940	74	18	0.44	19581	0.2218	1.8	2.5266	2.6	0.0826	1.8	0.71	1291	22	1280	19	1260	36	102
BF21-60-90-seq3-	1601	13	3	0.29	2066	0.2382	2.7	2.5915	8.0	0.0789	7.5	0.34	1378	34	1298	60	1169	149	118
BF21-60-90-seq3-	3355	124	10	0.64	6079	0.0721	3.6	0.5556	6.9	0.0559	5.9	0.52	449	15	449	25	449	130	100
BF21-60-90-seq3-	3478	35	7	0.52	3301	0.1890	2.1	1.8714	4.8	0.0718	4.3	0.44	1116	22	1071	32	981	87	114
BF21-60-90-seq3-	81974	99	68	0.53	39343	0.5520	2.6	15.7865	2.8	0.2074	1.1	0.93	2834	61	2864	27	2885	17	98
BF21-60-90-seq3-	19138	96	34	0.81	19235	0.2828	2.2	3.8828	2.7	0.0996	1.6	0.80	1606	31	1610	22	1616	30	99
BF21-60-90-seq3-	22496	217	45	0.31	29320	0.1961	2.0	2.1054	2.4	0.0779	1.4	0.81	1154	21	1151	17	1143	29	101
BF21-60-90-seq3-	7874	310	25	0.74	14465	0.0683	2.2	0.5214	3.4	0.0553	2.6	0.64	426	9	426	12	426	58	100
BF21-60-90-seq3-	1788	19	5	1.43	2509	0.1769	2.1	1.7962	4.8	0.0736	4.3	0.44	1050	21	1044	32	1032	87	102
BF21-60-90-seq3-	3797	140	12	0.64	7234	0.0706	2.4	0.5181	4.3	0.0532	3.6	0.56	440	10	424	15	338	81	130
BF21-60-90-seq3-	22598	113	42	0.92	22620	0.2802	1.9	3.9077	2.4	0.1012	1.5	0.79	1592	27	1615	20	1645	28	97
BF21-60-90-seq3-	8906	79	17	0.38	11353	0.1982	2.7	2.1788	3.4	0.0797	2.1	0.78	1166	28	1174	24	1190	42	98
BF21-60-90-seq3-	3422	166	14	0.40	8497	0.0810	2.1	0.6022	11.0	0.0539	10.7	0.19	502	10	479	43	367	242	137
BF21-60-90-seq3-	41196	206	69	0.41	40683	0.3002	1.6	4.2596	2.0	0.1029	1.0	0.84	1692	25	1686	16	1677	19	101
BF21-60-90-seq3-	12429	53	17	0.37	11771	0.2949	2.3	4.3580	3.3	0.1072	2.4	0.70	1666	34	1704	28	1752	44	95
BF21-60-90-seq3-	59653	618	126	0.38	78080	0.1875	2.3	2.0093	2.7	0.0777	1.4	0.85	1108	23	1119	18	1140	28	97
BF21-60-90-seq3-	23533	285	48	0.06	32286	0.1768	2.3	1.8163	2.7	0.0745	1.4	0.86	1049	23	1051	18	1056	29	99
BF21-60-90-seq3-	52073	655	101	0.45	2299	0.1428	4.7	1.5134	5.0	0.0769	1.8	0.94	860	38	936	31	1118	35	77
BF21-60-90-seq3-	7926	302	25	1.13	14631	0.0639	2.7	0.4835	3.5	0.0549	2.2	0.78	399	11	400	12	408	50	98
BF21-60-90-seq3-	17996	255	34	0.28	25986	0.1264	3.6	1.2243	4.4	0.0702	2.4	0.83	767	26	812	25	935	50	82
BF21-60-90-seq3-	14250	97	29	0.66	15834	0.2486	1.8	3.1501	2.4	0.0919	1.5	0.76	1431	23	1445	18	1465	29	98
BF21-60-90-seq3-	25330	150	47	0.52	26237	0.2762	2.5	3.6978	2.9	0.0971	1.4	0.87	1572	35	1571	23	1569	26	100
BF21-60-90-seq3-	40287	68	42	0.54	7978	0.5207	2.1	13.6907	2.3	0.1907	1.0	0.91	2702	46	2729	22	2748	16	98
BF21-60-90-seq3-	67773	191	68	0.34	59605	0.3272	1.6	5.2119	1.8	0.1155	0.9	0.87	1825	25	1855	16	1888	16	97
BF21-60-90-seq3-	7686	51	11	0.67	10263	0.1894	2.2	1.9941	4.2	0.0763	3.6	0.52	1118	22	1114	29	1104	72	101
BF21-60-90-seq3-	102951	477	128	0.32	113460	0.2489	2.4	3.1490	2.6	0.0918	1.1	0.91	1433	30	1445	20	1462	20	98
BF21-60-90-seq3-	36330	241	68	0.31	37350	0.2635	2.0	3.5949	2.5	0.0989	1.5	0.81	1508	27	1548	20	1604	28	94
BF21-60-90-seq3-	2999	128	12	0.63	5953	0.0808	2.0	0.5701	3.9	0.0511	3.4	0.52	501	10	458	15	247	77	203
BF21-60-90-seq3-	5971	63	15	0.47	7953	0.2094	2.5	2.1995	5.0	0.0762	4.4	0.50	1226	28	1181	36	1100	87	111
BF21-60-90-seq3-	12832	98	26	0.33	14875	0.2480	1.9	2.9923	2.7	0.0875	1.9	0.71	1428	25	1406	21	1372	37	104
BF21-60-90-seq3-	87795	447	144	0.19	82884	0.3124	2.0	4.6318	2.3	0.1075	1.0	0.90	1753	31	1755	19	1758	18	100

BF21-60-90-seq3-	13137	159	32	0.35	17636	0.1894	2.2	1.9921	2.9	0.0763	1.9	0.76	1118	22	1113	19	1102	37	101
BF21-60-90-seq3-	778	9	2	0.13	449	0.2304	4.5	1.9652	12.7	0.0619	11.8	0.36	1337	55	1104	89	669	254	200
BF21-60-90-seq3-	6515	71	16	0.25	3921	0.2092	3.2	2.3013	4.9	0.0798	3.7	0.66	1224	36	1213	35	1192	72	103
BF21-60-90-seq3-	8111	117	28	1.23	11959	0.1732	1.9	1.6457	2.8	0.0689	2.0	0.70	1030	19	988	18	897	41	115
BF21-60-90-seq3-	8123	111	20	0.35	12227	0.1714	2.6	1.5930	3.1	0.0674	1.7	0.84	1020	24	967	19	850	35	120
BF21-60-90-seq3-	11190	162	33	0.90	4462	0.1613	2.6	1.5913	3.3	0.0716	2.1	0.79	964	24	967	21	973	42	99
BF21-60-90-seq3-	9276	55	18	0.42	9668	0.2922	2.6	3.9731	3.8	0.0986	2.8	0.68	1652	38	1629	31	1598	52	103
BF21-60-90-seq3-	8588	50	18	0.42	8831	0.3297	1.5	4.5028	2.6	0.0991	2.2	0.57	1837	24	1731	22	1607	40	114
BF21-60-90-seq3-	104317	321	118	0.75	8894	0.2993	3.6	8.2642	3.9	0.2002	1.5	0.92	1688	53	2260	36	2828	24	60
BF21-60-90-seq3-	26066	212	43	0.01	28742	0.2131	3.5	2.6934	4.7	0.0917	3.1	0.74	1245	39	1327	35	1460	60	85
BF21-60-90-seq3-	42497	203	74	0.44	39460	0.3199	1.9	4.8230	2.3	0.1094	1.4	0.81	1789	29	1789	20	1789	25	100
BF21-60-90-seq3-	2753	122	11	0.67	5291	0.0780	2.2	0.6245	10.9	0.0581	10.7	0.20	484	10	493	43	533	234	91
BF21-60-90-seq3-	29190	166	63	0.82	28095	0.2980	2.3	4.3189	2.6	0.1051	1.3	0.87	1681	34	1697	22	1716	23	98
BF21-60-90-seq3-	10763	451	36	0.30	9009	0.0780	1.9	0.6111	2.4	0.0568	1.5	0.78	484	9	484	9	484	34	100
BF21-60-90-seq3-	3927	42	11	0.51	4302	0.2480	2.6	3.1827	6.6	0.0931	6.0	0.40	1428	34	1453	52	1490	115	96
BF21-60-90-seq3-	-	-	-	-	-	-	-	-	-	-	-	-	-	-	-	-	-	-	-
Sample BF22	Gortanimill Formation					Location (decimal degrees) 52.027 8.112033 W						Datum: D_WGS_1984							
BF22-seq1-a1	8880	115	10	0.41	16266	0.0839	2.4	0.6425	3.6	0.0556	2.6	0.67	519	12	504	14	435	59	119
BF22-seq1-a2	44039	111	32	0.42	49431	0.2529	2.2	3.1695	2.6	0.0909	1.3	0.86	1453	29	1450	20	1444	25	101
BF22-seq1-a3	49640	111	46	0.47	43777	0.3621	2.4	5.7874	3.1	0.1159	2.0	0.76	1992	41	1945	27	1894	37	105
BF22-seq1-a4	18787	213	25	0.29	27575	0.1122	2.8	1.0773	4.4	0.0696	3.3	0.65	686	19	742	23	917	68	75
BF22-seq1-a5	31270	223	43	0.36	43137	0.1757	2.0	1.7934	2.4	0.0740	1.2	0.86	1044	20	1043	15	1042	24	100
BF22-seq1-a6	2101	13	4	0.82	1263	0.2261	2.4	2.1332	6.2	0.0684	5.7	0.38	1314	28	1160	44	881	119	149
BF22-seq1-a7	4947	115	10	0.47	7968	0.0812	2.1	0.6029	5.7	0.0539	5.3	0.37	503	10	479	22	365	119	138
BF22-seq1-a8	15661	113	21	0.54	21496	0.1565	3.7	1.6047	4.2	0.0744	1.9	0.89	937	33	972	27	1051	39	89
BF22-seq1-a9	18629	33	16	0.42	14392	0.4448	2.1	8.1191	2.9	0.1324	2.0	0.71	2372	41	2244	26	2130	35	111
BF22-seq1-a10	45748	40	26	0.47	25456	0.5348	2.2	13.5314	2.9	0.1835	1.8	0.77	2762	51	2717	28	2685	30	103
BF22-seq1-a11	9812	72	14	0.25	9531	0.1825	3.2	1.9204	4.9	0.0763	3.7	0.65	1080	32	1088	33	1104	74	98
BF22-seq1-a12	26235	108	30	0.41	28968	0.2480	2.6	3.1613	3.2	0.0924	1.8	0.82	1428	34	1448	25	1476	35	97
BF22-seq1-a13	3642	81	7	0.22	1274	0.0835	2.3	0.6276	5.3	0.0545	4.7	0.44	517	12	495	21	393	106	132
BF22-seq1-a14	10863	51	16	0.81	1576	0.2578	1.8	3.0046	2.9	0.0845	2.3	0.62	1479	24	1409	23	1305	45	113
BF22-seq1-a15	15932	75	22	0.58	7184	0.2468	1.9	2.9720	2.8	0.0873	2.0	0.69	1422	25	1400	21	1368	39	104
BF22-seq1-a16	1224	18	2	0.47	525	0.1159	2.8	0.8620	11.1	0.0539	10.7	0.26	707	19	631	54	369	242	192
BF22-seq1-a17	5928	131	12	0.51	4850	0.0814	1.9	0.6404	3.6	0.0571	3.0	0.54	504	9	503	14	494	66	102
BF22-seq1-a18	6669	231	19	0.36	17425	0.0784	2.0	0.4064	6.9	0.0376	6.6	0.29	487	9	346	20	-515	176	-95
BF22-seq1-a19	6881	197	16	0.53	13056	0.0728	2.8	0.5396	4.4	0.0537	3.4	0.64	453	12	438	16	359	76	126
BF22-seq1-a20	19138	460	36	0.29	7917	0.0761	1.9	0.6088	2.9	0.0581	2.2	0.66	473	9	483	11	532	48	89
BF22-seq1-a21	5000	91	10	0.44	8430	0.0964	2.7	0.8045	5.1	0.0605	4.3	0.53	593	16	599	24	622	94	95
BF22-seq1-a22	51832	197	70	0.73	54178	0.2863	2.5	3.8545	2.9	0.0977	1.5	0.86	1623	35	1604	23	1580	27	103
BF22-seq1-a23	13404	344	31	0.66	19563	0.0761	2.4	0.5917	2.9	0.0564	1.7	0.81	473	11	472	11	469	38	101
BF22-seq1-a24	10239	61	18	0.90	2722	0.2186	2.0	2.5530	3.4	0.0847	2.7	0.59	1274	23	1287	25	1309	53	97

BF22-seq1-a25	17554	606	30	0.35	31847	0.0504	3.3	0.3890	3.7	0.0559	1.8	0.88	317	10	334	11	450	40	70
BF22-seq1-a26	16594	80	22	0.27	8114	0.2679	1.9	3.2535	2.5	0.0881	1.6	0.76	1530	26	1470	19	1384	30	111
BF22-seq1-a27	33486	167	47	0.32	38140	0.2571	2.2	3.1842	2.8	0.0898	1.7	0.80	1475	30	1453	22	1422	32	104
BF22-seq1-a28	18269	318	26	0.37	32994	0.0756	2.2	0.5894	3.3	0.0566	2.5	0.66	470	10	470	13	474	55	99
BF22-seq1-a29	93582	640	133	0.28	134316	0.1492	2.2	1.4651	2.8	0.0712	1.7	0.79	896	19	916	17	964	35	93
BF22-seq1-a30	536820	502	146	0.07	312128	0.2745	3.2	6.6458	3.7	0.1756	1.7	0.89	1564	45	2065	33	2612	28	60
BF22-seq1-a31	17146	64	24	0.63	17351	0.3183	2.0	4.4241	2.7	0.1008	1.8	0.75	1782	31	1717	23	1639	33	109
BF22-seq1-a32	14845	145	39	1.34	20592	0.1754	2.4	1.7829	3.2	0.0737	2.1	0.76	1042	23	1039	21	1034	42	101
BF22-seq1-a33	4581	131	13	0.65	8645	0.0856	1.7	0.6388	3.0	0.0541	2.4	0.59	530	9	502	12	375	54	141
BF22-seq1-a34	8987	295	23	0.40	16452	0.0701	1.9	0.5397	4.8	0.0559	4.5	0.39	436	8	438	17	448	99	97
BF22-seq1-a35	14150	120	22	0.04	19078	0.1957	2.1	2.0416	3.0	0.0757	2.2	0.69	1152	22	1129	21	1086	44	106
BF22-seq1-a36	55485	249	75	0.48	57245	0.2554	2.1	3.4850	3.1	0.0990	2.3	0.68	1466	27	1524	25	1605	42	91
BF22-seq1-a37	16985	242	27	0.48	3295	0.0959	2.3	0.7988	3.3	0.0604	2.4	0.70	590	13	596	15	618	51	95
BF22-seq1-a38	11556	74	15	0.38	16264	0.1852	2.2	1.8474	3.1	0.0724	2.3	0.69	1095	22	1062	21	996	47	110
BF22-seq1-a39	140196	210	112	0.17	64428	0.4879	2.1	11.7861	2.5	0.1752	1.2	0.87	2562	46	2588	23	2608	21	98
BF22-seq1-a40	3213	98	10	0.84	6238	0.0826	2.7	0.6000	6.1	0.0527	5.5	0.44	512	13	477	24	316	125	162
BF22-seq1-a41	227902	113	117	0.21	66440	0.8312	2.4	40.2000	2.8	0.3508	1.4	0.87	3900	72	3776	28	3710	21	105
BF22-seq1-a42	4716	120	15	1.10	4228	0.0916	1.9	0.8217	8.5	0.0651	8.2	0.23	565	10	609	40	777	173	73
BF22-seq1-a43	4053	148	14	0.91	8076	0.0734	2.7	0.5187	4.4	0.0512	3.4	0.62	457	12	424	15	252	79	181
BF22-seq1-a44	44082	195	73	0.51	43681	0.3231	2.4	4.5898	2.8	0.1030	1.5	0.85	1805	38	1747	24	1679	27	107
BF22-seq1-a45	9961	102	25	0.78	3143	0.1942	2.9	2.0645	5.2	0.0771	4.3	0.56	1144	31	1137	36	1124	85	102
BF22-seq1-a46	3254	79	10	0.56	5898	0.1169	2.5	0.8983	4.9	0.0557	4.2	0.52	713	17	651	24	441	93	162
BF22-seq1-a47	1099	8	2	0.50	426	0.2823	3.4	3.0586	15.0	0.0786	14.6	0.23	1603	49	1422	121	1161	289	138
BF22-seq1-a48	9851	102	19	0.40	13597	0.1715	2.5	1.7485	4.3	0.0740	3.6	0.57	1020	23	1027	28	1040	72	98
BF22-seq1-a49	6559	241	22	0.49	12074	0.0822	2.6	0.6282	5.3	0.0554	4.6	0.49	509	13	495	21	429	103	119
BF22-seq1-a50	17369	90	37	0.77	18040	0.3329	1.8	4.5149	2.7	0.0984	2.0	0.68	1852	30	1734	23	1593	37	116
BF22-seq1-a51	53710	541	108	0.30	69930	0.1868	2.0	2.0194	2.4	0.0784	1.4	0.82	1104	20	1122	17	1157	28	95
BF22-seq1-a52	8532	346	29	0.48	15758	0.0768	1.9	0.5761	3.0	0.0544	2.3	0.65	477	9	462	11	389	51	123
BF22-seq1-a53	18220	93	34	0.52	7083	0.3117	2.1	4.4862	2.6	0.1044	1.6	0.80	1749	32	1728	22	1704	29	103
BF22-seq1-a54	46337	291	81	0.32	49886	0.2550	2.0	3.3328	2.4	0.0948	1.2	0.85	1464	27	1489	19	1524	23	96
BF22-seq1-a55	9364	399	28	0.18	17414	0.0705	2.4	0.5347	3.0	0.0550	1.9	0.77	439	10	435	11	411	43	107
BF22-seq1-a56	2586	100	10	0.56	5054	0.0859	2.0	0.6170	4.5	0.0521	4.1	0.43	531	10	488	18	288	93	184
BF22-seq1-a57	1165	18	4	0.50	2105	0.1995	3.7	1.6402	10.1	0.0596	9.4	0.37	1172	40	986	66	591	205	199
BF22-seq1-a58	5787	232	23	0.64	5328	0.0832	2.3	0.6206	3.8	0.0541	3.0	0.62	515	12	490	15	376	67	137
BF22-seq1-a59	37847	131	47	0.42	37487	0.3159	2.2	4.4976	2.7	0.1033	1.7	0.80	1770	34	1731	23	1684	31	105
BF22-seq1-a60	11440	97	22	0.47	16181	0.2041	1.9	2.0331	2.8	0.0722	2.0	0.70	1198	21	1127	19	992	40	121
BF22-seq2-b1	18934	102	29	0.41	21454	0.2573	2.4	3.2056	2.8	0.0904	1.5	0.84	1476	31	1459	22	1433	29	103
BF22-seq2-b2	25869	108	44	0.93	26490	0.3098	1.7	4.2760	2.4	0.1001	1.7	0.71	1740	26	1689	20	1626	32	107
BF22-seq2-b3	2808	119	14	0.76	532	0.0956	3.0	0.8491	11.5	0.0644	11.1	0.26	588	17	624	55	756	235	78
BF22-seq2-b4	71605	543	92	0.01	92383	0.1809	2.3	1.9816	2.8	0.0795	1.6	0.82	1072	23	1109	19	1184	32	91
BF22-seq2-b5	8530	43	15	0.73	9655	0.3001	1.7	3.7547	3.2	0.0908	2.7	0.53	1692	25	1583	26	1441	51	117
BF22-seq2-b6	14928	430	30	0.20	27354	0.0707	1.9	0.5475	2.7	0.0562	1.8	0.73	440	8	443	10	459	40	96

BF22-seq2-b7	20950	415	30	0.17	16568	0.0685	3.5	0.6726	6.1	0.0712	5.0	0.58	427	15	522	25	963	102	44
BF22-seq2-b8	7494	247	19	0.59	13765	0.0646	4.7	0.4997	5.9	0.0561	3.6	0.79	404	18	411	20	457	80	88
BF22-seq2-b9	2130	58	6	1.00	4049	0.0754	2.4	0.5597	5.5	0.0538	5.0	0.43	469	11	451	20	364	112	129
BF22-seq2-b10	25904	232	41	0.04	35348	0.1896	2.2	1.9622	2.6	0.0751	1.4	0.84	1119	22	1103	18	1070	29	105
BF22-seq2-b11	3672	29	7	0.49	4950	0.1981	2.3	2.0651	4.1	0.0756	3.4	0.56	1165	25	1137	29	1084	69	107
BF22-seq2-b12	62127	315	91	0.27	68525	0.2757	2.2	3.5248	2.5	0.0927	1.3	0.87	1570	31	1533	20	1482	24	106
BF22-seq2-b13	17397	96	22	0.60	23080	0.1960	2.1	2.0880	2.5	0.0773	1.3	0.84	1154	22	1145	17	1128	27	102
BF22-seq2-b14	16836	88	23	0.86	22128	0.2071	2.0	2.2249	2.6	0.0779	1.7	0.77	1213	22	1189	19	1145	34	106
BF22-seq2-b15	8118	62	18	0.73	10984	0.2509	2.1	2.6169	4.1	0.0757	3.5	0.51	1443	27	1305	31	1086	71	133
BF22-seq2-b16	4853	108	12	0.52	8879	0.0991	2.2	0.7491	4.2	0.0548	3.5	0.53	609	13	568	18	406	79	150
BF22-seq2-b17	34922	132	46	0.26	34323	0.3291	3.2	4.7274	3.5	0.1042	1.5	0.91	1834	51	1772	30	1700	27	108
BF22-seq2-b18	72744	84	58	0.60	37090	0.5398	2.3	15.0125	2.7	0.2017	1.5	0.84	2783	52	2816	26	2840	24	98
BF22-seq2-b19	1753	55	8	2.32	3673	0.0813	2.7	0.5486	9.8	0.0489	9.4	0.27	504	13	444	36	144	221	350
BF22-seq2-b20	6369	178	12	0.72	11359	0.0527	4.4	0.4163	6.0	0.0573	4.2	0.72	331	14	353	18	505	92	66
BF22-seq2-b21	4680	41	11	0.96	3863	0.2057	2.3	2.0651	5.0	0.0728	4.5	0.45	1206	25	1137	35	1009	91	120
BF22-seq2-b22	26332	171	45	0.22	30921	0.2568	2.7	3.0842	2.9	0.0871	1.1	0.92	1474	35	1429	22	1362	22	108
BF22-seq2-b23	8163	245	22	0.37	6285	0.0825	3.3	0.6549	5.2	0.0576	4.0	0.64	511	16	511	21	515	89	99
BF22-seq2-b24	21783	673	66	0.02	34458	0.1055	1.9	0.9446	5.4	0.0649	5.0	0.35	647	11	675	27	772	106	84
BF22-seq2-b25	2387	40	8	0.35	3528	0.2036	3.5	1.9480	8.2	0.0694	7.4	0.43	1194	38	1098	57	911	153	131
BF22-seq2-b26	3461	19	4	0.31	4866	0.2143	2.2	2.1515	6.1	0.0728	5.6	0.37	1252	25	1166	43	1009	114	124
BF22-seq2-b27	5989	299	26	0.30	11109	0.0863	2.3	0.6569	3.2	0.0552	2.3	0.70	534	12	513	13	420	51	127
BF22-seq2-b28	48067	86	55	0.65	15852	0.5432	5.4	14.6368	6.0	0.1954	2.6	0.90	2797	125	2792	59	2788	42	100
BF22-seq2-b29	6360	218	17	0.34	8608	0.0749	2.1	0.5578	3.1	0.0540	2.3	0.67	465	9	450	11	373	51	125
BF22-seq2-b30	41072	266	85	0.74	45266	0.2493	3.0	3.1985	4.3	0.0931	3.2	0.68	1435	38	1457	34	1489	60	96
BF22-seq2-b31	39050	431	37	0.06	53400	0.0898	3.3	0.9246	4.5	0.0747	3.0	0.74	554	18	665	22	1061	61	52
BF22-seq2-b32	3529	26	5	0.32	5119	0.1813	2.3	1.7711	4.8	0.0709	4.2	0.49	1074	23	1035	32	953	86	113
BF22-seq2-b33	6929	145	12	0.36	12556	0.0782	2.3	0.6095	3.3	0.0566	2.3	0.71	485	11	483	13	474	51	102
BF22-seq2-b34	8186	147	17	0.49	14352	0.1004	4.1	0.8081	5.2	0.0584	3.2	0.79	616	24	601	24	545	70	113
BF22-seq2-b35	19382	87	33	0.62	19660	0.3157	2.1	4.3920	2.9	0.1009	1.9	0.74	1769	33	1711	24	1641	36	108
BF22-seq2-b36	4654	103	13	0.68	8191	0.1038	2.4	0.8356	4.1	0.0584	3.3	0.58	637	15	617	19	544	73	117
BF22-seq2-b37	47774	129	54	0.14	37727	0.4034	2.2	7.2180	2.4	0.1298	1.0	0.92	2185	41	2139	22	2095	17	104
BF22-seq2-b38	5971	60	12	0.58	5218	0.1715	2.4	1.7026	4.2	0.0720	3.5	0.56	1021	22	1010	27	985	71	104
BF22-seq2-b39	3483	173	10	0.17	6484	0.0554	2.7	0.4194	11.0	0.0549	10.6	0.25	347	9	356	33	410	237	85
BF22-seq2-b40	97063	296	133	0.45	79184	0.3962	2.1	6.8324	2.5	0.1251	1.3	0.85	2151	39	2090	23	2030	23	106
BF22-seq2-b41	65986	516	123	0.27	79966	0.2269	2.1	2.6480	2.6	0.0847	1.6	0.81	1318	25	1314	20	1308	30	101
BF22-seq2-b42	146463	349	13	0.15	5392	0.0257	55.3	0.6129	55.5	0.1732	5.0	1.00	163	90	485	241	2589	83	6
BF22-seq2-b43	33423	100	32	0.13	33027	0.3226	2.3	4.6080	2.6	0.1036	1.3	0.88	1802	36	1751	22	1690	23	107
BF22-seq2-b44	33581	399	59	0.52	14280	0.1352	2.0	1.2216	2.5	0.0655	1.5	0.79	818	15	811	14	791	32	103
BF22-seq2-b45	84530	392	128	0.34	82763	0.2980	2.2	4.2952	2.5	0.1046	1.3	0.86	1681	33	1692	21	1706	24	99
BF22-seq2-b46	15407	346	42	0.56	26233	0.1072	2.0	0.8902	2.9	0.0602	2.1	0.68	656	12	646	14	612	46	107
BF22-seq2-b47	2731	103	9	0.41	5033	0.0841	2.2	0.6441	3.8	0.0556	3.0	0.59	520	11	505	15	435	68	120
BF22-seq2-b48	14725	56	17	0.39	18087	0.2803	1.9	3.2424	2.9	0.0839	2.1	0.68	1593	28	1467	23	1290	41	123

BF22-seq2-b49	4365	133	12	0.46	5259	0.0813	2.3	0.6417	8.5	0.0572	8.2	0.27	504	11	503	34	501	181	101
BF22-seq2-b50	2376	82	9	0.89	4663	0.0879	2.0	0.6318	4.7	0.0522	4.2	0.42	543	10	497	18	292	96	186
BF22-seq2-b51	9792	255	29	0.22	16734	0.1151	1.9	0.9414	3.2	0.0593	2.6	0.59	702	13	674	16	580	57	121
BF22-seq2-b52	35272	81	43	0.38	22736	0.4579	2.8	10.0184	3.1	0.1587	1.3	0.90	2430	56	2436	29	2442	22	100
BF22-seq2-b53	2108	77	6	0.37	4112	0.0682	3.1	0.4925	5.4	0.0524	4.4	0.58	425	13	407	18	301	99	141
BF22-seq2-b54	4411	158	15	0.21	8767	0.0981	2.2	0.6958	5.9	0.0514	5.4	0.37	603	12	536	25	260	125	232
BF22-seq2-b55	5094	55	13	0.66	1410	0.1965	3.0	1.9018	4.0	0.0702	2.7	0.74	1157	32	1082	27	934	56	124
BF22-seq1-a56	5094	56	13	0.66	1410	0.1966	3.0	1.9026	4.0	0.0702	2.7	0.74	1157	32	1082	27	934	56	124
BF22-seq2-b57	5972	148	15	0.17	9942	0.1053	1.8	0.8789	3.9	0.0605	3.4	0.47	645	11	640	18	623	74	104
BF22-seq2-b58	23261	538	47	0.36	41877	0.0826	2.4	0.6493	2.8	0.0570	1.6	0.83	512	12	508	11	492	35	104
BF22-seq2-b59	33042	160	56	0.36	31618	0.3172	3.2	4.6843	3.4	0.1071	1.3	0.93	1776	50	1764	29	1750	23	101
BF22-seq2-b60	24994	138	51	0.60	12419	0.3144	2.1	4.3191	3.0	0.0996	2.1	0.70	1762	32	1697	25	1617	40	109
BF22-seq3-c1	13475	424	35	0.46	24254	0.0761	1.8	0.5954	2.5	0.0567	1.7	0.73	473	8	474	10	480	38	98
BF22-seq3-c2	15835	381	40	0.37	26812	0.0982	2.7	0.8165	6.3	0.0603	5.7	0.43	604	16	606	29	615	122	98
BF22-seq3-c3	2337	73	6	0.42	4249	0.0754	3.8	0.5850	11.9	0.0563	11.2	0.32	469	17	468	45	463	249	101
BF22-seq3-c4	1805	47	4	0.55	2320	0.0761	2.6	0.5821	7.8	0.0555	7.3	0.34	473	12	466	29	433	163	109
BF22-seq3-c5	10717	143	23	0.37	9180	0.1504	2.8	1.4346	4.2	0.0692	3.1	0.67	903	24	903	25	904	64	100
BF22-seq3-c6	2304	59	6	0.53	4328	0.0982	1.1	0.7348	4.0	0.0543	3.8	0.29	604	7	559	17	381	86	158
BF22-seq3-c7	14169	49	23	0.84	12806	0.3562	2.8	5.5496	3.6	0.1130	2.3	0.78	1964	48	1908	31	1848	41	106
BF22-seq3-c8	3980	40	11	1.38	5655	0.1936	1.4	1.9222	4.1	0.0720	3.9	0.34	1141	15	1089	28	986	79	116
BF22-seq3-c9	2423	71	8	0.85	1350	0.0861	1.5	0.7082	4.7	0.0597	4.5	0.32	532	8	544	20	592	98	90
BF22-seq3-c10	20149	89	33	0.70	12331	0.2961	2.0	4.2140	3.4	0.1032	2.8	0.59	1672	30	1677	29	1683	51	99
BF22-seq3-c11	1490	37	4	0.65	2700	0.1036	1.5	0.8027	7.5	0.0562	7.4	0.19	635	9	598	35	461	164	138
BF22-seq3-c12	22747	99	40	0.73	22175	0.3278	1.4	4.7328	1.9	0.1047	1.3	0.73	1828	23	1773	16	1710	24	107
BF22-seq3-c13	33847	160	35	0.19	38859	0.2094	2.7	2.5688	3.4	0.0890	2.1	0.79	1225	30	1292	25	1404	40	87
BF22-seq3-c14	61002	180	62	0.34	60882	0.3141	1.5	4.4336	1.8	0.1024	1.0	0.83	1761	23	1719	15	1667	18	106
BF22-seq3-c15	6639	114	12	0.36	2097	0.0982	2.3	0.8980	12.0	0.0664	11.7	0.20	604	14	651	59	818	245	74
BF22-seq3-c16	7468	146	14	0.52	13205	0.0851	1.8	0.6790	3.7	0.0579	3.3	0.49	526	9	526	15	526	71	100
BF22-seq3-c17	15447	167	23	0.20	24252	0.1343	1.3	1.2052	2.1	0.0651	1.6	0.62	812	10	803	12	777	34	105
BF22-seq3-c18	33103	99	39	0.87	32952	0.2998	1.7	4.2428	2.4	0.1026	1.8	0.68	1690	25	1682	20	1672	33	101
BF22-seq3-c19	2568	48	5	0.64	1099	0.0839	1.7	0.6663	8.7	0.0576	8.6	0.19	520	8	518	36	513	188	101
BF22-seq3-c20	48091	145	52	0.60	47925	0.3006	1.5	4.2420	2.1	0.1024	1.4	0.74	1694	23	1682	17	1667	25	102
BF22-seq3-c21	7557	180	15	0.41	2703	0.0759	1.0	0.5746	2.5	0.0549	2.2	0.42	471	5	461	9	410	50	115
BF22-seq3-c22	12094	107	20	0.35	6529	0.1855	1.3	1.8182	2.9	0.0711	2.6	0.46	1097	14	1052	19	960	52	114
BF22-seq3-c23	976	24	3	0.98	2162	0.0815	1.5	0.5159	9.2	0.0459	9.0	0.16	505	7	422	32	-6	218	-8781
BF22-seq3-c24	5508	177	14	0.17	9751	0.0821	3.2	0.6524	5.2	0.0576	4.1	0.62	508	16	510	21	516	89	98
BF22-seq3-c25	84946	183	74	0.29	49450	0.3538	1.6	8.5756	2.1	0.1758	1.4	0.77	1953	28	2294	20	2614	23	75
BF22-seq3-c26	44965	219	51	0.26	52519	0.2198	1.6	2.6466	2.2	0.0873	1.5	0.74	1281	19	1314	16	1368	28	94
BF22-seq3-c27	25997	109	30	0.27	29925	0.2593	1.4	3.1717	2.1	0.0887	1.6	0.66	1486	19	1450	17	1398	31	106
BF22-seq3-c28	78040	248	103	1.02	50501	0.3080	1.8	4.3117	2.2	0.1015	1.2	0.83	1731	27	1696	18	1653	22	105
BF22-seq3-c29	26586	239	47	0.02	20613	0.2106	2.0	2.3311	2.5	0.0803	1.6	0.78	1232	22	1222	18	1204	31	102
BF22-seq3-c30	26302	30	21	0.60	13511	0.5605	1.6	15.3683	2.1	0.1989	1.4	0.75	2869	36	2838	20	2817	22	102

[a] within-run background-corrected mean ^{207}Pb signal in counts per second

[b] U and Pb content and Th/U ratio were calculated relative to GJ-1 and are accurate to approximately 10%.

[c] corrected for background, mass bias, laser induced U-Pb fractionation and common Pb (if detectable, see analytical method) using Stacey & Kramers (1975) model Pb composition. $^{207}Pb/^{235}U$ calculated using $^{207}Pb/^{206}Pb/(^{238}U/^{206}Pb \times 1/137.88)$. Errors are propagated by quadratic addition of within-run errors (2SE) and the reproducibility of GJ-1 (2SD).

[d] Rho is the error correlation defined as $err^{206}Pb/^{238}U/err^{207}Pb/^{235}U$.

Table IV. LA ICP MS U, Pb and Th isotopic data for detrital zircons from all 15 samples from the NCSB, SCSB, Fastnet Basin and Goban Spur Basin arranged by basin and stratigraphic

Number	$^{207}Pb^a$ (cps)	U^b (ppm)	Pb^b (ppm)	Th^b / U	^{206}Pb / ^{204}Pb	$^{206}Pb^c$ / ^{238}U	2 s %	$^{207}Pb^c$ / ^{235}U	2 s %	$^{207}Pb^c$ / ^{206}Pb	2 s %	rho[d]	^{206}Pb / ^{238}U	2 s (Ma)	^{207}Pb / ^{235}U	2 s (Ma)	^{207}Pb / ^{206}Pb	2 s (Ma)	conc %
Sample 57/09-1 (AK29)				**Well no.: 57/09-1**								**Locati**	**50.827**	**8.381836 W**	**Datum: IRENET95**				
AK29-seq1-A01	481	187	12	0.70	901	0.0584	2.1	0.4543	6.8	0.0564	6.5	0.31	366	8	380	22	469	143	78
AK29-seq1-A02	1101	327	40	0.89	1857	0.1133	1.5	0.9790	6.0	0.0627	5.9	0.24	692	10	693	31	696	125	99
AK29-seq1-A03	1584	123	12	0.26	2782	0.0976	1.0	0.8033	3.9	0.0597	3.8	0.25	600	6	599	18	593	83	101
AK29-seq1-A04	1520	159	21	0.21	2508	0.1292	1.6	1.1547	5.0	0.0648	4.7	0.32	783	12	779	28	768	100	102
AK29-seq1-A05	2244	133	35	0.32	2723	0.2511	3.3	2.9911	4.9	0.0864	3.6	0.67	1444	43	1405	38	1347	70	107
AK29-seq1-A06	19773	192	78	0.20	17804	0.3963	1.2	6.3461	1.9	0.1161	1.5	0.64	2152	22	2025	17	1897	26	113
AK29-seq1-A07	561	137	9	0.58	942	0.0583	2.0	0.4968	10.5	0.0618	10.3	0.19	365	7	410	36	668	220	55
AK29-seq1-A08	4052	129	54	0.68	3667	0.3499	1.6	5.5806	3.1	0.1157	2.6	0.53	1934	28	1913	27	1890	47	102
AK29-seq1-A09	3586	93	26	0.41	3149	0.2492	3.1	4.1130	4.7	0.1197	3.5	0.66	1434	40	1657	39	1952	63	73
AK29-seq1-A10	2196	218	19	0.47	4028	0.0814	1.2	0.6402	3.5	0.0570	3.3	0.35	504	6	502	14	493	73	102
AK29-seq1-A11	14664	824	142	0.54	409	0.1491	2.3	1.3732	4.6	0.0668	4.0	0.49	896	19	878	28	831	84	108
AK29-seq1-A12	494	108	12	0.44	858	0.1001	2.3	0.8272	8.3	0.0599	8.0	0.28	615	14	612	39	600	173	102
AK29-seq1-A13	356	49	5	0.35	614	0.1061	3.5	0.8927	11.0	0.0610	10.4	0.32	650	21	648	54	640	224	102
AK29-seq1-A14	849	286	14	0.19	1410	0.0495	1.7	0.3583	5.7	0.0525	5.4	0.30	311	5	311	15	308	123	101
AK29-seq1-A15	508	39	5	0.96	883	0.1008	1.8	0.8387	9.3	0.0603	9.1	0.19	619	11	618	44	615	196	101
AK29-seq1-A16	1333	235	12	0.50	2643	0.0479	2.0	0.3470	4.9	0.0525	4.5	0.41	302	6	302	13	309	102	98
AK29-seq1-A17	933	346	27	1.13	1767	0.0607	1.7	0.4608	5.2	0.0550	4.9	0.33	380	6	385	17	413	109	92
AK29-seq1-A18	1226	207	18	0.13	2183	0.0907	1.8	0.7366	5.2	0.0589	4.9	0.34	559	10	560	23	564	107	99
AK29-seq1-A19	1676	54	17	0.36	1794	0.2845	2.1	3.8603	4.9	0.0984	4.4	0.43	1614	30	1605	40	1594	82	101
AK29-seq1-A20	1132	187	18	0.41	2013	0.0917	1.6	0.7447	4.7	0.0589	4.5	0.34	565	9	565	21	564	97	100
AK29-seq1-A21	833	129	17	1.31	1450	0.0975	2.2	0.8092	6.5	0.0602	6.1	0.33	600	12	602	30	611	132	98
AK29-seq1-A22	21422	377	175	0.29	18257	0.4438	1.1	7.5383	1.9	0.1232	1.5	0.60	2367	22	2178	17	2003	27	118
AK29-seq1-A23	13034	251	102	0.10	10751	0.4074	1.3	7.0505	2.2	0.1255	1.7	0.60	2203	24	2118	19	2036	31	108
AK29-seq1-A24	183	17	2	0.46	321	0.0884	2.8	0.7067	16.6	0.0580	16.4	0.17	546	15	543	72	529	358	103
AK29-seq1-A25	670	60	7	1.15	1179	0.0940	2.3	0.7682	6.2	0.0593	5.8	0.37	579	13	579	28	578	126	100
AK29-seq1-A26	801	145	14	0.36	1332	0.0930	1.9	0.7505	6.1	0.0585	5.9	0.30	573	10	569	27	549	128	104
AK29-seq1-A27	173	25	3	0.55	303	0.1015	2.9	0.8425	20.0	0.0602	19.7	0.15	623	17	621	97	611	427	102
AK29-seq1-A28	2119	781	40	0.30	4221	0.0506	1.8	0.3668	4.1	0.0525	3.7	0.44	318	6	317	11	309	84	103
AK29-seq1-A29	1106	461	22	0.27	2192	0.0472	1.5	0.3407	6.8	0.0524	6.6	0.21	297	4	298	18	302	152	98
AK29-seq1-A30	610	163	12	0.43	1151	0.0664	1.8	0.5047	6.0	0.0551	5.8	0.30	414	7	415	21	418	129	99
AK29-seq1-A31	593	116	10	0.24	1041	0.0903	3.0	0.7384	8.4	0.0593	7.8	0.35	558	16	561	37	577	170	97
AK29-seq1-A32	1980	191	19	0.54	3507	0.0924	1.4	0.7576	4.1	0.0594	3.8	0.35	570	8	573	18	584	82	98
AK29-seq1-A33	701	121	13	0.34	1203	0.1012	1.9	0.8525	6.9	0.0611	6.6	0.28	622	11	626	33	642	143	97
AK29-seq1-A34	1496	565	32	0.53	2968	0.0524	1.4	0.3836	4.4	0.0531	4.2	0.31	329	4	330	13	331	96	99
AK29-seq1-A35	2053	701	37	0.34	4085	0.0517	2.0	0.3765	3.9	0.0528	3.3	0.52	325	6	324	11	321	75	101
AK29-seq1-A36	734	118	14	0.72	1257	0.1051	2.7	0.8976	7.6	0.0619	7.1	0.36	644	17	650	37	672	153	96

AK29-seq1-A37	1630	277	32	0.67	2842	0.1036	1.8	0.8545	4.7	0.0598	4.4	0.39	635	11	627	22	598	95	106
AK29-seq1-A38	416	77	8	0.38	727	0.0985	2.2	0.8170	9.2	0.0601	9.0	0.23	606	13	606	43	609	194	99
AK29-seq1-A39	1812	310	36	0.63	3147	0.1022	1.8	0.8479	3.9	0.0602	3.5	0.45	627	11	624	18	611	76	103
AK29-seq1-A40	866	217	28	0.50	1419	0.1201	4.6	1.0457	7.7	0.0632	6.1	0.60	731	32	727	41	714	131	102
AK29-seq1-A41	769	212	20	1.11	1421	0.0737	2.0	0.5765	7.3	0.0567	7.0	0.27	458	9	462	27	482	155	95
AK29-seq1-A42	297	99	7	0.68	566	0.0619	2.4	0.4616	12.8	0.0541	12.6	0.19	387	9	385	42	376	283	103
AK29-seq1-A43	1622	287	31	0.40	2814	0.1008	1.9	0.8429	4.8	0.0606	4.4	0.39	619	11	621	23	626	96	99
AK29-seq1-A44	480	94	9	0.32	843	0.0937	2.4	0.7695	9.0	0.0596	8.7	0.27	577	13	579	40	589	188	98
AK29-seq1-A45	2720	65	28	0.47	2266	0.3830	1.7	6.6428	4.2	0.1258	3.9	0.40	2090	30	2065	38	2040	68	102
AK29-seq1-A46	6085	162	60	0.27	5259	0.3498	1.4	5.8585	2.8	0.1215	2.4	0.50	1934	23	1955	25	1978	43	98
AK29-seq1-A47	761	72	17	0.30	915	0.2241	2.6	2.6911	6.4	0.0871	5.8	0.40	1303	30	1326	48	1363	112	96
AK29-seq1-A48	1490	294	30	0.47	2609	0.0958	2.2	0.7988	4.8	0.0605	4.3	0.46	590	13	596	22	620	92	95
AK29-seq1-A49	1394	259	32	0.91	2416	0.1005	1.9	0.8350	5.0	0.0603	4.6	0.37	617	11	616	23	613	100	101
AK29-seq1-A50	1359	194	25	0.23	2192	0.1278	1.6	1.1380	5.2	0.0646	5.0	0.30	775	11	772	29	761	105	102
AK29-seq1-A51	555	120	12	0.50	980	0.0939	1.5	0.7671	7.2	0.0592	7.1	0.21	579	8	578	32	576	154	101
AK29-seq1-A52	771	124	11	0.12	1239	0.0912	4.7	0.8242	8.7	0.0656	7.3	0.54	562	25	610	41	793	153	71
AK29-seq1-A53	1086	760	38	0.21	2147	0.0511	2.1	0.3726	5.2	0.0529	4.8	0.41	321	7	322	15	324	108	99
AK29-seq1-A54	429	87	5	0.37	815	0.0581	1.2	0.4387	6.7	0.0547	6.6	0.18	364	4	369	21	401	148	91
AK29-seq1-A55	2475	166	34	0.29	2049	0.1961	1.6	2.3567	4.2	0.0872	3.8	0.39	1154	17	1230	30	1364	74	85
AK29-seq1-A56	432	88	11	0.85	769	0.0987	1.7	0.8164	7.0	0.0600	6.8	0.25	607	10	606	32	604	147	100
AK29-seq1-A57	1017	387	21	0.03	1967	0.0575	2.4	0.4258	6.7	0.0537	6.3	0.36	360	8	360	21	360	141	100
AK29-seq1-A58	944	180	22	0.83	1645	0.1015	2.5	0.8448	6.4	0.0604	5.9	0.39	623	15	622	30	616	128	101
AK29-seq1-A59	958	204	20	0.37	1704	0.0947	2.2	0.7668	5.9	0.0587	5.5	0.37	583	12	578	26	556	119	105
AK29-seq1-A60	1430	73	19	0.32	1580	0.2514	2.4	3.2847	4.7	0.0948	4.1	0.50	1446	31	1477	38	1523	78	95
AK29-seq2-B01	1745	170	18	0.16	2920	0.1105	1.7	0.9576	4.5	0.0628	4.2	0.38	676	11	682	23	703	89	96
AK29-seq2-B02	848	99	10	0.13	1466	0.1000	2.0	0.8309	5.4	0.0602	5.0	0.38	615	12	614	25	612	107	100
AK29-seq2-B03	2244	40	14	0.49	1997	0.3104	1.5	5.0275	4.0	0.1175	3.7	0.37	1743	23	1824	34	1918	66	91
AK29-seq2-B04	383	46	5	0.39	670	0.0934	2.7	0.7674	7.5	0.0596	7.0	0.35	576	15	578	34	588	152	98
AK29-seq2-B05	4994	191	56	0.31	5426	0.2770	2.9	3.6906	3.7	0.0966	2.2	0.80	1576	41	1569	30	1560	42	101
AK29-seq2-B06	5889	175	68	0.88	5746	0.3237	2.5	4.8287	4.0	0.1082	3.1	0.63	1808	40	1790	34	1769	57	102
AK29-seq2-B07	1054	59	15	1.67	1371	0.2269	3.0	2.5290	5.9	0.0808	5.0	0.51	1318	36	1280	44	1217	99	108
AK29-seq2-B08	26639	423	183	0.49	23891	0.3931	1.7	6.2504	2.2	0.1153	1.4	0.78	2137	31	2012	19	1885	24	113
AK29-seq2-B09	1537	209	17	0.18	2764	0.0824	1.8	0.6608	4.7	0.0582	4.4	0.37	510	9	515	19	537	96	95
AK29-seq2-B10	1057	260	15	0.74	1923	0.0499	1.8	0.3979	4.4	0.0578	4.0	0.41	314	6	340	13	523	88	60
AK29-seq2-B11	-	-	-	-	-	-	-	-	-	-	-	-	-	-	-	-	-	-	-
AK29-seq2-B12	1376	183	27	0.35	2114	0.1445	1.9	1.3660	4.7	0.0686	4.3	0.41	870	16	874	28	886	89	98
AK29-seq2-B13	1092	215	21	0.46	1905	0.0931	2.0	0.7780	5.6	0.0606	5.2	0.35	574	11	584	25	626	112	92
AK29-seq2-B14	932	111	11	0.27	1635	0.0995	2.4	0.8243	5.8	0.0601	5.3	0.41	612	14	610	27	606	114	101
AK29-seq2-B15	869	179	15	0.93	1666	0.0661	3.0	0.5011	10.5	0.0550	10.0	0.28	412	12	412	36	413	224	100
AK29-seq2-B16	5484	87	36	0.53	4695	0.3663	1.5	6.1766	2.6	0.1223	2.1	0.58	2012	26	2001	23	1990	37	101
AK29-seq2-B17	30905	252	145	0.47	12989	0.4571	1.9	15.7966	3.2	0.2506	2.6	0.58	2427	38	2865	31	3189	42	76
AK29-seq2-B18	3561	230	38	0.35	5132	0.1584	1.4	1.5849	3.2	0.0726	2.9	0.43	948	12	964	20	1001	59	95

AK29-seq2-B19	1138	139	14	0.50	2020	0.0945	2.6	0.7719	5.5	0.0592	4.9	0.47	582	14	581	25	576	106	101
AK29-seq2-B20	2460	247	42	0.54	3595	0.1561	1.6	1.5459	3.8	0.0718	3.4	0.42	935	14	949	23	981	69	95
AK29-seq2-B21	980	340	20	0.32	1848	0.0569	2.3	0.4363	4.3	0.0556	3.6	0.53	357	8	368	13	436	81	82
AK29-seq2-B22	876	139	18	0.50	1425	0.1190	2.5	1.0604	5.9	0.0646	5.3	0.42	725	17	734	31	762	112	95
AK29-seq2-B23	898	362	21	0.80	1720	0.0507	1.6	0.3841	4.9	0.0549	4.6	0.33	319	5	330	14	409	104	78
AK29-seq2-B24	1528	361	28	0.17	2655	0.0790	1.4	0.6516	4.2	0.0598	3.9	0.34	490	7	509	17	598	85	82
AK29-seq2-B25	1215	273	19	0.54	2335	0.0629	2.1	0.4747	4.5	0.0548	4.0	0.46	393	8	394	15	403	90	98
AK29-seq2-B26	1563	84	16	0.62	2192	0.1707	2.3	1.7643	4.7	0.0750	4.2	0.48	1016	21	1032	31	1067	84	95
AK29-seq2-B27	31340	119	100	0.52	12174	0.6644	1.9	24.8123	2.5	0.2709	1.6	0.78	3284	50	3301	25	3311	25	99
AK29-seq2-B28	1912	68	23	0.64	1943	0.2867	2.0	4.0741	4.2	0.1031	3.7	0.48	1625	29	1649	35	1680	68	97
AK29-seq2-B29	6670	57	39	0.73	3129	0.5324	2.1	16.3795	3.1	0.2231	2.3	0.67	2752	47	2899	30	3003	37	92
AK29-seq2-B30	745	103	10	0.62	1339	0.0874	2.3	0.7027	6.2	0.0583	5.8	0.37	540	12	540	26	542	127	100
AK29-seq2-B31	5761	347	63	0.35	8472	0.1746	1.6	1.7186	2.8	0.0714	2.3	0.56	1038	15	1016	18	968	48	107
AK29-seq2-B32	553	61	7	0.34	967	0.1018	2.2	0.8450	8.0	0.0602	7.6	0.28	625	13	622	38	611	165	102
AK29-seq2-B33	1554	437	28	1.12	3052	0.0513	1.6	0.3784	4.4	0.0535	4.1	0.36	323	5	326	12	349	94	92
AK29-seq2-B34	923	268	16	1.11	1801	0.0473	1.8	0.3410	5.3	0.0522	5.0	0.35	298	5	298	14	296	114	101
AK29-seq2-B35	2441	283	33	0.67	4149	0.1035	2.0	0.8690	3.7	0.0609	3.2	0.52	635	12	635	18	635	68	100
AK29-seq2-B36	1439	155	20	0.66	2420	0.1150	1.6	0.9960	4.5	0.0628	4.2	0.36	702	11	702	23	702	88	100
AK29-seq2-B37	645	116	15	1.08	1103	0.1050	1.4	0.8869	6.8	0.0613	6.7	0.21	644	9	645	33	649	143	99
AK29-seq2-B38	1855	256	23	0.29	3181	0.0871	1.7	0.7351	3.9	0.0612	3.5	0.45	538	9	560	17	647	75	83
AK29-seq2-B39	830	130	15	0.59	1925	0.1092	1.9	0.6824	4.9	0.0453	4.5	0.39	668	12	528	20	-39	109	-1694
AK29-seq2-B40	598	138	13	0.31	1901	0.0973	1.5	0.4423	9.9	0.0330	9.8	0.15	599	9	372	31	-879	283	-68
AK29-seq2-B41	2939	197	28	0.33	3373	0.1362	2.1	1.7066	4.4	0.0909	3.9	0.47	823	16	1011	29	1444	75	57
AK29-seq2-B42	3487	65	29	0.96	3110	0.3544	1.6	5.7725	3.6	0.1181	3.2	0.44	1956	26	1942	31	1928	57	101
AK29-seq2-B43	3259	712	45	0.12	6279	0.0659	1.4	0.4960	3.2	0.0546	2.8	0.45	411	6	409	11	397	63	104
AK29-seq2-B44	843	244	20	0.84	1568	0.0700	2.2	0.5445	5.5	0.0564	5.0	0.40	436	9	441	20	470	111	93
AK29-seq2-B45	1013	162	21	0.59	1699	0.1164	1.9	1.0042	6.0	0.0626	5.7	0.31	710	13	706	31	693	122	102
AK29-seq2-B46	2844	133	28	0.31	3788	0.2030	1.9	2.2196	4.1	0.0793	3.6	0.46	1191	20	1187	29	1180	72	101
AK29-seq2-B47	12554	182	82	0.32	10670	0.4181	1.5	7.1526	2.3	0.1241	1.8	0.63	2252	28	2131	21	2015	32	112
AK29-seq2-B48	975	128	13	0.43	1702	0.0992	1.4	0.8226	5.4	0.0602	5.2	0.27	610	8	609	25	609	113	100
AK29-seq2-B49	880	275	21	0.59	1736	0.0688	1.9	0.5043	5.9	0.0532	5.6	0.31	429	8	415	20	335	128	128
AK29-seq2-B50	8622	161	68	0.73	7971	0.3536	1.3	5.5386	2.7	0.1136	2.3	0.50	1952	23	1907	23	1858	42	105
AK29-seq3-C01	2590	55	24	1.10	1941	0.3217	4.7	6.1782	6.5	0.1393	4.4	0.73	1798	75	2001	58	2218	76	81
AK29-seq3-C02	1366	171	18	0.35	2348	0.0995	1.3	0.8289	4.3	0.0604	4.1	0.31	611	8	613	20	620	89	99
AK29-seq3-C03	732	142	11	0.54	1376	0.0697	2.0	0.5345	5.4	0.0556	5.0	0.37	434	8	435	19	437	111	99
AK29-seq3-C04	1149	132	15	0.54	1935	0.1029	1.6	0.8776	5.2	0.0618	5.0	0.30	632	10	640	25	669	106	94
AK29-seq3-C05	3477	458	46	0.30	6116	0.0989	1.7	0.8107	3.6	0.0595	3.1	0.49	608	10	603	16	584	68	104
AK29-seq3-C06	1000	128	13	0.27	1723	0.0990	1.7	0.8182	4.4	0.0599	4.1	0.38	609	10	607	21	601	89	101
AK29-seq3-C07	1718	222	25	0.68	2969	0.0955	1.2	0.7921	4.3	0.0602	4.1	0.28	588	7	592	20	609	89	96
AK29-seq3-C08	216	24	4	1.39	362	0.1109	3.4	0.9670	13.7	0.0632	13.2	0.25	678	22	687	71	715	281	95
AK29-seq3-C09	2174	308	28	0.30	3837	0.0904	1.1	0.7370	3.8	0.0591	3.6	0.30	558	6	561	16	572	78	97
AK29-seq3-C10	1112	155	15	0.37	1975	0.0915	1.8	0.7396	5.5	0.0586	5.2	0.33	564	10	562	24	553	113	102

AK29-seq3-C11	1048	153	14	0.23	1852	0.0891	1.8	0.7255	5.8	0.0591	5.5	0.31	550	10	554	25	570	120	97
AK29-seq3-C12	1772	247	23	0.25	3100	0.0934	2.0	0.7673	4.6	0.0596	4.1	0.44	575	11	578	21	589	90	98
AK29-seq3-C13	1827	255	26	0.42	3238	0.0969	1.6	0.7904	4.0	0.0591	3.7	0.39	596	9	591	18	572	80	104
AK29-seq3-C14	12963	186	114	0.26	7745	0.5587	2.8	13.4582	3.2	0.1747	1.6	0.87	2861	65	2712	31	2603	27	110
AK29-seq3-C15	577	165	8	0.30	1086	0.0472	2.9	0.3630	5.7	0.0558	4.9	0.51	297	8	314	15	444	108	67
AK29-seq3-C16	1691	191	24	0.61	2871	0.1076	1.4	0.9082	3.8	0.0612	3.6	0.36	659	9	656	19	646	77	102
AK29-seq3-C17	2856	375	38	0.22	4911	0.1011	1.3	0.8457	2.9	0.0607	2.6	0.46	621	8	622	14	628	55	99
AK29-seq3-C18	870	115	11	0.63	1521	0.0809	2.4	0.6544	6.5	0.0586	6.0	0.38	502	12	511	26	554	131	91
AK29-seq3-C19	21056	410	125	0.04	19168	0.3100	1.6	4.9061	2.1	0.1148	1.4	0.77	1741	25	1803	18	1876	24	93
AK29-seq3-C20	750	104	10	0.44	1303	0.0925	2.3	0.7663	6.0	0.0601	5.5	0.38	570	12	578	27	606	119	94
AK29-seq3-C21	972	140	8	0.43	1846	0.0519	2.1	0.3937	5.3	0.0551	4.9	0.39	326	7	337	15	414	109	79
AK29-seq3-C22	500	19	4	0.78	564	0.1210	14.4	1.5479	15.6	0.0928	6.0	0.92	736	101	950	101	1484	114	50
AK29-seq3-C23	3982	264	50	0.48	5803	0.1701	1.5	1.6804	2.7	0.0716	2.3	0.53	1013	14	1001	18	976	47	104
AK29-seq3-C24	1105	150	16	0.50	1922	0.0934	2.2	0.7773	5.1	0.0603	4.6	0.43	576	12	584	23	616	99	93
AK29-seq3-C25	754	104	11	0.29	1273	0.1001	1.3	0.8507	6.2	0.0616	6.0	0.21	615	8	625	29	661	129	93
AK29-seq3-C26	622	194	11	0.63	1236	0.0503	1.8	0.3645	6.5	0.0526	6.3	0.27	316	6	316	18	310	143	102
AK29-seq3-C27	398	110	6	0.43	769	0.0545	2.4	0.4025	8.4	0.0535	8.1	0.28	342	8	343	25	351	182	97
Sample 49/09-4 (BF6)		**Well no.: 49/09-4**					**Location (decimal degrees):**				**51.67**	**7.384328 W**		**Datum: IRENET95**					
BF6-60-90-seq1-a	33244	299	45	0.34	31785	0.1173	3.9	1.7129	5.3	0.1060	3.5	0.75	715	27	1013	34	1731	64	41
BF6-60-90-seq1-a	2521	81	12	1.20	4394	0.1140	1.4	0.9105	4.5	0.0579	4.2	0.32	696	9	657	22	527	93	132
BF6-60-90-seq1-a	12947	285	34	0.63	21957	0.1005	1.3	0.8319	2.7	0.0601	2.3	0.49	617	8	615	12	606	51	102
BF6-60-90-seq1-a	10294	100	19	0.21	14176	0.1906	1.4	1.9334	2.5	0.0736	2.0	0.58	1125	15	1093	17	1030	41	109
BF6-60-90-seq1-a	11351	64	23	0.39	10676	0.3231	1.6	4.8120	2.6	0.1080	2.0	0.61	1805	25	1787	22	1766	37	102
BF6-60-90-seq1-a	12736	37	16	0.29	7408	0.3886	2.5	9.3778	3.2	0.1750	2.1	0.76	2116	44	2376	30	2606	35	81
BF6-60-90-seq1-a	9206	351	35	0.49	15872	0.0899	1.5	0.7295	2.9	0.0588	2.5	0.52	555	8	556	13	561	54	99
BF6-60-90-seq1-a	4542	36	12	0.66	4341	0.2688	1.9	3.5779	4.7	0.0965	4.3	0.41	1535	27	1545	38	1558	80	98
BF6-60-90-seq1-a	43620	90	53	0.70	23028	0.4727	4.0	12.5276	4.3	0.1922	1.8	0.91	2495	82	2645	42	2761	30	90
BF6-60-90-seq1-a	3844	205	16	0.34	7004	0.0728	3.2	0.5625	7.3	0.0560	6.6	0.44	453	14	453	27	453	147	100
BF6-60-90-seq1-a	5378	173	22	0.83	3238	0.1048	1.8	0.8826	5.4	0.0611	5.1	0.33	642	11	642	26	643	109	100
BF6-60-90-seq1-a	863	13	3	0.43	1355	0.1972	2.2	1.8164	11.7	0.0668	11.5	0.19	1160	24	1051	80	832	240	139
BF6-60-90-seq1-a	872	33	4	0.87	1555	0.0968	1.5	0.7668	10.8	0.0574	10.7	0.14	596	8	578	49	508	236	117
BF6-60-90-seq1-a	3427	96	13	0.55	5950	0.1154	1.8	0.9410	4.0	0.0592	3.6	0.44	704	12	673	20	573	79	123
BF6-60-90-seq1-a	11296	367	46	0.67	18846	0.1053	1.2	0.8859	2.8	0.0610	2.5	0.42	645	7	644	13	640	54	101
BF6-60-90-seq1-a	4680	162	26	1.46	8431	0.1035	1.4	0.8014	3.1	0.0562	2.8	0.44	635	8	598	14	459	62	138
BF6-60-90-seq1-a	24202	152	53	0.45	23232	0.3097	1.7	4.5025	2.3	0.1054	1.6	0.74	1739	26	1731	19	1722	29	101
BF6-60-90-seq1-a	3264	16	7	0.59	3061	0.3514	2.1	5.3885	4.8	0.1112	4.3	0.45	1941	36	1883	42	1819	78	107
BF6-60-90-seq1-a	138503	2638	199	0.13	200	0.0706	5.0	0.8432	6.2	0.0867	3.6	0.81	440	21	621	29	1353	70	32
BF6-60-90-seq1-a	1726	36	5	0.86	3017	0.1156	2.6	0.9346	5.9	0.0586	5.3	0.44	705	17	670	29	553	116	128
BF6-60-90-seq2-b	24487	30	25	0.67	11134	0.6527	2.4	20.2723	3.3	0.2253	2.2	0.74	3239	63	3104	32	3019	35	107
BF6-60-90-seq2-b	20099	574	62	0.54	500	0.0962	4.9	0.8101	6.1	0.0611	3.7	0.80	592	28	603	28	643	79	92
BF6-60-90-seq2-b	3822	54	10	0.26	5510	0.1909	2.3	1.8813	4.8	0.0715	4.2	0.48	1126	24	1075	32	971	85	116
BF6-60-90-seq2-b	9782	305	42	0.81	16344	0.1109	2.7	0.9401	4.2	0.0615	3.3	0.63	678	17	673	21	657	71	103

BF6-60-90-seq2-b	5472	156	20	0.47	9509	0.1154	1.4	0.9391	3.2	0.0590	2.9	0.43	704	9	672	16	568	63	124
BF6-60-90-seq2-b	15573	220	39	0.08	21880	0.1846	1.6	1.8556	2.6	0.0729	2.0	0.62	1092	16	1065	17	1012	41	108
BF6-60-90-seq2-b	2737	25	5	0.43	3057	0.2004	1.8	1.9765	5.0	0.0715	4.7	0.36	1177	20	1108	34	973	95	121
BF6-60-90-seq2-b	113156	147	101	0.48	18723	0.5744	1.7	14.6489	2.0	0.1850	1.1	0.84	2926	39	2793	19	2698	18	108
BF6-60-90-seq2-b	9946	58	23	0.58	4186	0.3294	1.3	4.6734	2.7	0.1029	2.4	0.48	1836	20	1762	23	1677	44	109
BF6-60-90-seq2-b	15228	81	33	0.54	14611	0.3420	2.0	5.0880	2.7	0.1079	1.8	0.74	1896	33	1834	23	1764	34	107
BF6-60-90-seq2-b	5357	128	13	0.33	9565	0.0967	2.0	0.7664	3.6	0.0575	3.0	0.56	595	12	578	16	510	66	117
BF6-60-90-seq2-b	182411	233	155	0.44	99299	0.5563	1.2	14.4339	1.9	0.1882	1.4	0.65	2851	28	2779	18	2726	24	105
BF6-60-90-seq2-b	5164	145	20	0.55	3081	0.1174	2.0	1.0282	4.1	0.0635	3.6	0.49	716	14	718	21	726	76	99
BF6-60-90-seq2-b	13622	57	20	0.28	10755	0.3222	1.9	5.7008	2.9	0.1283	2.1	0.67	1800	31	1931	25	2075	38	87
BF6-60-90-seq2-b	6763	114	26	1.15	9914	0.1543	1.6	1.4854	2.9	0.0698	2.5	0.54	925	14	924	18	924	51	100
BF6-60-90-seq2-b	43186	54	33	0.38	21501	0.5012	2.2	14.0635	3.1	0.2035	2.1	0.73	2619	48	2754	30	2855	34	92
BF6-60-90-seq2-b	11525	425	44	0.49	19839	0.0895	1.4	0.7262	3.0	0.0589	2.7	0.47	552	7	554	13	562	58	98
BF6-60-90-seq2-b	107226	980	143	0.69	101	0.1085	2.8	1.1604	5.2	0.0775	4.4	0.54	664	18	782	29	1135	87	59
BF6-60-90-seq2-b	18658	259	51	0.25	24901	0.1922	1.4	2.0314	2.2	0.0767	1.7	0.64	1133	15	1126	15	1113	34	102
BF6-60-90-seq2-b	113622	248	130	0.22	1037	0.4634	5.6	12.8975	5.8	0.2019	1.7	0.96	2454	115	2672	57	2841	27	86
BF6-60-90-seq2-b	5778	155	14	0.14	10096	0.0923	1.4	0.7442	3.0	0.0585	2.6	0.46	569	7	565	13	548	57	104
BF6-60-90-seq2-b	4243	138	16	0.39	7233	0.1069	1.7	0.8868	3.6	0.0602	3.2	0.46	654	10	645	17	611	70	107
BF6-60-90-seq2-b	5615	60	14	0.25	6771	0.2218	1.9	2.5852	3.6	0.0845	3.0	0.52	1291	22	1296	26	1305	59	99
BF6-60-90-seq2-b	7800	490	31	0.21	5171	0.0626	3.4	0.5027	4.4	0.0582	2.8	0.77	391	13	414	15	539	62	73
BF6-60-90-seq2-b	1159	24	4	1.62	1688	0.1074	2.0	1.0542	9.8	0.0712	9.6	0.20	658	12	731	52	962	195	68
BF6-60-90-seq2-b	4351	246	20	0.59	8409	0.0732	1.7	0.5227	4.0	0.0518	3.7	0.41	456	7	427	14	275	84	166
BF6-60-90-seq2-b	6100	42	14	0.20	6314	0.3136	1.6	4.2775	3.0	0.0989	2.5	0.55	1759	25	1689	25	1604	46	110
BF6-60-90-seq2-b	352	8	1	0.03	386	0.0645	10.3	0.7349	35.8	0.0826	34.3	0.29	403	40	559	167	1261	671	32
BF6-60-90-seq2-b	4277	184	19	0.49	7879	0.0935	2.2	0.7150	4.3	0.0555	3.7	0.51	576	12	548	18	432	82	133
BF6-60-90-seq2-b	62987	131	89	0.65	28270	0.5306	1.9	13.7726	2.2	0.1882	1.0	0.87	2744	42	2734	21	2727	17	101
BF6-60-90-seq2-b	4572	75	16	0.47	6446	0.1873	2.4	1.8671	4.0	0.0723	3.3	0.58	1107	24	1069	27	994	67	111
BF6-60-90-seq2-b	2834	54	10	0.47	4112	0.1632	1.9	1.5871	5.4	0.0705	5.1	0.35	975	17	965	34	944	104	103
BF6-60-90-seq2-b	17496	132	50	0.81	17516	0.2987	1.5	4.1993	2.2	0.1020	1.6	0.70	1685	23	1674	18	1660	29	101
BF6-60-90-seq2-b	21312	109	38	0.55	19239	0.2988	1.5	4.1366	2.6	0.1004	2.1	0.57	1685	22	1662	21	1632	40	103
BF6-60-90-seq2-b	5721	63	14	0.53	8190	0.1908	1.6	1.8746	3.2	0.0713	2.7	0.52	1126	17	1072	21	965	55	117
BF6-60-90-seq2-b	27712	196	55	0.44	32539	0.2574	1.6	3.0888	2.4	0.0870	1.8	0.67	1477	22	1430	19	1361	35	108
BF6-60-90-seq2-b	8273	86	19	0.35	11163	0.2082	1.5	2.1779	2.5	0.0759	2.0	0.61	1219	17	1174	18	1091	40	112
BF6-60-90-seq2-b	11338	136	31	0.80	15604	0.1841	1.6	1.8709	2.8	0.0737	2.3	0.57	1089	16	1071	19	1033	47	105
BF6-60-90-seq2-b	19980	212	41	0.24	27847	0.1854	1.3	1.8697	2.2	0.0732	1.8	0.60	1096	14	1070	15	1018	37	108
BF6-60-90-seq2-b	17187	271	58	0.34	22467	0.2010	1.7	2.1695	2.6	0.0783	1.9	0.66	1181	18	1171	18	1154	39	102
BF6-60-90-seq2-b	12972	221	44	0.25	17535	0.1945	2.2	2.0187	3.2	0.0753	2.3	0.69	1146	23	1122	22	1076	47	106
BF6-60-90-seq2-b	3770	171	18	0.37	6874	0.1004	1.9	0.7785	3.9	0.0562	3.4	0.48	617	11	585	17	461	75	134
BF6-60-90-seq2-b	2230	102	14	0.95	4227	0.1035	1.6	0.7769	6.3	0.0544	6.1	0.26	635	10	584	28	389	136	163
BF6-60-90-seq2-b	4735	191	25	0.73	5210	0.1091	1.6	0.8695	3.8	0.0578	3.5	0.43	668	10	635	18	522	76	128
BF6-60-90-seq2-b	4425	432	26	0.65	9073	0.0519	1.4	0.3586	3.5	0.0501	3.2	0.40	326	5	311	9	202	75	162
BF6-60-90-seq2-b	6073	301	34	0.83	10686	0.0882	2.9	0.7046	4.4	0.0579	3.3	0.67	545	15	542	19	527	71	103

BF6-60-90-seq2-b	4084	174	19	0.38	6991	0.1024	1.3	0.8407	3.0	0.0595	2.7	0.44	629	8	620	14	586	59	107
BF6-60-90-seq2-b	2133	61	11	0.66	1450	0.1570	4.3	1.5149	7.3	0.0700	5.9	0.59	940	38	936	46	927	121	101
BF6-60-90-seq2-b	13692	72	30	0.31	8994	0.3818	1.8	6.6457	3.0	0.1262	2.4	0.60	2085	32	2065	27	2046	43	102
BF6-60-90-seq2-b	1936	35	9	1.01	2889	0.2061	1.9	1.8903	6.0	0.0665	5.6	0.33	1208	21	1078	40	823	118	147
BF6-60-90-seq2-b	10163	139	40	0.92	12247	0.2254	1.4	2.5621	3.2	0.0824	2.9	0.45	1311	17	1290	24	1256	56	104
BF6-60-90-seq2-b	26916	248	42	0.28	25598	0.1486	11.0	2.2028	11.1	0.1075	1.9	0.99	893	92	1182	81	1758	35	51
BF6-60-90-seq2-b	10504	50	23	0.37	2775	0.4172	1.3	7.5751	2.3	0.1317	1.9	0.59	2248	26	2182	21	2120	32	106
BF6-60-90-seq2-b	3435	66	13	0.40	468	0.1804	2.5	1.9439	7.7	0.0781	7.3	0.32	1069	25	1096	53	1150	145	93
BF6-60-90-seq2-b	7621	70	22	0.19	7973	0.3060	2.1	4.1491	3.7	0.0984	3.0	0.58	1721	32	1664	30	1593	56	108
BF6-60-90-seq2-b	42533	169	92	0.68	27718	0.4386	1.7	9.5038	2.2	0.1572	1.4	0.77	2344	33	2388	20	2425	23	97
BF6-60-90-seq2-b	14243	197	48	0.31	17040	0.2271	2.5	2.6630	3.3	0.0850	2.2	0.75	1319	29	1318	25	1317	42	100
BF6-60-90-seq2-b	1667	77	9	0.53	3084	0.1114	1.5	0.8338	7.9	0.0543	7.8	0.19	681	10	616	37	383	175	178
BF6-60-90-seq2-b	14812	865	41	0.50	217	0.0287	20.2	0.4785	22.3	0.1210	9.5	0.91	182	36	397	76	1971	169	9
BF6-60-90-seq2-b	3909	148	19	0.60	6770	0.1126	2.4	0.9294	4.2	0.0598	3.4	0.57	688	15	667	21	598	74	115
BF6-60-90-seq3-c	14038	111	23	0.28	18449	0.1996	1.7	2.1238	2.5	0.0772	1.9	0.67	1173	18	1157	18	1125	37	104
BF6-60-90-seq3-c	39346	176	55	0.46	40968	0.2728	1.4	3.6820	2.0	0.0979	1.4	0.71	1555	20	1567	16	1584	27	98
BF6-60-90-seq3-c	24582	53	24	0.25	18210	0.4184	1.7	7.8962	2.2	0.1369	1.4	0.77	2253	32	2219	20	2188	24	103
BF6-60-90-seq3-c	8302	276	19	0.47	15437	0.0624	1.4	0.4688	2.7	0.0545	2.3	0.50	390	5	390	9	392	53	99
BF6-60-90-seq3-c	204674	766	287	0.20	2561	0.3674	3.1	6.1531	3.3	0.1215	1.2	0.93	2017	54	1998	30	1978	21	102
BF6-60-90-seq3-c	92458	402	134	0.34	91893	0.3040	1.8	4.2981	2.4	0.1026	1.6	0.75	1711	27	1693	20	1671	29	102
BF6-90-180-seq1-	6787	42	8	0.23	9620	0.1865	1.7	1.8814	3.3	0.0732	2.8	0.50	1102	17	1075	22	1019	57	108
BF6-90-180-seq1-	26781	158	27	0.08	36468	0.1736	1.4	1.7980	2.1	0.0751	1.7	0.64	1032	13	1045	14	1072	33	96
BF6-90-180-seq1-	4331	28	6	0.88	6082	0.1732	2.2	1.7227	3.7	0.0721	3.0	0.60	1030	21	1017	24	990	61	104
BF6-90-180-seq1-	34469	409	41	0.21	55509	0.0965	1.7	0.8440	2.7	0.0634	2.0	0.64	594	10	621	12	723	43	82
BF6-90-180-seq1-	10858	65	14	0.44	14683	0.1873	1.7	1.9400	2.8	0.0751	2.2	0.60	1107	17	1095	19	1072	45	103
BF6-90-180-seq1-	15879	91	19	0.34	21696	0.1865	1.2	1.9236	2.4	0.0748	2.1	0.51	1102	13	1089	16	1063	42	104
BF6-90-180-seq1-	177794	165	100	0.58	16070	0.4604	3.1	11.8499	3.5	0.1867	1.6	0.89	2441	64	2593	34	2713	27	90
BF6-90-180-seq1-	30772	186	36	0.31	30394	0.1811	1.4	1.8725	2.1	0.0750	1.6	0.66	1073	14	1071	14	1069	32	100
BF6-90-180-seq1-	4643	77	8	0.51	8122	0.0856	1.4	0.6731	3.1	0.0570	2.8	0.44	529	7	523	13	493	61	107
BF6-90-180-seq1-	2362	37	4	0.59	2685	0.0967	1.7	0.7460	5.0	0.0559	4.7	0.35	595	10	566	22	450	104	132
BF6-90-180-seq1-	2848	50	5	0.46	5051	0.0824	1.3	0.6506	3.8	0.0573	3.6	0.35	510	7	509	15	502	79	102
BF6-90-180-seq1-	8130	105	13	0.48	6307	0.1112	2.0	0.9088	3.3	0.0593	2.7	0.59	680	13	656	16	578	58	118
BF6-90-180-seq1-	172739	202	112	0.36	37181	0.4817	1.1	10.3224	1.6	0.1554	1.1	0.71	2535	23	2464	15	2407	19	105
BF6-90-180-seq1-	15187	63	24	0.50	5706	0.3320	1.6	4.6135	2.5	0.1008	1.9	0.65	1848	26	1752	21	1638	35	113
BF6-90-180-seq1-	36727	126	41	0.55	39658	0.2755	2.5	3.5580	3.0	0.0937	1.6	0.85	1569	35	1540	24	1502	29	104
BF6-90-180-seq1-	95875	60	47	0.53	43527	0.6189	1.0	19.1021	1.8	0.2238	1.5	0.56	3106	25	3047	18	3009	24	103
BF6-90-180-seq1-	26694	168	32	0.21	29392	0.1885	1.5	1.9299	2.2	0.0742	1.6	0.70	1113	16	1092	15	1048	31	106
BF6-90-180-seq1-	44466	178	51	0.52	51014	0.2406	1.6	2.9387	2.0	0.0886	1.3	0.77	1390	20	1392	15	1396	25	100
BF6-90-180-seq1-	11025	58	13	0.35	6460	0.2000	1.4	2.2113	3.0	0.0802	2.7	0.46	1175	15	1185	21	1201	52	98
BF6-90-180-seq1-	105389	185	77	0.27	82509	0.3792	1.7	6.7959	2.1	0.1300	1.2	0.83	2073	31	2085	19	2098	20	99
BF6-90-180-seq1-	230948	527	186	0.15	66	0.2677	4.8	6.1794	6.0	0.1674	3.6	0.80	1529	65	2002	54	2532	60	60
BF6-90-180-seq1-	6300	36	9	0.62	8557	0.2126	1.9	2.1925	3.0	0.0748	2.4	0.62	1243	21	1179	21	1063	48	117

BF6-90-180-seq1-	129028	335	107	0.14	120446	0.3108	1.8	4.6705	2.2	0.1090	1.2	0.82	1745	27	1762	18	1783	22	98
BF6-90-180-seq1-	12379	66	15	0.26	15822	0.2124	1.6	2.3317	2.6	0.0796	2.1	0.60	1241	18	1222	19	1188	42	105
BF6-90-180-seq1-	17589	261	44	1.49	29556	0.1023	1.7	0.8544	2.8	0.0606	2.2	0.62	628	10	627	13	624	47	101
BF6-90-180-seq1-	38081	58	26	0.17	28132	0.4286	1.5	8.1435	2.0	0.1378	1.4	0.74	2299	29	2247	18	2200	24	105
BF6-90-180-seq1-	34420	511	47	0.02	32861	0.0981	1.7	0.8108	2.2	0.0599	1.4	0.77	603	10	603	10	601	30	100
BF6-90-180-seq1-	73148	235	57	0.25	75644	0.2243	2.7	3.0414	3.3	0.0984	1.9	0.82	1304	32	1418	25	1593	35	82
BF6-90-180-seq1-	9250	188	16	0.51	17057	0.0716	1.7	0.5462	3.2	0.0553	2.7	0.53	446	7	442	11	425	60	105
BF6-90-180-seq1-	27161	135	32	0.38	33376	0.2075	1.4	2.3745	2.3	0.0830	1.8	0.62	1216	16	1235	17	1269	36	96
BF6-90-180-seq1-	33089	182	37	0.13	41301	0.2009	1.8	2.2475	2.3	0.0812	1.5	0.77	1180	20	1196	17	1225	29	96
BF6-90-180-seq1-	6198	103	12	0.53	10872	0.0976	1.7	0.7826	3.3	0.0581	2.8	0.52	601	10	587	15	535	61	112
BF6-90-180-seq1-	46691	137	60	1.17	45805	0.2846	1.6	4.0709	2.2	0.1037	1.5	0.74	1615	23	1648	18	1692	27	95
BF6-90-180-seq1-	26076	383	42	0.36	20223	0.1010	1.8	0.8477	2.7	0.0609	2.0	0.67	620	11	623	13	635	43	98
BF6-90-180-seq1-	25179	258	37	0.16	38998	0.1431	1.7	1.2961	2.5	0.0657	1.8	0.69	862	14	844	14	796	38	108
BF6-90-180-seq1-	34845	105	37	0.50	7518	0.3030	1.4	4.2869	2.1	0.1026	1.6	0.66	1706	21	1691	17	1672	29	102
BF6-90-180-seq1-	4203	53	7	0.44	6930	0.1135	1.8	0.9645	3.1	0.0616	2.5	0.58	693	12	686	16	661	54	105
BF6-90-180-seq1-	8474	40	11	0.43	10371	0.2461	1.1	2.8172	2.8	0.0830	2.6	0.40	1418	15	1360	22	1270	51	112
BF6-90-180-seq1-	6611	47	8	0.18	9556	0.1640	1.6	1.5896	3.0	0.0703	2.6	0.54	979	15	966	19	937	52	104
BF6-90-180-seq1-	14876	104	18	0.00	20944	0.1823	1.5	1.8069	2.6	0.0719	2.1	0.57	1079	15	1048	17	983	43	110
BF6-90-180-seq1-	52536	42	29	0.27	26287	0.6003	2.9	16.8636	3.5	0.2037	1.9	0.84	3031	71	2927	34	2856	31	106
BF6-90-180-seq1-	31455	92	32	0.39	31778	0.3104	1.5	4.3551	2.3	0.1018	1.8	0.63	1743	22	1704	19	1656	34	105
BF6-90-180-seq1-	16055	108	21	0.22	8301	0.1879	1.8	1.9199	3.0	0.0741	2.4	0.61	1110	19	1088	20	1044	49	106
BF6-90-180-seq1-	10445	139	18	0.46	9836	0.1170	1.8	1.0279	3.6	0.0637	3.1	0.50	713	12	718	19	732	66	97
BF6-90-180-seq1-	43739	119	44	0.39	40926	0.3277	1.4	4.8828	1.9	0.1081	1.4	0.71	1827	22	1799	16	1767	25	103
BF6-90-180-seq1-	15388	237	25	0.24	25681	0.1024	1.3	0.8609	2.0	0.0610	1.6	0.62	629	8	631	10	638	34	99
BF6-90-180-seq1-	14117	293	26	0.38	25039	0.0824	1.9	0.6536	2.8	0.0575	2.1	0.67	510	9	511	11	512	45	100
BF6-90-180-seq1-	34066	82	29	0.08	30539	0.3542	1.6	5.5036	2.1	0.1127	1.3	0.78	1954	27	1901	18	1843	23	106
BF6-90-180-seq1-	8514	137	18	0.74	14710	0.1017	1.2	0.8253	2.6	0.0589	2.3	0.47	624	7	611	12	562	51	111
BF6-90-180-seq1-	9549	57	13	0.44	12559	0.2046	1.9	2.1753	2.8	0.0771	2.1	0.68	1200	21	1173	20	1124	42	107
BF6-90-180-seq1-	214920	671	196	0.22	4837	0.2777	1.6	4.2372	2.2	0.1107	1.5	0.72	1580	22	1681	18	1811	28	87
BF6-90-180-seq1-	7937	45	10	0.25	5585	0.2134	1.3	2.3352	2.7	0.0794	2.3	0.51	1247	15	1223	19	1181	45	106
BF6-90-180-seq1-	10449	128	19	0.55	16926	0.1298	1.2	1.1243	2.3	0.0628	1.9	0.54	786	9	765	12	703	41	112
BF6-90-180-seq1-	46782	149	50	0.29	46535	0.3112	1.4	4.3893	1.8	0.1023	1.1	0.79	1747	22	1710	15	1666	20	105
BF6-90-180-seq1-	14306	108	19	0.18	20106	0.1771	1.9	1.7648	2.7	0.0723	1.9	0.71	1051	19	1033	18	994	39	106
BF6-90-180-seq1-	131910	393	114	0.22	39716	0.2714	3.3	4.2539	3.6	0.1137	1.4	0.92	1548	45	1684	30	1859	25	83
BF6-90-180-seq1-	17080	86	21	0.25	21083	0.2326	1.8	2.6505	2.9	0.0827	2.3	0.62	1348	22	1315	22	1261	44	107
BF6-90-180-seq1-	93826	298	87	0.11	89094	0.2881	1.5	4.2505	1.9	0.1070	1.1	0.79	1632	21	1684	15	1749	21	93
BF6-90-180-seq1-	13035	462	27	0.46	25021	0.0510	2.2	0.3706	3.0	0.0528	2.0	0.75	320	7	320	8	318	45	101
BF6-90-180-seq1-	4644	24	6	0.20	5698	0.2332	1.8	2.6658	3.3	0.0829	2.8	0.54	1351	22	1319	25	1267	55	107
Sample 49/15-1 (BF10)			**Well no.: 49/15-1**				**Location (decimal degrees):**				**51.658**	**7.059775W**			**Datum:IRENET95**				
BF10-60-90-seq1-	2368	20	4	0.59	3310	0.1932	1.9	1.9412	7.1	0.0729	6.8	0.27	1138	20	1095	48	1011	138	113
BF10-60-90-seq1-	16707	54	20	0.24	15722	0.3453	1.7	5.1450	2.4	0.1081	1.8	0.69	1912	28	1844	21	1767	32	108
BF10-60-90-seq1-	100475	377	120	0.19	97617	0.3088	1.5	4.4578	1.9	0.1047	1.2	0.78	1735	22	1723	16	1709	22	102

BF10-60-90-seq1-	2513	53	7	1.00	1715	0.0899	2.7	0.7273	5.8	0.0587	5.1	0.47	555	15	555	25	556	112	100
BF10-60-90-seq1-	19835	120	39	0.97	23616	0.2328	2.0	2.7631	3.1	0.0861	2.4	0.65	1349	25	1346	24	1340	46	101
BF10-60-90-seq1-	2394	14	4	0.50	3051	0.2520	1.6	2.8110	4.9	0.0809	4.6	0.32	1449	20	1358	37	1219	90	119
BF10-60-90-seq1-	16825	467	53	0.32	27722	0.1064	2.3	0.9050	4.5	0.0617	3.9	0.50	652	14	654	22	663	83	98
BF10-60-90-seq1-	877	8	2	0.36	1131	0.2508	2.6	2.7416	12.0	0.0793	11.7	0.22	1443	34	1340	94	1179	232	122
BF10-60-90-seq1-	11903	110	34	0.91	9060	0.2342	3.4	2.7936	4.2	0.0865	2.4	0.81	1356	42	1354	32	1350	47	100
BF10-60-90-seq1-	4890	53	13	0.61	6421	0.2149	1.8	2.3030	3.4	0.0777	2.9	0.52	1255	20	1213	24	1140	58	110
BF10-60-90-seq1-	14960	84	24	0.60	17114	0.2311	2.7	2.8785	3.2	0.0903	1.8	0.83	1340	33	1376	25	1433	34	94
BF10-60-90-seq1-	8735	86	21	1.24	12345	0.1658	1.7	1.6503	3.2	0.0722	2.7	0.54	989	16	990	21	991	55	100
BF10-60-90-seq1-	4463	99	11	0.51	7680	0.0944	3.3	0.7704	4.8	0.0592	3.5	0.68	582	18	580	21	574	76	101
BF10-60-90-seq1-	5763	107	15	0.93	9810	0.1109	1.5	0.9145	2.7	0.0598	2.2	0.56	678	10	659	13	597	48	114
BF10-60-90-seq1-	18629	162	31	0.25	25443	0.1841	1.8	1.8915	2.4	0.0745	1.6	0.74	1089	18	1078	16	1056	33	103
BF10-60-90-seq1-	43382	139	54	0.27	4979	0.3664	1.5	5.6103	1.9	0.1111	1.3	0.75	2012	25	1918	17	1817	24	111
BF10-60-90-seq1-	12848	518	35	0.79	7626	0.0566	2.5	0.4545	3.1	0.0582	1.9	0.80	355	9	380	10	538	41	66
BF10-60-90-seq1-	56064	303	91	0.37	60272	0.2771	2.5	3.6030	2.9	0.0943	1.4	0.87	1577	35	1550	23	1514	26	104
BF10-60-90-seq1-	20854	85	31	0.71	21082	0.2951	1.6	4.0949	2.4	0.1006	1.7	0.69	1667	24	1653	19	1636	32	102
BF10-60-90-seq1-	5723	14	6	0.49	3066	0.3549	3.9	5.9660	5.9	0.1219	4.4	0.66	1958	66	1971	52	1984	78	99
BF10-60-90-seq1-	26553	223	44	0.42	14827	0.1826	2.0	1.9150	2.8	0.0761	2.0	0.71	1081	20	1086	19	1097	40	99
BF10-60-90-seq1-	16303	84	23	0.25	18389	0.2612	1.8	3.2484	2.4	0.0902	1.5	0.76	1496	24	1469	19	1430	29	105
BF10-60-90-seq1-	7320	139	15	0.38	12465	0.0978	2.4	0.8060	3.6	0.0598	2.7	0.66	601	14	600	17	595	59	101
BF10-60-90-seq1-	2862	54	7	0.52	4921	0.1121	1.5	0.9147	3.8	0.0592	3.5	0.40	685	10	660	18	574	75	119
BF10-60-90-seq1-	19538	75	28	0.60	19652	0.3115	1.1	4.3452	1.6	0.1012	1.2	0.69	1748	17	1702	13	1645	21	106
BF10-60-90-seq1-	2279	18	4	0.22	3214	0.2076	2.2	2.0789	4.4	0.0726	3.8	0.50	1216	24	1142	30	1004	76	121
BF10-60-90-seq1-	47437	159	56	0.22	42903	0.3373	1.7	5.2374	2.4	0.1126	1.6	0.72	1874	28	1859	20	1842	30	102
BF10-60-90-seq1-	9128	76	18	0.68	12192	0.1920	1.3	2.0154	2.5	0.0761	2.1	0.54	1132	14	1121	17	1099	41	103
BF10-60-90-seq1-	2606	76	9	0.45	4762	0.1110	2.0	0.8550	3.9	0.0559	3.4	0.52	679	13	627	19	447	75	152
BF10-60-90-seq1-	6782	136	18	0.73	11507	0.1046	1.5	0.8662	3.4	0.0600	3.1	0.43	642	9	633	16	605	67	106
BF10-60-90-seq1-	32324	158	55	0.71	33196	0.2739	2.5	3.7347	3.1	0.0989	1.8	0.80	1561	34	1579	25	1603	34	97
BF10-60-90-seq1-	5492	151	15	0.73	9839	0.0819	1.8	0.6380	3.5	0.0565	2.9	0.53	507	9	501	14	473	65	107
BF10-60-90-seq1-	4019	39	7	0.41	3402	0.1738	1.3	1.6875	3.6	0.0704	3.3	0.37	1033	13	1004	23	941	68	110
BF10-60-90-seq1-	40483	161	59	0.26	39182	0.3488	2.0	4.9929	2.3	0.1038	1.3	0.83	1929	33	1818	20	1693	24	114
BF10-60-90-seq1-	55517	277	70	0.21	57975	0.2401	1.7	3.2536	2.7	0.0983	2.1	0.62	1387	21	1470	21	1591	40	87
BF10-60-90-seq1-	4999	108	12	0.64	8695	0.0948	2.0	0.7671	3.5	0.0587	2.9	0.56	584	11	578	16	556	64	105
BF10-60-90-seq1-	9063	63	14	0.31	11678	0.2027	1.2	2.2070	2.6	0.0790	2.3	0.47	1190	14	1183	19	1171	46	102
BF10-60-90-seq1-	6733	181	16	0.41	6108	0.0800	1.5	0.6231	3.2	0.0565	2.8	0.46	496	7	492	13	472	63	105
BF10-60-90-seq1-	8592	63	15	0.37	11077	0.2118	1.6	2.3080	2.8	0.0790	2.3	0.57	1239	18	1215	20	1173	45	106
BF10-60-90-seq1-	29694	135	47	0.60	29955	0.2911	1.3	4.0269	2.5	0.1003	2.1	0.54	1647	20	1640	20	1630	39	101
BF10-60-90-seq1-	63601	65	46	0.31	30817	0.6089	1.7	17.6560	2.1	0.2103	1.3	0.80	3066	42	2971	21	2908	21	105
BF10-60-90-seq1-	2974	30	6	0.25	4384	0.1786	1.5	1.6933	4.1	0.0687	3.9	0.37	1060	15	1006	27	891	80	119
BF10-60-90-seq1-	19460	187	47	0.87	25352	0.2110	4.8	2.2677	5.1	0.0780	1.8	0.93	1234	54	1202	37	1146	36	108
BF10-60-90-seq1-	5691	159	15	0.62	10272	0.0786	2.2	0.6114	3.5	0.0564	2.7	0.63	488	11	484	14	470	61	104
BF10-60-90-seq1-	42453	143	52	0.10	38403	0.3636	1.6	5.6456	2.5	0.1126	1.9	0.64	1999	27	1923	22	1842	35	109

BF10-60-90-seq1-	6748	215	17	0.43	5084	0.0719	1.6	0.5499	3.2	0.0555	2.8	0.51	447	7	445	12	432	61	104
BF10-60-90-seq1-	7357	262	17	0.24	6915	0.0628	1.7	0.4704	5.9	0.0543	5.7	0.28	392	6	391	19	385	127	102
BF10-60-90-seq1-	3492	98	10	1.05	3986	0.0749	2.1	0.5691	4.0	0.0551	3.4	0.53	466	10	457	15	416	76	112
BF10-60-90-seq1-	24907	101	44	0.97	742	0.3240	1.6	4.6554	3.2	0.1042	2.7	0.52	1809	26	1759	27	1700	50	106
BF10-60-90-seq1-	12431	240	27	0.30	20646	0.1072	2.0	0.9046	2.7	0.0612	1.8	0.73	656	12	654	13	647	40	101
BF10-60-90-seq1-	4537	142	13	0.68	8583	0.0742	3.3	0.5507	6.1	0.0538	5.1	0.55	461	15	445	22	364	114	127
BF10-60-90-seq1-	107403	128	79	0.28	55467	0.5421	1.5	14.7319	2.0	0.1971	1.3	0.74	2792	33	2798	19	2802	22	100
BF10-60-90-seq1-	12712	57	20	0.52	12742	0.2931	2.1	4.1005	3.0	0.1015	2.1	0.70	1657	31	1654	25	1651	39	100
BF10-60-90-seq1-	9400	184	22	0.34	15428	0.1120	1.6	0.9588	2.8	0.0621	2.3	0.57	684	10	683	14	677	49	101
BF10-60-90-seq1-	15743	78	26	0.41	16733	0.3048	1.6	3.9888	2.7	0.0949	2.2	0.59	1715	24	1632	22	1526	41	112
BF10-60-90-seq1-	9939	94	19	0.35	13651	0.1932	1.3	1.9677	2.2	0.0739	1.8	0.60	1139	14	1105	15	1038	36	110
BF10-60-90-seq1-	2420	52	6	0.60	4129	0.0964	2.7	0.7979	4.9	0.0600	4.0	0.56	593	16	596	22	605	87	98
BF10-60-90-seq1-	3028	68	8	0.67	3419	0.0993	2.5	0.7864	5.0	0.0574	4.3	0.50	610	15	589	23	508	95	120
BF10-60-90-seq1-	11808	26	12	0.27	9038	0.4383	1.8	8.0588	2.6	0.1334	1.8	0.70	2343	35	2238	23	2143	32	109
BF10-60-90-seq1-	16506	613	40	0.52	959	0.0566	2.8	0.4232	5.5	0.0542	4.8	0.50	355	10	358	17	379	107	94
BF10-90-180-seq2	3660	21	6	0.74	4624	0.2404	1.6	2.7033	3.8	0.0816	3.5	0.43	1389	20	1329	29	1235	68	112
BF10-90-180-seq2	17486	147	30	0.37	23711	0.1940	1.7	2.0112	2.3	0.0752	1.6	0.73	1143	17	1119	16	1074	31	106
BF10-90-180-seq2	20297	76	29	0.71	20073	0.3099	1.9	4.4089	2.5	0.1032	1.6	0.78	1740	30	1714	21	1682	29	103
BF10-90-180-seq2	110055	335	121	0.27	96643	0.3305	1.6	5.3142	1.9	0.1166	1.1	0.82	1841	26	1871	17	1905	20	97
BF10-90-180-seq2	5703	31	7	0.17	913	0.2165	2.2	2.4842	11.7	0.0832	11.5	0.19	1263	25	1267	88	1275	224	99
BF10-90-180-seq2	51247	373	78	0.21	65742	0.2051	2.0	2.2493	2.6	0.0796	1.7	0.76	1202	22	1197	18	1186	33	101
BF10-90-180-seq2	21424	192	36	0.34	29206	0.1749	1.8	1.7880	2.5	0.0742	1.6	0.75	1039	18	1041	16	1046	33	99
BF10-90-180-seq2	37460	36	25	0.36	18531	0.6005	1.9	17.0829	2.4	0.2063	1.4	0.80	3032	46	2940	23	2877	23	105
BF10-90-180-seq2	1936	46	4	0.24	3314	0.0926	7.1	0.7590	10.4	0.0595	7.6	0.68	571	39	573	47	584	165	98
BF10-90-180-seq2	29343	128	42	0.69	30687	0.2632	1.6	3.5221	2.3	0.0970	1.6	0.69	1506	21	1532	18	1568	31	96
BF10-90-180-seq2	27566	129	42	0.65	28977	0.2635	1.6	3.4884	2.5	0.0960	1.9	0.63	1508	21	1525	20	1548	37	97
BF10-90-180-seq2	5976	22	8	0.59	1339	0.3062	1.8	4.4494	4.5	0.1054	4.2	0.39	1722	27	1722	38	1721	77	100
BF10-90-180-seq2	11450	71	18	0.36	10258	0.2359	1.9	2.6909	3.1	0.0827	2.5	0.60	1365	23	1326	24	1263	49	108
BF10-90-180-seq2	22582	654	47	0.22	10723	0.0717	1.7	0.5671	2.8	0.0574	2.3	0.60	446	7	456	10	506	50	88
BF10-90-180-seq2	81512	252	100	0.55	72307	0.3389	1.2	5.3274	1.7	0.1140	1.2	0.73	1881	20	1873	15	1864	21	101
BF10-90-180-seq2	25800	208	44	0.43	34717	0.1879	1.9	1.9654	2.5	0.0759	1.6	0.76	1110	20	1104	17	1092	33	102
BF10-90-180-seq2	28309	110	38	0.42	2626	0.3048	1.6	4.3070	3.2	0.1025	2.7	0.51	1715	24	1695	26	1669	50	103
BF10-90-180-seq2	31923	104	38	0.25	29120	0.3497	1.8	5.3924	2.3	0.1118	1.4	0.78	1933	30	1884	20	1830	26	106
BF10-90-180-seq2	7097	51	10	0.37	9316	0.1848	2.3	1.9430	4.6	0.0763	3.9	0.52	1093	24	1096	31	1102	78	99
BF10-90-180-seq2	581	10	2	0.81	961	0.1350	3.1	1.2269	15.9	0.0659	15.6	0.19	816	24	813	93	803	327	102
BF10-90-180-seq2	1881	23	5	0.93	2951	0.1677	1.9	1.5077	7.6	0.0652	7.3	0.25	1000	18	934	47	780	154	128
BF10-90-180-seq2	10254	80	16	0.25	13693	0.1958	2.0	2.0531	3.3	0.0761	2.7	0.61	1153	21	1133	23	1097	53	105
BF10-90-180-seq2	40907	153	50	0.17	40978	0.3176	2.0	4.4658	2.5	0.1020	1.4	0.81	1778	31	1725	21	1661	27	107
BF10-90-180-seq2	76009	249	88	0.21	69440	0.3363	2.2	5.1690	2.9	0.1115	1.9	0.75	1869	35	1848	25	1824	35	102
BF10-90-180-seq2	13775	136	24	0.23	19881	0.1764	1.6	1.7210	2.9	0.0708	2.5	0.55	1047	16	1016	19	951	50	110
BF10-90-180-seq2	8955	267	19	0.07	16832	0.0769	3.2	0.5759	4.4	0.0543	3.0	0.73	477	15	462	16	385	67	124
BF10-90-180-seq2	55300	358	82	0.20	67087	0.2244	1.7	2.5799	2.1	0.0834	1.3	0.80	1305	20	1295	15	1278	24	102

BF10-90-180-seq2	45455	118	47	0.25	37329	0.3718	1.8	6.3396	2.6	0.1237	1.8	0.71	2038	32	2024	23	2010	33	101
BF10-90-180-seq2	14308	575	35	0.27	27254	0.0590	1.5	0.4358	2.4	0.0535	1.9	0.62	370	5	367	8	352	43	105
BF10-90-180-seq2	74017	173	85	0.53	56836	0.4169	1.6	7.6380	2.1	0.1329	1.4	0.75	2246	30	2189	19	2136	25	105
BF10-90-180-seq2	11375	101	19	0.19	15303	0.1899	1.7	1.9821	2.7	0.0757	2.1	0.63	1121	18	1109	19	1087	42	103
BF10-90-180-seq2	915	9	2	1.20	1396	0.1771	2.6	1.6544	8.8	0.0677	8.4	0.29	1051	25	991	57	860	175	122
BF10-90-180-seq2	11739	43	17	0.95	11658	0.3056	2.4	4.2760	3.1	0.1015	2.1	0.75	1719	36	1689	26	1651	38	104
BF10-90-180-seq2	4072	41	8	0.32	6107	0.1802	1.9	1.6820	3.8	0.0677	3.3	0.49	1068	19	1002	25	859	69	124
BF10-90-180-seq2	17827	105	30	0.51	21994	0.2550	1.6	2.9007	2.3	0.0825	1.7	0.68	1464	21	1382	18	1258	33	116
BF10-90-180-seq2	5099	38	8	0.33	6855	0.2102	1.6	2.1901	2.9	0.0756	2.5	0.53	1230	17	1178	21	1084	50	113
BF10-90-180-seq2	2646	107	7	0.37	5483	0.0599	2.2	0.4055	6.7	0.0491	6.4	0.33	375	8	346	20	152	149	246
BF10-90-180-seq2	1244	9	2	0.84	1728	0.2151	2.6	2.2109	7.9	0.0746	7.4	0.34	1256	30	1184	57	1057	149	119
BF10-90-180-seq2	11155	80	17	0.18	12932	0.2162	1.6	2.3487	2.8	0.0788	2.3	0.58	1262	19	1227	20	1167	46	108
BF10-90-180-seq2	119404	343	126	0.17	98861	0.3510	2.0	5.9617	2.5	0.1232	1.5	0.81	1939	34	1970	22	2003	26	97
BF10-90-180-seq2	8925	198	20	0.38	15674	0.0947	2.2	0.7578	3.3	0.0580	2.5	0.67	583	12	573	15	531	54	110
BF10-90-180-seq2	41567	160	53	0.34	40710	0.3006	2.1	4.3211	2.6	0.1043	1.6	0.80	1694	31	1697	22	1701	29	100
BF10-90-180-seq2	23074	115	32	0.29	25486	0.2629	2.0	3.3480	2.5	0.0924	1.5	0.79	1505	27	1492	20	1475	29	102
BF10-90-180-seq2	166528	311	198	0.69	87280	0.4860	3.2	13.0984	3.8	0.1955	2.1	0.84	2553	68	2687	37	2789	34	92
BF10-90-180-seq2	206121	802	269	0.08	9788	0.3347	3.6	6.8839	3.7	0.1492	0.9	0.97	1861	58	2097	33	2336	16	80
BF10-90-180-seq2	71254	257	86	0.17	67367	0.3250	1.7	4.8395	2.2	0.1080	1.4	0.77	1814	27	1792	19	1766	26	103
BF10-90-180-seq2	20696	126	32	0.29	24471	0.2403	2.2	2.8496	2.7	0.0860	1.6	0.80	1388	27	1369	21	1338	32	104
BF10-90-180-seq2	16405	73	23	0.36	11016	0.2871	1.6	3.8166	2.5	0.0964	1.9	0.65	1627	23	1596	20	1556	36	105
BF10-90-180-seq2	63541	157	69	0.36	49788	0.3921	1.7	7.0603	2.0	0.1306	1.1	0.84	2133	31	2119	18	2106	19	101
BF10-90-180-seq2	9860	324	25	0.45	18103	0.0699	1.8	0.5353	2.7	0.0556	2.1	0.65	435	7	435	10	435	46	100
BF10-90-180-seq2	27453	112	38	0.47	27584	0.2943	1.5	4.1344	2.3	0.1019	1.7	0.65	1663	22	1661	19	1659	32	100
BF10-90-180-seq2	7036	164	19	0.51	424	0.1020	2.0	0.8342	7.3	0.0593	7.0	0.28	626	12	616	34	578	152	108
BF10-90-180-seq2	19804	68	25	0.36	18397	0.3262	1.9	4.8248	2.5	0.1073	1.7	0.75	1820	30	1789	22	1754	31	104
BF10-90-180-seq2	41081	408	71	0.28	55420	0.1650	1.6	1.6596	2.0	0.0729	1.3	0.78	985	14	993	13	1012	26	97
BF10-90-180-seq2	35517	54	30	0.29	21728	0.5002	1.5	11.4750	2.3	0.1664	1.7	0.67	2615	33	2563	21	2522	28	104
BF10-90-180-seq2	40841	126	63	1.07	36701	0.3601	1.5	5.6325	2.0	0.1135	1.3	0.75	1982	25	1921	17	1856	24	107
BF10-90-180-seq2	12553	114	27	0.83	16276	0.1758	1.9	1.7895	2.9	0.0738	2.2	0.65	1044	18	1042	19	1036	44	101
BF10-90-180-seq2	16344	127	32	0.57	21149	0.2140	1.9	2.3437	2.8	0.0794	2.0	0.68	1250	22	1226	20	1182	40	106
BF10-90-180-seq2	5591	50	13	0.90	7800	0.1918	2.4	1.9270	4.1	0.0729	3.3	0.60	1131	25	1091	28	1010	66	112
BF10-90-180-seq2	18330	135	30	0.20	23605	0.2163	1.8	2.3632	2.5	0.0792	1.8	0.70	1262	20	1232	18	1178	36	107
BF10-90-180-seq2	12001	376	30	0.32	1586	0.0736	2.8	0.5712	4.3	0.0563	3.3	0.65	458	13	459	16	464	73	99
BF10-90-180-seq2	4156	41	8	0.40	2389	0.1754	1.7	1.7500	3.2	0.0724	2.8	0.52	1042	16	1027	21	996	56	105
BF10-90-180-seq2	10636	63	15	0.18	12469	0.2356	2.6	2.8189	3.5	0.0868	2.3	0.76	1364	33	1361	26	1355	44	101
BF10-90-180-seq2	50880	160	54	0.09	45577	0.3337	1.6	5.2331	2.1	0.1137	1.4	0.75	1857	25	1858	18	1860	25	100
BF10-90-180-seq2	8227	71	15	0.38	11009	0.1896	1.8	1.9927	3.0	0.0762	2.5	0.59	1119	19	1113	21	1101	49	102
BF10-90-180-seq2	82051	234	90	0.20	69332	0.3673	2.0	6.0592	2.4	0.1196	1.4	0.82	2017	35	1984	22	1951	25	103
BF10-90-180-seq2	14678	50	18	0.44	14015	0.3210	1.6	4.7328	2.3	0.1069	1.6	0.70	1795	25	1773	19	1748	30	103
BF10-90-180-seq2	11296	101	22	0.44	15457	0.1923	1.2	1.9728	2.0	0.0744	1.7	0.57	1134	12	1106	14	1053	34	108
BF10-90-180-seq2	21179	129	34	0.43	24845	0.2347	1.6	2.8100	2.2	0.0868	1.5	0.73	1359	20	1358	17	1357	29	100

BF10-90-180-seq2	9490	55	14	0.25	11007	0.2439	2.2	3.0151	7.7	0.0896	7.3	0.28	1407	28	1411	60	1418	140	99
BF10-90-180-seq2	2168	44	6	0.73	4049	0.1095	2.1	0.8203	6.0	0.0543	5.7	0.34	670	13	608	28	385	128	174
BF10-90-180-seq2	6908	211	15	0.19	12527	0.0735	1.8	0.5700	3.0	0.0562	2.4	0.59	457	8	458	11	461	54	99
BF10-90-180-seq2	14471	69	20	0.29	15666	0.2799	1.7	3.6291	2.2	0.0940	1.5	0.75	1591	24	1556	18	1509	28	105
BF10-90-180-seq2	12054	177	24	0.30	19288	0.1273	2.2	1.1155	2.9	0.0635	2.0	0.74	773	16	761	16	727	42	106
BF10-90-180-seq2	4578	28	7	0.45	5701	0.2325	1.7	2.6128	3.5	0.0815	3.1	0.48	1347	20	1304	26	1234	60	109
BF10-90-180-seq2	39645	148	52	0.31	38265	0.3185	1.9	4.6495	2.7	0.1059	1.9	0.70	1782	29	1758	23	1730	35	103
BF10-90-180-seq2	52621	455	81	0.24	71143	0.1708	1.6	1.7808	2.4	0.0756	1.7	0.68	1017	15	1038	16	1085	35	94
BF10-90-180-seq2	14909	70	22	0.44	13835	0.2699	1.9	3.5333	2.8	0.0949	2.0	0.69	1541	26	1535	22	1527	38	101
BF10-90-180-seq2	18847	201	32	0.20	26677	0.1559	3.6	1.5490	4.1	0.0720	1.9	0.88	934	32	950	26	987	39	95
BF10-90-180-seq2	23122	29	20	0.49	13064	0.5559	2.1	13.8305	2.6	0.1805	1.6	0.79	2850	48	2738	25	2657	27	107
BF10-90-180-seq2	17322	79	26	0.56	2052	0.2753	2.0	3.6285	4.0	0.0956	3.4	0.50	1568	28	1556	32	1540	65	102
BF10-90-180-seq2	5485	47	9	0.14	7598	0.1879	1.9	1.9094	3.4	0.0737	2.9	0.54	1110	19	1084	23	1033	58	107
BF10-90-180-seq2	4925	144	11	0.21	9110	0.0733	1.1	0.5575	3.2	0.0552	3.0	0.35	456	5	450	12	419	67	109
BF10-90-180-seq2	10076	85	20	0.62	2947	0.1946	4.9	2.1052	5.8	0.0785	3.1	0.85	1146	52	1151	41	1159	62	99
BF10-90-180-seq2	12074	61	19	0.55	13127	0.2628	5.3	3.4088	5.7	0.0941	1.9	0.94	1504	72	1506	45	1510	37	100
BF10-90-180-seq2	14620	103	24	0.30	5884	0.2211	1.5	2.4594	2.5	0.0807	1.9	0.62	1288	18	1260	18	1213	38	106
BF10-90-180-seq2	62945	201	73	0.30	21353	0.3373	1.6	5.3622	2.0	0.1153	1.3	0.77	1874	25	1879	18	1885	23	99
BF10-90-180-seq2	33769	237	52	0.24	42520	0.2130	1.7	2.3769	2.3	0.0809	1.6	0.73	1245	19	1236	16	1220	31	102
BF10-90-180-seq2	31541	1065	71	0.22	58500	0.0661	1.4	0.5002	1.9	0.0549	1.2	0.76	413	6	412	6	408	28	101
BF10-90-180-seq2	10084	64	15	0.26	12304	0.2243	1.9	2.5836	3.1	0.0835	2.5	0.60	1304	22	1296	23	1282	49	102
BF10-90-180-seq2	3165	30	7	0.60	4575	0.1859	2.8	1.8094	5.3	0.0706	4.5	0.53	1099	29	1049	36	946	93	116
BF10-90-180-seq2	5620	48	10	0.38	7715	0.1927	4.2	1.9767	4.8	0.0744	2.1	0.89	1136	44	1108	33	1052	43	108
BF10-90-180-seq2	1056	9	2	0.67	1669	0.2107	2.5	1.9982	9.5	0.0688	9.1	0.27	1232	29	1115	66	892	188	138
BF10-90-180-seq2	27432	106	36	0.43	27373	0.2989	1.8	4.2099	2.2	0.1021	1.3	0.81	1686	27	1676	18	1663	24	101
BF10-90-180-seq2	9942	355	23	0.31	18661	0.0612	2.2	0.4590	3.5	0.0544	2.8	0.63	383	8	384	11	387	62	99
BF10-90-180-seq2	56861	274	69	0.12	62952	0.2539	1.7	3.2186	2.3	0.0919	1.5	0.76	1459	23	1462	18	1466	28	100
Sample 49/10-1 (BF7)			**Well no.: 49/10-1**				**Location (decimal degrees):**				**51.684**	**7.176539W**			**Datum:IRENET95**				
BF7-seq1-a01	11734	210	24	0.38	19910	0.1046	1.8	0.8749	3.0	0.0607	2.3	0.62	641	11	638	14	627	50	102
BF7-seq1-a02	5531	149	13	0.88	10303	0.0666	1.8	0.5048	2.8	0.0549	2.2	0.64	416	7	415	10	410	48	101
BF7-seq1-a03	28013	113	51	1.43	4273	0.2781	2.1	3.9482	2.7	0.1030	1.8	0.76	1582	29	1624	22	1679	33	94
BF7-seq1-a04	37122	83	38	0.37	28088	0.3998	3.1	7.3453	3.6	0.1333	1.8	0.86	2168	57	2154	32	2141	32	101
BF7-seq1-a05	3002	81	7	0.44	5977	0.0843	2.4	0.5986	4.7	0.0515	4.0	0.51	522	12	476	18	263	92	198
BF7-seq1-a06	28949	239	57	0.74	39308	0.1854	2.6	1.9327	3.3	0.0756	2.0	0.79	1096	26	1092	22	1085	41	101
BF7-seq1-a07	9940	196	19	0.03	14999	0.1030	4.6	0.8906	6.4	0.0627	4.5	0.71	632	28	647	31	698	96	91
BF7-seq1-a08	4591	84	10	0.56	8049	0.1037	1.9	0.8345	3.9	0.0583	3.4	0.49	636	12	616	18	543	75	117
BF7-seq1-a09	21971	661	48	0.30	38817	0.0666	4.9	0.5314	7.6	0.0579	5.7	0.65	415	20	433	27	526	125	79
BF7-seq1-a10	19166	274	38	0.44	27369	0.1140	3.7	1.1282	4.9	0.0718	3.2	0.76	696	25	767	27	980	65	71
BF7-seq1-a11	1555	66	6	0.76	3117	0.0797	2.4	0.5616	8.2	0.0511	7.8	0.29	494	11	453	30	246	180	201
BF7-seq1-a12	109026	298	109	0.20	93287	0.3454	2.1	5.7047	2.6	0.1198	1.5	0.83	1913	35	1932	23	1953	26	98
BF7-seq1-a13	4660	82	9	0.52	7987	0.0983	2.2	0.8088	3.8	0.0597	3.2	0.57	604	12	602	17	592	68	102
BF7-seq1-a14	11008	96	18	0.20	5114	0.1845	1.8	1.9057	3.5	0.0749	3.0	0.52	1092	18	1083	23	1066	60	102

BF7-seq1-a15	5696	101	13	0.54	2988	0.1131	2.1	0.9879	3.5	0.0633	2.8	0.60	691	14	698	18	720	59	96
BF7-seq1-a16	32335	54	33	0.22	17269	0.5439	3.2	14.3536	3.9	0.1914	2.3	0.82	2800	74	2773	38	2754	37	102
BF7-seq1-a17	1046	39	3	0.64	2490	0.0744	2.3	0.4436	7.3	0.0433	6.9	0.32	462	10	373	23	-152	172	-303
BF7-seq1-a18	4649	33	10	0.28	3630	0.2828	3.2	3.4147	6.1	0.0876	5.2	0.53	1605	46	1508	49	1373	100	117
BF7-seq1-a19	2034	65	9	0.75	4127	0.1124	2.2	0.7834	5.6	0.0506	5.1	0.40	687	15	587	25	221	119	311
BF7-seq1-a20	8746	60	13	0.33	2797	0.2084	2.0	2.3306	3.8	0.0811	3.2	0.54	1220	23	1222	27	1224	63	100
BF7-seq1-a21	60445	77	48	0.61	36226	0.5015	1.8	11.8451	2.2	0.1713	1.3	0.82	2620	39	2592	21	2570	21	102
BF7-seq1-a22	19595	56	26	1.02	17722	0.3457	1.8	5.4024	2.4	0.1134	1.7	0.73	1914	30	1885	21	1854	30	103
BF7-seq1-a23	2560	50	6	0.48	2956	0.1055	1.9	0.8026	5.2	0.0552	4.8	0.37	646	12	598	24	420	108	154
BF7-seq1-a24	696	6	1	0.72	647	0.1963	2.8	2.1594	24.0	0.0798	23.8	0.12	1155	30	1168	182	1192	471	97
BF7-seq1-a25	19098	38	21	0.48	14949	0.4904	1.8	8.8665	2.6	0.1311	1.9	0.69	2572	38	2324	24	2113	33	122
BF7-seq1-a26	5916	67	14	0.40	8056	0.1936	2.2	2.0160	3.7	0.0755	2.9	0.61	1141	23	1121	25	1083	59	105
BF7-seq1-a27	1753	14	3	0.66	2502	0.2016	2.3	2.0011	5.4	0.0720	4.9	0.42	1184	25	1116	37	986	100	120
BF7-seq1-a28	14705	570	33	0.25	28227	0.0556	1.8	0.4098	2.8	0.0534	2.1	0.65	349	6	349	8	347	48	101
BF7-seq1-a29	58302	128	54	0.26	46540	0.3914	1.7	6.9612	2.4	0.1290	1.7	0.72	2129	31	2106	21	2084	29	102
BF7-seq1-a30	7590	61	11	0.20	10573	0.1768	2.4	1.7921	4.2	0.0735	3.5	0.57	1050	24	1043	28	1028	70	102
BF7-seq1-a31	7495	69	13	0.21	11614	0.1850	1.8	1.6856	3.2	0.0661	2.6	0.58	1094	19	1003	21	809	55	135
BF7-seq1-a32	13888	361	41	0.49	3123	0.0981	2.2	0.9024	3.5	0.0667	2.7	0.64	603	13	653	17	830	56	73
BF7-seq1-a33	7854	228	27	0.50	13277	0.1049	2.7	0.8790	4.6	0.0608	3.7	0.59	643	17	640	22	632	79	102
BF7-seq1-a34	1526	34	4	0.49	3117	0.1033	2.3	0.7149	6.3	0.0502	5.8	0.37	634	14	548	27	204	135	311
BF7-seq1-a35	10432	38	13	0.46	10699	0.2936	2.1	4.0420	3.3	0.0999	2.6	0.63	1659	30	1643	27	1621	48	102
BF7-seq1-a36	1502	36	5	0.64	1204	0.1207	2.2	1.0694	6.5	0.0642	6.1	0.33	735	15	738	35	750	129	98
BF7-seq1-a37	7604	202	23	0.36	12664	0.1054	2.0	0.8932	3.5	0.0614	2.9	0.56	646	12	648	17	655	62	99
BF7-seq1-a38	16595	269	33	0.43	27307	0.1099	2.0	0.9433	2.8	0.0623	1.9	0.72	672	13	675	14	683	42	98
BF7-seq1-a39	1176	18	2	0.25	1092	0.1241	3.8	1.0394	11.1	0.0607	10.4	0.34	754	27	724	59	630	225	120
BF7-seq1-a40	205	10	1	1.02	784	0.0833	2.5	0.2849	56.1	0.0248	56.0	0.05	516	13	255	135	-1785	1993	-29
BF7-seq1-a41	4234	114	15	0.43	5684	0.1194	2.0	0.9836	4.7	0.0597	4.3	0.42	727	14	695	24	594	93	122
BF7-seq1-a42	9198	102	18	0.22	12515	0.1799	3.6	1.8721	4.6	0.0755	2.8	0.79	1066	35	1071	31	1082	56	99
BF7-seq1-a43	4631	20	9	0.73	4277	0.3858	2.0	5.9047	3.5	0.1110	2.9	0.58	2104	37	1962	31	1816	53	116
BF7-seq1-a44	2659	144	12	1.11	5423	0.0648	2.2	0.4504	5.0	0.0504	4.4	0.45	405	9	378	16	213	103	190
BF7-seq1-a45	4268	95	11	0.64	8026	0.0979	2.3	0.7354	3.6	0.0545	2.7	0.65	602	13	560	15	392	61	154
BF7-seq1-a46	-	-	-	-	-	-	-	-	-	-	-	-	-	-	-	-	-	-	-
BF7-seq1-a47	18275	62	21	0.32	17584	0.3132	1.9	4.5997	2.6	0.1065	1.8	0.74	1756	30	1749	22	1741	32	101
BF7-seq1-a48	1707	47	6	0.67	3051	0.1110	2.5	0.8760	6.2	0.0572	5.7	0.40	679	16	639	30	500	125	136
BF7-seq1-a49	1622	11	3	0.32	2297	0.2447	2.4	2.4391	7.7	0.0723	7.3	0.31	1411	30	1254	57	994	149	142
BF7-seq1-a50	13288	49	20	0.84	13177	0.3069	2.6	4.3802	3.5	0.1035	2.3	0.76	1725	40	1709	29	1688	42	102
BF7-seq1-a51	22277	208	40	0.49	31572	0.1718	1.9	1.7169	2.8	0.0725	2.0	0.70	1022	18	1015	18	999	40	102
BF7-seq1-a52	15801	58	20	0.51	15777	0.2997	2.3	4.2413	3.3	0.1026	2.4	0.69	1690	34	1682	27	1673	44	101
BF7-seq1-a53	480	15	1	0.35	1249	0.0873	2.8	0.4715	15.0	0.0391	14.7	0.18	540	14	392	50	-407	384	-133
BF7-seq1-a54	6726	220	15	0.14	13147	0.0718	1.8	0.5189	2.8	0.0524	2.1	0.64	447	8	424	10	302	49	148
BF7-seq1-a55	5313	157	10	0.13	10344	0.0667	2.3	0.4844	4.0	0.0527	3.3	0.58	416	9	401	13	315	74	132
BF7-seq1-a56	37982	94	39	0.38	31567	0.3653	2.5	6.2222	3.0	0.1235	1.6	0.84	2007	43	2008	27	2008	29	100

BF7-seq1-a57	11020	90	21	0.72	15301	0.1788	1.8	1.8215	2.7	0.0739	2.0	0.66	1061	17	1053	18	1038	40	102
BF7-seq1-a58	5031	100	11	0.47	8980	0.0972	2.3	0.7696	3.6	0.0574	2.8	0.64	598	13	580	16	508	61	118
BF7-seq1-a59	10240	19	9	0.38	2778	0.3883	2.3	7.2441	5.3	0.1353	4.8	0.43	2115	41	2142	48	2168	84	98
BF7-seq1-a60	3283	72	8	0.35	1120	0.1070	2.3	0.8539	6.1	0.0579	5.7	0.37	655	14	627	29	525	125	125
BF7-seq2-b01	1217	14	3	0.45	2004	0.1671	4.6	1.4326	9.6	0.0622	8.5	0.48	996	43	903	59	680	181	146
BF7-seq2-b02	37168	139	54	0.27	31676	0.3601	2.4	5.9855	3.0	0.1206	1.7	0.82	1983	42	1974	26	1964	30	101
BF7-seq2-b03	10484	62	21	0.51	10648	0.2980	2.3	4.1479	3.3	0.1010	2.4	0.70	1681	35	1664	28	1642	44	102
BF7-seq2-b04	2545	16	6	0.78	2938	0.2938	3.3	3.5941	5.2	0.0887	4.0	0.64	1660	49	1548	42	1398	77	119
BF7-seq2-b05	5186	216	16	0.36	9560	0.0689	2.4	0.5261	4.2	0.0554	3.4	0.57	430	10	429	15	428	77	100
BF7-seq2-b06	24255	118	43	0.34	22375	0.3349	2.2	5.1418	2.8	0.1114	1.6	0.81	1862	36	1843	24	1822	29	102
BF7-seq2-b07	76380	111	86	0.82	39957	0.5731	2.1	15.4952	2.5	0.1961	1.3	0.85	2921	49	2846	24	2794	21	105
BF7-seq2-b08	11186	57	15	0.38	13172	0.2396	2.3	2.8742	2.9	0.0870	1.8	0.80	1385	29	1375	22	1361	34	102
BF7-seq2-b09	27014	65	32	0.82	21274	0.3753	2.5	6.7321	3.3	0.1301	2.1	0.77	2054	44	2077	29	2099	37	98
BF7-seq2-b10	35626	28	17	0.02	14807	0.5488	4.5	16.8256	5.5	0.2223	3.1	0.82	2820	103	2925	54	2998	51	94
BF7-seq2-b11	2280	42	5	0.56	4031	0.1068	2.4	0.8517	5.1	0.0578	4.5	0.47	654	15	626	24	523	99	125
BF7-seq2-b12	43004	44	36	0.95	6840	0.6184	2.5	14.4084	3.2	0.1690	2.1	0.77	3103	61	2777	31	2548	35	122
BF7-seq2-b13	4370	32	7	0.36	6023	0.2053	2.4	2.1062	3.4	0.0744	2.4	0.70	1204	26	1151	24	1053	49	114
BF7-seq2-b14	2964	52	6	0.49	3020	0.1091	2.0	0.9263	4.0	0.0616	3.5	0.49	668	13	666	20	659	75	101
BF7-seq2-b15	14384	115	24	0.40	19584	0.1838	2.2	1.9115	3.3	0.0754	2.4	0.67	1088	22	1085	22	1080	49	101
BF7-seq2-b16	8239	245	18	0.35	15546	0.0700	2.2	0.5229	3.1	0.0542	2.2	0.72	436	9	427	11	379	49	115
BF7-seq2-b17	1932	60	5	0.61	3722	0.0698	2.7	0.5120	7.0	0.0532	6.4	0.39	435	11	420	24	337	146	129
BF7-seq2-b18	4749	90	12	0.55	8603	0.1126	2.4	0.9686	6.0	0.0624	5.5	0.40	688	16	688	31	687	118	100
BF7-seq2-b19	49146	135	50	0.21	43380	0.3482	2.2	5.5787	2.7	0.1162	1.6	0.81	1926	36	1913	23	1899	28	101
BF7-seq2-b20	7712	141	17	0.42	13351	0.1081	2.4	0.8815	3.4	0.0592	2.4	0.70	661	15	642	16	573	52	115
BF7-seq2-b21	6586	59	12	0.48	9451	0.1791	2.6	1.7629	3.5	0.0714	2.4	0.73	1062	25	1032	23	968	49	110
BF7-seq2-b22	18068	53	25	0.84	16850	0.3697	2.5	5.5992	3.2	0.1098	1.9	0.81	2028	44	1916	28	1797	34	113
BF7-seq2-b23	53291	351	77	0.22	68024	0.2104	2.3	2.3298	2.8	0.0803	1.5	0.84	1231	26	1221	20	1205	30	102
BF7-seq2-b24	1053	28	3	0.41	556	0.1130	3.4	0.9069	11.0	0.0582	10.4	0.31	690	22	655	54	537	228	129
BF7-seq2-b25	3372	17	7	0.79	3584	0.3344	2.4	4.5700	4.5	0.0991	3.8	0.54	1860	39	1744	38	1608	70	116
BF7-seq2-b26	18446	46	16	0.05	16021	0.3567	3.0	5.8222	3.9	0.1184	2.5	0.76	1967	50	1950	34	1932	45	102
BF7-seq2-b27	6327	128	16	0.49	10681	0.1031	2.9	0.8617	3.7	0.0606	2.3	0.78	633	17	631	17	625	50	101
BF7-seq2-b28	105245	364	121	0.21	73203	0.3114	2.4	4.6147	2.8	0.1075	1.5	0.85	1747	36	1752	24	1757	27	99
BF7-seq2-b29	8780	145	18	0.36	15291	0.1176	2.8	1.0195	6.3	0.0629	5.7	0.44	717	19	714	33	704	120	102
BF7-seq2-b30	133719	510	158	0.14	13673	0.3014	2.3	4.4170	3.1	0.1063	2.1	0.74	1698	35	1716	26	1737	38	98
BF7-seq2-b31	14959	64	21	0.47	15109	0.2793	3.7	3.7449	5.6	0.0973	4.2	0.66	1588	53	1581	46	1572	79	101
BF7-seq2-b32	124812	165	101	0.66	72586	0.4633	2.4	11.2545	2.6	0.1762	1.0	0.92	2454	49	2544	24	2617	16	94
BF7-seq2-b33	34060	67	30	0.25	25178	0.4113	2.3	7.8640	2.7	0.1387	1.4	0.85	2221	43	2216	24	2211	25	100
BF7-seq2-b34	7670	161	14	0.19	13459	0.0892	2.5	0.7177	3.4	0.0583	2.2	0.76	551	13	549	14	542	48	102
BF7-seq2-b35	12606	233	27	0.38	21403	0.1039	2.7	0.8669	4.0	0.0605	3.0	0.67	637	16	634	19	623	64	102
BF7-seq2-b36	54446	64	37	0.32	30388	0.5092	2.4	12.8658	2.8	0.1833	1.4	0.86	2653	53	2670	27	2683	23	99
BF7-seq2-b37	14293	370	33	0.36	25997	0.0870	2.0	0.6697	3.0	0.0559	2.1	0.69	538	11	521	12	446	47	120
BF7-seq2-b38	2657	25	5	0.64	4107	0.1829	2.3	1.6684	5.5	0.0662	5.0	0.42	1083	23	997	36	812	105	133

BF7-seq2-b39	10702	207	28	1.01	18291	0.0989	2.1	0.8186	3.3	0.0601	2.6	0.64	608	12	607	15	606	56	100
BF7-seq2-b40	158658	253	131	0.21	85309	0.4743	2.4	11.0676	3.0	0.1692	1.8	0.81	2502	50	2529	28	2550	29	98
BF7-seq2-b41	23478	62	26	0.62	20890	0.3409	2.4	5.3934	3.6	0.1148	2.6	0.69	1891	40	1884	31	1876	47	101
BF7-seq2-b42	12646	99	21	0.18	17352	0.2065	2.3	2.1286	3.8	0.0748	3.0	0.61	1210	25	1158	26	1062	60	114
BF7-seq2-b43	23350	72	26	0.12	22675	0.3632	2.6	5.2842	3.2	0.1055	1.8	0.82	1997	45	1866	27	1723	33	116
BF7-seq2-b44	21137	49	22	0.42	16742	0.3900	3.8	6.9059	4.5	0.1284	2.4	0.85	2123	70	2099	41	2077	42	102
BF7-seq2-b45	5861	257	19	0.37	5938	0.0692	2.0	0.5091	3.7	0.0534	3.1	0.53	431	8	418	13	345	71	125
BF7-seq2-b46	4252	125	9	0.27	8245	0.0724	3.0	0.5275	4.3	0.0528	3.1	0.69	451	13	430	15	321	71	140
BF7-seq2-b47	3912	54	8	0.26	6474	0.1352	2.5	1.1536	4.8	0.0619	4.1	0.53	818	20	779	26	670	87	122
BF7-seq2-b48	7665	139	17	0.55	2406	0.1052	2.6	0.8522	3.6	0.0588	2.5	0.72	645	16	626	17	559	54	115
BF7-seq2-b49	2862	83	8	0.36	1117	0.0934	2.9	0.7654	4.9	0.0594	3.9	0.59	576	16	577	22	582	86	99
BF7-seq2-b50	11765	30	10	0.35	1353	0.3053	2.9	4.9237	5.6	0.1169	4.8	0.52	1718	45	1806	49	1910	86	90
BF7-seq2-b51	48767	103	45	0.24	39156	0.4033	1.9	7.1006	2.5	0.1277	1.7	0.75	2184	35	2124	22	2066	29	106
BF7-seq2-b52	53357	1148	72	0.14	401	0.0583	3.5	0.4366	6.2	0.0543	5.1	0.56	365	13	368	19	383	116	95
BF7-seq2-b53	1714	36	4	0.35	3262	0.0963	2.6	0.7201	6.0	0.0543	5.4	0.44	592	15	551	26	382	121	155
BF7-seq2-b54	3008	84	7	0.33	5771	0.0810	2.2	0.5967	3.9	0.0534	3.2	0.57	502	11	475	15	346	72	145
BF7-seq2-b55	3253	60	8	0.49	2122	0.1142	2.9	0.8963	6.0	0.0569	5.2	0.49	697	19	650	29	489	116	143
BF7-seq2-b56	6356	117	15	0.55	11049	0.1068	3.4	0.8629	5.5	0.0586	4.3	0.62	654	21	632	26	553	94	118
BF7-seq2-b57	7869	57	7	0.33	8184	0.1030	3.6	1.4001	5.0	0.0986	3.5	0.71	632	22	889	30	1598	66	40
BF7-seq2-b58	5107	81	10	0.30	5459	0.1150	2.5	0.9907	6.9	0.0625	6.4	0.36	702	17	699	35	691	136	102
BF7-seq2-b59	43796	117	40	0.04	35081	0.3487	5.5	6.1734	7.9	0.1284	5.6	0.70	1929	92	2001	71	2076	99	93
BF7-seq2-b60	60798	283	74	0.17	67116	0.2555	2.3	3.2692	2.6	0.0928	1.2	0.88	1467	30	1474	20	1484	23	99
BF7-seq3-c01	3516	193	14	0.42	1797	0.0676	2.3	0.4612	4.3	0.0495	3.7	0.52	421	9	385	14	172	86	244
BF7-seq3-c02	14913	175	25	0.26	22849	0.1400	1.6	1.2879	2.2	0.0667	1.5	0.71	845	13	840	13	829	32	102
BF7-seq3-c03	52025	187	63	0.42	52355	0.2970	1.8	4.1630	2.4	0.1017	1.6	0.76	1676	27	1667	20	1655	29	101
BF7-seq3-c04	3972	109	11	0.81	7489	0.0769	1.8	0.5753	3.5	0.0543	3.0	0.51	477	8	461	13	383	68	125
BF7-seq3-c05	6840	132	14	0.28	11211	0.0969	3.4	0.8130	5.4	0.0609	4.2	0.63	596	19	604	25	634	90	94
BF7-seq3-c06	46505	117	47	0.13	36612	0.3882	2.8	6.9600	4.2	0.1300	3.1	0.68	2115	51	2106	38	2098	54	101
BF7-seq3-c07	8988	214	17	0.15	16526	0.0811	1.4	0.6206	2.5	0.0555	2.1	0.55	503	7	490	10	433	47	116
BF7-seq3-c08	3704	105	8	0.26	2388	0.0707	2.4	0.5483	8.2	0.0563	7.9	0.29	440	10	444	30	462	174	95
BF7-seq3-c09	658	31	3	0.37	1494	0.0904	3.6	0.5630	10.3	0.0452	9.7	0.35	558	19	454	39	-46	236	-1214
BF7-seq3-c10	7307	117	14	0.31	6866	0.1157	1.9	0.9545	3.0	0.0598	2.4	0.61	706	12	680	15	597	52	118
BF7-seq3-c11	22172	55	27	0.94	18405	0.3394	3.5	5.7587	4.0	0.1231	1.9	0.88	1884	58	1940	35	2001	34	94
BF7-seq3-c12	13567	73	20	0.40	15975	0.2425	2.0	2.9198	2.8	0.0873	2.0	0.72	1400	26	1387	22	1367	38	102
BF7-seq3-c13	21116	47	15	0.37	16026	0.2732	3.6	5.0690	4.1	0.1346	2.1	0.87	1557	50	1831	36	2158	36	72
BF7-seq3-c14	3094	24	5	0.46	4277	0.2059	2.8	2.1040	5.5	0.0741	4.7	0.51	1207	31	1150	39	1045	95	115
BF7-seq3-c15	30786	173	53	0.15	31043	0.3048	1.4	4.2650	3.5	0.1015	3.2	0.41	1715	22	1687	29	1652	58	104
BF7-seq3-c16	92184	143	67	0.14	51419	0.4371	2.3	11.0405	2.9	0.1832	1.7	0.81	2338	46	2527	27	2682	28	87
BF7-seq3-c17	21522	53	24	0.47	11450	0.3776	1.9	6.4603	2.6	0.1241	1.8	0.73	2065	33	2041	23	2016	31	102
BF7-seq3-c18	4617	101	11	0.59	8475	0.0941	2.3	0.7234	4.3	0.0558	3.6	0.54	580	13	553	19	442	81	131
BF7-seq3-c19	2449	44	6	0.63	4317	0.1106	1.8	0.8810	5.4	0.0578	5.0	0.33	676	11	642	26	522	111	129
BF7-seq3-c20	7148	252	16	0.38	13616	0.0574	1.6	0.4246	2.7	0.0537	2.1	0.61	360	6	359	8	358	47	101

BF7-seq3-c21	147153	193	107	0.23	89303	0.4958	2.0	11.5404	2.6	0.1688	1.7	0.75	2596	43	2568	25	2546	29	102
BF7-seq3-c22	41401	43	26	0.26	22000	0.5352	1.8	14.1025	2.5	0.1911	1.7	0.72	2764	41	2757	24	2752	28	100
BF7-seq3-c23	32598	107	46	0.23	6082	0.3974	2.5	7.3106	3.4	0.1334	2.3	0.74	2157	46	2150	31	2143	40	101
BF7-seq3-c25	4842	195	27	0.91	8136	0.1069	2.1	0.8991	3.8	0.0610	3.1	0.56	655	13	651	18	640	67	102
BF7-seq3-c26	4429	77	9	0.40	7741	0.1046	1.8	0.8418	3.9	0.0584	3.4	0.47	641	11	620	18	544	75	118
BF7-seq3-c27	13317	65	17	0.31	15191	0.2483	2.3	3.0652	3.0	0.0895	2.0	0.74	1430	29	1424	23	1415	39	101
BF7-seq3-c28	1548	83	5	0.26	2916	0.0595	2.0	0.4455	5.2	0.0543	4.9	0.37	373	7	374	17	382	109	98
Sample 49/09-3 (BF8)			**Well no.: 49/09-3**				**Location (decimal degrees):**				**51.683**	**7.346061W**			**Datum:IRENET95**				
BF8-60-90-seq1-a	92877	319	100	0.25	17718	0.2972	2.2	4.1590	2.6	0.1015	1.5	0.83	1677	32	1666	22	1652	27	102
BF8-60-90-seq1-a	49476	99	40	0.16	39082	0.3898	2.3	6.9105	2.5	0.1286	0.9	0.94	2122	42	2100	22	2078	15	102
BF8-60-90-seq1-a	7210	51	10	0.31	10040	0.1924	2.5	1.9197	3.8	0.0724	2.9	0.65	1134	26	1088	26	996	58	114
BF8-60-90-seq1-a	176275	431	156	0.29	148291	0.3342	1.7	5.5690	2.0	0.1208	1.0	0.87	1859	28	1911	17	1969	18	94
BF8-60-90-seq1-a	28932	51	23	0.36	8705	0.4005	2.4	7.4496	2.9	0.1349	1.7	0.82	2171	44	2167	27	2163	29	100
BF8-60-90-seq1-a	4450	146	15	0.85	8449	0.0801	2.3	0.5892	3.4	0.0533	2.5	0.68	497	11	470	13	343	56	145
BF8-60-90-seq1-a	599	12	2	0.87	982	0.1119	2.9	0.9755	13.3	0.0632	13.0	0.22	684	19	691	69	716	276	95
BF8-60-90-seq1-a	4218	60	8	0.63	6884	0.1090	2.0	0.9381	6.0	0.0624	5.6	0.33	667	13	672	30	689	120	97
BF8-60-90-seq1-a	8054	204	16	0.45	14639	0.0705	1.8	0.5453	3.5	0.0561	3.0	0.52	439	8	442	12	456	66	96
BF8-60-90-seq1-a	6146	94	11	0.52	10156	0.1082	2.1	0.9032	3.2	0.0605	2.4	0.67	662	13	653	15	623	51	106
BF8-60-90-seq1-a	146921	117	86	0.61	44374	0.5723	2.0	17.6746	2.3	0.2240	1.0	0.89	2917	48	2972	22	3009	16	97
BF8-60-90-seq1-a	10597	227	24	0.96	2171	0.0871	1.6	0.6992	2.7	0.0582	2.2	0.59	538	8	538	11	538	48	100
BF8-60-90-seq1-a	244635	580	215	0.24	210042	0.3467	2.5	5.6569	2.7	0.1183	0.9	0.94	1919	41	1925	23	1931	17	99
BF8-60-90-seq1-a	65786	225	78	0.56	65895	0.2928	2.0	4.0964	2.3	0.1015	1.2	0.86	1655	29	1654	19	1651	22	100
BF8-60-90-seq1-a	10988	325	22	0.34	19991	0.0667	1.9	0.5064	2.6	0.0551	1.8	0.71	416	8	416	9	415	41	100
BF8-60-90-seq1-a	9977	390	35	0.71	17890	0.0749	1.9	0.5812	4.2	0.0563	3.7	0.44	465	8	465	16	465	83	100
BF8-60-90-seq1-a	25666	84	32	1.02	8856	0.2766	2.3	3.7756	2.9	0.0990	1.7	0.81	1574	33	1588	23	1606	31	98
BF8-60-90-seq1-a	27278	203	37	0.22	12512	0.1795	2.0	1.8341	2.5	0.0741	1.5	0.80	1064	20	1058	17	1045	30	102
BF8-60-90-seq1-a	80532	150	64	0.23	17001	0.3944	2.3	7.3996	2.5	0.1361	1.0	0.91	2143	42	2161	23	2178	18	98
BF8-60-90-seq1-a	37467	115	41	0.55	36606	0.3011	1.6	4.3121	2.0	0.1039	1.2	0.80	1697	24	1696	17	1694	22	100
BF8-60-90-seq1-a	53684	94	47	0.47	7162	0.4225	1.9	8.4749	2.3	0.1455	1.3	0.83	2272	37	2283	22	2293	23	99
BF8-60-90-seq1-a	28129	170	43	0.64	34534	0.2136	1.7	2.4038	2.2	0.0816	1.4	0.77	1248	19	1244	16	1237	27	101
BF8-60-90-seq1-a	2438	181	14	0.28	1864	0.0763	3.2	0.5703	5.6	0.0542	4.6	0.58	474	15	458	21	379	104	125
BF8-60-90-seq1-a	6127	96	11	0.24	10353	0.1166	2.5	0.9667	3.2	0.0601	1.9	0.80	711	17	687	16	609	41	117
BF8-60-90-seq1-a	11803	97	17	0.22	10923	0.1705	2.0	1.7151	2.7	0.0730	1.8	0.73	1015	19	1014	17	1013	37	100
BF8-60-90-seq1-a	30816	198	44	0.38	38908	0.2018	2.3	2.2428	2.9	0.0806	1.7	0.81	1185	25	1195	21	1212	34	98
BF8-60-90-seq1-a	60307	217	74	0.52	22902	0.2894	2.0	4.0260	2.2	0.1009	1.0	0.89	1639	29	1639	18	1640	19	100
BF8-60-90-seq1-a	26146	507	36	0.60	372	0.0515	5.4	0.4258	9.3	0.0600	7.6	0.58	324	17	360	29	602	165	54
BF8-60-90-seq1-a	60973	93	61	0.48	31710	0.5380	1.6	14.4928	2.2	0.1954	1.4	0.77	2775	37	2783	21	2788	23	100
BF8-60-90-seq1-a	10319	93	16	0.35	14629	0.1626	1.7	1.6074	2.5	0.0717	1.7	0.71	971	16	973	15	978	35	99
BF8-60-90-seq1-a	7167	200	17	0.61	13353	0.0727	2.2	0.5457	3.1	0.0544	2.3	0.69	452	9	442	11	389	51	116
BF8-60-90-seq1-a	8814	128	19	0.43	14430	0.1334	2.2	1.2938	3.7	0.0703	3.0	0.60	807	17	843	21	938	61	86
BF8-60-90-seq1-a	5512	161	14	0.62	10485	0.0765	2.6	0.5957	9.5	0.0565	9.1	0.27	475	12	474	37	472	202	101
BF8-60-90-seq1-a	6579	129	12	0.28	11221	0.0934	2.1	0.7667	3.7	0.0595	3.1	0.56	575	11	578	16	587	66	98

BF8-60-90-seq1-a	6998	229	17	0.45	13565	0.0689	2.0	0.5467	7.1	0.0575	6.9	0.28	430	8	443	26	511	151	84
BF8-60-90-seq1-a	17274	111	24	0.20	22004	0.2090	2.0	2.3001	2.8	0.0798	1.9	0.72	1223	22	1212	20	1193	38	103
BF8-60-90-seq1-a	26707	56	27	0.59	12802	0.3980	1.9	7.3655	2.2	0.1342	1.2	0.85	2160	35	2157	20	2154	20	100
BF8-60-90-seq1-a	7101	59	11	0.19	9153	0.1848	3.3	2.0098	5.7	0.0789	4.6	0.58	1093	33	1119	39	1169	91	94
BF8-60-90-seq1-a	9090	82	22	0.66	11460	0.2306	2.3	2.5553	3.7	0.0804	2.8	0.64	1337	28	1288	27	1206	56	111
BF8-60-90-seq1-a	21803	78	33	0.46	17636	0.3672	2.5	6.3016	2.8	0.1245	1.3	0.89	2016	44	2019	25	2021	22	100
BF8-60-90-seq1-a	2751	36	7	0.34	3953	0.1957	2.6	1.9067	4.7	0.0707	3.9	0.56	1152	27	1083	31	948	79	122
BF8-60-90-seq1-a	23080	84	33	0.31	12066	0.3609	1.7	6.0198	2.1	0.1210	1.4	0.77	1986	28	1979	19	1971	24	101
BF8-60-90-seq1-a	30916	193	62	0.59	5885	0.2685	2.1	3.5377	2.5	0.0956	1.3	0.86	1533	29	1536	20	1539	24	100
BF8-60-90-seq1-a	1878	50	4	0.24	3350	0.0792	2.5	0.6283	9.0	0.0575	8.7	0.28	492	12	495	36	511	191	96
BF8-60-90-seq1-a	9091	274	22	0.37	17542	0.0744	1.7	0.5417	3.3	0.0528	2.8	0.52	463	8	440	12	320	63	145
BF8-60-90-seq1-a	23657	49	23	0.42	10057	0.4159	2.0	7.6745	2.6	0.1338	1.6	0.78	2242	39	2194	24	2149	29	104
BF8-60-90-seq1-a	15186	77	22	0.24	5607	0.2810	1.9	3.5121	3.1	0.0906	2.5	0.60	1596	27	1530	25	1439	48	111
BF8-60-90-seq1-a	239432	337	237	0.91	136666	0.5070	1.9	12.4052	2.1	0.1774	0.9	0.91	2644	40	2636	19	2629	14	101
BF8-90-180-seq1-	42652	33	25	0.78	22278	0.5700	1.9	15.3369	2.2	0.1951	1.2	0.86	2908	45	2836	22	2786	19	104
BF8-90-180-seq1-	1651	7	2	0.48	2097	0.2467	3.1	2.7047	5.8	0.0795	4.9	0.54	1421	40	1330	44	1185	96	120
BF8-90-180-seq1-	14816	231	24	0.33	26148	0.1017	1.8	0.8079	2.8	0.0576	2.2	0.64	624	11	601	13	515	47	121
BF8-90-180-seq1-	132468	112	75	0.57	70588	0.5333	2.1	14.0195	2.3	0.1907	0.9	0.91	2755	48	2751	22	2748	16	100
BF8-90-180-seq1-	13852	190	19	0.36	22960	0.0940	2.2	0.7999	3.3	0.0617	2.4	0.68	579	12	597	15	664	52	87
BF8-90-180-seq1-	30247	114	33	0.33	11287	0.2628	2.9	3.4692	3.5	0.0958	2.0	0.83	1504	39	1520	28	1543	37	97
BF8-90-180-seq1-	46683	118	40	0.30	32837	0.3138	2.2	4.6611	2.5	0.1077	1.1	0.89	1759	34	1760	21	1761	21	100
BF8-90-180-seq1-	100891	102	58	0.38	57463	0.4811	1.8	11.8280	2.3	0.1783	1.4	0.80	2532	38	2591	22	2637	23	96
BF8-90-180-seq1-	4138	26	5	0.43	5768	0.1792	1.9	1.7987	3.8	0.0728	3.2	0.52	1063	19	1045	25	1008	65	105
BF8-90-180-seq1-	9943	64	13	0.29	14048	0.1909	1.9	1.9020	2.8	0.0722	2.0	0.69	1126	20	1082	19	993	41	113
BF8-90-180-seq1-	15222	249	23	0.29	26369	0.0900	2.1	0.7283	3.0	0.0587	2.1	0.72	556	11	556	13	555	45	100
BF8-90-180-seq1-	1669	47	3	0.33	3338	0.0582	2.3	0.4074	5.2	0.0507	4.7	0.45	365	8	347	15	229	108	159
BF8-90-180-seq1-	14093	190	23	0.65	6479	0.1009	2.2	0.8421	3.0	0.0605	2.1	0.73	619	13	620	14	623	45	99
BF8-90-180-seq1-	8366	33	10	0.68	9712	0.2502	1.7	3.0345	2.9	0.0880	2.3	0.61	1439	23	1416	22	1382	44	104
BF8-90-180-seq1-	13547	244	21	0.30	23902	0.0821	1.9	0.6524	2.4	0.0576	1.5	0.79	509	9	510	10	515	32	99
BF8-90-180-seq1-	11332	172	16	0.06	19132	0.0990	1.8	0.8226	2.6	0.0602	1.9	0.68	609	10	610	12	612	41	99
BF8-90-180-seq1-	32918	107	30	0.16	34739	0.2729	2.0	3.6506	2.4	0.0970	1.4	0.82	1556	28	1561	19	1567	26	99
BF8-90-180-seq1-	8183	88	14	0.57	13511	0.1376	2.1	1.2900	4.5	0.0680	4.0	0.47	831	16	841	26	868	82	96
BF8-90-180-seq1-	15461	114	20	0.20	21887	0.1666	2.4	1.6465	3.0	0.0717	1.7	0.82	993	22	988	19	977	35	102
BF8-90-180-seq1-	4632	97	8	0.46	8758	0.0789	1.7	0.5816	3.6	0.0535	3.2	0.47	490	8	466	14	349	73	140
BF8-90-180-seq1-	26288	166	29	0.17	936	0.1689	2.1	1.7141	3.7	0.0736	3.0	0.58	1006	20	1014	24	1031	61	98
BF8-90-180-seq1-	16309	49	16	0.43	16733	0.2820	2.0	3.8517	2.6	0.0990	1.8	0.75	1602	28	1604	22	1606	33	100
BF8-90-180-seq1-	100428	294	84	0.07	100822	0.2909	2.0	4.0580	2.2	0.1012	1.0	0.89	1646	29	1646	18	1646	19	100
BF8-90-180-seq1-	57830	193	55	0.30	47185	0.2649	1.7	3.4540	2.2	0.0946	1.4	0.78	1515	23	1517	17	1519	26	100
BF8-90-180-seq1-	13986	96	17	0.24	19653	0.1685	2.4	1.6804	3.2	0.0723	2.1	0.74	1004	22	1001	21	995	44	101
BF8-90-180-seq1-	8487	249	16	0.19	16306	0.0633	2.1	0.4827	8.1	0.0553	7.9	0.26	396	8	400	27	423	175	94
BF8-90-180-seq1-	9209	28	8	0.44	9941	0.2494	3.3	3.2382	4.2	0.0942	2.6	0.78	1435	43	1466	33	1512	49	95
BF8-90-180-seq1-	496	11	1	0.43	1010	0.0860	2.4	0.5892	12.4	0.0497	12.2	0.19	532	12	470	48	181	285	294

BF8-90-180-seq1-	4077	33	7	0.50	5930	0.1745	1.9	1.7847	8.7	0.0742	8.5	0.22	1037	18	1040	59	1047	172	99
BF8-90-180-seq1-	29848	423	47	0.32	8704	0.1048	2.2	0.8840	3.0	0.0612	2.0	0.73	642	13	643	14	646	43	99
BF8-90-180-seq1-	6449	155	12	0.44	9521	0.0733	2.4	0.5905	6.2	0.0584	5.7	0.39	456	11	471	24	545	125	84
BF8-90-180-seq1-	7241	129	9	0.04	12850	0.0774	2.5	0.6116	3.2	0.0573	2.0	0.78	481	11	485	12	503	44	96
BF8-90-180-seq1-	1748	24	4	0.81	3221	0.1312	3.0	0.9427	5.7	0.0521	4.9	0.52	795	22	674	29	290	112	274
BF8-90-180-seq1-	21655	478	39	0.07	38159	0.0854	1.9	0.6859	3.2	0.0582	2.6	0.60	529	10	530	13	538	57	98
BF8-90-180-seq1-	6140	98	11	0.41	10813	0.0988	2.0	0.7873	3.1	0.0578	2.3	0.65	608	11	590	14	521	51	117
BF8-90-180-seq1-	81139	345	71	0.00	68755	0.2193	1.8	2.5764	2.3	0.0852	1.5	0.77	1278	21	1294	17	1321	29	97
BF8-90-180-seq1-	81474	267	76	0.12	17625	0.2812	2.1	3.8302	2.5	0.0988	1.5	0.81	1597	29	1599	21	1602	27	100
BF8-90-180-seq1-	8114	125	14	0.44	14011	0.1057	2.5	0.8583	3.3	0.0589	2.1	0.76	648	15	629	15	564	46	115
BF8-90-180-seq1-	3683	254	8	0.47	7541	0.0277	2.0	0.1898	3.0	0.0496	2.2	0.67	176	3	176	5	177	51	99
BF8-90-180-seq1-	3411	106	7	0.32	6950	0.0615	2.3	0.4220	4.4	0.0498	3.8	0.51	385	9	357	13	185	89	208
BF8-90-180-seq1-	22230	195	40	0.25	28498	0.2007	2.0	2.1941	2.6	0.0793	1.6	0.78	1179	22	1179	18	1179	33	100
BF8-90-180-seq1-	12539	99	19	0.28	17788	0.1797	2.2	1.8528	3.1	0.0748	2.2	0.71	1065	22	1064	21	1063	45	100
BF8-90-180-seq1-	4051	70	8	0.70	7565	0.1011	2.1	0.7583	4.0	0.0544	3.4	0.53	621	12	573	17	388	75	160
BF8-90-180-seq1-	2071	35	4	0.53	1769	0.1019	2.2	0.7738	6.3	0.0551	5.9	0.36	625	13	582	28	416	131	150
BF8-90-180-seq1-	18467	381	29	0.20	32460	0.0764	1.8	0.5974	2.7	0.0567	2.0	0.67	475	8	476	10	480	44	99
BF8-90-180-seq1-	12642	363	22	0.09	8331	0.0634	2.0	0.4611	2.5	0.0527	1.5	0.80	397	8	385	8	316	34	125
BF8-90-180-seq1-	12862	326	28	0.80	23741	0.0665	2.3	0.5052	3.0	0.0551	1.9	0.77	415	9	415	10	417	43	99
BF8-90-180-seq1-	53517	108	36	0.46	43835	0.2802	2.5	4.8032	3.1	0.1243	1.8	0.81	1592	35	1785	26	2019	32	79
BF8-90-180-seq1-	12389	183	21	0.36	20536	0.1084	1.8	0.9167	2.3	0.0613	1.5	0.75	664	11	661	11	650	33	102
BF8-90-180-seq1-	9330	60	14	0.56	12074	0.1981	1.7	2.1487	3.5	0.0787	3.0	0.48	1165	18	1165	24	1164	60	100
BF8-90-180-seq1-	109339	217	103	0.66	88027	0.3672	2.3	6.3633	2.8	0.1257	1.5	0.84	2016	40	2027	25	2039	27	99
BF8-90-180-seq1-	6130	212	13	0.32	12412	0.0559	2.3	0.4242	5.0	0.0550	4.5	0.45	351	8	359	15	414	100	85
BF8-90-180-seq1-	7312	120	15	0.44	13070	0.1108	2.0	0.9557	4.4	0.0626	4.0	0.44	677	13	681	22	694	85	98
BF8-90-180-seq1-	17685	93	20	0.25	21980	0.2069	1.9	2.3290	2.3	0.0816	1.3	0.82	1212	21	1221	17	1237	26	98
BF8-90-180-seq1-	3491	61	6	0.13	6391	0.0964	1.9	0.7199	5.2	0.0542	4.8	0.37	593	11	551	22	379	108	157
BF8-90-180-seq1-	4372	41	9	0.58	6087	0.1899	1.6	1.9030	2.8	0.0727	2.3	0.58	1121	17	1082	19	1005	47	112
BF8-90-180-seq1-	143161	332	109	0.04	121043	0.3346	2.7	5.5295	3.0	0.1199	1.2	0.92	1861	44	1905	26	1954	21	95
BF8-90-180-seq1-	32910	233	47	0.45	45029	0.1767	1.8	1.8108	2.2	0.0743	1.3	0.82	1049	18	1049	15	1050	26	100
BF8-90-180-seq1-	5970	52	13	0.51	7717	0.2289	2.1	2.4833	3.8	0.0787	3.2	0.54	1329	25	1267	28	1164	64	114
BF8-90-180-seq1-	155401	207	133	0.49	28438	0.5206	3.1	14.5132	3.4	0.2022	1.3	0.92	2702	69	2784	33	2844	21	95
BF8-90-180-seq2-	12512	84	17	0.41	16944	0.1801	1.8	1.8437	2.7	0.0743	2.0	0.65	1067	17	1061	18	1048	41	102
BF8-90-180-seq2-	21666	333	34	0.06	7812	0.1072	2.1	0.9087	2.8	0.0615	1.8	0.74	657	13	656	13	655	40	100
BF8-90-180-seq2-	3318	56	7	0.62	6084	0.1044	2.2	0.9099	8.7	0.0632	8.4	0.25	640	13	657	43	716	178	89
BF8-90-180-seq2-	4945	89	9	0.61	8546	0.0895	1.9	0.7260	3.3	0.0589	2.7	0.58	552	10	554	14	562	58	98
BF8-90-180-seq2-	42034	39	28	0.62	21223	0.5607	3.2	15.5789	3.5	0.2015	1.5	0.90	2869	74	2851	34	2839	25	101
BF8-90-180-seq2-	2494	54	5	0.41	4853	0.0900	1.9	0.6489	4.5	0.0523	4.1	0.41	555	10	508	18	299	95	186
BF8-90-180-seq2-	4694	121	10	0.61	2261	0.0713	2.7	0.5523	5.4	0.0562	4.6	0.51	444	12	446	20	459	102	97
BF8-90-180-seq2-	10815	23	10	0.46	9065	0.3625	1.9	6.1291	3.2	0.1226	2.6	0.58	1994	32	1994	29	1995	47	100
BF8-90-180-seq2-	8269	144	16	0.62	14357	0.0889	2.8	0.7173	3.9	0.0585	2.8	0.70	549	15	549	17	548	61	100
BF8-90-180-seq2-	14270	91	19	0.24	18582	0.1961	1.9	2.1077	2.7	0.0779	1.9	0.70	1155	20	1151	19	1145	39	101

BF8-90-180-seq2-	6423	88	12	0.21	10164	0.1416	2.1	1.2596	4.0	0.0645	3.4	0.52	854	16	828	23	759	72	112
BF8-90-180-seq2-	7941	20	8	0.56	7335	0.3264	1.6	5.0026	3.2	0.1111	2.8	0.50	1821	25	1820	28	1818	50	100
BF8-90-180-seq2-	22828	58	29	1.30	20222	0.3296	2.0	5.2220	2.5	0.1149	1.6	0.78	1837	31	1856	22	1878	29	98
BF8-90-180-seq2-	6760	49	8	0.24	9382	0.1591	2.8	1.6075	3.7	0.0733	2.4	0.76	952	25	973	23	1022	48	93
BF8-90-180-seq2-	84331	366	95	0.25	92440	0.2474	1.7	3.1702	2.2	0.0929	1.4	0.78	1425	22	1450	17	1487	26	96
BF8-90-180-seq2-	4325	338	10	0.46	8859	0.0277	1.6	0.1897	4.1	0.0497	3.7	0.40	176	3	176	7	179	87	98
BF8-90-180-seq2-	13360	84	19	0.42	18015	0.2102	2.5	2.1867	3.5	0.0754	2.5	0.70	1230	28	1177	25	1080	50	114
BF8-90-180-seq2-	1495	107	3	0.42	1690	0.0279	2.2	0.1919	5.5	0.0498	5.1	0.40	178	4	178	9	187	118	95
Sample 48/28-1 (BF5)			**Well no.: 48/28-1**				**Location (decimal degrees):**				**51.164**	**8.462889W**			**Datum:IRENET95**				
BF5-seq1-A01	1786	121	21	0.32	2505	0.1627	1.7	1.6712	3.8	0.0745	3.5	0.44	972	15	998	25	1055	70	92
BF5-seq1-A02	2384	152	27	0.27	3337	0.1744	1.7	1.7901	3.8	0.0744	3.4	0.44	1037	16	1042	25	1053	68	98
BF5-seq1-A03	1469	246	23	0.53	2644	0.0851	2.5	0.6824	4.8	0.0582	4.0	0.53	526	13	528	20	536	89	98
BF5-seq1-A04	712	209	12	0.38	1407	0.0563	1.9	0.4138	6.3	0.0533	6.0	0.30	353	7	352	19	342	135	103
BF5-seq1-A05	3366	422	48	0.18	5527	0.1150	1.5	1.0080	3.6	0.0636	3.3	0.41	702	10	708	19	727	70	97
BF5-seq1-A06	2644	425	46	0.11	2732	0.1146	2.4	0.9850	4.2	0.0623	3.4	0.57	700	16	696	21	685	73	102
BF5-seq1-A07	4269	178	45	0.36	4840	0.2309	3.3	2.9377	4.1	0.0923	2.4	0.81	1339	40	1392	32	1473	46	91
BF5-seq1-A08	1370	429	34	0.27	2326	0.0789	2.6	0.6727	4.5	0.0619	3.7	0.57	489	12	522	19	669	80	73
BF5-seq1-A09	1977	708	46	0.49	3516	0.0595	2.0	0.4863	5.5	0.0592	5.1	0.36	373	7	402	18	576	111	65
BF5-seq1-A10	1296	276	40	0.55	3000	0.1331	1.5	0.8245	6.0	0.0449	5.8	0.25	805	11	611	28	-59	142	-1362
BF5-seq1-A11	298	129	10	0.75	576	0.0614	2.4	0.4606	10.5	0.0544	10.2	0.23	384	9	385	34	387	230	99
BF5-seq1-A12	440	98	10	0.32	752	0.1014	2.5	0.8518	8.5	0.0610	8.1	0.30	622	15	626	40	638	174	98
BF5-seq1-A13	2913	83	34	0.49	2505	0.3590	2.2	6.0514	4.2	0.1223	3.6	0.53	1977	38	1983	37	1989	64	99
BF5-seq1-A14	178	79	5	0.47	346	0.0536	3.1	0.3924	13.3	0.0531	12.9	0.24	337	10	336	39	332	292	101
BF5-seq1-A15	9010	134	72	0.48	4983	0.4585	1.8	11.7053	2.8	0.1852	2.1	0.66	2433	37	2581	27	2700	35	90
BF5-seq1-A16	1952	198	39	0.24	2612	0.1966	2.4	2.1136	5.1	0.0780	4.6	0.46	1157	25	1153	36	1146	91	101
BF5-seq1-A17	789	397	33	2.35	1492	0.0492	2.6	0.3791	6.2	0.0559	5.6	0.43	310	8	326	17	447	124	69
BF5-seq1-A18	425	110	7	0.51	829	0.0584	2.6	0.4325	7.3	0.0537	6.9	0.35	366	9	365	23	359	155	102
BF5-seq1-A19	1390	92	16	0.20	1920	0.1748	2.2	1.8234	4.4	0.0757	3.8	0.51	1038	21	1054	29	1086	76	96
BF5-seq1-A20	3147	318	40	0.11	4999	0.1292	2.1	1.1709	3.5	0.0657	2.8	0.59	784	15	787	19	797	58	98
BF5-seq1-A21	510	119	13	1.02	737	0.0854	3.5	0.8557	9.8	0.0727	9.1	0.36	528	18	628	47	1005	184	53
BF5-seq1-A22	4368	279	48	0.16	6120	0.1736	1.9	1.7822	3.0	0.0745	2.2	0.65	1032	18	1039	19	1054	45	98
BF5-seq1-A23	804	142	12	0.26	1433	0.0850	1.6	0.6858	5.3	0.0585	5.1	0.31	526	8	530	22	549	111	96
BF5-seq1-A24	6843	128	87	1.34	4551	0.4872	1.8	10.5467	3.1	0.1570	2.5	0.60	2559	39	2484	29	2424	42	106
BF5-seq1-A25	401	99	10	0.68	708	0.0911	2.2	0.7394	10.6	0.0589	10.3	0.21	562	12	562	47	563	225	100
BF5-seq1-A26	694	148	18	0.75	1184	0.1002	2.0	0.8412	7.0	0.0609	6.7	0.28	616	12	620	33	635	145	97
BF5-seq1-A27	1915	196	26	0.32	3039	0.1289	2.3	1.1743	4.5	0.0661	3.9	0.50	782	17	789	25	808	82	97
BF5-seq1-A28	571	146	15	0.60	1037	0.0888	2.7	0.7154	9.3	0.0584	8.9	0.29	548	14	548	40	547	195	100
BF5-seq1-A29	1972	98	29	0.35	2089	0.2752	1.7	3.7258	4.0	0.0982	3.7	0.41	1567	23	1577	33	1590	69	99
BF5-seq1-A30	2350	200	41	0.34	3122	0.1971	1.6	2.1147	3.9	0.0778	3.6	0.41	1160	17	1154	27	1142	71	102
BF5-seq2-B01	674	75	9	0.64	1146	0.1059	2.3	0.9035	6.1	0.0619	5.7	0.37	649	14	654	30	670	122	97
BF5-seq2-B02	1089	273	14	0.40	2055	0.0491	2.3	0.3755	6.0	0.0554	5.6	0.39	309	7	324	17	429	124	72
BF5-seq2-B03	1361	525	29	0.14	2657	0.0577	1.4	0.4283	4.6	0.0538	4.4	0.31	362	5	362	14	364	99	99

BF5-seq2-B04	1187	183	23	0.72	1871	0.1045	1.5	0.9590	5.6	0.0666	5.4	0.27	641	9	683	28	824	113	78
BF5-seq2-B05	518	130	11	0.64	906	0.0717	2.4	0.5948	7.7	0.0601	7.3	0.32	447	10	474	29	609	157	73
BF5-seq2-B06	735	63	11	0.27	1087	0.1638	2.2	1.5991	5.8	0.0708	5.3	0.38	978	20	970	37	952	109	103
BF5-seq2-B07	1794	494	32	0.55	2282	0.0580	2.0	0.4320	5.7	0.0540	5.3	0.35	363	7	365	18	372	120	98
BF5-seq2-B08	437	45	5	0.42	731	0.1094	2.9	0.9398	10.4	0.0623	10.0	0.28	669	18	673	53	685	214	98
BF5-seq2-B09	812	221	16	0.31	1533	0.0698	2.1	0.5361	5.8	0.0557	5.4	0.35	435	9	436	21	442	121	98
BF5-seq2-B10	1884	101	19	0.21	2314	0.1841	2.3	1.9162	4.9	0.0755	4.3	0.47	1089	23	1087	33	1081	86	101
BF5-seq2-B11	1567	69	20	0.48	1735	0.2600	2.3	3.3603	5.0	0.0937	4.4	0.46	1490	30	1495	40	1503	84	99
BF5-seq2-B12	2059	84	29	0.86	1786	0.2642	1.6	4.5425	5.1	0.1247	4.9	0.32	1511	22	1739	44	2025	86	75
BF5-seq2-B13	1283	101	19	0.28	1756	0.1849	1.6	1.9426	4.1	0.0762	3.8	0.38	1094	16	1096	28	1100	77	99
BF5-seq2-B14	329	73	6	0.75	394	0.0745	2.9	0.7144	10.2	0.0696	9.8	0.29	463	13	547	44	916	201	51
BF5-seq2-B15	1834	148	27	0.26	2463	0.1802	1.7	1.9304	3.9	0.0777	3.6	0.42	1068	16	1092	27	1139	71	94
BF5-seq2-B16	5319	184	68	0.79	5325	0.3069	1.4	4.4540	3.1	0.1052	2.7	0.46	1726	21	1722	26	1719	50	100
BF5-seq2-B17	289	34	5	0.46	318	0.1281	4.9	1.7283	17.0	0.0979	16.3	0.29	777	36	1019	115	1584	304	49
BF5-seq2-B18	592	40	9	0.96	777	0.1753	2.6	1.9204	8.3	0.0794	7.9	0.31	1041	25	1088	57	1183	157	88
BF5-seq2-B19	1806	789	46	0.81	815	0.0527	4.1	0.4345	9.9	0.0598	9.0	0.42	331	13	366	31	596	195	56
BF5-seq2-B20	798	46	9	0.35	1126	0.1780	2.0	1.8290	7.6	0.0745	7.3	0.26	1056	19	1056	51	1056	147	100
BF5-seq2-B21	30097	251	133	0.23	1142	0.4824	3.8	11.7032	4.6	0.1760	2.7	0.81	2538	80	2581	44	2615	45	97
BF5-seq2-B22	1560	299	35	0.16	3370	0.1217	2.6	0.8036	5.4	0.0479	4.7	0.48	740	18	599	25	95	111	781
BF5-seq2-B23	1218	295	16	0.27	2301	0.0549	1.8	0.4203	4.6	0.0555	4.2	0.40	345	6	356	14	432	94	80
BF5-seq2-B24	596	192	11	0.16	1119	0.0592	2.4	0.4444	8.5	0.0544	8.2	0.28	371	9	373	27	388	183	96
BF5-seq2-B25	324	134	8	0.76	646	0.0511	2.1	0.3749	10.2	0.0532	10.0	0.21	321	7	323	29	339	226	95
BF5-seq2-B26	837	47	9	0.56	1063	0.1653	5.9	1.8983	12.2	0.0833	10.6	0.49	986	54	1080	84	1276	208	77
BF5-seq2-B27	1358	238	22	0.84	2488	0.0753	2.6	0.5909	5.2	0.0569	4.5	0.50	468	12	471	20	489	99	96
BF5-seq2-B28	384	49	5	0.49	668	0.0947	2.8	0.7821	8.2	0.0599	7.8	0.34	583	16	587	37	600	168	97
BF5-seq2-B29	2513	631	35	0.56	3032	0.0505	1.6	0.3952	4.3	0.0567	4.0	0.37	318	5	338	12	481	88	66
BF5-seq2-B30	2832	139	28	0.26	3830	0.1945	2.2	2.0859	4.9	0.0778	4.4	0.45	1146	23	1144	34	1141	87	100
BF5-seq2-B31	1526	206	21	0.32	2706	0.0996	2.4	0.8136	4.4	0.0592	3.7	0.54	612	14	604	20	575	81	106
BF5-seq2-B32	1218	306	18	0.48	2393	0.0524	1.5	0.3840	4.7	0.0532	4.5	0.32	329	5	330	13	337	101	98
BF5-seq2-B33	1580	184	21	0.41	2680	0.1047	1.4	0.8931	4.4	0.0619	4.1	0.33	642	9	648	21	669	88	96
BF5-seq2-B34	835	56	21	0.74	882	0.3124	2.0	4.2926	6.3	0.0996	5.9	0.32	1753	31	1692	53	1617	111	108
BF5-seq2-B35	3165	223	58	0.05	3344	0.2704	1.2	3.7113	3.5	0.0995	3.3	0.34	1543	16	1574	28	1615	61	96
BF5-seq2-B36	8630	193	76	1.05	8687	0.2960	1.7	4.2657	3.0	0.1045	2.5	0.58	1672	26	1687	25	1706	45	98
BF5-seq2-B37	6743	131	48	0.60	6114	0.3121	2.1	4.9219	2.8	0.1144	1.8	0.76	1751	32	1806	24	1870	32	94
BF5-seq2-B38	1489	101	15	0.41	1892	0.1365	2.2	1.4746	7.8	0.0784	7.5	0.28	825	17	920	48	1156	148	71
BF5-seq2-B39	303	32	4	0.79	512	0.1135	2.8	0.9782	10.5	0.0625	10.2	0.26	693	18	693	54	691	217	100
BF5-seq2-B40	3927	135	49	0.85	3879	0.2908	1.6	4.2674	2.8	0.1064	2.3	0.58	1646	24	1687	23	1739	42	95
BF5-seq2-B41	981	256	20	0.69	1535	0.0697	2.5	0.6475	6.7	0.0674	6.3	0.37	434	10	507	27	849	130	51
BF5-seq2-B42	167	20	3	1.53	291	0.1030	3.0	0.8593	13.8	0.0605	13.5	0.22	632	18	630	67	621	290	102
BF5-seq2-B43	3738	124	48	0.70	3479	0.3246	1.9	5.0466	3.5	0.1128	2.9	0.55	1812	30	1827	30	1845	53	98
BF5-seq2-B44	2220	438	44	1.64	4222	0.0686	1.9	0.5228	3.7	0.0553	3.2	0.50	427	8	427	13	424	72	101
BF5-seq2-B45	1726	191	23	0.63	2872	0.1057	1.7	0.9132	4.1	0.0626	3.7	0.42	648	10	659	20	696	79	93

BF5-seq2-B46	631	165	10	0.42	1214	0.0543	1.6	0.4016	6.1	0.0536	5.9	0.26	341	5	343	18	355	134	96
BF5-seq2-B47	733	169	14	0.22	1330	0.0837	3.2	0.6684	7.9	0.0579	7.2	0.40	518	16	520	33	526	158	99
BF5-seq2-B48	527	154	13	0.89	980	0.0728	2.3	0.5651	7.1	0.0563	6.7	0.33	453	10	455	26	465	148	97
BF5-seq2-B49	1405	194	21	0.63	2415	0.0904	3.0	0.7615	5.5	0.0611	4.7	0.54	558	16	575	25	643	100	87
BF5-seq2-B50	447	159	10	0.36	864	0.0617	2.8	0.4602	7.8	0.0541	7.2	0.36	386	11	384	25	374	163	103
BF5-seq2-B51	64590	691	409	0.11	27477	0.5539	1.8	14.9962	3.4	0.1964	2.9	0.54	2841	43	2815	33	2796	47	102
BF5-seq2-B52	5748	99	38	0.36	4933	0.3455	1.7	5.7300	2.6	0.1203	2.0	0.64	1913	28	1936	23	1961	35	98
BF5-seq2-B53	1462	281	29	0.26	2485	0.1034	2.4	0.8732	5.7	0.0613	5.2	0.42	634	15	637	27	649	111	98
BF5-seq2-B54	225	16	4	0.63	307	0.2068	3.7	2.1821	12.1	0.0765	11.5	0.30	1212	41	1175	88	1109	230	109
BF5-seq2-B55	10154	323	94	0.47	11803	0.2602	2.0	3.2050	3.0	0.0893	2.3	0.66	1491	27	1458	24	1411	43	106
BF5-seq2-B56	902	131	14	0.79	1578	0.0893	1.7	0.7460	6.2	0.0606	5.9	0.28	551	9	566	27	624	128	88
BF5-seq2-B57	3813	106	40	0.61	3310	0.3182	2.2	5.2443	4.4	0.1195	3.8	0.50	1781	34	1860	38	1949	69	91
BF5-seq2-B58	734	141	16	0.82	1298	0.0950	3.0	0.7757	7.4	0.0592	6.8	0.40	585	17	583	33	576	147	102
BF5-seq2-B59	1122	286	24	0.29	2023	0.0826	1.7	0.6575	5.3	0.0577	5.0	0.32	512	8	513	22	520	110	98
BF5-seq2-B60	1308	222	20	0.66	2316	0.0777	2.2	0.6407	5.0	0.0598	4.5	0.43	483	10	503	20	596	98	81
BF5-seq3-C01	674	94	9	0.47	1167	0.0909	2.1	0.7522	7.4	0.0600	7.1	0.28	561	11	570	33	605	154	93
BF5-seq3-C02	5385	314	57	0.25	7680	0.1787	1.6	1.8101	3.3	0.0735	2.9	0.49	1060	16	1049	22	1027	59	103
BF5-seq3-C03	2525	496	35	0.05	3600	0.0717	5.4	0.7273	10.1	0.0735	8.5	0.54	447	24	555	44	1029	172	43
BF5-seq3-C04	3063	1333	55	0.31	860	0.0401	6.6	0.2849	8.7	0.0515	5.6	0.76	254	16	255	20	262	129	97
BF5-seq3-C05	3637	369	41	0.11	5935	0.1157	1.6	1.0197	3.6	0.0639	3.3	0.44	706	11	714	19	738	69	96
BF5-seq3-C06	-	-	-	-	-	-	-	-	-	-	-	-	-	-	-	-	-	-	-
BF5-seq3-C07	1239	277	16	0.11	2370	0.0608	2.1	0.4548	5.2	0.0543	4.7	0.42	380	8	381	16	382	105	100
BF5-seq3-C08	-	-	-	-	-	-	-	-	-	-	-	-	-	-	-	-	-	-	-
BF5-seq3-C09	42148	360	215	0.18	25625	0.5626	1.6	13.0218	2.2	0.1679	1.5	0.72	2877	37	2681	21	2537	25	113
BF5-seq3-C10	2014	79	28	0.79	2044	0.2969	1.4	4.2208	4.6	0.1031	4.4	0.30	1676	20	1678	38	1681	81	100
BF5-seq3-C11	3301	983	59	0.03	785	0.0633	1.7	0.5448	7.8	0.0624	7.6	0.22	396	7	442	28	688	162	58
BF5-seq3-C12	449	121	10	0.54	834	0.0749	2.8	0.5790	8.3	0.0560	7.8	0.34	466	13	464	31	454	173	103
BF5-seq3-C13	1743	177	21	0.09	2417	0.1194	3.3	1.2491	6.2	0.0759	5.3	0.53	727	23	823	36	1091	105	67
BF5-seq3-C14	4768	523	67	0.28	416	0.1226	8.2	1.1065	9.8	0.0654	5.5	0.83	746	58	756	54	788	115	95
BF5-seq3-C15	1677	98	19	0.37	2375	0.1795	1.6	1.8326	4.3	0.0740	4.0	0.37	1064	15	1057	29	1042	80	102
BF5-seq3-C16	1020	188	13	0.22	1918	0.0667	2.8	0.5086	6.2	0.0553	5.5	0.45	416	11	417	21	423	124	98
BF5-seq3-C17	4001	79	36	0.92	3664	0.3563	1.5	5.6339	3.2	0.1147	2.9	0.48	1965	26	1921	28	1875	51	105
BF5-seq3-C18	197	103	8	0.58	317	0.0658	2.0	0.5800	14.3	0.0639	14.1	0.14	411	8	464	55	739	299	56
BF5-seq3-C19	774	226	17	0.42	1423	0.0725	2.3	0.5719	8.7	0.0572	8.4	0.27	451	10	459	33	500	184	90
BF5-seq3-C20	658	104	10	0.42	1036	0.0856	4.9	0.7790	8.9	0.0660	7.4	0.55	530	25	585	40	806	155	66
BF5-seq3-C21	2654	106	38	0.78	2705	0.2958	2.4	4.1728	4.3	0.1023	3.6	0.54	1671	35	1669	36	1666	67	100
BF5-seq3-C22	5634	147	58	0.30	4804	0.3703	2.0	6.2348	3.0	0.1221	2.2	0.68	2031	36	2009	27	1987	39	102
BF5-seq3-C23	1179	113	24	0.82	1687	0.1742	2.4	1.7623	5.9	0.0734	5.5	0.40	1035	23	1032	39	1024	110	101
BF5-seq3-C24	1608	131	28	0.49	2140	0.1962	1.4	2.0996	4.4	0.0776	4.2	0.31	1155	14	1149	31	1137	84	102
BF5-seq3-C25	1037	254	16	0.44	2007	0.0578	2.5	0.4323	5.9	0.0543	5.3	0.42	362	9	365	18	382	119	95
BF5-seq3-C26	3032	90	34	0.53	2685	0.3296	1.8	5.3511	3.2	0.1178	2.6	0.56	1836	28	1877	28	1923	47	96
BF5-seq3-C27	60	75	1	0.65	71	0.0169	7.5	0.2078	33.8	0.0890	32.9	0.22	108	8	192	61	1403	631	8

BF5-seq3-C28	1099	73	12	0.37	1622	0.1539	2.1	1.4940	5.5	0.0704	5.1	0.39	923	19	928	34	940	104	98
BF5-seq3-C29	8422	221	84	0.54	6956	0.3238	2.0	5.6487	2.8	0.1265	2.0	0.71	1808	32	1924	25	2050	36	88
BF5-seq3-C30	1038	179	23	0.77	1727	0.1096	1.8	0.9472	5.5	0.0627	5.2	0.33	670	12	677	28	698	111	96
BF5-seq3-C31	635	128	13	0.38	1118	0.0934	2.4	0.7626	6.0	0.0592	5.5	0.40	575	13	576	27	576	120	100
BF5-seq3-C32	10887	458	157	0.75	11585	0.2884	1.5	3.8653	2.3	0.0972	1.7	0.67	1633	22	1606	18	1571	31	104
BF5-seq3-C33	10887	458	156	0.75	11418	0.2885	1.5	3.9182	2.5	0.0985	2.0	0.61	1634	22	1617	20	1596	37	102
BF5-seq3-C34	4797	175	69	0.97	1198	0.3186	2.4	5.1928	6.3	0.1182	5.8	0.39	1783	38	1851	55	1929	104	92
BF5-seq3-C35	6123	305	85	0.31	7065	0.2681	1.5	3.3558	3.1	0.0908	2.7	0.50	1531	21	1494	24	1442	51	106
BF5-seq3-C36	1661	192	32	0.55	2398	0.1505	2.7	1.4856	5.2	0.0716	4.4	0.53	904	23	925	32	975	89	93
BF5-seq3-C37	7689	90	52	0.42	4301	0.5081	3.9	13.0564	4.5	0.1864	2.2	0.87	2648	85	2684	43	2710	36	98
BF5-seq3-C38	9825	102	72	0.53	5019	0.5920	1.6	16.6730	2.3	0.2043	1.6	0.71	2997	39	2916	22	2861	26	105
BF5-seq3-C39	827	107	16	0.72	1445	0.0976	2.2	0.8043	6.2	0.0598	5.8	0.35	600	13	599	29	596	126	101
BF5-seq3-C40	320	25	4	1.07	376	0.1236	6.7	1.4759	12.7	0.0866	10.7	0.53	751	48	921	80	1352	207	56
BF5-seq3-C41	645	144	14	0.41	1127	0.0930	1.7	0.7539	7.5	0.0588	7.3	0.22	573	9	570	33	560	160	102
BF5-seq3-C42	908	167	16	0.28	1581	0.0962	1.8	0.7939	5.5	0.0598	5.1	0.33	592	10	593	25	598	112	99
BF5-seq3-C43	2614	93	32	0.32	2553	0.3285	1.3	4.8724	3.6	0.1076	3.3	0.35	1831	20	1797	30	1759	61	104
BF5-seq3-C44	571	124	12	0.23	986	0.0936	2.6	0.7817	6.9	0.0606	6.4	0.38	577	15	586	31	624	138	92
BF5-seq3-C45	10439	436	127	0.46	767	0.2589	2.0	3.3398	3.9	0.0936	3.3	0.52	1484	27	1490	31	1499	63	99
BF5-seq3-C46	3180	288	52	0.13	4292	0.1826	2.0	1.9314	3.6	0.0767	3.0	0.55	1081	20	1092	24	1114	60	97
BF5-seq3-C47	632	91	9	0.44	1112	0.0936	3.0	0.7664	8.0	0.0594	7.4	0.38	577	17	578	36	582	160	99
Sample 48/24-4 (BF4)			**Well no.: 48/24-4**				**Location (decimal degrees):**				**51.331**	**8.296366W**			**Datum:IRENET95**				
BF4-seq1-a01	5067	171	18	0.55	8777	0.0939	3.5	0.7651	4.8	0.0591	3.2	0.74	578	19	577	21	571	70	101
BF4-seq1-a02	7463	314	28	0.59	5277	0.0797	3.1	0.6236	4.6	0.0568	3.3	0.68	494	15	492	18	483	74	102
BF4-seq1-a03	1577	45	6	0.74	2769	0.1211	2.7	0.9635	7.9	0.0577	7.4	0.34	737	19	685	40	519	163	142
BF4-seq1-a04	4076	173	14	0.21	7330	0.0786	3.3	0.6187	5.3	0.0571	4.1	0.63	488	16	489	21	496	90	98
BF4-seq1-a05	1970	317	24	0.28	11736	0.0782	3.0	0.1749	25.4	0.0162	25.2	0.12	485	14	164	39	-3683	1446	-13
BF4-seq1-a06	28349	350	63	0.08	32577	0.1867	2.9	2.3018	3.4	0.0894	1.7	0.87	1104	30	1213	24	1413	32	78
BF4-seq1-a07	4022	207	17	0.57	7347	0.0748	3.7	0.5786	5.0	0.0561	3.3	0.74	465	17	464	19	457	74	102
BF4-seq1-a08	6241	86	17	0.32	8673	0.1930	3.3	1.9522	6.2	0.0734	5.3	0.53	1137	35	1099	43	1024	107	111
BF4-seq1-a09	20628	260	83	0.44	21622	0.2920	3.1	3.9370	4.0	0.0978	2.6	0.77	1652	45	1621	33	1582	48	104
BF4-seq1-a10	3914	216	30	1.04	6552	0.1093	3.1	0.9322	10.7	0.0619	10.2	0.29	668	20	669	54	670	218	100
BF4-seq1-a11	5142	261	30	0.20	8466	0.1155	2.7	0.9937	4.0	0.0624	3.0	0.66	704	18	701	21	688	65	102
BF4-seq1-a12	11893	56	24	1.41	12660	0.2931	2.8	3.8948	3.4	0.0964	2.0	0.82	1657	41	1613	28	1555	37	107
BF4-seq1-a13	2870	29	6	0.56	4447	0.1874	3.0	1.7074	5.4	0.0661	4.5	0.56	1107	31	1011	35	809	94	137
BF4-seq1-a14	40766	48	32	0.45	21472	0.5600	3.0	15.0167	3.5	0.1945	1.8	0.86	2866	71	2816	34	2781	29	103
BF4-seq1-a15	1413	51	7	1.23	2821	0.1100	3.2	0.7793	8.6	0.0514	8.0	0.37	672	20	585	39	259	183	260
BF4-seq1-a16	61996	191	151	1.10	31224	0.5743	3.3	16.1559	4.3	0.2040	2.8	0.76	2925	77	2886	42	2859	45	102
BF4-seq1-a17	1318	44	6	0.77	2496	0.1176	4.6	0.8785	6.5	0.0542	4.6	0.71	717	31	640	31	377	103	190
BF4-seq1-a18	43399	416	146	0.07	35936	0.3525	2.8	6.0323	3.3	0.1241	1.8	0.83	1946	47	1981	29	2016	33	97
BF4-seq1-a19	8347	499	45	0.13	14451	0.0938	3.1	0.7634	4.2	0.0590	2.9	0.73	578	17	576	19	568	63	102
BF4-seq1-a20	1665	49	10	0.43	2686	0.1910	3.6	1.7103	10.4	0.0649	9.7	0.35	1127	37	1012	69	772	205	146
BF4-seq1-a21	4247	169	22	1.26	7964	0.0949	3.0	0.7148	5.3	0.0546	4.4	0.56	585	17	548	23	396	98	148

BF4-seq1-a22	7381	763	46	0.03	13877	0.0655	2.7	0.4943	4.5	0.0548	3.7	0.59	409	11	408	15	403	82	102
BF4-seq1-a23	707	35	4	0.41	1337	0.1236	3.6	0.9328	16.4	0.0547	16.0	0.22	751	25	669	84	401	359	187
BF4-seq1-a24	4276	184	27	0.70	6595	0.1292	3.8	1.1681	7.2	0.0656	6.1	0.53	783	28	786	40	793	128	99
BF4-seq1-a25	6033	306	35	0.38	6802	0.1119	3.1	0.9659	5.2	0.0626	4.2	0.60	684	20	686	26	694	89	98
BF4-seq1-a26	23952	90	42	0.49	18896	0.4135	2.7	7.4236	3.2	0.1302	1.7	0.84	2231	50	2164	29	2101	30	106
BF4-seq1-a27	1895	77	6	0.30	3890	0.0743	3.2	0.5103	11.4	0.0498	11.0	0.28	462	14	419	40	185	256	249
BF4-seq1-a28	6930	405	44	0.43	11706	0.1038	4.2	0.8691	5.6	0.0607	3.7	0.75	637	25	635	27	629	80	101
BF4-seq1-a29	2836	58	6	0.18	4667	0.1079	3.5	0.9265	8.3	0.0623	7.5	0.43	661	22	666	41	683	160	97
BF4-seq1-a30	348	37	3	0.71	569	0.0882	5.0	0.4966	47.4	0.0408	47.1	0.11	545	26	409	174	-297	1204	-183
BF4-seq1-a31	6790	74	16	0.41	8716	0.2061	4.0	2.2701	6.1	0.0799	4.7	0.64	1208	44	1203	44	1194	92	101
BF4-seq1-a32	3061	161	14	1.23	5731	0.0639	3.0	0.4810	5.1	0.0546	4.1	0.59	400	12	399	17	394	92	101
BF4-seq1-a33	24959	162	57	0.59	25081	0.3021	3.0	4.2586	3.6	0.1022	2.0	0.83	1702	45	1685	30	1665	36	102
BF4-seq1-a34	1594	94	11	0.64	2879	0.1040	4.6	0.8047	11.2	0.0561	10.2	0.41	638	28	599	52	458	225	139
BF4-seq1-a35	7799	188	46	1.15	10513	0.1846	3.8	1.9343	5.2	0.0760	3.5	0.73	1092	39	1093	36	1095	71	100
BF4-seq1-a36	690	52	8	0.38	1581	0.1582	3.3	0.9640	29.3	0.0442	29.1	0.11	947	29	685	158	-99	715	-952
BF4-seq1-a37	871	98	7	0.87	2322	0.0625	3.8	0.3271	25.0	0.0379	24.8	0.15	391	14	287	65	-489	658	-80
BF4-seq1-a38	25152	252	87	0.30	23799	0.3245	2.7	4.8519	3.5	0.1084	2.2	0.78	1812	43	1794	30	1773	40	102
BF4-seq1-a39	22522	228	85	0.40	11007	0.3417	2.7	5.2081	3.8	0.1105	2.7	0.70	1895	44	1854	33	1808	50	105
BF4-seq1-a40	6879	239	29	0.78	11658	0.1024	2.9	0.8563	4.1	0.0606	3.0	0.69	629	17	628	19	627	64	100
BF4-seq1-a41	1268	70	8	0.55	2379	0.1108	3.6	0.8345	8.8	0.0546	8.1	0.41	677	23	616	42	398	181	170
BF4-seq1-a42	16262	53	40	1.13	8800	0.5431	3.0	14.2822	3.5	0.1907	1.9	0.85	2797	69	2769	34	2748	31	102
BF4-seq1-a43	2437	137	18	0.45	4264	0.1266	3.2	1.0243	5.9	0.0587	5.0	0.54	768	23	716	31	555	108	138
BF4-seq1-a44	470	63	4	0.57	1376	0.0659	6.9	0.3237	39.7	0.0356	39.1	0.17	412	28	285	104	-661	1077	-62
BF4-seq1-a45	115217	535	181	0.02	94701	0.3453	2.8	5.9460	3.1	0.1249	1.3	0.90	1912	46	1968	27	2027	24	94
BF4-seq1-a46	3162	22	11	0.52	2561	0.4441	7.8	7.7813	14.0	0.1271	11.6	0.56	2369	157	2206	135	2058	205	115
BF4-seq1-a47	9661	564	65	0.76	16449	0.0965	2.5	0.7936	3.5	0.0596	2.5	0.72	594	14	593	16	591	53	101
BF4-seq1-a48	4883	256	33	1.00	8164	0.1011	3.3	0.8413	4.7	0.0604	3.4	0.70	621	19	620	22	616	73	101
BF4-seq1-a49	5347	166	27	1.16	9295	0.1190	2.8	0.9717	4.8	0.0592	3.9	0.59	725	19	689	24	574	84	126
BF4-seq1-a50	62600	255	101	0.16	50670	0.3852	2.8	6.7393	3.1	0.1269	1.3	0.90	2101	50	2078	28	2055	23	102
BF4-seq1-a51	2493	266	21	0.47	836	0.0747	2.9	0.5112	9.5	0.0497	9.1	0.30	464	13	419	33	179	212	259
BF4-seq1-a52	2759	167	20	0.47	4987	0.1144	3.8	0.8977	12.1	0.0569	11.5	0.31	698	25	650	60	489	254	143
BF4-seq1-a53	9763	119	37	0.66	10380	0.2604	3.7	3.4591	5.2	0.0964	3.6	0.72	1492	50	1518	42	1555	68	96
BF4-seq1-a54	1299	120	10	0.74	2701	0.0737	3.1	0.5000	9.4	0.0492	8.9	0.33	459	14	412	32	156	208	293
BF4-seq1-a55	19340	270	58	0.02	18530	0.2235	3.5	3.2663	4.5	0.1060	2.9	0.78	1300	42	1473	36	1732	53	75
BF4-seq1-a56	7270	149	14	0.02	12395	0.1002	3.2	0.8332	4.8	0.0603	3.6	0.66	616	19	615	22	614	77	100
BF4-seq1-a57	21331	482	80	0.82	160	0.1137	4.7	2.2778	7.3	0.1453	5.5	0.65	694	31	1205	52	2291	95	30
BF4-seq1-a58	57225	183	114	0.43	31712	0.5368	2.8	13.5758	3.3	0.1834	1.7	0.86	2770	63	2721	31	2684	28	103
BF4-seq1-a59	6188	98	27	0.33	4860	0.2668	2.6	3.2991	5.0	0.0897	4.2	0.53	1524	36	1481	39	1419	80	107
BF4-seq1-a60	2274	133	12	0.77	4808	0.0780	3.2	0.5204	5.5	0.0484	4.5	0.58	484	15	425	19	119	106	407
BF4-seq2-b01	80162	244	90	0.56	75802	0.3102	2.0	4.6230	2.7	0.1081	1.9	0.72	1742	30	1753	23	1767	35	99
BF4-seq2-b02	6517	290	26	0.13	10623	0.0909	2.4	0.7870	3.7	0.0628	2.8	0.64	561	13	589	17	701	61	80
BF4-seq2-b03	23450	150	44	0.47	25751	0.2602	2.4	3.3407	3.1	0.0931	2.0	0.77	1491	32	1491	25	1491	38	100

BF4-seq2-b04	1774	98	12	0.19	2755	0.1225	2.5	0.8973	8.4	0.0531	8.0	0.29	745	17	650	41	334	182	223
BF4-seq2-b05	422	41	3	0.57	1045	0.0703	5.3	0.4190	34.8	0.0432	34.4	0.15	438	23	355	110	-155	855	-283
BF4-seq2-b06	9167	75	30	1.56	6839	0.2624	3.3	3.3329	4.7	0.0921	3.3	0.72	1502	45	1489	37	1470	62	102
BF4-seq2-b07	2413	88	7	0.59	867	0.0753	2.3	0.5763	6.2	0.0555	5.8	0.37	468	10	462	23	433	129	108
BF4-seq2-b08	3587	105	11	0.44	4239	0.0974	2.2	0.7488	5.7	0.0557	5.2	0.38	599	12	568	25	442	117	135
BF4-seq2-b09	5178	197	21	0.01	8529	0.1144	2.2	0.9825	4.2	0.0623	3.5	0.53	698	15	695	21	683	76	102
BF4-seq2-b10	31555	518	102	0.01	39900	0.2108	2.1	2.3425	2.6	0.0806	1.6	0.80	1233	24	1225	19	1212	31	102
BF4-seq2-b11	4335	335	27	1.05	8100	0.0625	2.2	0.4712	4.3	0.0547	3.7	0.52	391	9	392	14	400	82	98
BF4-seq2-b12	32926	195	52	0.04	34270	0.2769	1.4	3.7529	6.4	0.0983	6.3	0.22	1576	20	1583	53	1592	117	99
BF4-seq2-b13	84341	315	125	0.20	67706	0.3788	2.4	6.6581	2.7	0.1275	1.3	0.88	2071	42	2067	24	2063	23	100
BF4-seq2-b14	6322	159	30	0.63	9043	0.1658	1.8	1.6361	3.3	0.0716	2.8	0.54	989	16	984	21	973	56	102
BF4-seq2-b15	5010	276	22	0.70	8929	0.0648	3.7	0.5125	6.3	0.0574	5.1	0.59	404	15	420	22	507	112	80
BF4-seq2-b16	5957	88	15	0.37	8547	0.1652	2.1	1.6240	3.2	0.0713	2.4	0.66	986	19	980	20	966	50	102
BF4-seq2-b17	15305	404	35	0.06	22722	0.0910	3.0	0.7981	5.9	0.0636	5.1	0.51	561	16	596	27	730	107	77
BF4-seq2-b18	39343	258	64	0.19	38299	0.2387	2.3	3.4573	2.9	0.1050	1.8	0.78	1380	29	1518	23	1715	34	80
BF4-seq2-b19	2781	218	19	0.77	5052	0.0737	2.2	0.5691	4.8	0.0560	4.3	0.46	458	10	457	18	454	95	101
BF4-seq2-b20	1284	64	9	1.09	2461	0.1082	2.5	0.7925	6.3	0.0531	5.8	0.39	662	16	593	29	333	132	199
BF4-seq2-b21	24336	143	48	0.74	25123	0.2669	2.3	3.6429	2.9	0.0990	1.7	0.80	1525	31	1559	23	1605	32	95
BF4-seq2-b22	2657	120	11	0.56	5323	0.0809	2.3	0.5773	6.5	0.0518	6.1	0.35	501	11	463	24	275	139	182
BF4-seq2-b23	7108	121	14	0.29	11892	0.1102	2.7	0.9301	4.3	0.0612	3.3	0.64	674	18	668	21	646	71	104
BF4-seq2-b24	21727	75	37	0.67	16404	0.4070	2.4	7.6108	4.1	0.1356	3.4	0.58	2201	44	2186	38	2172	58	101
BF4-seq2-b25	10756	291	34	0.36	17728	0.1128	1.8	0.9654	2.6	0.0621	1.8	0.71	689	12	686	13	677	38	102
BF4-seq2-b26	9342	488	55	0.67	15824	0.0968	2.3	0.8055	3.3	0.0604	2.4	0.69	595	13	600	15	617	51	96
BF4-seq2-b27	1444	119	10	1.24	2746	0.0617	2.8	0.4606	9.2	0.0541	8.7	0.30	386	10	385	30	377	196	102
BF4-seq2-b28	6241	312	39	0.67	10569	0.1090	2.4	0.9076	3.0	0.0604	1.8	0.80	667	15	656	15	617	39	108
BF4-seq2-b29	403493	677	593	0.41	134065	0.6968	3.4	29.6301	3.9	0.3084	1.9	0.87	3408	92	3475	39	3513	30	97
BF4-seq2-b30	98470	1121	195	0.87	54421	0.1436	10.9	3.3712	13.8	0.1702	8.5	0.79	865	89	1498	114	2560	141	34
BF4-seq2-b31	3581	114	19	1.61	7084	0.1172	2.3	0.8341	6.2	0.0516	5.8	0.37	715	15	616	29	268	132	267
BF4-seq2-b32	29483	710	53	0.29	31826	0.0695	3.8	0.6053	4.6	0.0631	2.6	0.83	433	16	481	18	713	55	61
BF4-seq2-b33	28653	136	44	0.50	15929	0.2868	2.0	3.9032	2.7	0.0987	1.8	0.75	1626	29	1614	22	1600	33	102
BF4-seq2-b34	5451	337	20	0.07	10302	0.0635	3.1	0.4764	8.5	0.0544	7.9	0.37	397	12	396	28	388	178	102
BF4-seq2-b35	26490	159	72	0.52	20704	0.3987	1.9	7.1968	3.0	0.1309	2.2	0.66	2163	36	2136	27	2110	39	102
BF4-seq2-b36	44593	172	76	0.58	34068	0.3714	2.0	6.8603	2.5	0.1340	1.4	0.81	2036	35	2094	22	2150	25	95
BF4-seq2-b37	1474	157	10	0.27	2768	0.0666	2.2	0.5031	6.8	0.0548	6.5	0.32	416	9	414	23	403	145	103
BF4-seq2-b38	4097	238	26	1.50	7801	0.0865	2.7	0.6393	4.7	0.0536	3.9	0.57	535	14	502	19	354	87	151
BF4-seq2-b39	2979	98	11	0.59	5058	0.1013	2.6	0.8417	5.8	0.0603	5.2	0.44	622	15	620	27	614	112	101
BF4-seq2-b40	13460	192	56	0.42	14731	0.2676	1.6	3.4460	2.5	0.0934	2.0	0.63	1529	22	1515	20	1496	37	102
BF4-seq2-b41	14763	260	62	0.28	17499	0.2333	2.0	2.7643	2.7	0.0859	1.8	0.74	1352	25	1346	21	1337	35	101
BF4-seq2-b42	11001	155	44	0.19	10948	0.2870	2.4	4.0545	3.4	0.1025	2.4	0.71	1626	35	1645	28	1669	45	97
BF4-seq2-b43	5108	175	19	0.36	8634	0.1027	2.6	0.8557	5.0	0.0604	4.3	0.52	630	16	628	24	618	93	102
BF4-seq2-b44	22260	274	86	0.33	3756	0.2937	2.6	4.4390	3.3	0.1096	2.1	0.78	1660	38	1720	28	1793	37	93
BF4-seq2-b45	260	52	3	0.75	745	0.0476	4.5	0.2356	27.6	0.0359	27.2	0.16	300	13	215	55	-639	746	-47

BF4-seq2-b46	17006	124	45	0.79	16996	0.2923	2.0	4.1300	3.4	0.1025	2.7	0.59	1653	29	1660	28	1670	50	99
BF4-seq2-b47	24047	190	65	0.77	24596	0.2789	1.9	3.8447	2.5	0.1000	1.6	0.77	1586	27	1602	20	1624	29	98
BF4-seq2-b48	5747	226	25	0.47	9797	0.1009	2.4	0.8356	5.7	0.0601	5.1	0.43	620	14	617	27	606	111	102
BF4-seq2-b49	1541	60	9	1.60	2771	0.1044	3.1	0.8177	12.9	0.0568	12.5	0.24	640	19	607	61	485	277	132
BF4-seq2-b50	4452	258	20	0.69	8324	0.0667	2.2	0.5051	7.2	0.0549	6.8	0.31	416	9	415	25	410	152	101
BF4-seq2-b51	3394	401	24	0.11	6985	0.0626	3.3	0.4250	5.4	0.0493	4.3	0.61	391	13	360	17	161	101	243
BF4-seq2-b52	2051	182	14	0.61	3835	0.0688	2.0	0.5174	8.1	0.0546	7.9	0.25	429	8	423	29	394	177	109
BF4-seq2-b53	3808	209	29	0.63	6617	0.1261	2.0	1.0083	4.6	0.0580	4.2	0.44	766	15	708	24	529	91	145
BF4-seq2-b54	4163	284	19	0.61	1988	0.0596	2.3	0.4430	4.9	0.0540	4.4	0.47	373	8	372	15	369	98	101
BF4-seq2-b55	20755	90	40	0.38	15973	0.4020	2.7	7.3945	3.7	0.1334	2.5	0.74	2178	51	2160	34	2143	44	102
BF4-seq2-b56	3928	228	17	0.15	7759	0.0781	2.5	0.5643	6.3	0.0524	5.8	0.40	485	12	454	23	304	132	159
BF4-seq2-b57	66646	323	122	0.07	53131	0.3789	2.3	6.6887	2.8	0.1280	1.5	0.84	2071	41	2071	25	2071	26	100
BF4-seq2-b58	13781	130	52	0.50	11591	0.3511	2.5	5.8824	3.4	0.1215	2.3	0.73	1940	42	1959	30	1979	41	98
BF4-seq2-b59	2458	162	11	0.32	2968	0.0661	2.4	0.4878	4.7	0.0535	4.0	0.52	412	10	403	16	352	90	117
BF4-seq2-b60	1931	128	13	1.06	3913	0.0797	2.4	0.5437	9.8	0.0495	9.5	0.25	495	12	441	36	169	222	292
BF4-seq3-c01	4196	239	18	0.53	7857	0.0664	1.9	0.5032	3.5	0.0549	2.9	0.55	415	8	414	12	409	66	101
BF4-seq3-c02	4591	135	13	0.21	8686	0.0956	2.3	0.7109	4.6	0.0539	3.9	0.51	589	13	545	20	368	89	160
BF4-seq3-c03	23512	179	68	0.79	23198	0.3080	2.2	4.4257	3.0	0.1042	2.0	0.73	1731	33	1717	25	1701	37	102
BF4-seq3-c04	2109	205	17	0.42	3838	0.0782	2.5	0.6118	6.7	0.0567	6.2	0.37	485	12	485	26	481	137	101
BF4-seq3-c05	1537	121	16	1.33	3241	0.0942	2.8	0.6245	12.7	0.0481	12.4	0.22	580	16	493	51	103	293	565
BF4-seq3-c06	1640	90	10	1.18	2775	0.0777	2.9	0.6123	11.7	0.0571	11.4	0.24	483	13	485	46	497	251	97
BF4-seq3-c07	62559	136	94	0.66	31333	0.5466	2.6	15.4723	3.3	0.2053	2.0	0.79	2811	60	2845	32	2869	33	98
BF4-seq3-c08	2470	244	18	0.66	4706	0.0646	2.7	0.4862	4.5	0.0546	3.6	0.60	404	11	402	15	395	82	102
BF4-seq3-c09	2490	104	10	0.20	4718	0.0969	2.8	0.7228	5.3	0.0541	4.5	0.52	596	16	552	23	375	101	159
BF4-seq3-c10	32028	202	78	0.63	29905	0.3267	2.6	4.9580	3.3	0.1101	1.9	0.81	1822	42	1812	28	1801	34	101
BF4-seq3-c11	1903	144	15	0.66	2650	0.0895	3.0	0.7304	7.6	0.0592	7.0	0.39	552	16	557	33	574	151	96
BF4-seq3-c12	9766	296	29	0.44	17064	0.0887	2.2	0.7137	3.4	0.0584	2.6	0.66	548	12	547	14	543	56	101
BF4-seq3-c13	8732	222	30	0.19	13311	0.1342	2.4	1.2478	3.7	0.0674	2.9	0.63	812	18	822	21	850	61	95
BF4-seq3-c14	91	29	3	1.32	587	0.0840	3.7	0.1736	90.2	0.0150	90.1	0.04	520	18	163	145	-4165	5840	-12
BF4-seq3-c15	990	41	5	0.57	1790	0.1072	2.6	0.8316	10.8	0.0563	10.4	0.24	657	16	615	51	463	231	142
BF4-seq3-c16	2538	97	11	0.66	4326	0.0988	3.1	0.8197	5.4	0.0602	4.5	0.56	607	18	608	25	610	97	100
BF4-seq3-c17	6126	117	24	0.70	8719	0.1707	2.0	1.7009	3.1	0.0723	2.5	0.62	1016	18	1009	20	994	50	102
BF4-seq3-c18	6176	167	18	0.73	4879	0.0866	3.0	0.6930	5.8	0.0580	5.0	0.51	535	15	535	24	531	109	101
BF4-seq3-c19	3194	217	24	0.28	5646	0.1121	2.4	0.8963	5.6	0.0580	5.1	0.43	685	16	650	27	530	112	129
BF4-seq3-c20	2230	129	10	0.63	4106	0.0703	2.7	0.5416	5.2	0.0559	4.4	0.53	438	12	439	19	447	98	98
BF4-seq3-c21	5744	224	24	0.41	6009	0.1024	1.7	0.8548	3.9	0.0605	3.5	0.45	629	10	627	18	622	75	101
Sample 48/18-01 (BF2)			**Well no.: 48/18-1**				**Location (decimal degrees):**				**51.425**	**8.422678W**			**Datum:IRENET95**				
BF2-seq1-A01	2269	297	35	0.27	625	0.1102	1.7	0.9369	11.0	0.0617	10.9	0.15	674	11	671	56	662	233	102
BF2-seq1-A02	934	125	14	0.59	1602	0.0996	1.6	0.8374	5.2	0.0610	4.9	0.32	612	10	618	24	639	105	96
BF2-seq1-A03	387	71	6	0.95	725	0.0696	2.0	0.5426	9.4	0.0565	9.2	0.21	434	8	440	34	473	203	92
BF2-seq1-A04	3031	70	36	0.45	2315	0.4618	3.1	8.7149	4.9	0.1369	3.8	0.64	2447	64	2309	46	2188	66	112
BF2-seq1-A05	1452	330	34	0.68	2597	0.0875	2.0	0.6998	4.9	0.0580	4.5	0.41	541	10	539	21	529	98	102

BF2-seq1-A06	325	82	7	0.21	588	0.0884	5.2	0.7157	13.4	0.0587	12.4	0.39	546	27	548	58	557	270	98
BF2-seq1-A07	1880	366	40	0.28	3120	0.1082	1.7	0.9332	5.3	0.0626	5.1	0.31	662	10	669	26	694	108	95
BF2-seq1-A08	12262	296	123	0.22	10040	0.3960	1.7	7.0008	2.5	0.1282	1.8	0.68	2151	31	2112	22	2074	32	104
BF2-seq1-A09	5385	178	67	0.48	4936	0.3327	1.7	5.2471	3.3	0.1144	2.8	0.53	1851	28	1860	28	1870	50	99
BF2-seq1-A10	7505	364	111	0.38	8505	0.2865	1.7	3.6632	2.9	0.0927	2.4	0.58	1624	24	1563	23	1482	45	110
BF2-seq1-A11	498	100	8	0.47	923	0.0765	2.9	0.5965	8.0	0.0566	7.5	0.36	475	13	475	31	475	165	100
BF2-seq1-A12	327	103	9	0.65	598	0.0739	2.4	0.5754	9.4	0.0565	9.0	0.26	459	11	461	35	472	200	97
BF2-seq1-A13	794	269	29	0.42	1347	0.1008	1.9	0.8568	5.3	0.0617	4.9	0.36	619	11	628	25	663	106	93
BF2-seq1-A14	8754	190	117	0.27	4883	0.5554	2.3	14.5735	3.2	0.1903	2.2	0.72	2848	53	2788	31	2745	37	104
BF2-seq1-A15	1120	630	47	0.52	2076	0.0674	1.7	0.5220	5.0	0.0562	4.7	0.34	421	7	426	18	458	104	92
BF2-seq1-A16	689	137	18	0.57	1238	0.1164	2.3	0.9384	6.2	0.0585	5.8	0.37	710	16	672	31	547	126	130
BF2-seq1-A17	324	64	8	0.85	561	0.1027	2.8	0.8679	10.5	0.0613	10.1	0.27	630	17	634	51	648	218	97
BF2-seq1-A18	1851	395	33	0.55	530	0.0713	2.2	0.7762	11.4	0.0789	11.2	0.20	444	10	583	52	1171	221	38
BF2-seq1-A19	541	97	10	0.46	587	0.0830	3.4	1.1408	9.6	0.0997	9.0	0.35	514	17	773	54	1619	168	32
BF2-seq1-A20	290	106	7	0.67	567	0.0525	2.1	0.3868	14.2	0.0535	14.1	0.15	330	7	332	41	349	318	95
BF2-seq1-A21	686	132	9	0.19	1172	0.0997	2.0	0.8356	6.9	0.0608	6.7	0.28	613	11	617	33	632	144	97
BF2-seq1-A22	1368	175	26	1.39	2323	0.1034	1.9	0.8790	4.9	0.0617	4.5	0.39	634	12	640	24	662	97	96
BF2-seq1-A23	1902	43	17	0.73	1818	0.3260	1.8	4.9716	5.5	0.1106	5.2	0.32	1819	28	1815	48	1809	95	101
BF2-seq1-A24	923	191	19	0.15	1608	0.1008	1.9	0.8342	6.2	0.0600	5.9	0.31	619	11	616	29	605	128	102
BF2-seq1-A25	667	65	13	0.33	932	0.1922	1.7	2.0295	8.8	0.0766	8.6	0.19	1133	17	1125	62	1110	173	102
BF2-seq1-A26	249	43	5	0.33	326	0.1199	5.4	1.3071	23.2	0.0790	22.5	0.23	730	37	849	143	1173	446	62
BF2-seq1-A27	2601	58	28	0.62	2055	0.4163	1.1	7.6257	3.4	0.1329	3.2	0.32	2244	20	2188	31	2136	56	105
BF2-seq1-A28	3380	83	43	0.95	2693	0.4016	1.5	7.2882	3.5	0.1316	3.1	0.43	2177	28	2147	32	2120	55	103
BF2-seq1-A29	4004	812	72	0.13	580	0.0761	3.3	1.1771	5.7	0.1121	4.6	0.58	473	15	790	32	1834	84	26
BF2-seq1-A30	947	198	21	0.45	1651	0.0966	2.5	0.7980	5.2	0.0599	4.6	0.48	595	14	596	24	599	99	99
BF2-seq1-A31	3259	246	23	0.03	5722	0.0991	1.6	0.8151	3.5	0.0596	3.1	0.46	609	9	605	16	590	67	103
BF2-seq1-A32	650	79	12	0.01	994	0.1605	2.7	1.6039	9.0	0.0725	8.5	0.30	959	24	972	58	1000	173	96
BF2-seq1-A33	427	53	8	0.34	654	0.1413	1.8	1.3388	9.6	0.0687	9.4	0.19	852	15	863	57	890	194	96
BF2-seq1-A34	831	126	18	0.50	1304	0.1265	1.5	1.1645	6.0	0.0667	5.8	0.26	768	11	784	33	830	120	93
BF2-seq1-A35	187	40	4	0.45	339	0.0917	3.9	0.7379	11.9	0.0583	11.3	0.33	566	21	561	53	542	246	104
BF2-seq1-A36	417	82	10	0.64	710	0.1079	2.0	0.9257	8.6	0.0622	8.3	0.23	661	13	665	43	681	178	97
BF2-seq1-A37	995	105	14	0.10	1270	0.1279	3.1	1.4509	6.3	0.0823	5.5	0.49	776	23	910	39	1252	107	62
BF2-seq1-A38	1427	342	38	0.81	2550	0.0924	1.9	0.7497	5.3	0.0588	5.0	0.35	570	10	568	24	560	109	102
BF2-seq1-A39	828	144	20	0.84	1379	0.1124	1.7	0.9710	5.9	0.0627	5.6	0.29	687	11	689	30	697	120	99
BF2-seq1-A40	3662	218	60	0.64	1861	0.2109	4.4	3.5531	5.3	0.1222	3.0	0.83	1234	49	1539	43	1988	53	62
BF2-seq1-A41	154	43	5	0.71	288	0.0967	3.8	0.7554	20.0	0.0567	19.6	0.19	595	22	571	91	479	433	124
BF2-seq1-A42	660	230	17	0.44	1249	0.0670	1.6	0.5096	6.0	0.0552	5.8	0.26	418	6	418	21	419	130	100
BF2-seq1-A43	634	192	15	0.16	1081	0.0772	2.0	0.6519	7.5	0.0612	7.2	0.26	479	9	510	30	648	155	74
BF2-seq1-A44	1048	159	16	0.39	1863	0.0928	2.1	0.7557	5.0	0.0590	4.6	0.41	572	11	572	22	568	100	101
BF2-seq1-A45	16166	311	131	0.38	13757	0.3852	1.7	6.4806	2.5	0.1220	1.9	0.68	2101	31	2043	23	1986	33	106
BF2-seq1-A46	557	114	14	0.55	944	0.1061	2.0	0.9100	7.8	0.0622	7.5	0.26	650	12	657	38	682	161	95
BF2-seq1-A47	1051	343	24	0.29	1903	0.0693	2.0	0.5576	6.5	0.0583	6.2	0.30	432	8	450	24	542	136	80

BF2-seq1-A48	263	65	7	0.83	476	0.0946	2.9	0.7768	12.1	0.0595	11.8	0.24	583	16	584	55	587	255	99
BF2-seq1-A49	1269	104	25	0.54	1601	0.2128	2.4	2.4194	6.3	0.0824	5.8	0.38	1244	27	1248	46	1256	113	99
BF2-seq1-A50	1114	242	32	1.00	1924	0.1031	2.2	0.8609	4.9	0.0606	4.3	0.46	632	13	631	23	624	94	101
BF2-seq1-A51	184	47	6	0.90	365	0.1048	2.9	0.7753	11.9	0.0536	11.6	0.24	643	18	583	54	356	261	180
BF2-seq1-A52	4893	157	52	0.25	3858	0.3087	2.1	5.6588	3.2	0.1329	2.5	0.64	1735	31	1925	28	2137	43	81
BF2-seq1-A53	188	30	2	0.33	265	0.0737	5.4	0.7405	22.2	0.0729	21.6	0.24	458	24	563	101	1011	437	45
BF2-seq1-A54	576	77	9	0.61	966	0.1049	2.8	0.9034	7.6	0.0625	7.1	0.37	643	17	654	38	691	152	93
BF2-seq1-A55	1330	192	24	0.79	2307	0.1036	2.1	0.8642	4.4	0.0605	3.9	0.48	635	13	632	21	622	84	102
BF2-seq1-A56	1368	307	21	0.15	2551	0.0713	2.7	0.5524	5.8	0.0562	5.1	0.47	444	12	447	21	461	113	96
BF2-seq1-A57	1113	163	18	0.47	1936	0.0981	1.6	0.8133	4.9	0.0602	4.7	0.32	603	9	604	23	609	101	99
BF2-seq1-A58	363	59	7	0.97	639	0.0977	1.7	0.8105	11.4	0.0602	11.2	0.15	601	10	603	53	610	242	98
BF2-seq1-A59	1281	181	21	0.38	2138	0.1092	2.7	0.9441	6.0	0.0627	5.4	0.45	668	17	675	30	697	114	96
BF2-seq1-A60	366	56	6	0.29	644	0.0994	1.7	0.8226	9.0	0.0600	8.9	0.19	611	10	610	42	603	192	101
BF2-seq2-B01	783	186	13	0.37	1481	0.0651	2.4	0.4967	5.7	0.0553	5.1	0.43	407	10	409	19	425	115	96
BF2-seq2-B02	3096	208	35	0.14	4457	0.1734	2.1	1.7499	4.1	0.0732	3.5	0.52	1031	20	1027	27	1019	70	101
BF2-seq2-B03	1125	172	18	0.53	1973	0.0954	1.7	0.7868	4.3	0.0598	4.0	0.39	588	9	589	19	596	86	99
BF2-seq2-B04	339	41	6	0.12	509	0.1617	3.2	1.5839	9.1	0.0710	8.6	0.35	966	29	964	59	959	175	101
BF2-seq2-B05	2169	272	34	0.12	3340	0.1284	3.8	1.1980	5.2	0.0677	3.6	0.72	779	28	800	29	859	75	91
BF2-seq2-B06	747	240	17	0.16	1372	0.0727	2.6	0.5642	9.4	0.0563	9.0	0.27	452	11	454	35	464	201	98
BF2-seq2-B07	695	144	13	0.47	981	0.0819	2.2	0.8492	8.2	0.0752	7.9	0.27	507	11	624	39	1074	159	47
BF2-seq2-B08	2836	147	34	0.56	3772	0.2013	2.2	2.1965	4.4	0.0791	3.8	0.49	1182	23	1180	31	1175	76	101
BF2-seq2-B09	300	107	11	0.35	514	0.1035	2.3	0.8724	11.6	0.0612	11.3	0.20	635	14	637	56	645	244	98
BF2-seq2-B10	224	74	8	0.52	395	0.1027	3.7	0.8675	12.3	0.0613	11.7	0.30	630	22	634	60	649	252	97
BF2-seq2-B11	198	72	8	0.76	347	0.0958	3.1	0.7869	11.8	0.0596	11.4	0.27	590	18	589	54	588	247	100
BF2-seq2-B12	715	100	13	0.66	1262	0.1126	2.8	0.9197	8.3	0.0593	7.8	0.34	688	18	662	41	576	170	119
BF2-seq2-B13	3110	431	87	0.14	3752	0.2044	2.1	2.4481	4.3	0.0868	3.8	0.49	1199	23	1257	32	1357	72	88
BF2-seq2-B14	3460	259	49	1.05	73	0.1324	3.1	4.2890	12.6	0.2350	12.2	0.24	801	23	1691	109	3087	195	26
BF2-seq2-B15	306	96	9	0.97	565	0.0727	3.2	0.5800	10.5	0.0578	10.0	0.30	453	14	464	40	524	220	86
BF2-seq2-B16	7553	154	77	0.33	252	0.4317	6.8	8.6949	8.9	0.1461	5.7	0.77	2313	134	2307	85	2301	98	101
BF2-seq2-B17	749	184	15	0.63	1193	0.0755	5.5	0.6530	11.0	0.0627	9.5	0.50	469	25	510	45	699	203	67
BF2-seq2-B18	2722	81	31	0.29	2225	0.3551	2.0	6.2657	5.4	0.1280	5.1	0.37	1959	34	2014	49	2070	89	95
BF2-seq2-B19	1181	453	26	0.12	2288	0.0612	1.7	0.4567	4.2	0.0541	3.8	0.41	383	6	382	13	375	86	102
BF2-seq2-B20	416	58	7	0.59	728	0.0990	3.2	0.8145	7.7	0.0597	7.0	0.41	609	19	605	36	591	153	103
BF2-seq2-B21	582	125	15	0.83	996	0.1004	1.5	0.8474	7.9	0.0612	7.7	0.20	617	9	623	37	646	166	96
BF2-seq2-B22	1680	82	26	0.75	1748	0.2702	2.1	3.7536	4.9	0.1008	4.4	0.43	1542	29	1583	40	1638	81	94
BF2-seq2-B23	1323	189	20	0.48	2293	0.0960	2.6	0.7969	5.4	0.0602	4.7	0.48	591	15	595	25	612	102	97
BF2-seq2-B24	7658	1533	76	0.29	524	0.0466	5.2	0.5790	6.7	0.0901	4.3	0.77	293	15	464	25	1429	81	21
BF2-seq2-B25	70375	390	311	0.36	6913	0.6800	1.6	23.1029	2.3	0.2464	1.7	0.70	3344	43	3231	23	3162	26	106
BF2-seq2-B26	337	72	8	0.59	577	0.1029	3.2	0.8685	11.3	0.0612	10.9	0.28	631	19	635	55	647	234	98
BF2-seq2-B27	976	239	23	0.55	1723	0.0883	2.1	0.7161	5.6	0.0588	5.1	0.38	546	11	548	24	560	112	97
BF2-seq2-B28	709	153	17	0.50	1238	0.0993	2.7	0.8220	7.0	0.0600	6.4	0.39	610	16	609	33	604	140	101
BF2-seq2-B29	1289	253	28	0.51	2194	0.1008	2.1	0.8562	5.2	0.0616	4.8	0.40	619	12	628	25	660	103	94

BF2-seq2-B30	2868	222	46	0.20	3792	0.2051	1.8	2.2464	3.6	0.0795	3.2	0.49	1202	20	1196	26	1183	62	102
BF2-seq2-B31	423	96	12	1.12	747	0.0934	1.6	0.7632	8.0	0.0593	7.9	0.19	575	9	576	36	577	171	100
BF2-seq2-B32	425	161	11	0.75	803	0.0547	2.5	0.4056	12.6	0.0538	12.4	0.19	343	8	346	38	361	279	95
BF2-seq2-B33	580	90	13	0.48	934	0.1290	2.1	1.1603	6.3	0.0652	6.0	0.33	782	16	782	35	782	126	100
BF2-seq2-B34	1223	402	29	0.34	2293	0.0701	1.7	0.5424	4.6	0.0561	4.3	0.37	437	7	440	16	456	94	96
BF2-seq2-B35	494	24	6	0.63	507	0.2172	6.2	3.0652	9.6	0.1024	7.4	0.64	1267	72	1424	77	1667	137	76
BF2-seq2-B36	381	133	10	0.39	750	0.0687	2.2	0.5249	8.1	0.0554	7.8	0.27	428	9	428	29	430	174	99
BF2-seq2-B37	299	109	12	0.36	524	0.1067	4.5	0.9223	19.2	0.0627	18.6	0.23	654	28	664	98	698	397	94
BF2-seq2-B38	5232	133	56	0.35	3486	0.3832	1.7	6.9095	3.0	0.1308	2.5	0.56	2091	30	2100	27	2108	43	99
BF2-seq2-B39	736	98	13	1.05	1279	0.1003	2.1	0.8391	7.4	0.0607	7.1	0.29	616	13	619	35	627	153	98
BF2-seq2-B40	769	311	18	0.12	1475	0.0618	2.8	0.4669	7.9	0.0548	7.4	0.36	386	11	389	26	404	165	96
BF2-seq2-B41	1853	362	48	0.14	2937	0.1357	2.1	1.2296	4.7	0.0657	4.2	0.45	820	16	814	26	797	87	103
BF2-seq2-B42	1645	325	35	0.42	2750	0.1010	1.4	0.8818	4.5	0.0633	4.2	0.31	620	8	642	21	719	90	86
BF2-seq2-B44	29793	304	208	0.20	14894	0.6180	1.5	17.9595	2.1	0.2108	1.5	0.70	3102	36	2988	21	2911	25	107
BF2-seq2-B45	475	124	12	0.90	476	0.0816	2.8	1.1607	17.5	0.1032	17.2	0.16	506	14	782	100	1682	318	30
BF2-seq2-B46	656	242	15	0.09	1264	0.0641	1.6	0.4828	6.6	0.0547	6.4	0.24	400	6	400	22	398	143	101
BF2-seq2-B47	1344	301	27	0.18	2326	0.0926	1.5	0.7733	5.4	0.0606	5.2	0.28	571	8	582	24	625	113	91
BF2-seq2-B48	567	169	13	0.18	1036	0.0798	2.1	0.6388	7.4	0.0580	7.1	0.28	495	10	502	30	531	155	93
BF2-seq2-B49	760	176	20	1.03	1089	0.0914	1.8	0.7585	5.9	0.0602	5.6	0.30	564	10	573	26	611	122	92
BF2-seq2-B50	3894	104	42	0.76	3133	0.3224	3.3	5.7363	4.4	0.1290	3.0	0.73	1801	52	1937	39	2085	53	86
BF2-seq3-C01	440	47	6	0.55	686	0.1020	3.0	0.9596	9.2	0.0682	8.6	0.33	626	18	683	47	875	179	72
BF2-seq3-C02	930	103	17	0.33	1390	0.1542	2.8	1.4873	6.3	0.0699	5.7	0.44	925	24	925	39	927	116	100
BF2-seq3-C03	727	144	15	0.52	1234	0.0916	3.1	0.7563	6.4	0.0599	5.6	0.48	565	17	572	29	599	122	94
BF2-seq3-C04	1102	129	14	0.38	1870	0.1041	2.7	0.8787	5.1	0.0612	4.3	0.53	638	16	640	25	647	93	99
BF2-seq3-C05	7306	175	75	0.50	6042	0.3714	2.5	6.4951	3.8	0.1268	2.8	0.67	2036	44	2045	34	2054	49	99
BF2-seq3-C06	635	187	14	0.34	679	0.0730	4.3	0.5656	11.3	0.0562	10.5	0.38	454	19	455	42	461	232	98
BF2-seq3-C07	10600	226	102	0.36	8128	0.4050	2.4	7.6053	3.1	0.1362	1.9	0.77	2192	44	2185	28	2179	34	101
BF2-seq3-C08	2189	549	65	0.15	3346	0.1202	3.2	1.1316	6.0	0.0683	5.0	0.54	732	22	769	33	876	104	84
BF2-seq3-C09	258	49	6	0.69	443	0.1059	3.5	0.8877	12.1	0.0608	11.6	0.29	649	22	645	60	632	250	103
BF2-seq3-C10	294	53	5	0.12	467	0.0928	3.9	0.8332	11.2	0.0651	10.5	0.35	572	21	615	53	777	221	74
BF2-seq3-C11	2558	429	56	0.66	1661	0.1111	2.4	1.0662	4.7	0.0696	4.0	0.52	679	16	737	25	916	82	74
BF2-seq3-C12	1954	255	37	0.46	3037	0.1291	3.3	1.1732	5.5	0.0659	4.4	0.60	783	24	788	31	803	92	97
BF2-seq3-C13	1737	363	38	0.52	2953	0.0921	2.7	0.7823	4.5	0.0616	3.5	0.61	568	15	587	20	660	76	86
BF2-seq3-C14	433	142	12	0.67	802	0.0699	3.2	0.5413	6.9	0.0561	6.1	0.46	436	13	439	25	458	136	95
BF2-seq3-C15	593	64	11	0.39	880	0.1585	2.8	1.5432	6.9	0.0706	6.3	0.41	948	25	948	43	947	129	100
BF2-seq3-C16	397	131	10	0.44	759	0.0677	3.1	0.5180	8.1	0.0555	7.5	0.38	422	13	424	29	433	168	97
BF2-seq3-C17	441	133	17	0.64	663	0.1085	3.8	1.0450	11.0	0.0699	10.3	0.35	664	24	726	59	924	212	72
BF2-seq3-C18	1016	187	18	0.51	1961	0.0868	2.9	0.6326	6.3	0.0528	5.6	0.46	537	15	498	25	321	127	167
BF2-seq3-C19	2928	78	36	0.58	2317	0.3916	3.0	7.1137	4.7	0.1317	3.6	0.64	2130	55	2126	43	2121	64	100
BF2-seq3-C20	547	116	14	0.62	953	0.1025	3.4	0.8494	6.8	0.0601	5.9	0.50	629	21	624	32	607	128	104
BF2-seq3-C21	1094	127	25	0.80	1613	0.1603	2.7	1.5731	5.8	0.0712	5.2	0.46	958	24	960	37	963	105	100

Sample 49/09-2 (BF1) **Well no.: 49/09-2** **Location (decimal degrees):** **51.683 7.346094W** **Datum:IRENET95**

BF1-seq1-a01	9840	23	9	0.56	8808	0.3432	1.7	5.3896	11.4	0.1139	11.3	0.15	1902	29	1883	103	1863	204	102
BF1-seq1-a02	6184	40	8	0.28	3184	0.1860	2.5	1.8890	3.8	0.0737	2.9	0.66	1100	26	1077	26	1032	58	107
BF1-seq1-a03	5231	115	10	0.40	7380	0.0816	2.3	0.6267	12.4	0.0557	12.1	0.19	505	11	494	50	442	270	114
BF1-seq1-a04	3614	77	7	0.45	3883	0.0779	2.2	0.5694	4.2	0.0530	3.6	0.51	484	10	458	16	330	82	147
BF1-seq1-a05	2009	42	4	0.66	3660	0.0744	2.0	0.5722	6.3	0.0558	6.0	0.32	462	9	459	24	444	133	104
BF1-seq1-a06	10384	228	18	0.39	19030	0.0714	1.9	0.5452	3.0	0.0554	2.3	0.65	444	8	442	11	428	51	104
BF1-seq1-a07	7797	156	13	0.37	10165	0.0786	1.5	0.6130	3.2	0.0566	2.8	0.48	488	7	485	12	474	62	103
BF1-seq1-a08	3099	45	4	0.30	5362	0.0939	2.0	0.7587	4.4	0.0586	4.0	0.44	579	11	573	20	552	87	105
BF1-seq1-a09	2633	12	3	0.37	3328	0.2316	4.0	2.5455	6.7	0.0797	5.4	0.59	1343	48	1285	50	1190	106	113
BF1-seq1-a10	3294	15	4	0.62	4139	0.2379	2.3	2.6671	8.5	0.0813	8.2	0.26	1376	28	1319	65	1229	162	112
BF1-seq1-a11	11984	75	14	0.19	16012	0.1852	2.1	1.9389	3.2	0.0759	2.4	0.66	1096	21	1095	22	1093	49	100
BF1-seq1-a12	11636	264	23	0.47	21550	0.0757	1.7	0.5721	2.6	0.0548	1.9	0.66	470	8	459	10	405	43	116
BF1-seq1-a13	4906	68	8	0.34	8337	0.1084	2.1	0.8903	4.0	0.0595	3.4	0.52	664	13	647	19	587	74	113
BF1-seq1-a14	36163	83	34	0.49	32939	0.3452	1.8	5.3334	2.5	0.1120	1.7	0.72	1912	30	1874	22	1833	32	104
BF1-seq1-a15	8347	59	10	0.22	11808	0.1694	1.9	1.6700	3.1	0.0715	2.5	0.61	1009	18	997	20	971	50	104
BF1-seq1-a16	3294	19	4	0.48	4537	0.1940	2.6	1.9537	6.1	0.0730	5.6	0.42	1143	27	1100	42	1015	113	113
BF1-seq1-a17	6466	22	8	0.77	7206	0.2861	1.9	3.5921	3.3	0.0910	2.6	0.59	1622	28	1548	26	1448	50	112
BF1-seq1-a18	23909	98	25	0.15	27229	0.2512	2.2	3.0834	2.9	0.0890	1.8	0.77	1444	29	1429	22	1405	35	103
BF1-seq1-a19	8354	51	10	0.31	11322	0.1870	2.3	1.9429	3.3	0.0753	2.4	0.69	1105	24	1096	23	1078	48	103
BF1-seq1-a20	12757	150	19	0.35	20572	0.1195	1.3	1.0343	2.0	0.0628	1.5	0.66	727	9	721	10	701	32	104
BF1-seq1-a21	7482	49	11	0.47	10510	0.2023	1.6	2.0142	3.1	0.0722	2.7	0.52	1188	18	1120	21	992	54	120
BF1-seq1-a22	3344	78	6	0.42	6586	0.0738	2.3	0.5256	6.0	0.0517	5.6	0.38	459	10	429	21	271	128	169
BF1-seq1-a23	60144	174	66	0.66	58800	0.3139	1.9	4.4947	2.3	0.1039	1.3	0.83	1760	29	1730	19	1694	23	104
BF1-seq1-a24	2549	50	5	0.53	4539	0.0826	1.6	0.6435	4.1	0.0565	3.7	0.39	511	8	504	16	473	83	108
BF1-seq1-a25	12099	54	14	0.38	14403	0.2346	2.1	2.7528	2.8	0.0851	1.8	0.75	1359	25	1343	21	1318	36	103
BF1-seq1-a26	31542	179	35	0.13	39594	0.1920	1.4	2.1400	2.1	0.0809	1.5	0.69	1132	15	1162	15	1218	30	93
BF1-seq1-a27	65676	219	62	0.22	63583	0.2715	2.2	3.9215	2.6	0.1048	1.3	0.87	1548	31	1618	21	1710	24	91
BF1-seq1-a28	10109	77	13	0.24	14374	0.1630	1.4	1.5935	2.3	0.0709	1.9	0.59	974	12	968	15	954	39	102
BF1-seq1-a29	2632	16	3	0.36	818	0.1919	3.1	2.0882	23.8	0.0789	23.6	0.13	1132	32	1145	178	1170	467	97
BF1-seq1-a30	91873	353	100	0.54	3825	0.2219	3.6	2.9587	3.8	0.0967	1.5	0.92	1292	42	1397	30	1561	27	83
BF1-seq1-a31	1313	8	2	0.77	1799	0.2135	1.7	2.1959	5.8	0.0746	5.6	0.29	1248	19	1180	42	1057	112	118
BF1-seq1-a32	8864	42	11	0.44	10918	0.2348	2.3	2.6652	3.8	0.0823	3.1	0.60	1359	28	1319	29	1254	60	108
BF1-seq1-a33	13224	87	18	0.30	17781	0.1980	2.2	2.0142	3.0	0.0738	2.1	0.73	1164	24	1120	21	1036	42	112
BF1-seq1-a34	31278	110	35	0.47	33048	0.2779	2.1	3.6075	2.7	0.0941	1.7	0.77	1581	30	1551	22	1511	33	105
BF1-seq1-a35	369	3	1	0.18	571	0.1760	8.2	1.6321	35.3	0.0673	34.4	0.23	1045	80	983	251	846	715	124
BF1-seq1-a36	18310	16	11	0.73	10068	0.5597	1.7	14.3855	2.5	0.1864	1.8	0.70	2865	40	2775	24	2711	29	106
BF1-seq1-a37	17563	113	22	0.21	23410	0.1889	2.1	1.9860	3.2	0.0762	2.4	0.65	1116	21	1111	22	1101	49	101
BF1-seq1-a38	378	7	1	0.43	654	0.0905	3.1	0.7280	16.0	0.0583	15.8	0.19	558	16	555	71	543	344	103
BF1-seq1-a39	8394	797	19	0.59	17432	0.0201	2.4	0.1348	4.0	0.0487	3.2	0.60	128	3	128	5	131	75	98
BF1-seq1-a40	65894	287	76	0.32	76129	0.2446	1.8	2.9602	2.4	0.0878	1.6	0.74	1411	23	1397	19	1377	31	102
BF1-seq1-a41	8243	54	12	0.50	11189	0.1960	1.3	2.0187	2.9	0.0747	2.6	0.45	1154	14	1122	20	1061	52	109
BF1-seq1-a42	7540	51	12	0.67	10559	0.1973	1.5	1.9667	2.5	0.0723	2.0	0.60	1161	16	1104	17	994	41	117

BF1-seq1-a43	11400	27	23	3.51	10315	0.3529	1.4	5.4414	2.8	0.1118	2.5	0.50	1948	24	1891	25	1829	45	107
BF1-seq1-a44	19283	57	20	0.45	19556	0.2995	1.5	4.1360	2.3	0.1002	1.8	0.63	1689	22	1661	19	1627	33	104
BF1-seq1-a45	36280	106	39	0.33	35016	0.3338	3.7	4.8376	4.0	0.1051	1.3	0.94	1857	60	1791	34	1716	25	108
BF1-seq1-a46	8823	39	10	0.29	10237	0.2446	1.7	2.9527	3.2	0.0876	2.7	0.52	1410	21	1396	24	1373	52	103
BF1-seq1-a47	8406	131	16	0.71	13938	0.0954	2.9	0.7865	3.8	0.0598	2.6	0.74	587	16	589	17	597	56	98
BF1-seq1-a48	42832	126	42	0.15	41943	0.3269	2.0	4.6491	2.4	0.1032	1.4	0.81	1823	31	1758	20	1682	26	108
BF1-seq1-a49	187150	174	121	0.50	5110	0.5616	1.9	14.3033	2.1	0.1847	0.9	0.91	2873	45	2770	21	2696	15	107
BF1-seq1-a50	32631	215	43	0.20	18726	0.1945	1.8	2.0478	2.4	0.0764	1.6	0.75	1146	19	1132	17	1105	32	104
BF1-seq1-a51	11459	53	17	0.83	8781	0.2322	3.0	2.6380	4.0	0.0824	2.5	0.77	1346	37	1311	30	1255	49	107
BF1-seq1-a52	11908	89	18	0.73	16592	0.1670	1.9	1.6626	2.6	0.0722	1.7	0.74	995	18	994	17	992	35	100
BF1-seq1-a53	22949	69	26	0.46	22797	0.3301	1.6	4.6498	2.4	0.1022	1.8	0.67	1839	26	1758	20	1664	33	111
BF1-seq1-a54	46048	74	40	0.86	34019	0.3999	1.4	7.5738	2.0	0.1373	1.4	0.71	2169	26	2182	18	2194	24	99
BF1-seq1-a55	5890	81	11	0.64	3254	0.1079	3.3	0.9263	5.7	0.0622	4.7	0.57	661	21	666	28	682	101	97
BF1-seq1-a56	6765	56	12	0.72	10241	0.1767	1.9	1.6318	3.5	0.0670	2.9	0.54	1049	18	983	22	837	60	125
BF1-seq1-a57	3336	78	7	0.45	6190	0.0778	2.8	0.5880	5.2	0.0548	4.4	0.53	483	13	470	20	404	99	120
BF1-seq1-a58	37999	258	51	0.22	50728	0.1899	1.5	1.9906	2.5	0.0760	2.0	0.60	1121	16	1112	17	1096	41	102
BF1-seq1-a59	18795	55	22	0.67	18483	0.3244	2.6	4.6138	3.1	0.1031	1.6	0.84	1811	41	1752	26	1681	30	108
BF1-seq1-a60	61273	65	38	0.35	34299	0.4985	1.8	12.4726	2.4	0.1815	1.6	0.75	2608	38	2641	23	2666	26	98
BF1-seq2-b01	36273	153	42	0.34	41191	0.2532	1.5	3.1179	2.0	0.0893	1.3	0.76	1455	20	1437	15	1411	25	103
BF1-seq2-b02	27536	163	33	0.09	34610	0.2073	1.9	2.3075	2.7	0.0807	1.8	0.73	1214	21	1215	19	1215	36	100
BF1-seq2-b03	21629	114	27	0.31	26482	0.2232	1.2	2.5483	2.0	0.0828	1.6	0.59	1299	14	1286	15	1265	31	103
BF1-seq2-b04	4427	100	11	1.03	7970	0.0768	1.7	0.5971	3.9	0.0564	3.6	0.44	477	8	475	15	468	79	102
BF1-seq2-b05	65601	178	62	0.24	61166	0.3323	1.4	4.9505	2.0	0.1081	1.4	0.72	1849	23	1811	17	1767	25	105
BF1-seq2-b06	57576	158	54	0.21	53203	0.3291	2.4	4.8957	3.1	0.1079	1.9	0.77	1834	38	1802	26	1764	35	104
BF1-seq2-b07	74120	180	70	0.48	981	0.3237	3.6	4.8797	3.9	0.1093	1.6	0.91	1808	57	1799	34	1788	30	101
BF1-seq2-b08	119010	139	85	0.49	71529	0.5078	2.2	11.7728	3.1	0.1682	2.3	0.69	2647	47	2587	30	2539	38	104
BF1-seq2-b09	7262	165	14	0.58	13245	0.0723	2.2	0.5519	3.6	0.0554	2.9	0.59	450	9	446	13	428	65	105
BF1-seq2-b10	20032	62	25	0.86	9364	0.3077	1.5	4.3289	2.5	0.1020	2.1	0.58	1729	23	1699	21	1661	38	104
BF1-seq2-b11	21086	100	27	0.26	25404	0.2587	1.3	3.0035	2.1	0.0842	1.7	0.60	1483	17	1409	16	1297	33	114
BF1-seq2-b12	86789	338	99	0.25	3434	0.2837	4.0	3.9656	4.4	0.1014	1.8	0.91	1610	58	1627	37	1649	34	98
BF1-seq2-b13	3365	24	6	0.51	5048	0.2038	2.2	1.9448	5.1	0.0692	4.6	0.43	1196	24	1097	35	905	94	132
BF1-seq2-b14	23174	83	28	0.53	23850	0.2863	1.8	3.8887	3.4	0.0985	2.9	0.53	1623	25	1611	27	1596	53	102
BF1-seq2-b15	27079	150	37	0.37	7550	0.2214	1.9	2.4753	3.1	0.0811	2.5	0.60	1289	22	1265	23	1223	50	105
BF1-seq2-b16	22835	83	24	0.31	24674	0.2674	2.1	3.4613	3.0	0.0939	2.2	0.69	1528	29	1518	24	1506	42	101
BF1-seq2-b17	17466	119	22	0.13	15580	0.1922	1.8	2.0230	2.7	0.0764	2.0	0.67	1133	19	1123	19	1104	40	103
BF1-seq2-b18	2559	19	4	0.42	3503	0.1778	2.0	1.8225	4.8	0.0743	4.3	0.43	1055	20	1054	32	1050	87	100
BF1-seq2-b19	288323	281	160	0.14	7401	0.5215	2.7	13.6984	3.1	0.1905	1.6	0.87	2706	61	2729	30	2747	26	99
BF1-seq2-b20	-	-	-	-	-	-	-	-	-	-	-	-	-	-	-	-	-	-	-
BF1-seq2-b21	4169	22	6	0.78	4875	0.2350	3.1	2.7389	5.9	0.0845	5.1	0.51	1361	38	1339	45	1305	99	104
BF1-seq2-b22	1085	22	2	0.55	1510	0.0637	4.7	0.6440	19.7	0.0733	19.1	0.24	398	18	505	81	1023	386	39
BF1-seq2-b23	9935	32	13	0.79	10184	0.3209	2.2	4.3853	3.2	0.0991	2.3	0.68	1794	34	1710	27	1608	44	112
BF1-seq2-b24	12544	104	23	1.01	17809	0.1710	1.7	1.6845	2.4	0.0714	1.8	0.69	1018	16	1003	16	970	36	105

BF1-seq2-b25	30568	79	43	0.38	17070	0.5056	1.4	11.3731	4.4	0.1631	4.2	0.32	2638	31	2554	42	2488	71	106
BF1-seq2-b26	6442	46	9	0.23	3579	0.1901	1.1	1.9517	2.5	0.0745	2.3	0.42	1122	11	1099	17	1054	46	106
BF1-seq2-b27	4828	31	8	0.70	6469	0.2139	1.9	2.2447	3.3	0.0761	2.7	0.57	1249	21	1195	23	1098	54	114
BF1-seq2-b28	34132	109	40	0.59	33272	0.3087	1.8	4.4180	2.5	0.1038	1.7	0.73	1734	28	1716	21	1693	32	102
BF1-seq2-b29	8590	60	14	0.55	11764	0.1996	2.8	2.0407	3.7	0.0742	2.3	0.77	1173	30	1129	25	1046	47	112
BF1-seq2-b30	28536	102	34	0.24	28209	0.3175	2.8	4.4034	3.2	0.1006	1.6	0.86	1778	43	1713	27	1635	30	109
BF1-seq2-b31	13654	50	15	0.29	14602	0.2817	2.1	3.6800	2.9	0.0948	2.0	0.73	1600	30	1567	24	1523	38	105
BF1-seq2-b32	93072	91	49	0.51	23419	0.4553	2.6	13.4585	2.9	0.2144	1.1	0.92	2419	54	2712	27	2939	18	82
BF1-seq2-b33	42544	38	26	0.48	21732	0.5567	1.7	15.2102	2.3	0.1982	1.6	0.71	2853	39	2828	23	2811	27	101
BF1-seq2-b34	4167	68	11	1.26	7323	0.1070	2.2	0.8517	3.8	0.0578	3.1	0.57	655	13	626	18	520	69	126
BF1-seq2-b35	6536	47	9	0.26	5488	0.1918	2.2	1.9870	3.7	0.0751	2.9	0.60	1131	23	1111	25	1072	59	106
BF1-seq2-b36	24949	189	36	0.15	31477	0.1929	1.6	1.9587	2.3	0.0736	1.7	0.70	1137	17	1101	16	1032	34	110
BF1-seq2-b37	41510	132	44	0.35	39879	0.3000	1.6	4.3716	2.6	0.1057	2.0	0.62	1691	24	1707	21	1726	37	98
BF1-seq2-b38	22264	69	24	0.37	3192	0.3149	1.8	4.4703	2.9	0.1030	2.3	0.62	1765	28	1725	24	1678	42	105
BF1-seq2-b39	74219	311	95	0.48	80547	0.2630	2.0	3.3934	2.4	0.0936	1.4	0.82	1505	27	1503	19	1500	27	100
BF1-seq2-b40	17354	19	12	0.57	10491	0.5183	2.0	12.0239	2.7	0.1682	1.8	0.74	2692	45	2606	26	2540	31	106
BF1-seq2-b41	15362	89	23	0.59	13025	0.2257	1.0	2.5573	2.0	0.0822	1.7	0.51	1312	12	1289	15	1250	34	105
BF1-seq2-b42	28741	30	18	0.25	16084	0.5177	2.7	12.9113	3.5	0.1809	2.2	0.77	2689	60	2673	34	2661	37	101
BF1-seq2-b43	83492	276	94	0.48	6409	0.2867	1.7	3.9801	2.2	0.1007	1.5	0.76	1625	24	1630	18	1637	27	99
BF1-seq2-b44	10124	247	23	0.54	18863	0.0785	1.1	0.5901	2.5	0.0545	2.2	0.45	487	5	471	9	392	50	124
BF1-seq2-b45	17294	72	23	0.54	18714	0.2784	1.5	3.6036	2.4	0.0939	1.8	0.64	1583	22	1550	19	1506	35	105
BF1-seq2-b46	21102	55	21	0.22	19036	0.3746	1.2	5.7820	2.0	0.1119	1.5	0.64	2051	22	1944	17	1831	28	112
BF1-seq2-b47	997	7	1	0.72	1655	0.1341	6.3	1.1335	16.4	0.0613	15.1	0.38	811	48	769	92	650	325	125
BF1-seq2-b48	22248	138	28	0.15	14709	0.2057	1.6	2.2642	2.1	0.0798	1.5	0.73	1206	17	1201	15	1193	29	101
BF1-seq2-b49	3809	83	6	0.24	1311	0.0734	2.8	0.5477	4.5	0.0541	3.6	0.61	457	12	443	16	376	81	121
BF1-seq2-b50	54041	200	72	0.59	56294	0.3021	2.0	4.0773	2.8	0.0979	1.9	0.72	1702	31	1650	23	1584	36	107
BF1-seq2-b51	115723	107	70	0.31	58275	0.5599	2.0	15.5729	2.3	0.2017	1.2	0.86	2866	46	2851	22	2840	19	101
BF1-seq2-b52	16094	46	17	0.41	15004	0.3206	1.8	4.8142	2.8	0.1089	2.2	0.63	1793	28	1787	24	1781	40	101
BF1-seq2-b53	4184	26	7	0.85	5476	0.2030	1.8	2.1736	3.6	0.0777	3.1	0.50	1191	20	1173	25	1138	62	105
BF1-seq2-b54	6723	7	5	1.01	4011	0.5585	2.6	13.0607	3.7	0.1696	2.6	0.71	2860	61	2684	36	2554	44	112
BF1-seq2-b55	85551	358	99	0.08	92774	0.2818	1.6	3.6348	2.0	0.0936	1.3	0.79	1600	23	1557	16	1499	24	107
BF1-seq2-b56	10146	66	13	0.18	13452	0.1921	2.3	2.0153	3.6	0.0761	2.8	0.63	1133	24	1121	25	1098	56	103
BF1-seq2-b57	141485	130	83	0.21	68621	0.5625	2.0	16.1139	2.6	0.2078	1.6	0.79	2877	47	2884	25	2888	26	100
BF1-seq2-b58	37130	96	33	0.09	33208	0.3417	1.5	5.3439	1.9	0.1134	1.2	0.76	1895	24	1876	17	1855	23	102
BF1-seq2-b59	22069	22	18	1.38	12098	0.5569	1.8	14.3563	2.3	0.1870	1.5	0.75	2854	41	2774	22	2716	25	105
BF1-seq2-b60	26240	215	55	1.38	2876	0.1744	1.2	1.7374	2.5	0.0722	2.2	0.47	1037	11	1022	16	993	44	104
BF1-seq3-c01	18312	75	22	0.27	20198	0.2820	1.4	3.5956	2.2	0.0925	1.7	0.65	1602	20	1549	17	1477	32	108
BF1-seq3-c02	35784	178	40	0.13	40147	0.2222	1.7	2.7905	2.8	0.0911	2.2	0.62	1293	20	1353	21	1449	42	89
BF1-seq3-c03	21084	47	20	0.37	17271	0.3712	1.6	6.3087	2.4	0.1233	1.7	0.67	2035	28	2020	21	2004	31	102
BF1-seq3-c04	5623	89	11	0.67	9276	0.1057	1.8	0.8971	3.8	0.0615	3.3	0.48	648	11	650	18	658	71	98
BF1-seq3-c05	7312	39	10	0.31	8713	0.2352	1.4	2.8250	4.4	0.0871	4.2	0.33	1362	18	1362	33	1363	80	100
BF1-seq3-c06	29512	93	33	0.43	28415	0.3142	1.7	4.5938	2.7	0.1060	2.1	0.63	1761	26	1748	23	1732	38	102

BF1-seq3-c07	4914	38	9	1.26	6913	0.1657	3.5	1.6472	4.9	0.0721	3.4	0.71	988	32	988	31	989	69	100
BF1-seq3-c08	13079	78	18	0.35	16826	0.2196	1.8	2.4095	2.7	0.0796	2.1	0.65	1280	21	1245	20	1187	41	108
BF1-seq3-c09	16778	159	28	0.35	24366	0.1640	1.4	1.5865	2.2	0.0702	1.7	0.64	979	13	965	14	934	35	105
BF1-seq3-c10	6466	48	10	0.47	4290	0.1869	1.9	1.9184	3.4	0.0744	2.9	0.54	1105	19	1087	23	1054	58	105
BF1-seq3-c11	11335	132	18	0.16	15351	0.1386	1.6	1.4377	2.6	0.0752	2.0	0.62	837	13	905	16	1075	41	78
BF1-seq3-c12	-	-	-	-	-	-	-	-	-	-	-	-	-	-	-	-	-	-	-
BF1-seq3-c13	53322	260	89	0.75	13640	0.2736	6.5	3.3376	8.6	0.0885	5.5	0.76	1559	91	1490	69	1393	106	112
BF1-seq3-c14	3413	25	5	0.53	4626	0.1830	2.5	1.8987	4.3	0.0753	3.5	0.57	1083	24	1081	29	1075	71	101
BF1-seq3-c15	9614	259	18	0.07	17997	0.0732	1.7	0.5521	3.2	0.0547	2.7	0.53	455	7	446	12	400	61	114
BF1-seq3-c16	20147	570	35	0.00	37834	0.0682	1.7	0.5103	2.4	0.0543	1.7	0.69	425	7	419	8	383	39	111
BF1-seq3-c17	13253	96	19	0.26	17670	0.1880	1.8	1.9821	2.7	0.0765	2.0	0.66	1110	18	1109	18	1108	40	100
BF1-seq3-c18	28318	536	47	0.03	24618	0.0936	0.9	0.7836	1.5	0.0607	1.2	0.59	577	5	588	7	630	26	92
BF1-seq3-c19	27579	525	46	0.03	21905	0.0942	1.1	0.7784	1.9	0.0599	1.5	0.60	580	6	585	8	601	33	97
BF1-seq3-c20	27743	533	46	0.03	47417	0.0926	1.2	0.7617	1.6	0.0597	1.0	0.76	571	7	575	7	591	22	97
Sample 56/26-2A (AK24)			**Well no.: 56/26-2A**				**Location (decimal degrees):**				**50.007**	**9.897846W**			**Datum:IRENET95**				
AK24-seq1-a01	13344	345	27	0.80	5970	0.0668	2.4	0.5087	5.0	0.0552	4.4	0.48	417	10	418	17	422	98	99
AK24-seq1-a02	137714	236	111	0.68	43482	0.3861	2.1	7.1976	2.4	0.1352	1.0	0.90	2105	38	2136	21	2167	18	97
AK24-seq1-a03	17192	589	29	0.23	17358	0.0488	2.3	0.3562	2.8	0.0529	1.6	0.82	307	7	309	7	324	36	95
AK24-seq1-a04	10402	146	16	0.34	17298	0.1048	2.0	0.8807	2.9	0.0610	2.0	0.71	642	13	641	14	638	43	101
AK24-seq1-a05	3581	37	5	0.81	6244	0.1201	3.1	0.9587	5.4	0.0579	4.4	0.58	731	22	683	27	525	96	139
AK24-seq1-a06	14848	203	25	0.57	24454	0.1076	2.3	0.9134	3.1	0.0616	2.1	0.73	659	14	659	15	660	45	100
AK24-seq1-a07	17031	26	12	0.25	12909	0.4320	2.5	7.9710	3.1	0.1338	1.8	0.82	2315	49	2228	28	2149	31	108
AK24-seq1-a08	1927	29	3	0.35	3419	0.1045	2.0	0.8062	5.0	0.0560	4.6	0.41	640	12	600	23	452	101	142
AK24-seq1-a09	7960	198	19	0.33	3966	0.0904	2.3	0.7332	3.9	0.0588	3.1	0.60	558	12	558	17	561	68	99
AK24-seq1-a10	14835	378	24	0.23	27532	0.0638	2.5	0.4810	2.9	0.0547	1.4	0.87	399	10	399	10	398	32	100
AK24-seq1-a11	14318	381	23	0.23	26485	0.0594	2.1	0.4433	3.1	0.0542	2.3	0.67	372	8	373	10	378	53	98
AK24-seq1-a12	10055	251	17	0.23	18503	0.0686	2.1	0.5236	3.7	0.0554	3.1	0.55	427	9	428	13	428	70	100
AK24-seq1-a13	10616	260	16	0.14	19581	0.0641	2.3	0.4842	3.1	0.0548	2.1	0.74	400	9	401	10	404	47	99
AK24-seq1-a14	7608	224	14	0.49	14372	0.0568	2.4	0.4205	3.1	0.0537	2.0	0.77	356	8	356	9	358	45	99
AK24-seq1-a15	87597	289	82	0.23	91141	0.2744	2.3	3.6906	2.7	0.0976	1.3	0.87	1563	32	1569	22	1578	25	99
AK24-seq1-a16	4221	304	18	0.37	8301	0.0565	2.6	0.4020	5.3	0.0516	4.6	0.48	354	9	343	16	268	107	132
AK24-seq1-a17	210601	401	142	0.05	160693	0.3543	1.9	6.4821	2.4	0.1327	1.5	0.78	1955	32	2043	22	2134	27	92
AK24-seq1-a18	1503	59	7	0.80	2812	0.1062	2.4	0.7896	6.1	0.0539	5.6	0.40	650	15	591	28	368	125	177
AK24-seq1-a19	6095	244	16	0.19	11329	0.0662	1.9	0.4995	3.6	0.0547	3.0	0.52	413	7	411	12	400	68	103
AK24-seq1-a20	48943	99	39	0.29	18215	0.3625	2.4	6.0337	2.6	0.1207	1.0	0.92	1994	42	1981	23	1967	18	101
AK24-seq1-a21	3367	64	7	0.56	6327	0.0958	2.9	0.8155	9.0	0.0617	8.6	0.32	590	16	606	42	665	184	89
AK24-seq1-a22	35599	64	33	0.94	27570	0.3880	2.2	6.9879	2.8	0.1306	1.6	0.81	2113	41	2110	25	2107	28	100
AK24-seq1-a23	61797	152	66	0.85	56380	0.3220	2.2	4.9378	2.4	0.1112	0.9	0.93	1799	35	1809	20	1820	16	99
AK24-seq1-a24	17519	296	33	0.71	29573	0.0923	2.2	0.7517	2.7	0.0591	1.5	0.82	569	12	569	12	569	33	100
AK24-seq1-a25	21307	595	33	0.09	39575	0.0583	2.6	0.4387	2.9	0.0546	1.3	0.89	365	9	369	9	396	30	92
AK24-seq1-a26	8262	64	11	0.31	12211	0.1715	2.2	1.6258	3.1	0.0688	2.2	0.70	1020	21	980	20	892	46	114
AK24-seq1-a27	58877	206	60	0.32	61689	0.2728	2.1	3.6150	2.5	0.0961	1.2	0.86	1555	29	1553	20	1550	23	100

AK24-seq1-a28	6749	124	15	0.95	12189	0.0950	2.1	0.8195	6.0	0.0626	5.6	0.34	585	12	608	28	694	120	84
AK24-seq1-a29	5945	250	29	0.54	2797	0.1070	2.3	0.8598	3.4	0.0583	2.5	0.67	655	14	630	16	540	55	121
AK24-seq1-a30	35205	81	30	0.40	31211	0.3350	2.3	5.2782	2.8	0.1143	1.6	0.81	1863	37	1865	24	1868	29	100
AK24-seq1-a31	2525	41	4	0.32	4599	0.1035	2.6	0.7891	4.2	0.0553	3.3	0.63	635	16	591	19	425	73	149
AK24-seq1-a32	4932	74	9	0.43	8710	0.1067	2.2	0.9080	7.2	0.0617	6.9	0.30	654	13	656	35	664	147	99
AK24-seq1-a33	5535	75	10	0.43	1291	0.1230	2.1	1.0139	3.1	0.0598	2.3	0.67	748	15	711	16	595	50	126
AK24-seq1-a34	3107	61	8	0.65	4979	0.1172	2.3	1.0215	4.2	0.0632	3.5	0.55	714	16	715	22	716	75	100
AK24-seq1-a35	52292	117	48	0.58	45784	0.3490	2.1	5.5771	2.7	0.1159	1.7	0.78	1930	36	1913	24	1894	31	102
AK24-seq1-a36	37799	1167	163	0.31	56663	0.1429	2.2	1.3332	2.9	0.0677	1.9	0.76	861	18	860	17	859	39	100
AK24-seq1-a37	7146	113	13	0.39	5913	0.1054	2.3	0.8448	3.6	0.0581	2.8	0.64	646	14	622	17	535	60	121
AK24-seq1-a38	157354	297	134	0.63	40838	0.4022	2.4	7.5569	2.8	0.1363	1.4	0.87	2179	45	2180	25	2180	24	100
AK24-seq1-a39	28202	90	26	0.21	29783	0.2767	1.9	3.6628	2.5	0.0960	1.6	0.76	1575	27	1563	20	1548	31	102
AK24-seq1-a40	17138	299	23	0.42	528	0.0671	3.1	0.5158	6.0	0.0558	5.1	0.52	419	13	422	21	443	114	95
AK24-seq1-a41	10749	48	13	0.68	3519	0.2313	2.0	2.7497	3.1	0.0862	2.3	0.66	1342	24	1342	23	1343	45	100
AK24-seq1-a42	12004	305	19	0.13	22886	0.0649	2.3	0.4753	3.1	0.0531	2.1	0.74	405	9	395	10	334	47	121
AK24-seq1-a43	4000	64	7	0.39	7127	0.1062	2.3	0.8326	3.8	0.0569	3.1	0.59	651	14	615	18	486	68	134
AK24-seq1-a44	11900	26	13	1.13	9740	0.3624	2.3	6.1168	3.1	0.1224	2.0	0.76	1993	40	1993	27	1992	35	100
AK24-seq1-a45	16199	86	18	0.26	11232	0.2025	2.4	2.2296	3.0	0.0799	1.8	0.80	1189	26	1190	21	1193	36	100
AK24-seq1-a46	53140	124	49	0.43	47593	0.3393	2.5	5.4192	2.9	0.1158	1.6	0.84	1883	40	1888	25	1893	29	99
AK24-seq1-a47	6072	75	11	0.55	10037	0.1264	2.2	1.0675	3.8	0.0613	3.1	0.58	767	16	738	20	648	66	118
AK24-seq1-a48	3908	65	7	0.47	7023	0.0982	2.3	0.7585	4.1	0.0560	3.4	0.56	604	13	573	18	454	75	133
AK24-seq1-a49	16337	58	20	0.85	17270	0.2696	2.1	3.5471	2.9	0.0954	1.9	0.74	1539	29	1538	23	1537	36	100
AK24-seq1-a50	2168	85	14	0.81	4155	0.1361	2.7	0.9751	9.9	0.0520	9.5	0.27	822	21	691	51	284	218	289
AK24-seq1-a51	14139	151	28	0.89	21321	0.1468	2.0	1.3574	2.8	0.0671	1.8	0.74	883	17	871	16	840	38	105
AK24-seq1-a52	2711	48	5	0.56	2158	0.0989	2.3	0.7571	5.3	0.0555	4.8	0.43	608	13	572	23	433	107	141
AK24-seq1-a53	31462	32	19	0.49	11822	0.4913	2.6	11.5850	3.0	0.1710	1.5	0.86	2576	55	2571	29	2568	25	100
AK24-seq1-a54	2669	46	5	0.31	4936	0.1010	2.5	0.8457	9.8	0.0607	9.5	0.25	620	15	622	47	629	205	99
AK24-seq1-a55	5726	200	12	0.34	11688	0.0580	2.3	0.4514	6.7	0.0565	6.3	0.34	363	8	378	21	471	138	77
AK24-seq1-a56	13299	178	21	0.33	21566	0.1101	2.4	0.9463	3.1	0.0623	1.9	0.77	674	15	676	15	685	42	98
AK24-seq1-a57	7617	124	14	0.44	13186	0.1041	2.4	0.8417	3.3	0.0586	2.3	0.72	639	15	620	16	553	51	116
AK24-seq1-a58	3156	83	7	0.33	6185	0.0765	2.5	0.6031	12.3	0.0572	12.0	0.21	475	12	479	48	498	265	95
AK24-seq1-a59	4946	58	9	0.69	2605	0.1349	2.5	1.1420	3.9	0.0614	3.1	0.62	815	19	773	22	654	66	125
AK24-seq1-a60	19517	541	31	0.22	2452	0.0567	2.0	0.4545	3.2	0.0581	2.5	0.63	356	7	380	10	534	54	67
AK24-seq2-b01	29370	133	31	0.34	34331	0.2155	2.5	2.5718	3.3	0.0865	2.3	0.73	1258	28	1293	25	1350	44	93
AK24-seq2-b02	13580	206	22	0.38	22867	0.0971	2.1	0.8009	2.9	0.0598	2.0	0.73	597	12	597	13	598	43	100
AK24-seq2-b03	30069	82	27	0.45	28104	0.2900	2.4	4.3493	3.0	0.1088	1.8	0.80	1642	35	1703	25	1779	33	92
AK24-seq2-b04	182401	422	142	0.19	130790	0.3180	2.3	5.6232	2.6	0.1283	1.2	0.89	1780	36	1920	23	2074	21	86
AK24-seq2-b05	15579	102	19	0.16	19786	0.1840	2.5	1.8996	3.0	0.0749	1.7	0.83	1089	25	1081	20	1065	34	102
AK24-seq2-b06	64768	410	86	0.39	47620	0.1905	2.2	2.1001	2.9	0.0799	1.9	0.75	1124	22	1149	20	1195	37	94
AK24-seq2-b07	53975	50	37	0.47	30021	0.6278	2.1	15.7680	2.5	0.1822	1.2	0.87	3141	53	2863	24	2673	20	118
AK24-seq2-b08	14272	300	28	0.29	25825	0.0905	2.2	0.7037	2.8	0.0564	1.7	0.79	559	12	541	12	467	38	120
AK24-seq2-b09	6363	227	15	0.79	12706	0.0544	2.4	0.4006	8.9	0.0534	8.6	0.26	341	8	342	26	346	195	99

AK24-seq2-b10	12865	377	26	0.51	24088	0.0615	2.1	0.4601	2.8	0.0543	1.9	0.73	385	8	384	9	383	43	100
AK24-seq2-b11	6601	195	14	0.37	12953	0.0694	2.1	0.4959	3.4	0.0518	2.7	0.62	433	9	409	12	278	62	156
AK24-seq2-b12	94857	186	80	0.51	75474	0.3643	2.2	6.4071	2.5	0.1276	1.3	0.86	2002	37	2033	22	2065	22	97
AK24-seq2-b13	24087	53	20	0.22	20799	0.3562	2.3	5.7885	2.9	0.1179	1.8	0.78	1964	39	1945	25	1924	32	102
AK24-seq2-b14	11766	175	21	0.34	20294	0.1126	2.4	0.9812	4.4	0.0632	3.7	0.55	688	16	694	22	715	78	96
AK24-seq2-b15	4642	78	10	0.65	8141	0.1052	2.4	0.9606	7.7	0.0662	7.3	0.31	645	15	684	39	814	152	79
AK24-seq2-b16	3962	73	8	0.67	7144	0.0980	2.3	0.7618	3.7	0.0564	2.9	0.62	603	13	575	17	467	65	129
AK24-seq2-b17	4228	69	8	0.32	7446	0.1069	2.2	0.8490	4.1	0.0576	3.5	0.53	654	14	624	19	515	76	127
AK24-seq2-b18	2056	30	3	0.33	3387	0.1052	2.9	0.8933	5.9	0.0616	5.1	0.50	645	18	648	29	660	110	98
AK24-seq2-b19	2621	83	5	0.38	4873	0.0610	2.3	0.4585	4.3	0.0545	3.6	0.54	382	9	383	14	391	81	98
AK24-seq2-b20	1952	25	3	0.44	3337	0.1223	2.3	1.0032	5.3	0.0595	4.7	0.44	744	16	705	27	585	103	127
AK24-seq2-b21	10648	303	19	0.17	19761	0.0654	2.0	0.4941	2.7	0.0548	1.8	0.75	408	8	408	9	404	40	101
AK24-seq2-b22	5471	89	11	0.57	9699	0.1069	2.3	0.9091	8.4	0.0617	8.1	0.27	655	14	657	41	663	173	99
AK24-seq2-b23	1245	22	2	0.34	2522	0.1132	2.3	0.7807	6.4	0.0500	6.0	0.35	691	15	586	29	197	139	352
AK24-seq2-b24	329824	258	192	0.33	136764	0.6247	3.8	20.7583	4.7	0.2410	2.7	0.82	3129	96	3127	46	3127	42	100
AK24-seq2-b25	11954	371	23	0.32	5701	0.0589	2.2	0.4389	3.3	0.0540	2.4	0.68	369	8	369	10	372	54	99
AK24-seq2-b26	1480	25	3	0.35	2770	0.1011	2.7	0.7500	8.2	0.0538	7.8	0.33	621	16	568	36	363	175	171
AK24-seq2-b27	20205	555	40	0.56	24845	0.0623	2.2	0.4712	2.6	0.0549	1.4	0.85	390	8	392	8	407	31	96
AK24-seq2-b28	7594	209	14	0.21	2713	0.0677	2.2	0.5161	3.3	0.0553	2.4	0.69	422	9	423	11	423	53	100
AK24-seq2-b29	1797	77	4	0.50	3921	0.0481	1.9	0.3745	11.8	0.0564	11.6	0.16	303	6	323	33	469	257	65
AK24-seq2-b30	6076	89	12	0.62	9909	0.1126	2.7	0.9678	3.5	0.0624	2.3	0.75	688	17	687	18	686	50	100
AK24-seq2-b31	824	45	5	0.24	1811	0.1156	2.6	1.2565	29.9	0.0788	29.8	0.09	705	18	826	185	1167	591	60
AK24-seq2-b32	2023	33	4	0.51	3647	0.1155	2.8	0.9073	5.7	0.0570	5.0	0.48	704	18	656	28	491	111	143
AK24-seq2-b33	3075	51	6	0.37	5685	0.1092	2.2	0.8247	4.8	0.0548	4.3	0.45	668	14	611	22	403	96	166
AK24-seq2-b34	3970	57	7	0.60	1802	0.1126	2.4	0.9728	4.8	0.0627	4.2	0.51	688	16	690	25	697	89	99
AK24-seq2-b35	1873	47	3	0.33	3433	0.0687	2.8	0.5275	6.2	0.0557	5.5	0.45	428	12	430	22	441	123	97
AK24-seq2-b36	45500	50	32	0.50	24886	0.5308	2.3	13.6032	2.6	0.1859	1.3	0.86	2745	51	2722	25	2706	22	101
AK24-seq2-b37	8098	112	14	0.52	2914	0.1114	2.9	0.9566	4.0	0.0623	2.7	0.73	681	19	682	20	683	57	100
AK24-seq2-b38	7314	250	16	0.40	14467	0.0596	2.2	0.4474	6.1	0.0544	5.7	0.36	373	8	375	19	390	128	96
AK24-seq2-b39	9544	59	15	0.94	12723	0.1897	2.4	1.9915	3.4	0.0762	2.4	0.71	1120	25	1113	23	1099	48	102
AK24-seq2-b40	38546	70	32	0.54	28941	0.3850	2.0	7.1900	2.3	0.1354	1.1	0.88	2100	36	2135	20	2170	19	97
AK24-seq2-b41	1744	29	4	0.52	3287	0.1118	2.4	0.8314	6.1	0.0539	5.6	0.39	683	15	614	29	368	127	186
AK24-seq2-b42	6619	201	14	0.32	12957	0.0688	2.3	0.5301	7.5	0.0559	7.2	0.31	429	10	432	27	449	159	96
AK24-seq2-b43	3290	52	7	0.97	489	0.0952	4.0	0.7974	12.1	0.0608	11.4	0.33	586	22	595	56	631	246	93
AK24-seq2-b44	108553	232	93	0.27	90458	0.3745	2.4	6.3048	2.8	0.1221	1.4	0.86	2051	42	2019	25	1987	26	103
AK24-seq2-b45	2990	52	6	0.32	5473	0.1131	2.5	0.9851	10.3	0.0632	10.0	0.25	691	17	696	53	713	212	97
AK24-seq2-b46	1849	33	4	0.42	3626	0.1071	2.7	0.7599	5.0	0.0515	4.2	0.54	656	17	574	22	262	97	250
AK24-seq2-b47	32731	565	61	0.39	14206	0.1013	2.8	0.8447	3.3	0.0605	1.7	0.86	622	17	622	16	620	37	100
AK24-seq2-b48	6671	86	13	0.56	11304	0.1291	2.4	1.0694	3.5	0.0601	2.5	0.70	783	18	738	18	606	54	129
AK24-seq2-b49	97022	137	66	0.29	51074	0.4315	2.2	8.7933	2.3	0.1478	0.8	0.94	2313	42	2317	21	2321	14	100
AK24-seq2-b50	37907	103	39	0.46	35781	0.3229	2.3	4.7922	2.6	0.1077	1.3	0.86	1804	36	1784	22	1760	25	102
AK24-seq2-b51	6238	101	11	0.36	10805	0.1072	2.2	0.8685	3.7	0.0587	3.0	0.60	657	14	635	18	558	65	118

AK24-seq2-b52	115565	231	99	0.32	42037	0.3887	2.2	7.0602	2.6	0.1317	1.4	0.85	2117	40	2119	23	2121	24	100
AK24-seq2-b53	7217	38	9	0.22	9136	0.2326	2.3	2.5781	3.7	0.0804	2.9	0.63	1348	28	1294	28	1207	57	112
AK24-seq2-b54	4124	53	9	0.73	6385	0.1401	2.7	1.1421	3.7	0.0591	2.5	0.72	845	21	774	20	572	55	148
AK24-seq2-b55	9407	332	16	0.28	18191	0.0477	2.9	0.3454	3.6	0.0525	2.1	0.80	301	8	301	9	307	49	98
AK24-seq2-b56	2591	70	8	0.40	2266	0.1050	2.3	0.8226	4.4	0.0568	3.8	0.51	644	14	610	20	484	83	133
AK24-seq2-b57	2064	96	6	0.43	3940	0.0622	2.2	0.4591	5.3	0.0535	4.9	0.41	389	8	384	17	351	110	111
AK24-seq2-b58	2354	43	6	0.33	3560	0.1295	3.4	1.1797	5.5	0.0660	4.3	0.62	785	25	791	30	808	90	97
AK24-seq2-b59	7227	104	13	0.39	5769	0.1187	2.4	1.0287	3.5	0.0629	2.5	0.69	723	17	718	18	704	54	103
AK24-seq2-b60	6624	109	13	0.37	11511	0.1099	2.1	0.9963	4.9	0.0657	4.4	0.44	672	14	702	25	798	92	84
AK24-seq3-c01	2657	78	5	0.44	5236	0.0607	2.3	0.4282	3.8	0.0512	3.1	0.59	380	8	362	12	249	71	153
AK24-seq3-c02	3962	65	9	0.81	7047	0.1108	2.1	0.9655	8.7	0.0632	8.4	0.24	677	13	686	44	715	179	95
AK24-seq3-c03	4932	80	7	0.04	8411	0.0932	1.9	0.7599	4.3	0.0591	3.9	0.45	574	11	574	19	572	84	100
AK24-seq3-c04	16334	173	22	0.48	674	0.1105	1.9	0.9423	5.0	0.0619	4.6	0.39	675	12	674	25	670	99	101
AK24-seq3-c05	15171	241	27	0.64	13804	0.0924	2.3	0.7576	3.1	0.0595	2.1	0.75	570	13	573	14	584	45	98
Sample 63/10-1 (AK27)			**Well no.: 63/10-1**				**Location (decimal degrees):**				**49.961**	**10.17114W**			**Datum: IRENET95**				
AK27-seq1-A01	5310	84	39	0.64	4231	0.3905	1.7	7.1103	3.1	0.1321	2.5	0.57	2125	31	2125	28	2126	44	100
AK27-seq1-A02	4252	45	35	0.76	2180	0.6094	1.8	17.2804	3.2	0.2057	2.6	0.57	3068	44	2951	31	2872	43	107
AK27-seq1-A03	795	51	10	0.59	1107	0.1703	2.6	1.7937	7.6	0.0764	7.1	0.35	1014	25	1043	51	1106	142	92
AK27-seq1-A04	3865	97	32	0.35	3690	0.3070	1.9	4.5581	3.6	0.1077	3.1	0.53	1726	29	1742	31	1761	56	98
AK27-seq1-A05	692	11	5	0.57	547	0.3967	2.4	7.4016	5.9	0.1353	5.4	0.41	2154	45	2161	54	2168	94	99
AK27-seq1-A06	3302	48	23	0.86	2338	0.3632	1.7	7.4335	3.8	0.1485	3.4	0.44	1997	28	2165	34	2328	58	86
AK27-seq1-A07	6594	161	57	0.52	6433	0.3115	1.7	4.5894	2.8	0.1069	2.1	0.63	1748	26	1747	23	1746	39	100
AK27-seq1-A08	10015	91	53	0.32	5726	0.5203	2.3	13.2457	3.2	0.1846	2.1	0.74	2700	52	2697	30	2695	35	100
AK27-seq1-A09	3496	105	33	0.49	3716	0.2833	1.4	3.8731	3.3	0.0992	2.9	0.43	1608	20	1608	27	1608	55	100
AK27-seq1-A10	18369	107	89	0.69	8423	0.6541	1.5	20.7347	2.1	0.2299	1.4	0.73	3244	39	3126	21	3051	23	106
AK27-seq1-A11	1994	57	19	0.58	2021	0.2873	1.6	4.1022	4.4	0.1035	4.1	0.35	1628	23	1655	37	1689	76	96
AK27-seq1-A12	13997	368	134	0.45	14423	0.3311	1.8	4.6708	2.5	0.1023	1.7	0.71	1844	28	1762	21	1666	32	111
AK27-seq1-A13	1209	81	17	0.75	1751	0.1790	2.3	1.7906	5.2	0.0725	4.6	0.45	1062	23	1042	34	1001	93	106
AK27-seq1-A14	3666	192	39	0.19	4924	0.2002	1.5	2.1706	3.4	0.0786	3.0	0.44	1176	16	1172	24	1163	60	101
AK27-seq1-A15	12125	710	146	0.08	15921	0.2163	1.6	2.0869	2.5	0.0700	2.0	0.62	1262	18	1145	18	928	41	136
AK27-seq1-A16	4621	124	40	0.29	4609	0.3066	1.7	4.4241	3.1	0.1046	2.5	0.55	1724	26	1717	26	1708	47	101
AK27-seq1-A17	4046	105	35	0.37	4096	0.3089	1.2	4.4345	2.8	0.1041	2.5	0.43	1735	18	1719	23	1699	46	102
AK27-seq1-A18	28729	359	143	0.01	18871	0.3970	2.0	8.6472	2.6	0.1580	1.6	0.77	2155	36	2302	24	2434	28	89
AK27-seq1-A19	832	280	21	0.22	1549	0.0756	2.2	0.5893	6.0	0.0565	5.6	0.37	470	10	470	23	474	124	99
AK27-seq1-A20	1448	125	28	0.58	1875	0.1968	1.7	2.2073	4.1	0.0813	3.7	0.43	1158	18	1183	29	1230	72	94
AK27-seq1-A21	6173	321	41	0.13	2612	0.1202	2.8	1.7496	3.5	0.1055	2.2	0.78	732	19	1027	23	1724	41	42
AK27-seq1-A22	737	277	17	0.01	1405	0.0671	2.1	0.5067	7.7	0.0548	7.5	0.27	419	8	416	27	404	167	104
AK27-seq1-A23	6550	355	77	0.17	9031	0.2187	1.5	2.3016	2.9	0.0763	2.5	0.51	1275	17	1213	21	1104	50	115
AK27-seq1-A24	18557	442	157	0.08	19376	0.3652	1.3	5.1387	2.6	0.1020	2.2	0.51	2007	23	1843	22	1662	42	121
AK27-seq1-A25	2012	137	26	0.33	2898	0.1831	2.1	1.8574	4.1	0.0736	3.5	0.52	1084	21	1066	27	1030	71	105
AK27-seq1-A26	3523	104	37	0.38	433	0.3124	1.8	4.5150	7.8	0.1048	7.6	0.23	1752	28	1734	67	1711	140	102
AK27-seq1-A27	3061	107	32	0.34	3414	0.2817	1.9	3.6653	3.8	0.0944	3.3	0.49	1600	26	1564	31	1516	62	106

AK27-seq1-A28	1322	89	21	1.04	1860	0.1882	2.0	1.9372	4.5	0.0747	4.0	0.44	1111	20	1094	30	1060	81	105
AK27-seq1-A29	5858	162	64	0.88	5940	0.3181	1.5	4.5640	2.8	0.1040	2.4	0.52	1781	23	1743	24	1698	44	105
AK27-seq1-A30	5144	99	39	0.26	4367	0.3747	2.0	6.4049	3.3	0.1240	2.6	0.60	2052	35	2033	29	2014	47	102
AK27-seq2-B01	341	69	4	0.00	653	0.0693	2.5	0.5295	8.4	0.0554	8.0	0.30	432	11	431	30	429	179	101
AK27-seq2-B02	2597	46	20	0.67	2296	0.3504	2.1	5.7654	4.0	0.1193	3.4	0.53	1936	36	1941	35	1946	61	99
AK27-seq2-B03	3926	86	31	0.46	3834	0.3244	1.8	4.8443	3.3	0.1083	2.7	0.54	1811	28	1793	28	1771	50	102
AK27-seq2-B04	1419	251	20	0.25	2626	0.0780	1.7	0.6126	4.0	0.0569	3.6	0.42	484	8	485	15	489	79	99
AK27-seq2-B05	1682	166	20	0.23	2817	0.1136	3.0	0.9812	5.1	0.0626	4.1	0.59	694	20	694	26	695	88	100
AK27-seq2-B06	990	182	14	0.37	1859	0.0733	1.6	0.5696	5.2	0.0563	4.9	0.31	456	7	458	19	466	109	98
AK27-seq2-B07	5183	121	42	0.32	5318	0.3221	1.5	4.5693	3.0	0.1029	2.6	0.50	1800	24	1744	25	1677	48	107
AK27-seq2-B08	12535	263	94	0.18	12575	0.3523	1.4	5.1128	2.1	0.1052	1.7	0.63	1946	23	1838	18	1719	31	113
AK27-seq2-B09	1541	36	15	0.99	1541	0.3042	1.6	4.4337	5.1	0.1057	4.9	0.32	1712	24	1719	43	1726	89	99
AK27-seq2-B10	3513	113	31	0.26	3971	0.2673	1.5	3.4414	2.9	0.0934	2.6	0.49	1527	20	1514	23	1496	48	102
AK27-seq2-B11	1571	60	20	0.67	1516	0.2942	2.1	4.4395	4.0	0.1095	3.4	0.52	1662	31	1720	34	1790	62	93
AK27-seq2-B12	9635	246	98	1.02	10221	0.3118	1.9	4.2542	3.0	0.0990	2.4	0.63	1749	30	1685	25	1605	44	109
AK27-seq2-B13	1811	107	30	0.62	2276	0.2392	1.6	2.8697	7.1	0.0870	6.9	0.23	1383	20	1374	55	1361	133	102
AK27-seq2-B14	2386	66	21	0.47	2544	0.2851	2.0	3.8904	3.8	0.0990	3.2	0.52	1617	28	1612	31	1605	60	101
AK27-seq2-B15	1248	56	13	0.59	1656	0.2045	2.2	2.2520	6.4	0.0799	6.0	0.35	1199	24	1197	46	1194	119	100
AK27-seq2-B16	13930	108	67	0.36	7985	0.5440	1.6	13.8259	2.5	0.1843	1.8	0.66	2800	37	2738	23	2692	31	104
AK27-seq2-B17	1633	104	25	0.43	2071	0.2230	1.9	2.5580	4.5	0.0832	4.1	0.43	1298	23	1289	34	1274	80	102
AK27-seq2-B18	5235	117	43	0.54	5110	0.3194	1.7	4.8149	3.2	0.1094	2.7	0.54	1787	27	1788	28	1789	50	100
AK27-seq2-B19	6995	52	34	0.50	3903	0.5421	1.6	14.1323	3.0	0.1891	2.5	0.55	2792	37	2759	28	2734	41	102
AK27-seq2-B20	2066	73	24	0.29	1949	0.3122	1.5	4.8254	3.9	0.1121	3.6	0.38	1752	23	1789	33	1834	65	96
AK27-seq2-B21	257	98	6	0.03	522	0.0638	3.6	0.4793	16.6	0.0545	16.2	0.22	398	14	398	56	393	364	101
AK27-seq2-B22	3661	122	47	0.92	3285	0.3375	1.5	5.5049	3.4	0.1183	3.0	0.45	1875	25	1901	29	1931	54	97
AK27-seq2-B23	1160	367	23	0.07	2205	0.0673	1.7	0.5140	5.1	0.0554	4.8	0.34	420	7	421	18	429	106	98
AK27-seq2-B24	7055	224	85	0.55	6324	0.3295	1.5	5.3573	2.7	0.1179	2.2	0.57	1836	25	1878	24	1925	40	95
AK27-seq2-B25	1419	110	23	0.38	1866	0.1902	1.6	2.0923	4.5	0.0798	4.2	0.36	1122	17	1146	32	1192	84	94
AK27-seq2-B26	25361	592	208	0.10	28546	0.3587	1.5	4.6492	2.2	0.0940	1.6	0.68	1976	26	1758	19	1508	31	131
AK27-seq2-B27	23189	396	163	0.16	21843	0.4064	1.6	6.2853	2.2	0.1122	1.6	0.71	2198	29	2016	20	1835	29	120
AK27-seq2-B28	10878	84	54	0.40	5970	0.5380	3.3	14.5326	4.5	0.1959	3.0	0.74	2775	75	2785	43	2792	49	99
AK27-seq2-B29	1191	33	10	0.42	1279	0.2811	1.9	3.8285	4.7	0.0988	4.3	0.40	1597	27	1599	39	1601	81	100
AK27-seq2-B30	3128	23	19	1.31	1696	0.5591	1.3	15.0453	3.5	0.1952	3.2	0.38	2863	31	2818	34	2786	53	103
AK27-seq2-B31	4343	106	35	0.38	4315	0.3018	1.6	4.4223	4.8	0.1063	4.6	0.32	1700	23	1717	41	1737	84	98
AK27-seq2-B32	740	31	8	0.31	899	0.2380	1.5	2.8680	6.9	0.0874	6.8	0.22	1376	19	1374	54	1369	130	101
AK27-seq2-B33	1674	195	27	0.06	2474	0.1463	2.4	1.4411	6.5	0.0714	6.1	0.37	880	20	906	40	970	124	91
AK27-seq2-B34	2658	30	22	1.02	1431	0.5446	2.0	14.6920	3.8	0.1957	3.2	0.53	2803	46	2796	37	2790	53	100
AK27-seq2-B35	2576	63	29	0.59	2124	0.3869	1.1	6.8223	3.6	0.1279	3.4	0.31	2108	20	2089	32	2069	60	102
AK27-seq2-B36	4925	128	51	0.35	4293	0.3649	2.1	6.0824	3.3	0.1209	2.6	0.62	2005	35	1988	29	1970	46	102
AK27-seq2-B37	2666	21	16	1.12	1449	0.5547	2.2	14.8703	3.8	0.1944	3.1	0.57	2845	50	2807	37	2780	51	102
AK27-seq2-B38	10991	144	50	0.35	11902	0.3257	1.4	4.3738	2.2	0.0974	1.7	0.63	1817	22	1707	19	1575	32	115
AK27-seq2-B39	1800	92	19	0.27	2390	0.2035	2.1	2.2355	4.4	0.0797	3.9	0.47	1194	23	1192	32	1189	77	100

AK27-seq2-B40	12230	117	66	0.38	7460	0.4948	1.6	11.7773	2.5	0.1726	2.0	0.62	2592	34	2587	24	2583	33	100
AK27-seq2-B41	1440	78	17	0.46	1980	0.1981	2.2	2.0912	4.8	0.0766	4.2	0.47	1165	24	1146	33	1110	84	105
AK27-seq2-B42	34995	379	187	0.15	22016	0.4692	1.3	10.8454	1.8	0.1677	1.2	0.74	2480	28	2510	17	2534	21	98
AK27-seq2-B43	5693	163	65	0.31	5030	0.3730	1.3	6.1832	2.8	0.1202	2.4	0.48	2043	23	2002	24	1960	43	104
AK27-seq2-B44	14131	211	106	0.27	7437	0.4452	1.7	12.1572	2.2	0.1981	1.5	0.75	2374	33	2617	21	2810	24	84
AK27-seq2-B45	18233	639	125	0.19	27996	0.2001	1.4	1.8196	1.8	0.0659	1.3	0.74	1176	15	1053	12	804	26	146
AK27-seq2-B46	31047	673	258	0.02	33250	0.4000	1.5	5.4449	2.2	0.0987	1.6	0.70	2169	29	1892	19	1600	29	136
AK27-seq2-B47	1805	68	18	0.36	2121	0.2421	1.7	2.9821	4.3	0.0893	3.9	0.39	1398	21	1403	33	1412	75	99
AK27-seq2-B48	4847	268	73	0.32	5665	0.2601	1.6	3.2142	3.0	0.0896	2.5	0.54	1490	22	1461	24	1417	48	105
AK27-seq2-B49	15478	421	145	0.25	17302	0.3352	1.7	4.3672	2.3	0.0945	1.6	0.71	1863	27	1706	19	1518	31	123
AK27-seq2-B50	637	7	2	0.00	578	0.3562	2.5	5.6842	7.5	0.1157	7.1	0.34	1964	43	1929	67	1892	127	104
AK27-seq2-B51	4770	544	39	0.21	1320	0.0669	8.9	0.8060	9.9	0.0874	4.1	0.91	417	36	600	46	1369	80	30
AK27-seq2-B52	15120	188	72	0.32	15540	0.3602	1.2	5.1242	2.1	0.1032	1.7	0.58	1983	21	1840	18	1682	32	118
AK27-seq2-B53	2196	104	23	0.22	2756	0.2123	1.4	2.4673	4.4	0.0843	4.1	0.31	1241	16	1263	32	1299	80	96
AK27-seq2-B54	3861	87	31	0.28	3621	0.3466	1.8	5.3852	3.1	0.1127	2.5	0.59	1918	30	1882	27	1843	46	104
AK27-seq2-B55	5247	110	42	0.33	4970	0.3492	1.5	5.3618	2.7	0.1114	2.2	0.57	1931	25	1879	23	1822	40	106
AK27-seq2-B56	7843	271	99	0.23	7451	0.3521	1.7	5.3534	2.6	0.1103	2.0	0.66	1944	29	1877	23	1804	36	108
AK27-seq2-B57	1764	141	31	0.34	2345	0.2080	1.6	2.2806	4.1	0.0795	3.7	0.40	1218	18	1206	29	1185	74	103
AK27-seq2-B58	11900	414	163	0.14	10970	0.3924	2.0	6.2781	2.9	0.1160	2.1	0.69	2134	37	2015	26	1896	38	113
AK27-seq2-B59	1641	42	15	0.50	1631	0.3042	2.0	4.4456	4.6	0.1060	4.2	0.44	1712	31	1721	39	1731	77	99
AK27-seq2-B60	2797	74	26	0.53	2828	0.3104	2.4	4.4765	4.2	0.1046	3.4	0.57	1743	36	1727	35	1707	63	102
AK27-seq3-C01	7771	181	78	0.79	7338	0.3461	1.6	5.3175	2.8	0.1114	2.2	0.59	1916	27	1872	24	1823	41	105
AK27-seq3-C02	3986	153	43	0.25	4434	0.2739	1.9	3.5554	3.6	0.0941	3.1	0.53	1561	27	1540	29	1511	58	103
AK27-seq3-C03	281	34	5	0.10	414	0.1574	2.6	1.5410	10.4	0.0710	10.0	0.25	942	23	947	66	958	205	98
AK27-seq3-C04	1717	167	30	0.25	2331	0.1728	1.6	1.8324	4.1	0.0769	3.8	0.38	1028	15	1057	28	1119	76	92
AK27-seq3-C05	732	264	17	0.00	1342	0.0682	2.3	0.5371	6.7	0.0571	6.3	0.34	425	9	437	24	497	138	85
AK27-seq3-C06	5890	228	84	0.31	5548	0.3436	1.5	5.3572	3.0	0.1131	2.7	0.48	1904	24	1878	26	1849	48	103
AK27-seq3-C07	3270	119	35	0.38	3638	0.2668	2.1	3.4770	3.6	0.0945	3.0	0.58	1524	29	1522	29	1519	56	100
AK27-seq3-C08	4174	163	56	0.17	4098	0.3381	1.5	4.9733	3.1	0.1067	2.7	0.49	1878	25	1815	27	1743	50	108
AK27-seq3-C09	30332	969	348	0.10	1789	0.3522	8.5	7.3334	9.3	0.1510	3.8	0.91	1945	144	2153	87	2357	65	83
AK27-seq3-C10	988	331	21	0.03	1859	0.0694	1.7	0.5315	5.9	0.0556	5.7	0.28	433	7	433	21	434	126	100
AK27-seq3-C11	1368	91	22	0.39	1622	0.2304	1.6	2.8183	4.5	0.0887	4.2	0.36	1337	20	1360	34	1398	80	96
AK27-seq3-C12	1516	47	17	0.68	1571	0.2976	2.1	4.1712	5.5	0.1016	5.1	0.38	1680	31	1668	46	1654	94	102
AK27-seq3-C13	2742	124	48	1.10	2792	0.2944	1.6	4.1857	3.2	0.1031	2.8	0.49	1663	23	1671	26	1681	51	99
AK27-seq3-C14	1518	104	21	0.52	2150	0.1750	1.9	1.7821	5.3	0.0738	4.9	0.36	1040	18	1039	35	1037	100	100
AK27-seq3-C15	6349	55	36	0.54	3418	0.5430	1.9	14.5215	3.3	0.1940	2.7	0.58	2796	44	2784	32	2776	44	101
AK27-seq3-C16	2615	77	27	0.67	2665	0.2954	1.3	4.1848	3.7	0.1028	3.4	0.36	1668	19	1671	31	1675	63	100
AK27-seq3-C17	3900	165	41	0.32	4616	0.2336	1.9	2.8623	3.4	0.0889	2.9	0.54	1353	23	1372	26	1401	56	97
AK27-seq3-C18	8635	295	110	0.27	7568	0.3500	1.9	5.7643	2.9	0.1194	2.2	0.67	1935	33	1941	26	1948	39	99
AK27-seq3-C19	2129	131	38	0.61	2404	0.2540	1.9	3.2620	3.9	0.0931	3.4	0.48	1459	25	1472	31	1491	65	98
AK27-seq3-C20	3759	115	40	0.64	3837	0.2878	1.8	4.0942	3.3	0.1032	2.8	0.54	1631	26	1653	27	1682	51	97
AK27-seq3-C21	1911	76	22	0.48	2185	0.2595	1.6	3.2933	4.4	0.0920	4.1	0.37	1487	22	1479	35	1468	78	101

AK27-seq3-C22	4617	444	83	0.28	6296	0.1804	2.5	1.9213	3.3	0.0772	2.2	0.75	1069	24	1089	22	1128	43	95
AK27-seq3-C23	2409	130	30	0.32	3098	0.2190	1.6	2.4701	3.4	0.0818	3.0	0.47	1277	19	1263	25	1241	59	103
AK27-seq3-C24	36381	1487	512	0.03	22140	0.3597	1.6	4.8885	2.3	0.0986	1.7	0.67	1981	27	1800	20	1597	33	124
AK27-seq3-C25	1364	317	21	0.03	2395	0.0705	1.7	0.5838	5.0	0.0600	4.7	0.34	439	7	467	19	605	102	73
AK27-seq3-C26	5412	50	36	0.85	3032	0.5464	1.9	14.1728	3.4	0.1881	2.7	0.58	2810	44	2761	32	2726	45	103
AK27-seq3-C27	11454	841	164	0.11	17084	0.2088	3.3	2.0195	3.8	0.0701	1.8	0.88	1223	37	1122	26	932	36	131
AK27-seq3-C28	2204	181	28	0.08	3259	0.1612	1.4	1.5777	4.0	0.0710	3.8	0.34	964	12	961	25	957	78	101
AK27-seq3-C29	3230	111	39	0.18	2806	0.3417	2.6	5.6678	4.0	0.1203	3.0	0.65	1895	43	1926	35	1961	54	97
AK27-seq3-C30	4287	146	56	0.27	3719	0.3586	1.5	5.9900	2.9	0.1212	2.5	0.53	1975	26	1974	25	1973	44	100
AK27-seq3-C31	1271	94	17	0.27	1839	0.1788	1.9	1.7915	4.3	0.0727	3.8	0.44	1060	18	1042	28	1005	78	106
AK27-seq3-C32	17950	839	267	0.31	18572	0.3152	2.2	4.4140	2.6	0.1016	1.5	0.81	1766	33	1715	22	1653	28	107
AK27-seq3-C33	10299	87	58	0.36	5429	0.5792	2.1	15.9419	3.0	0.1996	2.1	0.70	2946	50	2873	29	2823	35	104
AK27-seq3-C34	10249	658	140	0.30	5630	0.2007	2.1	2.9791	3.0	0.1077	2.2	0.69	1179	22	1402	23	1760	40	67
AK27-seq3-C35	1258	26	11	0.44	1050	0.3513	2.5	6.1308	6.1	0.1266	5.6	0.41	1941	43	1995	55	2051	99	95
AK27-seq3-C36	6013	448	101	0.01	6974	0.2386	1.7	2.9802	3.0	0.0906	2.4	0.58	1380	21	1403	23	1438	46	96
AK27-seq3-C37	2733	108	37	0.96	2522	0.2624	1.7	3.4587	3.8	0.0956	3.4	0.44	1502	23	1518	31	1540	65	98
AK27-seq3-C38	2653	70	24	0.27	2514	0.3240	1.4	4.9897	3.7	0.1117	3.5	0.38	1809	23	1818	32	1827	63	99
AK27-seq3-C39	5493	107	49	0.40	3430	0.3989	2.4	9.3362	4.1	0.1697	3.3	0.58	2164	44	2372	39	2555	56	85
AK27-seq3-C40	3320	43	31	0.63	1833	0.5721	1.4	15.0250	3.0	0.1905	2.6	0.47	2916	33	2817	29	2746	43	106
AK27-seq3-C41	4488	366	68	0.43	6622	0.1719	1.9	1.6965	3.5	0.0716	2.9	0.54	1023	18	1007	22	974	59	105
AK27-seq3-C42	3294	223	44	0.31	4521	0.1894	1.5	1.9954	3.5	0.0764	3.1	0.44	1118	15	1114	24	1105	62	101
AK27-seq3-C43	3323	141	59	0.89	3147	0.3335	2.0	5.1205	3.6	0.1113	3.1	0.54	1855	32	1840	31	1822	56	102
AK27-seq3-C44	4335	132	45	0.28	4225	0.3230	2.2	4.8620	3.9	0.1092	3.2	0.56	1805	34	1796	33	1785	59	101
AK27-seq3-C45	10601	300	100	0.14	10610	0.3316	1.4	4.8175	2.4	0.1054	2.0	0.57	1846	22	1788	21	1721	36	107
AK27-seq3-C46	1572	160	39	0.98	1539	0.2026	1.9	2.2481	5.2	0.0805	4.9	0.36	1189	21	1196	37	1209	96	98
AK27-seq3-C47	1051	91	13	0.03	1553	0.1564	3.5	1.5185	8.0	0.0704	7.2	0.44	937	30	938	50	941	147	100
AK27-seq3-C48	7601	75	54	0.77	4333	0.5620	2.0	14.2428	3.1	0.1838	2.3	0.65	2875	47	2766	30	2688	38	107
AK27-seq3-C49	10753	285	98	0.16	10287	0.3409	1.6	5.0053	2.5	0.1065	1.9	0.64	1891	27	1820	22	1740	36	109
AK27-seq3-C50	853	61	12	0.46	1201	0.1807	1.8	1.8618	5.9	0.0747	5.6	0.30	1071	18	1068	40	1062	113	101
AK27-seq3-C51	1390	95	18	0.40	1892	0.1707	2.0	1.8138	4.7	0.0771	4.2	0.44	1016	19	1050	31	1123	84	90
AK27-seq3-C52	1566	46	19	1.01	1537	0.3046	2.0	4.4738	5.2	0.1065	4.8	0.39	1714	30	1726	44	1741	88	98
AK27-seq3-C53	373	45	8	0.65	558	0.1583	2.6	1.5158	9.9	0.0695	9.5	0.27	947	23	937	63	912	197	104
AK27-seq3-C54	1727	79	27	0.53	1696	0.3005	1.9	4.4310	4.5	0.1069	4.1	0.41	1694	28	1718	38	1748	75	97
AK27-seq3-C55	759	79	16	0.32	1020	0.1993	3.4	2.1526	6.6	0.0783	5.6	0.51	1172	36	1166	47	1155	112	101
AK27-seq3-C56	11549	357	116	0.45	11240	0.2896	1.8	4.3260	2.9	0.1083	2.3	0.62	1640	26	1698	24	1772	41	93
AK27-seq3-C57	3830	77	32	0.83	340	0.3101	2.5	4.3605	6.5	0.1020	6.0	0.39	1741	39	1705	55	1661	110	105
AK27-seq3-C58	4514	154	46	0.33	4695	0.2793	1.8	3.9195	3.2	0.1018	2.7	0.55	1588	25	1618	26	1657	50	96
AK27-seq3-C59	7604	70	44	0.25	4187	0.5525	2.3	15.0106	3.5	0.1970	2.6	0.66	2836	54	2816	34	2802	43	101
AK27-seq3-C60	919	64	15	0.98	1251	0.1760	2.4	1.8712	5.5	0.0771	4.9	0.44	1045	23	1071	37	1124	98	93
AK27-seq4-D01	6978	450	132	0.26	8033	0.2823	1.6	3.6077	2.8	0.0927	2.2	0.59	1603	23	1551	22	1482	43	108
AK27-seq4-D02	1620	142	38	0.80	2056	0.2181	1.5	2.4941	4.9	0.0829	4.6	0.31	1272	18	1270	36	1268	91	100
AK27-seq4-D03	4210	40	28	0.66	2304	0.5590	1.5	14.7984	3.6	0.1920	3.3	0.41	2862	35	2802	35	2760	55	104

AK27-seq4-D04	24276	201	147	0.44	13107	0.6202	1.4	16.6021	1.9	0.1941	1.3	0.74	3111	34	2912	18	2778	21	112
AK27-seq4-D05	3709	104	36	0.41	3503	0.3137	2.0	4.7684	3.8	0.1102	3.2	0.54	1759	32	1779	32	1803	58	98
AK27-seq4-D06	1099	49	14	0.81	1262	0.2242	1.9	2.8586	5.2	0.0925	4.9	0.35	1304	22	1371	40	1477	93	88
AK27-seq4-D07	447	34	7	0.61	634	0.1708	2.8	1.7432	8.2	0.0740	7.7	0.34	1017	26	1025	54	1042	155	98
AK27-seq4-D08	506	36	7	0.49	704	0.1809	2.5	1.8792	8.1	0.0753	7.7	0.30	1072	24	1074	55	1077	155	100
AK27-seq4-D09	15157	443	147	0.17	14467	0.3246	1.7	4.8895	2.3	0.1093	1.5	0.75	1812	28	1800	20	1787	28	101
AK27-seq4-D10	3018	214	56	0.29	3568	0.2490	1.1	3.0515	3.6	0.0889	3.5	0.31	1433	14	1421	28	1402	66	102
AK27-seq4-D11	565	24	9	0.46	532	0.3339	2.9	5.1737	9.1	0.1124	8.6	0.32	1857	47	1848	80	1838	156	101
AK27-seq4-D12	9571	90	55	0.25	5222	0.5436	1.5	14.3645	2.8	0.1917	2.4	0.52	2798	33	2774	27	2756	39	102
AK27-seq4-D13	2805	234	50	0.18	3572	0.2135	1.6	2.4307	3.6	0.0826	3.2	0.46	1248	19	1252	26	1259	62	99
AK27-seq4-D14	310	78	6	0.52	581	0.0712	3.0	0.5497	9.1	0.0560	8.6	0.33	443	13	445	33	452	192	98
Sample 56/26-2B (AK25)			**Well no.: 56/26-2B**				**Location (decimal degrees):**				**50.007**	**9.897846W**			**Datum: IRENET95**				
AK25-seq1-a01	2485	87	21	0.38	2940	0.2240	2.1	2.7461	3.8	0.0889	3.2	0.54	1303	25	1341	29	1402	62	93
AK25-seq1-a02	1166	197	19	0.20	1842	0.0969	2.1	0.8893	4.9	0.0665	4.4	0.44	596	12	646	24	823	93	72
AK25-seq1-a03	854	110	12	0.78	1492	0.0962	2.4	0.7979	5.9	0.0602	5.3	0.41	592	14	596	27	610	115	97
AK25-seq1-a04	943	76	12	0.62	1494	0.1391	2.3	1.2769	6.0	0.0666	5.5	0.38	840	18	835	35	824	116	102
AK25-seq1-a05	708	88	10	0.50	1222	0.1011	2.4	0.8451	6.1	0.0606	5.7	0.39	621	14	622	29	625	122	99
AK25-seq1-a06	2583	57	21	0.51	2551	0.3205	2.3	4.7449	3.7	0.1074	2.8	0.64	1792	37	1775	31	1755	51	102
AK25-seq1-a07	543	119	8	0.68	1030	0.0606	2.7	0.4661	6.8	0.0558	6.2	0.40	379	10	388	22	445	138	85
AK25-seq1-a08	1493	448	29	0.31	2773	0.0633	2.1	0.4954	4.4	0.0567	3.8	0.49	396	8	409	15	481	84	82
AK25-seq1-a09	3322	735	42	0.28	6169	0.0569	2.1	0.4478	3.3	0.0571	2.5	0.64	357	7	376	10	494	56	72
AK25-seq1-a10	3588	195	35	0.15	4868	0.1818	2.1	1.9501	3.3	0.0778	2.5	0.64	1077	21	1098	22	1142	50	94
AK25-seq1-a11	1471	338	19	0.08	2847	0.0583	2.4	0.4370	5.1	0.0543	4.5	0.47	366	9	368	16	385	101	95
AK25-seq1-a12	9385	437	102	0.24	6065	0.2262	2.2	3.2568	3.1	0.1044	2.2	0.70	1314	26	1471	24	1704	40	77
AK25-seq1-a13	23663	237	83	0.37	22681	0.3255	2.1	4.9605	2.7	0.1105	1.7	0.79	1817	34	1813	23	1808	30	100
AK25-seq1-a14	497	105	7	0.54	963	0.0616	2.9	0.4614	7.4	0.0544	6.7	0.40	385	11	385	24	386	151	100
AK25-seq1-a15	1296	177	18	0.54	2275	0.0935	2.2	0.7731	4.2	0.0600	3.6	0.53	576	12	582	19	602	78	96
AK25-seq1-a16	4523	113	23	0.38	5954	0.1953	1.9	2.1549	2.8	0.0800	2.1	0.67	1150	20	1167	19	1197	41	96
AK25-seq1-a17	672	234	17	0.48	1300	0.0665	2.4	0.5048	6.9	0.0550	6.4	0.34	415	9	415	24	414	144	100
AK25-seq1-a18	4212	69	32	0.98	3458	0.3579	2.3	6.3397	3.9	0.1285	3.1	0.59	1972	39	2024	35	2077	55	95
AK25-seq1-a19	16687	443	91	0.26	23808	0.2017	1.9	2.0553	2.2	0.0739	1.1	0.86	1185	20	1134	15	1038	23	114
AK25-seq1-a20	952	137	13	0.55	1583	0.0849	2.0	0.7422	6.3	0.0634	6.0	0.32	525	10	564	28	722	127	73
AK25-seq1-a21	2175	102	28	0.39	2441	0.2574	2.0	3.3621	3.7	0.0948	3.0	0.55	1476	27	1496	29	1523	57	97
AK25-seq1-a22	-347	50	5	0.26	658	0.0972	3.0	0.6555	-	0.0489	-	-	598	17	512	-	145	-	413
AK25-seq1-a23	1312	155	17	0.33	2270	0.1047	2.8	0.8816	5.5	0.0611	4.7	0.52	642	17	642	26	642	101	100
AK25-seq1-a24	679	100	10	0.78	1218	0.0869	2.5	0.7049	5.4	0.0588	4.8	0.47	537	13	542	23	561	104	96
AK25-seq1-a25	1477	510	30	0.26	2794	0.0587	2.3	0.4506	4.2	0.0557	3.6	0.53	368	8	378	13	440	79	84
AK25-seq1-a26	1534	369	43	0.17	2747	0.1222	2.3	0.9935	5.2	0.0590	4.7	0.45	743	16	700	27	566	102	131
AK25-seq1-a27	749	95	10	0.90	1142	0.0838	3.1	0.8004	7.2	0.0693	6.5	0.43	519	15	597	33	907	134	57
AK25-seq1-a28	560	106	12	0.36	966	0.1065	2.3	0.9002	9.1	0.0613	8.8	0.25	653	14	652	45	650	189	100
AK25-seq1-a29	1311	283	18	0.38	2497	0.0617	2.1	0.4661	5.5	0.0548	5.1	0.39	386	8	388	18	405	113	95
AK25-seq1-a30	658	213	15	0.46	1260	0.0650	2.8	0.4922	6.4	0.0549	5.8	0.43	406	11	406	22	407	130	100

AK25-seq1-a31	768	138	15	0.39	1271	0.1038	2.1	0.9122	6.1	0.0637	5.8	0.35	637	13	658	30	733	122	87
AK25-seq1-a32	7799	90	38	0.49	4560	0.3580	2.4	8.9025	4.6	0.1804	3.9	0.53	1972	41	2328	43	2656	64	74
AK25-seq1-a33	407	52	6	0.96	724	0.0844	5.1	0.6860	10.8	0.0590	9.5	0.48	522	26	530	46	566	206	92
AK25-seq1-a34	3727	51	16	0.39	3876	0.2874	2.2	4.0205	3.5	0.1015	2.7	0.63	1628	31	1638	29	1651	50	99
AK25-seq1-a35	7286	180	63	0.80	7477	0.2856	2.0	4.0463	2.9	0.1028	2.0	0.70	1619	29	1644	24	1675	38	97
AK25-seq1-a36	2694	108	37	0.74	2682	0.2978	2.0	4.3530	3.9	0.1060	3.3	0.52	1680	30	1703	33	1732	61	97
AK25-seq1-a37	20079	237	136	0.14	11306	0.5407	2.1	13.9340	2.9	0.1869	2.1	0.71	2786	47	2745	28	2715	34	103
AK25-seq1-a38	1292	358	27	0.40	1932	0.0697	5.7	0.6724	9.5	0.0700	7.6	0.60	434	24	522	40	928	157	47
AK25-seq1-a39	7488	248	84	0.12	7021	0.3391	2.0	5.2959	2.9	0.1133	2.2	0.67	1882	32	1868	25	1853	39	102
AK25-seq1-a40	19590	422	138	0.21	18906	0.3171	2.5	4.7790	2.8	0.1093	1.4	0.88	1775	38	1781	24	1788	25	99
AK25-seq1-a41	3685	295	60	0.38	4851	0.1927	2.3	2.0971	4.2	0.0789	3.6	0.54	1136	24	1148	30	1170	70	97
AK25-seq1-a42	957	110	14	0.81	1553	0.1031	2.9	0.9211	4.8	0.0648	3.8	0.60	632	17	663	24	769	81	82
AK25-seq1-a43	1640	194	21	0.47	2824	0.0992	2.8	0.8397	4.3	0.0614	3.2	0.67	610	17	619	20	653	68	93
AK25-seq1-a44	1181	231	16	0.24	2226	0.0699	2.3	0.5397	4.8	0.0560	4.2	0.49	436	10	438	17	451	93	97
AK25-seq1-a45	5787	165	45	0.18	6361	0.2713	2.7	3.5929	3.8	0.0960	2.6	0.72	1548	38	1548	30	1548	49	100
AK25-seq1-a46	3409	92	32	0.88	3623	0.2769	2.2	3.7825	3.8	0.0991	3.1	0.59	1576	31	1589	31	1606	57	98
AK25-seq1-a47	5992	140	43	0.25	5805	0.2936	2.1	4.4056	3.3	0.1088	2.6	0.62	1660	30	1713	28	1780	47	93
AK25-seq1-a48	579	137	9	0.53	1180	0.0583	2.5	0.4180	7.4	0.0520	6.9	0.34	365	9	355	22	285	158	128
AK25-seq1-a49	1092	52	10	0.27	1432	0.1943	2.7	2.1409	5.9	0.0799	5.2	0.45	1145	28	1162	42	1195	103	96
AK25-seq1-a50	995	80	15	0.37	1313	0.1773	2.4	1.9510	5.0	0.0798	4.4	0.48	1052	23	1099	34	1192	87	88
AK25-seq1-a51	1643	413	26	0.36	3178	0.0613	2.5	0.4617	5.4	0.0547	4.8	0.46	383	9	385	17	399	107	96
AK25-seq1-a52	5349	78	35	0.56	4252	0.3825	2.0	7.0094	3.2	0.1329	2.4	0.64	2088	36	2113	29	2137	43	98
AK25-seq1-a53	643	133	9	0.45	1232	0.0654	2.7	0.4958	6.0	0.0550	5.4	0.44	409	11	409	20	411	120	99
AK25-seq1-a54	478	76	10	0.69	786	0.1132	2.6	1.0027	8.6	0.0642	8.2	0.30	692	17	705	45	749	174	92
AK25-seq1-a55	881	264	19	0.54	1640	0.0655	2.8	0.5133	5.6	0.0568	4.8	0.50	409	11	421	19	485	106	84
AK25-seq1-a56	879	32	9	0.72	1060	0.2263	2.5	2.7318	5.3	0.0876	4.7	0.46	1315	29	1337	40	1373	91	96
AK25-seq1-a57	509	155	11	0.65	962	0.0643	2.5	0.4883	8.7	0.0551	8.3	0.29	402	10	404	29	416	186	96
AK25-seq1-a58	393	135	8	0.34	786	0.0578	2.6	0.4199	9.2	0.0527	8.8	0.28	362	9	356	28	314	201	115
AK25-seq1-a59	12912	291	123	0.39	10281	0.3842	2.3	6.9593	2.9	0.1314	1.7	0.81	2096	42	2106	26	2116	30	99
AK25-seq1-a60	588	110	10	1.15	1060	0.0650	2.4	0.5250	5.5	0.0585	5.0	0.43	406	9	428	20	550	109	74
AK25-seq2-b01	341	58	5	0.88	654	0.0713	2.5	0.5235	10.2	0.0532	9.9	0.25	444	11	427	36	339	223	131
AK25-seq2-b02	1853	724	35	0.42	3355	0.0445	2.8	0.3446	4.9	0.0562	4.0	0.58	280	8	301	13	461	88	61
AK25-seq2-b03	4613	117	33	0.21	4950	0.2763	2.2	3.6383	3.1	0.0955	2.2	0.72	1573	31	1558	25	1538	41	102
AK25-seq2-b04	841	157	12	0.77	1643	0.0628	2.8	0.4547	5.4	0.0525	4.7	0.51	392	11	381	17	309	106	127
AK25-seq2-b05	3439	138	37	1.15	4568	0.1912	2.5	2.0332	3.8	0.0771	2.9	0.66	1128	26	1127	27	1124	58	100
AK25-seq2-b06	11871	177	79	0.48	9927	0.3929	2.2	6.6410	2.8	0.1226	1.8	0.79	2136	41	2065	25	1994	31	107
AK25-seq2-b07	4500	78	30	0.53	4055	0.3368	2.5	5.3834	3.2	0.1159	2.0	0.78	1871	41	1882	28	1894	36	99
AK25-seq2-b08	29149	338	188	0.41	13329	0.4932	2.6	12.8449	2.9	0.1889	1.2	0.90	2584	56	2668	28	2733	20	95
AK25-seq2-b09	431	124	8	0.46	780	0.0619	2.5	0.4841	7.3	0.0567	6.8	0.34	387	9	401	24	480	151	81
AK25-seq2-b10	11201	113	36	0.21	10834	0.3076	2.3	4.4885	2.7	0.1058	1.4	0.86	1729	36	1729	23	1729	26	100
AK25-seq2-b11	1722	33	14	1.11	1652	0.3114	2.3	4.5830	4.7	0.1067	4.1	0.50	1747	36	1746	40	1745	75	100
AK25-seq2-b12	7644	351	74	0.53	10416	0.1888	2.3	1.9571	3.1	0.0752	2.0	0.77	1115	24	1101	21	1074	39	104

AK25-seq2-b13	6036	199	47	0.18	7087	0.2366	2.5	2.8465	3.2	0.0873	2.0	0.79	1369	31	1368	24	1366	38	100
AK25-seq2-b14	1067	111	12	0.49	1733	0.0932	2.4	0.8118	4.9	0.0632	4.3	0.50	575	13	603	23	713	91	81
AK25-seq2-b15	1361	231	23	0.31	2236	0.0973	3.1	0.8474	6.1	0.0631	5.3	0.50	599	18	623	29	713	113	84
AK25-seq2-b16	1236	21	7	0.26	1045	0.3064	2.8	5.1244	4.7	0.1213	3.7	0.61	1723	43	1840	41	1976	66	87
AK25-seq2-b17	446	97	5	0.23	847	0.0552	3.5	0.4079	9.3	0.0536	8.6	0.38	346	12	347	28	354	194	98
AK25-seq2-b18	1202	213	14	0.13	2214	0.0696	2.4	0.5344	5.2	0.0557	4.6	0.46	433	10	435	19	442	103	98
AK25-seq2-b19	16747	446	134	0.37	18227	0.2804	2.5	3.6408	2.9	0.0942	1.3	0.89	1593	36	1559	23	1512	25	105
AK25-seq2-b20	1147	61	14	0.30	1340	0.2246	2.6	2.7075	5.7	0.0874	5.0	0.46	1306	31	1331	43	1370	97	95
AK25-seq2-b21	5113	115	37	0.42	5036	0.2925	2.5	4.1974	3.5	0.1041	2.4	0.71	1654	36	1674	29	1698	45	97
AK25-seq2-b22	1075	209	17	1.00	2013	0.0621	3.0	0.4669	7.3	0.0545	6.7	0.40	389	11	389	24	392	151	99
AK25-seq2-b23	445	56	6	0.58	734	0.0955	2.5	0.8178	7.3	0.0621	6.8	0.34	588	14	607	34	678	146	87
AK25-seq2-b24	1695	236	14	0.87	3313	0.0486	2.6	0.3525	4.0	0.0526	3.1	0.64	306	8	307	11	310	71	99
AK25-seq2-b25	895	194	11	0.16	1685	0.0554	2.7	0.4165	5.0	0.0545	4.2	0.54	348	9	354	15	391	95	89
AK25-seq2-b26	614	117	8	0.42	1086	0.0619	3.2	0.4956	6.8	0.0580	6.0	0.46	387	12	409	23	531	132	73
AK25-seq2-b27	419	77	6	0.57	732	0.0646	2.7	0.5219	7.9	0.0586	7.4	0.35	404	11	426	28	551	162	73
AK25-seq2-b28	1591	360	21	0.18	3010	0.0596	2.4	0.4444	4.0	0.0541	3.2	0.60	373	9	373	12	375	71	100
AK25-seq2-b29	1625	100	17	0.45	2306	0.1513	2.9	1.4698	5.2	0.0705	4.3	0.56	908	25	918	32	942	89	96
AK25-seq2-b30	1228	155	18	0.72	1859	0.0965	3.0	0.8066	5.7	0.0606	4.8	0.53	594	17	601	26	625	104	95
AK25-seq2-b31	11259	329	93	0.34	12979	0.2668	2.4	3.2881	3.0	0.0894	1.8	0.80	1525	32	1478	23	1412	34	108
AK25-seq2-b32	22496	763	195	0.05	13144	0.2632	3.3	3.8567	3.6	0.1063	1.3	0.93	1506	45	1605	29	1737	25	87
AK25-seq2-b33	4541	123	38	0.58	4697	0.2667	2.6	3.6444	3.4	0.0991	2.2	0.76	1524	35	1559	28	1607	42	95
AK25-seq2-b34	8631	151	66	0.94	7361	0.3369	2.6	5.5652	3.2	0.1198	2.0	0.80	1872	42	1911	28	1953	35	96
AK25-seq2-b35	925	81	12	0.48	1327	0.1304	2.5	1.2510	6.6	0.0696	6.1	0.38	790	19	824	38	916	126	86
AK25-seq2-b36	959	211	18	0.49	1716	0.0776	2.6	0.6093	5.8	0.0570	5.1	0.46	482	12	483	22	490	113	98
AK25-seq2-b37	7627	162	56	0.38	7325	0.3161	2.4	4.6531	3.5	0.1068	2.6	0.68	1771	37	1759	30	1745	47	101
AK25-seq2-b38	5368	78	31	0.18	4222	0.3862	2.5	6.9487	3.4	0.1305	2.2	0.75	2105	45	2105	30	2105	39	100
AK25-seq2-b39	1830	54	14	1.67	2506	0.1708	2.7	1.7641	4.5	0.0749	3.6	0.61	1017	26	1032	30	1066	72	95
AK25-seq2-b40	1023	95	11	0.26	1574	0.1176	3.4	1.0810	6.6	0.0667	5.6	0.52	717	23	744	35	828	117	87
AK25-seq2-b41	7103	198	81	0.68	6425	0.3380	2.6	5.3351	3.6	0.1145	2.5	0.72	1877	42	1875	31	1872	45	100
AK25-seq2-b42	697	91	12	0.33	1035	0.1275	2.7	1.2285	6.8	0.0699	6.2	0.40	774	20	814	39	924	128	84
AK25-seq2-b43	1110	224	18	0.74	2039	0.0671	2.6	0.5160	4.8	0.0558	4.1	0.54	419	11	422	17	443	90	94
AK25-seq2-b44	3085	62	24	0.68	2811	0.3280	2.5	5.0870	4.5	0.1125	3.7	0.56	1829	41	1834	39	1840	67	99
AK25-seq2-b45	23966	303	128	0.01	17257	0.4261	3.3	8.4692	4.1	0.1441	2.4	0.80	2288	64	2283	38	2278	42	100
AK25-seq2-b46	971	136	17	1.23	1673	0.0910	3.1	0.7416	5.5	0.0591	4.6	0.56	561	16	563	24	571	99	98
AK25-seq2-b47	8345	137	49	0.04	6945	0.3601	2.5	6.1159	3.1	0.1232	2.0	0.78	1983	42	1993	28	2003	35	99
AK25-seq2-b48	1697	338	33	0.25	2906	0.0978	2.9	0.8087	4.6	0.0600	3.6	0.63	602	17	602	21	602	78	100
AK25-seq2-b49	646	67	12	0.42	910	0.1699	3.0	1.7087	6.5	0.0729	5.8	0.46	1012	28	1012	42	1012	117	100
AK25-seq2-b50	2264	300	43	0.23	3430	0.1406	3.5	1.3097	4.9	0.0675	3.5	0.70	848	28	850	29	854	73	99
AK25-seq2-b51	1643	40	14	0.62	1538	0.2936	3.0	4.4318	4.9	0.1095	3.8	0.62	1659	45	1718	41	1791	70	93
AK25-seq2-b52	6013	284	77	0.26	6669	0.2615	2.6	3.3290	3.0	0.0923	1.5	0.86	1498	34	1488	23	1474	28	102
AK25-seq2-b53	1474	277	33	0.70	2546	0.1039	2.5	0.8485	4.7	0.0592	3.9	0.54	637	15	624	22	576	86	111
AK25-seq2-b54	5952	204	72	0.55	5771	0.3103	2.3	4.5211	3.2	0.1057	2.1	0.74	1742	36	1735	27	1726	39	101

AK25-seq2-b55	4474	199	57	0.47	4933	0.2567	2.9	3.3191	4.4	0.0938	3.3	0.67	1473	39	1486	35	1503	62	98
AK25-seq2-b56	8553	303	119	0.52	5734	0.3568	3.0	5.1026	3.9	0.1037	2.5	0.76	1967	50	1837	33	1692	46	116
AK25-seq2-b57	6042	62	33	0.33	3636	0.4839	2.5	11.3671	3.4	0.1704	2.3	0.74	2544	53	2554	32	2561	38	99
AK25-seq2-b58	658	217	17	0.71	1207	0.0685	3.0	0.5299	7.6	0.0561	7.0	0.40	427	13	432	27	455	156	94
AK25-seq2-b59	507	108	11	0.46	851	0.1001	2.5	0.8384	6.9	0.0607	6.5	0.35	615	14	618	33	630	140	98
AK25-seq2-b60	5241	386	88	0.43	6586	0.2131	2.4	2.3762	3.4	0.0809	2.4	0.72	1245	28	1235	25	1218	47	102
AK25-seq3-c01	2726	314	59	0.62	3838	0.1631	1.9	1.6341	3.1	0.0726	2.4	0.62	974	17	983	20	1004	49	97
AK25-seq3-c02	4076	32	23	0.46	1790	0.5654	2.0	18.2002	3.3	0.2335	2.7	0.60	2889	47	3000	32	3076	42	94
AK25-seq3-c03	4510	165	43	0.26	5109	0.2478	2.4	3.0536	3.4	0.0894	2.4	0.71	1427	31	1421	26	1412	46	101
AK25-seq3-c04	1029	167	16	0.23	1767	0.0924	2.1	0.7600	5.8	0.0596	5.4	0.36	570	11	574	26	590	117	97
AK25-seq3-c05	1946	141	27	0.62	2769	0.1648	2.1	1.6273	4.2	0.0716	3.6	0.50	983	19	981	27	975	74	101
AK25-seq3-c06	501	68	8	0.80	777	0.0944	2.3	0.8714	8.2	0.0670	7.8	0.28	581	13	636	39	836	163	70
AK25-seq3-c07	19990	153	96	0.25	10301	0.5493	2.1	15.0682	2.7	0.1989	1.7	0.77	2822	48	2820	26	2818	28	100
AK25-seq3-c08	26563	441	226	0.11	16098	0.4863	1.8	11.3300	2.3	0.1690	1.4	0.80	2555	39	2551	22	2548	23	100
AK25-seq3-c09	627	169	9	0.14	1193	0.0549	2.7	0.4053	7.1	0.0535	6.5	0.38	345	9	345	21	351	148	98
AK25-seq3-c10	2853	238	48	0.16	3793	0.2018	1.9	2.1422	2.9	0.0770	2.2	0.64	1185	20	1163	20	1121	44	106
Sample 56/22-1 (AK26)			**Well no.: 56/22-1**				**Location (decimal degrees):**				**50.185**	**9.636133W**			**Datum: IRENET95**				
AK26-seq1-A01	652	110	13	0.85	1144	0.0915	2.1	0.7561	8.6	0.0599	8.3	0.24	565	11	572	38	600	180	94
AK26-seq1-A02	1440	476	40	0.50	2648	0.0763	1.5	0.5988	4.5	0.0569	4.3	0.34	474	7	476	17	489	94	97
AK26-seq1-A03	2509	222	41	0.32	3257	0.1713	2.7	1.9144	4.9	0.0811	4.1	0.56	1019	26	1086	33	1223	80	83
AK26-seq1-A04	1530	454	26	0.08	2920	0.0602	1.7	0.4505	5.9	0.0543	5.7	0.28	377	6	378	19	384	128	98
AK26-seq1-A05	4810	149	50	0.60	4902	0.2845	2.3	4.0204	3.6	0.1025	2.8	0.63	1614	32	1638	30	1670	52	97
AK26-seq1-A06	712	113	15	0.47	1158	0.1216	2.8	1.0702	7.0	0.0638	6.4	0.40	740	20	739	37	737	135	100
AK26-seq1-A07	513	208	13	0.14	983	0.0654	2.3	0.4933	7.6	0.0547	7.3	0.30	409	9	407	26	399	163	102
AK26-seq1-A08	4308	79	34	0.25	3407	0.3979	1.9	7.2610	3.8	0.1324	3.2	0.51	2159	35	2144	34	2130	57	101
AK26-seq1-A09	1546	378	44	0.33	2532	0.1164	4.0	1.0108	6.3	0.0630	4.8	0.64	710	27	709	33	708	103	100
AK26-seq1-A10	374	103	7	0.69	720	0.0617	2.3	0.4647	8.9	0.0546	8.6	0.26	386	9	388	29	398	193	97
AK26-seq1-A11	1108	43	18	0.81	1031	0.3260	2.3	5.0696	6.3	0.1128	5.9	0.36	1819	36	1831	55	1845	107	99
AK26-seq1-A12	324	50	8	0.68	492	0.1379	2.7	1.3014	9.5	0.0684	9.1	0.29	833	21	846	56	881	188	95
AK26-seq1-A13	791	315	23	0.34	1498	0.0711	1.5	0.5443	7.6	0.0555	7.4	0.20	443	6	441	27	434	165	102
AK26-seq1-A14	483	49	10	0.37	675	0.1891	2.8	1.9841	8.1	0.0761	7.7	0.34	1117	28	1110	57	1097	153	102
AK26-seq1-A15	846	235	26	0.78	1486	0.0913	2.0	0.7457	6.1	0.0592	5.7	0.33	563	11	566	27	575	124	98
AK26-seq1-A16	1203	321	38	0.73	2069	0.1032	2.6	0.8686	5.7	0.0611	5.1	0.46	633	16	635	28	642	110	99
AK26-seq1-A17	1452	382	36	0.21	2069	0.0941	2.4	0.9579	6.7	0.0738	6.3	0.35	580	13	682	34	1037	126	56
AK26-seq1-A18	1764	122	26	0.47	2363	0.1914	2.1	2.0670	5.0	0.0783	4.5	0.43	1129	22	1138	34	1155	89	98
AK26-seq1-A19	422	110	8	0.56	808	0.0659	2.4	0.5016	8.7	0.0552	8.3	0.27	411	10	413	30	421	186	98
AK26-seq1-A20	1836	450	54	0.72	3101	0.1039	1.6	0.8841	3.7	0.0617	3.3	0.45	637	10	643	18	664	70	96
AK26-seq1-A21	45	20	2	0.62	140	0.0956	5.6	0.4457	29.6	0.0338	29.1	0.19	589	31	374	97	-806	826	-73
AK26-seq1-A22	393	101	9	0.22	667	0.0923	3.0	0.8050	9.2	0.0633	8.7	0.33	569	16	600	42	717	184	79
AK26-seq1-A23	432	153	13	0.36	793	0.0791	2.1	0.6181	7.3	0.0567	7.0	0.29	490	10	489	29	480	154	102
AK26-seq1-A24	468	100	12	0.31	798	0.1161	2.0	0.9786	6.0	0.0611	5.6	0.34	708	14	693	30	644	121	110
AK26-seq1-A25	5014	293	113	1.16	5678	0.2898	1.3	3.6838	2.6	0.0922	2.3	0.49	1641	18	1568	21	1471	43	112

AK26-seq1-A26	1076	170	20	0.59	1753	0.0993	2.0	0.8779	4.7	0.0641	4.2	0.43	610	12	640	22	747	89	82
AK26-seq1-A27	3045	39	19	0.29	1752	0.4186	2.6	10.5133	5.7	0.1822	5.1	0.44	2254	49	2481	55	2673	85	84
AK26-seq1-A28	2592	446	48	0.38	4435	0.1053	1.7	0.8852	3.9	0.0610	3.5	0.43	646	10	644	19	638	76	101
AK26-seq1-A29	388	122	14	0.91	694	0.0912	2.6	0.7367	9.6	0.0586	9.2	0.27	563	14	560	42	551	201	102
AK26-seq1-A30	1229	36	15	0.19	991	0.4020	1.9	7.2888	4.8	0.1315	4.4	0.39	2178	35	2147	44	2118	77	103
AK26-seq2-B01	3476	228	46	0.26	4191	0.1937	2.2	2.3292	3.4	0.0872	2.7	0.63	1141	23	1221	25	1365	51	84
AK26-seq2-B02	1357	428	31	0.46	2540	0.0675	1.7	0.5210	4.4	0.0560	4.0	0.40	421	7	426	15	451	89	93
AK26-seq2-B03	647	147	17	1.05	1165	0.0895	2.0	0.7220	7.6	0.0585	7.3	0.27	553	11	552	33	548	160	101
AK26-seq2-B04	254	48	6	0.49	430	0.1106	2.8	0.9471	9.9	0.0621	9.4	0.29	676	18	677	50	677	202	100
AK26-seq2-B05	249	49	5	0.51	445	0.0916	3.9	0.7526	13.3	0.0596	12.7	0.30	565	21	570	60	589	276	96
AK26-seq2-B06	302	61	6	0.35	519	0.1008	2.6	0.8491	10.1	0.0611	9.8	0.26	619	15	624	48	643	210	96
AK26-seq2-B07	4859	97	57	0.56	3813	0.5251	1.3	9.6656	2.8	0.1335	2.4	0.48	2721	30	2403	26	2145	42	127
AK26-seq2-B08	10153	95	41	0.56	8461	0.3732	1.5	6.4941	2.3	0.1262	1.7	0.65	2044	26	2045	20	2046	30	100
AK26-seq2-B09	942	130	14	0.49	1655	0.0950	2.0	0.7835	5.9	0.0598	5.6	0.34	585	11	587	27	597	121	98
AK26-seq2-B10	1008	323	16	0.11	526	0.0514	6.8	0.4077	9.8	0.0576	7.1	0.69	323	21	347	29	514	156	63
AK26-seq2-B11	360	115	11	1.20	685	0.0709	2.5	0.5436	9.8	0.0556	9.4	0.26	442	11	441	36	435	210	101
AK26-seq2-B12	2837	227	53	0.58	3824	0.2094	1.5	2.2466	3.6	0.0778	3.2	0.43	1226	17	1196	25	1142	64	107
AK26-seq2-B13	1394	315	31	0.39	2480	0.0933	1.8	0.7610	4.9	0.0591	4.5	0.38	575	10	575	22	573	98	100
AK26-seq2-B14	727	159	14	0.88	1354	0.0758	1.7	0.5917	6.8	0.0566	6.6	0.25	471	8	472	26	476	146	99
AK26-seq2-B15	2967	51	29	1.43	2439	0.3878	2.1	6.8514	3.5	0.1281	2.8	0.61	2113	38	2092	31	2072	49	102
AK26-seq2-B16	3086	183	38	0.44	4278	0.1893	2.1	1.9849	3.4	0.0760	2.7	0.61	1118	21	1110	24	1096	55	102
AK26-seq2-B17	266	35	4	0.76	462	0.1018	2.5	0.8578	10.4	0.0611	10.1	0.24	625	15	629	50	643	217	97
AK26-seq2-B18	999	132	14	0.43	1712	0.0988	2.4	0.8375	5.2	0.0615	4.6	0.47	607	14	618	24	656	98	93
AK26-seq2-B19	3802	186	40	0.24	4976	0.2095	1.9	2.3200	3.1	0.0803	2.4	0.61	1226	21	1218	22	1205	48	102
AK26-seq2-B20	459	56	7	0.40	780	0.1083	2.1	0.9337	8.2	0.0625	8.0	0.26	663	13	670	41	693	170	96
AK26-seq2-B21	6357	109	43	0.17	5297	0.3819	1.9	6.6196	2.9	0.1257	2.2	0.65	2085	34	2062	26	2039	40	102
AK26-seq2-B22	560	73	9	0.58	963	0.1085	2.5	0.9183	6.7	0.0614	6.3	0.37	664	16	661	33	654	134	102
AK26-seq2-B23	1030	383	24	0.21	1990	0.0631	1.6	0.4734	5.9	0.0544	5.7	0.28	394	6	394	19	388	127	102
AK26-seq2-B24	4265	236	71	0.31	4937	0.2921	2.2	3.6325	3.4	0.0902	2.7	0.63	1652	32	1557	28	1429	51	116
AK26-seq2-B25	13879	312	105	0.41	12225	0.3012	2.2	4.9192	2.7	0.1184	1.5	0.82	1697	34	1806	23	1933	28	88
AK26-seq2-B26	1046	220	17	0.47	1960	0.0694	1.9	0.5367	4.4	0.0561	4.0	0.43	433	8	436	16	456	88	95
AK26-seq2-B27	757	115	10	0.30	1317	0.0864	2.1	0.7174	6.1	0.0602	5.7	0.35	534	11	549	26	612	123	87
AK26-seq2-B28	294	59	6	0.23	508	0.0953	2.1	0.7893	11.5	0.0601	11.3	0.18	587	12	591	53	606	245	97
AK26-seq2-B29	7625	90	48	0.44	5065	0.4596	2.2	10.0401	3.3	0.1584	2.4	0.66	2438	44	2438	31	2439	41	100
AK26-seq2-B30	2070	420	65	2.01	2057	0.0954	1.8	0.8213	3.7	0.0625	3.2	0.48	587	10	609	17	690	69	85
AK26-seq2-B31	1096	223	26	0.21	1783	0.1174	2.6	1.0445	5.4	0.0645	4.8	0.47	716	17	726	29	759	101	94
AK26-seq2-B32	331	54	5	0.56	586	0.0862	3.6	0.6938	14.4	0.0584	13.9	0.25	533	18	535	62	544	304	98
AK26-seq2-B33	451	98	12	0.68	775	0.1006	1.8	0.8373	7.4	0.0603	7.2	0.25	618	11	618	35	615	156	100
AK26-seq2-B34	570	113	14	0.61	972	0.1103	2.5	0.9421	7.5	0.0619	7.0	0.34	675	16	674	37	671	150	101
AK26-seq2-B35	4890	174	60	0.30	4682	0.3229	1.7	4.8962	3.3	0.1100	2.8	0.52	1804	28	1802	29	1799	52	100
AK26-seq2-B36	370	126	8	0.20	704	0.0677	3.2	0.5179	9.2	0.0555	8.6	0.35	422	13	424	32	432	193	98
AK26-seq2-B37	13150	137	71	0.48	8159	0.4281	1.7	9.9966	2.6	0.1694	2.0	0.65	2297	32	2434	24	2551	33	90

AK26-seq2-B38	1765	250	27	0.34	3055	0.1020	2.1	0.8535	3.8	0.0607	3.1	0.56	626	13	627	18	629	68	100
AK26-seq2-B39	1798	50	17	0.61	1849	0.2959	2.1	4.1719	4.4	0.1023	3.9	0.48	1671	31	1669	37	1665	72	100
AK26-seq2-B40	1784	77	27	0.62	1845	0.2968	2.2	4.1586	4.6	0.1016	4.0	0.48	1675	33	1666	38	1654	74	101
AK26-seq2-B41	3146	82	40	0.81	2564	0.4010	2.2	7.1410	3.7	0.1292	3.0	0.59	2174	40	2129	33	2086	52	104
AK26-seq2-B42	10263	335	127	0.35	7200	0.3332	1.8	6.8693	2.7	0.1495	2.0	0.68	1854	30	2095	24	2341	34	79
AK26-seq2-B43	22823	844	312	0.24	1252	0.3564	2.3	5.6657	3.0	0.1153	1.9	0.77	1965	39	1926	26	1884	34	104
AK26-seq2-B44	1220	413	30	0.64	2128	0.0626	2.5	0.5100	8.4	0.0591	8.0	0.30	391	10	418	29	571	175	69
AK26-seq2-B45	522	172	13	0.71	876	0.0623	2.4	0.5562	10.4	0.0647	10.1	0.23	390	9	449	39	765	214	51
AK26-seq2-B46	5584	212	79	0.56	5420	0.3212	1.5	4.8075	2.8	0.1085	2.4	0.55	1796	24	1786	24	1775	43	101
AK26-seq2-B47	314	61	8	0.81	531	0.1080	3.1	0.9281	10.6	0.0623	10.1	0.29	661	19	667	53	685	216	97
AK26-seq2-B48	546	131	13	0.43	969	0.0931	1.8	0.7549	7.7	0.0588	7.5	0.23	574	10	571	34	560	164	102
AK26-seq2-B49	953	186	23	0.70	1613	0.1055	2.3	0.8984	6.3	0.0618	5.9	0.37	646	14	651	31	666	126	97
AK26-seq2-B50	12179	111	66	0.32	7199	0.5236	2.3	12.8353	3.0	0.1778	1.9	0.78	2715	51	2668	28	2632	31	103
AK26-seq2-B51	715	281	17	0.42	1332	0.0547	2.7	0.4260	7.0	0.0565	6.4	0.39	343	9	360	21	472	142	73
AK26-seq2-B52	3135	73	32	0.31	2384	0.4010	1.7	7.6908	3.6	0.1391	3.1	0.48	2174	31	2196	33	2216	54	98
AK26-seq2-B53	3605	38	16	0.61	3207	0.3486	1.7	5.6714	3.0	0.1180	2.5	0.57	1928	29	1927	26	1926	44	100
AK26-seq2-B54	451	34	4	0.26	781	0.1018	2.0	0.8557	8.6	0.0610	8.4	0.23	625	12	628	41	639	181	98
AK26-seq2-B55	303	59	7	0.54	482	0.0992	3.7	0.9040	10.8	0.0661	10.1	0.35	610	22	654	53	810	212	75
AK26-seq2-B56	334	113	9	0.58	633	0.0700	2.8	0.5355	10.3	0.0555	9.9	0.27	436	12	435	37	431	221	101
AK26-seq2-B58	395	153	9	0.11	762	0.0627	2.4	0.4845	9.4	0.0560	9.1	0.26	392	9	401	32	454	202	86
AK26-seq2-B59	561	190	14	0.62	1021	0.0658	3.0	0.5220	7.6	0.0575	7.0	0.39	411	12	426	27	513	154	80
AK26-seq2-B60	9329	306	106	0.01	8177	0.3568	1.5	5.9120	2.9	0.1202	2.4	0.54	1967	26	1963	25	1959	43	100
AK26-seq3-C01	4701	88	36	0.41	4004	0.3649	1.8	6.2057	3.3	0.1234	2.8	0.54	2005	31	2005	30	2005	50	100
AK26-seq3-C02	439	145	11	0.59	756	0.0652	1.8	0.5473	7.7	0.0608	7.5	0.24	407	7	443	28	633	162	64
AK26-seq3-C03	371	129	9	0.46	712	0.0622	3.9	0.4660	8.2	0.0544	7.2	0.48	389	15	388	27	387	161	101
AK26-seq3-C04	454	51	7	0.64	707	0.1137	3.3	1.0563	7.9	0.0674	7.2	0.41	694	21	732	42	850	149	82
AK26-seq3-C05	434	154	12	0.42	817	0.0735	1.9	0.5710	9.8	0.0563	9.6	0.19	457	8	459	37	465	212	98
AK26-seq3-C06	1789	29	19	0.82	1140	0.4869	2.1	11.0214	4.3	0.1642	3.8	0.48	2557	43	2525	41	2499	64	102
AK26-seq3-C07	395	84	9	0.54	683	0.0990	2.3	0.8264	8.9	0.0606	8.6	0.25	608	13	612	42	624	186	98
AK26-seq3-C08	913	327	27	0.67	1726	0.0688	3.0	0.5284	7.6	0.0557	7.0	0.39	429	12	431	27	442	156	97
AK26-seq3-C09	549	88	9	0.59	974	0.0882	2.5	0.7165	6.3	0.0589	5.8	0.39	545	13	549	27	564	127	97
AK26-seq3-C11	7526	163	83	0.45	5834	0.4454	2.3	8.3186	3.2	0.1355	2.3	0.70	2375	45	2266	30	2170	40	109
AK26-seq3-C12	904	133	15	0.45	1564	0.0993	2.0	0.8248	5.9	0.0602	5.5	0.34	610	12	611	27	612	120	100
AK26-seq3-C13	717	210	27	2.33	1332	0.0735	3.5	0.5663	7.9	0.0559	7.1	0.44	457	16	456	30	448	158	102
AK26-seq3-C14	1240	407	37	0.96	2319	0.0704	1.4	0.5423	4.3	0.0559	4.1	0.33	438	6	440	15	448	90	98
AK26-seq3-C15	13469	142	78	0.04	6096	0.5280	2.3	16.9191	3.0	0.2324	1.9	0.78	2733	52	2930	29	3069	30	89
AK26-seq3-C16	595	77	9	0.62	1307	0.0987	2.7	0.8226	10.4	0.0604	10.0	0.26	607	16	610	49	620	217	98
AK26-seq3-C17	2844	63	32	0.51	2128	0.4299	1.8	8.2818	3.8	0.1397	3.4	0.46	2305	34	2262	35	2224	59	104
AK26-seq3-C18	284	23	4	2.27	493	0.1060	10.8	0.8844	19.1	0.0605	15.8	0.56	650	67	643	95	621	340	105
Sample 58/03-1 (BF9)			**Well no.: 58/03-1**				**Location (decimal degrees):**				**50.891**	**7.585781W**			**Datum: IRENET95**				
BF9-seq1-a01	72404	311	33	0.57	322	0.0891	2.0	0.7375	4.0	0.0601	3.5	0.49	550	10	561	17	605	76	91
BF9-seq1-a02	10140	8	3	0.35	2118	0.3613	2.0	5.9411	2.7	0.1193	1.7	0.76	1988	35	1967	24	1945	31	102

BF9-seq1-a03	9278	54	6	0.36	3508	0.1082	2.2	0.8795	3.1	0.0590	2.3	0.69	662	14	641	15	566	49	117
BF9-seq1-a04	145332	169	55	0.38	1779	0.2861	1.9	4.0402	2.1	0.1024	1.0	0.88	1622	27	1642	18	1668	19	97
BF9-seq1-a05	10669	34	6	0.40	11240	0.1589	2.2	1.5386	2.8	0.0702	1.7	0.80	951	19	946	17	935	34	102
BF9-seq1-a06	69635	86	40	1.57	23450	0.2748	2.3	3.8455	2.5	0.1015	1.0	0.92	1565	32	1602	20	1652	18	95
BF9-seq1-a07	3521	24	3	0.93	6161	0.0991	2.1	0.7873	4.4	0.0576	3.9	0.47	609	12	590	20	515	86	118
BF9-seq1-a08	16358	94	13	0.91	27566	0.1000	2.0	0.8316	2.4	0.0603	1.4	0.82	615	12	615	11	615	30	100
BF9-seq1-a09	36548	39	12	0.69	28778	0.2385	5.1	4.0197	5.8	0.1222	2.9	0.87	1379	63	1638	49	1989	52	69
BF9-seq1-a10	24372	20	8	0.46	6682	0.3508	2.0	5.7485	2.6	0.1188	1.6	0.79	1938	34	1939	22	1939	28	100
BF9-seq1-a11	8999	27	5	0.43	10967	0.1781	2.0	1.7284	2.5	0.0704	1.6	0.79	1057	20	1019	16	940	32	112
BF9-seq1-a12	127235	33	23	0.37	59290	0.5800	1.9	17.4508	2.1	0.2182	0.9	0.90	2949	46	2960	21	2968	15	99
BF9-seq1-a13	49665	33	16	0.67	10800	0.3969	1.6	7.5851	1.9	0.1386	1.1	0.84	2155	30	2183	18	2210	18	97
BF9-seq1-a14	4506	13	2	0.36	6281	0.1780	2.1	1.8156	4.0	0.0740	3.3	0.54	1056	21	1051	26	1041	67	101
BF9-seq1-a15	17255	25	8	0.78	17999	0.2422	2.0	3.2469	2.5	0.0972	1.5	0.79	1398	25	1468	19	1571	28	89
BF9-seq1-a16	4936	49	4	0.30	8901	0.0754	2.0	0.5852	4.5	0.0563	4.0	0.44	469	9	468	17	464	90	101
BF9-seq1-a17	6828	72	5	0.40	12534	0.0678	2.0	0.5188	3.2	0.0555	2.5	0.63	423	8	424	11	431	56	98
BF9-seq1-a18	1124	11	1	0.61	2365	0.0726	2.1	0.4910	6.5	0.0491	6.1	0.33	452	9	406	22	151	143	300
BF9-seq1-a19	3868	28	4	0.95	6681	0.1040	2.1	0.8370	4.1	0.0584	3.5	0.51	638	13	618	19	545	77	117
BF9-seq1-a20	9968	64	7	0.47	17208	0.0925	2.3	0.7477	2.8	0.0586	1.4	0.85	570	13	567	12	554	32	103
BF9-seq1-a21	8644	51	6	0.64	14268	0.1081	2.3	0.9182	3.3	0.0616	2.4	0.70	662	15	661	16	660	51	100
BF9-seq1-a22	224704	210	77	0.13	85826	0.3552	2.8	6.2466	3.2	0.1275	1.5	0.88	1960	47	2011	28	2064	26	95
BF9-seq1-a23	514	3	0	0.79	1028	0.1117	4.8	0.8158	12.4	0.0530	11.5	0.39	683	31	606	58	327	260	209
BF9-seq1-a24	39531	253	28	0.41	2471	0.1019	2.6	0.8858	3.7	0.0630	2.6	0.71	626	16	644	18	709	55	88
BF9-seq1-a25	6252	56	5	0.54	11307	0.0726	2.0	0.5612	3.4	0.0560	2.8	0.58	452	9	452	13	453	62	100
BF9-seq1-a26	5893	32	4	0.60	9986	0.0925	3.1	0.7579	4.3	0.0594	3.0	0.72	570	17	573	19	582	65	98
BF9-seq1-a27	1718	16	1	0.48	3228	0.0792	2.0	0.5889	5.6	0.0540	5.3	0.35	491	9	470	21	370	118	133
BF9-seq1-a28	148351	140	43	0.08	115530	0.3098	2.2	5.5660	2.6	0.1303	1.3	0.87	1740	34	1911	22	2102	22	83
BF9-seq1-a29	13195	208	11	0.42	24563	0.0469	1.8	0.3531	3.0	0.0546	2.4	0.61	296	5	307	8	395	53	75
BF9-seq1-a30	77276	87	34	0.60	10065	0.3200	1.8	5.0251	1.9	0.1139	0.7	0.92	1790	27	1824	16	1862	13	96
BF9-seq1-a31	100912	241	45	0.02	76425	0.1960	2.9	2.6120	3.7	0.0966	2.3	0.78	1154	30	1304	27	1560	44	74
BF9-seq1-a32	1038	42	1	0.85	2170	0.0172	2.9	0.1164	7.9	0.0490	7.3	0.37	110	3	112	8	146	172	76
BF9-seq1-a33	4483	37	4	0.93	1686	0.0887	2.4	0.6926	4.5	0.0566	3.9	0.52	548	12	534	19	476	86	115
BF9-seq1-a34	7770	55	6	0.34	13187	0.0964	1.8	0.7961	3.1	0.0599	2.5	0.59	593	10	595	14	600	54	99
BF9-seq1-a35	17410	126	12	0.10	29480	0.0960	2.2	0.7936	2.9	0.0599	1.9	0.76	591	12	593	13	601	40	98
BF9-seq1-a36	23117	111	15	0.10	27420	0.1384	1.9	1.2704	2.2	0.0666	1.2	0.85	836	15	833	13	824	25	101
BF9-seq1-a37	67573	91	28	0.35	61216	0.2753	2.5	4.2150	3.0	0.1110	1.6	0.84	1568	34	1677	25	1816	30	86
BF9-seq1-a38	7136	87	5	0.40	694	0.0513	2.6	0.3856	5.3	0.0545	4.6	0.49	323	8	331	15	391	104	82
BF9-seq1-a39	96766	77	37	0.42	70256	0.4127	1.8	7.9423	2.1	0.1396	1.1	0.85	2227	35	2224	20	2222	19	100
BF9-seq1-a40	21117	52	12	0.40	26712	0.2019	3.5	2.2410	4.0	0.0805	1.9	0.88	1185	38	1194	28	1210	38	98
BF9-seq1-a41	4483	36	4	0.29	7894	0.0982	2.2	0.7825	3.7	0.0578	2.9	0.60	604	13	587	16	521	64	116
BF9-seq1-a42	11117	83	10	0.30	18914	0.1131	1.7	0.9759	3.5	0.0626	3.1	0.49	691	11	691	18	694	66	100
BF9-seq1-a43	8370	101	8	0.55	15753	0.0654	1.9	0.4862	2.7	0.0539	1.9	0.71	409	7	402	9	366	42	112
BF9-seq1-a44	3723	28	4	0.70	6675	0.1083	1.7	0.8426	4.3	0.0564	3.9	0.41	663	11	621	20	469	86	141

BF9-seq1-a45	77655	68	28	0.26	61241	0.3744	1.9	6.6485	2.1	0.1288	1.0	0.87	2050	33	2066	19	2082	18	98
BF9-seq1-a46	6602	33	6	0.95	9863	0.1385	1.8	1.2817	3.0	0.0671	2.4	0.61	836	14	838	17	841	49	99
BF9-seq1-a47	5319	62	5	0.48	10027	0.0696	2.0	0.5140	3.2	0.0535	2.4	0.64	434	9	421	11	352	55	123
BF9-seq1-a48	3421	41	3	0.43	6703	0.0790	2.1	0.5644	3.5	0.0518	2.8	0.61	490	10	454	13	278	63	176
BF9-seq1-a49	3640	24	3	0.47	5913	0.1105	2.1	0.9507	3.4	0.0624	2.7	0.61	675	14	678	17	689	58	98
BF9-seq1-a50	6506	89	6	0.28	12873	0.0603	2.1	0.4241	3.2	0.0510	2.4	0.65	377	8	359	10	242	55	156
BF9-seq1-a51	816	6	1	0.40	1472	0.1139	2.7	0.8929	10.1	0.0569	9.8	0.26	695	18	648	50	487	216	143
BF9-seq1-a52	30464	215	25	0.40	47395	0.1099	1.6	0.9666	4.3	0.0638	4.0	0.37	672	10	687	22	734	85	92
BF9-seq1-a53	3512	18	3	0.51	5317	0.1357	2.1	1.2463	3.8	0.0666	3.1	0.56	820	16	822	22	825	66	99
BF9-seq1-a54	7678	69	8	0.57	13760	0.0984	1.8	0.8385	6.9	0.0618	6.7	0.25	605	10	618	33	668	144	91
BF9-seq1-a55	75827	127	40	0.33	77956	0.2847	1.8	3.8786	2.1	0.0988	1.1	0.86	1615	26	1609	17	1602	20	101
BF9-seq1-a56	8564	141	9	0.39	9477	0.0609	2.1	0.4421	2.9	0.0526	1.9	0.74	381	8	372	9	313	44	122
BF9-seq1-a57	41740	65	21	0.52	44586	0.2669	1.6	3.4931	2.1	0.0949	1.4	0.75	1525	21	1526	17	1527	26	100
BF9-seq1-a58	18964	95	14	0.06	26427	0.1556	2.1	1.5237	6.0	0.0710	5.6	0.35	932	18	940	37	958	114	97
BF9-seq1-a59	4068	19	3	0.38	6177	0.1402	2.1	1.2911	3.6	0.0668	2.9	0.58	846	16	842	21	830	60	102
BF9-seq1-a60	157713	153	59	0.06	124240	0.3809	1.9	6.7769	2.2	0.1290	1.1	0.87	2081	33	2083	19	2085	19	100
BF9-seq2-b01	3508	56	7	0.68	6107	0.1083	2.7	0.8748	4.3	0.0586	3.3	0.63	663	17	638	20	552	72	120
BF9-seq2-b02	8577	142	16	0.50	10657	0.1002	2.1	0.8372	3.0	0.0606	2.1	0.71	616	12	618	14	625	46	99
BF9-seq2-b03	9359	220	21	0.03	11797	0.1037	2.0	0.8721	2.9	0.0610	2.2	0.67	636	12	637	14	638	47	100
BF9-seq2-b04	128257	596	115	0.34	963	0.1746	3.1	2.4290	3.2	0.1009	1.1	0.94	1037	29	1251	24	1641	20	63
BF9-seq2-b05	3163	140	12	0.58	6236	0.0731	2.4	0.5690	11.5	0.0565	11.3	0.21	455	10	457	43	471	250	97
BF9-seq2-b06	14949	88	25	0.36	16394	0.2637	2.0	3.3730	2.8	0.0928	1.9	0.72	1509	27	1498	22	1484	37	102
BF9-seq2-b07	12442	149	32	0.81	17303	0.1697	2.1	1.7125	2.8	0.0732	1.9	0.75	1011	20	1013	18	1019	38	99
BF9-seq2-b08	8799	259	28	0.50	15715	0.0964	2.9	0.8324	5.5	0.0626	4.7	0.53	593	16	615	26	695	99	85
BF9-seq2-b09	5617	229	20	0.60	10967	0.0755	2.1	0.5399	3.7	0.0519	3.1	0.56	469	10	438	13	280	71	168
BF9-seq2-b10	14913	650	47	0.35	28161	0.0681	2.2	0.5253	3.6	0.0559	2.9	0.60	425	9	429	13	449	64	95
BF9-seq2-b11	5142	341	18	0.29	7505	0.0519	2.3	0.3805	7.4	0.0532	7.1	0.31	326	7	327	21	337	160	97
BF9-seq2-b12	72545	252	99	0.40	57691	0.3481	2.9	6.1499	3.4	0.1281	1.9	0.84	1926	48	1997	31	2072	33	93
BF9-seq2-b13	60414	162	92	0.92	45015	0.4284	2.1	7.9604	2.4	0.1348	1.1	0.90	2299	41	2227	22	2161	18	106
BF9-seq2-b14	7385	187	18	0.11	13215	0.1014	2.4	0.8424	5.9	0.0603	5.3	0.41	622	14	620	28	613	116	101
BF9-seq2-b15	35780	1954	102	0.15	68448	0.0535	2.0	0.3923	2.3	0.0532	1.3	0.84	336	6	336	7	337	29	100
BF9-seq2-b16	3836	123	11	0.26	7020	0.0869	3.1	0.6682	4.8	0.0558	3.7	0.64	537	16	520	20	443	82	121
BF9-seq2-b17	34869	240	65	0.22	37953	0.2596	2.5	3.3176	3.3	0.0927	2.2	0.75	1488	33	1485	26	1481	42	100
BF9-seq2-b18	5372	160	22	1.31	5100	0.1034	3.2	0.8133	4.0	0.0571	2.3	0.81	634	20	604	18	494	52	128
BF9-seq2-b19	4830	122	15	0.52	8449	0.1096	2.8	1.0191	7.4	0.0674	6.8	0.38	671	18	713	39	851	142	79
BF9-seq2-b20	27050	151	61	1.20	28775	0.2746	2.4	3.6202	2.7	0.0956	1.2	0.89	1564	33	1554	21	1540	23	102
BF9-seq2-b21	19862	305	45	0.27	7657	0.1421	3.2	1.4508	4.3	0.0740	2.9	0.74	857	25	910	26	1042	58	82
BF9-seq2-b22	1871	39	4	0.46	3009	0.1046	2.9	0.8948	6.8	0.0621	6.1	0.43	641	18	649	33	676	131	95
BF9-seq2-b23	118618	459	131	0.40	596	0.2280	3.4	3.7777	3.8	0.1202	1.8	0.88	1324	41	1588	31	1959	32	68
BF9-seq2-b24	6217	21	9	1.41	6449	0.2928	3.4	3.9509	4.5	0.0979	2.9	0.75	1655	49	1624	37	1584	55	105
BF9-seq2-b25	26939	460	48	0.46	3794	0.0935	2.3	0.7666	2.9	0.0595	1.8	0.78	576	13	578	13	584	40	99
BF9-seq2-b26	4966	55	6	0.36	335	0.0985	2.6	1.2964	7.4	0.0954	6.9	0.35	606	15	844	43	1537	130	39

BF9-seq2-b27	8991	241	16	0.36	3692	0.0611	2.4	0.4580	3.4	0.0544	2.4	0.70	382	9	383	11	387	54	99
BF9-seq2-b28	8680	142	16	0.31	15023	0.1051	2.4	0.8539	3.3	0.0589	2.2	0.72	644	14	627	15	564	49	114
BF9-seq2-b29	13042	58	14	0.36	15876	0.2198	2.3	2.5334	2.9	0.0836	1.8	0.79	1281	26	1282	21	1283	34	100
BF9-seq2-b30	15119	62	17	0.23	16772	0.2627	2.1	3.3239	2.9	0.0917	2.0	0.72	1504	28	1487	23	1462	39	103
BF9-seq2-b31	6121	174	11	0.16	8443	0.0621	2.5	0.4661	3.8	0.0544	2.8	0.67	388	9	388	12	388	63	100
BF9-seq2-b32	2210	38	5	0.48	4044	0.1070	2.2	0.8189	4.4	0.0555	3.9	0.49	655	14	607	21	434	86	151
BF9-seq2-b33	28494	229	39	0.40	39777	0.1539	2.0	1.5484	2.4	0.0730	1.4	0.82	923	17	950	15	1013	28	91
BF9-seq2-b34	22206	162	35	0.43	14112	0.1950	1.9	2.0852	2.6	0.0775	1.8	0.73	1149	20	1144	18	1135	35	101
BF9-seq2-b35	7336	135	17	0.50	13081	0.1110	2.1	0.9701	3.9	0.0634	3.3	0.55	678	14	689	20	722	69	94
BF9-seq2-b36	4394	142	10	0.47	8569	0.0599	3.5	0.4294	6.2	0.0520	5.1	0.57	375	13	363	19	286	116	131
BF9-seq2-b37	3887	101	10	0.26	3475	0.0971	2.4	0.8025	3.8	0.0599	2.9	0.63	598	14	598	17	600	63	100
BF9-seq2-b38	49064	337	97	0.38	5643	0.2619	2.4	3.3824	2.7	0.0937	1.3	0.89	1499	33	1500	22	1502	24	100
BF9-seq2-b39	21462	173	29	0.10	30000	0.1715	2.3	1.7208	2.8	0.0728	1.6	0.82	1020	22	1016	18	1008	32	101
BF9-seq2-b40	56289	194	58	0.22	57005	0.2886	2.1	4.0040	2.4	0.1006	1.2	0.86	1635	31	1635	20	1636	23	100
BF9-seq2-b41	4234	92	10	0.44	7286	0.0970	2.1	0.7903	3.8	0.0591	3.1	0.57	597	12	591	17	571	67	104
BF9-seq2-b42	9702	263	33	0.78	16342	0.0981	2.4	0.8122	3.3	0.0601	2.3	0.72	603	14	604	15	606	50	100
BF9-seq2-b43	6298	23	10	0.80	5342	0.3551	4.2	5.8602	5.5	0.1197	3.5	0.77	1959	72	1955	49	1952	63	100
BF9-seq2-b44	15565	366	46	0.60	25581	0.1079	2.6	0.9203	3.2	0.0618	1.8	0.83	661	17	663	16	669	38	99
BF9-seq2-b45	8779	244	22	0.17	14936	0.0908	2.4	0.7387	3.3	0.0590	2.2	0.75	561	13	562	14	566	47	99
BF9-seq2-b46	3173	78	11	0.88	5677	0.1163	2.3	0.9086	4.2	0.0566	3.5	0.56	709	16	656	20	478	77	149
BF9-seq2-b47	5550	147	16	0.29	9561	0.1056	2.7	0.9082	7.8	0.0624	7.3	0.34	647	16	656	38	687	156	94
BF9-seq2-b48	32587	279	71	0.28	37813	0.2417	2.1	2.9460	2.5	0.0884	1.3	0.84	1396	26	1394	19	1391	26	100
BF9-seq2-b49	3080	74	8	0.16	5448	0.1072	2.5	0.8528	4.4	0.0577	3.6	0.58	657	16	626	21	518	79	127
BF9-seq2-b50	4779	205	14	0.31	9184	0.0654	2.8	0.5641	7.4	0.0626	6.9	0.38	408	11	454	28	694	146	59
BF9-seq2-b51	2408	64	8	0.69	4430	0.1051	2.9	0.7916	5.2	0.0546	4.3	0.56	644	18	592	24	397	97	162
BF9-seq2-b52	5577	168	19	0.48	10048	0.1026	2.6	0.8932	7.2	0.0632	6.7	0.37	629	16	648	35	714	142	88
BF9-seq2-b53	94076	1234	184	0.01	6874	0.1594	2.1	1.5950	2.2	0.0726	0.7	0.95	954	19	968	14	1002	14	95
BF9-seq2-b54	1340	38	5	0.76	2547	0.1065	2.8	0.7878	6.6	0.0537	5.9	0.43	652	18	590	30	357	134	183
BF9-seq2-b55	69514	992	163	0.00	3373	0.1754	3.6	1.7940	3.8	0.0742	1.3	0.94	1042	34	1043	25	1047	27	100
BF9-seq2-b56	7048	214	13	0.17	5970	0.0633	2.5	0.4718	3.6	0.0541	2.6	0.70	395	10	392	12	375	58	105
BF9-seq2-b57	4551	122	10	0.66	3440	0.0693	2.4	0.5314	3.6	0.0556	2.7	0.67	432	10	433	13	437	59	99
BF9-seq2-b58	5123	217	18	0.42	4684	0.0748	2.2	0.5853	3.8	0.0567	3.1	0.58	465	10	468	14	482	69	97
BF9-seq2-b59	2858	74	6	0.67	5004	0.0641	3.1	0.5117	6.6	0.0579	5.9	0.47	400	12	420	23	528	128	76
BF9-seq2-b60	4266	167	15	0.95	1452	0.0678	2.3	0.5620	8.0	0.0601	7.6	0.29	423	9	453	30	607	165	70
BF9-seq3-c01	18553	91	33	0.49	17438	0.3130	2.0	4.6745	3.0	0.1083	2.3	0.66	1755	31	1763	25	1771	41	99
BF9-seq3-c02	59124	120	69	0.33	3059	0.5033	3.2	12.3890	3.3	0.1785	0.8	0.97	2628	69	2634	31	2639	14	100
BF9-seq3-c03	562	19	2	0.61	1174	0.0971	2.9	0.6509	14.9	0.0486	14.7	0.20	597	17	509	62	130	345	461
BF9-seq3-c04	43377	91	53	0.71	27118	0.4407	1.7	9.8796	2.1	0.1626	1.3	0.80	2354	34	2424	20	2483	21	95
BF9-seq3-c05	181292	428	228	0.49	13951	0.4378	2.9	9.4918	3.0	0.1573	0.9	0.95	2341	57	2387	28	2426	15	96
BF9-seq3-c06	31092	186	49	0.19	2774	0.2534	1.6	3.1627	3.0	0.0905	2.5	0.53	1456	21	1448	23	1436	48	101
BF9-seq3-c07	12694	333	35	0.41	6295	0.0952	3.1	0.8181	4.8	0.0624	3.6	0.66	586	18	607	22	686	78	85
BF9-seq3-c08	7392	444	28	0.11	14494	0.0657	2.2	0.4997	5.4	0.0551	4.9	0.41	410	9	411	18	418	110	98

BF9-seq3-c09	4160	53	11	0.32	3171	0.1914	2.1	1.8450	3.8	0.0699	3.1	0.56	1129	22	1062	25	926	64	122
BF9-seq3-c10	2880	32	6	0.30	3914	0.1864	2.1	1.9206	4.5	0.0747	4.0	0.47	1102	21	1088	31	1061	81	104
BF9-seq3-c11	3192	99	10	0.32	5870	0.1010	2.7	0.8820	11.6	0.0633	11.2	0.23	620	16	642	57	719	238	86
BF9-seq3-c12	5291	133	15	0.52	8965	0.0984	2.2	0.8177	3.6	0.0603	2.8	0.63	605	13	607	17	614	61	99
BF9-seq3-c13	17714	146	37	0.38	20922	0.2279	2.0	2.7077	2.5	0.0862	1.6	0.79	1323	24	1331	19	1342	30	99
BF9-seq3-c14	893	34	3	0.47	1641	0.0990	2.1	0.7383	13.2	0.0541	13.0	0.16	608	12	561	58	375	293	162
BF9-seq3-c15	8553	240	29	0.56	10165	0.1032	2.1	0.8651	2.8	0.0608	1.8	0.76	633	13	633	13	631	40	100
BF9-seq3-c16	9802	173	22	0.63	16755	0.1072	2.4	0.8794	2.8	0.0595	1.5	0.84	656	15	641	14	586	33	112
BF9-seq3-c17	20888	275	38	0.10	8037	0.1454	2.1	1.3703	2.8	0.0684	1.9	0.73	875	17	876	17	880	40	99
BF9-seq3-c18	5215	115	18	1.74	9408	0.0980	1.7	0.7620	3.8	0.0564	3.4	0.43	602	10	575	17	469	76	129
BF9-seq3-c19	4210	200	14	0.40	8153	0.0689	2.2	0.4957	3.9	0.0522	3.2	0.57	430	9	409	13	292	73	147
BF9-seq3-c20	11831	197	25	0.30	20273	0.1197	2.1	0.9799	3.0	0.0594	2.1	0.71	729	15	694	15	580	46	126
BF9-seq3-c21	10568	290	24	0.35	19756	0.0778	3.0	0.6098	4.5	0.0568	3.3	0.67	483	14	483	18	485	74	100
Sample 62/07-1 (AK22)			**Well no.: 62/07-1**				**Location (decimal degrees):**				**49.667**	**11.76303W**			**Datum: IRENET95**				
AK22-seq1-a01	11605	38	11	0.59	13250	0.2496	1.6	3.0543	2.4	0.0887	1.9	0.64	1436	20	1421	19	1399	36	103
AK22-seq1-a02	115648	293	93	0.26	54226	0.3004	1.4	4.3039	1.6	0.1039	0.8	0.87	1693	21	1694	13	1695	15	100
AK22-seq1-a03	17312	334	27	0.48	31326	0.0728	1.6	0.5623	2.2	0.0560	1.5	0.75	453	7	453	8	452	32	100
AK22-seq1-a04	54368	94	39	0.39	18709	0.3768	1.7	6.5246	2.2	0.1256	1.4	0.77	2061	30	2049	20	2037	25	101
AK22-seq1-a05	12984	81	16	0.67	15837	0.1688	1.8	1.7022	2.4	0.0731	1.6	0.75	1005	17	1009	15	1018	32	99
AK22-seq1-a06	80618	161	66	0.76	29739	0.3166	2.0	5.2146	2.2	0.1195	1.0	0.90	1773	31	1855	19	1948	17	91
AK22-seq1-a07	238832	629	182	0.15	208464	0.2781	5.1	4.4428	7.2	0.1159	5.0	0.72	1582	72	1720	61	1894	90	84
AK22-seq1-a08	45278	122	37	0.31	46390	0.2815	1.5	3.8431	2.0	0.0990	1.4	0.73	1599	21	1602	17	1606	26	100
AK22-seq1-a09	22219	62	18	0.40	1520	0.2528	1.9	3.2335	4.1	0.0928	3.6	0.47	1453	25	1465	33	1483	69	98
AK22-seq1-a10	405372	317	176	0.16	81052	0.5103	1.2	14.2160	1.6	0.2021	1.0	0.78	2658	27	2764	15	2843	16	93
AK22-seq1-a11	25123	71	24	0.68	7685	0.2826	1.6	3.8575	2.0	0.0990	1.2	0.79	1604	23	1605	16	1606	23	100
AK22-seq1-a12	50253	155	46	0.42	19248	0.2709	1.4	3.6192	1.8	0.0969	1.1	0.79	1545	19	1554	14	1565	21	99
AK22-seq1-a13	3832	127	9	0.41	6951	0.0691	1.5	0.5330	3.9	0.0559	3.6	0.39	431	6	434	14	449	80	96
AK22-seq1-a14	22195	142	37	0.44	8128	0.2350	1.5	2.8246	2.1	0.0872	1.5	0.71	1361	18	1362	16	1364	28	100
AK22-seq1-a15	61274	320	87	0.29	26058	0.2582	1.9	3.3135	2.3	0.0931	1.4	0.81	1481	25	1484	18	1489	26	99
AK22-seq1-a16	5115	158	13	0.64	792	0.0716	1.7	0.5537	4.1	0.0560	3.7	0.42	446	7	447	15	454	82	98
AK22-seq1-a17	35710	106	36	0.67	29738	0.2769	1.9	3.8129	2.3	0.0999	1.3	0.83	1576	27	1595	19	1622	24	97
AK22-seq1-a18	71522	202	77	0.92	71147	0.2952	1.3	4.1473	1.6	0.1019	0.9	0.83	1667	19	1664	13	1659	16	100
AK22-seq1-a19	140109	430	141	0.69	13593	0.2660	2.1	3.6658	2.2	0.1000	0.8	0.93	1520	28	1564	18	1623	15	94
AK22-seq1-a20	18384	52	16	0.35	18490	0.2883	2.3	4.0083	3.1	0.1008	2.0	0.74	1633	33	1636	25	1640	38	100
AK22-seq2-b01	31134	176	39	0.31	8328	0.2087	2.4	2.3712	3.1	0.0824	2.0	0.76	1222	27	1234	23	1255	40	97
AK22-seq2-b02	399352	168	150	0.20	121397	0.7271	2.3	33.3928	2.8	0.3331	1.6	0.81	3522	63	3592	28	3631	25	97
AK22-seq2-b03	8228	271	24	0.59	14687	0.0760	2.6	0.6000	4.3	0.0573	3.4	0.61	472	12	477	17	501	75	94
AK22-seq2-b04	26382	114	38	0.22	25176	0.3225	2.1	4.7412	2.6	0.1066	1.5	0.82	1802	33	1775	22	1743	27	103
AK22-seq2-b05	56147	234	76	0.24	51434	0.3071	2.3	4.7137	2.6	0.1113	1.2	0.89	1727	35	1770	22	1821	21	95
AK22-seq2-b06	34474	133	46	0.26	10057	0.3274	2.2	5.0516	2.5	0.1119	1.2	0.88	1826	35	1828	21	1830	22	100
AK22-seq2-b07	15752	210	57	0.76	8380	0.2271	3.0	2.6759	3.4	0.0855	1.6	0.88	1319	36	1322	26	1326	31	99
AK22-seq2-b08	43367	581	123	0.09	29177	0.2178	2.4	2.5490	2.8	0.0849	1.4	0.86	1270	27	1286	20	1313	27	97

AK22-seq2-b09	26553	204	38	0.53	7491	0.1605	2.2	1.6257	2.7	0.0735	1.6	0.82	960	20	980	17	1026	32	93
AK22-seq2-b10	163544	383	158	0.52	138939	0.3511	2.1	5.8069	2.5	0.1199	1.4	0.83	1940	35	1947	22	1955	25	99
AK22-seq2-b11	14270	80	19	0.28	2749	0.2316	1.9	2.5549	2.7	0.0800	1.9	0.70	1343	22	1288	20	1197	38	112
AK22-seq2-b12	11179	268	23	0.70	2050	0.0731	2.2	0.5874	2.9	0.0583	1.9	0.77	455	10	469	11	541	40	84
AK22-seq2-b13	3961	27	6	0.53	5470	0.2104	2.5	2.1548	4.7	0.0743	4.0	0.53	1231	28	1167	33	1049	80	117
AK22-seq2-b14	110028	135	78	0.50	65937	0.4886	1.8	11.4195	2.3	0.1695	1.4	0.79	2565	38	2558	21	2553	23	100
AK22-seq2-b15	113912	121	81	0.82	41912	0.5107	1.9	12.7733	2.2	0.1814	1.0	0.88	2660	42	2663	21	2666	17	100
AK22-seq2-b16	16517	119	22	0.33	22974	0.1778	2.2	1.7904	2.5	0.0731	1.3	0.86	1055	21	1042	17	1015	26	104
AK22-seq2-b17	20314	68	24	0.78	20594	0.2830	2.4	3.9152	2.9	0.1003	1.7	0.82	1607	34	1617	24	1630	31	99
AK22-seq2-b18	79679	299	110	0.75	16749	0.2897	2.3	3.9917	3.3	0.0999	2.4	0.69	1640	34	1633	28	1623	45	101
AK22-seq2-b19	94544	103	58	0.26	53420	0.5030	2.2	12.5732	2.5	0.1813	1.2	0.88	2627	48	2648	24	2665	20	99
AK22-seq2-b20	48794	49	33	0.71	26144	0.5088	2.5	13.1015	3.0	0.1868	1.5	0.86	2651	56	2687	28	2714	25	98
AK22-seq2-b21	57869	137	53	0.25	48425	0.3611	2.5	6.0583	2.9	0.1217	1.4	0.87	1988	43	1984	26	1981	26	100
AK22-seq2-b22	84798	222	82	0.39	17970	0.3343	2.3	5.5060	2.4	0.1195	0.8	0.94	1859	37	1902	21	1948	14	95
AK22-seq2-b23	129706	148	87	0.62	21100	0.4763	2.1	12.3115	2.3	0.1875	1.0	0.90	2511	43	2628	22	2720	16	92
AK22-seq2-b24	15110	69	18	0.28	17011	0.2436	2.1	3.0371	2.7	0.0904	1.8	0.76	1405	26	1417	21	1435	34	98
AK22-seq2-b25	22062	186	63	0.48	21694	0.3007	2.0	4.2937	2.6	0.1036	1.6	0.78	1695	30	1692	21	1689	29	100
AK22-seq2-b26	912	31	2	0.72	1905	0.0678	2.5	0.4605	10.3	0.0492	10.0	0.24	423	10	385	34	159	234	266
AK22-seq2-b27	68359	65	47	0.84	36028	0.5378	2.1	14.3182	2.4	0.1931	1.1	0.89	2774	48	2771	23	2769	18	100
AK22-seq2-b28	55633	142	63	0.91	23421	0.3392	2.2	5.4981	2.8	0.1176	1.7	0.80	1883	37	1900	24	1920	30	98
AK22-seq2-b29	11262	84	16	0.27	15177	0.1809	2.2	1.8809	3.0	0.0754	2.0	0.75	1072	22	1074	20	1079	40	99
AK22-seq2-b30	28769	184	57	0.43	1546	0.2834	3.2	3.7974	3.8	0.0972	2.1	0.84	1608	46	1592	31	1571	39	102
AK22-seq2-b31	25562	85	30	0.52	25817	0.3028	2.1	4.2090	2.9	0.1008	2.0	0.73	1705	32	1676	24	1639	37	104
AK22-seq2-b32	34759	147	40	0.21	37035	0.2665	2.3	3.4763	3.0	0.0946	2.0	0.75	1523	31	1522	24	1520	38	100
AK22-seq2-b33	9269	63	14	0.60	12372	0.1866	2.2	1.9597	3.0	0.0762	2.0	0.74	1103	22	1102	20	1099	40	100
AK22-seq2-b34	7989	43	11	0.29	9978	0.2606	2.8	2.9285	4.0	0.0815	2.8	0.71	1493	38	1389	30	1234	55	121
AK22-seq2-b35	23242	107	27	0.30	15411	0.2380	2.3	2.8749	2.8	0.0876	1.5	0.84	1376	29	1375	21	1374	29	100
AK22-seq2-b36	53410	392	73	0.04	70684	0.1954	1.9	2.0753	2.4	0.0770	1.4	0.81	1151	20	1141	16	1122	28	103
AK22-seq2-b37	36624	126	43	0.51	35139	0.2941	2.2	4.3010	2.8	0.1061	1.7	0.79	1662	32	1694	23	1733	31	96
AK22-seq2-b38	203822	396	192	0.52	44503	0.4179	2.1	8.3355	2.4	0.1447	1.3	0.84	2251	39	2268	22	2284	23	99
AK22-seq2-b39	32611	973	75	0.31	3649	0.0736	2.8	0.5797	3.6	0.0571	2.2	0.79	458	12	464	13	497	48	92
AK22-seq2-b40	8360	64	14	0.52	11806	0.1931	2.2	1.9166	2.7	0.0720	1.6	0.81	1138	23	1087	18	986	32	115
AK22-seq2-b41	88586	326	106	0.36	87403	0.2952	2.1	4.1912	2.6	0.1030	1.6	0.78	1668	30	1672	22	1678	30	99
AK22-seq2-b42	13110	34	16	0.69	11667	0.3831	2.6	6.0731	3.6	0.1150	2.6	0.71	2091	46	1986	32	1880	46	111
AK22-seq2-b43	44354	160	62	0.52	44083	0.3467	2.1	4.8460	2.6	0.1014	1.5	0.81	1919	35	1793	22	1650	28	116
AK22-seq2-b44	27558	198	46	0.66	35686	0.1955	2.2	2.1186	2.5	0.0786	1.1	0.90	1151	24	1155	17	1162	22	99
AK22-seq2-b45	60104	95	60	0.98	24596	0.4768	2.0	10.0972	2.2	0.1536	0.9	0.91	2513	42	2444	21	2386	16	105
AK22-seq2-b46	36656	180	45	0.32	42681	0.2349	2.1	2.8167	2.6	0.0870	1.5	0.82	1360	26	1360	19	1359	28	100
AK22-seq2-b47	22223	78	26	0.44	21874	0.2950	2.0	4.1844	2.5	0.1029	1.5	0.80	1666	29	1671	21	1677	28	99
AK22-seq2-b48	5987	44	10	0.51	8359	0.2015	2.3	2.0157	3.4	0.0725	2.5	0.68	1184	25	1121	24	1001	51	118
AK22-seq2-b49	77788	571	223	0.45	67378	0.3483	2.2	5.6444	2.5	0.1175	1.1	0.90	1927	37	1923	21	1919	19	100
AK22-seq2-b50	50140	201	79	0.25	42138	0.3725	2.4	6.2354	2.9	0.1214	1.6	0.84	2041	43	2009	26	1977	28	103

AK22-seq2-b51	7878	70	13	0.23	11336	0.1855	2.2	1.8096	3.3	0.0707	2.5	0.67	1097	23	1049	22	950	50	115
AK22-seq2-b52	13245	122	24	0.65	18516	0.1631	2.6	1.6448	3.5	0.0731	2.3	0.75	974	24	988	22	1018	46	96
AK22-seq2-b53	9564	208	17	0.03	3690	0.0905	2.3	0.7340	3.6	0.0588	2.8	0.63	559	12	559	15	560	60	100
AK22-seq2-b54	43502	173	53	0.28	20138	0.2870	2.2	3.9673	2.6	0.1003	1.3	0.86	1626	32	1628	21	1629	25	100
AK22-seq2-b55	70916	75	49	0.37	36971	0.5522	2.0	14.7452	2.4	0.1937	1.3	0.85	2834	47	2799	23	2774	21	102
AK22-seq2-b56	35430	285	51	0.16	47685	0.1806	2.4	1.8820	2.8	0.0756	1.3	0.88	1070	24	1075	18	1084	27	99
AK22-seq2-b57	27310	62	27	0.65	19868	0.3626	2.1	6.1103	2.4	0.1222	1.1	0.88	1994	36	1992	21	1989	20	100
AK22-seq2-b58	59979	184	76	0.79	53493	0.3308	1.8	5.2038	2.1	0.1141	1.1	0.86	1842	28	1853	18	1865	19	99
AK22-seq2-b59	11697	51	15	0.32	12682	0.2746	2.4	3.5527	2.9	0.0938	1.6	0.83	1564	34	1539	23	1505	31	104
AK22-seq2-b60	47327	221	63	0.30	50258	0.2687	2.5	3.5201	2.9	0.0950	1.5	0.85	1534	34	1532	23	1528	29	100
AK22-seq3-c01	6959	26	9	0.66	2068	0.3017	2.3	4.0780	3.5	0.0980	2.6	0.67	1700	35	1650	29	1587	48	107
AK22-seq3-c02	49426	49	33	0.54	24420	0.5554	1.9	15.8049	2.4	0.2064	1.5	0.79	2848	44	2865	23	2877	24	99
AK22-seq3-c03	11248	81	17	0.36	14571	0.1952	1.9	2.1119	2.6	0.0785	1.7	0.75	1150	21	1153	18	1158	34	99
AK22-seq3-c04	4007	34	7	0.42	5821	0.1859	2.8	1.7966	4.8	0.0701	3.9	0.58	1099	28	1044	32	931	80	118
AK22-seq3-c05	25866	217	41	0.27	34568	0.1833	2.4	1.9231	2.7	0.0761	1.3	0.88	1085	24	1089	19	1098	26	99
AK22-seq3-c06	4562	373	23	0.00	8381	0.0691	2.6	0.5285	3.7	0.0555	2.6	0.70	431	11	431	13	432	59	100
AK22-seq3-c07	6007	51	11	0.47	8315	0.1941	2.3	1.9731	3.4	0.0737	2.4	0.69	1144	24	1106	23	1034	49	111
AK22-seq3-c08	351027	373	233	0.40	180631	0.5305	2.1	14.4637	2.2	0.1977	0.9	0.92	2744	47	2781	22	2807	14	98
AK22-seq3-c09	16879	87	22	0.32	12473	0.2386	2.2	2.9089	2.8	0.0884	1.8	0.76	1380	27	1384	22	1391	35	99
AK22-seq3-c10	26352	121	36	0.49	28841	0.2595	1.9	3.2906	2.2	0.0920	1.2	0.85	1487	25	1479	17	1467	22	101
AK22-seq3-c11	7574	230	16	0.45	14025	0.0634	2.5	0.4797	3.4	0.0549	2.4	0.73	396	10	398	11	406	53	98
AK22-seq3-c12	151141	166	103	0.33	77309	0.5309	2.0	14.5647	2.1	0.1990	0.8	0.93	2745	45	2787	21	2818	13	97
AK22-seq3-c13	28978	187	42	0.25	35689	0.2133	2.3	2.4276	2.7	0.0825	1.4	0.85	1247	26	1251	20	1258	28	99
AK22-seq3-c14	35041	112	41	0.43	32858	0.3280	1.9	4.9095	2.3	0.1086	1.4	0.82	1829	31	1804	20	1776	25	103
AK22-seq3-c15	8851	260	19	0.31	16129	0.0714	2.2	0.5497	3.3	0.0559	2.4	0.67	444	9	445	12	447	54	100
AK22-seq3-c16	17381	60	20	0.24	16499	0.3143	2.5	4.6418	3.2	0.1071	2.0	0.78	1762	39	1757	27	1751	37	101
AK22-seq3-c17	32137	125	40	0.53	32379	0.2674	2.2	3.7239	2.8	0.1010	1.7	0.79	1528	30	1577	23	1642	32	93
AK22-seq3-c18	77323	88	50	0.17	40492	0.5170	2.4	13.8475	3.0	0.1943	1.8	0.80	2686	53	2739	29	2779	29	97
AK22-seq3-c19	14512	48	28	0.46	8537	0.4895	2.7	11.6569	4.3	0.1727	3.4	0.62	2568	57	2577	41	2584	57	99
AK22-seq3-c20	3293	103	7	0.22	4647	0.0716	2.3	0.5064	4.1	0.0513	3.3	0.57	446	10	416	14	254	77	176
AK22-seq3-c21	3532	35	6	0.33	3978	0.1772	2.3	1.6581	4.8	0.0679	4.2	0.48	1051	22	993	31	865	87	122
AK22-seq3-c22	22089	397	49	0.02	32981	0.1313	2.0	1.1902	5.1	0.0657	4.7	0.40	795	15	796	29	798	98	100
AK22-seq3-c23	63956	176	67	0.39	1339	0.3341	2.7	5.4916	2.9	0.1192	1.1	0.92	1858	44	1899	26	1944	20	96
AK22-seq3-c24	12738	51	16	0.47	13393	0.2700	2.8	3.6013	3.1	0.0967	1.3	0.90	1541	38	1550	25	1562	25	99
AK22-seq3-c25	11993	77	18	0.47	13573	0.2091	2.4	2.2900	3.3	0.0794	2.2	0.74	1224	27	1209	23	1183	43	103
AK22-seq3-c26	22427	88	27	0.22	21657	0.2960	2.7	4.3173	3.1	0.1058	1.7	0.85	1672	39	1697	26	1728	31	97
AK22-seq3-c27	15548	108	25	0.57	20220	0.1966	2.4	2.1202	3.0	0.0782	1.7	0.81	1157	26	1155	21	1152	34	100
AK22-seq3-c28	53651	184	59	0.21	51393	0.3037	2.6	4.4511	2.8	0.1063	1.0	0.94	1709	40	1722	24	1737	17	98

[a] within-run background-corrected mean ^{207}Pb signal in counts per second

[b] U and Pb content and Th/U ratio were calculated relative to GJ-1 and are accurate to approximately 10%.

[c] corrected for background, mass bias, laser induced U-Pb fractionation and common Pb (if detectable, see analytical method) using

Stacey & Kramers (1975) model Pb composition. $^{207}Pb/^{235}U$ calculated using $^{207}Pb/^{206}Pb/(^{238}U/^{206}Pb \times 1/137.88)$. Errors are propagated by quadratic addition of within-run errors (2SE) and the reproducibility of GJ-1 (2SD).
[a] Rho is the error correlation defined as $err^{206}Pb/^{238}U/err^{207}Pb/^{235}U$.

: age

Table V. LA ICP MS data for all detrital apatite samples taken across the LORS of the Dingle Basin.

Analysis	U (ppm)	$f^{206}Pb$	$\frac{^{207}Pb}{^{235}U}$	2σ	$\frac{^{206}Pb}{^{238}U}$	2σ	ρ	$\frac{^{238}U}{^{206}Pb}$	2σ	$\frac{^{207}Pb}{^{206}Pb}$	2σ	ρ	$\frac{206}{238}$ Age	2σ (Ma)	$\frac{207}{235}$ Age	2σ (Ma)	$\frac{207}{206}$ Age	2σ (Ma)	^{207}Pb-corr. Age	2σ (Ma)	err. %
Sample Mb	**Ballymore Sandstone Formation**		**Location (**	**52.235 N 10.25446 W**				**Datum:**	**IRENET95 Irish Transverse Mercator**												
Mb_1_0	14.0	0.806	33.30	1.00	0.3451	0.0180	0.36	2.8977	0.1511	0.707	0.022	0.37	1911	100	3590	108	4745	148	418	64	15
Mb_1_1	15.0	0.783	28.93	0.93	0.3146	0.0170	0.09	3.1786	0.1718	0.689	0.028	0.50	1763	95	3451	111	4708	191	425	72	17
Mb_1_10	8.0	0.893	120.50	2.50	1.1080	0.0570	0.42	0.9025	0.0464	0.798	0.016	0.46	4807	247	4874	101	4918	99	724	147	20
Mb_1_11	14.6	0.692	17.63	0.73	0.2101	0.0110	0.40	4.7596	0.2492	0.614	0.023	0.19	1229	64	2970	123	4542	170	404	43	11
Mb_1_12	24.1	0.492	7.82	0.31	0.1274	0.0068	-0.01	7.8493	0.4190	0.452	0.020	0.54	773	41	2211	88	4092	181	405	29	7
Mb_1_13	29.1	0.763	29.64	0.65	0.3187	0.0160	0.39	3.1377	0.1575	0.675	0.015	0.36	1783	90	3475	76	4678	104	470	46	10
Mb_1_14	9.1	0.726	24.90	1.30	0.2798	0.0160	0.39	3.5740	0.2044	0.646	0.032	0.19	1590	91	3304	173	4615	229	476	73	15
Mb_1_15	49.2	0.533	9.30	0.25	0.1406	0.0070	-0.01	7.1124	0.3541	0.486	0.015	0.41	848	42	2368	64	4199	130	410	26	6
Mb_1_16	12.9	0.715	20.07	0.79	0.2298	0.0120	0.11	4.3516	0.2272	0.633	0.030	0.46	1334	70	3095	122	4586	217	409	57	14
Mb_1_17	18.1	0.301	4.08	0.28	0.1024	0.0059	0.08	9.7656	0.5627	0.300	0.020	0.32	629	36	1650	113	3470	231	445	30	7
Mb_1_18	23.9	0.768	24.30	0.68	0.2661	0.0140	0.21	3.7580	0.1977	0.674	0.021	0.44	1521	80	3281	92	4676	146	387	49	13
Mb_1_19	6.1	0.715	17.80	1.20	0.2107	0.0130	0.02	4.7461	0.2928	0.631	0.050	0.44	1233	76	2979	201	4581	363	376	84	22
Mb_1_2	17.4	0.558	10.03	0.48	0.1460	0.0078	0.22	6.8493	0.3659	0.506	0.024	0.35	879	47	2438	117	4259	202	403	34	9
Mb_1_20	9.0	0.670	16.85	0.91	0.2047	0.0120	0.06	4.8852	0.2864	0.597	0.035	0.45	1201	70	2926	158	4501	264	422	60	14
Mb_1_21	9.7	0.752	25.06	0.99	0.2752	0.0160	0.26	3.6337	0.2113	0.664	0.030	0.42	1567	91	3311	131	4655	210	425	68	16
Mb_1_22	1.3	1.038	56.00	6.10	0.4720	0.0450	0.22	2.1186	0.2020	0.858	0.094	0.47	2492	238	4105	447	5021	550	-115	372	-322
Mb_1_23	14.2	0.937	87.20	1.90	0.7880	0.0400	0.49	1.2690	0.0644	0.806	0.017	0.37	3746	190	4549	99	4932	104	313	115	37
Mb_1_3	28.3	0.502	8.83	0.34	0.1413	0.0075	0.10	7.0771	0.3756	0.462	0.020	0.53	852	45	2321	89	4124	179	439	32	7
Mb_1_4	6.0	0.867	153.30	5.70	1.3660	0.0760	0.38	0.7321	0.0407	0.801	0.032	0.52	5552	309	5116	190	4924	197	1073	313	29
Mb_1_5	20.0	0.520	8.98	0.38	0.1349	0.0074	-0.08	7.4129	0.4066	0.475	0.024	0.60	816	45	2336	99	4165	211	405	33	8
Mb_1_6	24.5	0.471	7.56	0.34	0.1266	0.0068	0.10	7.8989	0.4243	0.436	0.023	0.43	768	41	2180	98	4038	213	418	31	8
Mb_1_7	17.4	0.623	13.81	0.53	0.1772	0.0093	0.18	5.6433	0.2962	0.559	0.023	0.41	1052	55	2737	105	4405	181	417	38	9
Mb_1_8	25.5	0.550	10.63	0.40	0.1510	0.0080	0.01	6.6225	0.3509	0.500	0.023	0.50	907	48	2491	94	4241	195	424	35	8
Mb_1_9	14.7	0.673	15.08	0.60	0.1856	0.0100	0.23	5.3879	0.2903	0.597	0.028	0.45	1098	59	2820	112	4501	211	380	45	12
Sample Mb	**Ballymore Sandstone Formation**		**Location(**	**52.229 N 10.26369 W**				**Datum:**	**IRENET95 Irish Transverse Mercator**												
Mb_4_0	6.0	0.828	50.50	1.80	0.5030	0.0260	0.19	1.9881	0.1028	0.732	0.029	0.38	2627	136	4002	143	4795	190	536	115	21
Mb_4_1	4.6	0.990	91.80	3.20	0.8150	0.0450	0.29	1.2270	0.0677	0.832	0.028	0.48	3843	212	4600	160	4978	168	50	192	386
Mb_4_10	21.1	0.875	70.00	1.20	0.6580	0.0330	0.35	1.5198	0.0762	0.769	0.014	0.55	3259	164	4328	74	4865	89	509	82	16

Mb_4_11	3.4	0.970	80.70	3.70	0.7120	0.0390	0.05	1.4045	0.0769	0.821	0.041	0.48	3466	190	4471	205	4959	248	136	237	174
Mb_4_12	8.0	0.855	50.10	1.70	0.4920	0.0270	0.51	2.0325	0.1115	0.748	0.024	0.38	2579	142	3994	136	4826	155	446	96	22
Mb_4_13	12.2	0.801	45.50	1.40	0.4594	0.0240	0.40	2.1768	0.1137	0.712	0.020	0.30	2437	127	3899	120	4755	134	565	77	14
Mb_4_14	26.9	0.831	37.29	0.93	0.3736	0.0190	0.40	2.6767	0.1361	0.726	0.017	0.25	2046	104	3701	92	4783	112	394	56	14
Mb_4_15	4.9	0.892	51.50	3.30	0.4910	0.0310	0.35	2.0367	0.1286	0.771	0.046	0.32	2575	163	4022	258	4869	291	333	177	53
Mb_4_16	13.1	0.701	19.13	0.80	0.2231	0.0120	0.38	4.4823	0.2411	0.622	0.025	0.26	1298	70	3048	128	4560	183	416	49	12
Mb_4_17	10.4	0.856	45.30	2.00	0.4450	0.0240	0.28	2.2472	0.1212	0.746	0.036	0.31	2373	128	3894	172	4822	233	402	126	31
Mb_4_18	10.1	0.700	18.80	0.87	0.2244	0.0130	0.21	4.4563	0.2582	0.621	0.032	0.39	1305	76	3032	140	4558	235	421	60	14
Mb_4_19	20.4	0.460	7.21	0.31	0.1235	0.0067	0.02	8.0972	0.4393	0.427	0.021	0.52	751	41	2138	92	4007	197	416	30	7
Mb_4_2	9.6	0.644	14.65	0.84	0.1861	0.0110	0.22	5.3735	0.3176	0.576	0.036	0.38	1100	65	2793	160	4449	278	413	57	14
Mb_4_3	2.0	1.043	565.00	19.00	4.7800	0.2700	0.77	0.2092	0.0118	0.870	0.018	0.21	11310	639	6436	216	5041	104	-1465	945	-65
Mb_4_4	5.2	0.758	25.00	1.50	0.2792	0.0170	0.29	3.5817	0.2181	0.668	0.041	0.41	1587	97	3308	199	4663	286	422	91	22
Mb_4_6	14.4	0.688	20.14	0.84	0.2387	0.0130	0.24	4.1894	0.2282	0.614	0.026	0.42	1380	75	3098	129	4542	192	463	54	12
Mb_4_7	7.3	0.831	60.50	2.20	0.6040	0.0330	0.48	1.6556	0.0905	0.741	0.022	0.26	3046	166	4182	152	4812	143	625	108	17
Mb_4_8	12.3	0.865	43.90	2.10	0.4250	0.0230	0.45	2.3529	0.1273	0.751	0.031	0.18	2283	124	3863	185	4832	199	359	105	29
Mb_4_9	1.3	1.014	95.90	7.30	0.8440	0.0590	0.31	1.1848	0.0828	0.843	0.066	0.42	3945	276	4644	354	4996	391	-79	465	-589
Sample Mb	**Ballymore Sandstone Formation**				**Location(c**	**52.227 N 10.26807 W**			**Datum:**	**IRENET95 Irish Transverse Mercator**											
Mb5_0	31.3	0.488	7.99	0.34	0.1315	0.0049	0.27	7.6046	0.2834	0.450	0.020	0.46	796	30	2230	95	4085	182	420	26	6
Mb5_1	32.8	0.870	58.40	3.10	0.5610	0.0270	0.93	1.7825	0.0858	0.761	0.016	-0.25	2871	138	4147	220	4850	102	454	78	17
Mb5_10	18.7	0.818	37.97	0.82	0.3851	0.0100	0.25	2.5967	0.0674	0.718	0.017	0.41	2100	55	3719	80	4767	113	436	55	13
Mb5_11	4.4	0.358	4.92	0.73	0.1055	0.0070	0.15	9.4787	0.6289	0.345	0.054	0.32	647	43	1806	268	3685	577	422	51	12
Mb5_12	22.1	0.739	22.01	0.69	0.2466	0.0069	0.18	4.0552	0.1135	0.652	0.021	0.36	1421	40	3184	100	4628	149	402	43	11
Mb5_13	2.9	0.802	36.10	2.20	0.3810	0.0160	0.28	2.6247	0.1102	0.707	0.047	0.41	2081	87	3669	224	4745	315	469	137	29
Mb5_14	10.9	0.504	8.48	0.75	0.1359	0.0050	-0.03	7.3584	0.2707	0.463	0.043	0.42	821	30	2284	202	4128	383	420	47	11
Mb5_15	19.9	0.749	23.96	0.82	0.2648	0.0073	0.28	3.7764	0.1041	0.661	0.023	0.28	1514	42	3267	112	4648	162	414	49	12
Mb5_16	10.1	0.761	21.50	1.10	0.2380	0.0081	0.35	4.2017	0.1430	0.667	0.032	0.26	1376	47	3161	162	4661	224	356	61	17
Mb5_17	7.3	0.890	49.80	2.10	0.4670	0.0150	0.23	2.1413	0.0688	0.769	0.034	0.40	2470	79	3988	168	4865	215	322	126	39
Mb5_18	14.7	1.023	486.70	6.80	4.1480	0.1100	0.72	0.2411	0.0064	0.854	0.009	0.35	10563	280	6285	88	5014	52	-639	448	-70
Mb5_19	20.2	0.159	4.87	0.26	0.1773	0.0054	0.21	5.6402	0.1718	0.201	0.011	0.19	1052	32	1797	96	2834	155	896	30	3
Mb5_2	42.6	0.406	6.06	0.23	0.1156	0.0034	0.25	8.6505	0.2544	0.384	0.014	0.25	705	21	1985	75	3848	140	428	18	4
Mb5_20	9.1	0.647	20.54	0.89	0.2483	0.0086	0.21	4.0274	0.1395	0.585	0.028	0.36	1430	50	3117	135	4471	214	542	56	10
Mb5_21	12.8	0.825	47.00	1.20	0.4563	0.0140	0.30	2.1915	0.0672	0.727	0.019	0.40	2423	74	3931	100	4785	125	496	71	14
Mb5_3	20.8	0.722	21.54	0.95	0.2517	0.0095	0.39	3.9730	0.1500	0.640	0.030	0.30	1447	55	3163	140	4602	216	436	60	14

Mb5_4	11.7	0.584	10.47	0.90	0.1486	0.0062	0.02	6.7295	0.2808	0.526	0.048	0.37	893	37	2477	213	4316	394	386	57	15
Mb5_5	36.5	0.865	57.60	1.20	0.5551	0.0150	0.33	1.8015	0.0487	0.758	0.014	0.36	2846	77	4133	86	4845	90	465	67	14
Mb5_6	8.2	0.802	38.70	1.40	0.3987	0.0130	0.26	2.5082	0.0818	0.708	0.026	0.52	2163	71	3738	135	4747	174	491	82	17
Mb5_7	9.1	0.740	22.80	1.50	0.2599	0.0110	0.16	3.8476	0.1628	0.654	0.047	0.45	1489	63	3218	212	4633	333	421	95	23
Mb5_8	12.9	0.747	24.72	0.81	0.2746	0.0092	0.35	3.6417	0.1220	0.660	0.019	0.45	1564	52	3297	108	4646	134	433	44	10
Mb5_9	34.7	0.595	11.24	0.41	0.1552	0.0050	0.16	6.4433	0.2076	0.535	0.021	0.47	930	30	2543	93	4341	170	393	28	7
Sample Mb	**Ballymore Sandstone Formation**				**Location(c**	**52.215 N**		**10.27879 W**		**Datum:**		**IRENET95 Irish Transverse Mercator**										
Mb7_0	3.8	0.817	61.40	3.90	0.6070	0.0420	0.01	1.6474	0.1140	0.733	0.059	0.67	3058	212	4197	267	4797	386	678	265	39
Mb7_1	7.1	0.841	35.80	1.10	0.3565	0.0120	0.18	2.8050	0.0944	0.731	0.028	0.52	1966	66	3661	113	4793	184	356	80	22
Mb7_10	7.6	0.735	22.70	1.20	0.2544	0.0100	0.09	3.9308	0.1545	0.650	0.039	0.47	1461	57	3214	170	4624	277	420	78	19
Mb7_11	18.8	0.631	13.62	0.51	0.1764	0.0058	0.13	5.6689	0.1864	0.565	0.026	0.47	1047	34	2724	102	4421	203	406	38	9
Mb7_12	17.9	0.761	24.20	0.95	0.2629	0.0091	0.29	3.8037	0.1317	0.669	0.025	0.47	1505	52	3277	129	4666	174	393	53	14
Mb7_13	13.3	0.781	30.90	1.30	0.3243	0.0097	0.24	3.0836	0.0922	0.688	0.029	0.29	1811	54	3516	148	4706	198	443	74	17
Mb7_14	9.6	0.763	24.50	1.00	0.2614	0.0084	0.01	3.8256	0.1229	0.670	0.031	0.47	1497	48	3289	134	4668	216	388	64	17
Mb7_15	15.0	0.821	39.03	0.98	0.3923	0.0110	0.12	2.5491	0.0715	0.720	0.021	0.47	2134	60	3746	94	4771	139	439	67	15
Mb7_16	19.6	0.855	50.60	1.20	0.4891	0.0130	0.48	2.0446	0.0543	0.748	0.016	0.21	2567	68	4004	95	4826	103	442	66	15
Mb7_17	3.3	0.847	95.10	3.30	0.8790	0.0300	0.16	1.1377	0.0388	0.767	0.028	0.47	4066	139	4636	161	4862	178	811	183	23
Mb7_18	22.8	0.777	29.22	0.89	0.3094	0.0088	0.23	3.2321	0.0919	0.684	0.022	0.34	1738	49	3461	105	4698	151	431	55	13
Mb7_19	4.9	0.985	327.70	6.30	2.8020	0.0860	0.73	0.3569	0.0110	0.851	0.014	0.25	8609	264	5884	113	5010	82	260	353	136
Mb7_2	20.3	0.829	35.35	0.87	0.3534	0.0096	0.30	2.8297	0.0769	0.723	0.018	0.40	1951	53	3649	90	4777	119	378	53	14
Mb7_20	42.8	0.358	5.06	0.20	0.1053	0.0030	-0.03	9.4967	0.2706	0.345	0.015	0.46	645	18	1829	72	3685	160	422	17	4
Mb7_21	45.4	0.712	21.56	0.70	0.2461	0.0074	0.25	4.0634	0.1222	0.632	0.023	0.42	1418	43	3164	103	4583	167	442	46	10
Mb7_22	30.0	0.803	31.10	1.30	0.3206	0.0110	0.74	3.1192	0.1070	0.703	0.023	-0.15	1793	62	3522	147	4737	155	395	60	15
Mb7_23	21.4	0.763	23.87	0.65	0.2589	0.0082	0.51	3.8625	0.1223	0.670	0.016	0.30	1484	47	3263	89	4668	112	384	36	9
Mb7_3	1.1	1.042	723.00	22.00	5.9900	0.2200	0.70	0.1669	0.0061	0.870	0.020	0.32	12535	460	6686	203	5041	116	-1887	1369	-73
Mb7_4	9.3	0.975	102.60	3.80	0.9010	0.0340	0.67	1.1099	0.0419	0.826	0.025	0.22	4141	156	4712	175	4967	150	142	189	133
Mb7_5	3.4	0.994	85.20	4.20	0.7330	0.0330	0.50	1.3643	0.0614	0.833	0.041	0.25	3545	160	4525	223	4979	245	30	249	821
Mb7_6	16.1	0.631	13.62	0.51	0.1764	0.0058	0.13	5.6689	0.1864	0.565	0.026	0.47	1047	34	2724	102	4421	203	406	38	9
Mb7_7	11.3	0.887	106.90	2.10	0.9740	0.0250	0.38	1.0267	0.0264	0.790	0.015	0.37	4384	113	4753	93	4904	93	671	121	18
Mb7_8	16.2	0.428	6.55	0.37	0.1202	0.0038	0.14	8.3195	0.2630	0.402	0.023	0.37	732	23	2053	116	3917	224	428	25	6
Mb7_9	3.4	0.919	78.60	3.50	0.6950	0.0280	0.23	1.4388	0.0580	0.794	0.044	0.44	3402	137	4444	198	4911	272	354	238	67
Sample Mb	**Farran Sandstone Formation**				**Location**	**52.238 N**		**10.30877 W**		**Datum:**		**IRENET95 Irish Transverse Mercator**										
Mb9_0	18.7	0.819	47.80	1.00	0.4759	0.0130	0.38	2.1013	0.0574	0.725	0.015	0.44	2509	69	3948	83	4781	99	532	60	11

Mb9_10	5.4	0.718	19.50	1.00	0.2207	0.0091	0.09	4.5310	0.1868	0.634	0.037	0.49	1286	53	3067	157	4588	268	389	65	17
Mb9_11	3.4	0.829	93.80	3.90	0.8880	0.0330	0.50	1.1261	0.0418	0.759	0.026	0.27	4097	152	4622	192	4847	166	909	171	19
Mb9_12	1.0	1.020	288.00	15.00	2.4600	0.1200	0.54	0.4065	0.0198	0.851	0.035	0.22	8002	390	5754	300	5010	206	-329	752	-228
Mb9_13	4.5	0.845	170.80	4.70	1.5130	0.0430	0.38	0.6609	0.0188	0.802	0.021	0.31	5940	169	5226	144	4925	129	1356	227	17
Mb9_14	8.1	0.536	8.59	0.57	0.1265	0.0062	0.02	7.9051	0.3874	0.486	0.041	0.58	768	38	2296	152	4199	354	368	44	12
Mb9_15	8.7	0.684	18.50	1.10	0.2159	0.0095	0.05	4.6318	0.2038	0.609	0.039	0.46	1260	56	3016	179	4530	290	425	67	16
Mb9_16	6.6	0.732	24.90	1.90	0.2870	0.0130	0.24	3.4843	0.1578	0.651	0.053	0.36	1627	74	3304	252	4626	377	477	117	24
Mb9_17	1.9	0.871	50.60	3.40	0.4680	0.0230	0.19	2.1368	0.1050	0.757	0.055	0.52	2475	122	4004	269	4843	352	378	199	53
Mb9_18	10.0	0.831	58.30	2.00	0.5620	0.0180	0.21	1.7794	0.0570	0.738	0.027	0.40	2875	92	4145	142	4807	176	585	117	20
Mb9_19	2.4	0.925	98.90	3.90	0.8770	0.0340	0.34	1.1403	0.0442	0.803	0.036	0.44	4059	157	4675	184	4927	221	411	245	60
Mb9_2	22.1	0.587	12.49	0.51	0.1701	0.0048	0.07	5.8789	0.1659	0.531	0.021	0.40	1013	29	2642	108	4330	171	438	30	7
Mb9_21	6.6	0.443	7.71	0.62	0.1330	0.0062	-0.09	7.5188	0.3505	0.415	0.040	0.53	805	38	2198	177	3964	382	461	45	10
Mb9_22	42.4	0.298	3.92	0.23	0.0955	0.0027	0.13	######	0.2960	0.296	0.017	-0.09	588	17	1618	95	3449	198	418	17	4
Mb9_23	18.9	0.836	34.30	0.92	0.3379	0.0089	0.16	2.9595	0.0779	0.727	0.021	0.40	1877	49	3619	97	4785	138	347	58	17
Mb9_24	13.5	0.561	11.77	0.56	0.1664	0.0058	0.26	6.0096	0.2095	0.511	0.027	0.23	992	35	2586	123	4273	226	454	38	8
Mb9_3	10.7	0.319	4.30	0.39	0.0968	0.0037	0.22	######	0.3949	0.313	0.028	0.33	596	23	1693	154	3536	316	411	26	6
Mb9_4	19.8	0.498	9.42	0.45	0.1473	0.0047	0.03	6.7889	0.2166	0.460	0.024	0.39	886	28	2380	114	4118	215	460	31	7
Mb9_5	9.5	0.750	24.00	1.00	0.2634	0.0100	0.49	3.7965	0.1441	0.661	0.025	0.34	1507	57	3268	136	4648	176	412	54	13
Mb9_6	5.1	0.426	6.42	0.62	0.1206	0.0061	0.03	8.2919	0.4194	0.400	0.042	0.64	734	37	2035	197	3909	411	432	44	10
Mb9_8	9.9	0.920	88.20	2.70	0.7910	0.0260	0.58	1.2642	0.0416	0.798	0.021	0.27	3757	124	4560	140	4918	129	394	136	34
Mb9_9	12.7	0.610	11.55	0.56	0.1547	0.0050	0.30	6.4641	0.2089	0.546	0.026	0.26	927	30	2569	125	4371	208	378	34	9

Table VI. LA ICP MS data for all detrital apatite samples taken across the UORS of the Munster Basin.

Analysis	U (ppm)	$f^{206}Pb$	$\frac{^{207}Pb}{^{235}U}$	2σ	$\frac{^{206}Pb}{^{238}U}$	2σ	ρ	$\frac{^{238}U}{^{206}Pb}$	2σ	$\frac{^{207}Pb}{^{206}Pb}$	2σ	ρ	$\frac{206}{238}$ Age	2σ (Ma)	$\frac{207}{235}$ Age	2σ (Ma)	$\frac{207}{206}$ Age	2σ (Ma)	^{207}Pb-corr. Age	2σ (Ma)	err. %
Sample Ca-1		**Ballinskelligs Sandstone Form**			**Locatio 51.993 N**			**9.737518 W**		**Datum:**	**IRENET95**										
Ca_1_0	5.6	0.815	36.90	1.60	0.3550	0.0170	0.12	2.8169	0.1349	0.714	0.035	0.54	1958	94	3691	160	4759	233	409	98	24
Ca_1_1	38.3	0.468	8.93	0.30	0.1508	0.0062	0.23	6.6313	0.2726	0.437	0.016	0.44	905	37	2331	78	4042	148	498	27	5
Ca_1_10	10.2	0.474	6.94	0.41	0.1196	0.0059	0.07	8.3612	0.4125	0.437	0.030	0.31	728	36	2104	124	4042	277	394	33	9
Ca_1_11	19.2	0.350	4.66	0.35	0.0997	0.0046	0.22	10.0301	0.4628	0.338	0.026	0.16	613	28	1760	132	3654	281	405	27	7
Ca_1_12	64.4	0.348	4.80	0.39	0.1043	0.0056	0.81	9.5877	0.5148	0.337	0.019	-0.47	640	34	1785	145	3649	206	424	27	6
Ca_1_13	6.4	0.615	31.90	1.70	0.4140	0.0200	0.29	2.4155	0.1167	0.584	0.030	0.27	2233	108	3547	189	4469	230	953	98	10
Ca_1_14	7.5	0.784	32.20	1.20	0.3430	0.0160	0.11	2.9155	0.1360	0.692	0.031	0.48	1901	89	3556	133	4714	211	460	84	18
Ca_1_15	36.3	0.678	19.06	0.47	0.2339	0.0093	0.30	4.2753	0.1700	0.606	0.016	0.41	1355	54	3045	75	4522	119	469	35	7
Ca_1_16	17.3	0.730	18.80	1.20	0.2193	0.0110	0.42	4.5600	0.2287	0.643	0.037	0.28	1278	64	3032	194	4608	265	370	65	18
Ca_1_17	11.4	0.687	23.90	2.00	0.2710	0.0140	0.67	3.6900	0.1906	0.617	0.044	-0.34	1546	80	3264	273	4549	324	525	93	18
Ca_1_18	31.1	0.411	6.27	0.29	0.1186	0.0048	0.20	8.4317	0.3412	0.388	0.017	0.27	723	29	2014	93	3863	169	436	23	5
Ca_1_19	15.0	0.644	16.42	0.66	0.2070	0.0087	0.19	4.8309	0.2030	0.578	0.025	0.41	1213	51	2902	117	4454	193	459	44	10
Ca_1_2	26.6	0.691	194.30	2.60	1.8710	0.0740	0.44	0.5345	0.0211	0.785	0.012	0.45	6799	269	5356	72	4895	75	0	236	-
Ca_1_20	44.1	0.243	3.29	0.15	0.0944	0.0039	0.06	10.5932	0.4376	0.253	0.013	0.31	582	24	1479	67	3204	165	445	20	5
Ca_1_21	17.4	0.518	10.53	0.44	0.1603	0.0070	0.09	6.2383	0.2724	0.477	0.023	0.43	958	42	2483	104	4172	201	480	35	7
Ca_1_22	14.1	0.723	18.80	1.20	0.2158	0.0094	0.11	4.6339	0.2018	0.637	0.037	0.49	1260	55	3032	194	4595	267	375	64	17
Ca_1_23	9.6	0.705	23.40	2.10	0.2720	0.0150	0.40	3.6765	0.2027	0.630	0.056	0.20	1551	86	3244	291	4579	407	497	117	24
Ca_1_24	23.6	0.831	96.30	1.60	0.9240	0.0350	0.40	1.0823	0.0410	0.762	0.013	0.32	4219	160	4648	77	4852	83	937	102	11
Ca_1_25	24.7	0.461	6.60	0.38	0.1124	0.0049	0.09	8.8968	0.3878	0.426	0.026	0.10	687	30	2059	119	4003	244	379	28	7
Ca_1_3	26.3	0.667	177.30	3.40	1.6470	0.0630	0.45	0.6072	0.0232	0.773	0.014	0.32	6275	240	5263	101	4873	88	2816	225	8
Ca_1_4	13.9	0.614	12.55	0.47	0.1663	0.0074	0.19	6.0132	0.2676	0.551	0.025	0.45	992	44	2646	99	4384	199	401	37	9
Ca_1_5	19.3	0.547	10.15	0.83	0.1526	0.0081	0.36	6.5531	0.3478	0.498	0.038	0.17	916	49	2449	200	4235	323	431	49	11
Ca_1_6	73.5	0.178	2.09	0.09	0.0780	0.0031	0.13	12.8205	0.5095	0.198	0.009	0.22	484	19	1145	52	2812	130	401	17	4
Ca_1_7	10.1	0.620	17.70	0.83	0.2303	0.0100	0.15	4.3422	0.1885	0.563	0.029	0.42	1336	58	2974	139	4415	227	541	55	10
Ca_1_8	9.2	0.672	17.76	0.85	0.2146	0.0091	0.12	4.6598	0.1976	0.600	0.032	0.40	1253	53	2977	142	4508	240	438	56	13
Ca_1_9	41.6	0.235	2.97	0.14	0.0916	0.0037	0.13	10.9170	0.4410	0.246	0.012	0.32	565	23	1400	66	3159	154	436	19	4
Sample Ca-4		**Lough Acoose Sandstone Forr**			**Locatio 51.9994 N**			**9.743 W**		**Datum:**	**IRENET95**										
Ca_4_0	21.9	0.689	15.42	0.55	0.1807	0.0074	-0.02	5.5340	0.2266	0.609	0.024	0.52	1071	44	2842	101	4530	179	352	37	11
Ca_4_1	10.1	0.483	7.87	0.53	0.1313	0.0065	0.14	7.6161	0.3770	0.446	0.033	0.42	795	39	2216	149	4072	301	423	39	9
Ca_4_10	10.0	0.763	20.40	1.10	0.2202	0.0098	-0.09	4.5413	0.2021	0.667	0.039	0.16	1283	57	3111	168	4661	273	328	68	21
Ca_4_11	13.0	0.670	18.13	0.82	0.2126	0.0090	-0.12	4.7037	0.1991	0.598	0.031	0.55	1243	53	2997	136	4503	233	437	54	12
Ca_4_12	24.4	0.856	48.20	1.20	0.4601	0.0180	0.30	2.1734	0.0850	0.747	0.019	0.44	2440	95	3956	98	4824	123	414	73	18
Ca_4_13	14.3	0.474	7.12	0.45	0.1201	0.0056	0.01	8.3264	0.3882	0.437	0.032	0.42	731	34	2127	134	4042	296	395	35	9
Ca_4_14	12.0	0.691	18.01	0.98	0.2103	0.0100	0.27	4.7551	0.2261	0.613	0.033	0.45	1230	59	2990	163	4539	244	406	57	14

Ca_4_15	12.3	0.524	9.75	0.54	0.1428	0.0065	0.19	7.0028	0.3188	0.479	0.029	0.40	860	39	2411	134	4178	253	424	37	9
Ca_4_16	21.8	0.590	11.54	0.49	0.1526	0.0062	-0.16	6.5531	0.2662	0.531	0.026	0.54	916	37	2568	109	4330	212	391	34	9
Ca_4_17	8.0	0.398	6.83	0.52	0.1261	0.0066	0.03	7.9302	0.4151	0.379	0.034	0.32	766	40	2090	159	3828	343	472	40	9
Ca_4_18	12.1	0.759	23.36	0.89	0.2453	0.0100	-0.06	4.0766	0.1662	0.666	0.031	0.55	1414	58	3242	124	4659	217	370	61	16
Ca_4_19	13.5	0.673	18.16	0.70	0.2134	0.0088	0.01	4.6860	0.1932	0.600	0.026	0.44	1247	51	2998	116	4508	195	435	46	11
Ca_4_2	15.6	0.773	28.80	1.10	0.3055	0.0130	0.09	3.2733	0.1393	0.681	0.027	0.48	1719	73	3447	132	4691	186	433	67	15
Ca_4_20	18.3	0.553	12.04	0.48	0.1688	0.0073	-0.01	5.9242	0.2562	0.505	0.023	0.53	1005	43	2608	104	4256	194	469	36	8
Ca_4_21	12.0	0.741	25.00	1.00	0.2740	0.0120	0.23	3.6496	0.1598	0.656	0.030	0.41	1561	68	3308	132	4637	212	442	66	15
Ca_4_22	13.2	0.678	15.52	0.86	0.1848	0.0087	0.45	5.4113	0.2548	0.601	0.032	0.24	1093	51	2848	158	4510	240	372	49	13
Ca_4_3	10.4	0.791	37.90	1.30	0.3862	0.0160	0.28	2.5893	0.1073	0.700	0.024	0.50	2105	87	3717	128	4731	162	500	75	15
Ca_4_4	9.4	0.628	13.59	0.70	0.1666	0.0076	0.07	6.0024	0.2738	0.561	0.034	0.47	993	45	2722	140	4410	267	388	47	12
Ca_4_5	20.2	0.524	9.51	0.41	0.1427	0.0066	0.13	7.0077	0.3241	0.479	0.024	0.48	860	40	2389	103	4178	209	424	33	8
Ca_4_6	23.4	0.463	8.10	0.31	0.1342	0.0058	0.03	7.4516	0.3220	0.431	0.019	0.48	812	35	2242	86	4021	177	449	27	6
Ca_4_7	17.6	0.741	23.90	1.00	0.2551	0.0110	0.31	3.9200	0.1690	0.654	0.028	0.28	1465	63	3264	137	4633	198	413	58	14
Ca_4_8	4.3	0.483	7.53	0.72	0.1225	0.0073	-0.12	8.1633	0.4865	0.445	0.052	0.67	745	44	2177	208	4069	475	396	54	14
Ca_4_9	21.9	0.347	4.86	0.28	0.1037	0.0045	0.04	9.6432	0.4185	0.336	0.020	0.42	636	28	1795	103	3645	217	422	24	6
Sample Ca-6		**Ballinskelligs Sandstone Form**				**Locatio**	**51.994 N**	**9.734737 W**			**Datum:**		**IRENET95**								
Ca_6_0	11.6	0.591	12.44	0.62	0.1691	0.0079	0.08	5.9137	0.2763	0.534	0.033	0.44	1007	47	2638	131	4338	268	431	47	11
Ca_6_1	24.7	0.562	10.70	0.44	0.1500	0.0063	0.03	6.6667	0.2800	0.509	0.025	0.52	901	38	2497	103	4267	210	410	34	8
Ca_6_10	14.3	0.340	4.75	0.40	0.1057	0.0048	0.01	9.4607	0.4296	0.331	0.029	0.36	648	29	1776	150	3622	317	435	30	7
Ca_6_11	16.5	0.526	7.66	0.45	0.1207	0.0054	0.26	8.2850	0.3707	0.478	0.032	0.17	735	33	2192	129	4175	279	358	34	9
Ca_6_12	14.4	0.643	13.76	0.61	0.1836	0.0083	0.08	5.4466	0.2462	0.575	0.030	0.51	1087	49	2733	121	4446	232	409	46	11
Ca_6_13	12.2	0.682	15.68	0.66	0.1884	0.0088	0.10	5.3079	0.2479	0.604	0.032	0.56	1113	52	2858	120	4518	239	375	50	13
Ca_6_14	10.9	0.614	10.91	0.76	0.1501	0.0074	0.01	6.6622	0.3285	0.549	0.044	0.46	902	44	2515	175	4378	351	363	54	15
Ca_6_15	34.5	0.531	9.31	0.33	0.1463	0.0062	0.20	6.8353	0.2897	0.485	0.018	0.45	880	37	2369	84	4196	156	428	27	6
Ca_6_16	32.0	0.359	4.70	0.24	0.0973	0.0043	0.24	10.2775	0.4542	0.344	0.018	0.43	599	26	1767	90	3681	193	390	22	6
Ca_6_17	26.8	0.479	6.64	0.33	0.1122	0.0049	0.26	8.9127	0.3892	0.440	0.022	0.32	686	30	2065	103	4052	203	366	25	7
Ca_6_18	25.2	0.405	6.04	0.28	0.1192	0.0052	0.12	8.3893	0.3660	0.384	0.020	0.37	726	32	1982	92	3848	200	441	26	6
Ca_6_19	12.0	0.460	6.97	0.45	0.1169	0.0059	0.15	8.5543	0.4317	0.426	0.027	0.29	713	36	2108	136	4003	254	395	31	8
Ca_6_2	18.2	0.523	9.17	0.45	0.1401	0.0063	0.17	7.1378	0.3210	0.478	0.025	0.43	845	38	2355	116	4175	218	417	33	8
Ca_6_20	26.9	0.120	1.83	0.14	0.0850	0.0036	0.01	11.7647	0.4983	0.154	0.013	0.33	526	22	1056	81	2391	202	465	21	5
Ca_6_21	20.0	0.481	6.60	0.37	0.1129	0.0051	0.14	8.8574	0.4001	0.442	0.023	0.34	690	31	2059	115	4059	211	367	26	7
Ca_6_3	14.4	0.722	18.99	0.90	0.2117	0.0092	0.20	4.7237	0.2053	0.636	0.030	0.37	1238	54	3041	144	4592	217	369	52	14
Ca_6_4	20.7	0.828	30.45	0.74	0.3143	0.0120	0.09	3.1817	0.1215	0.720	0.019	0.52	1762	67	3501	85	4771	126	339	51	15
Ca_6_5	15.0	0.696	16.71	0.73	0.2038	0.0092	0.49	4.9068	0.2215	0.616	0.024	0.28	1196	54	2918	127	4546	177	388	42	11
Ca_6_6	15.3	0.504	8.74	0.49	0.1393	0.0063	0.19	7.1788	0.3247	0.463	0.027	0.30	841	38	2311	130	4128	241	431	35	8
Ca_6_7	13.5	0.619	14.89	0.78	0.2003	0.0085	0.21	4.9925	0.2119	0.559	0.030	0.28	1177	50	2808	147	4405	236	474	50	11
Ca_6_8	53.2	0.217	2.49	0.11	0.0796	0.0032	0.02	12.5628	0.5050	0.230	0.011	0.37	494	20	1269	56	3052	146	390	17	4
Ca_6_9	18.6	0.465	7.50	0.42	0.1287	0.0056	0.08	7.7700	0.3381	0.432	0.028	0.43	780	34	2173	122	4024	261	429	33	8
Sample Ca-8		**Lough Acoose Sandstone Forr**				**Locatio**	**52.00 N**	**9.723767 W**			**Datum:**		**IRENET95**								
Ca_8_0	8.1	0.416	5.56	0.50	0.1003	0.0057	0.07	9.9701	0.5666	0.389	0.035	0.38	616	35	1910	172	3867	348	367	34	9
Ca_8_1	11.3	0.304	11.39	0.68	0.2474	0.0100	0.22	4.0420	0.1634	0.328	0.018	0.11	1425	58	2556	153	3608	198	1024	50	5

Ca_8_10	40.6	0.196	2.54	0.15	0.0852	0.0035	0.10	11.7371	0.4822	0.214	0.013	0.03	527	22	1284	76	2936	178	427	19	4
Ca_8_11	22.2	0.490	7.57	0.83	0.1305	0.0100	0.80	7.6628	0.5872	0.451	0.033	-0.18	791	61	2181	239	4089	299	416	45	11
Ca_8_12	12.0	0.518	8.84	0.72	0.1389	0.0075	0.27	7.1994	0.3887	0.474	0.039	0.19	838	45	2322	189	4162	342	418	47	11
Ca_8_13	10.0	0.503	10.66	0.81	0.1676	0.0085	0.08	5.9666	0.3026	0.467	0.045	0.38	999	51	2494	190	4140	399	515	62	12
Ca_8_14	15.0	0.470	8.02	0.44	0.1306	0.0058	0.25	7.6570	0.3400	0.436	0.025	0.27	791	35	2233	123	4038	232	431	31	7
Ca_8_15	15.1	0.435	7.20	0.41	0.1306	0.0062	0.33	7.6570	0.3635	0.409	0.022	0.24	791	38	2137	122	3942	212	459	31	7
Ca_8_2	13.9	0.365	6.12	0.42	0.1229	0.0054	0.07	8.1367	0.3575	0.353	0.026	0.28	747	33	1993	137	3720	274	485	32	7
Ca_8_3	13.6	0.568	14.14	0.71	0.1904	0.0086	0.23	5.2521	0.2372	0.519	0.024	0.38	1124	51	2759	139	4296	199	510	41	8
Ca_8_4	38.2	0.339	4.77	0.23	0.1056	0.0044	0.24	9.4697	0.3946	0.330	0.018	0.23	647	27	1780	86	3617	197	435	23	5
Ca_8_5	21.1	0.214	2.84	0.19	0.0882	0.0041	0.17	11.3379	0.5270	0.229	0.017	0.28	545	25	1366	91	3045	226	432	23	5
Ca_8_6	10.1	0.612	13.52	0.66	0.1750	0.0079	0.07	5.7143	0.2580	0.550	0.031	0.47	1040	47	2717	133	4381	247	424	46	11
Ca_8_7	14.3	0.473	8.30	0.42	0.1353	0.0064	0.18	7.3910	0.3496	0.439	0.025	0.41	818	39	2264	115	4048	231	444	33	7
Ca_8_8	3.9	0.773	34.10	2.40	0.3660	0.0180	-0.19	2.7322	0.1344	0.686	0.055	0.25	2011	99	3613	254	4702	377	515	153	30
Ca_8_9	25.9	0.280	3.68	0.23	0.0948	0.0040	0.07	10.5485	0.4451	0.282	0.018	0.24	584	25	1567	98	3374	215	426	22	5
Sample Ca-9		**Lough Acoose Sandstone Forr**				**Locatio 52.012 N**		**9.71606 W**			**Datum:**	**IRENET95**									
Ca_9_0	15.3	0.514	8.45	0.46	0.1317	0.0069	0.16	7.5930	0.3978	0.470	0.026	0.36	798	42	2281	124	4150	230	400	33	8
Ca_9_1	28.5	0.349	4.42	0.23	0.0963	0.0047	-0.03	10.3842	0.5068	0.336	0.020	0.41	593	29	1716	89	3645	217	392	24	6
Ca_9_10	17.1	0.776	25.54	0.73	0.2656	0.0130	0.07	3.7651	0.1843	0.680	0.024	0.55	1518	74	3329	95	4689	165	372	54	14
Ca_9_11	26.5	0.357	4.90	0.27	0.1051	0.0053	0.18	9.5147	0.4798	0.344	0.020	0.26	644	32	1802	99	3681	214	422	26	6
Ca_9_12	19.1	0.797	34.11	0.93	0.3517	0.0170	0.33	2.8433	0.1374	0.701	0.019	0.34	1943	94	3613	99	4733	128	446	58	13
Ca_9_13	18.6	0.693	17.11	0.63	0.2014	0.0100	-0.07	4.9652	0.2465	0.614	0.025	0.53	1183	59	2941	108	4541	185	386	44	11
Ca_9_14	23.6	0.205	2.65	0.21	0.0853	0.0045	0.05	11.7233	0.6185	0.221	0.018	0.30	528	28	1315	104	2988	243	423	25	6
Ca_9_15	20.4	0.701	18.48	0.54	0.2117	0.0100	0.17	4.7237	0.2231	0.621	0.020	0.40	1238	58	3015	88	4558	147	395	38	10
Ca_9_16	4.1	0.596	11.80	1.20	0.1567	0.0110	0.16	6.3816	0.4480	0.536	0.060	0.43	938	66	2589	263	4343	486	396	77	19
Ca_9_17	22.7	0.461	7.33	0.40	0.1221	0.0060	0.07	8.1900	0.4025	0.428	0.025	0.30	743	36	2152	117	4010	234	411	31	7
Ca_9_18	39.2	0.202	2.89	0.16	0.0952	0.0047	0.01	10.5042	0.5186	0.220	0.013	0.44	586	29	1379	76	2981	176	472	25	5
Ca_9_19	13.0	0.556	12.20	0.63	0.1720	0.0085	0.09	5.8140	0.2873	0.508	0.028	0.35	1023	51	2620	135	4265	235	474	43	9
Ca_9_2	11.5	0.489	8.98	0.55	0.1430	0.0079	0.02	6.9930	0.3863	0.452	0.032	0.49	862	48	2336	143	4092	290	455	43	9
Ca_9_20	5.6	0.713	15.90	1.00	0.1793	0.0110	0.16	5.5772	0.3422	0.626	0.044	0.46	1063	65	2871	181	4570	321	324	64	20
Ca_9_21	9.2	0.680	15.20	1.40	0.1837	0.0120	0.07	5.4437	0.3556	0.602	0.056	0.57	1087	71	2828	260	4513	420	369	82	22
Ca_9_22	12.2	0.542	9.93	0.87	0.1354	0.0091	0.26	7.3855	0.4964	0.492	0.044	0.22	819	55	2428	213	4217	377	388	52	13
Ca_9_23	8.0	0.713	32.30	1.60	0.3540	0.0200	0.19	2.8249	0.1596	0.644	0.035	0.46	1954	110	3559	176	4611	251	624	98	16
Ca_9_3	13.0	0.446	7.15	0.53	0.1286	0.0073	0.15	7.7760	0.4414	0.417	0.030	0.25	780	44	2130	158	3972	286	444	38	9
Ca_9_4	27.0	0.417	6.16	0.26	0.1136	0.0055	0.03	8.8028	0.4262	0.392	0.019	0.39	694	34	1999	84	3879	188	414	26	6
Ca_9_5	10.1	0.656	13.54	0.65	0.1637	0.0089	0.05	6.1087	0.3321	0.582	0.032	0.45	977	53	2718	130	4464	245	353	45	13
Ca_9_6	32.5	0.768	29.39	0.76	0.3122	0.0160	0.21	3.2031	0.1642	0.678	0.019	0.49	1752	90	3467	90	4685	131	451	52	12
Ca_9_7	5.9	0.654	12.67	0.88	0.1583	0.0092	0.29	6.3171	0.3671	0.580	0.041	0.33	947	55	2655	184	4459	315	344	54	16
Ca_9_8	39.6	0.275	3.56	0.20	0.0912	0.0045	0.00	10.9649	0.5410	0.277	0.017	0.44	563	28	1541	87	3346	205	413	23	6
Ca_9_9	10.3	0.562	13.35	0.69	0.1873	0.0110	0.16	5.3390	0.3136	0.514	0.026	0.43	1107	65	2705	140	4282	217	509	47	9
Sample Ga-1		**Lough Muskry Formation**				**Locatio 52.366 N**		**8.182 W**			**Datum:**	**IRENET95**									
Ga1_0	51.8	0.364	4.93	0.22	0.1002	0.0056	0.36	9.9800	0.5578	0.349	0.014	0.12	616	34	1807	81	3703	149	398	24	6
Ga1_1	10.9	0.594	14.40	1.00	0.1819	0.0120	0.32	5.4975	0.3627	0.538	0.035	0.32	1077	71	2776	193	4349	283	459	57	12

Ga1_2	17.8	0.669	14.79	0.70	0.1772	0.0110	0.24	5.6433	0.3503	0.593	0.029	0.37	1052	65	2802	133	4491	220	368	46	12
Ga1_3	14.7	0.512	12.74	0.75	0.1826	0.0110	0.06	5.4765	0.3299	0.476	0.027	0.48	1081	65	2661	157	4169	236	550	49	9
Ga1_4	37.7	0.438	6.50	0.31	0.1123	0.0063	0.06	8.9047	0.4996	0.408	0.021	0.42	686	38	2046	98	3939	203	395	28	7
Ga1_5	16.9	0.534	10.40	0.72	0.1491	0.0089	0.05	6.7069	0.4003	0.488	0.036	0.37	896	53	2471	171	4205	310	433	48	11
Ga1_6	51.0	0.383	5.95	0.29	0.1155	0.0065	0.22	8.6580	0.4872	0.366	0.018	0.33	705	40	1969	96	3775	186	444	29	7
Ga1_7	58.2	0.317	4.22	0.18	0.0961	0.0055	0.19	10.4058	0.5955	0.311	0.015	0.28	592	34	1678	72	3526	170	410	26	6
Ga1_8	11.8	0.799	27.60	1.40	0.2774	0.0160	0.33	3.6049	0.2079	0.697	0.034	0.26	1578	91	3405	173	4725	230	350	76	22
Ga1_9	32.5	0.483	7.63	0.38	0.1231	0.0075	0.47	8.1235	0.4949	0.445	0.020	0.16	748	46	2188	109	4069	183	398	30	8
Ga1_10	41.9	0.373	6.00	0.29	0.1164	0.0065	0.07	8.5911	0.4797	0.358	0.018	0.34	710	40	1976	95	3741	188	454	30	7
Ga1_11	61.8	0.400	5.42	0.25	0.1027	0.0063	0.35	9.7371	0.5973	0.377	0.016	0.34	630	39	1888	87	3820	162	386	27	7
Ga1_12	25.8	0.740	34.80	1.20	0.3670	0.0220	0.56	2.7248	0.1633	0.664	0.020	0.31	2015	121	3633	125	4655	140	587	66	11
Ga1_13	9.9	0.221	3.43	0.45	0.1029	0.0083	0.28	9.7182	0.7839	0.237	0.033	0.27	631	51	1511	198	3100	432	497	47	9
Ga1_14	45.3	0.420	6.11	0.30	0.1127	0.0065	0.02	8.8731	0.5118	0.394	0.025	0.21	688	40	1992	98	3886	247	408	32	8
Ga1_15	43.3	0.429	6.47	0.28	0.1148	0.0065	0.23	8.7108	0.4932	0.402	0.017	0.34	701	40	2042	88	3917	166	409	27	7
Ga1_16	37.7	0.344	4.65	0.27	0.0995	0.0061	0.11	10.0503	0.6161	0.333	0.023	0.42	611	37	1758	102	3631	251	408	30	7
Ga1_17	21.4	0.451	7.49	0.49	0.1247	0.0076	0.22	8.0192	0.4887	0.420	0.028	0.28	758	46	2172	142	3982	265	427	37	9
Ga1_18	30.1	0.383	5.60	0.32	0.1075	0.0067	0.10	9.3023	0.5798	0.365	0.024	0.49	658	41	1916	109	3771	248	414	32	8
Ga1_19	60.3	0.304	4.02	0.17	0.0950	0.0053	0.26	10.5263	0.5873	0.301	0.012	0.19	585	33	1638	69	3475	139	413	24	6
Ga1_20	17.0	0.525	9.11	0.70	0.1379	0.0098	0.13	7.2516	0.5153	0.479	0.044	0.45	833	59	2349	181	4178	384	409	54	13
Ga1_21	37.9	0.483	8.90	0.54	0.1423	0.0100	0.44	7.0274	0.4938	0.448	0.023	0.32	858	60	2328	141	4079	209	457	40	9
Ga1_22	8.3	0.567	11.90	1.30	0.1630	0.0140	-0.14	6.1350	0.5269	0.515	0.069	0.58	973	84	2597	284	4285	574	439	93	21
Ga1_23	22.0	0.639	13.93	0.70	0.1774	0.0120	0.48	5.6370	0.3813	0.571	0.026	0.34	1053	71	2745	138	4436	202	400	45	11
Ga1_24	69.7	0.380	5.41	0.22	0.1054	0.0062	0.03	9.4877	0.5581	0.362	0.016	0.56	646	38	1886	77	3758	166	408	27	7
Ga1_25	37.3	0.438	7.13	0.46	0.1218	0.0083	0.51	8.2102	0.5595	0.410	0.022	0.25	741	50	2128	137	3946	212	427	35	8
Ga1_26	24.7	0.535	8.70	0.55	0.1302	0.0086	0.39	7.6805	0.5073	0.486	0.031	0.30	789	52	2307	146	4199	268	379	40	10
Ga1_27	35.2	0.417	6.43	0.40	0.1166	0.0067	0.14	8.5763	0.4928	0.393	0.026	0.25	711	41	2036	127	3883	257	424	33	8
Ga1_28	47.2	0.310	4.03	0.25	0.0942	0.0054	0.07	10.6157	0.6085	0.305	0.020	0.35	580	33	1640	102	3496	229	406	27	7
Ga1_29	55.9	0.400	5.73	0.31	0.1099	0.0069	0.24	9.0992	0.5713	0.378	0.022	0.38	672	42	1936	105	3824	223	412	31	8
Sample Ga-2		**Galtymore Formation**				**Locatio**	**52.358 N**	**8.187 W**		**Datum:**	**IRENET95**										
Ga2_0	30.7	0.651	14.43	1.00	0.1799	0.0096	0.81	5.5586	0.2966	0.580	0.020	-0.13	1066	57	2778	193	4459	154	393	35	9
Ga2_1	16.3	0.535	8.64	0.89	0.1288	0.0071	0.80	7.7640	0.4280	0.486	0.038	0.21	781	43	2301	237	4199	328	375	43	11
Ga2_2	30.3	0.598	12.92	1.00	0.1743	0.0100	0.90	5.7372	0.3292	0.540	0.023	0.07	1036	59	2674	207	4354	185	436	40	9
Ga2_3	18.3	0.613	12.25	0.95	0.1655	0.0076	0.67	6.0423	0.2775	0.550	0.029	0.09	987	45	2624	203	4381	231	400	41	10
Ga2_4	36.4	0.526	9.20	0.78	0.1380	0.0079	0.76	7.2464	0.4148	0.480	0.023	0.06	833	48	2358	200	4181	200	409	34	8
Ga2_5	54.2	0.463	6.98	0.48	0.1220	0.0065	0.83	8.1967	0.4367	0.429	0.020	0.18	742	40	2109	145	4014	187	409	29	7
Ga2_6	39.8	0.423	5.78	0.48	0.1081	0.0052	0.91	9.2507	0.4450	0.396	0.019	-0.37	662	32	1943	161	3894	187	390	24	6
Ga2_7	23.8	0.615	12.01	0.87	0.1607	0.0073	0.71	6.2228	0.2827	0.551	0.027	0.06	961	44	2605	189	4384	215	387	38	10
Ga2_8	11.3	0.813	30.40	1.90	0.3040	0.0160	0.52	3.2895	0.1731	0.709	0.033	0.43	1711	90	3500	219	4749	221	356	81	23
Ga2_9	25.7	0.556	9.41	0.71	0.1323	0.0070	0.73	7.5586	0.3999	0.502	0.023	0.24	801	42	2379	179	4247	195	368	30	8
Ga2_10	27.4	0.498	8.07	0.67	0.1279	0.0062	0.64	7.8186	0.3790	0.457	0.028	-0.04	776	38	2239	186	4108	252	401	33	8
Ga2_11	43.5	0.430	6.20	0.51	0.1133	0.0060	0.79	8.8261	0.4674	0.402	0.020	-0.02	692	37	2004	165	3917	195	404	27	7
Ga2_12	10.3	0.745	17.50	1.40	0.1930	0.0120	0.54	5.1813	0.3222	0.651	0.043	0.38	1138	71	2963	237	4626	306	310	67	22

Ga2_13	57.9	0.432	6.14	0.47	0.1085	0.0054	0.42	9.2166	0.4587	0.403	0.022	0.12	664	33	1996	153	3920	214	386	26	7
Ga2_14	9.6	0.756	25.70	1.80	0.2840	0.0160	0.69	3.5211	0.1984	0.667	0.035	0.29	1611	91	3335	234	4661	245	433	80	18
Ga2_15	26.8	0.542	8.95	0.73	0.1308	0.0076	0.74	7.6453	0.4442	0.491	0.027	0.08	792	46	2333	190	4214	232	375	35	9
Ga2_16	16.7	0.610	11.87	1.10	0.1579	0.0087	0.82	6.3331	0.3489	0.547	0.033	0.00	945	52	2594	240	4373	264	385	45	12
Ga2_17	45.1	0.503	7.21	0.55	0.1200	0.0066	0.61	8.3333	0.4583	0.460	0.030	0.38	731	40	2138	163	4118	269	373	34	9
Ga2_18	54.2	0.600	13.17	0.79	0.1754	0.0085	0.48	5.7013	0.2763	0.541	0.020	0.40	1042	50	2692	161	4357	161	438	34	8
Ga2_19	36.0	0.480	8.46	0.76	0.1389	0.0091	0.85	7.1994	0.4717	0.445	0.022	-0.11	838	55	2282	205	4069	201	449	37	8
Ga2_20	22.4	0.581	10.07	1.00	0.1362	0.0080	0.91	7.3421	0.4313	0.522	0.028	-0.04	823	48	2441	242	4305	231	358	36	10
Ga2_21	44.4	0.496	8.25	0.61	0.1311	0.0061	0.92	7.6278	0.3549	0.456	0.019	-0.12	794	37	2259	167	4105	171	412	27	7
Ga2_22	38.3	0.442	6.19	0.49	0.1080	0.0052	0.30	9.2593	0.4458	0.411	0.023	-0.20	661	32	2003	159	3950	221	377	26	7
Ga2_23	42.4	0.657	14.70	1.00	0.1829	0.0088	0.71	5.4675	0.2631	0.585	0.019	0.05	1083	52	2796	190	4471	145	392	33	8
Ga2_24	21.1	0.524	9.10	1.20	0.1346	0.0110	0.94	7.4294	0.6072	0.478	0.035	-0.31	814	67	2348	310	4175	306	400	48	12
Ga2_25	4.3	0.896	198.00	12.00	1.7270	0.0780	0.73	0.5790	0.0262	0.822	0.024	0.23	6467	292	5375	326	4960	145	1063	304	29
Ga2_26	5.3	0.842	25.80	2.10	0.2730	0.0170	0.07	3.6630	0.2281	0.727	0.051	0.42	1556	97	3339	272	4785	336	272	110	41
Ga2_27	20.0	0.643	15.09	1.10	0.1897	0.0084	0.74	5.2715	0.2334	0.575	0.027	0.13	1120	50	2821	206	4446	209	423	44	10
Ga2_28	42.2	0.422	5.51	0.42	0.1045	0.0047	0.77	9.5694	0.4304	0.395	0.022	-0.02	641	29	1902	145	3890	217	378	24	6
Ga2_29	34.6	0.511	8.12	0.61	0.1281	0.0057	0.82	7.8064	0.3474	0.467	0.023	0.03	777	35	2244	169	4140	204	392	29	7
Sample Ga-4		**Slievenamuck Conglomerate F**			**Locatio**	**52.321 N**		**8.176 W**			**Datum:**		**IRENET95**								
Ga4_0	53.6	0.384	5.71	0.29	0.1111	0.0064	0.09	9.0009	0.5185	0.366	0.020	0.36	679	39	1933	98	3775	206	427	29	7
Ga4_1	7.3	0.499	9.80	1.10	0.1491	0.0110	0.13	6.7069	0.4948	0.461	0.049	0.35	896	66	2416	271	4121	438	464	64	14
Ga4_2	11.0	0.591	16.60	0.90	0.2175	0.0140	0.03	4.5977	0.2959	0.540	0.038	0.59	1269	82	2912	158	4354	306	550	71	13
Ga4_3	29.1	0.402	6.44	0.35	0.1186	0.0070	0.20	8.4317	0.4977	0.381	0.022	0.27	723	43	2038	111	3836	221	442	32	7
Ga4_4	23.6	0.505	8.56	0.55	0.1320	0.0089	0.42	7.5758	0.5108	0.463	0.029	0.27	799	54	2292	147	4128	259	408	40	10
Ga4_5	54.7	0.353	4.74	0.22	0.1000	0.0057	-0.07	10.0000	0.5700	0.340	0.017	0.55	614	35	1774	82	3663	183	404	26	6
Ga4_6	8.0	0.543	12.36	0.94	0.1744	0.0120	0.08	5.7339	0.3945	0.498	0.042	0.35	1036	71	2632	200	4235	357	495	64	13
Ga4_7	4.2	0.748	24.00	1.80	0.2650	0.0210	0.53	3.7736	0.2990	0.660	0.055	0.38	1515	120	3268	245	4646	387	417	116	28
Ga4_8	6.3	0.753	30.30	2.00	0.3160	0.0240	0.30	3.1646	0.2403	0.668	0.048	0.33	1770	134	3497	231	4663	335	485	120	25
Ga4_9	22.2	0.627	13.20	0.80	0.1699	0.0120	0.44	5.8858	0.4157	0.561	0.030	0.28	1012	71	2694	163	4410	236	396	48	12
Ga4_10	31.8	0.438	6.80	0.34	0.1182	0.0074	0.28	8.4602	0.5297	0.409	0.021	0.37	720	45	2086	104	3942	202	415	32	8
Ga4_11	19.1	0.570	10.73	0.77	0.1492	0.0090	0.15	6.7024	0.4043	0.515	0.039	0.34	896	54	2500	179	4285	324	401	50	13
Ga4_12	51.5	0.322	4.23	0.22	0.0945	0.0055	0.13	10.5820	0.6159	0.315	0.018	0.32	582	34	1680	87	3546	203	400	26	7
Ga4_13	36.0	0.513	8.19	0.51	0.1246	0.0084	0.49	8.0257	0.5411	0.468	0.025	0.32	757	51	2252	140	4143	221	380	35	9
Ga4_14	39.2	0.388	5.45	0.38	0.1078	0.0074	0.33	9.2764	0.6368	0.369	0.025	0.38	660	45	1893	132	3787	257	412	35	8
Ga4_15	4.3	0.821	22.00	2.80	0.2360	0.0220	0.25	4.2373	0.3950	0.710	0.100	0.55	1366	127	3184	405	4751	669	266	186	70
Ga4_16	29.5	0.404	5.97	0.41	0.1093	0.0065	0.01	9.1491	0.5441	0.381	0.028	0.46	669	40	1971	135	3836	282	407	33	8
Ga4_17	20.3	0.421	6.72	0.49	0.1206	0.0075	-0.01	8.2919	0.5157	0.396	0.034	0.48	734	46	2075	151	3894	334	435	41	9
Ga4_18	28.2	0.453	6.62	0.40	0.1132	0.0071	0.07	8.8339	0.5541	0.420	0.029	0.39	691	43	2062	125	3982	275	387	35	9
Ga4_19	13.7	0.650	18.30	1.30	0.2290	0.0170	0.27	4.3668	0.3242	0.585	0.040	0.42	1329	99	3006	214	4471	306	497	78	16
Ga4_20	39.5	0.437	6.59	0.37	0.1156	0.0066	-0.15	8.6505	0.4939	0.408	0.026	0.53	705	40	2058	116	3939	251	406	32	8
Ga4_21	42.4	0.316	4.41	0.33	0.1002	0.0067	0.00	9.9800	0.6673	0.311	0.022	0.36	616	41	1714	128	3526	249	427	33	8
Ga4_22	35.1	0.391	5.55	0.31	0.1062	0.0062	0.19	9.4162	0.5497	0.371	0.021	0.32	651	38	1908	107	3796	215	404	29	7
Ga4_23	5.4	0.667	17.00	1.70	0.2120	0.0180	0.37	4.7170	0.4005	0.596	0.060	0.36	1239	105	2935	293	4498	453	439	103	23

Ga4_24	36.6	0.460	7.67	0.43	0.1318	0.0091	0.53	7.5873	0.5239	0.428	0.023	0.32	798	55	2193	123	4010	216	444	38	9
Ga4_25	22.9	0.554	12.44	0.86	0.1684	0.0110	0.22	5.9382	0.3879	0.506	0.037	0.43	1003	66	2638	182	4259	311	466	56	12
Ga4_26	45.2	0.375	5.23	0.29	0.1031	0.0061	0.12	9.6993	0.5739	0.358	0.020	0.32	633	37	1858	103	3741	209	402	28	7
Ga4_27	8.8	0.753	28.90	1.40	0.3180	0.0210	0.21	3.1447	0.2077	0.668	0.035	0.38	1780	118	3450	167	4663	244	488	90	18
Ga4_28	52.9	0.326	4.21	0.26	0.0949	0.0062	0.41	10.5374	0.6884	0.318	0.018	0.21	584	38	1676	104	3560	202	400	29	7
Ga4_29	42.9	0.374	5.60	0.43	0.1101	0.0081	0.40	9.0827	0.6682	0.358	0.030	0.21	673	50	1916	147	3741	314	430	40	9
Sample Bg-1		**Ballystrasna Formation**				**Locatio 52.063 N**		**8.695 W**		**Datum:**	**IRENET95**										
Bg1_25	10.2	0.641	13.10	1.20	0.1647	0.0120	0.17	6.0716	0.4424	0.571	0.052	0.31	983	72	2687	246	4436	404	370	71	19
Bg1_28	27.0	0.450	6.60	0.44	0.1150	0.0071	0.01	8.6957	0.5369	0.418	0.034	0.40	702	43	2059	137	3975	323	395	38	10
Bg1_12	65.7	0.144	1.75	0.14	0.0751	0.0043	0.23	13.3156	0.7624	0.171	0.014	0.08	467	27	1027	82	2567	210	402	24	6
Bg1_7	22.0	0.473	7.37	0.45	0.1223	0.0076	0.14	8.1766	0.5081	0.437	0.030	0.38	744	46	2157	132	4042	277	403	37	9
Bg1_22	22.8	0.422	6.36	0.57	0.1142	0.0076	0.08	8.7566	0.5827	0.396	0.037	0.29	697	46	2027	182	3894	364	412	42	10
Bg1_13	40.6	0.347	4.74	0.27	0.1039	0.0060	0.35	9.6246	0.5558	0.336	0.018	0.11	637	37	1774	101	3645	195	423	28	7
Bg1_16	88.4	0.364	5.20	0.23	0.1075	0.0060	0.38	9.3023	0.5192	0.350	0.014	0.09	658	37	1853	82	3707	148	426	26	6
Bg1_2	32.7	0.323	4.52	0.36	0.1018	0.0066	0.22	9.8232	0.6369	0.317	0.025	0.13	625	41	1735	138	3555	280	429	33	8
Bg1_23	14.7	0.548	11.47	0.94	0.1551	0.0110	0.10	6.4475	0.4573	0.499	0.049	0.40	929	66	2562	210	4238	416	437	65	15
Bg1_10	32.0	0.665	17.44	0.63	0.2097	0.0120	0.11	4.7687	0.2729	0.594	0.025	0.53	1227	70	2959	107	4493	189	438	47	11
Bg1_24	25.2	0.443	7.42	0.52	0.1263	0.0085	0.20	7.9177	0.5329	0.414	0.030	0.30	767	52	2163	152	3961	287	439	41	9
Bg1_20	12.1	0.635	15.20	1.00	0.1965	0.0120	0.11	5.0891	0.3108	0.570	0.043	0.34	1156	71	2828	186	4433	334	447	69	16
Bg1_26	7.8	0.642	16.70	1.30	0.2022	0.0130	-0.05	4.9456	0.3180	0.576	0.053	0.52	1187	76	2918	227	4449	409	451	86	19
Bg1_18	12.0	0.646	16.00	1.20	0.2082	0.0140	0.24	4.8031	0.3230	0.580	0.046	0.40	1219	82	2877	216	4459	354	458	78	17
Bg1_9	17.8	0.579	13.16	0.73	0.1770	0.0110	0.34	5.6497	0.3511	0.526	0.029	0.34	1051	65	2691	149	4316	238	463	48	10
Bg1_6	5.5	0.684	19.50	1.80	0.2370	0.0180	0.23	4.2194	0.3205	0.611	0.061	0.37	1371	104	3067	283	4534	453	466	114	25
Bg1_29	23.1	0.111	1.77	0.26	0.0905	0.0066	0.11	11.0497	0.8058	0.147	0.023	0.21	558	41	1035	152	2311	362	499	39	8
Bg1_0	37.9	0.398	7.30	0.32	0.1356	0.0076	-0.02	7.3746	0.4133	0.381	0.019	0.46	820	46	2149	94	3836	191	506	34	7
Bg1_1	54.6	0.808	41.85	0.88	0.4273	0.0230	0.41	2.3403	0.1260	0.714	0.014	0.25	2294	123	3816	80	4759	93	509	57	11
Bg1_17	12.8	0.543	12.85	0.87	0.1812	0.0120	0.20	5.5188	0.3655	0.499	0.036	0.42	1074	71	2669	181	4238	306	513	59	12
Bg1_19	14.2	0.504	11.10	1.40	0.1705	0.0120	0.32	5.8651	0.4128	0.468	0.056	-0.07	1015	71	2532	319	4143	496	523	80	15
Bg1_8	13.4	0.485	10.56	0.83	0.1677	0.0110	-0.01	5.9630	0.3911	0.453	0.041	0.44	999	66	2485	195	4095	371	534	62	12
Bg1_5	7.1	0.599	17.40	1.40	0.2240	0.0160	0.21	4.4643	0.3189	0.547	0.046	0.38	1303	93	2957	238	4373	368	554	86	15
Bg1_21	8.8	0.625	19.70	1.30	0.2470	0.0180	0.17	4.0486	0.2950	0.569	0.043	0.53	1423	104	3077	203	4431	335	571	89	16
Bg1_3	13.4	0.657	22.30	1.30	0.2700	0.0170	0.30	3.7037	0.2332	0.595	0.035	0.30	1541	97	3197	186	4496	264	571	79	14
Bg1_4	16.2	0.796	45.90	1.80	0.4640	0.0300	0.61	2.1552	0.1393	0.709	0.027	0.43	2457	159	3907	153	4749	181	584	102	17
Bg1_11	21.3	0.229	8.97	0.52	0.2364	0.0150	0.22	4.2301	0.2684	0.268	0.016	0.36	1368	87	2335	135	3294	197	1079	71	7
Bg1_27	8.5	0.777	31.20	2.20	0.3280	0.0220	0.22	3.0488	0.2045	0.686	0.051	0.41	1829	123	3525	249	4702	350	454	130	29
Bg1_15	2.0	0.917	152.30	9.40	1.3480	0.0950	0.54	0.7418	0.0523	0.815	0.045	0.39	5502	388	5110	315	4948	273	685	448	65
Bg1_14	2.8	0.745	418.00	69.00	3.6800	0.5800	0.98	0.2717	0.0428	0.804	0.033	0.20	9949	1568	6131	1012	4929	202	0	1251	-

Table VII. Adjusted detrital mica ages from Ennis et al. (2015) based on the standard age of Kuiper e

Experiment	Adjusted Age (Ma)	1 s
Sample 030207-2		
C1304701	408	6.3
C1304702	433.9	4.2
C1304703	418	5.2
C1304704	439.5	7.2
C1304705	404.8	7.7
C1304706	429.6	6.6
C1304707	430	7.2
C1304708	396.9	6.6
C1304709	435.3	4.2
C1304710	399.4	5.9
C1304711	379.9	7.4
C1304712	407.3	7.3
C1304713	385.3	13.1
C1304714	421.9	4.2
C1304715	387.5	4.6
C1304716	388.2	5.6
C1304717	419	5.2
C1304718	379.9	10.3
C1304719	381	11
C1304720	352.9	19.6
C1304721	367.2	15
C1304722	385.7	10.9
C1304723	392.6	7.4
C1304724	417.6	6.6
C1304725	400.1	7.3
C1304726	358.8	17.3
C1304727	382.4	8.5
C1304728	372.3	10.7
C1304729	380.3	8.5
C1304730	383.2	12.4
C1304731	407.3	6.6
C1304732	370.5	13.2
C1304733	410.8	8.7
C1304734	411.9	7.6
C1304735	363.5	16.2
C1304736	307.8	10.3
C1304737	369.4	8.9
C1304738	378.1	8.8
C1304739	385.3	9.9
C1304740	381.4	15.6
C1304741	417.2	6.2
C1304742	420.4	7.6
C1304743	330.3	33.9
Sample 150206-2		
C1200501	423.8	1.8
C1200502	404.8	3.8
C1200503	415.0	2.5
C1200504	396.0	4.1
C1200505	427.9	3.4
C1200506	405.1	1.9
C1200507	385.6	2.4
C1200508	455.2	2.8
C1200509	397.9	2.7
C1200510	392.5	2.7
C1200511	432.8	1.8
C1200512	414.3	3.8
C1200513	384.0	1.6
C1200514	419.6	3.4
C1200515	413.9	1.9

Fish Canyon sanidine

Decay constant

C1200516	407.4	1.7
C1200517	417.3	4.5
C1200518	417.7	1.6
C1200519	405.5	4.1
C1200520	412.8	3.4
C1200521	402.5	4.1
C1200522	386.0	3.4
C1200523	416.2	5.2
C1200524	382.1	5.6
C1200525	379.0	2.1
C1200526	415.0	2.8
C1200527	396.3	2.7
C1200528	403.6	2.2
C1200529	418.5	3.4
C1200530	377.4	2.1
C1200531	414.3	2.5
C1200532	409.0	1.7
C1200533	381.3	1.6
C1200534	400.9	2.4
C1200535	377.4	1.8
C1200536	403.6	2.8
C1200537	423.0	2.0
C1200538	458.6	2.1
C1200539	365.4	3.4
C1200540	419.6	4.5
C1200541	366.2	1.6
C1200542	415.8	1.6
C1200543	400.9	2.2
Sample 121105-3		
C1200601	414.8	1.9
C1200602	391.1	1.9
C1200603	423.5	2.0
C1200604	388.8	1.9
C1200607	423.5	2.0
C1200608	410.6	2.2
C1200609	408.3	1.6
C1200610	422.3	1.8
C1200611	396.8	2.7
C1200612	378.0	1.5
C1200613	383.8	1.6
C1200614	395.3	1.7
C1200615	400.7	1.7
C1200616	396.1	1.9
C1200617	379.5	1.5
C1200618	381.1	2.4
C1200619	417.8	1.7
C1200620	378.3	2.1
C1200621	395.7	1.5
C1200622	378.0	2.1
C1200623	394.9	1.7
C1200624	412.1	1.7
C1200625	372.1	1.8
C1200626	431.8	2.5
C1200627	371.0	1.8
C1200628	426.5	1.8
C1200629	406.4	1.9
C1200630	411.7	2.5
C1200631	365.9	2.1
C1200632	414.8	2.2
C1200633	454.2	2.0
C1200634	410.6	1.7
C1200635	379.1	2.4
C1200636	424.2	1.8

C1200637	443.7	1.8
C1200638	379.5	1.6
C1200639	414.0	1.7
C1200640	452.7	2.0
C1200641	368.6	1.8
C1200642	447.5	1.8
Sample 121105-1A		
C1200701	403.6	1.7
C1200702	389.8	1.9
C1200703	400.5	1.9
C1200704	409.3	2.2
C1200705	419.2	1.6
C1200706	415.4	1.7
C1200707	430.5	1.8
C1200708	448.8	1.8
C1200709	432.0	1.8
C1200710	406.6	1.7
C1200711	438.0	1.8
C1200712	447.3	1.8
C1200713	403.2	1.7
C1200714	407.4	1.9
C1200715	418.0	1.6
C1200716	413.1	1.9
C1200717	374.7	1.8
C1200718	379.4	1.8
C1200719	412.7	1.7
C1200720	382.1	4.9
C1200721	400.5	1.7
C1200722	380.2	1.5
C1200723	401.3	4.1
C1200724	422.9	1.6
C1200725	391.7	7.1
C1200726	420.7	2.2
C1200727	443.2	1.8
C1200728	429.0	2.2
C1200729	405.9	1.9
C1200730	415.0	1.9
C1200731	375.1	1.5
C1200732	462.9	1.9
C1200733	397.5	1.9
C1200734	449.9	4.1
C1200735	405.1	3.1
C1200736	410.1	1.6
C1200737	356.0	1.8
C1200738	411.6	1.7

et al. (2008)

Age (years)	1 sigma
28200677.31	22383.02

per year	1 sigma
5.46E-10	5.35E-12

Table VIII. Total fusion $^{40}Ar/^{39}Ar$ ages for white micas for samples from the UORS and offshore basins.

Experiment no.	^{36}Ar [fA]	%1s	^{37}Ar [fA]	%1s	^{38}Ar [fA]	%1s	^{39}Ar [fA]	%1s	^{40}Ar [fA]	%1s	ł0(r)/39(k) ± 1s	Age ± 1s (Ma)	$^{40}Ar(r)$ (%)	$^{39}Ar(k)$ (%)
Sample BF22														
092_VU107-M5	0.00038	58.004	0.00457	102.654	0.00331	6.403	0.314755	3.385	14.3659	0.183	45.2863 ± 1.549	363.2 ± 11.3	99.22	0.57
073_VU107-M5	0.00555	6.780	-0.00358	137.188	0.03318	1.165	2.686494	0.994	129.1166	0.149	47.4432 ± 0.479	378.8 ± 3.5	98.71	4.87
105_VU107-M5	0.00120	21.595	0.01130	46.183	0.01268	2.441	1.085876	1.691	52.2418	0.151	47.7793 ± 0.815	381.2 ± 5.9	99.31	1.97
101_VU107-M5	0.00564	7.725	0.00242	242.547	0.04579	0.963	3.742002	0.393	182.2971	0.152	48.2657 ± 0.206	384.7 ± 1.5	99.07	6.78
071_VU107-M5	0.00329	8.764	-0.00330	168.998	0.01849	2.525	1.518499	0.679	74.7904	0.151	48.6052 ± 0.343	387.2 ± 2.5	98.69	2.75
103_VU107-M5	0.00014	243.382	0.00320	143.074	0.00402	8.014	0.372583	6.911	18.1509	0.297	48.6056 ± 3.373	387.2 ± 24.2	99.77	0.68
083_VU107-M5	0.00402	6.795	-0.00115	517.190	0.01369	3.009	1.062187	1.247	53.1136	0.152	48.8724 ± 0.619	389.1 ± 4.4	97.74	1.92
091_VU107-M5	0.00152	24.024	0.00877	61.578	0.00931	3.300	0.768674	1.548	38.1093	0.157	48.9890 ± 0.775	389.9 ± 5.6	98.81	1.39
066_VU107-M5	0.00213	12.740	0.00234	252.799	0.00718	4.593	0.539562	2.386	27.0746	0.162	49.0013 ± 1.181	390.0 ± 8.5	97.65	0.98
082_VU107-M5	0.00720	4.771	0.00838	76.660	0.03122	1.597	2.498662	0.636	124.6621	0.151	49.0308 ± 0.324	390.2 ± 2.3	98.27	4.53
087_VU107-M5	0.00063	49.949	0.00725	77.772	0.00930	3.909	0.791512	1.915	39.0007	0.157	49.0361 ± 0.950	390.3 ± 6.8	99.52	1.43
072_VU107-M5	0.00358	7.702	-0.00461	96.123	0.01204	2.708	0.976954	1.130	49.1446	0.158	49.2081 ± 0.568	391.5 ± 4.1	97.82	1.77
093_VU107-M5	0.00271	10.362	0.00044	1444.410	0.02601	2.098	2.234281	0.535	110.9166	0.155	49.2801 ± 0.277	392.0 ± 2.0	99.27	4.05
106_VU107-M5	0.00082	27.655	0.01308	42.670	0.01112	3.035	0.978579	1.503	48.6252	0.158	49.4408 ± 0.750	393.2 ± 5.4	99.50	1.77
088_VU107-M5	0.00387	7.018	-0.00195	217.047	0.04400	1.263	3.584537	0.387	178.5928	0.148	49.4999 ± 0.207	393.6 ± 1.5	99.35	6.49
070_VU107-M5	0.00236	14.220	-0.00337	151.465	0.01691	2.166	1.336528	0.794	66.9735	0.149	49.5808 ± 0.408	394.2 ± 2.9	98.94	2.42
069_VU107-M5	0.00354	8.105	-0.01328	33.257	0.01633	1.929	1.324838	0.658	66.8554	0.153	49.6625 ± 0.342	394.7 ± 2.4	98.41	2.40
064_VU107-M5	0.00455	7.210	-0.00297	208.546	0.01295	2.897	1.044928	1.169	53.2987	0.167	49.7071 ± 0.595	395.1 ± 4.3	97.45	1.89
104_VU107-M5	0.00710	5.143	0.00119	476.389	0.02327	1.608	1.854211	0.903	94.3445	0.148	49.7375 ± 0.459	395.3 ± 3.3	97.75	3.36
099_VU107-M5	0.00362	8.734	-0.00470	112.737	0.02443	1.871	2.071988	0.639	104.1440	0.147	49.7397 ± 0.330	395.3 ± 2.4	98.96	3.75
097_VU107-M5	0.00792	4.194	-0.00153	294.672	0.02225	1.087	1.744753	0.643	89.2315	0.149	49.7859 ± 0.334	395.6 ± 2.4	97.35	3.16
089_VU107-M5	0.00324	11.608	0.00132	356.555	0.04230	1.211	3.600576	0.412	181.3273	0.172	50.0911 ± 0.226	397.8 ± 1.6	99.46	6.52
080_VU107-M5	0.00087	30.251	-0.01212	46.089	0.01223	2.654	1.023418	1.312	51.5335	0.157	50.0989 ± 0.666	397.9 ± 4.8	99.49	1.85
095_VU107-M5	0.00441	8.074	0.00072	645.596	0.01789	2.317	1.428248	0.816	73.0580	0.151	50.2290 ± 0.424	398.8 ± 3.0	98.20	2.59
098_VU107-M5	0.00115	23.492	-0.00454	121.202	0.01243	3.041	1.035113	1.181	52.4739	0.154	50.3614 ± 0.605	399.7 ± 4.3	99.34	1.88
094_VU107-M5	0.00316	10.923	0.01061	48.864	0.02505	1.526	1.986540	0.643	101.1570	0.151	50.4462 ± 0.337	400.3 ± 2.4	99.07	3.60
061_VU107-M5	0.00417	7.185	-0.00071	737.393	0.02827	1.583	2.322307	0.548	118.7690	0.152	50.6061 ± 0.290	401.5 ± 2.1	98.95	4.21
085_VU107-M5	0.00098	35.834	0.00310	174.772	0.00936	3.280	0.761521	2.050	38.8370	0.159	50.6130 ± 1.050	401.5 ± 7.5	99.24	1.38
081_VU107-M5	0.00334	8.888	0.00337	146.047	0.00918	4.443	0.713563	1.798	37.2452	0.160	50.7993 ± 0.926	402.8 ± 6.6	97.32	1.29
063_VU107-M5	0.00360	7.199	0.00707	73.380	0.01847	1.766	1.543862	0.756	79.5544	0.153	50.8321 ± 0.395	403.1 ± 2.8	98.65	2.80
060_VU107-M5	0.00210	11.410	-0.00456	117.901	0.01439	2.541	1.174339	0.889	60.4392	0.186	50.9308 ± 0.467	403.8 ± 3.3	98.96	2.13
067_VU107-M5	0.00076	34.839	0.00887	62.441	0.00887	3.878	0.761038	1.878	39.3607	0.155	51.4235 ± 0.975	407.3 ± 6.9	99.43	1.38
059_VU107-M5	0.00307	11.620	-0.00024	1983.293	0.02266	1.751	1.860463	0.803	96.6188	0.148	51.4390 ± 0.424	407.4 ± 3.0	99.05	3.37
086_VU107-M5	0.00318	9.071	-0.00209	293.704	0.01387	2.558	1.074857	1.271	56.2578	0.164	51.4545 ± 0.664	407.5 ± 4.7	98.31	1.95
100_VU107-M5	0.00130	18.567	-0.00070	679.372	0.01114	2.705	0.904282	1.410	47.1051	0.229	51.6614 ± 0.742	409.0 ± 5.3	99.17	1.64
079_VU107-M5	0.00239	11.665	0.00101	488.395	0.02039	2.136	1.619755	0.856	84.6564	0.153	51.8244 ± 0.454	410.1 ± 3.2	99.16	2.93
065_VU107-M5	0.00018	164.572	-0.00002	29303.073	0.01032	2.744	0.850206	1.483	45.5949	0.160	53.5641 ± 0.806	422.4 ± 5.7	99.88	1.54
Sample BF21														
143_VU107-M7_2	0.00361	8.651	-0.01290	108.354	0.00482	5.435	0.326754	0.435	14.3382	0.106	40.5766 ± 0.339	328.6 ± 2.5	92.47	0.60
146_VU107-M7_2	0.00232	13.280	-0.00523	270.525	0.01498	1.721	1.222451	0.163	60.4025	0.055	48.8440 ± 0.113	388.9 ± 0.8	98.85	2.24
189_VU107-M7	-0.00003	1138.993	-0.00086	484.685	0.00857	3.269	0.704381	2.536	35.2810	0.161	50.0986 ± 1.280	397.9 ± 9.1	100.02	1.29
166_VU107-M7	0.00008	309.838	-0.00020	2232.114	0.00241	12.093	0.217380	7.316	11.0328	0.234	50.6446 ± 3.722	401.7 ± 26.5	99.79	0.40
163_VU107-M7	-0.00064	39.212	0.00969	44.137	0.00388	7.054	0.297375	4.633	15.3108	0.179	52.1364 ± 2.431	412.3 ± 17.2	101.26	0.54
194_VU107-M7	0.00101	22.142	0.00896	69.549	0.00505	4.676	0.468328	5.113	25.3367	0.163	53.4584 ± 2.738	421.7 ± 19.3	98.81	0.86
199_VU107-M7	-0.00026	104.206	-0.00094	594.694	0.00501	4.406	0.379891	3.303	20.5641	0.180	54.3314 ± 1.809	427.8 ± 12.7	100.37	0.69
201_VU107-M7	0.00307	10.218	0.00129	485.182	0.00921	3.346	0.730607	1.766	40.6340	0.156	54.3623 ± 0.972	428.0 ± 6.8	97.74	1.34
178_VU107-M7	0.00094	32.287	-0.00921	61.268	0.01436	2.877	1.121545	1.368	62.3560	0.152	55.3462 ± 0.766	434.9 ± 5.4	99.55	2.05
200_VU107-M7	0.00046	70.089	0.00629	97.145	0.00708	4.901	0.612501	3.163	34.1869	0.162	55.5915 ± 1.768	436.6 ± 12.4	99.60	1.12
188_VU107-M7	-0.00009	253.012	-0.00142	420.275	0.00218	11.883	0.167657	9.505	9.3444	0.234	55.8968 ± 5.331	438.8 ± 37.2	100.29	0.31
135_VU107-M7_2	0.00932	4.083	-0.01137	86.766	0.00699	3.830	0.507355	0.299	31.4196	0.093	56.4430 ± 0.286	442.6 ± 2.0	91.14	0.93
195_VU107-M7	0.00135	23.420	-0.00697	88.619	0.01926	1.603	1.642638	1.348	93.3066	0.161	56.5553 ± 0.770	443.4 ± 5.4	99.56	3.00
140_VU107-M7_2	0.00069	34.788	-0.00631	217.314	0.00992	3.430	0.788142	0.342	44.7904	0.059	56.5678 ± 0.216	443.5 ± 1.5	99.54	1.44
165_VU107-M7	0.00148	17.168	-0.00490	88.500	0.00691	4.919	0.602096	2.452	34.5161	0.162	56.5887 ± 1.396	443.6 ± 9.7	98.71	1.10
114_VU107-M7_2	0.00038	71.640	0.00760	161.729	0.00186	12.189	0.147943	0.563	8.5005	0.133	56.6920 ± 0.642	444.3 ± 4.5	98.66	0.27
162_VU107-M7	0.00877	4.425	0.00014	4474.885	0.01071	2.971	0.768223	1.287	46.3192	0.152	56.8838 ± 0.753	445.7 ± 5.2	94.34	1.41
181_VU107-M7	0.00151	20.945	-0.00791	56.504	0.01597	2.072	1.321612	1.207	75.7616	0.157	56.9818 ± 0.698	446.3 ± 4.8	99.40	2.42
142_VU107-M7_2	0.00075	36.725	-0.01844	66.025	0.00362	5.700	0.288176	0.379	16.6534	0.093	57.0036 ± 0.362	446.5 ± 2.5	98.65	0.53
137_VU107-M7_2	0.00275	8.947	-0.02458	55.848	0.00596	3.001	0.470000	0.383	27.6205	0.082	57.0117 ± 0.273	446.5 ± 1.9	97.02	0.86
125_VU107-M7_2	0.00081	27.176	0.00731	185.025	0.01114	2.793	0.913621	0.259	52.4577	0.078	57.1534 ± 0.170	447.5 ± 1.2	99.54	1.67
108_VU107-M7_2	0.00045	65.718	-0.00513	300.077	0.00635	3.706	0.517444	0.296	29.7360	0.104	57.2055 ± 0.248	447.9 ± 1.7	99.55	0.95
133_VU107-M7_2	0.00045	59.152	0.00285	415.144	0.00596	3.985	0.498855	0.253	28.7216	0.075	57.3049 ± 0.220	448.6 ± 1.5	99.53	0.91
161_VU107-M7	0.00011	259.910	0.00629	60.517	0.01534	2.848	1.296724	0.996	74.3946	0.159	57.3458 ± 0.582	448.9 ± 4.0	99.96	2.37
206_VU107-M7	0.00059	48.652	-0.00299	201.532	0.01992	1.413	1.598672	0.985	91.8644	0.173	57.3520 ± 0.576	448.9 ± 4.0	99.81	2.92
193_VU107-M7	0.00094	36.602	-0.00362	117.540	0.01073	3.396	0.899195	2.580	51.9095	0.157	57.4143 ± 1.488	449.3 ± 10.3	99.46	1.64
123_VU107-M7_2	0.00107	19.623	0.02009	78.372	0.01250	2.730	0.998788	0.144	57.6919	0.074	57.4447 ± 0.112	449.5 ± 0.8	99.45	1.83
141_VU107-M7_2	0.00271	10.107	-0.01435	81.000	0.01325	1.386	1.026127	0.233	59.8036	0.050	57.4904 ± 0.158	449.9 ± 1.1	98.64	1.88
109_VU107-M7_2	0.00174	16.106	-0.00606	264.519	0.00971	3.171	0.755241	0.252	43.9887	0.091	57.5549 ± 0.190	450.3 ± 1.3	98.82	1.38
124_VU107-M7_2	0.00225	13.940	0.01289	104.247	0.00823	4.496	0.650984	0.254	38.1593	0.055	57.5886 ± 0.208	450.5 ± 1.4	98.24	1.19
129_VU107-M7_2	0.00047	37.623	0.00305	333.676	0.00814	3.847	0.627094	0.259	36.2596	0.071	57.5972 ± 0.176	450.6 ± 1.2	99.61	1.15
197_VU107-M7	0.00017	161.082	-0.00231	242.762	0.01214	2.906	1.001401	2.729	57.7848	0.155	57.6523 ± 1.578	451.0 ± 10.9	99.91	1.83
121_VU107-M7_2	0.00115	21.639	0.02217	66.073	0.00308	8.160	0.247591	0.428	14.6244	0.097	57.6950 ± 0.392	451.3 ± 2.7	97.67	0.45
196_VU107-M7	0.00111	28.903	0.00060	990.913	0.01196	3.538	1.022044	2.481	59.3034	0.168	57.6995 ± 1.438	451.3 ± 10.0	99.44	1.87
207_VU107-M7	-0.00009	311.820	-0.00279	170.137	0.00960	3.216	0.775916	1.751	44.7483	0.191	57.7037 ± 1.021	451.3 ± 7.1	100.06	1.42